

UNIVERSITY OF CALIFORNIA, DAVIS  
MCCLELLAN NUCLEAR RESEARCH CENTER  
TRIGA RESEARCH REACTOR  
LICENSE NO. R-130  
DOCKET NO. 50-607

LICENSE RENEWAL APPLICATION  
UPDATED SAFETY ANALYSIS REPORT  
FOR THE  
UNIVERSITY OF CALIFORNIA, DAVIS  
MCCLELLAN NUCLEAR RESEARCH CENTER  
RESEARCH REACTOR  
JUNE 11, 2018

REDACTED VERSION\*

SECURITY-RELATED INFORMATION REMOVED

\*REDACTED TEXT AND FIGURES BLACKED OUT OR DENOTED BY BRACKETS

**CHAPTER 1**

**INTRODUCTION AND GENERAL**

**DESCRIPTION OF PLANT**

Chapter 1 - Valid Pages  
Rev. 6 04/30/18

i	Rev. 6	04/30/18
1-1	Rev. 6	04/30/18
1-2	Rev. 6	04/30/18
1-3	Rev. 6	04/30/18
1-4	Rev. 6	04/30/18
1-5	Rev. 6	04/30/18
1-6	Rev. 6	04/30/18
1-7	Rev. 6	04/30/18
1-8	Rev. 6	04/30/18
1-9	Rev. 6	04/30/18
1-10	Rev. 6	04/30/18
1-11	Rev. 6	04/30/18
1-12	Rev. 6	04/30/18
1-13	Rev. 6	04/30/18
1-14	Rev. 6	04/30/18
1-15	Rev. 6	04/30/18
1-16	Rev. 6	04/30/18
1-17	Rev. 6	04/30/18
1-18	Rev. 6	04/30/18

TABLE OF CONTENTS

1.0 INTRODUCTION AND GENERAL DESCRIPTION OF PLAN..... 1-1

1.1 Introduction..... 1-1

1.1.1 Purpose of Facility ..... 1-1

1.1.2 Location of Facility ..... 1-1

1.2 General Plant Description..... 1-2

1.2.1 Building..... 1-2

1.2.2 Reactor ..... 1-10

1.3 Relation of UCD/MNRC to Other TRIGA® Reactors..... 1-12

1.4 Safety Summary..... 1-14

1.4.1 Nuclear ..... 1-14

1.4.2 Building..... 1-17

LIST OF TABLES

1-1 TYPICAL PRINCIPAL DESIGN PARAMETERS..... 1-13

LIST OF FIGURES

1.1 ARTIST’S AXONOMETRIC VIEW OF MAIN UCD/MNRC FACILITY 1-3

1.2 UNIVERSITY OF CALIFORNIA - DAVIS/McCLELLAN NUCLEAR RADIATION CENTER 1-4

1.3 UCD/MNRC PLAN VIEW - MAIN FLOOR..... 1-5

1.4 UCD/MNRC PLAN VIEW - SECOND FLOOR ..... 1-6

1.5 UCD/MNRC ELEVATION SECTION A-A ..... 1-7

1.6 UCD/MNRC ELEVATION SECTION B-B ..... 1-8

1.7 UCD/MNRC ELEVATION SECTIONS..... 1-9

1.8 UCD/MNRC REACTOR..... 1-11

## 1.0 INTRODUCTION AND GENERAL DESCRIPTION OF PLAN

### 1.1 Introduction

This Safety Analysis Report supports an application to the Nuclear Regulatory Commission (NRC) by the University of California - Davis (UCD) for the utilization of a steady-state 2000 kW TRIGA<sup>®</sup> fueled reactor with a pulsing capability with a maximum reactivity step insertion of  $\beta$ 1.75. The reactor is owned and operated by UCD for neutron radiography and irradiation services for both university and non-university tasks. The facility is known as the University of California - Davis/McClellan Nuclear Research Center (UCD/MNRC).

This document addresses only the safety issues associated with the operation of the UCD/MNRC reactor. This document reflects the as-built condition of the facility and includes experience with the operation and performance of the reactor systems, radiation surveys, and personnel exposure histories related to operation of the UCD/MNRC at 1 MW and 2 MW. Accident scenarios are analyzed in Chapter 13. The industrial safety issues involving the handling of radiographic parts and irradiation experiments are addressed in the UCD/MNRC Operational Safety Hazards Analysis and support documents.

#### 1.1.1 Purpose of Facility

The UCD/MNRC provides a broad range of radiographic and irradiation services to the military and non-military sector. The facility presently provides four radiography bays and consequently four beams of neutrons for radiography purposes. In addition to the radiography bays, the UCD/MNRC reactor core and associated experiment facilities are completely accessible for the irradiation of material. These irradiation services include silicon doping, isotope production, both medical and industrial, and neutron activation analysis (e.g., geological samples). Although all four radiography bays are capable of using radiography film techniques, Bays 1, 2, and 3 are equipped with electronic imaging devices as well. All bays contain the equipment required to position parts for inspection as well as the radiography equipment. To meet facility use requirements, the reactor system and associated experiment facilities are designed to operate three shifts per day.

#### 1.1.2 Location of Facility

The reactor is located in the UCD/MNRC Building [REDACTED] on the former McClellan AFB, an industrial park of 2600 acres located approximately 8 miles northeast of Sacramento, California.

The industrial park is adequately suited for the location of the UCD/MNRC reactor. This is substantiated by this document and by the fact there are dozens of TRIGA<sup>®</sup> reactors in operation worldwide, including 16 in the United States. Many of these reactors are located on university campuses and in hospitals with surrounding high populated areas.

## 1.2 General Plant Description

### 1.2.1 Building

The UCD/MNRC is a three-level 18,000 ft<sup>2</sup> rectangular shaped building that incorporates a TRIGA<sup>®</sup> reactor, as shown in Figures 1.1 through 1.7. This facility provides space, shielding, and environmental control for the radiography and irradiation services work. Adequate room has been provided to handle the experiments and components in the facility in a safe manner.

The ground-level elements of the UCD/MNRC are constructed of reinforced concrete and concrete unit masonry with minor elements of exposed steel. The exterior walls of the upper portions feature factory-colored metal panels, concrete, and concrete unit masonry walls.

The exterior walls of the radiography bays are made of reinforced concrete and vary in thickness from 2 to 3 feet. The interior walls and the roofs of the radiography bays are constructed of 2-ft thick reinforced concrete.

The reactor room is above the radiography bays. Its walls are constructed of standard-filled reinforced concrete block and it has a typical metal deck built-up roof.

The reactor is located in a cylindrical aluminum walled tank with the core positioned approximately 4.5 ft below grade (i.e., tank bottom is ~6.5 ft below grade) (Figure 1.2). The reactor tank is surrounded by a monolithic block of reinforced concrete. Below ground level, the concrete is approximately 11 ft thick. Above ground level, the concrete varies in thickness from approximately 10 ft to 3.25 ft with the smaller dimension at the tank top. The tank is supported by a concrete pad approximately 9.5 ft thick.

The basic purpose of the massive concrete structures is to provide biological shielding for personnel working in and around the UCD/MNRC. However, due to the massiveness of these structures, they provide excellent protection for the reactor core against natural phenomena.

Another irradiation facility had been added to the original UCD/MNRC structural design. This facility is located in the lower level of Bay 4 and is called Bay 5. This facility was created by cutting a cavity into the biological shield so that a fifth neutron beam can be extracted from approximately the core centerline. The cavity extends from the outer surface of the biological shield to the tank wall. The cavity cross section is 10 feet high by 8.5 feet wide until about six inches from the tank wall. The last six inches has a window that exposes about a 3 feet high by 3.5 feet wide rectangular area of the tank wall. For now, the cavity has been filled with concrete block to keep the radiation levels below allowable limits (Section 11.1.1.3.1).

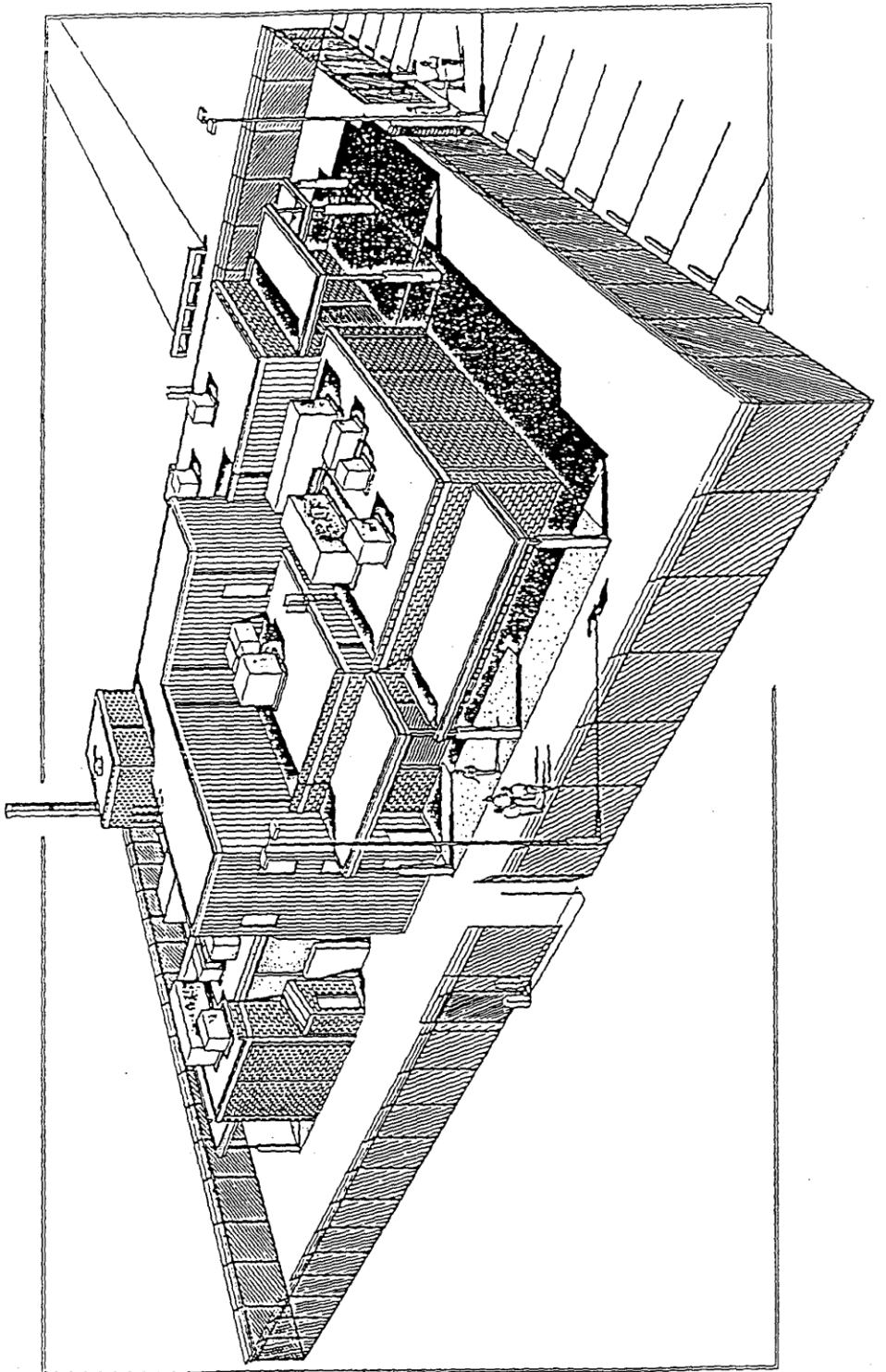
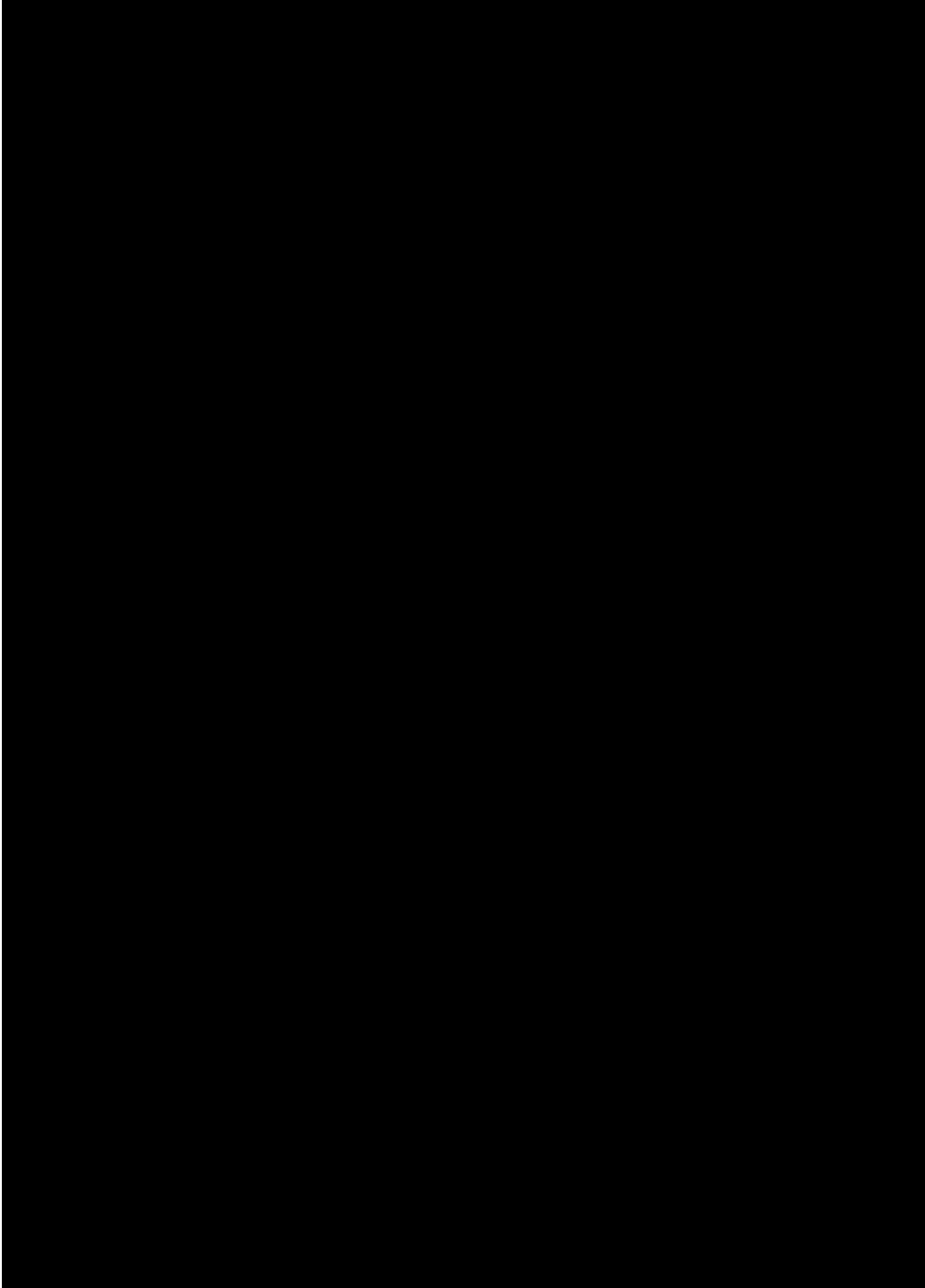
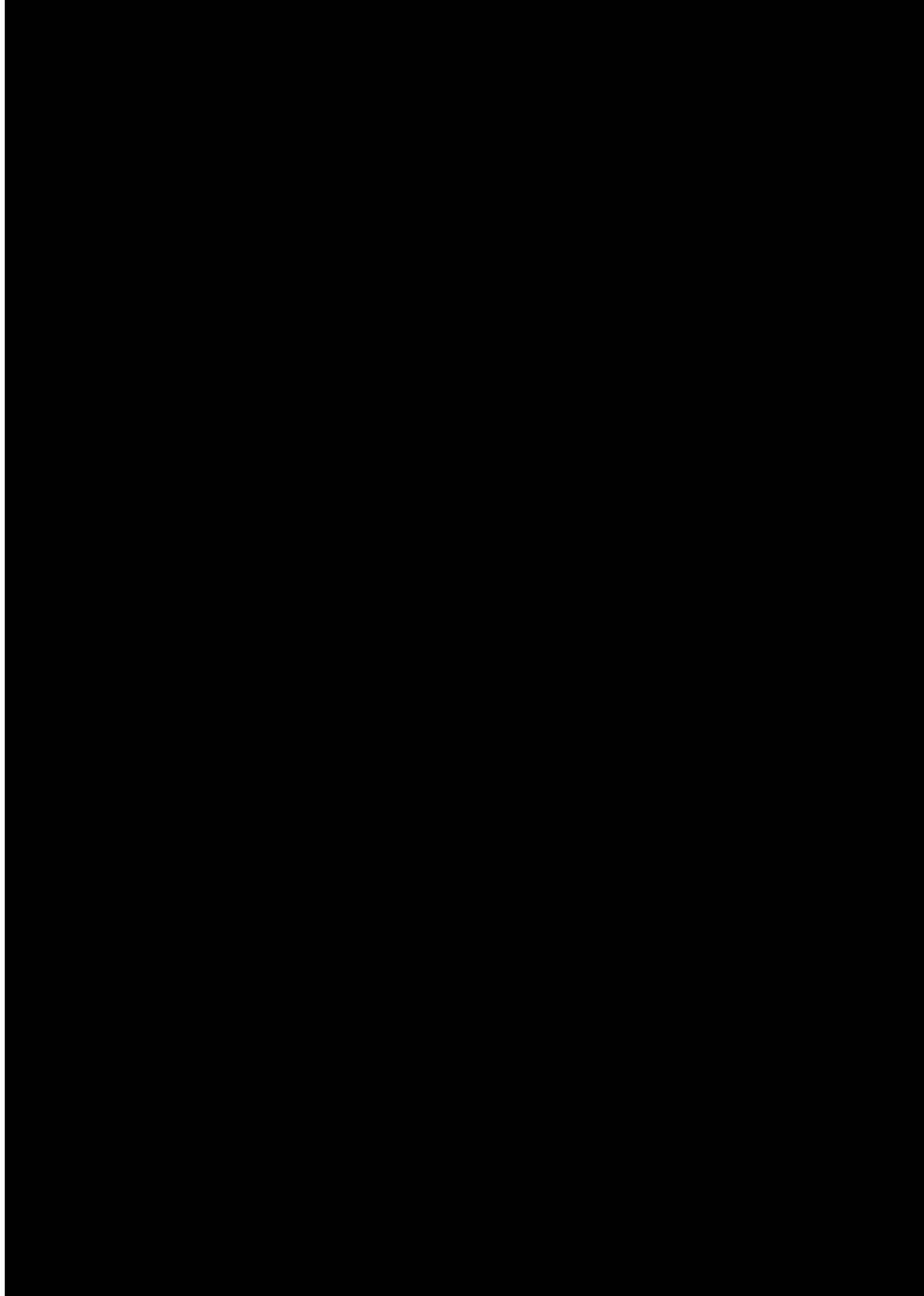


FIGURE 1.1 ARTIST'S AXONOMETRIC VIEW OF MAIN UCD/MNRC FACILITY



**FIGURE 1.2 UNIVERSITY OF CALIFORNIA - DAVIS/McCLELLAN NUCLEAR RESEARCH CENTER**



**FIGURE 1.3 UCD/MNRC PLAN VIEW - MAIN FLOOR**

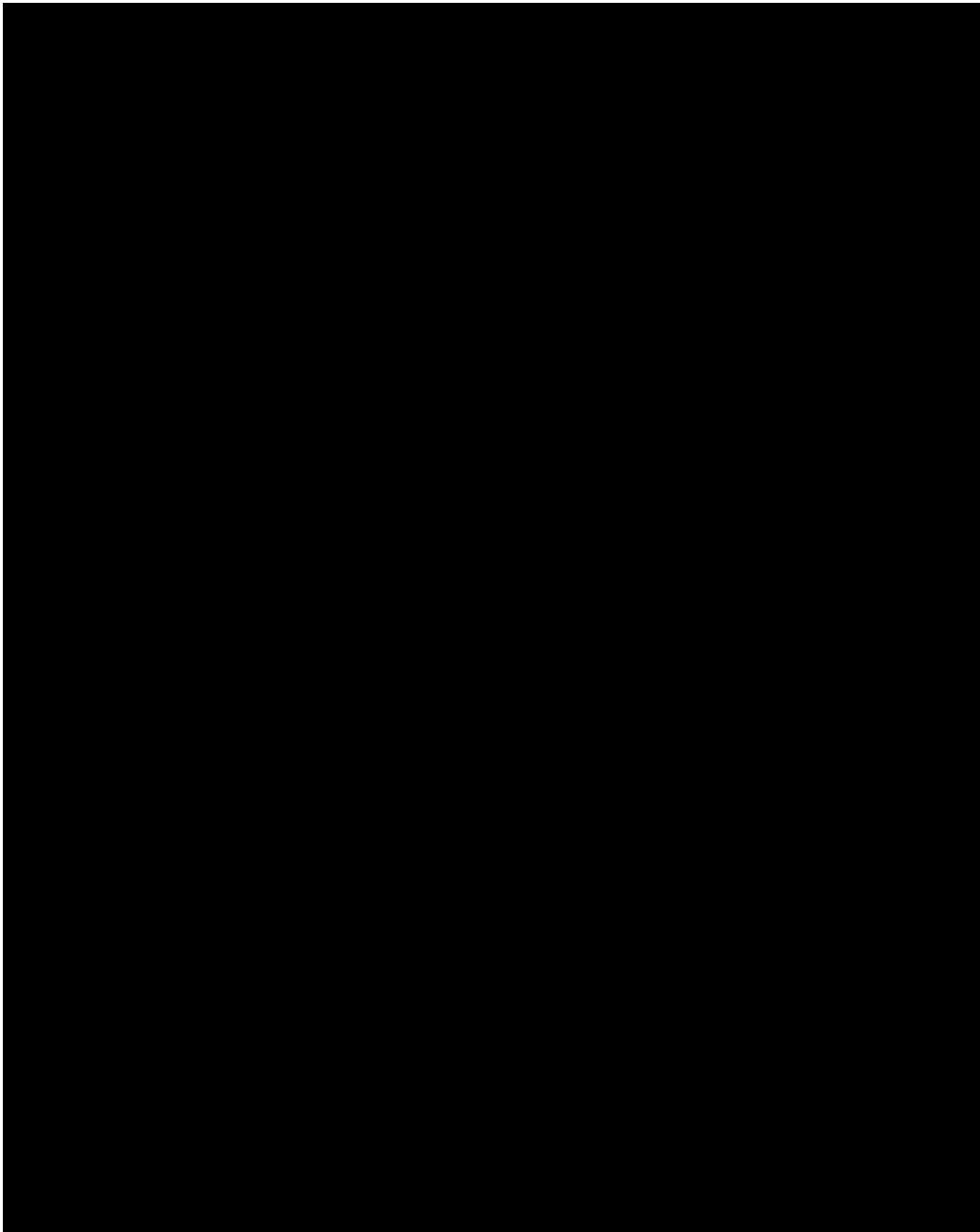


**FIGURE 1.4 UCD/MNRC PLAN VIEW - SECOND FLOOR**

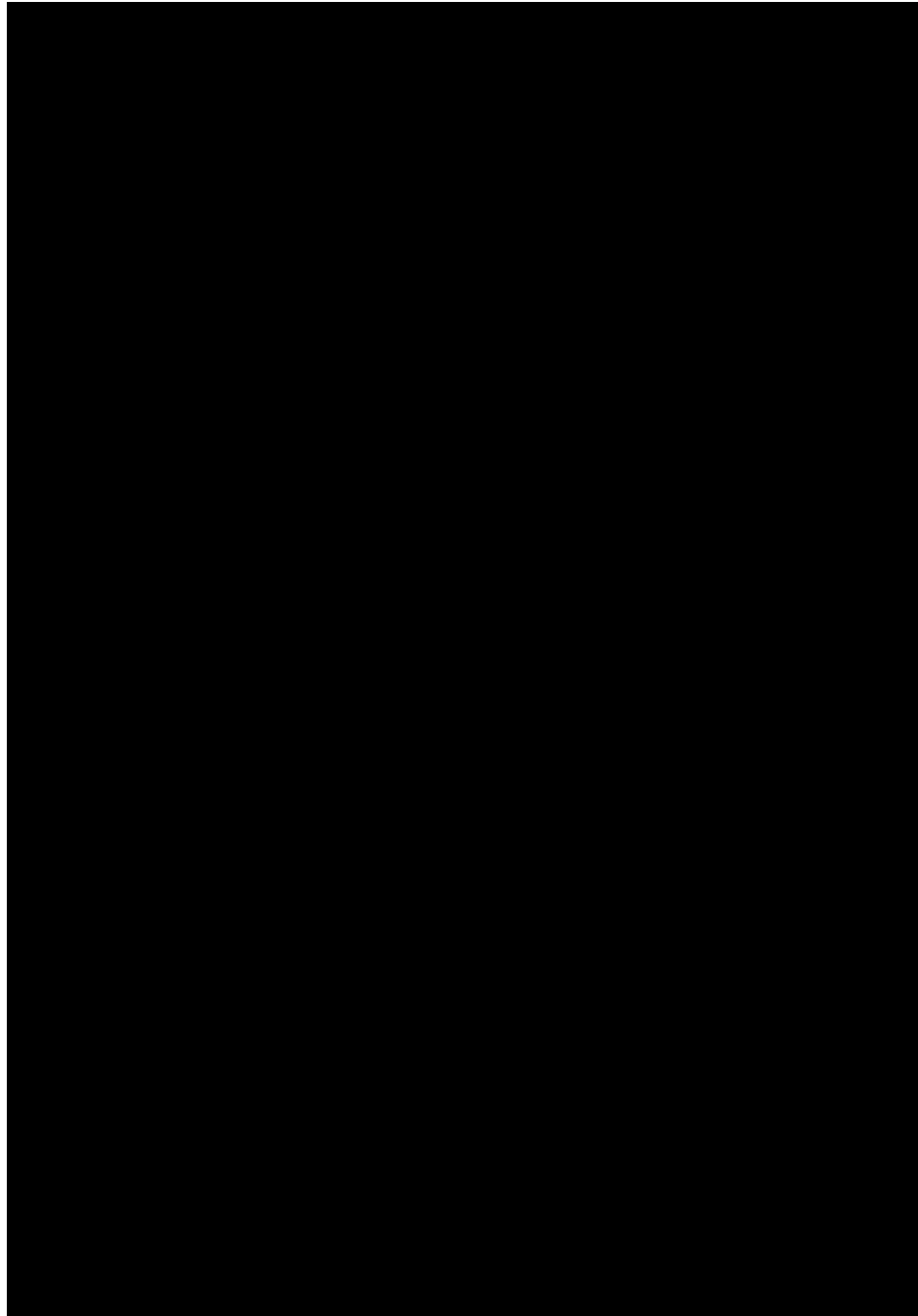


**FIGURE 1.5 UCD/MNRC ELEVATION SECTION A-A**

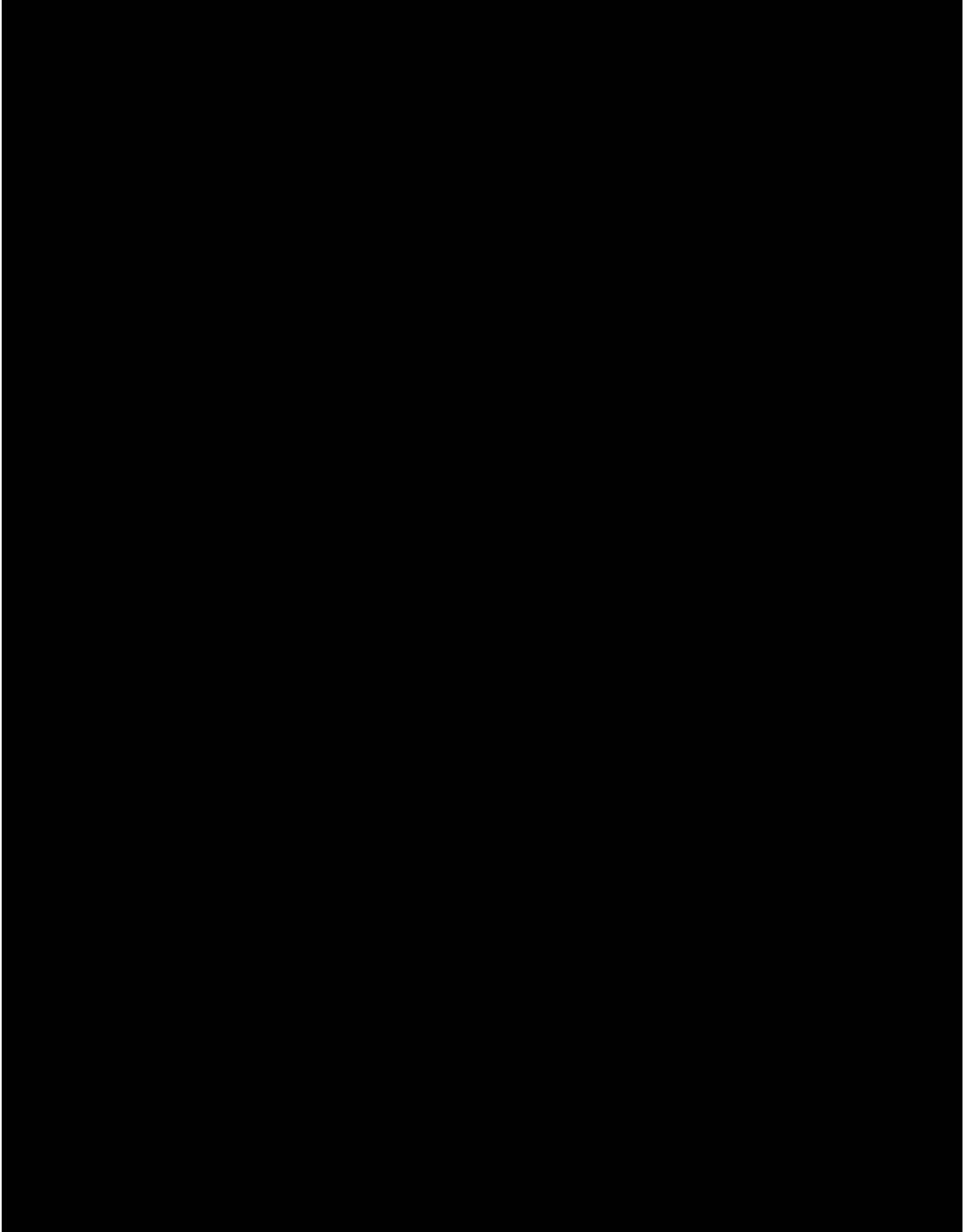


**FIGURE 1.6 UCD/MNRC ELEVATION SECTION B-B**

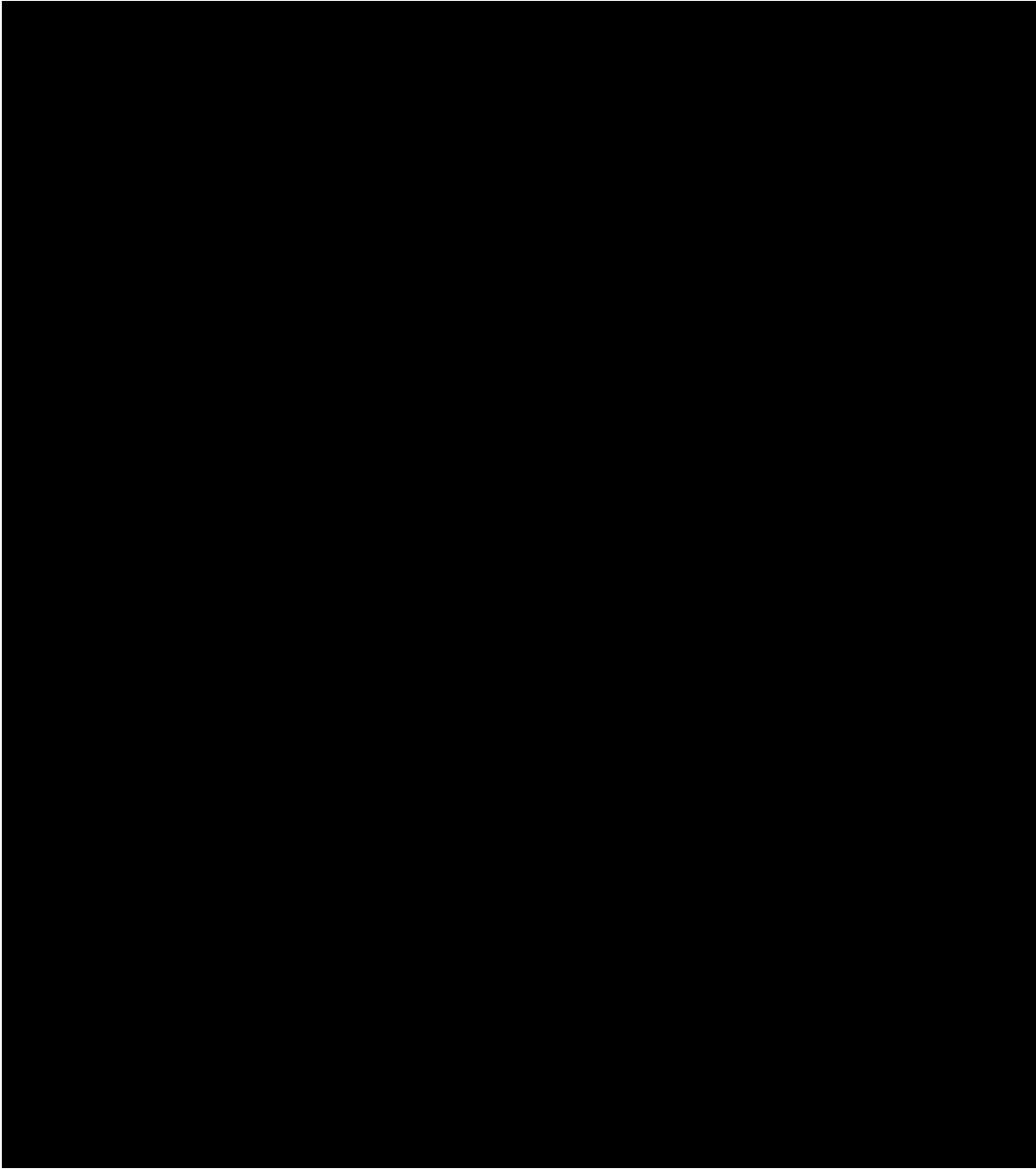


**FIGURE 1.7 UCD/MNRC ELEVATION SECTIONS**

The facility exhaust systems are designed to maintain the reactor room and radiography bays at a slightly negative pressure with respect to surrounding areas to prevent the spread of radioactive contamination. These systems also maintain concentrations of radioactive gases in the reactor room and the radiography bays to levels that are below the 10 CFR Part 20 limits for restricted areas. The reactor and radiography control rooms each have their own air handling systems.

There is a system of interlocks and warning devices to prevent personnel from inadvertent exposure to high radiation levels. Interlocks prevent personnel from entering the radiography bays whenever the beam tube shutters are open and the reactor is operating. This system also prevents the beam tube shutters from being opened when the reactor is operating and personnel are in the radiography bays when the bay doors are open. There are "Reactor On" lights throughout the facility that indicates the reactor operating status. Beam tube shutter positions are monitored in the reactor and radiography control rooms. Audible and visual alarms are sounded in the radiography bays when the shutters are opening. Manual and automatic reactor shutdown devices are located in the reactor room, and each radiography bay, so immediate reactor shutdown can be initiated by anyone occupying these areas should it become necessary.

The UCD/MNRC contains the electrical, water, and sewer utilities required for operation. In addition, the facility has both fire detection and suppression systems, intercom systems, radiation monitoring systems, security systems, parts positioning equipment, irradiation and radiography equipment.

### 1.2.2 Reactor

The UCD/MNRC reactor is a 2 MW, natural-convection-cooled TRIGA<sup>®</sup> reactor with a graphite reflector presently designed to accept the source ends of the four neutron radiography beam tubes which terminate in four separate neutron radiography bays. The reactor is located near the bottom of a water-filled aluminum tank 7 ft in diameter and about 24.5 ft deep (Figure 1.8). Direct visual and mechanical access to the core and mechanical components are available from the top of the tank for inspection, maintenance, and fuel handling. The water provides adequate shielding for personnel standing at the top of the tank. The control rod drives are mounted above the tank on a bridge structure spanning the diameter of the tank. The reactor is monitored and controlled by a computer-based instrumentation and control system featuring color graphics display and automatic logging of vital information. Both manual and automatic control options are available to the operator.

The reactor console is located in the reactor control room and manages all control rod movements, accounting for such things as interlocks and choice of particular operating modes. It processes and displays information on control rod positions, power level, fuel temperatures, pulse characteristics, and other system parameters. The reactor console performs many other functions, such as monitoring reactor usage and storage of historical operating data for replay at a later time.

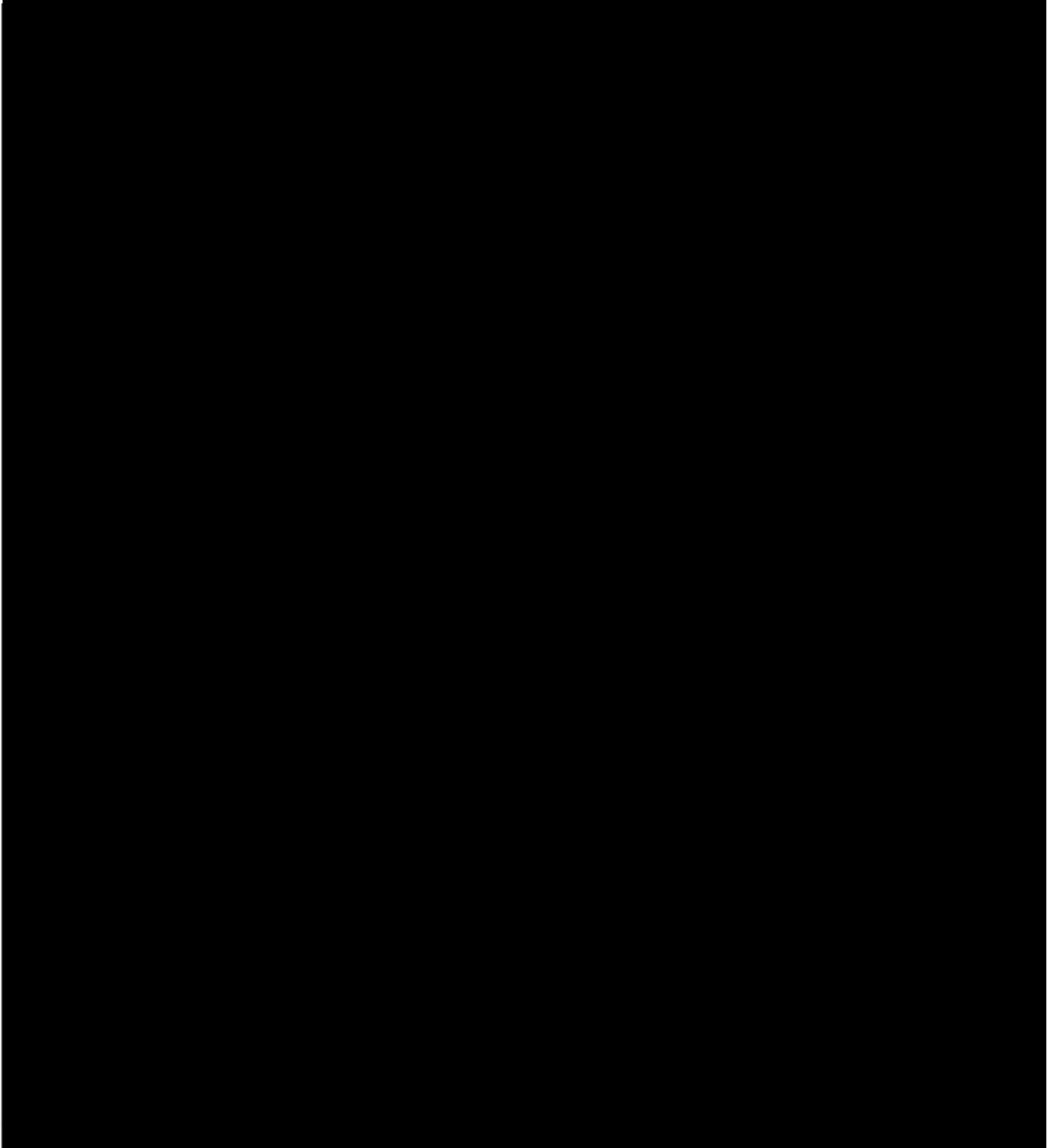


**FIGURE 1.8 UCD/MNRC REACTOR**

Fuel for the UCD/MNRC reactor is standard TRIGA<sup>®</sup> reactor fuel having 20%, or 30% by weight of uranium enriched to less than 20% <sup>235</sup>U. TRIGA<sup>®</sup> reactor fuel is characterized by inherent safety, high fission product retention, and the demonstrated ability to withstand water quenching with no adverse reaction from temperatures to 1150°C. The inherent safety of TRIGA<sup>®</sup> reactors has been demonstrated by extensive experience acquired from similar TRIGA<sup>®</sup> systems throughout the world. This safety arises from the large prompt negative temperature coefficient that is characteristic of uranium-zirconium hydride fuel-moderator elements used in TRIGA<sup>®</sup> systems. As the fuel temperature increases, this coefficient immediately compensates for reactivity insertions. This results in a mechanism whereby reactor power excursions are limited/terminated quickly and safely.

Heat produced by the reactor core is removed by the primary and secondary cooling systems. The primary system circulates tank water through a water-to-water heat exchanger. The secondary water system gains heat in the heat exchanger and rejects it by use of a cooling tower. A purification system circulates a small amount of tank water through a filter and resin tanks to maintain purity and optical clarity. All of these systems contain the necessary instruments and controls for operations and monitoring performance.

### 1.3 Relation of UCD/MNRC to Other TRIGA<sup>®</sup> Reactors

The design of the UCD/MNRC fuel is similar to those of approximately 30 TRIGA<sup>®</sup> type reactors currently operating world-wide with 16 in the United States. Most of these reactors were constructed in the late 1950s and 1960s. Since a large number of these reactors have been in operation for many years, considerable operational information is available and their characteristics are well documented.

Four of the ten TRIGA<sup>®</sup> reactors licensed for 1 MW steady-state operation in the United States have characteristics similar to the UCD/MNRC reactor. These four reactors are located at Penn State (1966), the U.S. Geological Survey Center - Denver (1969), Oregon State University - Corvallis (1967), and the University of Texas - Austin (1990). Worldwide, there have been five TRIGA<sup>®</sup> reactors operated at powers equal to or above 2 MW.

Table 1-1 lists the principal design parameters for the 2 MW UCD/MNRC Reactor and the Thailand 2 MW Reactor. It should be noted that these parameters may vary slightly depending on the use and core loading.

TABLE 1-1 TYPICAL PRINCIPAL DESIGN PARAMETERS

Parameter	UCD/MNRC	Thailand
Maximum steady-state power level	2000	2000
Fuel-Moderator material	U-ZrH1.6-1.7	U-ZrH1.6
Uranium Enrichment	Up to 20% U <sup>235</sup>	Up to 20% U <sup>235</sup>
Uranium Content	20 to 30 wt %	8.5 wt %
Shape	Cylindrical	Cylindrical
Length of Fuel	38 cm (15 in) overall	38 cm (15 in) overall
Diameter of Fuel	3.63 cm (1.43 in) OD	3.63 cm (1.43 in) OD
Cladding Material	0.051 cm (0.020 in) 304 SS	0.051 cm (0.020 in) 304 SS
Number of Fuel Elements	100 <sup>(a)</sup>	100
Excess Reactivity	7.0 <sup>(a)</sup> % $\Delta k/k$ (cold, clean) <sup>(a)</sup>	6.3% $\Delta k/k$ (cold, clean)
Number of Control Rods	6	5
Regulating	1	1
Safety-Transient	1	3
Shim	4	1
Total Reactivity Worth of Rods	8.7% $\Delta k/k$ <sup>(a)</sup>	10.12% $\Delta k/k$
Reactor Cooling	Natural Convection of Pool Water	Natural Convection of Pool Water

(a) = approximate value.

The functional characteristics of the UCD/MNRC Reactor's Instrumentation and Control (I&C) System are the same as for the approximately 30 TRIGA<sup>®</sup> reactors operating in the United States and throughout the world. However, the standard instrument and control system has been replaced by one with a computer-based design incorporating the use of a GA developed, multifunction, NM-1000 microprocessor based neutron monitor channel and a NPP-1000 analog-type neutron monitoring channel. The channels are completely independent and provide redundant safety channels. In addition, the NM-1000 channel provides wide-range log power, period, and multi-range linear power. The control system logic is contained in a separate control system computer with a color graphics display which is the interface between operator and the reactor.

Both the control rod and pulse rod drives are slightly different than those used on the earlier standard TRIGA<sup>®</sup> systems. The UCD/MNRC control rod drives, with the exception of the motor are essentially the same as the drives used on other TRIGA<sup>®</sup> systems. The UCD/MNRC drives use a stepping-type motor rather than the non-synchronous, single-phase motors used on earlier drives. The design and operation of the stepping motor type drive has been fully developed and has been used on the University of Texas - Austin, U.S. Geological Survey Center - Denver, and the Armed Forces Radiobiological Research Institute TRIGA<sup>®</sup> Reactor Systems.

The adjustable fast transient rod drive used on the UCD/MNRC is a modified version of the standard fast transient rod drive. The modified design consists of a combination of the standard rack-and-pinion control rod drive and the standard fast transient control rod drive and is used on the Sandia National Laboratory TRIGA<sup>®</sup> Reactor System. This design has been thoroughly developed, tested, and operationally proven.

The only other significant difference between the UCD/MNRC reactor and others is that the reflector has been modified to accept the source-end of the beam tube. This modification is of minor significance and discussed in more detail in Chapter 10.

#### 1.4 Safety Summary

##### 1.4.1 Nuclear

The analyses presented in this report demonstrate that the UCD/MNRC reactor has been designed and constructed and can be operated, as described herein, without undue risk to the health and safety of UCD/MNRC employees and the general public.

The approach taken in this document to demonstrate the safety of the UCD/MNRC reactor is to:

- (a) Show that the UCD/MNRC reactor fuel and instrumentation and control systems are of proven design, based on past operating experience of systems with the same or similar designs, which have been approved for operation by U.S. Government agencies;

- (b) Show that the operating and accident conditions of the UCD/MNRC reactor are no greater than those of other similar reactors using the same fuel systems, and therefore present no undue risk to the health and safety of the public.

The UCD/MNRC reactor fuel, control-rod drives, control rods, and experimental systems are similar to many other systems used throughout the United States. These items have well-established operating experience and no new significant reactor-design activity was required.

The UCD/MNRC facility has been specially designed to accommodate the reactor. The tank is embedded in a massive reinforced-concrete block, which is, in turn, surrounded by the reinforced concrete walls and roofs of the radiography bays. The core is approximately 4.5 ft below ground level. The reactor shielding configuration is similar to other TRIGA<sup>®</sup> reactors. The reactor bulk shielding and the radiography bay walls and reinforced roofs provide biological shielding to keep personnel exposures as low as reasonably achievable, and protects the reactor from natural phenomena. The reactor room air handling system maintains the reactor room at a negative pressure with respect to surrounding areas to control and prevent the spread of airborne radioactive materials. The air from the reactor room passes through a HEPA filter prior to being discharged to the atmosphere. In the event of a release of radioactive material within the reactor room, the reactor room air handling system automatically isolates the room preventing the release of activity to the atmosphere. The room air can then be recirculated within the reactor room and through the HEPA and charcoal filters to remove particulates.

The reactor operates at a nominal steady-state power of 2 MW. The average power density is approximately 20 kW/element, whereas the same fuel has successfully operated at other facilities with power densities in excess of 30 kW/element. The reactor is also equipped with a pulsing capability. This is the same type of pulsing operation that has been successfully demonstrated with many other TRIGA<sup>®</sup>-type reactors.

The inherent safety of the reactor lies primarily in the large, prompt negative temperature coefficient of reactivity characteristic of the TRIGA<sup>®</sup> fuel-moderator material. Thus, even when large sudden insertions of reactivity are made and the reactor power rises on a short period, the prompt negative reactivity feedback produced by an increase in temperature causes the power excursion to be terminated before the fuel temperature approaches its safety limit. The prompt shutdown and safety characteristics of reactors fueled with TRIGA<sup>®</sup> fuel have been demonstrated during transient tests conducted at GA in La Jolla, California as well as other facilities. This demonstrated safety has permitted the location of TRIGA<sup>®</sup> fueled reactors in urban areas in buildings without the pressure-type containment usually required for power reactors. Chapters 4 and 13 discuss this characteristic in detail.

Abnormal conditions or postulated accidents discussed in this report (See Chapter 13) include:

- a. Maximum Hypothetical Accident (MHA);
- b. Reactivity insertion;
- c. Loss of coolant;
- d. Loss of heat-removal system;
- e. Fuel cladding failure;
- f. Aircraft crashes;
- g. Pyrotechnic detonation.

In the first three postulated accidents (using actual measured rod worths), fuel and cladding temperatures remain at levels below those sufficient to produce cladding failure, and thus, no release of fission products would occur.

The limiting fault condition (i.e., the Maximum Hypothetical Accident (MHA), which assumes failure of fuel clad and an air release of fission products from one fuel element, will result in radiation doses to operations and base personnel and the general public for both thyroid and whole body that is orders of magnitude of those of ANS 15.7 (see Section 2.1.2 for boundary definitions). Chapter 13 contains a detailed discussion of this accident scenario.

The calculations of the probability of an airplane impacting the facility and damaging the reactor has been analyzed. It has been found that the probability of such an accident is less than  $10^{-8}$ /year and is, therefore, considered incredible. The aircraft impact accident analysis is summarized in Chapter 13. The complete bounding probabilistic assessment of an aircraft impact risk at the former McClellan AFB is contained in Appendix C.

The amount of explosive material allowed in the radiological bays at any given time will be limited to prevent damage to the reactor (Chapters 10 and 13).

Radiation exposures to personnel working in the UCD/MNRC from both direct and airborne radiation during normal operation have been analyzed. In addition, actual radiation levels were measured during one megawatt operation and have been extrapolated to two megawatt operation. This analysis and measurements show that the highest exposures occur when personnel are working in the radiography bays when the reactor is operating (beam tube bulk shutters closed). Under these conditions, personnel will be subjected to a maximum radiation field of less than 10 mrem/hr. Making a conservative assumption on the time personnel will be in this field if film radiography is used, the total dose will be 100 mrem/wk. Chapter 11 contains the personnel exposure analysis. In actuality personnel exposure is significantly lower than this, primarily due to the fact the reactor typically operates at 1 MW. All personnel entering the areas will be closely monitored, exposures kept as low as possible, and in no case will they be allowed to exceed the 10 CFR Part 20 guidelines.

The effects of Ar-41 and N-16 concentrations during normal operation of the reactor have also been evaluated for both operations personnel and the general public. These isotopes result in exposures of only a few mrem/yr to operating personnel. Their release to the atmosphere, through the UCD/MNRC stack, results in a maximum downwind concentration well below the 10 CFR Part 20 guidelines for unrestricted areas, see Chapter 11 and Appendix A for analysis.

The effects of a single fuel element clad failure in air have been evaluated for both operations personnel and the general public. The results show exposures below the 10 CFR Part 20 limits, see Chapter 13 and Appendix B for analysis.

Radiation-monitoring equipment has been installed at key locations to monitor radiation levels and to sound alarms if preset values are exceeded. Also, a system of reactor scrams, interlocks and administrative controls have been provided to prevent operating personnel from entering high radiation areas, namely the radiography bays. Included in the reactor scram chains are a number of ripcords in the radiography bays. These rip cords allow personnel in the radiography bays to terminate reactor operations if radiation levels become abnormally high.

#### 1.4.2 Building

The UCD/MNRC reactor is housed in a building specifically designed for reactor operation. It includes the many systems needed to support this type of operation. The UCD/MNRC Reactor Facility consists of one building which houses the reactor, radiography bays, and support areas. The UCD/MNRC is a three-story facility. The exterior walls are constructed from reinforced concrete and block to a height of 24 ft, and the remaining superstructure is covered with corrugated steel. The roof is a weather-sealed steel deck. The interior walls of the radiography bays are constructed of reinforced standard concrete ranging from 2 to 3 ft thick. The roof of these areas is constructed of 2-ft thick reinforced concrete. The reactor room is constructed of standard reinforced concrete block with a built-up roof.

The structural design of the UCD/MNRC conforms to the Air Force General Design Criteria (AFM 88-15), the Uniform Building Code, the AISC Specifications, and to the ACI Code. The UCD/MNRC design seismic load is in accordance with Uniform Building Code Zone 3 criteria. The massive concrete walls and roof that surround the reactor tank provide protection from natural phenomenon. This, coupled with the fact that the reactor can withstand reactivity-insertion and loss-of-coolant accidents without release of fission products, and the low exposures associated with the design-basis accident, demonstrates that the structure is adequate for housing the UCD/MNRC reactor.

Fire detection and suppression systems have been installed throughout the facility. In addition, the instrument cabinets and the reactor and radiography control consoles have been equipped with fire suppression systems.

The reactor room and equipment room cranes have been designed and constructed in accordance with OSHA 29 CFR Part 1910.184, Overhead and Monorail Cranes. All parts have been designed for resultant static loads based on rated capacity with a factor of safety of at least five based on the ultimate strength of the material used. The fuel transfer cask lifting lugs have been designed using the ANSI/ASME code as guidelines. The design analysis shows a margin greater than six when the entire load of the cask is on one lifting lug. In addition, all of the fuel transfer hoisting equipment will be load tested, maintained and operated in accordance with ANSI/ASME during all fuel handling operations. This design, fabrication and testing approach coupled with the low exposures associated with fuel element clad failures shows that this system is adequate for its intended use (Section 9.1).

**CHAPTER 2**

**SITE CHARACTERISTICS**

Chapter 2 - Valid Pages  
Rev. 6 01/30/18

i	Rev. 6	01/30/18	2-40	Rev. 6	01/30/18
ii	Rev. 6	01/30/18	2-41	Rev. 6	01/30/18
iii	Rev. 6	01/30/18			
iv	Rev. 6	01/30/18			
2-1	Rev. 6	01/30/18			
2-2	Rev. 6	01/30/18			
2-3	Rev. 6	01/30/18			
2-4	Rev. 6	01/30/18			
2-5	Rev. 6	01/30/18			
2-6	Rev. 6	01/30/18			
2-7	Rev. 6	01/30/18			
2-8	Rev. 6	01/30/18			
2-9	Rev. 6	01/30/18			
2-10	Rev. 6	01/30/18			
2-11	Rev. 6	01/30/18			
2-12	Rev. 6	01/30/18			
2-13	Rev. 6	01/30/18			
2-14	Rev. 6	01/30/18			
2-15	Rev. 6	01/30/18			
2-16	Rev. 6	01/30/18			
2-17	Rev. 6	01/30/18			
2-18	Rev. 6	01/30/18			
2-19	Rev. 6	01/30/18			
2-20	Rev. 6	01/30/18			
2-21	Rev. 6	01/30/18			
2-22	Rev. 6	01/30/18			
2-23	Rev. 6	01/30/18			
2-24	Rev. 6	01/30/18			
2-25	Rev. 6	01/30/18			
2-26	Rev. 6	01/30/18			
2-27	Rev. 6	01/30/18			
2-28	Rev. 6	01/30/18			
2-29	Rev. 6	01/30/18			
2-30	Rev. 6	01/30/18			
2-31	Rev. 6	01/30/18			
2-32	Rev. 6	01/30/18			
2-33	Rev. 6	01/30/18			
2-34	Rev. 6	01/30/18			
2-35	Rev. 6	01/30/18			
2-36	Rev. 6	01/30/18			
2-37	Rev. 6	01/30/18			
2-38	Rev. 6	01/30/18			
2-39	Rev. 6	01/30/18			

TABLE OF CONTENTS

2.0 SITE CHARACTERISTICS..... 2-1

2.1. Geography and Demography ..... 2-1

2.1.1. Site Location and Description ..... 2-1

2.1.2. Exclusion Area Authority and Control..... 2-6

2.1.3. Population Distribution..... 2-11

2.2. Nearby Industrial, Transportation, and Military Facilities ..... 2-19

2.2.1. Industry ..... 2-19

2.2.2. Transportation ..... 2-19

2.2.3. Military Facilities ..... 2-20

2.2.4. Evaluation of Potential Accidents ..... 2-23

2.3. Meteorology ..... 2-23

2.3.1. Regional Climatology..... 2-23

2.3.2. Local Meteorology ..... 2-23

2.3.2.1. Temperatures..... 2-24

2.3.2.2. Precipitation..... 2-24

2.3.2.3. Humidity..... 2-24

2.3.2.4. Winds and Stability ..... 2-24

2.3.2.5. Severe Weather..... 2-28

2.4. Hydrologic Engineering ..... 2-28

2.4.1. Hydrologic Description..... 2-28

2.4.2. Floods..... 2-29

2.4.3. Accidental Release of Liquid Effluents in Surface Waters..... 2-32

2.5. Geology, Seismology, and Geotechnical Engineering ..... 2-32

LIST OF TABLES

2-1 Sacramento Valley Region Census Data ..... 2-12

2-2 Summary Of Public Use And Military Airports In Sacog Region 1983 ..... 2-21

2-3 Summary Of Public Use And Military Airports In Sacog Region 2016 ..... 2-22

2-4 Normal And Extreme Temperatures..... 2-27

LIST OF FIGURES

2.1	California Map .....	2-2
2.2	UCD/MNRC General Location Map .....	2-3
2.3	McClellan Industrial Park General Area .....	2-7
2.4	Map Of McClellan Industrial Park .....	2-8
2.5	UCD/MNRC Plot Plan.....	2-9
2.6	Top And Axonometric View Main UCD/MNRC Facility .....	2-10
2.7	Regions Of Interest For Census Data.....	2-13
2.8	North Highlands Land Use Map .....	2-14
2.9	Rio Linda Land Use Map.....	2-15
2.10	Arden Arcade Land Use Map .....	2-16
2.11	Sacramento County Land Use .....	2-17
2.12	Regional Airport System – 1983.....	2-18
2.13	Annual Wind Rose For The Former McClellan AFB 1953-1957 .....	2-25
2.14	Annual Wind Rose For The Former McClellan AFB 1992-1996 .....	2-26
2.15	UCD/MNRC Site Hydrology.....	2-30
2.16	Sacramento County Hydrology.....	2-31
2.17	McClellan Park - 100 Year Floodplain North West Quadrant .....	2-33
2.18	McClellan Park - 100 Year Floodplain North East Quadrant.....	2-33
2.19	McClellan Park - 100 Year Floodplain South West Quadrant .....	2-33
2.20	McClellan Park - 100 Year Floodplain South East Quadrant.....	2-33
2.21	Earthquake Fault Epicenter Map Of California (Partial) .....	2-33
2.22	Sacramento Area Significant Faults.....	2-33

## REFERENCES

- 2.1. Hurt, C. B., "Natural Regions of the United States and Canada," W. H. Freeman and Co., 1967.
- 2.2. "McClellan AFB Compatible Land Use Report," June 1983.
- 2.3. U.S. Soil Conservation Service, "Soil Survey of Sacramento Area," Washington, D.C., 1954.
- 2.4. U.S. Department of Commerce, "Statistical Abstract of the United States 1984," 104th Ed.
- 2.5. U.S. Geological Survey, Sacramento, California, 1:250,000 Scale, Land Use and Land Cover and Associated Maps, Washington, D.C., 1979.
- 2.6. National Oceanic and Atmospheric Administration, "Climates of the States," 2 Vols, Second Edition, Gale Research Co., Detroit, 1980.
- 2.7. Climatology of the National Reactor Testing Station, January 1966.
- 2.8. Meteorology and Atomic Energy, 1968, TID 24190.
- 2.9. Bander, T. J. "PAVAN: An Atmospheric Dispersion Program for Evaluating Design Basis Accidental Releases of Radioactive Materials from Nuclear Power Stations," NUREG/CR-2858 Pacific Northwest Laboratory, November 1982.
- 2.10. U.S. Geological Survey, "National Atlas of the United States of America," Washington, D.C., 1970, p. 66, Major Recorded Earthquakes.
- 2.11. Bennett, J. H., "Foothills Fault Systems and the Auburn Dam," Calif. Geology, August 1978.
- 2.12. Toppazada, Tousson R., et al., "Annual Technical Report - Fiscal Year 1981-1981, Preparation of Iseismic Maps and Summaries of Reported Effects for Pre-1900 Calif. Earthquakes," September 1981.
- 2.13. Toppazada, Tousson R., "Annual Technical Report - Fiscal Year 1981-1982, Areas Damaged by California Earthquakes."
- 2.14. Meehan, J. F., Earthquakes and Faults Affecting Sacramento - Reprinted from Seismic Study, Westwing California State Capitol, by the Office of Architecture and Construction; Fred Hommel, State Architect, June 1972.
- 2.15. Kiger, K., Interoffice Memo, Population Demographics, June 1996.
- 2.16. U.S. Census Bureau QuickFacts 2010 Census, Retrieved January 01, 2018, from <https://www.census.gov/quickfacts>

- 2.17. Federal Aviation Administration, Traffic Flow Management System Counts (TFMSC), Aviation System Performance Metrics (ASPM), Retrieved January 01, 2018, from <https://aspm.faa.gov/tfms/sys/Airport.asp>
- 2.18. California Geological Survey Interactive Map Historical Earthquakes, Retrieved January 01, 2018, from <http://maps.conservation.ca.gov/cgs/historicearthquakes/>
- 2.19. Topozada, T. R., C. R. Real, and D. L. Parke (1981). Preparation of isoseismal maps and summaries of reported effects for pre-1900 California earthquakes, Calif. Div. Mines Geol. Open-File Rept. 81-11 SAC, 182 pp.
- 2.20. Topozada, T. R. and D. L. Parke (1982). Areas damaged by California earthquakes, 1900-1949, Calif. Div. Mines Geol. Open-File Rept. 82-17, 65 pp.
- 2.21. USGS Quaternary Faults and Folds Database Interactive Map, Retrieved January 01, 2018, <http://usgs.maps.arcgis.com/apps/webappviewer/index.html?id=db287853794f4555b8e93e42290e9716>

## 2.0 SITE CHARACTERISTICS

This chapter provides information on the site characteristics of Sacramento County and vicinity as they relate to the safety considerations for operation of the UCD/MNRC reactor.

The conclusion reached in this chapter and throughout this document is that the selected site is well suited for the UCD/MNRC facility when considering the relatively benign operating characteristics of the reactor including the Maximum Hypothetical Accident (MHA). This is consistent with the conclusions reached for the other 34 TRIGA<sup>®</sup> reactors operating throughout the world, 18 in the United States. Many of them are located on university campuses, in hospitals, and other highly populated areas.

### 2.1. Geography and Demography

#### 2.1.1. Site Location and Description

The UCD/MNRC reactor is located a few miles northeast of downtown Sacramento, California on the former site of McClellan AFB. Sacramento lies in the Central Valley between the coast range and the Sierra Nevada, about 90 miles northeast of San Francisco, California (Figure 2.1). The adjacent lands are located in the Great Valley subdivision of the Pacific Border Physiographic Province (Reference 2.1). The area is situated on the alluvial plains of the Sacramento River and its tributaries (Reference 2.2). The land is relatively flat, ranging in elevation from 50-75 ft (15-23 m) above mean sea level. Soil cover of about 4 ft (1.2 m) consists of sandy loam (Reference 2.3). The surface soil is moderately permeable but the subsoil has low permeability. The soils have moderate water-holding capacity and pose a slight erosion hazard.

The UCD/MNRC reactor is located approximately eight miles northeast of downtown Sacramento, California in the city of North Highlands (Figure 2.2). The reactor and the city of North Highlands are in Sacramento County, California located northwest of the intersection of Watt Avenue, Roseville Road, and I-80 and is between the communities of North Highlands- Foothills Farms, Arden-Arcade, and Rio Linda-Elverta.

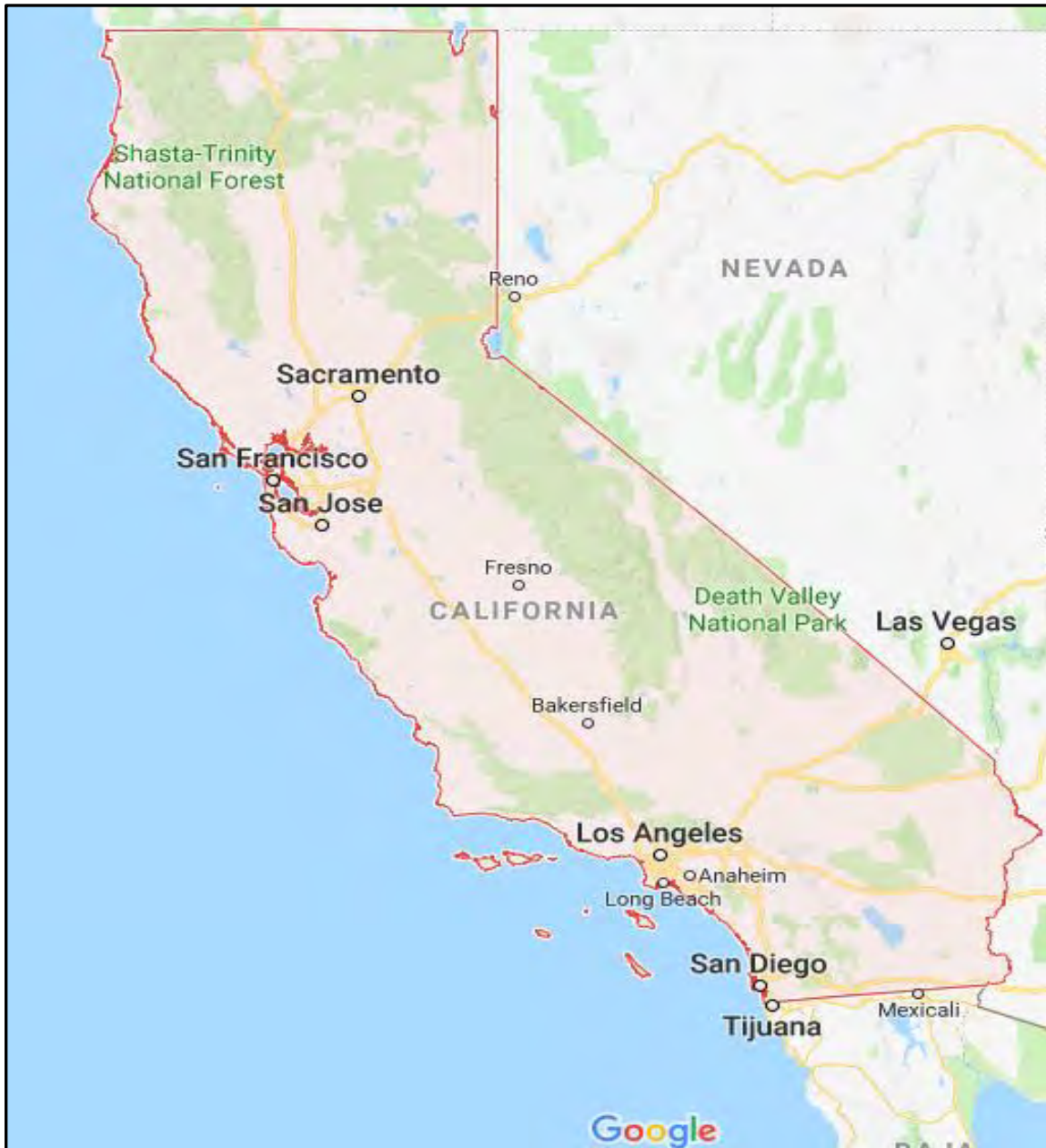


FIGURE 2.1 CALIFORNIA MAP

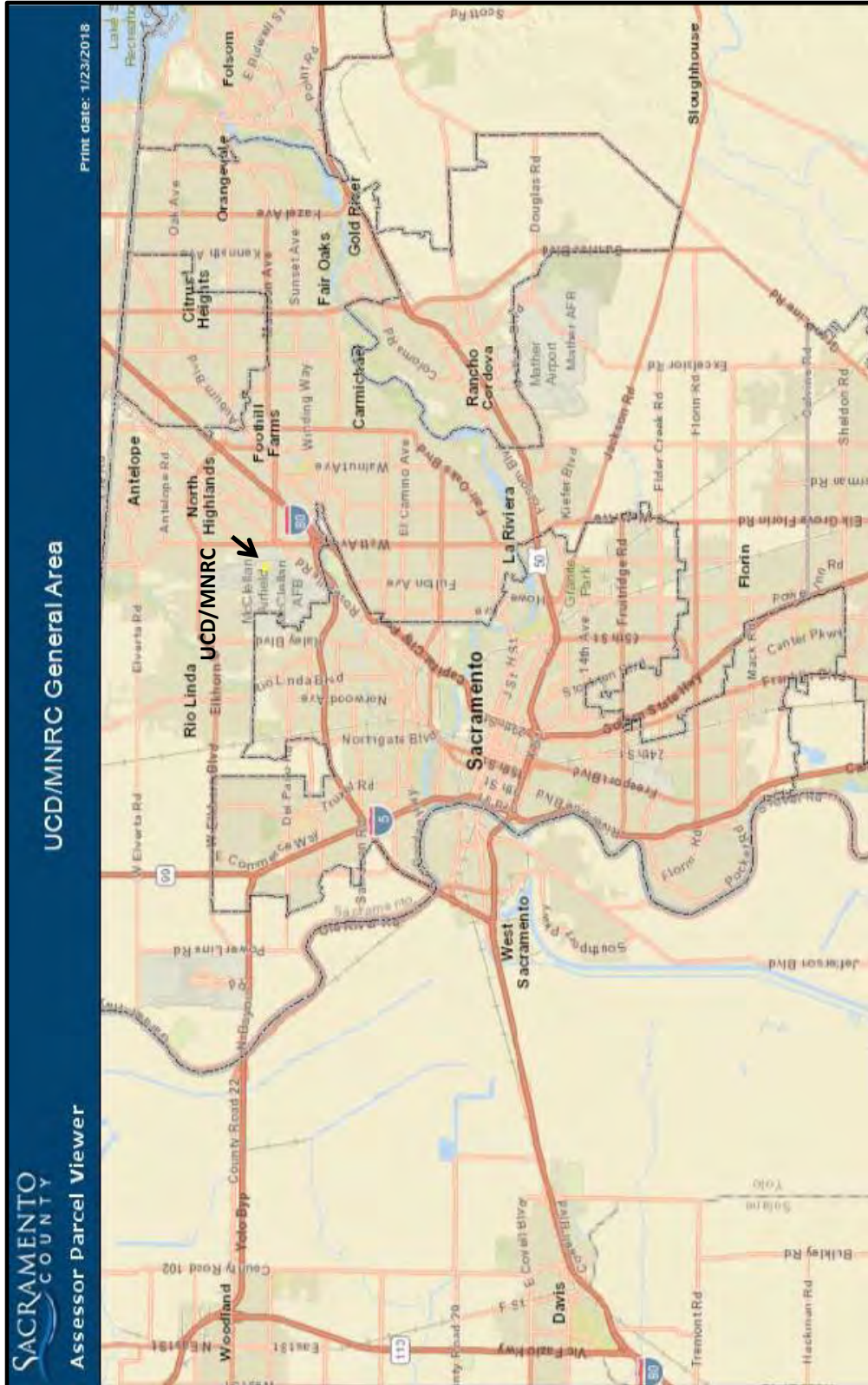


FIGURE 2.2 UCD/MNRC GENERAL LOCATION MAP

The former McClellan AFB had one active runway, 10,600 ft long and 200 ft wide, made of concrete. The south end has a 1,100 ft asphalt overrun, while the north end has a 1,000 ft asphalt overrun. The runway was capable of handling any aircraft in the Air Force inventory. The taxi- way system consists of 383,276 square yards of paved surface. Aircraft aprons total 18.9 acres.

The Air Force maintained a 1,000 ft safety zone on each side of the runway centerline, 3,000 x 3,000 ft clear zones at the ends of the runway, a 200 ft safety zone from the center of each taxi- way, and 125 ft minimum safety zone from the outside of aprons. Hazardous cargo pads are located nearby, with a 1,250 ft safety distance required between hazardous cargos and inhabited structures.

Navigational aids include high intensity runway lights, high intensity approach lighting, Visual Approach Slope Indicator (VASI) lights, Solid-State Instrument Landing System (SSILS), Area Surveillance Radar (ASR), VHF Omni-range and Tactical Navigation Station (VORTAC), and UHF transmitters and receivers.

During the 26 years, from 1970 to 1995, annual aircraft operations at McClellan AFB varied from a low of 43,516 to a high of 104,955. During the 26 year period, there were a total of 1,955,788 operations, which is an annual average of 75,223. The following table summarizes these operations.

ANNUAL AIRCRAFT OPERATIONS 1970-1995<sup>1</sup>

1970	104,955	1979	68,858	1988	83,333
1971	99,927	1980	76,467	1989	85,826
1972	98,125	1981	82,985	1990	78,811
1973	91,081	1982	87,713	1991	59,055
1974	84,720	1983	79,251	1992	52,138
1975	75,404	1984	76,381	1993	58,593
1976	58,734	1985	72,160	1994	50,717
1977	57,180	1986	90,175	1995	43,516
1978	58,822	1987	80,861		

26 year total = 1,955,788  
Annual Average = 75,223

---

<sup>1</sup>Source: McClellan Control Tower

During the last 17 years, from 2000 to 2016, annual aircraft operations at McClellan Air Field are substantially lower than shown in the previous table. During this latest 17 year period, there were a total of 103,518 operations, which results in an annual average of 6,089, a factor of 12 less than the average annual operations from earlier years. The following table summarizes these latest numbers (Reference 2.17).

ANNUAL AIRCRAFT OPERATIONS 2000 – 2016<sup>2</sup>

2000	1,404	2009	6,507
2001	2,396	2010	7,264
2002	4,716	2011	6,216
2003	6,028	2012	6,008
2004	6,039	2013	5,823
2005	6,712	2014	6,094
2006	7,456	2015	7,340
2007	8,283	2016	7,534
2008	7,698	2017	NA

17 year total = 103,518  
Annual Average = 6,089

Use of airspace around the former McClellan AFB is controlled by the Federal Aviation Administration (FAA). In the Sacramento area, responsibility for control of terminal airspace lies with four local air traffic control (ATC) towers located at Metropolitan, Mather Field, Executive airports, and Beale Air Force Bases. Responsibility for transitional area airspace lies with the Terminal Radar Approach Control Facility (TRACON) located adjacent to the former McClellan AFB. The Air Route Traffic Control (ARTCC), located in Fremont, is responsible for enroute airspace.

The UCD/MNRC facility is located as shown in Figures 2.3 and 2.4. It is approximately 1,800 ft (550 m) to the east of the former main runway and 3,000 ft (915 m) from the nearest urban area, Watt Avenue to the east. The next closest urban area is "E" street approximately 4,500 ft (1,375 m) to the north. This area of the former base is the location of other large repair shops.

<sup>2</sup>Source: Federal Aviation Administration, Traffic Flow Management System Counts (TFMSC), Aviation System Performance Metrics (ASPM) <https://aspm.faa.gov/tfms/sys/Airport.asp>

### 2.1.2. Exclusion Area Authority and Control

From the UCD/MNRC normal operations, safety, and emergency action standpoint there are two areas of concern (Figures 2.5, and 2.6). The first is the area inside the perimeter fence (with outriggers and barbed wire) surrounding the UCD/MNRC enclosure. This area is the exclusion area. It is a "restricted access" area and control of activities within this area during normal operations and emergencies is the responsibility of the UCD/MNRC Director/Emergency Director.

The second area of concern is the area outside the UCD/MNRC perimeter fence. The general public has free access to this area and direction of emergencies is by local city/county civilian authorities. This is defined as the unrestricted area. The closest urban area to the UCD/MNRC is about 3000 m to the east, Watt Avenue.

The area definitions for purposes of addressing radiation exposure in Chapter 11 are restricted and unrestricted areas. The operations boundary (i.e., the UCD/MNRC perimeter fence) is the boundary between these areas; inside the fence is the restricted area and outside the fence is the unrestricted area.



FIGURE 2.3 MCCLELLAN INDUSTRIAL PARK GENERAL AREA

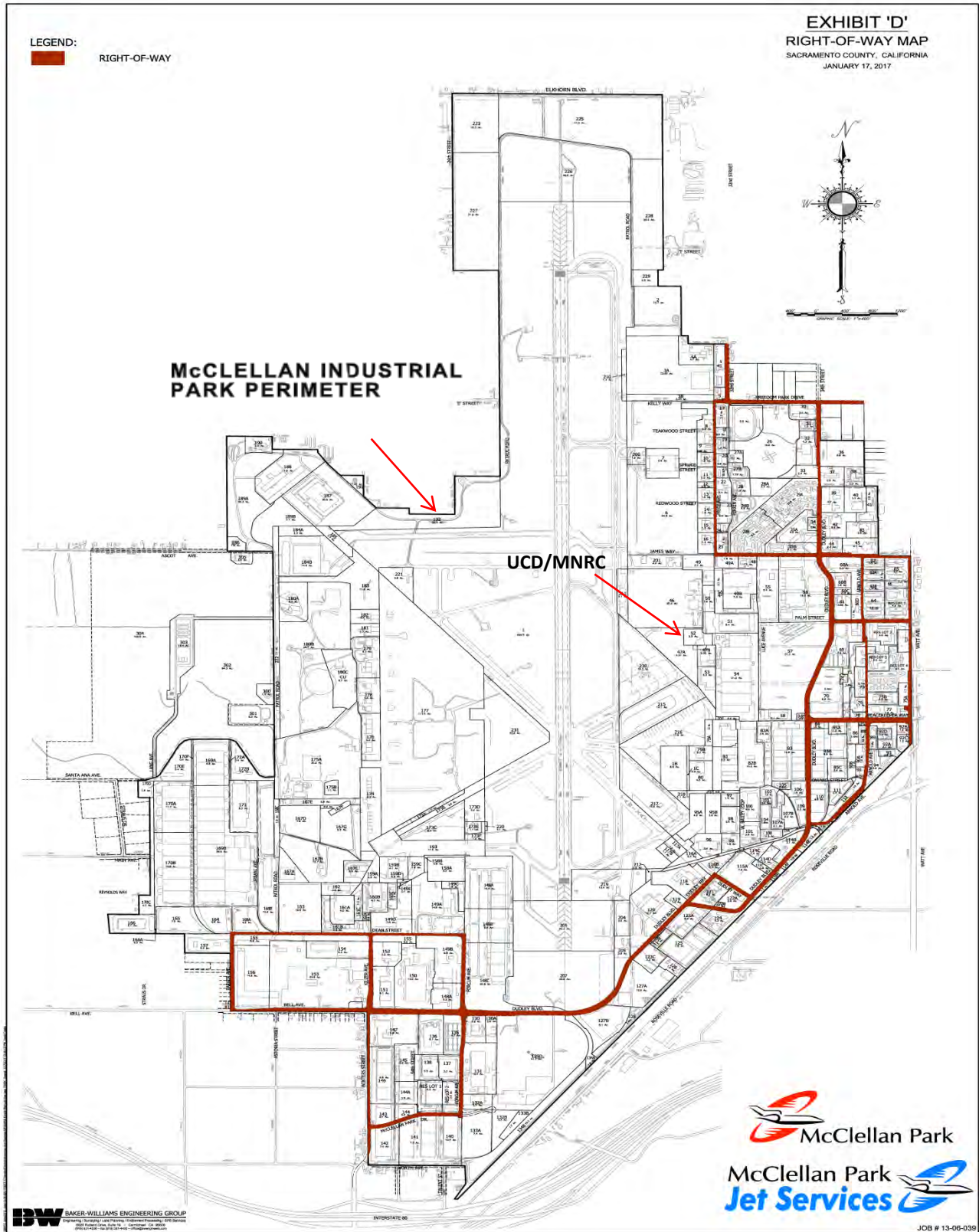


FIGURE 2.4 MAP OF MCCLELLAN INDUSTRIAL PARK

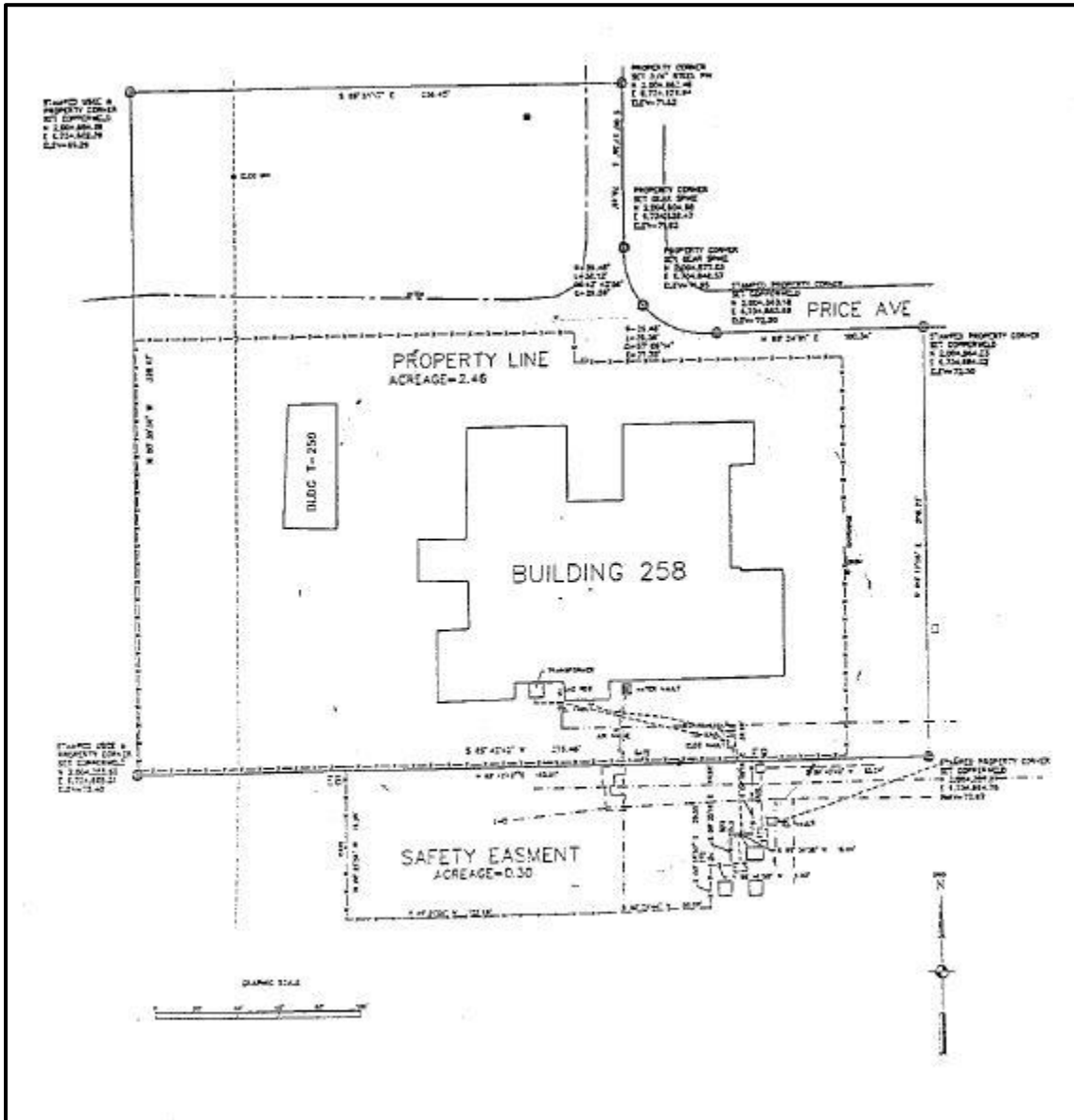


FIGURE 2.5 UCD/MNRC PLOT PLAN



FIGURE 2.6 TOP AND AXONOMETRIC VIEW MAIN UCD/MNRC FACILITY

### 2.1.3. Population Distribution

The UCD/MNRC is situated approximately 8 miles (13 km) north-by-northeast of downtown Sacramento, California. Sacramento county has a population of about 1,418,788 (2010 census), an increase of about 23% since the 1992 census which reported a population of about 1,093,000, which was in turn an increase of about 26% since 1970 (References 2.4, and 2.16). The major population center of Sacramento lies south-by southwest of the McClellan Business Park. (References 2.15, 2.16).

The UCD/MNRC is surrounded by communities. To the east and northeast is North Highlands; to the northwest, Rio Linda; to the west is North Sacramento and Del Paso Heights (which are generally considered as part of Sacramento City according to the US Census Bureau); and to the south is Arden-Arcade. The highest density developments are directly to the east, in North Highlands; to the southwest, in the Del Paso Heights area of the city of Sacramento; and to the south in Sacramento County.

Existing land uses, according to the Sacramento Area Council of Governments Comprehensive Land Use Plan (1987), around the base were generally:

North Highlands: Mostly single family residential development of about six units per acre, with retail and other business uses centered along Watt Avenue and Elkhorn Boulevard. There are also some commercial and light industrial uses along Elkhorn Boulevard. Scattered in the residential areas within about a mile of the UCD/MNRC, are 12 elementary schools. Some multi-family housing is scattered in the area. Industrial development is centered along Orange Grove Avenue.

Rio Linda: Mostly single family residential uses with few retail or business uses. There are four elementary schools, a junior high school, and a high school located in this community. There is also a small airport located about two miles to the west of the UCD/MNRC.

North Sacramento: Mostly single family residential uses, with lower densities near Rio Linda and high densities in Del Paso Heights. There are some commercial and business uses along Marysville Boulevard and Grand Avenue. There are nine elementary schools, a junior high school, a high school, and a hospital located in this area.

Arden-Arcade: A highly urbanized area with single family and multiple family residential uses, with retail, commercial, and business uses centered on arterial streets: Marconi Avenue, El Camino Avenue, Howe Avenue, Auburn Boulevard, Fulton Avenue, Watt Avenue, and Arden Way. There are 13 elementary schools, three high schools, a hospital, major shopping centers, and a community park located in the area.

No significant population variations due to transient population or transient land use occur in the area surrounding the UCD/MNRC. Although there are some recreational areas within 10 miles (16 km) of the UCD/MNRC, none attract large numbers of people and most are used by local residents.

Table 2-1 portrays the 2010 census demographics of the surrounding counties, and neighboring areas. Figures 2.7 through 2.11, and 2.12 depict the general areas of interest shown in Table 2-1, the regional airport locations (which will be discussed in more detail in the next section), and current general land use according to Sacramento County.

TABLE 2-1 Sacramento Valley Region Census Data

	Sacramento city	Arden-Arcade	North Highlands	Rio Linda	Sacramento County	Placer County	Sutter County	Yolo County	Solano County
Population, Census, April 1, 2010	466,488	92,186	42,694	15,106	1,418,788	348,432	94,737	200,849	413,344
Persons under 5 years, percent, April 1, 2010	7.50%	6.40%	8.20%	6.70%	7.10%	6.00%	7.60%	6.30%	6.50%
Persons under 18 years, percent, April 1, 2010	24.90%	20.90%	27.70%	27.10%	25.60%	24.40%	27.60%	22.70%	24.60%
Persons 65 years and over, percent, April 1, 2010	10.60%	15.70%	11.10%	10.40%	11.20%	15.40%	12.70%	9.80%	11.30%
Veterans, 2012-2016	23,480	5,586	2,922	903	85,177	27,830	6,393	8,827	33,653
Housing units, April 1, 2010	190,911	44,813	16,093	5,129	555,932	152,648	33,858	75,054	152,698
Owner-occupied housing unit rate, 2012-2016	46.80%	43.90%	43.10%	74.70%	55.20%	70.10%	57.10%	51.30%	59.20%
Median value of owner-occupied housing units, 2012-2016	\$259,400	\$309,300	\$157,600	\$194,200	\$271,300	\$380,900	\$213,100	\$346,200	\$305,900
Households, 2012-2016	179,865	41,028	15,244	4,747	527,335	136,730	32,028	72,544	145,315
Persons per household, 2012-2016	2.65	2.33	3.05	3.13	2.76	2.68	2.95	2.78	2.88
In civilian labor force, total, 2012-2016	62.90%	61.80%	55.40%	54.40%	62.30%	60.50%	59.20%	60.10%	62.10%
Total retail sales, 2012 (\$1,000)	4,363,259	1,986,474	550,287	51,730	15,227,280	6,437,879	1,069,489	1,968,762	5,106,627
Mean travel time to work (minutes), 2012-2016	24.9	23.9	26.6	27.9	26.5	27.1	26.2	22.4	30.8
All firms, 2012	38,244	8,360	3,531	1,064	110,172	31,846	5,461	13,884	25,724
Population per square mile, 2010	4,764.20	5,170.60	4,834.60	1,525.20	1,470.80	247.6	157.3	197.9	503
Land area in square miles, 2010	97.92	17.83	8.83	9.9	964.64	1,407.01	602.41	1,014.69	821.77
FIPS Code	"0664000"	"0602553"	"0651924"	"0660942"	"06067"	"06061"	"06101"	"06113"	"06095"

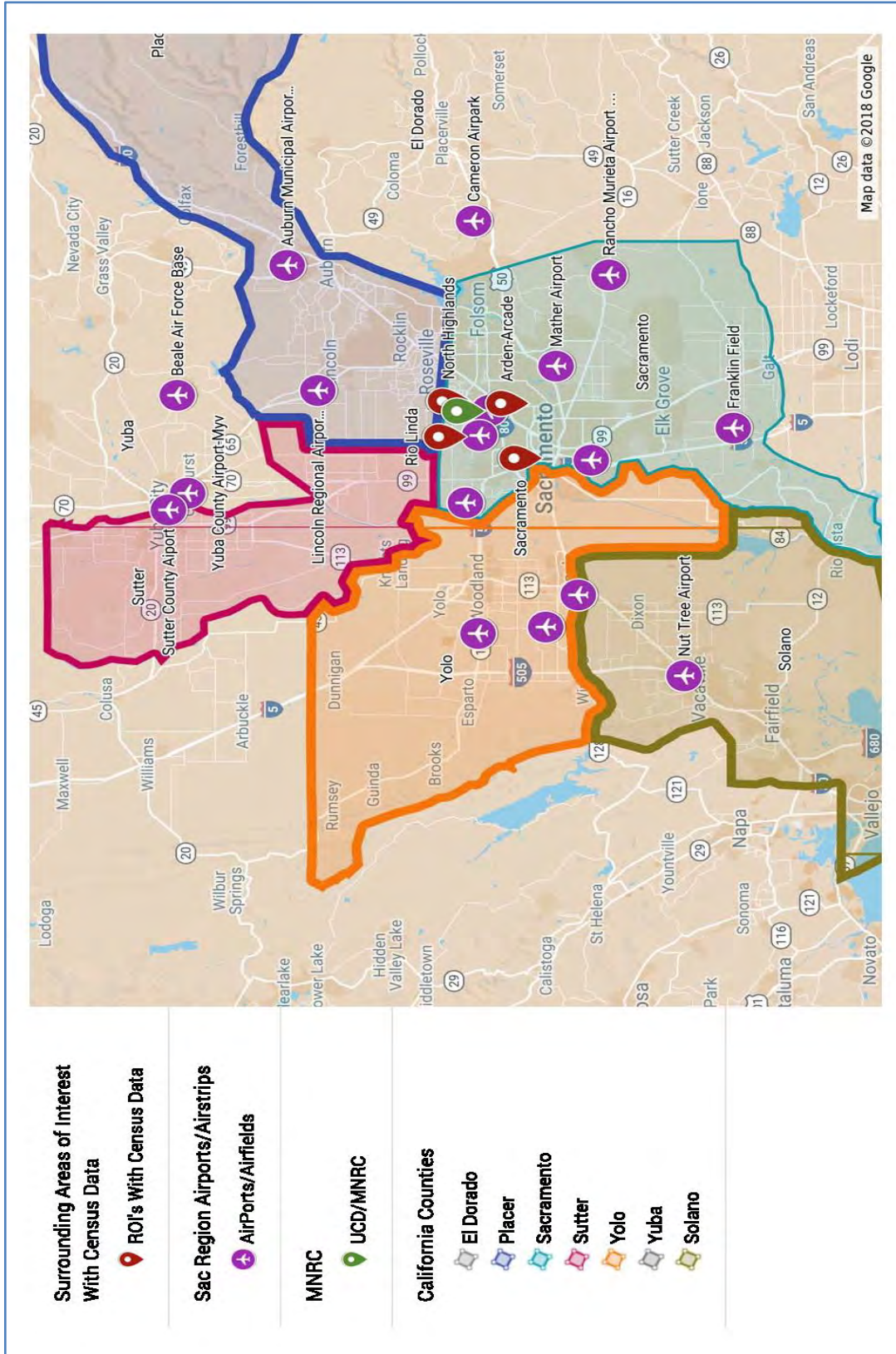


FIGURE 2.7 REGIONS OF INTEREST FOR CENSUS DATA

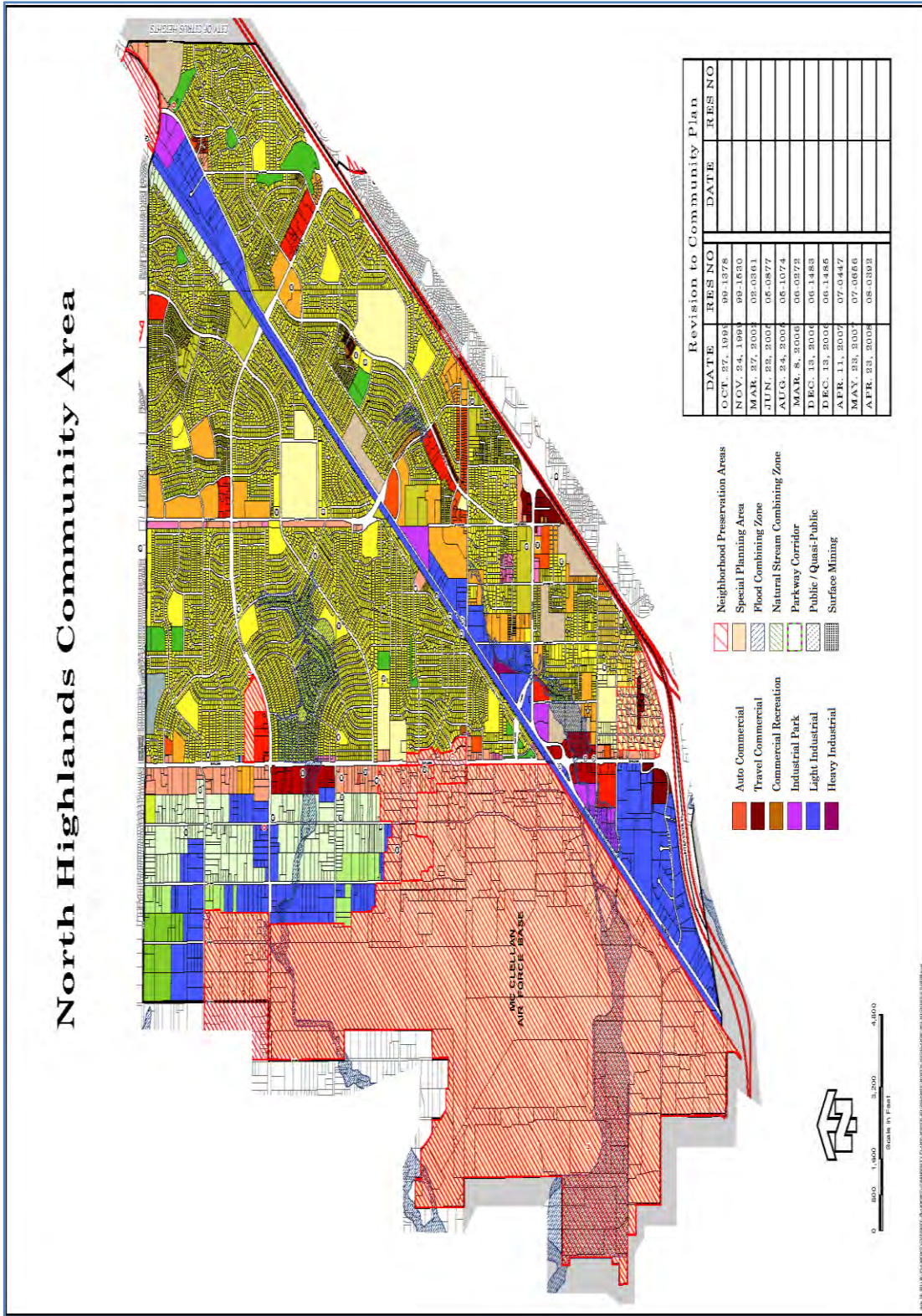


FIGURE 2.8 NORTH HIGHLANDS LAND USE MAP

# Rio Linda and Elverta Community Plan

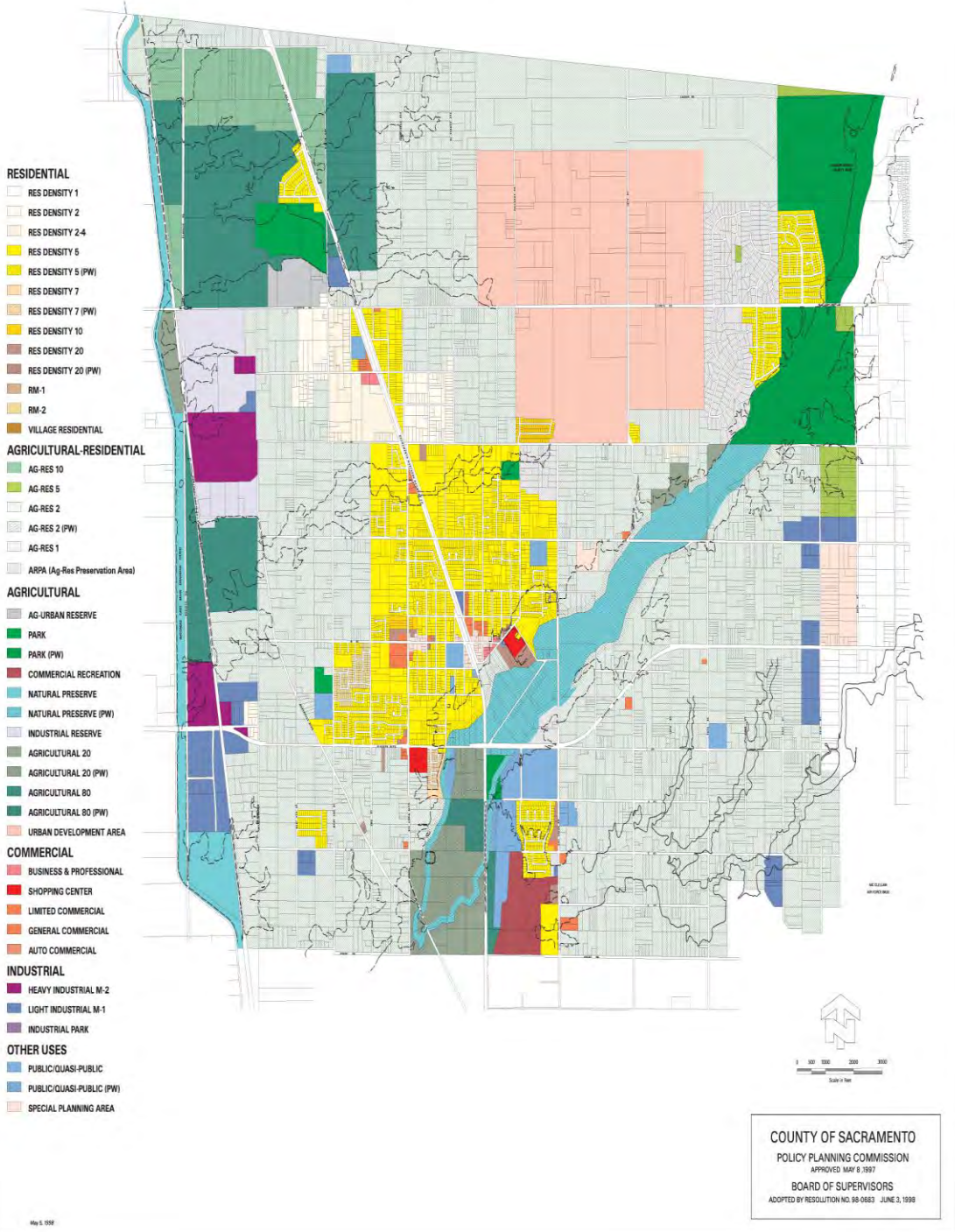


FIGURE 2.9 RIO LINDA LAND USE MAP



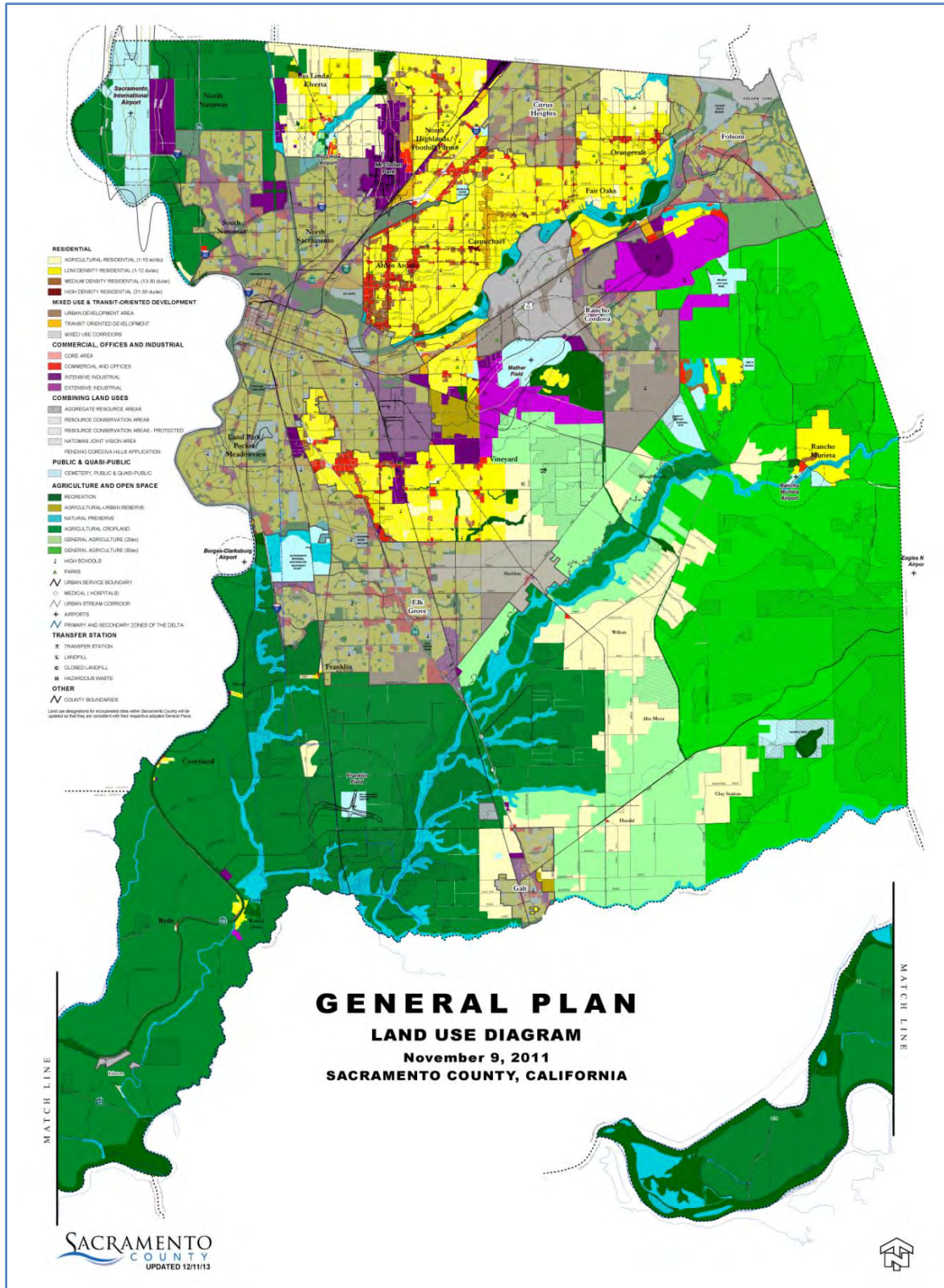


FIGURE 2. 11 SACRAMENTO COUNTY LAND USE

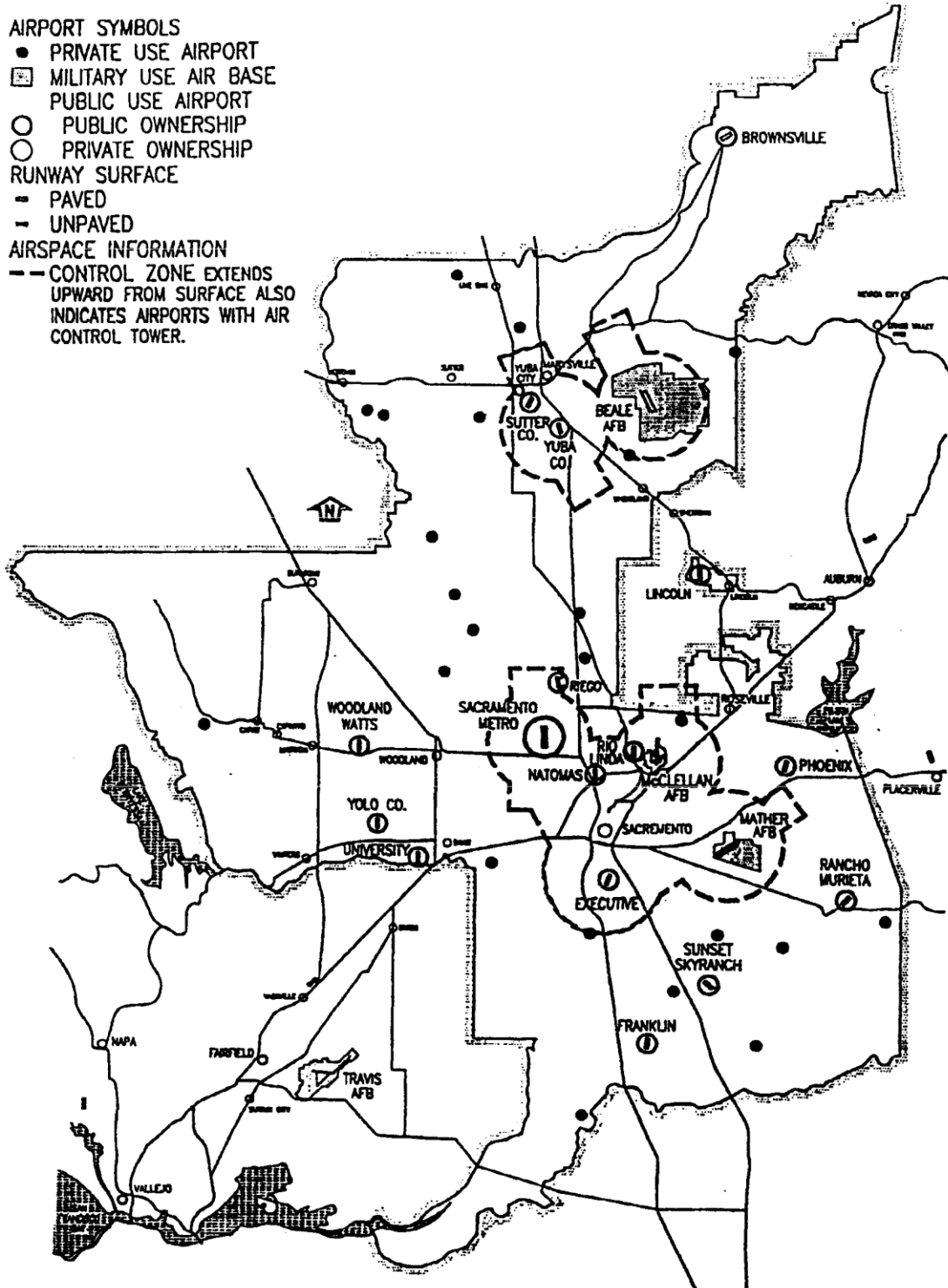


FIGURE 2. 12 REGIONAL AIRPORT SYSTEM – 1983

## 2.2. Nearby Industrial, Transportation, and Military Facilities

### 2.2.1. Industry

There are no major industrial facilities in the Sacramento area that need be of concern from the UCD/MNRC safety standpoint. The area's economy is primarily based on agriculture and government with much smaller contributions by such things as mining, manufacturing of durable goods, lumber and wood products, and metal fabrication. The closest oil refinery is located at Martinez, California, approximately 85 miles to the southwest.

### 2.2.2. Transportation

- Highway Transportation

The Sacramento area is at the cross-roads of two interstate highways: the transcontinental I-80, and N/S I-5. I-80 goes to San Francisco to the west, and to Reno to the east. Business 80 passes through the downtown area and connects with I-80 in west Sacramento, and in northeast Sacramento at Watt Avenue. Three main gates into the Industrial Park are located on Watt Avenue about a mile north of the I-80/Watt Avenue intersection.

Interstate 5 passes through downtown near the Sacramento River; traveling north, it leads to Oregon and Washington; south I-5 leads to Los Angeles and San Diego.

Highway 50 links the downtown area to points east; Rancho Cordova, Folsom, El Dorado Hills, Placerville, and South Lake Tahoe.

State Highway 99 generally parallels I-5 to southern California, joining I-5 south of Bakersfield.

- Airports

As of 1983 there were 71 airports within the Sacramento Area Council of Governments, SACOG, the Region on which records were kept. Of those, 16 were public use, 53 were private, and two (including the former McClellan AFB) were military. Since the early 80's the use of the aircraft runways to present day, at the former McClellan AFB site, continued to involve military; however, it now includes commercial usage. The current usage of the runways was shown earlier in this chapter to be significantly less than the former military usage in the 80's.

Table 2-2 and 2-3 (Reference 2.17) summarizes the items of interest for the public use and military airports in the SACOG region as of 1983 and then 2016 for comparison. The location of these airports with respect to the UCD/MNRC is shown in Figure 2.7 and 2.12.

- Water Transportation

Sacramento has the largest river system in California. A ship channel between Rio Vista and Sacramento was dredged by the Army Corps of Engineers where there was an existing lake area. It is the Port of Sacramento, operated by the Sacramento-Yolo Port district, and lies 79 nautical miles from the Pacific Ocean and approximately 11 miles from the UCD/MNRC.

Since its opening in 1963, the port has developed extensive cargo storage and handling facilities, largely focusing on rice, wheat, and wood chips commodities.

- Rail Transportation

Union Pacific operates the tracks that parallel Roseville Road, and along the south-east corner of the Industrial Park. The closest approach to the reactor facility is approximately 3500 feet. Union Pacific connects Sacramento with 21 western, central, and southern states. On a daily basis there are nine scheduled AMTRACK passenger trains and fourteen freight trains that utilize the tracks just southeast of the reactor facility. All shipments aboard these trains are in accordance with the Code of Federal Regulations 49 CFR - Transportation. All normal shipments are not expected to threaten the reactor facility. The California State Office of Emergency Services has the UCD/MNRC listed as a critical facility for notification during planning of any hazardous material shipments along this route.

There are other feeder, connector and inter-tie services provided to the Sacramento area by Sacramento Northern and Central Traction Company and Western Pacific Railroad. However, these facilities are all to the south and beyond consideration.

### 2.2.3. Military Facilities

There is one military facility in the vicinity of Sacramento: Beale AFB. Beale AFB is located in Yuba County approximately 13 miles east of Marysville and 75 miles from McClellan. The present 12,000 ft x 300 ft runway was completed in 1959. As of the late 90's, early 2000's, Beale AFB employed approximately 4,800 military and civilian personnel.

Three very different major operations are housed at Beale AFB. These are an air refueling mission, a reconnaissance wing, and missile warning squadron. These operations use four different types of aircraft, each with varying speeds and airspace requirements. The aircraft presently used are: U-2 High Altitude Photographic, T-38 Trainer, and RC-12 SIGINT.

The facilities at Beale AFB are not available for use by the general aviation or air carrier operators. There were an estimated 85,000 aircraft operations at Beale AFB in 1981.

TABLE 2-2 SUMMARY OF PUBLIC USE AND MILITARY AIRPORTS IN SACOG REGION 1983

<b><i>FAA ID - Airport</i></b>	<b><i>Use</i></b>	<b><i>Runways</i></b>	<b><i>1983 Total Operations</i></b>
<b>BAB - Beale AFB</b>	Military	12,000' x 300'	85,000
<b>BRO - Brownsville Airport*</b>	Public	2,240' x 40'	3,800
<b>F72 - Franklin Field</b>	Public	3,105' x 60' 3,030' x 60'	70,000
<b>LHM - Lincoln Regional</b>	Public	6,000' x 100'	40,000
<b>MHR - Mather</b>	Public	11,300' x 300'	25,600
<b>MCC - McClellan Airfield</b>	Military	10,600' x 200'	88,000
<b>Natomas Field*</b>	Public	2,600' x 30'	20,000
<b>RIU - Rancho Murieta</b>	Public	3,800' x 75'	15,500
<b>Riego Flight Strip*</b>	Public	2,380' x 35'	4,500
<b>L36 - Rio Linda</b>	Public	2,620' x 30'	34,000
<b>SAC - Sacramento Executive</b>	Public	5,503' x 150' 3,482' x 150' 3,834' x 100'	115,000
<b>SMF - Sacramento</b>	Public	8,600' x 150'	175,000
<b>Q40 - Sunset Sky ranch*</b>	Public	2,780' x 150'	18,000
<b>O52 - Sutter County</b>	Public	3,040' x 75'	352,000
<b>EDU - UC Davis</b>	Public	3,185' x 50'	37,300
<b>O41 - Watts-woodland</b>	Public	3,770' x 60'	63,000
<b>DWA - Yolo County</b>	Public	6,000' x 100'	60,000
<b>MYV - Yuba County</b>	Public	6,000' x 150'	63,000

\*No longer in operation, existence, or no current FAA records exist as of 2016

TABLE 2-3 SUMMARY OF PUBLIC USE AND MILITARY AIRPORTS IN SACOG REGION 2016

<b><u>FAA ID - Airport</u></b>	<b><u>Use</u></b>	<b><u>Runways</u></b>	<b><u>2016 Total Operations</u></b>
<b>AUN - Auburn Muni</b>	Public	3700' x 75'	935
<b>BAB - Beale AFB</b>	Military	12,000' x 300'	7806
<b>DWA - Yolo County</b>	Public	6000' x 150'	870
<b>EDU - UC Davis</b>	Public	3176' x 50'	359
<b>F72 - Franklin Field</b>	Public	3123' x 60' 3031' x 60'	7
<b>L36 - Rio Linda</b>	Public	2625' x 42'	17
<b>LHM - Lincoln Regional</b>	Public	6,001' x 100'	1130
<b>MCC - McClellan Airfield</b>	Public	10,600' x 200'	7534
<b>MHR - Mather</b>	Public	11301' x 150'	16622
<b>MYV - Yuba County</b>	Public	6007' x 150'	678
<b>O41 - Watts-woodland</b>	Public	3759' x 60'	234
<b>O52 - Sutter County</b>	Public	3045' x 75'	24
<b>O61 - Cameron Airpark</b>	Public	4051' x 50'	276
<b>RIU - Rancho Murieta</b>	Public	3798' x 75'	99
<b>SAC - Sacramento Executive</b>	Public	5503' x 150' 3837' x 100' 3505' x 150'	7120
<b>SMF - Sacramento</b>	Public	8605' x 150' 8598' x 150'	104673
<b>VCB - Nut Tree</b>	Public	4700' x 75'	1043

#### 2.2.4. Evaluation of Potential Accidents

There are no nearby industrial, transportation, or military facilities with the potential of causing a credible accident that would result in a release of radioactive material from UCD/MNRC that would exceed the general public exposure limits of 10 CFR Part 20.

The basic UCD/MNRC design and structure provide significant protection for the reactor. As described in Chapter 1, the reactor core is below grade and surrounded by a monolithic block of reinforced concrete from six to nine ft thick. Also, the above grade structures of the facility that surround the reactor tank are constructed of reinforced concrete and reinforced concrete block.

The accident, from sources outside the UCD/MNRC that is worthy of further discussion is one involving an aircraft since the facility is located near an airstrip. The possibility of an aircraft impact involving the UCD/MNRC reactor has been evaluated (assuming airstrip operation numbers from the early 80's as they are more conservative than current values), see Chapter 13, and it has been determined that the probability of such an event occurring is less than  $10^{-8}$  per year. Therefore, this type of accident is considered incredible.

### 2.3. Meteorology

#### 2.3.1. Regional Climatology

Sacramento is situated in California's Central Valley between the Sierra Nevada and Coastal Range. The area is characterized by hot summers (July mean maximum temperature 105°F) and cold winters (January mean minimum temperature 28°F) (Reference 2.6). As in most of California, the majority of the annual average precipitation, about 17 in. (40 cm), falls in the winter months as rain. The prevailing winds in the area are from the south to south-by-southeast.

The eastern most mountain chains form a barrier that protects much of California from the extremely cold air from the Great Basin in the winter. There are occasions when cold air from an extensive high pressure area spreads westward and southward over California. Even in these cases, the warming by compression as the air flows down the slopes of the mountains into the valleys prevents severe cold damage. The ranges of mountains to the west offer some protection to the interior from the strong flow of air off the Pacific Ocean. Between the two mountain chains and over much of the desert area the temperature regime is intermediate between the maritime and the continental models. Hot summers are the rule while winters are moderate to cold.

#### 2.3.2. Local Meteorology

The summary of meteorological conditions for the UCD/MNRC site is based on the records obtained by officials of the National Oceanic and Atmospheric Administration, U.S. Department of Commerce and published in Volume II of "Climates of the States." The specific data, for the most part, is from the weather station at the Sacramento Executive Airport.

#### 2.3.2.1. Temperatures

The normal and extreme temperatures for the Sacramento area are shown in Table 2-4. The normal temperatures are climatological standard normal (1931-1960). The normal daily minimum temperature of 37.2°F occurs in January and the normal daily maximum temperature, 93.4°F, occurs in July. Extreme temperatures have ranged from a low of 23°F in January of 1963 to 115°F in June of 1961.

#### 2.3.2.2. Precipitation

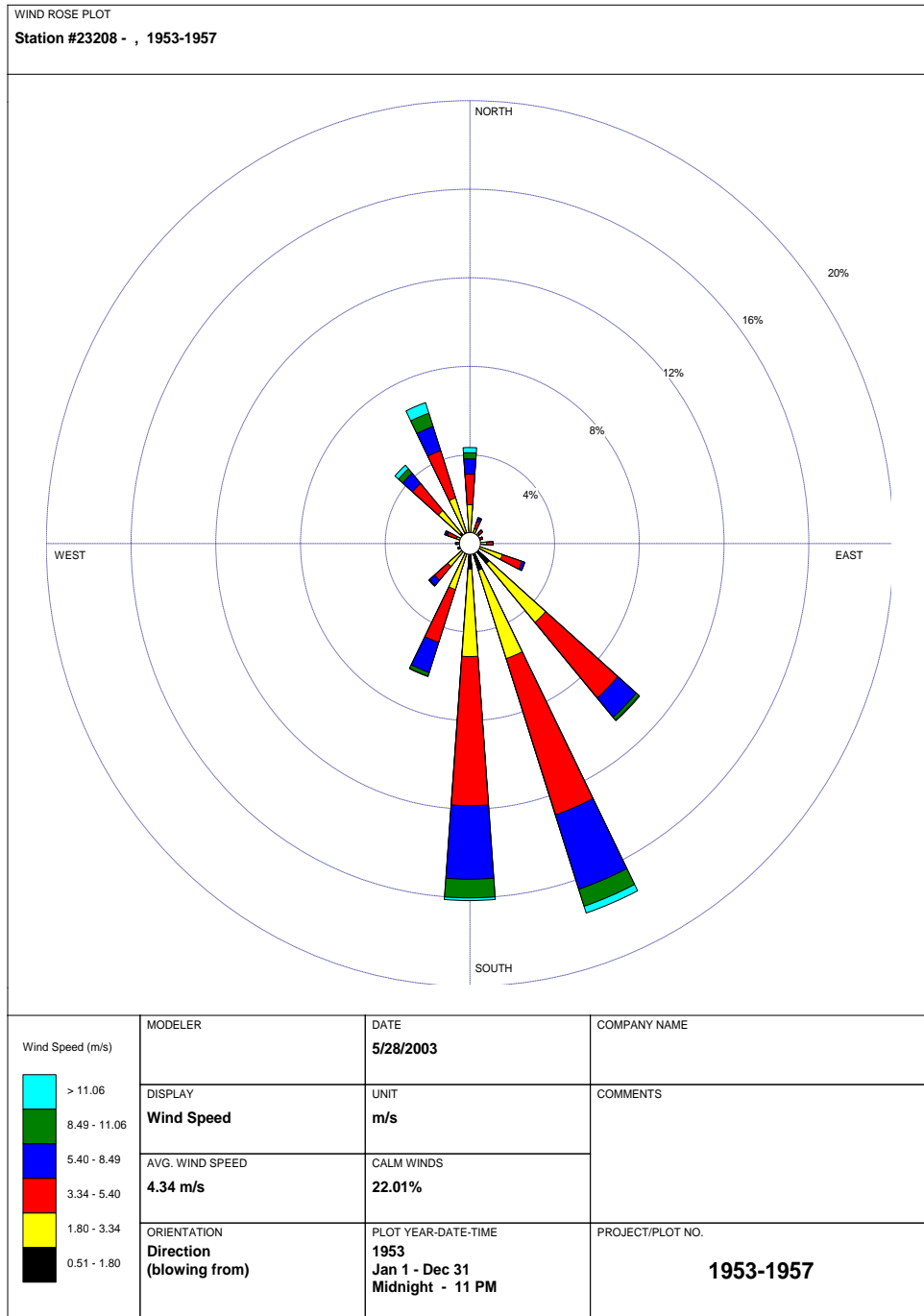
The normal precipitation for the Sacramento area is 16.29 in./yr with the highest amounts, approximately 3.2 in. occurring in the months of December and January. The maximum monthly rainfall, 12.64 in., fell in December 1955. The maximum rainfall over a 24-hour period of time, 5.59 in., occurred in October 1962.

#### 2.3.2.3. Humidity

The humidity in the Sacramento area range from a low of 28% in July to a high of 91% in December and January.

#### 2.3.2.4. Winds and Stability

The annual wind rose for the Sacramento area is shown in Figure 2.13 and 2.14. The data to prepare these two wind roses was collected for the periods 1953-57 and 1992-96. As can be seen, the prevailing winds in the area are from the south to south-by-southeast.



WRPLOT View 3.5 by Lakes Environmental Software - www.lakes-environmental.com

FIGURE 2.13 ANNUAL WIND ROSE FOR THE FORMER MCCLELLAN AFB 1953-1957

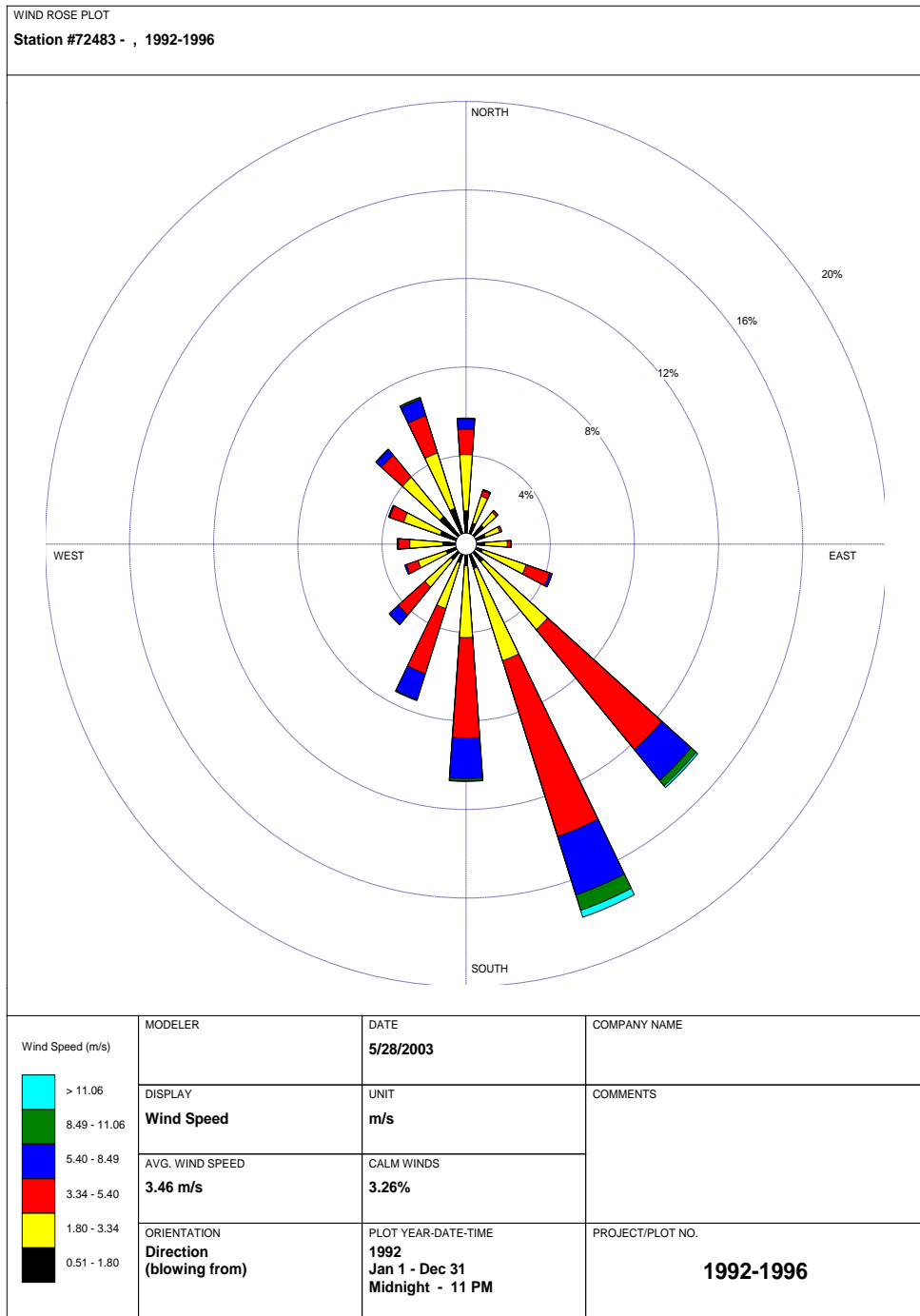


**FIGURE 2. 14 ANNUAL WIND ROSE FOR THE FORMER MCCLELLAN AFB 1992-1996**

TABLE 2-4 NORMAL AND EXTREME TEMPERATURES

Temperature							
Normal				Extreme			
Month	Daily Maximum	Daily Minimum	Monthly	Record High	Year	Record Low	Year
J	53.2	37.2	45.2	67	1966	23	1963
F	58.6	39.8	49.2	76	1964	28	1962
M	64.8	42.0	53.4	86	1966	28	1966
A	71.4	45.3	58.4	91	1968+	34	1967+
M	78.2	49.7	64.0	101	1967	37	1964
J	86.5	54.4	70.5	115	1961	43	1966
J	93.4	57.4	75.4	113	1961	50	1960
A	91.9	56.3	74.1	107	1968+	49	1966
S	88.2	55.0	71.6	104	1969+	43	1965
O	77.6	49.4	63.5	99	1963	38	1969+
N	64.2	41.6	52.9	87	1960	26	1961
D	54.6	38.1	46.4	72	1967	24	1965
YR	73.6	47.2	60.4	115	June 1961	23	Jan. 1963

### 2.3.2.5. Severe Weather

Tornadoes have been reported in California, but they are infrequent. They are generally not severe and most cases cause only minor damage to trees or light buildings.

## 2.4. Hydrologic Engineering

### 2.4.1. Hydrologic Description

The base and adjacent lands are located in the Great Valley subdivision of the Pacific Border Physiographic Province (Reference 2.1). They are situated on the alluvial plains of the Sacramento River and its tributaries (Reference 2.2). The land is relatively flat, ranging in elevation from 50-75 ft above mean sea level. Soil cover of about 4 ft consists of sandy loam (Reference 2.3). The surface soil is moderately permeable but the subsoil has low permeability. The soils have moderate water-holding capacity and pose a slight erosion hazard.

The UCD/MNRC site is underlain by a thick (>1,000 ft) section of unconsolidated sediments deposited by streams draining the Sierra Nevada. The uppermost deposits are termed the Victor Formation which is approximately 50 to 100 ft thick at the UCD/MNRC site. The Victor Formation is composed of the heterogeneous shifting streams that drained the Sierra Nevada in Pleistocene time. These streams left sand and gravel in channel-like structures that grade laterally and vertically into silt and clay in a manner that provides little correlation of materials from area to area. This is characteristic of floodplain or low-sloping alluvial fan deposits.

Underlying the Victor Formation is a series of alluvial deposits, termed the Laguna or Fair Oaks Formations. These alluvial deposits are composed of a heterogeneous assemblage of beds of silt, clay, and sand with lenticles of gravel deposited on westward-sloping floodplains by meandering, sluggish streams. Some of the sands are clean and well sorted while some of the gravels are extremely silty and poorly sorted. Sediments of the Laguna are variable; for example, in one area the formation consists of compact silt, clay with lenses of poorly sorted gravel, sand, and silt, and in others it contains sand with only a few interbeds of clay and silt.

Underlying the Victor, Laguna, and Fair Oaks Formations is a volcanic unit termed the Mehtren Formation. In the vicinity of the UCD/MNRC site, this formation is composed of sedimentary deposits derived from reworking of andesitic tuff-breccias which issued from volcanic vents in the Sierra Nevada. Typically, these are referred to as "black sands" in drillers logs. The black sands generally are fairly soft and well sorted. They are formed as fluvial deposits, having been derived from andesitic detritus washed down the slopes of the Sierra Nevada. Beds of black sand are commonly about 2 meters thick, although beds up to 6 meters or more have been reported. Where exposed in road cuts, these beds exhibit crossbedding, indicating a steam-laid mode of origin. Associated with the black sands are lenticular beds of stream gravel containing andesitic cobbles and boulders up to a meter or more in diameter. Also associated with the sands are beds of brown to blue clay and silt. In addition to these sedimentary units, volcanic mudflow units have apparently also been encountered.

The Mehtren Formation is the major aquifer of the Sacramento area. The thickness of the Mehtren formation in the vicinity of the base is unknown, but probably exceeds 300 ft.

#### 2.4.2. Floods

The natural surface drainage around the UCD/MNRC site has been altered by construction of a series of storm drains. The North Sacramento, Del Paso Heights, Robla, Rio Linda, and Elverta areas drain storm water runoff to the west through Arcade Creek, Magpie Creek, Rio Linda Creek, Dry Creek, and a series of shallow natural ditches and swales (Figure 2.15). Rather than emptying onto the flat farmland of the Natomas area, as they once did, these creeks and ditches are intercepted by the East Natomas Main Drainage Canal and carried via Bannon Slough to the Sacramento River. In the area, elevation above sea level ranges from about 90 ft in the northeast to 50 ft in the southwest. The extensively-wooded, double channel Dry Creek is the most important component of the natural drainage system serving the study area. Dry Creek begins to the east in Placer County where it collects from a large watershed in the Roseville vicinity.

Two rivers, the Sacramento and American, flow through the Sacramento area (Figure 2.16). The American River flows approximately five miles south of the UCD/MNRC site. There are two flood control dams on this river approximately 20 miles upstream. The major dam which forms Folsom Lake is an earthen structure. Directly downstream of Folsom Dam is Nimbus Dam. This is a concrete structure and forms Lake Natomas. The Sacramento River flows approximately five miles west of the UCD/MNRC site. This river handles the runoff from areas north of Sacramento.

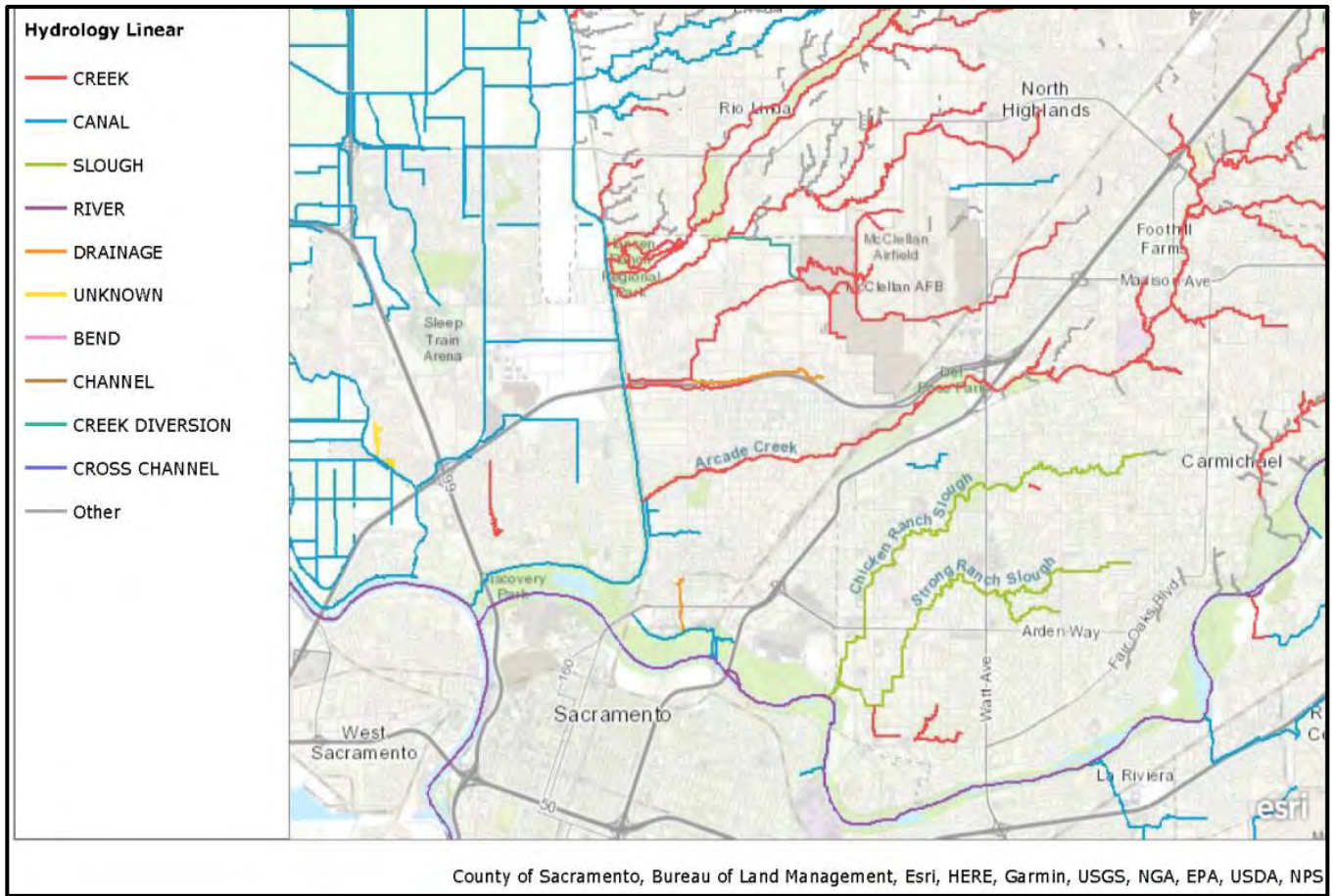


**FIGURE 2.15 UCD/MNRC SITE HYDROLOGY**

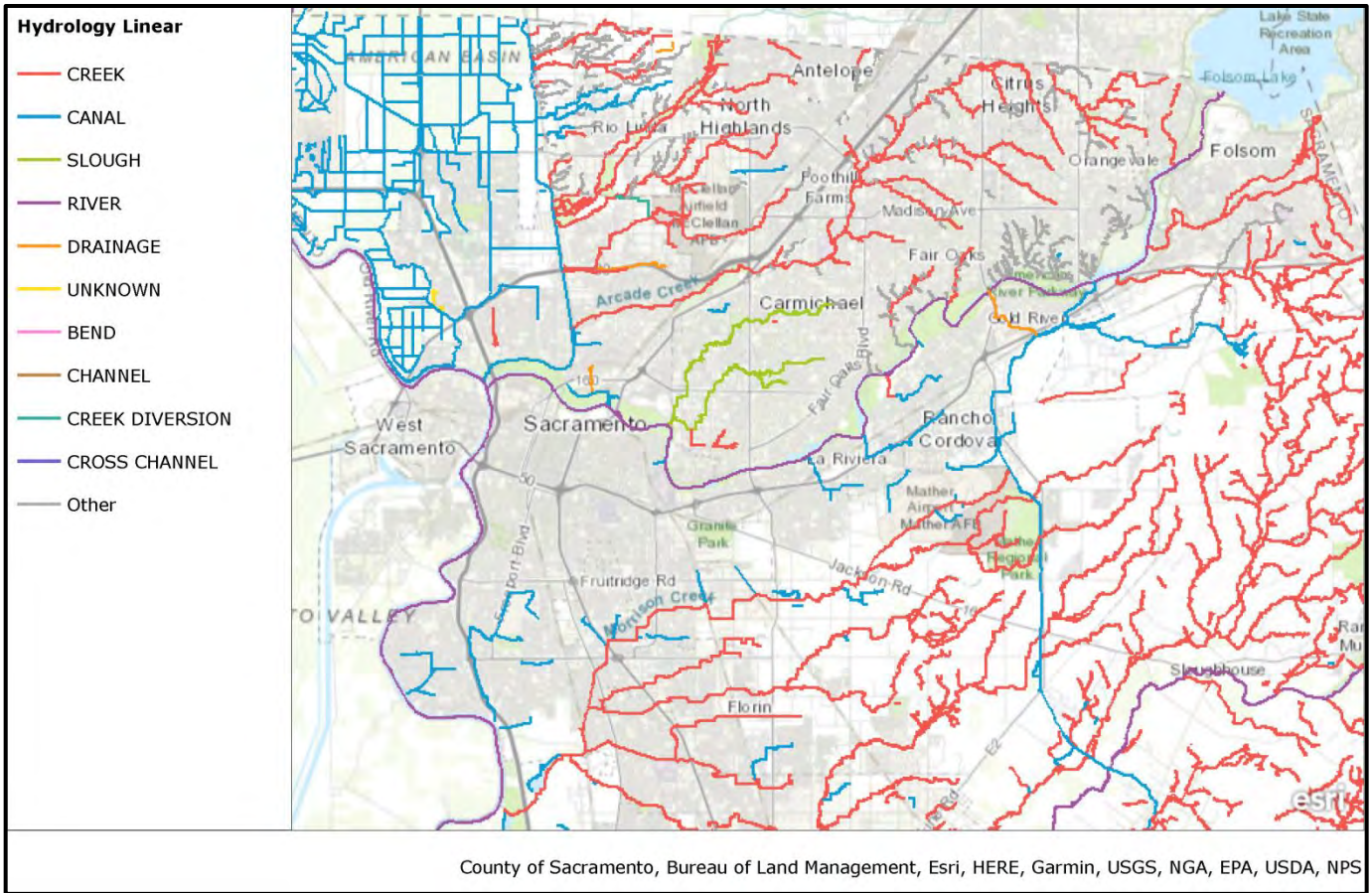


**FIGURE 2.16 SACRAMENTO COUNTY HYDROLOGY**

Neither of these rivers presents a flood hazard to the UCD/MNRC facility. The nearest 100 yr floodplain is about 3,400 ft (1,037 m) from the site of the UCD/MNRC (Figures 2.17 through 2.20).

#### 2.4.3. Accidental Release of Liquid Effluents in Surface Waters

The probability of an accidental release of radioactive liquid effluents from the UCD/MNRC in surface waters is extremely low. Two (2) UCD/MNRC systems may contain radioactive liquid: the reactor primary cooling system and the water purification systems. All of the components for these systems; reactor tank, pumps, heat exchangers, filters, resin tanks, valves, and piping, are located within the UCD/MNRC reactor and equipment rooms. Any contaminated water leakage from this equipment will be wiped up and disposed of as discussed in Chapter 11. The only other areas where contaminated water may be encountered is in the radiography bays and the men's washroom. The radiography bays have a drain system that leads to a sump in Bay 1. Any water collected in the sump is pumped into an above ground liquid storage tank. The decontamination shower located in the men's washroom also drains into the storage tank. There are no floor drains in the men's washroom that lead to the industrial waste. Any water entering the tank, even if other than the reactor systems, will be analyzed for radioactive materials. If radioactive materials are found it will be disposed of as discussed in Chapter 11.

#### 2.5. Geology, Seismology, and Geotechnical Engineering

The Sacramento area is located in Seismic Zone 3 of the Uniform Building Code. In general, seismic activity is not as great in the area as it is in the coastal areas (References 2.10, 2.11, 2.12 and 2.13). Based on a review of historical records, the maximum-intensity earthquake in Sacramento in historical times has been about VII on the Modified Mercalli scale (References 2.12 and 2.13). This intensity was the result of earthquakes centered about 20 mi (32 km) west of Sacramento with an estimated magnitude of 6.0 to 6.5 on the Richter scale. Earthquakes of the intensity of VII are characterized by collapse of weak chimneys, moderate damage to masonry walls, fall of cornices from high buildings, and fall of some nonstructural, unreinforced brick walls (References 2.12 and 2.13). However, earthquakes of higher intensity could have occurred prior to the coverage of the historical record, and higher intensity earthquakes are possible in the future Figure 2.21 (References 2.18 through 2.20) is a historical summary of the seismic activity in the area.









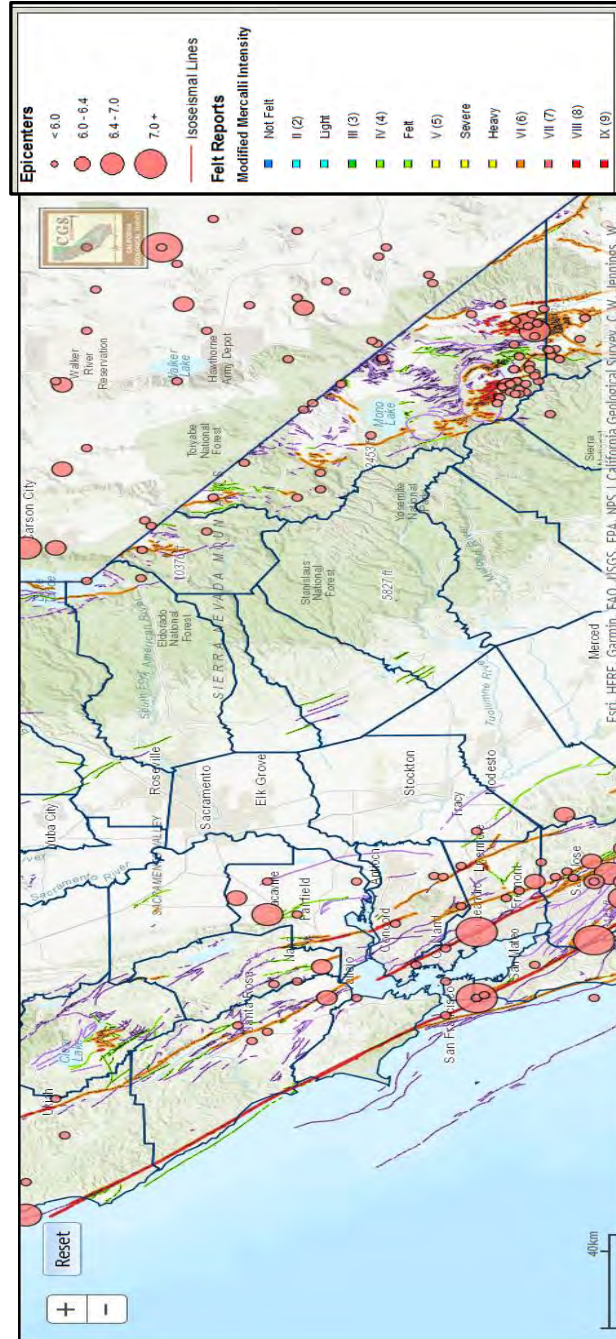


FIGURE 2.21 EARTHQUAKE FAULT EPICENTER MAP OF CALIFORNIA (PARTIAL)

California contains innumerable earthquake faults. Some of these faults are shown in Figure 2.22, including the known faults around Sacramento (Reference 2.14, 2.21). It is quite probable that other surface and subsurface faults also exist; however, this can only be positively determined by adequate explorations. The fact that no surface faults appear on the map in the Sacramento or San Joaquin Valleys may only indicate that sediments laid down during late geologic time cover the fault scars. On the other hand, rock or the firmer sediments usually found in the hill and mountain areas retain the evidence of faults over long time periods.

As shown in the figure, surface faulting has been identified in the Bear Mountain fault zone some 25 miles east of Sacramento and in the Rumsey Hills area west of Woodland. A number of subsurface faults have been found during explorations for gas near Sacramento as reported by the Division of Oil and Gas of the California Department of Conservation. Such subsurface faulting is reported near Freeport and Clarksburg just to the south of Sacramento; in the Todhunter Lake area a few miles north and east of Davis; and in the Rio Vista area, to identify a few areas near Sacramento. Data are not available to indicate the existence of subsurface faulting nearer to or within the City of Sacramento.

Geologic investigations to date have not discovered evidence indicating movement on subsurface faults in the Sacramento Valley more recent than Eocene time, about 40 million years ago. Eocene rocks extend generally from the surface of the ground to 0.5 to 0.75 kilometer depth. One fault in the Folsom area, recently mapped by the California Division of Mines and Geology, has been interpreted as having moved during the Quaternary Period.

One conclusion based on this evidence is that except for the possibly more recent movement on the fault in the Folsom area, there has been no near surface fault displacement in, or within close proximity of Sacramento during the past 40 million years. The focal depth of California earthquakes (the depth below the surface of the earth to the start of the rupture in the rock that provides the energy for the quake) ranges from a few kilometers to 15 to 20 kilometers, and therefore earthquakes of a smaller magnitude could have originated here during the past 40 million years, but the faulting might not have extended into or through this layer of post-Eocene rocks.

A second conclusion is that faulting did extend to the surface, but the evidence for this surface breaking either has not yet been found or is undiscernible in the sediments which fill the valley.

USGS Quaternary Faults and Folds Database

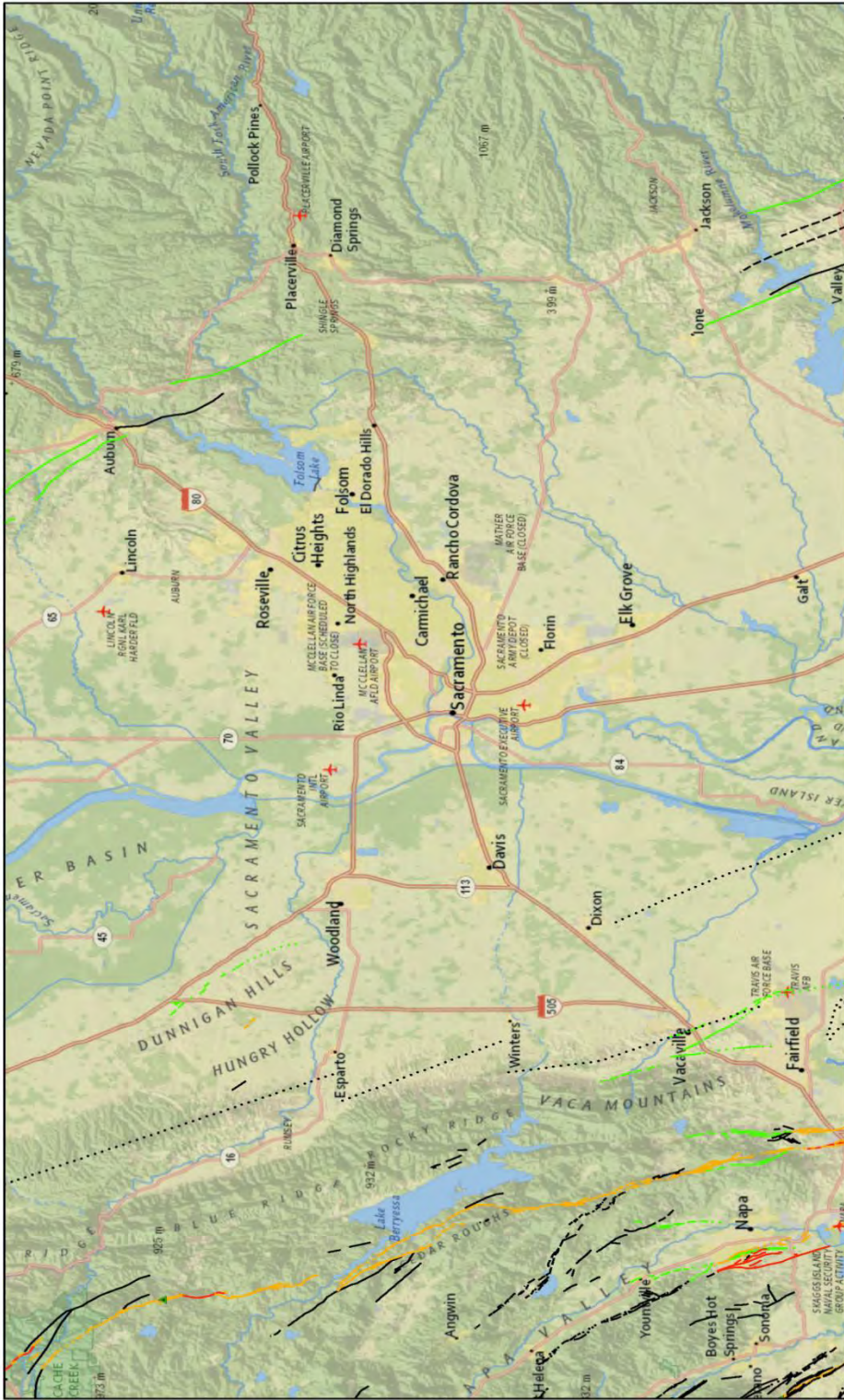


FIGURE 2.22 SACRAMENTO AREA SIGNIFICANT FAULTS

1/25/2018, 1:51:46 PM

1:577,791

0 5 10 20 mi  
0 5 10 20 km

▲ Site Investigations  
— Quaternary Faults  
— historical (<150 years), well constrained location  
- - historical (<150 years), moderately constrained location  
- · - historical (<150 years), inferred location  
— latest Quaternary (<15,000 years), well constrained location  
- - latest Quaternary (<15,000 years), moderately constrained location  
- · - latest Quaternary (<15,000 years), inferred location  
— latest Quaternary (<15,000 years), inferred location  
- - late Quaternary (<130,000 years), well constrained location  
- · - late Quaternary (<130,000 years), moderately constrained location  
- · - late Quaternary (<130,000 years), inferred location  
— middle and late Quaternary (<750,000 years), well constrained location  
- - middle and late Quaternary (<750,000 years), moderately constrained location  
- · - middle and late Quaternary (<750,000 years), inferred location  
— undifferentiated Quaternary (<1.6 million years), well constrained location  
- - undifferentiated Quaternary (<1.6 million years), moderately constrained location  
- · - undifferentiated Quaternary (<1.6 million years), inferred location  
- · - Class B (various age), well constrained location  
- - Class B (various age), moderately constrained location  
- · - Class B (various age), inferred location

Content may not reflect National Geographic's current map policy. Sources: National Geographic, Esri, DeLorme, HERE, UNEP-WCMC, USGS, NASA, ESA, METI, NRCAN, GEBCO, NOAA, increment P Corp.

U.S. Geological Survey

California's approximately 200-year recorded history is short, indeed, compared with the estimated 4.5 billion year age of the earth. It is a certainty that the Sacramento area has experienced violent earthquake motion during a part of this geologic time. From recorded information readily available for the past 200 years, however, it appears that Sacramento has not experienced violent earthquake motion of a nature compared with that experienced by several other areas within California.

Probably the greatest amount of earthquake shaking experienced in Sacramento during the recent past occurred on April 21, 1892. This earthquake produced extensive damage to towns some 25 miles west of Sacramento.

As noted above, the April 21, 1892 earthquake, along with the quake two days earlier, probably produced the most vigorous earthquake shaking in Sacramento during recorded history. There is some evidence that the epicenters of these shocks were in the area between Winters and Vacaville. Both of these towns, as well as Davis, Dixon, and Woodland experienced significant damage to many structures. Although the location for the fault responsible for the 1892 earthquakes is not known, the California Division of Mines and Geology and the U.S. Geological Survey have recently found (May 1972) that the Green Valley fault, west of Fairfield, is showing active fault creep or slip movements just to the south of Interstate 80 highway.

A lineament on the east flank of the Dunnigan Hills has been mapped recently by the U.S. Geological Survey..It may be the surface expression of a fault that has moved recently.

In recent time there was about \$10,000 damage at the Sacramento Filtration Plant resulting from the Dixie Valley earthquake, east of Fallon, Nevada, December 16, 1954 - a Richter magnitude 7.2 earthquake. This was about 185 miles northeast of Sacramento and clearly indicates that the long period earthquake waves resulting from distant earthquakes can have definite effects upon structures or their contents. Damage also occurred to the digestion tanks at the Sacramento Sewage Treatment Plant and to a clarifier tank at the Campbell Soup Company.

There appears to be a strong northwesterly structural "grain" to California geology. Earthquakes having epicenters towards the west have not affected Sacramento in the past to the same extent as those centered east and south of Sacramento. The 1892 Winters earthquake appears to be an exception to the general statement. To explain further, the April 18, 1906, San Francisco shock of Richter magnitude 8.25 with its epicenter about 80 miles west of Sacramento was probably felt in Sacramento with about the same intensity as the Owens Valley quake of March 12, 1872, which has been estimated to be between 8.0 and 8.25 Richter magnitude and was about 230 miles southeast of Sacramento. Also, the Boca Reservoir earthquake of Richter magnitude 6.0 on August 12, 1966, 95 miles northeast of Sacramento was strongly felt in the Sacramento area as well as the above mentioned Dixie Valley earthquake 185 miles northeast of Sacramento.

The University of California Seismographic Station Reports that since 1932 there have been approximately 700 earthquakes of Richter magnitude 4 and greater in the area bounded between longitudes 118°W and 124°W and between latitudes 36.5°N and 40.5°N. In general, this area is from Eastgate, located in west central Nevada, to the Pacific Ocean and from south of Fresno to Redding. Also within this area there were approximately 90 earthquakes of magnitude 5 and some 15 earthquakes of magnitude 6 during this period.

As noted above, the distance of the closest fault to the UCD/MNRC site far exceeds the siting requirements of ANSI 15.7, Section 3.2, which states “no proposed facility shall be located closer than 400 meters from the surface location of a known capable fault.”

**CHAPTER 3**

**DESIGN OF STRUCTURES, COMPONENTS,  
EQUIPMENT AND SYSTEMS**

Chapter 3 - Valid Pages  
Rev. 6 03/27/18

i	Rev. 6	03/27/18
ii	Rev. 6	03/27/18
3-1	Rev. 6	03/27/18
3-2	Rev. 6	03/27/18
3-3	Rev. 6	03/27/18
3-4	Rev. 6	03/27/18
3-5	Rev. 6	03/27/18
3-6	Rev. 6	03/27/18
3-7	Rev. 6	03/27/18
3-8	Rev. 6	03/27/18
3-9	Rev. 6	03/27/18
3-10	Rev. 6	03/27/18
3-11	Rev. 6	03/27/18
3-12	Rev. 6	03/27/18
3-13	Rev. 6	03/27/18
3-14	Rev. 6	03/27/18
3-15	Rev. 6	03/27/18
3-16	Rev. 6	03/27/18
3-17	Rev. 6	03/27/18
3-18	Rev. 6	03/27/18
3-19	Rev. 6	03/27/18
3-20	Rev. 6	03/27/18
3-21	Rev. 6	03/27/18
3-22	Rev. 6	03/27/18
3-23	Rev. 6	03/27/18
3-24	Rev. 6	03/27/18
3-25	Rev. 6	03/27/18
3-26	Rev. 6	03/27/18

TABLE OF CONTENTS

3.0 DESIGN OF STRUCTURES, COMPONENTS, EQUIPMENT AND SYSTEMS.....3-1

3.1 Conformance with NRC General Design Criteria.....3-1

3.1.1 Introduction.....3-1

3.1.2 Overall Requirements (Criteria 1-5) .....3-1

3.1.3 Protection by Multiple Fission - Product Barriers (Criteria 10-19).....3-7

3.1.4 Protection and Reactivity Control Systems (Criteria 20-29) .....3-11

3.1.5 Fluid Systems (Criteria 30-46) .....3-14

3.1.6 Reactor Containment (Criterion 50-57) .....3-16

3.1.7 Fuel Radioactivity Control (Criteria 60-64).....3-18

3.2 Classification of Structures, Components, and Systems .....3-20

3.2.1 Seismic Classification.....3-20

3.2.2 Systems-Quality-Group Classifications.....3-20

3.3 Wind and Tornado Considerations.....3-20

3.4 Flood Protection.....3-20

3.5 Missile Protection.....3-21

3.6 Protection Against Dynamic Effects Associated with the Postulated Rupture of Piping .....3-21

3.7 Seismic Design .....3-21

3.8 Design of Category I Structures.....3-21

3.9 Mechanical Systems and Components .....3-21

3.9.1 Control-Rod Drives .....3-21

3.9.2 Core-Support Structure .....3-23

3.9.3 Instrument Guide Tubes.....3-23

3.9.4 Neutron Source .....3-23

3.9.5 Fuel Storage Assemblies.....3-23

3.9.6 Beam-Tube Assemblies .....3-23

LIST OF TABLES

3-1 Applicability Of Compliance With General Design Criteria .....3-2

LIST OF FIGURES

3.1	Typical Rack-And-Pinion Control-Rod-Drive Mechanism.....	3-22
3.2	Typical Adjustable Fast Transient Rod Drive.....	3-24
3.3	Triga® Reactor .....	3-25
3.4	Typical In-Tank Reactor Core And Beam Tube Assembly.....	3-26

### 3.0 DESIGN OF STRUCTURES, COMPONENTS, EQUIPMENT AND SYSTEMS

#### 3.1 Conformance with NRC General Design Criteria

##### 3.1.1 Introduction

This chapter discusses the “General Design Criteria for Nuclear Power Plants” as set forth in 10CFR50, Appendix A, as they apply to the UCD/MNRC. These General Design Criteria were formulated for the purpose of establishing minimum requirements for the principal design criteria to be utilized for water-cooled nuclear power plants. Further, they are to be applied to new design and construction of plants similar in design for which construction permits have been previously issued. Since the UCD/MNRC is a research facility, many of the systems cannot be logically categorized according to power-plant application. Therefore, the discussions here are oriented with regard to the individual criterion, rather than toward identification of areas of noncompliance and corrective actions.

The nominal UCD/MNRC steady-state power level is 2 MW.

The maximum peak power for a \$1.75 pulse is predicted to be 2,000 MW, with a half-width of a few msec. Thus, the fission-product inventory is orders of magnitude less than those of the conventional power reactors for which General Design Criteria were primarily prepared. A conservative upper limit of energy released for an entire year of operation would be about 700 MW-days. These comparisons illustrate why the UCD/MNRC may be placed in a category of much lower risk, and treated accordingly, in a rigorous review for compliance with the General Design Criteria.

The accidents described in Chapter 13 conservatively demonstrate that instrumented shutdown actions and building confinement are not necessary to ensure that radiological doses will not exceed allowable limits. In the event of an improbable instantaneous loss of coolant from the reactor tank, an ECCS system has been provided for which ample time is available for initiation through operator action. Table 3-1 presents a synopsis of the conclusions regarding application of the General Design Criteria to the UCD/MNRC.

##### 3.1.2 Overall Requirements (Criteria 1-5)

###### Criterion 1: Quality Standards and Records

Original structures, systems, and components important to safety were designed, fabricated, constructed, and/or tested to design specifications (MAN-NDI-86-03) and associated standards.

TABLE 3-1 APPLICABILITY OF COMPLIANCE WITH GENERAL DESIGN CRITERIA

Criterion Number and Title	Compliance	Compliance Not Required	Conditional Noncompliance	Conditional Compliance
1. Quality Standards and Records	X			
2. Design Basis for Protections Against Natural Phenomena	X			
3. Fire Protection	X			
4. Environmental and Missile Design Basis	X			
5. Sharing of Structures, Systems and Components	X			

Criterion Number and Title	Compliance	Compliance Not Required	Conditional Noncompliance	Conditional Compliance
PROTECTION BY MULTIPLE FISSION PRODUCT BARRIERS				
10. Reactor Design	X			
11. Reactor Inherent Protection	X			
12. Suppressions of Reactor Power Oscillations	X			
13. Instrumentation and Control	X			
14. Reactor Coolant Pressure Boundary	X			
15. Reactor Coolant System Design	X			
16. Containment Design	X			
17. Electrical Power Systems	X			
18. Inspection and Testing of Electrical Power Systems	X			
19. Control Room				X

Criterion Number and Title	Compliance	Compliance Not Required	Conditional Noncompliance	Conditional Compliance
PROTECTION AND REACTIVITY CONTROL SYSTEMS				
20. Protection Systems Functions	X			
21. Protection System Reliability and Testability	X			
22. Protection System Independence	X			

Criterion Number and Title	Compliance	Compliance Not Required	Conditional Noncompliance	Conditional Compliance
PROTECTION AND REACTIVITY CONTROL SYSTEMS (CONT.)				
23. Protection System Failure Modes	X			
24. Separation of Protection and Control System	X			
25. Protection System Requirements for Reactivity Control Malfunctions	X			
26. Reactivity Control System Redundancy and Capability	X			
27. Combined Reactivity Control Systems Capability	X			
28. Reactivity Limits	X			
29. Protection Against Anticipated Operational Occurrences	X			

Criterion Number and Title	Compliance	Compliance Not Required	Conditional Noncompliance	Conditional Compliance
FLUIDSYSTEMS				
30. Quality of Reactor Coolant Pressure Boundary		X		
31. Fracture Prevention of Reactor Coolant Pressure Boundary		X		
32. Inspection of Reactor Coolant Pressure Boundary	X			
33. Reactor Coolant Makeup	X			
34. Residual Heat Removal	X			
35. Emergency Core Cooling	X			
36. Inspection of Emergency Core Cooling System	X			
37. Testing of Emergency Core Cooling System	X			
38. Containment Heat Removal		X		
39. Inspection of Containment Heat Removal System		X		
40. Testing of Containment Heat Removal System	X			
41. Containment Atmosphere Cleanup		X		
42. Inspection of Containment Atmosphere Cleanup System		X		
43. Testing of Containment Atmosphere Cleanup System	X			
44. Cooling Water				X
45. Inspection of Cooling Water System				X

Criterion Number and Title	Compliance	Compliance Not Required	Conditional Noncompliance	Conditional Compliance
REACTOR CONTAINMENT				
50. Containment Design Basis	X			
51. Fracture Prevention of Containment Pressure Boundary	X			
52. Capability for Containment Leakage Rate Testing		X		
53. Provisions for Containment Testing and Inspection		X		
54. System Penetrating Containment		X		
55. Reactor Coolant Pressure Boundary Penetrating Containment				X
56. Primary Containment Isolation		X		
57. Closed Systems Isolation Valves		X		

Criterion Number and Title	Compliance	Compliance Not Required	Conditional Noncompliance	Conditional Compliance
FUEL AND RADIOACTIVITY CONTROL				
60. Control of Releases of Radioactive Materials to the Environment	X			
61. Fuel Storage and Handling and Radioactivity Control	X			
62. Prevention of Criticality in Fuel Storage and Handling	X			
63. Monitoring Fuel and Waste Storage	X			
64. Monitoring Radioactivity Releases	X			

All design and construction work was monitored by McClellan AFB engineers to assure that the specifications incorporated appropriate standards, and the design and construction were in accordance with these specifications. Modifications have been made in accordance with existing standards and requirements.

#### Criterion 2: Design Bases for Protection Against Natural Phenomena

Hurricanes, tsunamis, and seiches do not occur in the Sacramento area. Flooding in the area could be caused by run-off from local rainstorm activity or by a catastrophic failure of Folsom Dam. However, the UCD/MNRC is situated some 3,400 ft from the 100-yr floodplain.

Only a small number of tornadoes, one or two per year, have been reported in California. Based on the small probability of occurrences, postulated low intensity, the intermittent type of reactor operation and low fission-product inventory, no criteria for tornadoes have been established for the UCD/MNRC structure. However, the buildings are designed to withstand the area wind loads.

The Sacramento area is classified as being in Seismic Zone 3 as defined in the Uniform Building Code. The UCD/MNRC structures have been designed and constructed in accordance with this code, with an importance factor of 1.5 and to AFM-88-15, Chapter 13. Seismic activity in the region has registered as high as Richter 6.0-6.5 in historical time which indicates an upper limit on the most likely seismic event (Section 2.5). Since the UCD/MNRC is designed to the Uniform Building Code for Zone 3 with an importance factor of 1.5, there is ample conservatism in the design for the maximum expected event. The UCD/MNRC structures may suffer some damage from a seismic event of the highest possible yield, but, as previously noted, even in the event of the incredible scenario that a seismic event would cause instantaneous loss of tank coolant water, an ECCS has been provided for which there is ample time for operators to initiate actions to minimize the consequences of such an event, and resultant radiological doses would be within the ranges evaluated in Chapter 13.

#### Criterion 3: Fire Protection

The reactor room and reactor control room structures, built of steel, concrete, and concrete block, are highly fire resistant. However, material inventories inside the rooms could include various flammable materials (paper, wood, etc.), and these, coupled with potential ignition sources, require that fires be considered.

Several features reduce both the likelihood and the consequences of a fire. First, periodic fire-safety inspections are made by Fire Safety engineers. Second, periodic in-house inspections are made for the explicit purpose of reducing nonessential combustible material inventory. Third, fire detection and suppression systems are installed in the facility. If these systems are activated, or a fire alarm is tripped, the Sacramento Metropolitan Fire Department is automatically alerted and will respond to the UCD/MNRC within a few minutes. Fourth, a closed circuit television camera in the reactor room with a monitor in the control room permits the reactor operator to continuously observe the reactor room, so that immediate action can be taken to minimize the effects of a fire; established emergency procedures will be put into effect in the event of a fire.

Fifth, the large volume of water in the reactor tank would protect the core from any conceivable fire. Sixth, the reactor is fail safe and will shutdown should a fire damage the instrumentation or control system.

#### Criterion 4: Environmental and Missile Design Bases

The construction of the facility precludes catastrophic rupturing of the reactor tank. There is no source in the reactor room for generating large, sustained positive pressure differentials which would breach the reactor room integrity.

The amount of explosive materials allowed in the radiography bays has been limited to preclude damage to the reactor should they detonate. Plates covering the entrance to beam tubes have been sized, as discussed in Chapters 10 and 13, so that these will not fail from a pressure pulse explosive generated from the maximum allowable quantities of explosives. Further, each experiment containing explosives will be analyzed to show that detonation will not produce pressure or fragments that will damage the reactor. The reactor core is protected from missiles by being below ground level and surrounded by a large block of reinforced concrete. Dynamic effects of such conditions as whipping pipes are not a problem because there are no high pressure systems. The piping systems are anchored and do not penetrate the tank walls and they could not conceivably affect the reactor. The probability of an event or condition resulting from dynamic effects of missiles, aircraft, etc., causing a reactor incident, is very small. "Probability Assessment of the Airplane Crash Risk for McClellan Air Force Base TRIGA® Reactor" shows that the probability of an aircraft accident impacting the facility is  $10^{-8}$ /year and is, therefore, considered incredible (Appendix C).

#### Criterion 5: Sharing of Structures, Systems, and Components

Electrical power constitutes the only system shared by the UCD/MNRC. Sharing is based on the fact that the UCD/MNRC electric power is supplied from a distribution point within the adjacent facility. Loss of power results in the shutdown of the reactor since all control circuits are fail-safe, and no power is required for safe shutdown or to maintain safe shutdown conditions. An electric power failure at any point in the UCD/MNRC network will not detrimentally affect the reactor.

### 3.1.3 Protection by Multiple Fission - Product Barriers (Criteria 10-19)

#### Criterion 10: Reactor Design

The safety limit placed on the temperature of the reactor fuel for UCD/MNRC operations is 1100°C when the clad is less than 500°C and 930°C when the clad temperature is equal to the fuel temperature.

Accident analyses presented in Chapter 13 show that under credible accident conditions, the safety limit on the temperature of the reactor fuel will not be exceeded. Consequently, there would be no fission product release that would exceed 10CFR Part 20 allowable radiation levels.

#### Criterion 11: Reactor Inherent Protection

Because of the fuel material (U-ZrH) and core design, there is a significant prompt negative temperature reactivity coefficient. Routine steady-state power operation is performed with the transient, shim, and regulating rods partially withdrawn. As shown in Chapters 4 and 13, the most rapid possible reactivity insertion rates are adequately compensated for by the negative temperature reactivity coefficient of 0.01 %/°C ( $1 \times 10^{-4} \Delta k/k/^\circ\text{C}$ ).

#### Criterion 12: Suppression of Reactor Power Oscillations

Due to the small dimensions of the core and low power levels, the reactor is inherently stable to space-time and xenon oscillations.

#### Criterion 13: Instrumentation and Control

The instrumentation and control system for the UCD/MNRC TRIGA<sup>®</sup> reactor is a computer-based system incorporating the use of a GA-developed, multifunction, NM-1000 microprocessor-based neutron monitoring channel and a NPP-1000 analog type neutron monitoring channel (refer to Chapter 7 for further detail). The NM-1000 system provides a safety channel (percent power with scram), a wide-range log percent power channel (below source level to full power), period indication, and a multirange linear power channel (source level to full power). The NPP-1000 system provides a second safety channel for redundancy (percent power with scram). In the pulse mode of operation, the Data Acquisition Computer (DAC) makes a gain change in the NPP-1000 safety channel to provide NV and NVT indication along with a peak pulse power scram. The NM-1000 is bypassed once a pulse has been initiated.

The control system logic is contained in a separate Control System Computer (CSC) with a color graphics display. While information from the NM-1000, NPP-1000, and fuel temperature channels is processed and displayed by the CSC, each is direct wired to its own output display, and the safety channel connects directly to the protective system scram circuit. That is, signals to the scram circuits are not processed by the Data Acquisition computer or the control computer.

The nuclear information goes directly from the detectors to either the NM-1000 or NPP-1000 where it is processed. The processed signals connect directly to the scram circuit switches. Fuel temperature information goes directly to "action pack modules" for amplification and then to the scram circuit switches.

The NM-1000 digital neutron monitor channels were developed for the nuclear power industry and are fully qualified for use in the demanding and restrictive conditions of a nuclear power generating plant. Their design is based on a special GA-designed fission chamber and low-noise ultra-fast pulse amplifier. The NPP-1000 safety channel was designed to the same criteria as the NM-1000 channels.

The CSC manages all control rod movements, accounting for such things as interlocks and choice of particular operating modes. It also processes and displays information on control rod positions, power level, fuel and water temperature, and pulse characteristics. The CSC also performs many other functions, such as monitoring reactor usage, and storing historical operating data for replay at a later time. A computer-based control system has many advantages over an analog system: speed, accuracy, reliability, the ability for self-calibration, improved diagnostics, graphic displays, and the logging of vital information.

The UCD/MNRC reactor can be operated in four modes: manual, automatic, square wave, and pulse. The operations are controlled from the reactor console mode control and the rod control panels. The manual and automatic modes are steady-state reactor conditions; the square-wave and pulse modes are the conditions implied by their names and require the use of the pulse rod.

The manual and automatic reactor control modes are used for reactor operation from source level to 100% power. These two modes are used for manual reactor startup, change in power level, and steady-state operation.

Interlocks prevent the movement of the rods in the up direction under the following conditions:

1. Scrams not reset;
2. Source level below minimum count;
3. Two UP switches depressed at the same time;
4. Mode switch in the PULSE position;
5. Mode switch in the AUTOMATIC position [servo-controlled rod(s) only];
6. Mode switch in the SQUARE WAVE position.

Automatic power control can be obtained by switching from manual operation to automatic operation on the mode control panel. All the instrumentation, safety, and interlock circuitry for steady operation applies to this mode. However, the servo-controlled rod(s) is (are) controlled automatically to a power level and period signal. The reactor power level is compared with the demand level set by the operator, on the mode control panel, and used to bring the reactor power to the demand level on a fixed preset period. The purpose of this feature is to maintain automatically the preset power level during long-term power runs.

The square-wave mode allows the reactor power to be quickly raised to a desired power level. In a square-wave operation, the reactor is first brought to criticality below one kW in the manual mode, leaving the transient rod partially in the core. The desired power level is set by the reactor operator using the power demand selector located on the mode control panel. All of the steady-state instrumentation is in operation. The transient rod is ejected from the core by means of the transient rod FIRE pushbutton located on the rod control panel. When the power level reaches the demand level, it is maintained in the automatic mode.

Reactor control in the pulsing mode consists of manually establishing criticality at a flux level below one kW in the steady-state mode. This is accomplished by the use of the control rods, leaving the transient rod either fully or partially inserted. The pulse mode selector switch located on the mode control panel is then depressed. The MODE SELECTOR switch automatically causes the DAC to make a gain change in the NPP-1000 safety channel to monitor and record peak flux (NV), energy release (NVT), and to provide a peak pulse power scram. The pulse is initiated by activating the FIRE pushbutton. Once a pulse has been initiated and it is detected by the DAC, the NM-1000 safety scram is bypassed. Pulsing can be initiated from either the critical or subcritical reactor state.

#### Criterion 14: Reactor Coolant Pressure Boundary

The reactor tank and cooling systems operate at low pressure and temperature. The vessel is open to the atmosphere, and there are no means for pressurizing the system. The reactor tank is constructed of aluminum and the primary coolant system components are aluminum or stainless steel. The system components outside the reactor tank have a low probability of serious leakage or of gross failure.

#### Criterion 15: Reactor Coolant System Design

The reactor tank is an open system and the maximum pressure in the primary system is that due to the static head (about 23-1/2 ft). The primary cooling system, the secondary cooling system, and the purification system are pressurized by small capacity pumps. The secondary system water pressure is maintained slightly higher than the primary system. This feature prevents any radioactive primary water from entering the secondary system, and the environment, should a leak develop in the heat exchanger. There are no instrumentation systems that derive signals from any portion of the reactor coolant systems to initiate either control or protection actions. Piping and valves in the primary and purification systems are stainless steel or aluminum and of such size to provide adequate operating margins. The secondary system components are carbon steel. Chapter 5 describes the cooling system in detail.

#### Criterion 16: Containment Design

The structure surrounding the reactor constitutes a confinement building rather than providing absolute containment. Because of the low fission-product inventory, leakage from the structure can be tolerated.

#### Criterion 17: Electric Power Systems

An uninterruptible power supply (UPS) provides electrical power to the reactor console, DAC, and translator rack during normal reactor operations. An additional emergency generator is provided to supply power to the Auxiliary Make Up Water System (AMUWS) and the reactor room exhaust fan (EF-1) should these systems be called upon to provide backup to the reactor ECCS system. The UPS provides a filtered and regulated power source to the computers and electronic components of the reactor control systems. If there was a loss of electrical power the UPS will supply electrical power to all components for fifteen minutes. Because the reactor is cooled by natural convection, and there is no requirement to provide forced cooling flow for the removal of heat, there is sufficient time for the reactor operator to shut down the reactor and confirm the reactor is shutdown. The UPS also provides an additional four hours of power to the stack continuous air monitor (CAM) and all remote area radiation monitors (RAM).

#### Criterion 18: Inspection and Testing of Electric Power Systems

The primary power distribution system supplying commercial power to UCD/MNRC is maintained by electrical utility maintenance crews. Routine inspections of the systems are performed.

The UCD/MNRC can tolerate a total loss of electric power with no adverse effects on the safety of the facility. There are no electrical power (distribution) systems designated as necessary to provide power to the UCD/MNRC during either normal or abnormal conditions except for the emergency generator which supplies the AMUWS and EF-1 which is considered only as a backup system to the primary ECCS system (Chapter 13).

#### Criterion 19: Control Room

In the event of an accident where operations instructions require shutdown of the reactor, continuous or even partial occupancy of the control room is not a requirement since the reactor has been shut down and experiments in progress terminated. The control room is equipped with a separate exhaust system and can monitor those accidents which do not result in a breach of the control room structure. Exposure levels from radiation sources resulting from an accident would be significantly reduced in magnitude (due to the location of the control room with respect to the reactor room). Consequently, control room radiation levels may not be higher than the allowable tolerance levels. In the event that the ECCS requires activation, this system is actuated by the operator through coupling a quick connect on the reactor building roof. The backup systems to the ECCS, can be controlled from either the reactor room or other remote locations. Nevertheless, the UCD/MNRC Emergency Plan describes actions for mitigating accident situations which require control room evacuation.

### 3.1.4 Protection and Reactivity Control Systems (Criteria 20-29)

#### Criterion 20: Protection System Functions

The UCD/MNRC Reactor Protection System has been designed to initiate automatic actions to assure that fuel design limits are not exceeded by anticipated operational occurrences or accident conditions. The automatic actions are initiated by two nuclear power channels and two fuel temperature channels. The Reactor Protective System automatically scrams the control rods when trip settings are exceeded (Chapter 7). There are no other automatic actions required by UCD/MNRC systems to keep fuel temperature limits from being exceeded. The Reactor Protective System satisfies the intent of IEEE-323-1974 in the areas of redundancy, diversity, power-loss fail-safe protection, isolation and surveillance.

#### Criterion 21: Protection System Reliability and Testability

The UCD/MNRC Reactor Protection System is designed to be fail-safe: any sub-channel loss that causes the channel to lose its ability to perform its intended function results in initiation of shutdown action. Protective action is manifested through several independent scram inputs arranged in series such that action by any one interrupts current to the scram magnets resulting in shutdown of the reactor. Redundancy of channels is provided and in addition, a loss of any channel due to open circuit or loss-of-power will result in a scram. Scram action is, therefore, on a one-out-of-one basis. All instrumentation is provided with testing capability. The Reactor Protective System satisfies the intent of the IEEE-323-1974 standard.

#### Criterion 22: Protection System Independence

The protective system satisfies the intent of IEEE-323-1974 "Criteria for Protective Systems for Nuclear Power Generating Stations." Protective functions are initiated through two independent nuclear and two independent fuel temperature channels, and there is a diversity of scram modes. Furthermore, the protective system is fail-safe upon loss of power.

The Reactor Protective System and the magnet power supply are, for the most part, physically and electrically isolated from the remainder of the control system. The cables between the control room and reactor room are enclosed in conduit. There is a separate conduit for each safety channel and one for the magnet power supply.

### Criterion 23: Protection System Failure Modes

The reactor protective system is designed and constructed to fail safe in event of a failure of a safety channel. Failure of a safety channel will result in removal of power to the control rod and transient rod magnets, allowing the control rods to fall into the core. Simultaneously, loss of a safety channel causes the transient rod's solenoid valve to de-energize thus removing any gas pressure that may be on the pneumatic cylinder. This causes the transient rod to fall into the core. The reactor protective system contains no control functions. Therefore, loss of a protective function will not necessarily affect the operation of the reactor, such as initiating an uncontrolled reactivity

### Criterion 24: Separation of Protection and Control Systems

The UCD/MNRC has two nuclear instrumentation and two fuel temperature channels. One of the nuclear channels utilizes a fission chamber and a GA NM-1000. This channel provides signals for both safety (scram) and control action as well as signals for monitoring operations over a wide power range. The second channel utilizes an ion chamber and a GA NPP-1000. This channel provides % power for safety (scram) action as well as neutron monitoring capability for pulse operation. Fuel temperature is measured by thermocouples placed within the special instrumented fuel elements. While information from these channels is processed and displayed by the control system computer, each channel is independent, has its own output displays, and connects directly to the safety system scram circuit, see Criterion 13, second paragraph, for technique used to separate protection and control functions. The ability of this configuration to meet the intent of protection system requirements for reliability, redundancy, and independence for TRIGA<sup>®</sup>-type reactors has been accepted by the NRC.

Separate conduits are used for the safety channel and control system cabling from the NM- 1000 and the NPP-1000 (located in the reactor room) to the control console.

Finally, the control and safety systems are fail safe and will scram the reactor should they malfunction. No control or safety systems are required to maintain a safe shutdown condition.

### Criterion 25: Protection System Requirements for Reactivity Control Malfunction

The UCD/MNRC Protection System is designed to assure that fuel temperature limits are not exceeded for any single malfunction of the reactivity control system. However Chapter 13 shows that accidental runout of all rods simultaneously from the core at their normal drive speed will not result in exceeding fuel temperature limits.

### Criterion 26: Reactivity Control System Redundancy and Capability

The UCD/MNRC has six independent reactivity control rods: four shim rods, one regulating rod and one transient rod. Each of the rods has its own drive mechanism and control circuit and they are operated individually.

The shim and regulating rods and drives are similar. The regulating rod is used to control power either manually or by automatic control.

Upon receipt of a scram signal, all six rods are released from their drives and dropped into the core. Insertion of five of the six rods ensures reactor shutdown.

#### Criterion 27: Combined Reactivity Control System Capability

Emergency core cooling is only required for MNRC if reactor power level exceeds 1.5 MW. The description for the requirement of emergency core cooling is given in chapter 13.

The addition of a neutron absorbing material in the emergency cooling water is not required as the total worth of the rods is more than adequate to maintain the core at a subcritical level, with the most reactive rod stuck out of the core.

#### Criterion 28: Reactivity Limits

No conceivable malfunction of the reactivity control systems could result in a reactivity accident worse than the conditions encountered during a maximum-yield pulse. As shown in Chapter 13, neither continuous rod withdrawal nor loss of coolant will cause undue heating of the fuel. Identified accidents will not result in significant movement of adjacent fuel elements or otherwise disturb the core so as to add reactivity to the system.

Since the primary coolant system operates at atmospheric pressure, control-rod ejection is not a credible event. The shim rods, the regulating rod, and the transient rod cannot drop out of the core because the rods in the full down position are approximately one inch above the safety plate located near the bottom of the tank. The possibility of traveling out of the core in the downward position is therefore eliminated. The transient-rod system is specially designed for rapid reactivity insertion, and an accidental rod system ejection might cause a reactivity accident in the sense that it was not planned; rapid reactivity additions constitute the normal pulse mode, however, and the maximum reactivity change and the rate of addition are limited by the design of the rods, the rod drive system, and the available excess reactivity such that the reactor is protected against the consequences of this type of accident.

#### Criterion 29: Protection Against Anticipated Operational Occurrences

There are two scram loops, using different input signals, to provide redundancy in scram capability. The protection and reactivity control systems satisfy all existing design standards. Periodic checks (i.e., startup, shutdown, and maintenance procedures) of all reactor protective system channels and reactivity control systems demonstrate that they perform their intended function.

If there was a loss of electrical power the UPS will supply electrical power to all components for fifteen minutes. Because the reactor is cooled by natural convection, and there is no requirement to provide forced cooling flow for the removal of heat, there is sufficient time for the reactor operator to shut down the reactor and confirm the reactor is shut down.

### 3.1.5 Fluid Systems (Criteria 30-46)

#### Criterion 30: Quality of Reactor Coolant Pressure Boundary

The reactor tank is open to the atmosphere and is subjected only to ambient conditions. All components containing primary coolant (i.e., reactor tank, primary coolant system, and the purification system) are constructed of aluminum and stainless steel, using standard codes for quality control. There is no requirement for leak detection in the primary coolant or purification loop since no conceivable leak condition can result in the tank water level to lower more than approximately three feet.

#### Criterion 31: Fracture Prevention of Reactor Coolant Pressure Boundary

Since the coolant system is open to the atmosphere, no reactor coolant pressure boundary exists.

#### Criterion 32: Inspection of Reactor Coolant Pressure Boundary

The reactor tank is surrounded by a thick reinforced-concrete block which prevents external forces from being directly transmitted to the tank and precludes movement of the tank. The tank wall cannot be inspected by any means other than visual observation through the water from inside the tank. All piping, valves, meters, etc., associated with the primary water system are located in open spaces and are readily accessible for periodic inspections.

The UCD/MNRC operates at relatively low powers and temperatures. Because of the moderate fluence levels and low temperature factors, no significant change in material properties is expected.

#### Criterion 33: Reactor Coolant Makeup

The UCD/MNRC water purification system design includes an Auxiliary Make Up Water System (AMUWS) for makeup of primary coolant water. This system is manually operated and contains 4600 gal water. This system can also act as a backup to the ECCS system should the need ever arise (Chapter 5).

#### Criterion 34: Residual Heat Removal

Natural convection cooling is adequate to dissipate core afterheat. Many years of operations with TRIGA<sup>®</sup> reactors have shown that natural convection will provide adequate flow for the removal of heat after several hours of maximum steady-state operation.

Calculations performed for loss of coolant show that an ECCS connected to the domestic water supply is sufficient to assure that fuel temperatures will not reach the safety limit even under loss-of-coolant conditions (Chapter 13).

The AMUWS and the reactor room exhaust fan also provide a back-up capability to the ECCS system sufficient to provide the emergency cooling function should the domestic water supply also fail.

#### Criterion 35: Emergency Core Cooling System

An emergency core-cooling system has been provided in the case of the unlikely probability that an accident such as a severe seismic event occurs which results in the instantaneous loss of all reactor coolant. Analyses presented in Chapter 13 show that sufficient capability resides in a simple ECCS requiring only a supply of domestic water for spraying over the uncovered reactor core. Ample time is present during the accident sequence to initiate the ECCS through operator action without any threat to the fuel cladding material.

#### Criterion 36: Inspection of Emergency Core Cooling System

All components of the ECCS system are located in open spaces and are readily available for periodic inspection. Verification of the availability of the domestic water system is checked on a daily basis.

#### Criterion 37: Testing of Emergency Core Cooling System

The UCD/MNRC ECCS is routinely checked, tested, and maintained.

#### Criterion 38: Containment Heat Removal

There are no systems, devices, equipment, experiments, etc., with sufficient stored energy to require a primary containment heat-removal capability.

#### Criterion 39: Inspection of Containment Heat Removal System

This criterion is not applicable.

#### Criterion 40: Testing of Containment Heat Removal System

This criterion is not applicable.

#### Criterion 41: Containment Atmosphere Cleanup

Post-accident activities are not contingent upon maintaining the integrity of the building structure. Accident analyses in Chapter 13 have shown that downwind doses would not exceed 10 CFR Part 20 or ANSI 15.7 guidelines in any credible accident.

Routine operations result in two isotopes of concern being produced: Argon-41 in the reactor room and radiography bays and Nitrogen-16 from the irradiation of oxygen in the tank water. Analysis in Chapter 11 show concentrations to be below ANSI 15.7 guidelines for accident situations and below 10 CFR Part 20 guidelines for normal operations.

Criterion 42: Inspection of Containment Atmosphere Cleanup Systems

This criterion is not applicable.

Criterion 43: Testing of Containment Atmosphere Cleanup Systems

This criterion is not applicable.

Criterion 44: Cooling Water

A coolant system is utilized to cool reactor tank water during normal operation of the reactor. The UCD/MNRC requires no auxiliary cooling system for cooling of reactor tank water upon shutdown.

Criterion 45: Inspection of Cooling Water System

Cooling equipment used in normal operation of the reactor is located either in the reactor room, equipment room, or outside the building with adequate space provided to permit inspection and testing of all components. Operation of the bulk coolant and cooling tower system is checked on a daily basis prior to reactor operation. During this checkout, the performance of each system is monitored with emphasis on pump outlet pressures, pressure differentials and system flow rates.

Criterion 46: Testing of Cooling Water System

UCD/MNRC reactor cooling systems are routinely checked, tested, and maintained.

3.1.6 Reactor Containment (Criterion 50-57)

Criterion 50: Containment Design Basis

Under the conditions of a loss of coolant, it is conceivable that the temperature at the reactor room could increase slightly due to heating of the air flowing through the core. However, since the building is not leak tight, it will not pressurize from the heating of the air.

Further, there is no requirement from a radiological-exposure viewpoint for a containment structure; hence, only confinement capability is provided. In addition, there is no source of energy (from an accident) which would provide a significant driving force ( $\Delta P$ ) if no corrective action were taken.

Criterion 51: Fracture Prevention Boundary

The confinement structure (the reactor room) is a reinforced filled concrete block structure with a conventional built-up roof. The entire structure is exposed to only normal external environmental conditions and internal environmental conditions are maintained at regulated conditions.

The structure will not be subjected to significant internal pressures during normal operations. Postulated accident conditions cannot result in significant changes in the pressure differential due to the non-leak tightness of the structure.

Criterion 52: Capability for Containment Leakage Rate Testing

This criterion is not applicable.

Criterion 53: Provisions for Containment Testing and Inspection

The reactor room confinement capability is checked on a daily basis prior to reactor operation and routinely during reactor operations. This check involves monitoring the pressure differentials between the reactor room and the surrounding areas. The reactor room exhaust recirculation system is checked monthly to confirm proper operation.

Criterion 54: Piping Systems Penetrating Containment

Piping systems which involve penetrations through the reactor building walls have no effect on the safety of operation; therefore, isolation, redundancy, and secondary containment of these systems is not required.

Criterion 55: Reactor Coolant Pressure Boundary Penetrating Containment

The reactor room was neither designed nor constructed as a containment structure but provides only a minor confinement capability. As pointed out in the responses to previous criteria, there are no requirements for containment (or confinement) capabilities. The only systems that penetrate the reactor room are the ventilation system, primary coolant system, ECCS/AMUWS, demineralizer system, helium pressurization system, Ar -41 production lines, electrical wiring ports, and air monitor lines for CAM and remote sampling. Reactor room wall penetrations are packed with fill material.

Criterion 56: Primary Containment Isolation

Penetrations through the building walls have no effect on the safety of reactor operations, therefore, isolation systems are not required in the UCD/MNRC.

Criterion 57: Closed System Isolation Valves

The UCD/MNRC reactor building was designed to provide only confinement capability; isolation valves are not required.

## 3.1.7 Fuel Radioactivity Control (Criteria 60-64)

Criterion 60: Control of Release of Radioactive Materials to the Environment

There is no readily available path for liquid waste to be discharged directly to the environment. Liquids in the reactor room which could subsequently be injected into the environment may result from spills, washdown of the floor, etc. These liquids are collected in a storage tank within the UCD/MNRC, analyzed for radioactivity, and disposed of accordingly.

Significant dilution of gaseous materials released to the atmosphere, and soil permeability coefficients are such that transmissibility times of ground fluids are very long (Chapter 13).

Criterion 61: Fuel Storage and Handling and Radioactivity Control

The major concern relative to storage, handling, and control of radioactivity of irradiated fuel is shielding. All irradiated fuel elements are either stored in special racks (Criterion 62) in the reactor tank or storage pits [REDACTED] (Chapter 9). When fuel is stored in the reactor tank, the water provides a minimum shield thickness of at least 18 ft. This amount of water also provides scavenging of any fission products should any escape from the fuel elements. Lead covers provide shielding for elements stored in the [REDACTED] storage pits. Cooling is not required due to low burnup and no large decay heat source is present in the UCD/MNRC fuel. Irradiated fuel elements are handled either under water or with a cask. The elements are transferred one at a time so they are in a criticality-safe configuration (Chapter 9).

Some spare, unirradiated, UCD/MNRC fuel elements may be stored in a criticality-safe configuration [REDACTED]. These elements require no special handling arrangements or radiation shields.

For some experiments, special core loadings may be required. Fuel elements removed from the core can be placed in a criticality-safe fuel storage rack [REDACTED].

#### Criterion 62: Prevention of Criticality in Fuel Storage and Handling

Fuel-storage capability is provided by storage racks mounted in the tank and fuel storage pits [REDACTED]. The storage locations are criticality safe due to the geometry utilized and the limited quantity of fuel elements which can be stored (Chapter 9).

Since only one fuel element can be handled at a time, handling does not present a criticality problem.

#### Criterion 63: Monitoring Fuel and Waste Storage

No residual heat removal or temperature measuring capability is required for irradiated UCD/MNRC fuel elements. Fuel burnup is low, therefore, only a minimum decay heat source is present.

The reactor room and the UCD/MNRC fuel storage area radiation level is monitored with both a RAM system and a CAM system.

#### Criterion 64: Monitoring Radioactivity Releases

The radiation monitoring system for the UCD/MNRC consists of the RAM's and CAM's. RAM's monitor the reactor room, and selected areas outside the reactor room for gamma activity. There are three CAMs in the facility.

The UCD/MNRC exhaust stack is equipped with a CAM which provides continuous readings of radiation from Ar-41 and beta/gamma particulates released from the facility.

The reactor room CAM monitors the air exhausted from the reactor room for radioactive iodine, beta/gamma particulates, and noble gases. Actions initiated to reduce the release of radioactivity if the set points of this instrument are exceeded are discussed in Chapter 9 and Chapter 11. A third CAM monitors the radiography bays for Ar-41 and beta/gamma particulates. The sample lines to this unit are manifolded and valved so that one bay may be monitored at a time. In addition to providing routine surveillance of the bays, this unit will be used to help determine the source of activity should the stack monitor alarm. All three of these CAMs have local readouts and alarms as well as remote readouts and alarms in the reactor control room.

### 3.2 Classification of Structures, Components, and Systems

The UCD/MNRC reactor does not have structures, components, or systems that are important to safety in the same context as nuclear power plants. For the UCD/MNRC, a loss of coolant event, failure of the protection system, or any other credible accident does not have the potential for causing off-site exposure comparable to those listed in the guideline for accident exposures of ANSI 15.7.

Thus, the UCD/MNRC facility does not have structures, components, and systems requiring a Category I classification. However, certain structures, components, and systems have been designed to withstand natural phenomena. These design considerations are discussed in the following subsections.

#### 3.2.1 Seismic Classification

The UCD/MNRC site is in a UBC Zone 3 risk area (Chapter 2). The UCD/MNRC building, reactor foundation, shielding structure, reactor tank, and core support structure are designed in accordance with AFM-88-15, Chapter 13 and UBC Zone 3 requirements with an importance factor of 1.5. Meeting these requirements will ensure that the reactor can be returned to operation without structural repairs following an earthquake likely to occur during the plant lifetime. Furthermore, failure of the reactor tank and loss of the coolant in the event of a very large earthquake has been considered in Chapter 13 and the consequences found acceptable from the standpoint of public safety.

#### 3.2.2 Systems-Quality-Group Classifications

Classification of the UCD/MNRC fluid systems into quality groups in accordance with the Regulatory Guide 1.26 quality-group classification system is considered inappropriate, because these systems with the exception of the ECCS which has defense in depth need not remain functional to ensure that the reactor can be maintained in a safe shutdown condition and to prevent the release of significant quantities of radioactive material to the environment.

### 3.3 Wind and Tornado Considerations

The UCD/MNRC reactor core is protected from damage by high winds or tornadoes by virtue of its below grade location and the thick reinforced concrete structure surrounding the reactor tank. The superstructure of the UCD/MNRC has been designed for area wind loads.

### 3.4 Flood Protection

As discussed in Chapter 2, flooding is not expected at the UCD/MNRC site. However, even if flooding occurred, reactor safety would not be an issue since the core is located in a water pool.

### 3.5 Missile Protection

Missile protection is provided for the UCD/MNRC reactor by virtue of the building design and the below grade location of the core which is surrounded by a seven (7) ft thick reinforced concrete block (see Chapter 1 for building design). Chapter 13 also shows that an aircraft accident damaging the facility is not probable.

### 3.6 Protection Against Dynamic Effects Associated with the Postulated Rupture of Piping

There are no pipes in the UCD/MNRC facility capable of flooding the radiography bays to the first floor level. Furthermore, the lowest elevation in the UCD/MNRC (Bay 1 floor) contains a sump. If a predetermined water level is reached, the sump pump will automatically start.

### 3.7 Seismic Design

Seismic considerations applicable to the UCD/MNRC facility are discussed in Chapter 2.

### 3.8 Design of Category I Structures

The UCD/MNRC facility does not have any Category I structures.

### 3.9 Mechanical Systems and Components

#### 3.9.1 Control-Rod Drives

The control-rod-drive assemblies for all control rods are mounted on the reactor bridge structure. The drives are standard TRIGA<sup>®</sup> drive mechanisms manufactured by GA. A drive mechanism for the shim and regulating rods is shown in Figure 3.1. The mechanism consists of a stepping motor and reduction gear, a rack and pinion, an electromagnet and armature, a dashpot assembly, and a control-rod extension shaft. Rod-position data are obtained from potentiometers. Limit switches are provided to indicate the up and down positions of the magnet and the down position of the rod. The drive motor is of the stepping type and is instantly reversible. The nominal drive speed for the shim and the regulating rods is 24 in./min.. The stepping motor speeds are adjustable with a maximum rod speed of 42 in./min.. The ability to change the rod drive speed is administratively controlled and access to the area is limited to authorized personnel only. Rod withdrawal reactivity insertion accidents use this maximum rate (Chapter 13).

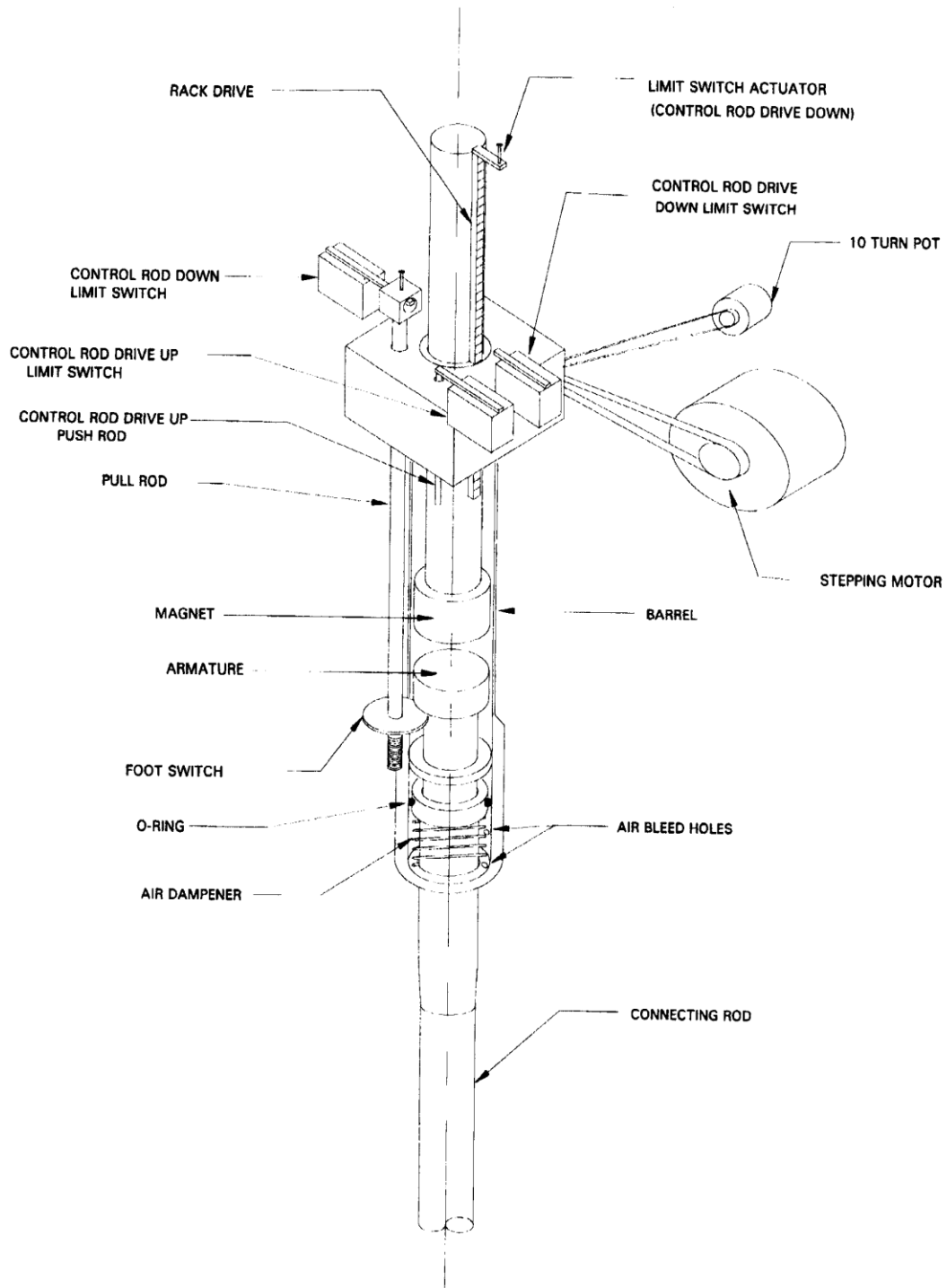


FIGURE 3.1 TYPICAL RACK-AND-PINION CONTROL-ROD-DRIVE MECHANISM

During a scram, the control rod, rod extension, and magnet armature are detached from the electromagnet and drop by gravity. The dashpot assembly slows the rate of insertion near the bottom of the stroke to limit deceleration forces.

The transient rod drive mechanism is shown in Figure 3.2. This is an adjustable fast transient TRIGA<sup>®</sup> pneumatic pulse drive system. The operability and reliability of this system has been proven over many years of use at Sandia National Laboratories.

### 3.9.2 Core-Support Structure

The fuel elements and graphite assemblies are supported by the core-support structure shown in Figure 3.3. The UCD/MNRC grid plate has been designed to have a thickness and hole pattern identical to those of other TRIGA<sup>®</sup> reactors with hexagonal grids.

### 3.9.3 Instrument Guide Tubes

The nuclear instrument chamber guide tubes for UCD/MNRC are supported by the core support structure as shown in Figure 3.4. There are three guide tubes, but only two are used during normal operations.

### 3.9.4 Neutron Source

The startup source is approximately 4 Ci of Americium-Beryllium held in a triple encapsulated stainless steel container approximately 3 in. long by 1 in. in diameter. The capsule is held in a container that positions the source near the reactor core centerline (Figure 3.3). Chapter 4 gives a detailed description of the source capsule and holder.

### 3.9.5 Fuel Storage Assemblies

Five fuel storage racks capable of holding 20 elements each are mounted in the reactor tank. Out-of-tank storage for a complete core is provided by five pits [REDACTED]. Each pit has a storage capacity for 38 elements. The storage systems are described in Chapter 9.

### 3.9.6 Beam-Tube Assemblies

Four beam tubes originate within the graphite reflector approximately 90° apart. The beam tubes are described in Chapter 10 and mounting arrangements are shown in Figure 3.4.

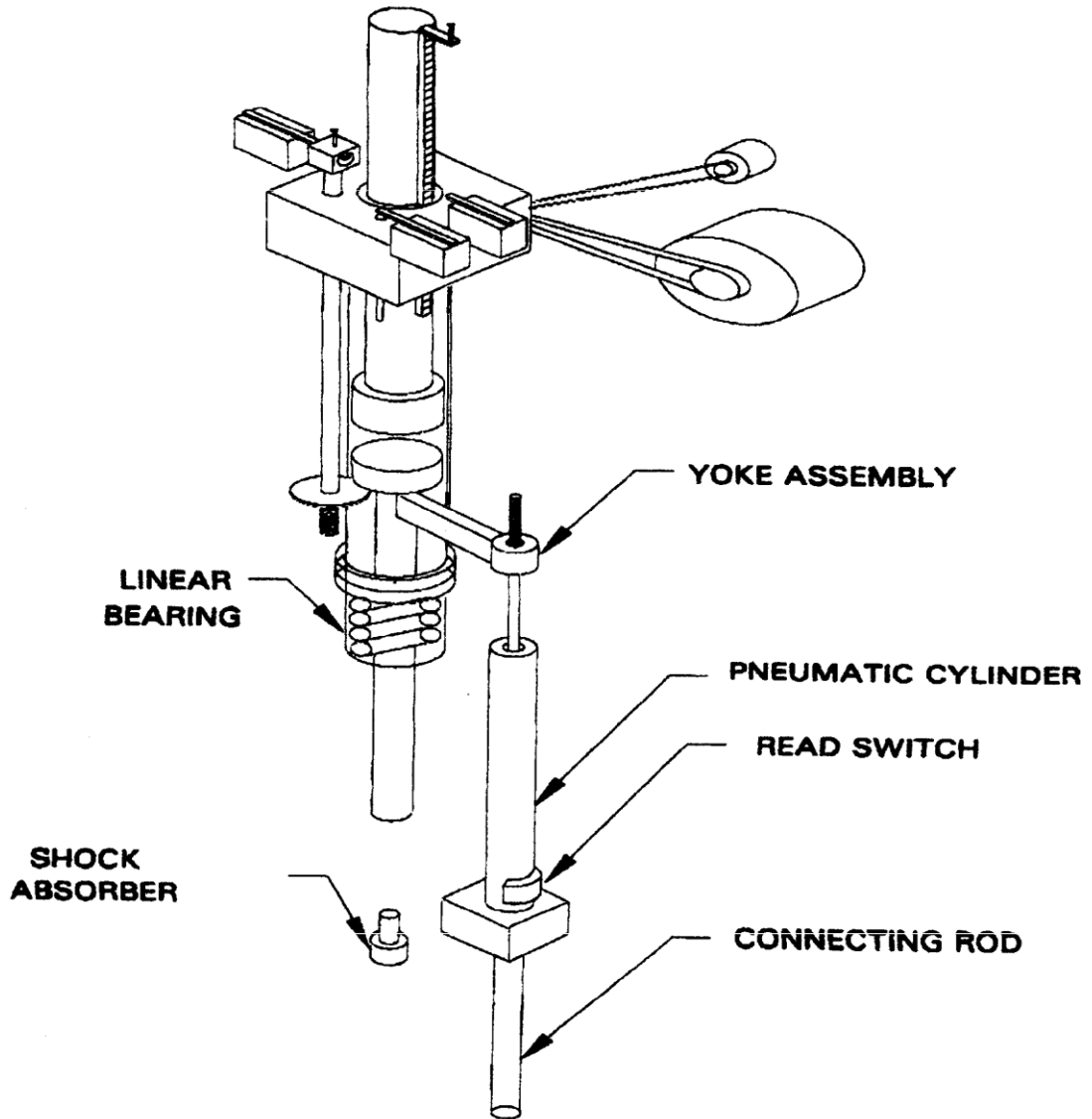
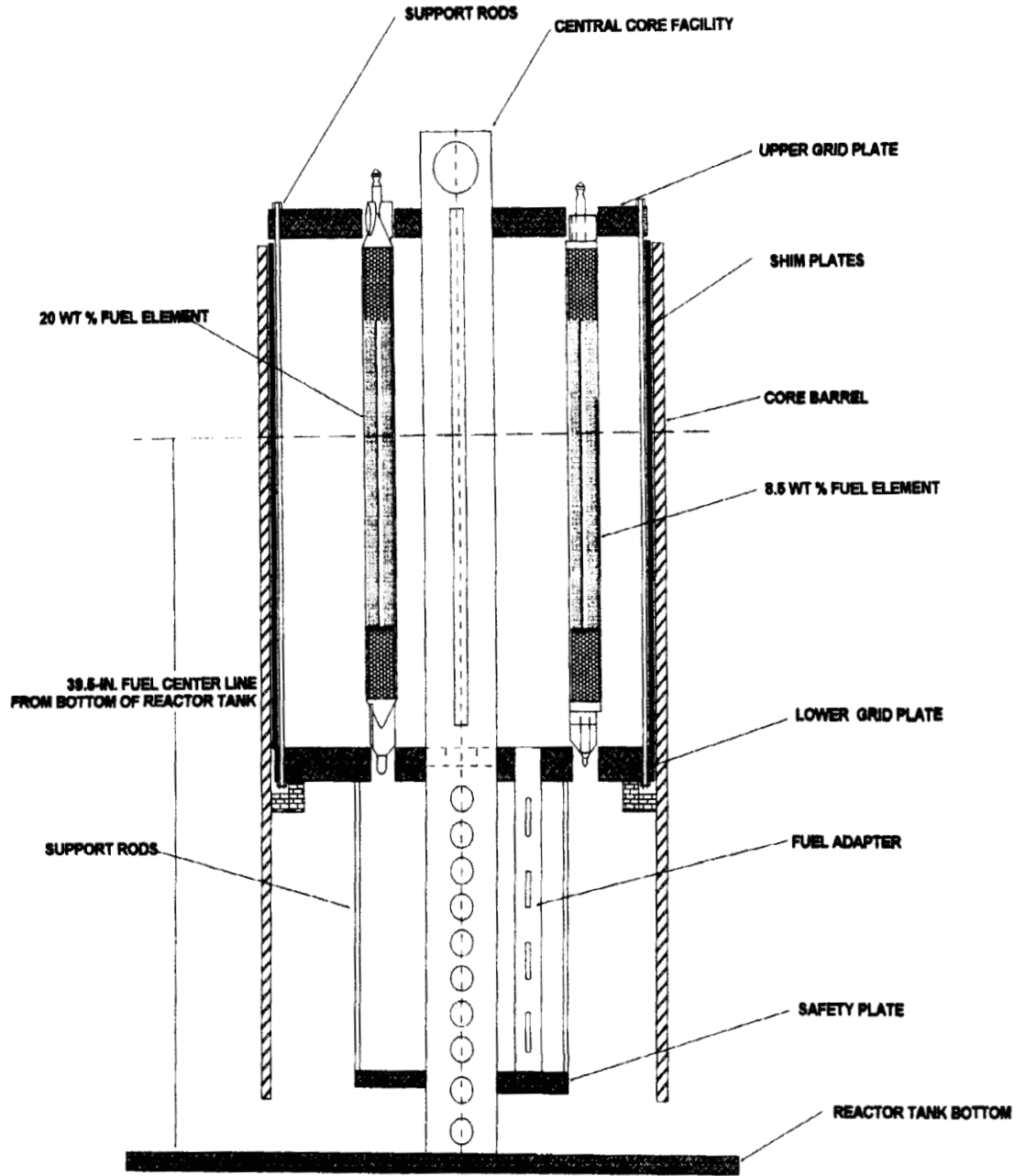


FIGURE 3.2 TYPICAL ADJUSTABLE FAST TRANSIENT ROD DRIVE



NOTE: CORE BARREL IS SUPPORTED BY THE REFLECTOR ASSEMBLY BASE SUPPORT (SEE FIG. 3.4)

FIGURE 3.3 TRIGA® REACTOR

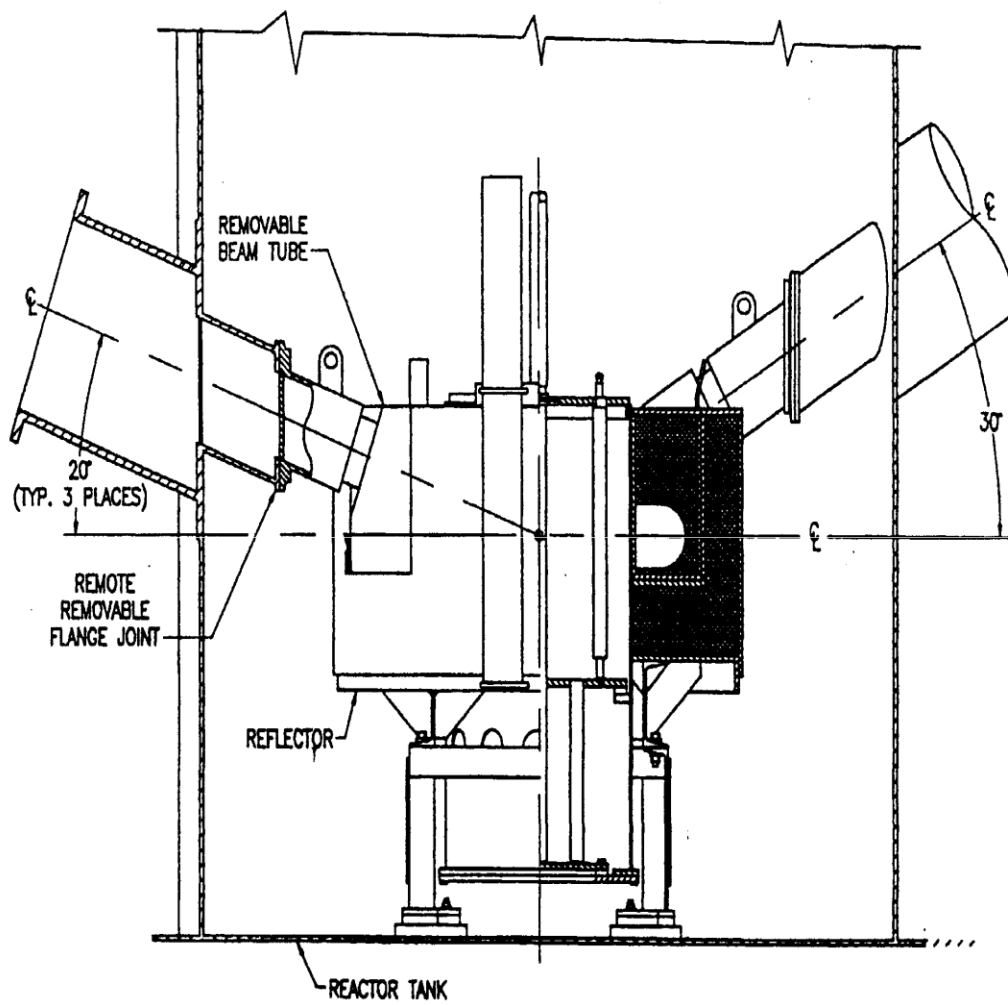


FIGURE 3.4 TYPICAL IN-TANK REACTOR CORE AND BEAM TUBE ASSEMBLY

**CHAPTER 4**

**UCD/MNRC TRIGA<sup>®</sup> REACTOR**

Chapter 4 - Valid Pages  
Rev. 5 04/09/18

i	Rev. 5	04/09/18	4-32	Rev. 5	04/09/18	4-72	Rev. 5	04/09/18
ii	Rev. 5	04/09/18	4-33	Rev. 5	04/09/18	4-73	Rev. 5	04/09/18
iii	Rev. 5	04/09/18	4-34	Rev. 5	04/09/18	4-74	Rev. 5	04/09/18
iv	Rev. 5	04/09/18	4-35	Rev. 5	04/09/18	4-75	Rev. 5	04/09/18
v	Rev. 5	04/09/18	4-36	Rev. 5	04/09/18	4-76	Rev. 5	04/09/18
vi	Rev. 5	04/09/18	4-37	Rev. 5	04/09/18	4-77	Rev. 5	04/09/18
vii	Rev. 5	04/09/18	4-38	Rev. 5	04/09/18	4-78	Rev. 5	04/09/18
viii	Rev. 5	04/09/18	4-39	Rev. 5	04/09/18	4-79	Rev. 5	04/09/18
ix	Rev. 5	04/09/18	4-40	Rev. 5	04/09/18	4-80	Rev. 5	04/09/18
4-1	Rev. 5	04/09/18	4-41	Rev. 5	04/09/18	4-81	Rev. 5	04/09/18
4-2	Rev. 5	04/09/18	4-42	Rev. 5	04/09/18	4-82	Rev. 5	04/09/18
4-3	Rev. 5	04/09/18	4-43	Rev. 5	04/09/18	4-83	Rev. 5	04/09/18
4-4	Rev. 5	04/09/18	4-44	Rev. 5	04/09/18	4-84	Rev. 5	04/09/18
4-5	Rev. 5	04/09/18	4-45	Rev. 5	04/09/18	4-85	Rev. 5	04/09/18
4-6	Rev. 5	04/09/18	4-46	Rev. 5	04/09/18	4-86	Rev. 5	04/09/18
4-7	Rev. 5	04/09/18	4-47	Rev. 5	04/09/18	4-87	Rev. 5	04/09/18
4-8	Rev. 5	04/09/18	4-48	Rev. 5	04/09/18	4-88	Rev. 5	04/09/18
4-9	Rev. 5	04/09/18	4-49	Rev. 5	04/09/18	4-89	Rev. 5	04/09/18
4-10	Rev. 5	04/09/18	4-50	Rev. 5	04/09/18	4-90	Rev. 5	04/09/18
4-11	Rev. 5	04/09/18	4-51	Rev. 5	04/09/18	4-91	Rev. 5	04/09/18
4-12	Rev. 5	04/09/18	4-52	Rev. 5	04/09/18	4-92	Rev. 5	04/09/18
4-13	Rev. 5	04/09/18	4-53	Rev. 5	04/09/18	4-93	Rev. 5	04/09/18
4-14	Rev. 5	04/09/18	4-54	Rev. 5	04/09/18	4-94	Rev. 5	04/09/18
4-15	Rev. 5	04/09/18	4-55	Rev. 5	04/09/18	4-95	Rev. 5	04/09/18
4-16	Rev. 5	04/09/18	4-56	Rev. 5	04/09/18	4-96	Rev. 5	04/09/18
4-17	Rev. 5	04/09/18	4-57	Rev. 5	04/09/18	4-97	Rev. 5	04/09/18
4-18	Rev. 5	04/09/18	4-58	Rev. 5	04/09/18	4-98	Rev. 5	04/09/18
4-19	Rev. 5	04/09/18	4-59	Rev. 5	04/09/18	4-99	Rev. 5	04/09/18
4-20	Rev. 5	04/09/18	4-60	Rev. 5	04/09/18	4-100	Rev. 5	04/09/18
4-21	Rev. 5	04/09/18	4-61	Rev. 5	04/09/18	4-101	Rev. 5	04/09/18
4-22	Rev. 5	04/09/18	4-62	Rev. 5	04/09/18	4-102	Rev. 5	04/09/18
4-23	Rev. 5	04/09/18	4-63	Rev. 5	04/09/18	4-103	Rev. 5	04/09/18
4-24	Rev. 5	04/09/18	4-64	Rev. 5	04/09/18	4-104	Rev. 5	04/09/18
4-25	Rev. 5	04/09/18	4-65	Rev. 5	04/09/18			
4-26	Rev. 5	04/09/18	4-66	Rev. 5	04/09/18			
4-27	Rev. 5	04/09/18	4-67	Rev. 5	04/09/18			
4-28	Rev. 5	04/09/18	4-68	Rev. 5	04/09/18			
4-29	Rev. 5	04/09/18	4-69	Rev. 5	04/09/18			
4-30	Rev. 5	04/09/18	4-70	Rev. 5	04/09/18			
4-31	Rev. 5	04/09/18	4-71	Rev. 5	04/09/18			

TABLE OF CONTENTS

4.0	UCD/MNRC TRIGA® REACTOR .....	4-1
4.1	Introduction .....	4-1
4.2	Reactor Core, Associated Structures, and Reactor Experiment Facilities.....	4-7
4.2.1	Reactor Fuel.....	4-7
4.2.1.1	Fuel-Moderator Element .....	4-7
4.2.1.2	Instrumented Fuel-Moderator Element.....	4-9
4.2.1.3	Evaluation of Fuel Element Design .....	4-9
4.2.2	Graphite Dummy Elements.....	4-13
4.2.3	Control Rods .....	4-13
4.2.3.1	Control Function .....	4-13
4.2.3.2	Evaluation of Control Rod System.....	4-15
4.2.4	Reflector Assembly.....	4-15
4.2.5	Neutron Source and Holder.....	4-17
4.2.6	Grid Plates.....	4-17
4.2.6.1	Top Grid Plate .....	4-17
4.2.6.2	Bottom Grid Plate .....	4-20
4.2.6.3	Safety Plate .....	4-20
4.3	Reactor Tank.....	4-24
4.4	Biological Shield.....	4-24
4.5	Nuclear Design .....	4-24
4.5.1	TRIGA® Fuels.....	4-24
4.5.1.1	Description of TRIGA® Fuels .....	4-24
4.5.1.2	Performance of Erbium Loaded Fuels.....	4-27
4.5.1.3	Materials Properties .....	4-28
4.5.2	Design Bases .....	4-30
4.5.3	Design Criteria - Reference Cores.....	4-31
4.5.4	Reactor Core Parameters .....	4-36
4.5.4.1	Reactor Fuel Temperature.....	4-36
4.5.4.1.1	Fuel and Clad Temperature.....	4-43
4.5.4.1.2	Hydrogen Pressure in TRIGA® Fuel Elements.....	4-56
4.5.4.1.3	ZrH Fuel Temperature Limits.....	4-60
4.5.4.1.4	Performance of High Uranium wt% Fuels .....	4-62
4.5.4.2	Prompt Negative Temperature Coefficient .....	4-64
4.5.4.3	Cross Section Generation .....	4-69

- 4.5.5 Reactor Physics Analysis - Reference Cores 1998 Analysis ..... 4-74
  - 4.5.5.1 Original Hexagonal-Z Computational Model ..... 4-74
    - 4.5.5.1.1 Validation of Hexagonal - Z Model Analysis ..... 4-77
  - 4.5.5.2 Reference Core 20E ..... 4-79
  - 4.5.5.3 Reference Core 30B..... 4-83
  - 4.5.5.4 Reference Core Considerations ..... 4-86
  - 4.5.5.5 Power Peaking Factor Analysis..... 4-88
  - 4.5.5.6 The Future of the 30 B Core and the 2017 Core Model..... 4-90
  - 4.5.5.7 Neutron Flux Analysis..... 4-93
  - 4.5.5.8 Fission Product Release Fraction..... 4-94
- 4.6 Thermal and Hydraulic Design..... 4-95
  - 4.6.1 Thermal and Hydraulic Analysis ..... 4-96
  - 4.6.2 Steady State Results..... 4-99
- 4.7 Operating Limits..... 4-102
  - 4.7.1 Operating Parameters..... 4-102
  - 4.7.2 Limiting Safety System Settings ..... 4-104

LIST OF FIGURES

4.1	UCD/MNRC Operating & Megawatt Hours.....	4-1
4.2	Typical Six-Control-Rod Core Arrangement .....	<b>4-3.</b>
4.3	Reactor Core Structure - Elevation .....	4-4
4.4	Reactor Core Structure And Reflector Assembly - Plan View .....	4-5
4.5	Image Of Current MNRC Reactor With Associated Irradiation Facilities (NIF, CIF, PTS, NTD).....	4-6
4.6	Typical TRIGA® Fuel Element Assembly .....	4-8
4.7	Typical TRIGA® Instrumented Fuel Element .....	4-11
4.8	Graphite Dummy Element .....	4-14
4.9	Reactor And Beam Tube Assembly .....	4-16
4.10	Top Grid Plate .....	4-18
4.11	Bottom Grid Plate .....	4-21
4.12	Operational Grid Nomenclature .....	4-22
4.13	Safety Plate .....	4-23
4.14	Reactor Tank .....	4-25
4.15	Typical In-Tank Reactor Core And Beam Tube Assembly .....	4-26
4.16	20E Reference Core Fuel Loading .....	<b>4-32</b>
4.17	30B Reference Core Fuel Loading .....	4-33
4.18	October 2017 Core Loading And Likely Future Core Loading .....	4-35
4.19	Phase Diagram Of The Zirconium-Hydrogen System.....	4-37
4.20	Equilibrium Hydrogen Pressures Over Zrhx Versus Temperature .....	4-40
4.21	Strength Of Type 304 Stainless Steel As A Function Of Temperature .....	4-41
4.22	Strength And Applied Stress As A Function Of Temperature .....	4-42
4.23	Radial Power Distribution In U-ZrH Fuel Element.....	4-44
4.24	Axial Power Distribution In A Fuel Element Assumed For Thermal Analysis.....	4-45
4.25	Subcooled Boiling Heat Transfer For Water .....	4-47
4.26	Clad Temperature At Midpoint Of Well Bonded Fuel Element .....	4-48
4.27	Fuel Body Temperatures At Midplane Of Well-Bonded U-Zr-H Element After Pulse.....	4-49
4.28	Surface Heat Flux At Midplane Of Well Bonded U-Zr-H Element.....	4-50
4.29	Surface Heat Flux Distribution For Standard Non-Gapped Fuel Element After Pulse, $h_{gap} = 500$ .....	4-52
4.30	Surface Heat Flux Distribution For Standard Non-Gapped Fuel Element After Pulse, $h_{gap} = 375$ .....	4-53
4.31	Surface Heat Flux Distribution For Standard Non-Gapped Fuel Element After Pulse, $h_{gap} = 250$ .....	4-54
4.32	Surface Heat Flux At Midpoint Versus Time For Standard Non-Gapped Fuel Element After Pulse.....	4-55
4.33	Thermal Neutron Spectra Versus Fuel Temperature Relative To $\sigma_a$ Versus Energy For Er-167.....	4-66
4.34	Prompt Negative Temperature Coefficient For TRIGA® LEU Fuel [20 Wt-% Uranium (19.7% Enriched), 0.47 Wt-% Erbium] .....	4-68
4.35	Prompt Negative Temperature Coefficient For 20/20 Fuel.....	4-70
4.36	Reference Core 20E Fuel Loading .....	4-81
4.37	Reference Core 30B Fuel Loading .....	4-84
4.38	Cross Section Of Central Irradiation Fixture-1 (CIF-1).....	4-87
4.39	UCD/MNRC RELAP5 Model .....	4-98
4.40	UCD/MNRC Power Distribution .....	4-100
4.41	Calculated Coolant Temperature And Void Distribution .....	4-103

LIST OF TABLES

4-1	Summary Of Fuel Element Specifications .....	4-10
4-2	Thermocouple Specifications .....	4-12
4-3	Grid Position Conversion Table .....	4-19
4-4	Parameters For TRIGA® LEU Fuels.....	4-27
4-5	Physical Properties Of Delta Phase U-ZrH.....	4-38
4-6	ORR In-Pile Irradiation Parameters .....	4-63
4-7	Cross Section Accuracy Test - Infinite Lattice Of 20/20 Fuel Cells .....	4-72
4-8	Test Of <sup>10</sup> B Cell Average Microscopic Absorption Cross Sections .....	4-73
4-9	Descriptions Of Some Important Element Cell Types .....	4-75
4-10	Compositions Used In The Hex-Z UCD/MNRC Model .....	4-76
4-11	Comparison Of Measured And Calculated Excess Reactivity Of Hex-Z Modeled Cores .....	4-78
4-12	Comparison Of Measured And Calculated Rod Worths Of Hex-Z Modeled Cores .....	4-79
4-13	Fuel-Dummy Substitution Worth In 20E .....	4-80
4-14	Calculated Rod Worths In 20E.....	4-82
4-15	Fuel-Dummy Substitution Worth In 30B.....	4-85
4-16	Calculated Rod Worths In 30B .....	4-85
4-17	Power Peaking Factors .....	4-89
4-18	Core Average Neutron Fluxes .....	4-94
4-19	Heat Transfer And Hydraulic Parameters For Operation With 101 Fuel Elements .....	4-101
4-20	Limiting Safety System Settings .....	4-104

REFERENCES

- 4.1 U. S. Nuclear Regulatory Commission, Office of Nuclear Reactor Regulation, "Safety Evaluation Report on High-Uranium Content, Low-Enriched Uranium- Zirconium Hydride Fuels for TRIGA<sup>®</sup> Reactor," NUREG-1282, August 1987.
- 4.2 UZR-14A, "TRIGA<sup>®</sup> LEU Shrouded Fuel Cluster Design for Operation Between 2 MW and 10 MW (Thermal)," GA Technologies.
- 4.3 UZR-23, "Special 4-Rod Unshrouded Cluster TRIGA<sup>®</sup>-LEU Fuel Description," GA Technologies, February 1988.
- 4.4 ANL Supplement to Final Safety Analysis Report, 2 MW Upgrade, 1996
- 4.5 Steady State Neutronics Analysis of MNRC Reactor Loadings with 30/20 Fuel, ANL, July 1997.
- 4.6 Merten, U., et al., "Thermal Migration of Hydrogen in Uranium-Zirconium Alloys," General Dynamics, General Atomic Division Report GA-3618, 1962.
- 4.7 G. A. Report, "Low Enriched TRIGA<sup>®</sup> Fuel-Water Quench Safety Test," GA- 15413, June 1979.
- 4.8 Simnad, M. T., "The U-ZrHx Alloy: Its Properties and Use in TRIGA<sup>®</sup> Fuel," General Atomics, E-117-833, February 1980.
- 4.9 Johnson, H. A., et al., "Temperature Variation, Heat Transfer, and Void Volume Development in the Transient Atmosphere Boiling of Water," SAN-1001, University of California, Berkeley, 1961.
- 4.10 McAdams, W.H., Heat Transmission, 3rd Ed, McGraw-Hill Book Co., New York, 1954.
- 4.11 Sparrow, E. M. and R. D. Cess, "The Effect of Subcooled Liquid on Film Boiling," Heat Transfer, 84, pp. 149-156, 1962.
- 4.12 Speigler, P., et al., "Onset of Stable Film Boiling and the Foam Limit," Int. J. Heat and Mass Transfer, 6, pp. 987-989, 1963.
- 4.13 Zuber, W., "Hydrodynamic Aspects of Boiling Heat Transfer," AEC Report AECV- 4439, TIS, ORNL, 1959.

- 4.14 Rohsenow, W., and H. Choi, Heat, Mass and Momentum Transfer, Prentice-Hall, pp. 231-232, 1961.
- 4.15 Ellion, M. E., "A Study of the Mechanism of Boiling Heat Transfer," Jet Propulsion Laboratory Memo, No. 20-88, 1954.
- 4.16 Coffey, C. O., et al., "Characteristics of Large Reactivity Insertions in a High Performance TRIGA<sup>®</sup> U-ZrH Core," General Dynamics, General Atomic Division Report GA-6216, 1965.
- 4.17 Fenech, H., and W. Rosenow, "Thermal Conductance of Metallic Surfaces in Contact," USAEC NYO-2130, 1959.
- 4.18 Graff, W. J., "Thermal Conductance Across Metal Joints," Machine Design, pp. 166-172, September 15, 1960.
- 4.19 Fenech, H., and J. J. Henry, "An Analysis of a Thermal Contact Resistance," Trans. Am. Nucl. Soc., 5, p. 476, 1962.
- 4.20 Bernath, L., "A Theory of Local Boiling Burnout and Its Application to Existing Data," Heat Transfer - Chemical Engineering Progress Symposium Series, Storrs.
- 4.21 Spano, A. H., "Quarterly Technical Report, SPERT Project," pp. 150-170, April, May and June 1964.
- 4.22 Dee, J. B., et. al., "Annular Core Pulse Reactor," General Dynamics, General Atomic Division Report GACD-6977, Supplement 2, 1966.
- 4.23 Johnson, H. E., "Hydrogen Disassociation Pressures of Modified SNAP Fuel," Report NAA-SR-9295, Atomics International, 1964.
- 4.24 West, G. B., M. T. Simnad, and G. L. Copeland, "Final Results from TRIGA<sup>®</sup> LEU Fuel Post-Irradiation Examination and Evaluation Following Long Term Irradiation Testing in the ORR," GA-A18641, November 1986.
- 4.25 Baldwin, N. L., F. C. Foushee, and J. S. Greenwood, "Fission Product Release from TRIGA<sup>®</sup> LEU Reactor Fuels," GA-A16287, November 1980.
- 4.26 Simnad, M. T. and G. B. West, "Post-Irradiation Examination and Evaluation of TRIGA<sup>®</sup> LEU Fuel Irradiated in the Oak Ridge Research Reactor," GA-A18599, May 1986.

- 4.27 Beyster, J. R., et al., "Neutron Thermalization in Zirconium Hydride," USAEC Report, General Dynamics, General Atomic Division Report GA-4581, 1963.
- 4.28 Chien-Hsiang Chen, "Development of SUNMAN: A Graphically Driven Steady State Neutronic and Thermal Hydraulic Model of the Nuclear Science Center Reactor at Texas A&M University," Ph.D. Dissertation, August 1997.
- 4.29 Research Reactor Core Conversion Guidebook, IAEA-TECDOC-643, April 1992; reprinted as UZR-27 by General Atomics.
- 4.30 "Documentation for CCC-576/WIMS-D4 Code Package," RSIC Computer Code Collection, Oak Ridge National Laboratory, 1990.
- 4.31 Woodruff, W. L., Argonne National Laboratory, Personal Communication, 1995.
- 4.32 Blomquist, R. N., "VIM," Proc. Int. Topl. Mtg. Advances in Mathematics, Computations, and Reactor Physics, Pittsburgh, PA, April 28 - May 2, 1991, Vol. 5, p. 39.4 2-1, American Nuclear Society, ISBN: 0-89448-161-4, 1991.
- 4.33 Wade, D. C., "Monte Carlo-Based Validation of the ENDF/MC<sup>2</sup>-II/SDX Cell Homogenization Path," ANL-79-5, Argonne National Laboratory, 1979.
- 4.34 Lawrence, R. D., "The DIF3D Nodal Neutronics Option for Two- and Three-Dimensional Diffusion Theory Calculations in Hexagonal Geometry," ANL-83-1, Argonne National Laboratory, 1983.
- 4.35 Whittemore, W. L., General Atomics, Personal Communication, 1995.
- 4.36 Yang, W. S., P.J. Finck, and H. Khalil, "Reconstruction of Pin Burnup Characteristics from Nodal Calculations in Hexagonal Geometry," Proc. Of Intl. Conf. On the Physics of Reactors: Operation, Design and Computation, Marseille, France, Vol. 2, VIII-22, April 23-27, 1990.
- 4.37 Carlson, K. E., et al., "RELAP5/MOD3 Code Manual Volume I: Code Structure, System Models, and Solution Methods", NUREG/CR-5535, EGG-2596, EG&G Idaho, Inc., June 1990.
- 4.38 Del Bene, J. V., General Atomics, Personal Communication, June 1995.
- 4.39 Indonesia SAR

- 4.40 Nelson, R. C., "Re-evaluation of the Thermal and Hydraulic Analyses and Operating Limits for the McClellan Nuclear Radiation Center 2 MW TRIGA<sup>®</sup> Reactor," RRSAS-99-66-1, Rev. 1, Research Reactor Safety Analysis Services, December 1999.
- 4.41 Safety Analysis Report for the Torrey Pines TRIGA<sup>®</sup> Mark III Reactor, GA-9064, January 5, 1990.
- 4.42 West, G. B. and R. H. Chesworth, "Update on World-Wide Use of TRIGA<sup>®</sup>-LEU Fuel Including Loss of Flow Tests," Proc. 1990 Int. Mtg. On Reduced Enrichment for Research and Test Reactors, Newport, Rhode Island, September 23-27, 1990, p. 249, ANL/RERTR/TM-18, CONF-9009108, Argonne National Laboratory, 1990.
- 4.43 Chesworth, R. H., J. Razvi and W. L. Whittemore, "TRIGA<sup>®</sup> Research Reactor Activities Around the World," Trans. Am. Nucl. Soc., 41, p. 237, 1991.
- 4.44 Liu, B. H. (2018, March 1). Memorandum [Letter to W. Steingass and W. Frey]. "Safety analysis for making a direct comparison between the current and future 30B core loading and the original SAR's reference core loading 20E at the UCD/ MNRC."

#### 4.0 UCD/MNRC TRIGA<sup>®</sup> REACTOR

##### 4.1 Introduction

The UCD/MNRC reactor is a hexagonal grid, natural convection water cooled TRIGA<sup>®</sup> reactor designed to operate at a nominal 2 MW steady state power as well as pulse and square wave operation. The reactor utilizes a specially designed graphite radial reflector to currently accept the source ends of four neutron radiography beam tubes. These beams terminate in four separate neutron radiography bays. The reactor core is located near the bottom of a water-filled aluminum tank 2.13 m (7.0 ft) in diameter and 7.47 m (24.5 ft) deep. The water provides adequate radiation shielding at the top of the tank.

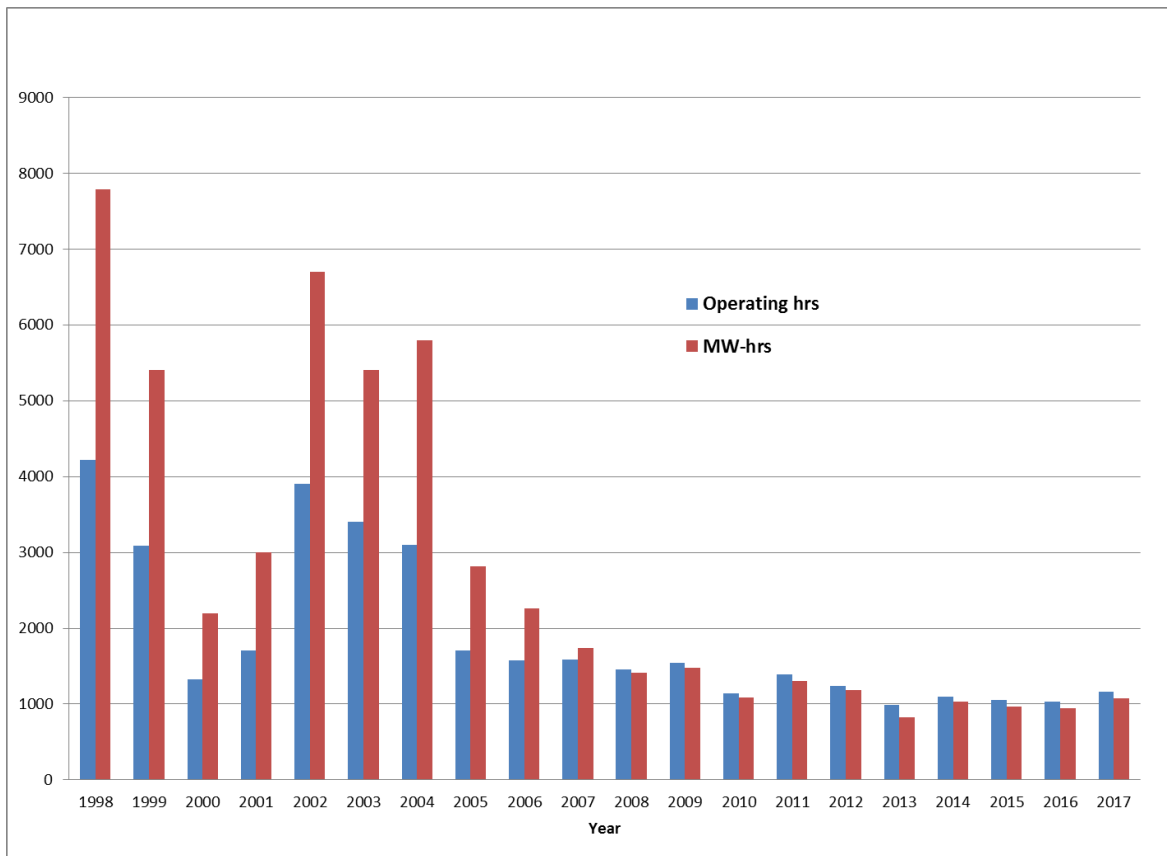


**FIGURE 4.1 UCD/MNRC OPERATING & MEGAWATT HOURS**

While the MNRC reactor is licensed for continuous 2.0 MW steady state operation it can be seen in Figure 4.1 that since 2007 the MNRC has essentially operated as a single shift 1 MW reactor. This change in reactor operation is due to historical decrease in workload and little need for higher fluxes (i.e. silicon doping). For the foreseeable future the MNRC will primarily function to support commercial neutron radiography and education/outreach programs. These programs can be accomplished by 1 MW single shift operations. Therefore the technical description of a 2.0 MW reactor provided in this chapter provided a binding description of reactor characteristics for all operations up to continuous 2.0 MW steady state operations.

Standard TRIGA<sup>®</sup> fuel of two types 20, and 30 wt% uranium, each having an enrichment slightly less than 20 % <sup>235</sup>U, can be utilized in UCD/MNRC reactor core loadings. Data on 8.5, 12, and 45 wt% will be provided in this chapter as reference only. These fuel types are sometimes referred to here as 20/20 and 30/20 fuel, respectively, where the number preceding the slash is the weight percent of uranium and the number following it is the nominal percent enrichment. Initial operation of the 2 MW core was with a mixed core fuel loading (e.g., 8.5/20 and 20/20) followed by an immediate transition to a 30B core (see 30B core Section 4.5.5.3). Results of the analyses of reference core loadings utilizing 20 and 30 wt% fuels are presented in this section to illustrate the safe operation of these fuel loadings. Mixed core loadings utilizing 12 wt% standard TRIGA<sup>®</sup> fuel can also be operated safely at 2 MW; however, no core loading of this type is presently planned and shall be analyzed (requiring a license amendment) prior to use. Likewise, 8.5 wt% is unlikely to be used again at MNRC and shall be analyzed (requiring a license amendment) prior to use. Although reference data for fuels of up to 45 wt% are presented to envelope the fuels authorized at the UCD/MNRC and to quote actual representative data, no fuel above a nominal 30 wt% is authorized.

TRIGA<sup>®</sup> fuel is characterized by inherent safety, high fission product retention, and the demonstrated ability to withstand water quenching with no adverse reaction from temperatures up to 1100°C (2012°F). The inherent safety of this TRIGA<sup>®</sup> reactor has been demonstrated by the extensive experience acquired from similar TRIGA<sup>®</sup> systems throughout the world. This safety arises from the large prompt negative temperature coefficient that is characteristic of uranium-zirconium-hydride fuel-moderator elements used in TRIGA<sup>®</sup> systems. As the fuel temperature increases, this coefficient immediately compensates for reactivity insertions. The negative compensation results in a mechanism whereby reactor power excursions are terminated quickly and safely (Section 4.5.4.2).

Power distributions were predicted by neutronics calculations and these values were input to thermal-hydraulic calculations so that the fuel and coolant temperatures could be predicted. The main thrust of the reactor physics analysis, as far as safety is concerned, is to identify reactor grid loading patterns that have acceptable values of peak power (temperature), excess reactivity and shutdown reactivity. The reactor physics analysis includes evaluation of the flux that will be attained there, as well as reactivity and power peaking issues associated with this facility.

A typical mixed core arrangement of reactor fuel elements, graphite elements, and control rods is shown in Figure 4.2. The core is made up of approximately 100 fuel-moderator elements including fuel followed control rods and approximately 10 graphite elements.

The reactor core structure is shown in Figure 4.3. The reactor grid plates and fuel/loading are contained within a core barrel approximately 24 inches in diameter by 40 inches in height. The reactor core structure and reflector assembly, shown in Figure 4.4, is a cylinder approximately 43 in. in diameter and 23 in. high currently accommodating four tangential neutron radiography beam tubes. Submerged in the reactor tank, the reflector assembly rests on a platform, which raises the lower edge of the reflector assembly about 2 ft above the tank floor. Coolant water occupies about one-third of the core volume. Cooling of the reactor fuel elements is provided by natural convection of the tank water. The heat dissipated to the tank water is removed by circulating the tank water to a primary to secondary heat exchanger. The heat from the primary system (reactor tank water) is removed by a secondary system cooling tower.

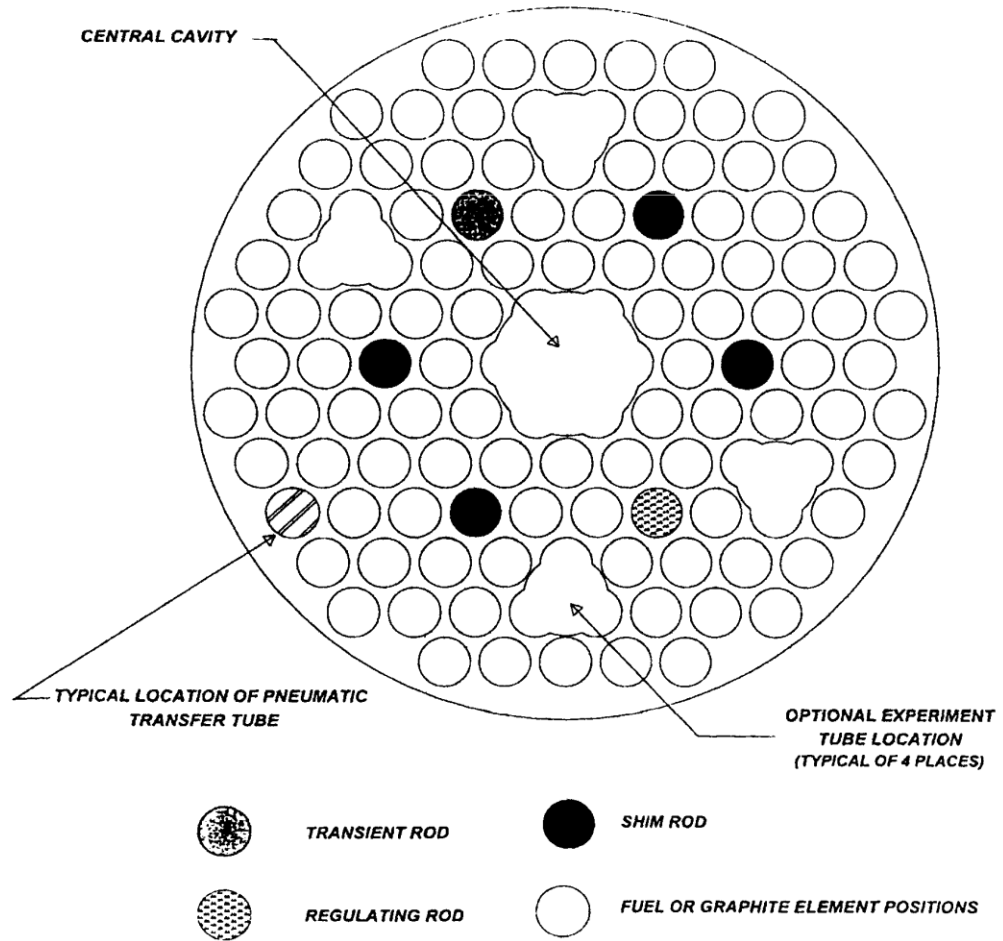
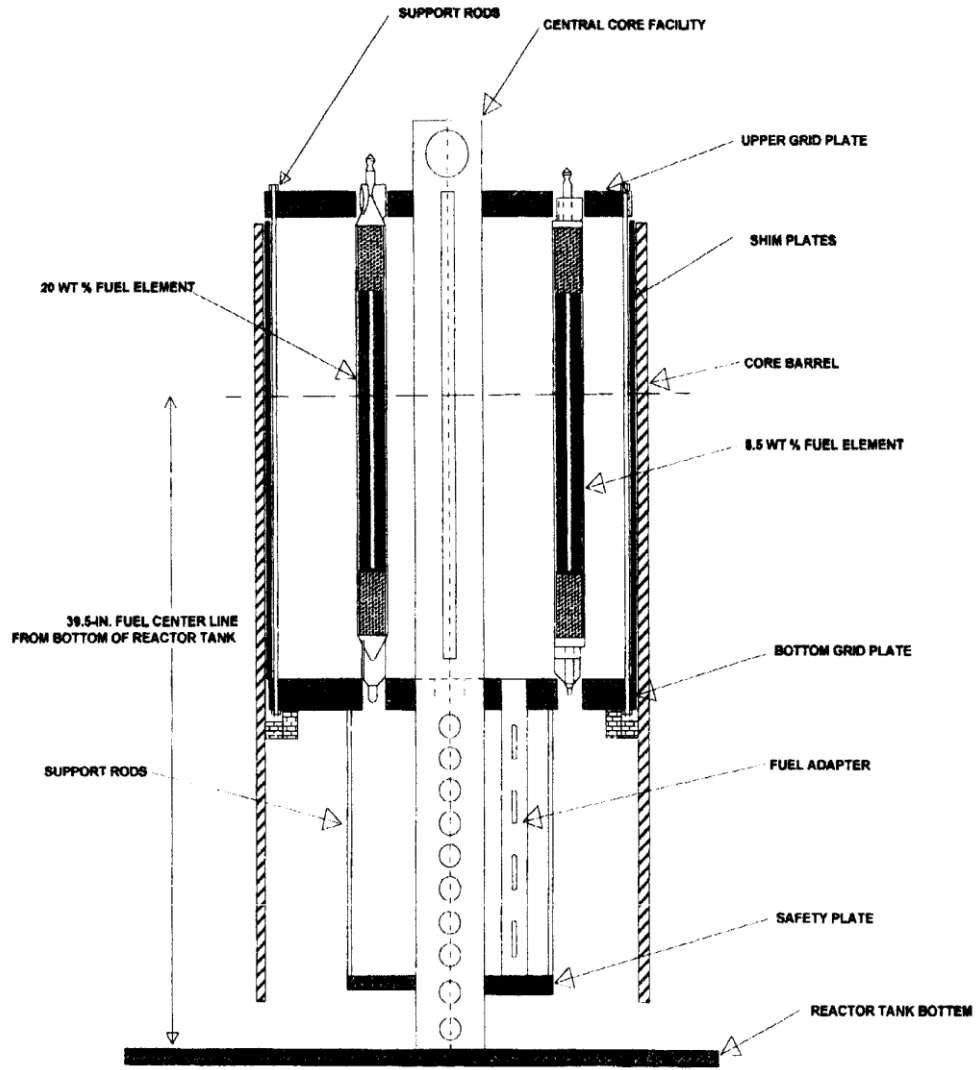


**FIGURE 4.2 TYPICAL SIX-CONTROL-ROD CORE ARRANGEMENT**



NOTE: CORE BARREL IS SUPPORTED BY THE REFLECTOR ASSEMBLY BASE SUPPORT ( SEE FIG. 4.15)

FIGURE 4.3 REACTOR CORE STRUCTURE - ELEVATION

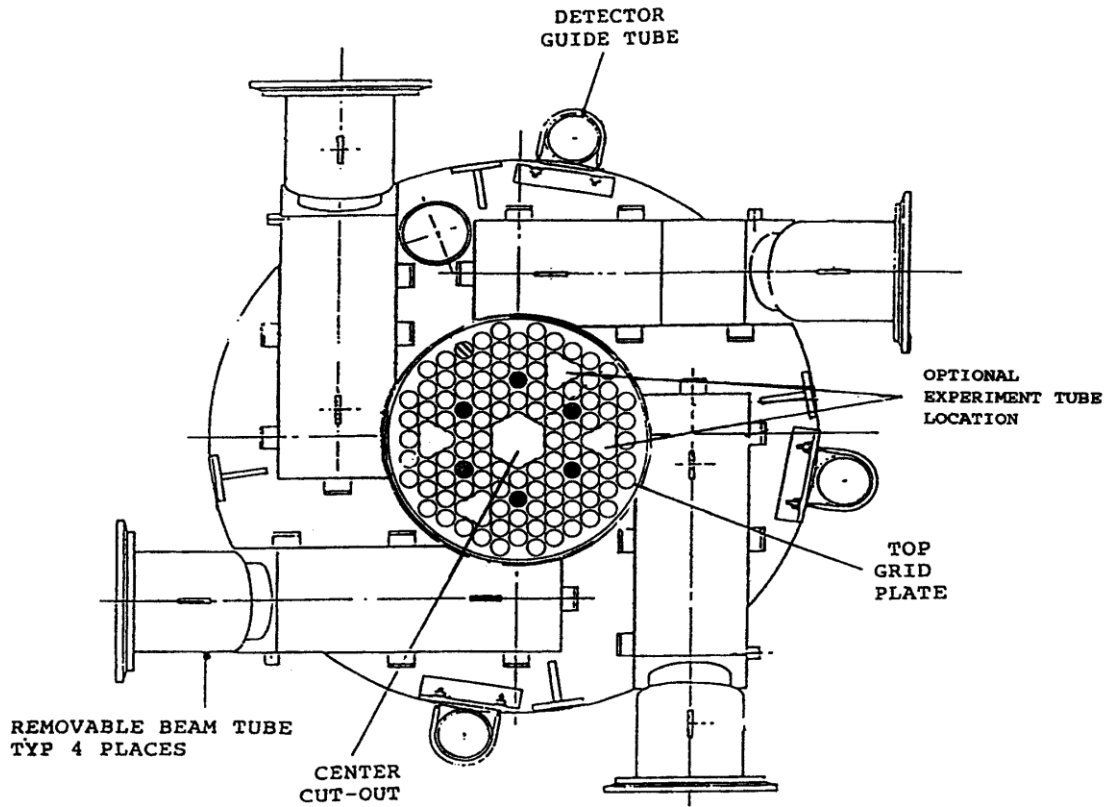


FIGURE 4.4 REACTOR CORE STRUCTURE AND REFLECTOR ASSEMBLY - PLAN VIEW

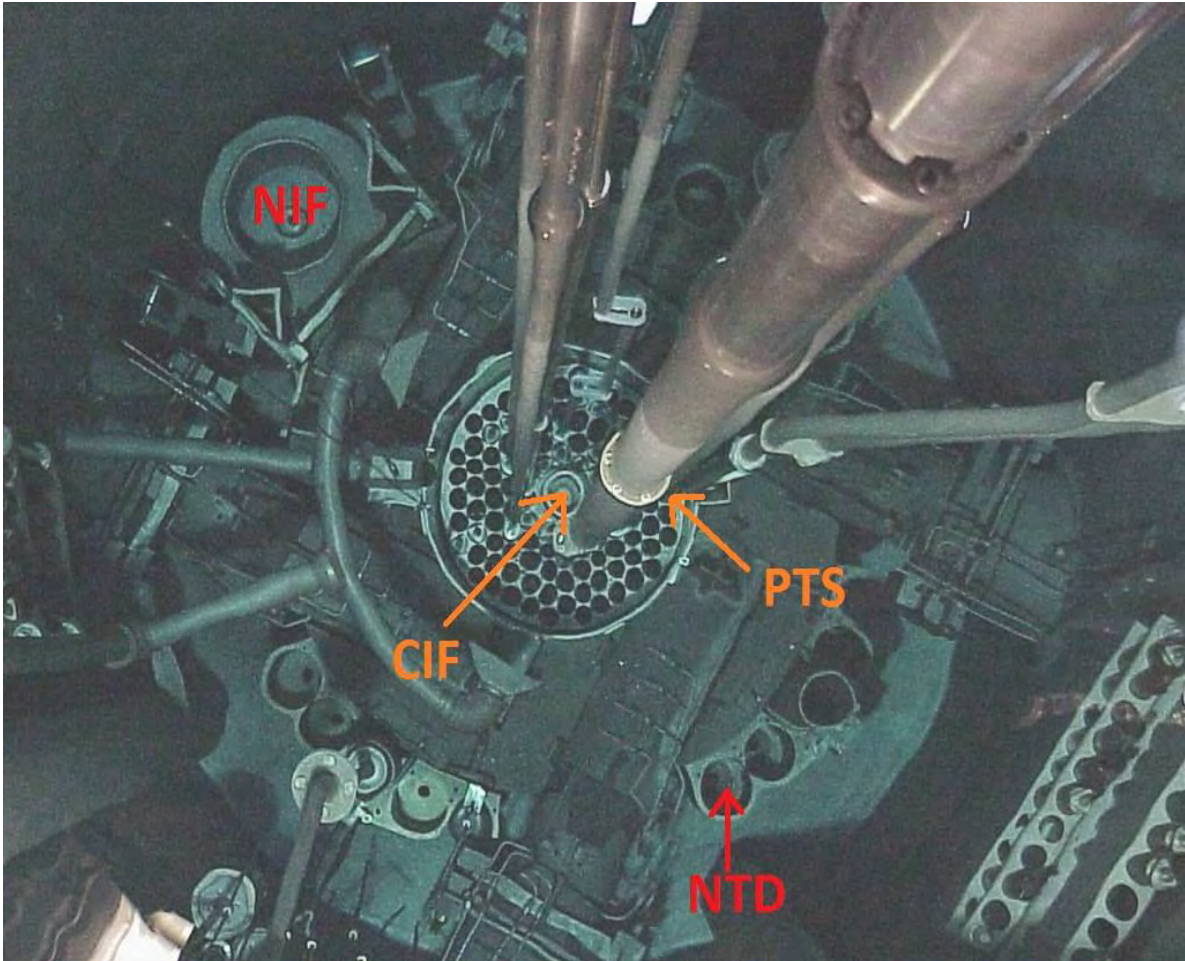


FIGURE 4.5 Image of current MNRC reactor with associated irradiation facilities (NIF, CIF, PTS, and NTD)

The UCD/MNRC reactor normally operates in the steady-state mode, however, pulse and square wave modes of operation are also possible. During steady-state operation, the reactivity in the reactor core is controlled by up to five standard control rods and drives and one transient rod and drive. The standard control rods have fuel followers and are sealed in Type 304 stainless steel tubes approximately 43 in. long by 1.35 in. in diameter. The uppermost section contains a neutron absorber (boron carbide in solid form) and immediately below the neutron absorber is a fuel follower section containing 20, or 30 wt % uranium enriched to less than 20%  $^{235}\text{U}$ . These control rods are attached to drive assemblies mounted on a bridge that spans the tank top. The drive assembly consists of a motor and reduction gear driving a rack-and-pinion. The control rod together with its segmented connecting rod is connected to the rack through an electromagnet and armature.

Pulsing is accomplished by the use of a rod attached to an adjustable fast transient drive. The transient rod drive is also mounted on the reactor bridge and is a combination of the standard GA rack-and-pinion control rod drive and the standard pneumatic fast transient rod drive. The rod is a 44.25 in. long by 1.25 in. in diameter aluminum tube. The top portion of the rod contains solid boron carbide for neutron absorption; the bottom is an air followed section. A complete description of both the pulse and steady-state control rods and drives is contained in Section 4.2.3 and Chapter 7.

The Instrumentation and Control System (ICS) for the TRIGA<sup>®</sup> reactor is a computer-based design incorporating a GA-developed, multifunction microprocessor-based neutron monitor channel and an analog-type neutron monitoring channel. These two units provide redundant safety channels (percent power with scram), wide-range log power (below source level to full power), period, and multirange linear power (source level to full power). The control system logic is contained in a separate Control System Computer (CSC) with a color graphics display which is the interface between the operator and the reactor. Details of the control system logic can be found in Chapter 7.

## 4.2 Reactor Core, Associated Structures, and Reactor Experiment Facilities

This section describes, and where appropriate, evaluates the following: the reactor core assembly, the reflector assembly, the grid plates, the safety plate, the fuel-moderator elements, including instrumented elements, the neutron source, the graphite dummy elements, the control rods and drives, the experiment facilities, and the beam tubes. A detailed description of the control rod system can be found in Chapter 7.

### 4.2.1 Reactor Fuel

#### 4.2.1.1 Fuel-Moderator Element

The active part of each fuel element, shown in Figure 4.6, is approximately 1.43 in. in diameter and 15 in. long. The reactor fuel is a solid, homogeneous mixture of uranium-zirconium hydride alloy containing 20, or 30 % by weight of uranium enriched to 20%  $^{235}\text{U}$ . The hydrogen-to-zirconium atom ratio within the UCD/MNRC fuel varies from 1.6 to 1.7. To facilitate hydriding, a small hole is drilled through the center of the active fuel section and a zirconium rod is inserted in this hole after hydriding is complete.

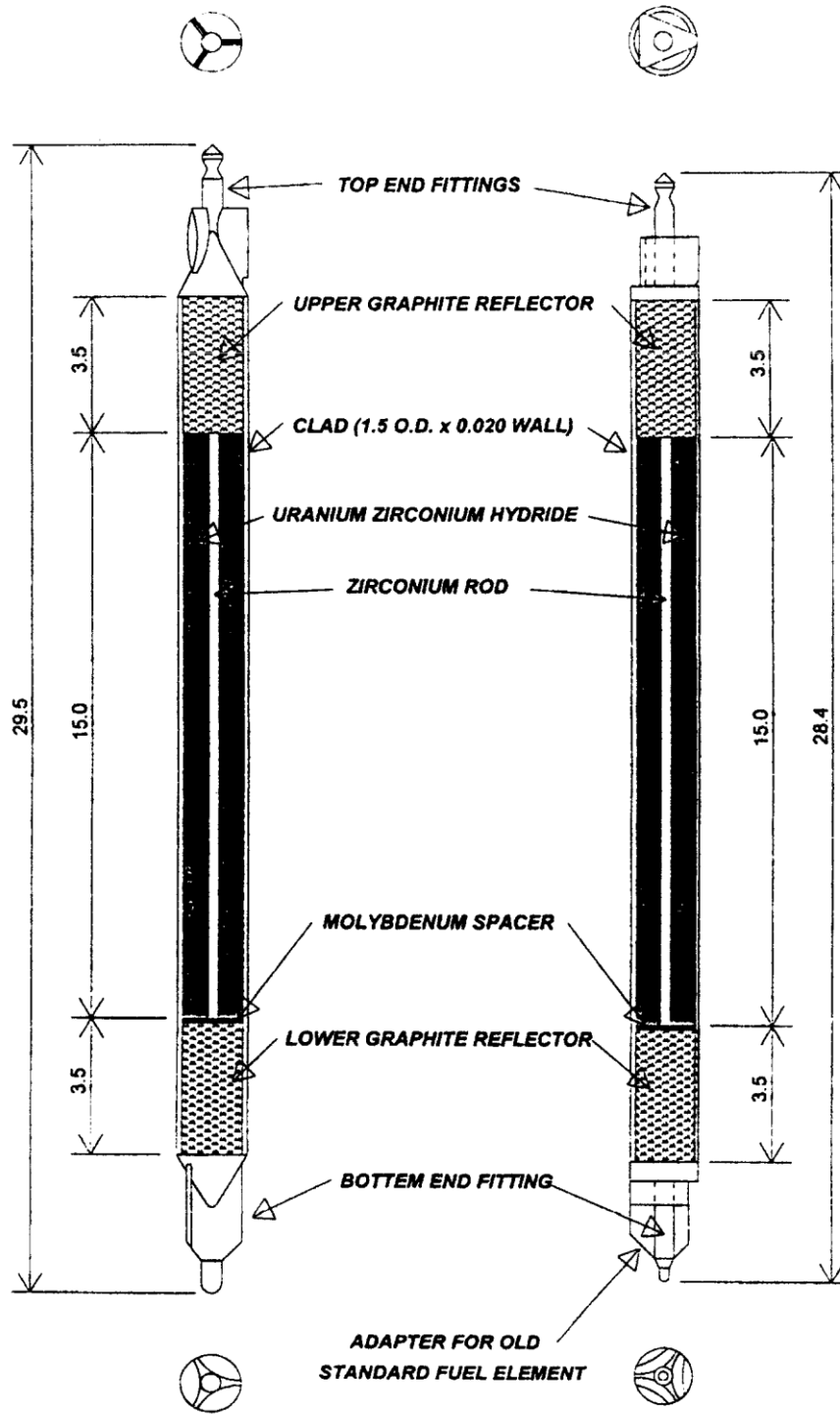


FIGURE 4.6 TYPICAL TRIGA® FUEL ELEMENT ASSEMBLY

Each element is clad with a 0.020 in. thick stainless steel can, and all closures are made by heliarc welding. Two sections of graphite are inserted in the can, one above and one below the fuel, to serve as top and bottom reflectors for the core. Stainless steel end fixtures are attached to both ends of the can, making the overall length of the fuel-moderator element approximately 29.0 inches. Table 4-1 gives a summary of fuel element specifications.

The lower end fixture supports the fuel moderator element on the bottom grid plate. The upper end fixture consists of a knob for attachment of the fuel-handling tool and a triangular spacer (tri-flute), which permits cooling water to flow through the upper grid plate. The total weight of a fully-loaded fuel element is about 3.18 kg (7 lb).

#### 4.2.1.2 Instrumented Fuel-Moderator Element

An instrumented fuel-moderator element has three thermocouples embedded in the fuel. As shown in Figure 4.7, the sensing tips of the fuel element thermocouples are located about 0.3 in. radially from the vertical centerline.

The thermocouple leadout wires pass through a seal in the upper end fixture. A leadout tube provides a watertight conduit carrying the leadout wires above the water surface in the reactor tank. Thermocouple specifications are listed in Table 4-2. In other respects, the instrumented fuel-moderator element is identical to the standard element.

#### 4.2.1.3 Evaluation of Fuel Element Design

The safety limits are determined by the chemical stability of the fuel-moderator material,  $U-ZrH_x$ , described in Section 4.5.4.1. At sufficiently high temperatures the zirconium hydride dissociates, creating hydrogen gas pressure that the cladding must be able to contain without deforming or failing. It is the pressure-induced stress compared to the tensile strength of the cladding that determines the safety limits. The chemical stability has been shown to be nearly independent of the uranium weight percent over a range that encompasses the 20% to 30% range for the UCD/MNRC reactor fuel (Section 4.5.4.1.4). The chemical stability of  $ZrH_x$  depends on  $x$  as well as temperature and, for the high-hydride ( $1.6 < x < 1.7$ ) fuel used in the UCD/MNRC reactor, the temperature dependence is known quantitatively. Likewise, the tensile strength of Type 304 stainless steel, which is the cladding material for the UCD/MNRC reactor fuel, is known quantitatively as a function of temperature. Using this information, the limit of safe operation, which depends only on the temperatures of the fuel and the cladding, has been determined. Two safety limits have been established in the form of a maximum fuel temperature, one for steady-state operation, where the cladding is assumed conservatively to be at the same temperature as the fuel, and the other for pulse operation, where the cladding temperature is assumed to be less than 500°C. It is shown in other sections of this Safety Analysis Report that fuel temperatures remain below these limits in all modes of operation, normal and abnormal. The dimensional stability of the overall fuel element has been excellent for the TRIGA<sup>®</sup> reactors in operation. Dimensional stability results from experimental irradiations are summarized in Reference 4.1.

**TABLE 4-1 SUMMARY OF FUEL ELEMENT SPECIFICATIONS**

	Nominal Value	
Fuel-Moderator Material		
H/Zr ratio	1.6 to 1.7 (actual)	
Uranium content	8.5, 12, 20, 30 wt%	
Enrichment (U-235)	≤ 20%	
20 wt%-Uranium-235	99 g/element	
30 wt%-Uranium-235	162 g/element	
Diameter	1.43 in.	
Length	15 in.	
Graphite End Reflectors	Upper	Lower
Porosity	20%	20%
Diameter	1.35 in.	1.35 in.
Length	Varies	3.47 in.
Cladding		
Material	Type 304 SS	
Wall thickness	0.020 in.	
Length	22.10 in.	
End Fixtures and Spacer	Type 304 SS	
Overall Element		
Outside diameter	1.47 in.	
Length	28.4 in. and 29.5 in.	
Weight	7 lb	

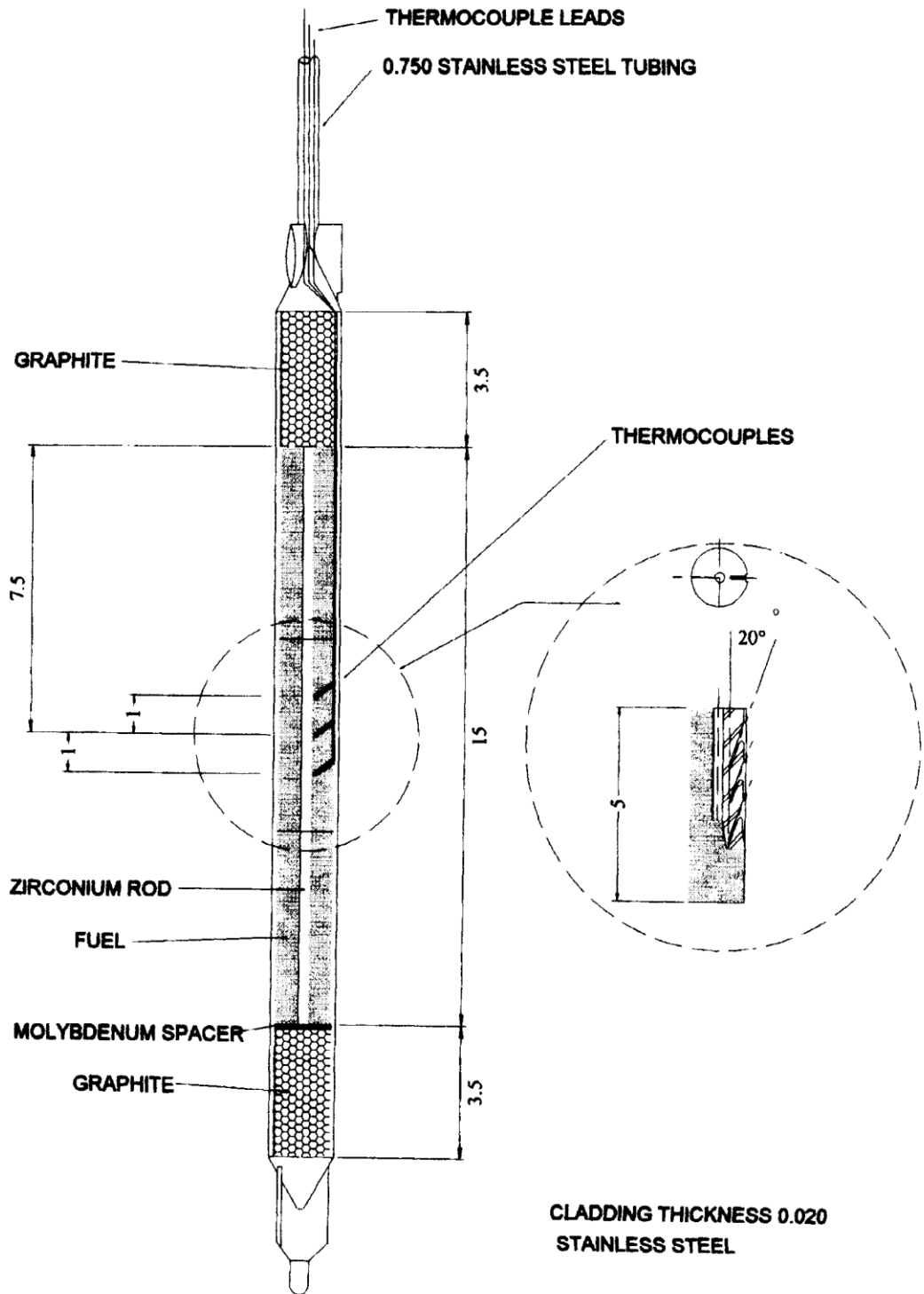


FIGURE 4.7 TYPICAL TRIGA® INSTRUMENTED FUEL ELEMENT

**TABLE 4-2 THERMOCOUPLE SPECIFICATIONS**

Type	Chromel-alumel
Wire diameter	0.005 in.
Resistance	24.08 ohms/double foot at 68°F
Junction	Grounded
Sheath material	Stainless Steel
Sheath diameter	0.040 in.
Insulation	MgO
Lead-out wire	
Material	Chromel-alumel
Size	20 AWG
Color code	Chromel - yellow (positive)
	Alumel - red (negative)
Resistance	0.59 ohms/double foot at 75°F

#### 4.2.2 Graphite Dummy Elements

Graphite dummy elements, shown in Figure 4.8, may be used to fill grid positions not filled by the fuel-moderator elements or other core components. They are of the same general dimensions and construction as the fuel-moderator elements, but are filled entirely with graphite and are clad with aluminum. Graphite dummy elements can be an integral part of core loadings.

#### 4.2.3 Control Rods

##### 4.2.3.1 Control Function

The reactivity of the UCD/MNRC reactor is controlled by up to five standard control rods and a transient rod. The control and transient rod drives are mounted on a bridge at the top of the reactor tank. The drives are connected to the control and transient rods through a connecting rod assembly.

Every core loading includes four or five fuel-followed control rods, i.e., control rods that have a fuel section below the absorber section. The uppermost section is a solid boron carbide neutron absorber. Immediately below the absorber is the fuel section consisting of U-ZrH<sub>1.7</sub> enriched in <sup>235</sup>U to less than 20%. The weight percent of uranium in the fuel is either 20, or 30, depending on the core loading. The bottom section of the rod has an air-filled void. The fuel and absorber sections are sealed in Type 304 stainless steel tubes approximately 43 inches long by 1.35 inches in diameter.

A detailed description of the control rod system, control rods, and drives is provided in Chapter 7.

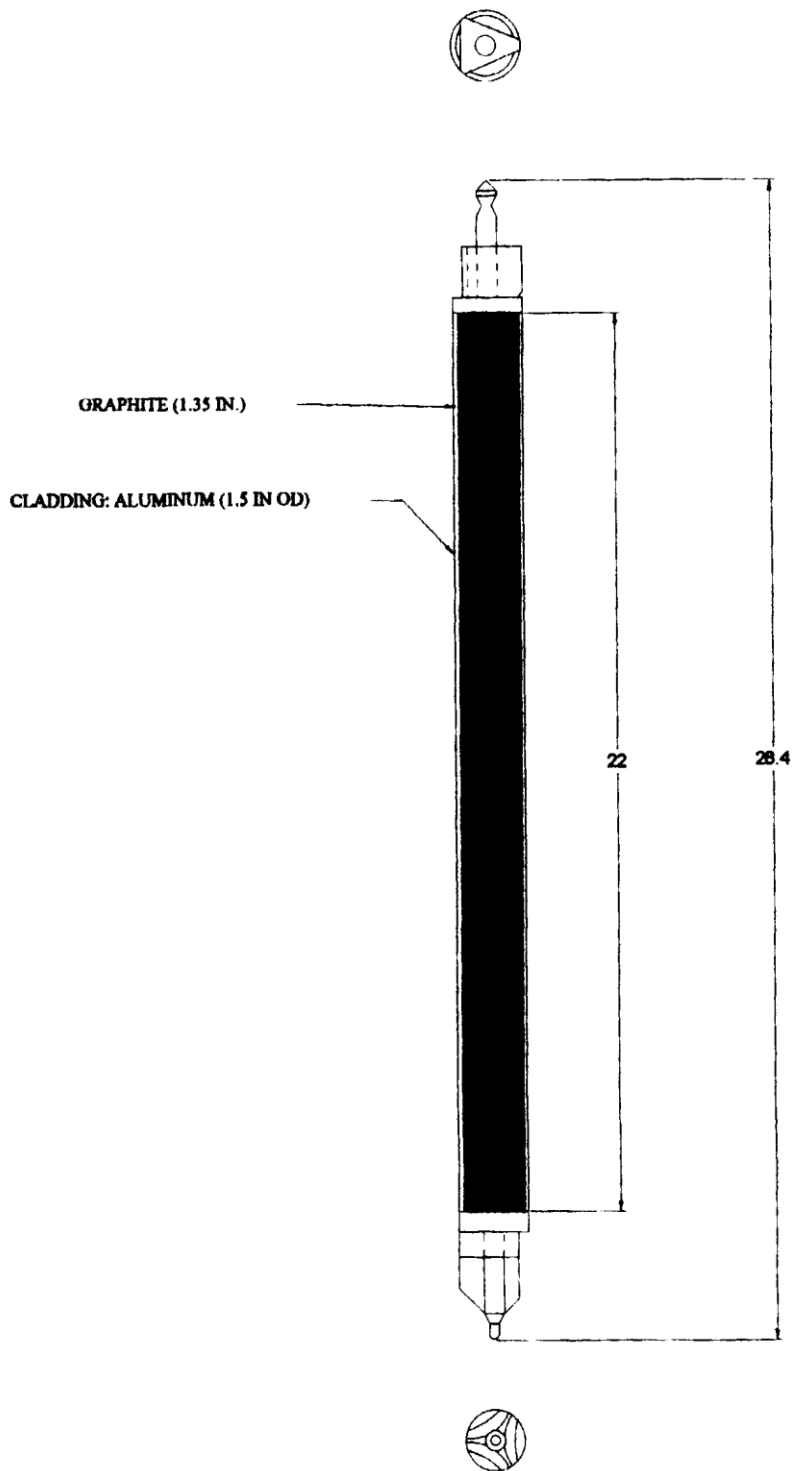


FIGURE 4.8 GRAPHITE DUMMY ELEMENT

#### 4.2.3.2 Evaluation of Control Rod System

The reactivity worth and speed of travel for the control rods are adequate to allow complete control of the reactor system during operation from a shutdown condition to full power. The scram times for the rods are quite adequate since the TRIGA<sup>®</sup> system does not rely on speed of control as being paramount to the safety of the reactor. The inherent shutdown mechanism of the TRIGA<sup>®</sup> prevents unsafe excursions and the control system is used only for the planned shutdown of the reactor and to control the power level in steady-state operation.

The reactivity worth of the control system can be varied by the placement of the control rods in the core. The control system has been configured to provide for the excess reactivity needed for 2 MW operation 24 hours per day (including xenon override) and will be capable of providing a shutdown reactivity greater than 50 cents, even with the most reactive control rod in its most reactive position and moveable experiments in their most reactive position.

The nominal speed of the control rods is about 24 in. per minute and the travel is about 15 in. However, the drive system is capable of moving the rods at a maximum speed of 42 in. per minute. Changing the rod speeds is administratively controlled and can only be accomplished by authorized personnel. The area where the control rod drives are located is a restricted access area, only authorized personnel are allowed in the area. The system is fail-safe, that is, multiple failures are required to get uncontrolled rod withdrawals at the maximum speed. It is very unlikely that control rod speed would ever be increased to its maximum.

#### 4.2.4 Reflector Assembly

The reflector, shown in Figure 4.9, is a ring-shaped block of graphite that surrounds the core radially. The graphite is 12.625 in. thick radially with an inside diameter of 21.5 in. and a height of about 22.125 in. The graphite is protected from water penetration by a leak-tight welded aluminum can. Vertical tubes attached to the outer diameter of the reflector assembly permit accurate and reproducible positioning of fission and ion chambers used to monitor reactor operation.

The reflector currently accommodates four tangential neutron radiography beam tubes. This design provides space for a removable in-tank beam tube section referred to as the reflector insert. Each insert begins the shaping of a gradually widening, conical neutron beam from the reactor core to the plane of radiography. Each insert is constructed from a block of graphite surrounded by a leak tight aluminum can. The inserts fit into four perpendicular cutouts in the reflector assembly with each perpendicular cutout being tangential to the reactor core.

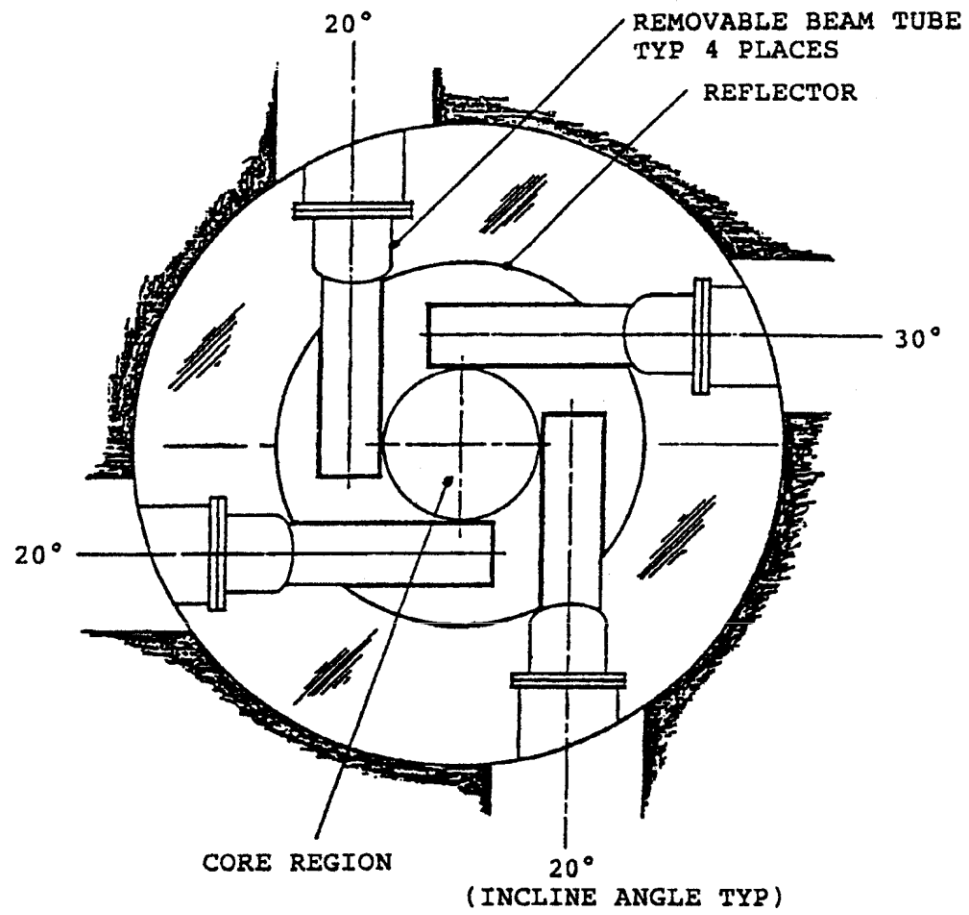


FIGURE 4.9 REACTOR AND BEAM TUBE ASSEMBLY

Since the reactor is located below grade level, the inserts are inclined to direct neutrons upward towards the plane of radiography. Three of the inserts are inclined at a 20° angle and one at a 30° angle.

The reflector assembly rests on an aluminum platform at the bottom of the tank. Four lugs are provided for lifting the assembly.

#### 4.2.5 Neutron Source and Holder

A 4 curie ( $\sim 9 \times 10^6$  n/sec) americium beryllium neutron source is used for reactor startup. The source material is triple encapsulated in welded stainless steel. The capsule is approximately 1 in. in diameter and approximately 3 in. long. The neutron source is contained in an aluminum cylindrical shaped source holder. The source holder can be installed in any fuel location in the top grid plate. A shoulder at the upper end of the holder supports the assembly on the upper grid plate. The neutron source is contained in a cavity in the lower portion of the source holder at the horizontal centerline of the core. The upper and lower portions of the holder are screwed together and pinned. Since the upper end fixture of the source holder is similar to that of the fuel element, the source holder can be installed or removed with the fuel handling tool. In addition, the upper end fixture has a small hole through which one end of a stainless steel wire may be inserted to facilitate handling operation from the top of the tank.

#### 4.2.6 Grid Plates

##### 4.2.6.1 Top Grid Plate

The top grid plate is an aluminum plate 21 in. in diameter and 1 1/4 in. thick (3/4 in. thick in the central region) that provides accurate lateral positioning for the core components. The top grid plate is supported by six 1/2 in. stainless steel rods that are attached to the bottom grid plate. Both plates are anodized to resist wear and corrosion.

One hundred twenty one (121) holes, on a 1.714 in. hexagonal pitch are drilled into the top grid plate in seven hexagonal rings to locate the fuel-moderator and graphite dummy elements, the control rods, guide tube, and the pneumatic transfer tube (Figure 4.10)\*. The 121 holes includes those associated with the hexagonal and triangular sections described below.

A hexagonal section can be removed from the center of the upper grid plate for the installation of irradiation fixtures into the region of highest flux; this displaces the central seven fuel element positions (Hex Rings A and B, or Grid Positions F-06, F-07, G-05, G-06, G-07, H-07, and H-06).

---

\*Two grid numbering systems have been utilized for describing individual positions in the hexagonal grid. The traditional system has numbered the hexagonal rings of the grid starting from A for the inner ring to G for the outer ring, with individual positions sequentially numbered. This grid nomenclature was utilized for the majority of the calculations performed. An operational grid pattern has however been created whereby grid columns are designated by letters and grid rows numerically. Specific grid positions in this document have been referenced by the column, row format for operational ease (Figures 4.12). Some reference calculations refer to the hexagonal ring system to simplify their explanation. A cross reference table has been provided (Table 4-3).

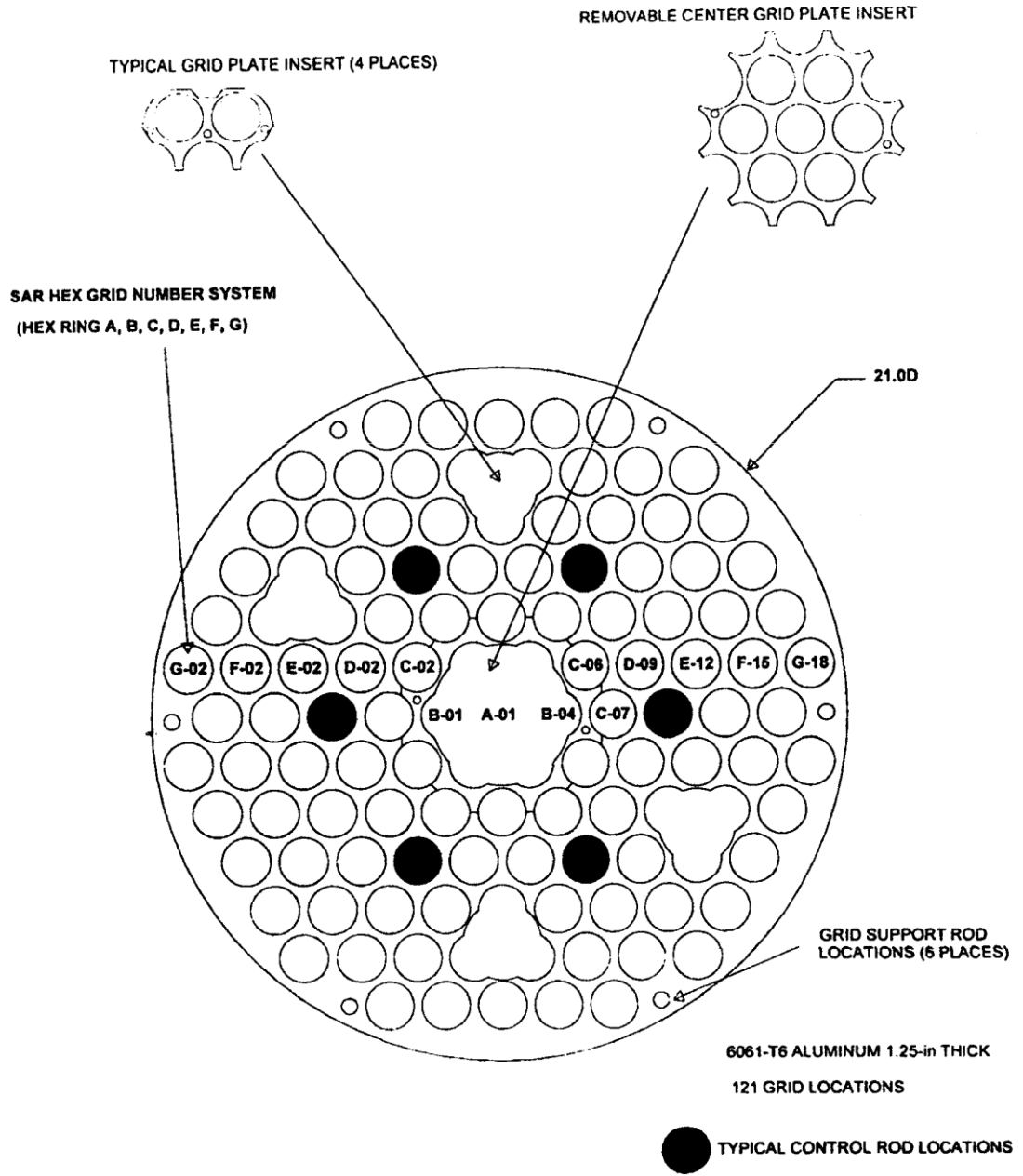


FIGURE 4.10 TOP GRID PLATE

TABLE 4-3 GRID POSITION CONVERSION TABLE

Hexagonal Grid No.	Operational Grid No.	Hexagonal Grid No.	Operational Grid No.	Hexagonal Grid No.	Operational Grid No.
A-01	G-06	E-06	H-10	F-24	D-02
B-01	F-07	E-07	I-09	F-25	C-02
B-02	G-07	E-08	J-08	F-26	B-02
B-03	H-07	E-09	K-07	F-27	B-03
B-04	H-06	E-10	K-06	F-28	B-04
B-05	G-05	E-11	K-05	F-29	B-05
B-06	F-06	E-12	K-04	F-30	B-06
C-01	E-07	E-13	K-03	G-02	B-08
C-02	F-08	E-14	J-03	G-03	C-09
C-03	G-08	E-15	I-03	G-04	D-10
C-04	H-08	E-16	H-03	G-05	E-11
C-05	I-07	E-17	G-02	G-06	F-12
C-06	I-06	E-18	F-03	G-08	H-12
C-07	I-05	E-19	E-03	G-09	I-11
C-08	H-05	E-20	D-03	G-10	J-10
C-09	G-04	E-21	C-03	G-11	K-09
C-10	F-05	E-22	C-04	G-12	L-08
C-11	E-05	E-23	C-05	G-14	M-05
C-12	E-06	E-24	C-06	G-15	M-04
D-01	D-07	F-01	B-07	G-16	M-03
D-02	E-08	F-02	C-08	G-17	M-02
D-03	F-09	F-03	D-09	G-18	M-01
D-04	G-10	F-04	E-10	G-20	L-01
D-05	H-09	F-05	F-11	G-21	K-01
D-06	I-08	F-06	G-12	G-22	J-01
D-07	J-07	F-07	H-11	G-23	I-01
D-08	J-06	F-08	I-10	G-24	H-01
D-09	J-05	F-09	J-09	G-25	F-01
D-10	J-04	F-10	K-08	G-27	E-01
D-11	I-04	F-11	L-07	G-28	D-01
D-12	H-04	F-12	L-06	G-29	C-01
D-13	G-03	F-13	L-05	G-30	B-01
D-14	F-04	F-14	L-04	G-32	A-01
D-15	E-04	F-15	L-03	G-33	A-02
D-16	D-04	F-16	L-02	G-34	A-03
D-17	D-05	F-17	K-02	G-35	A-04
D-18	D-06	F-18	J-02	G-36	A-05
E-01	C-07	F-19	I-02		
E-02	D-08	F-20	H-02		
E-03	E-09	F-21	G-01		
E-04	F-10	F-22	F-02		
E-05	G-11	F-23	E-02		

Four triangular-shaped sections are cut out of the upper grid plate. When fuel elements are placed in these locations, their lateral support is provided by a special fixture. When the fuel elements and support are removed, space is provided for the insertion of experiment tubes up to 2.4 in. outside diameter for placement of experiments.

The UCD/MNRC reactor is equipped with a TRIGA<sup>®</sup>-type pneumatic transfer system for irradiation of small specimens. The in-core section of this system is typically located in the outer portion of the reactor core.

The differential area between the fitting at the top of the fuel elements and the round holes in the top grid plate permits passage of cooling water through the plate. The grid plate holes are shaped to provide relief at the inlet and outlet edges; there is a taper on both the upper and lower sides of the plate, which reduces the resistance for the coolant flow. All outlet coolant flow is through the flow holes.

#### 4.2.6.2 Bottom Grid Plate

The bottom grid plate is an aluminum plate 1.25 in. thick, which supports the entire weight of the core and provides accurate spacing between the fuel-moderator elements (Figure 4.11). Six adapters are bolted to pads welded to a ring which is, in turn, welded to the core barrel to support the bottom grid plate.

Holes 1.25 in. in diameter in the bottom grid plate are aligned with fuel element holes in the top grid plate. They are countersunk to receive the adaptor end of the fuel-moderator elements and the adaptor-end of the pneumatic transfer tube.

Eight additional 1.505 in. diameter holes are aligned with upper grid plate holes to provide passage of fuel-follower control rods. Those holes in the bottom grid plate not occupied by control rod followers are plugged with removable fuel element adaptors that rest on the safety plate. These adaptors are aluminum tubing 1.5 in. OD x 1.25 in. ID by 18 in. long. Slotted channels are machined in the sides of the tubing to provide for coolant flow. At the lower end is a fitting that is accommodated by a hole in the safety plate. The upper end of the cylinder is flush with the upper surface of the bottom grid plate when the adaptor is in place. This end of the adaptor is countersunk similar to that in the bottom grid plate for accepting the fuel element lower end fitting. With the adaptor in place, a position formerly occupied by a control rod with a fuel follower will now accept a standard fuel element.

#### 4.2.6.3 Safety Plate

A safety plate is provided to preclude the possibility of control rods falling out of the core (Figure 4.13). It is a 1 inch thick machined aluminum plate that is suspended from the lower grid plate by 18.25 inch long stainless steel rods.

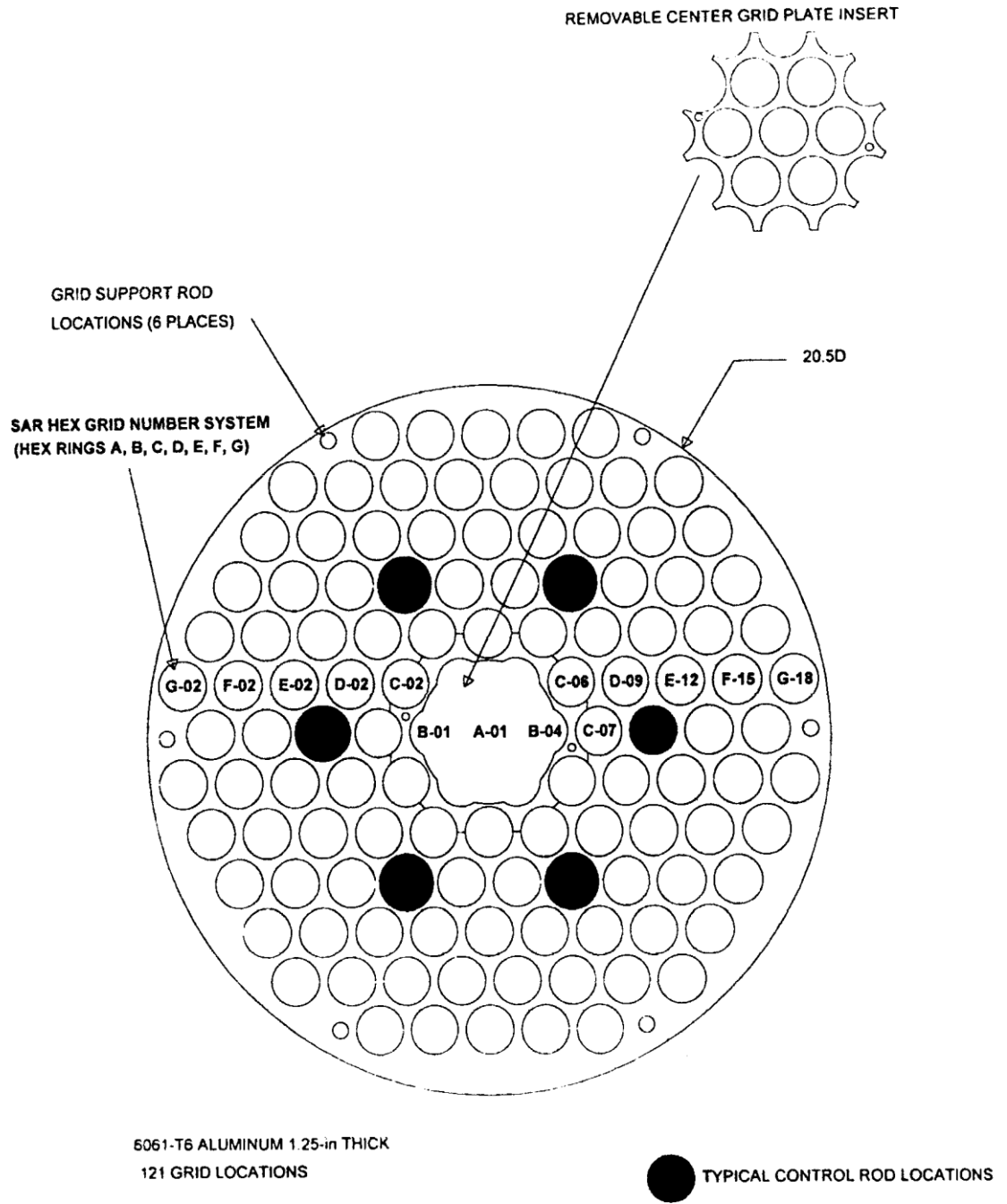


FIGURE 4.11 BOTTOM GRID PLATE

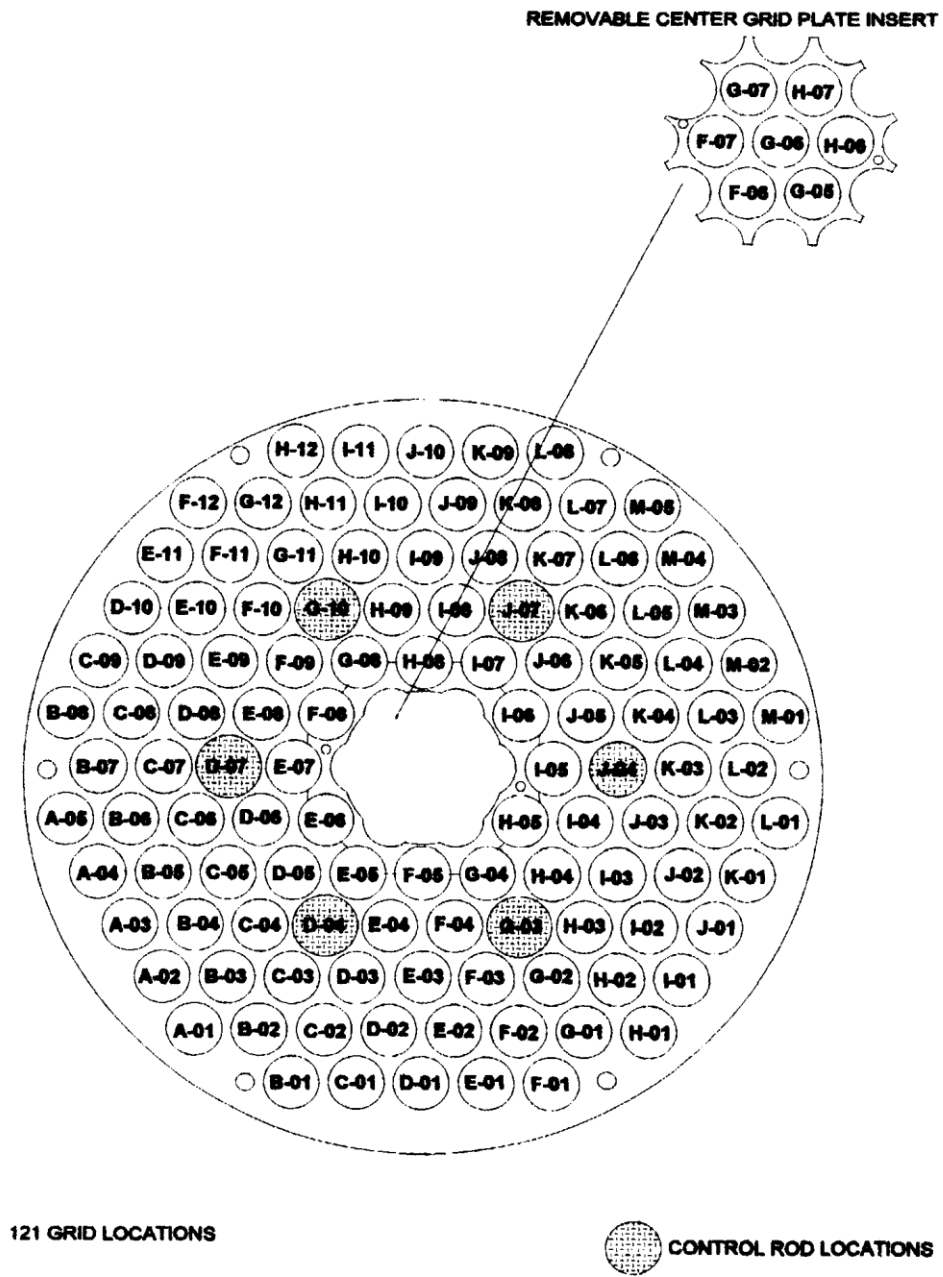
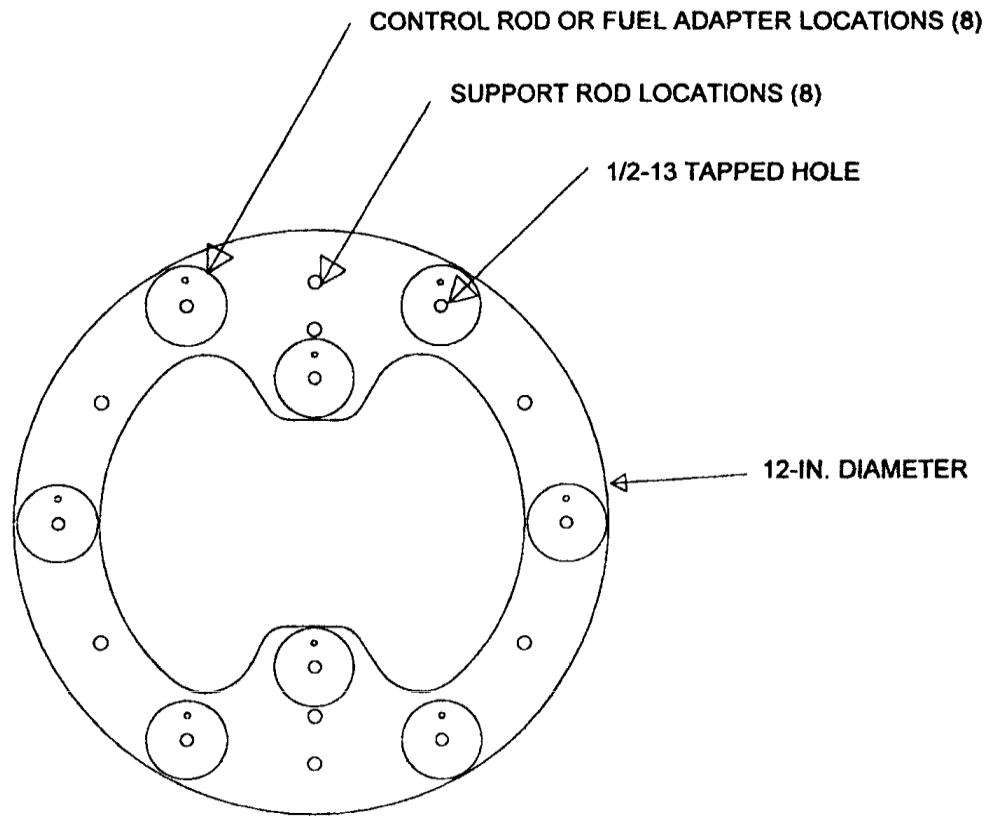


FIGURE 4.12 OPERATIONAL GRID NOMENCLATURE



**6061-T6 ALUMINUM 1-IN. THICK**

**FIGURE 4.13 SAFETY PLATE**

### 4.3 Reactor Tank

The UCD/MNRC reactor core assembly is located near the bottom of a cylindrical aluminum tank surrounded by a reinforced concrete structure (Figure 4.14). The reactor core and beam tube assembly installation is shown in Figure 4.15. The reactor tank is a welded aluminum vessel with 1/4 in. thick walls, a diameter of approximately 7 ft., and a depth of approximately 24-1/2 ft.. The tank is all-welded for water tightness. The integrity of the weld joints is verified by radiographic testing, dye penetrant checking, and leak testing. The outside of the tank is coated for corrosion protection.

Presently four beam tubes clamp onto the reactor tank at 90° interval spacing tangential to the reflector assembly and core (Figures 4.9 and 4.15). The tank wall section of the beam tubes consists of a 12-½ in. diameter pipe welded to the tank wall. These special flanges are welded to the in-tank end for water tightness. The beam tubes clamp onto the tank wall and extend through the bulk shielding concrete that surrounds the reactor tank. Three beam tubes are positioned at a 20° angle from horizontal and a fourth beam tube is positioned at a 30° angle from horizontal as shown in Figure 4.15.

### 4.4 Biological Shield

The reactor tank is surrounded by a monolithic reinforced standard concrete bulk shield structure. Below ground level, the concrete is approximately 11 ft. thick. Above ground level, the concrete varies in thickness from approximately 10 ft. to 3-1/4 ft., with the smaller dimension at the tank top. The tank is supported by a concrete pad approximately 9-1/2 ft. thick.

The massive concrete bulk shield structure provides radiation shielding for personnel working in and around the UCD/MNRC. Also, the massiveness of the concrete bulk shield structure provides excellent protection for the reactor core against natural phenomena that could result in damage to the reactor core.

### 4.5 Nuclear Design

#### 4.5.1 TRIGA® Fuels

This section provides a brief description of TRIGA® fuels followed by evaluations of neutron physics considerations, materials properties, irradiation performance, fission product release, pulse heating, and limiting design basis (Reference 4.1).

##### 4.5.1.1 Description of TRIGA® Fuels

The uranium-zirconium hydride fuel used in TRIGA® reactors is fabricated by hydriding an alloy that is a solid solution of uranium in zirconium. The zirconium is selectively hydrided, and the uranium remains as small metallic inclusions in the zirconium hydride matrix. The size of the uranium particles increases from 1 to 5 µm with increasing uranium content from 8.5 to 45 wt%. Some important parameters for TRIGA® fuels are provided in Table 4-4.

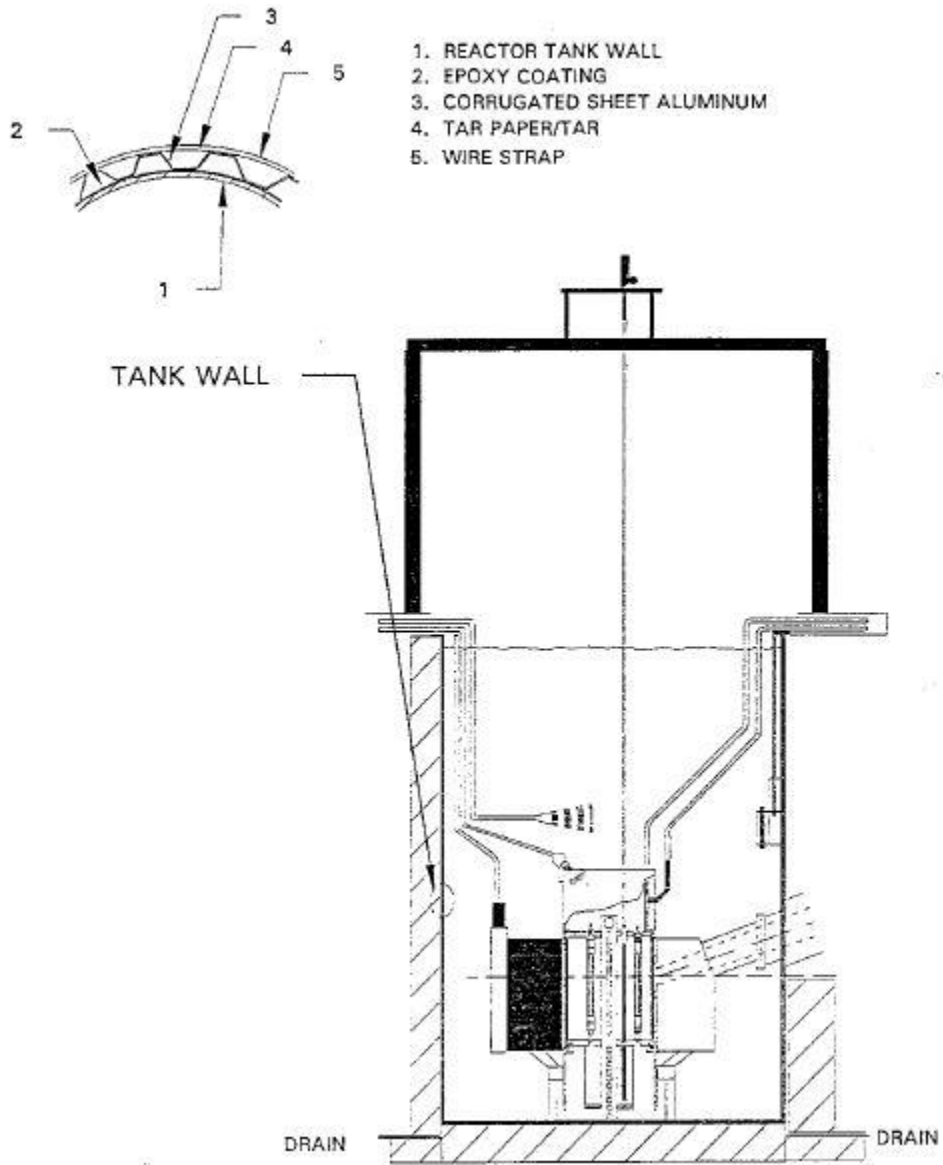


FIGURE 4.14 REACTOR TANK

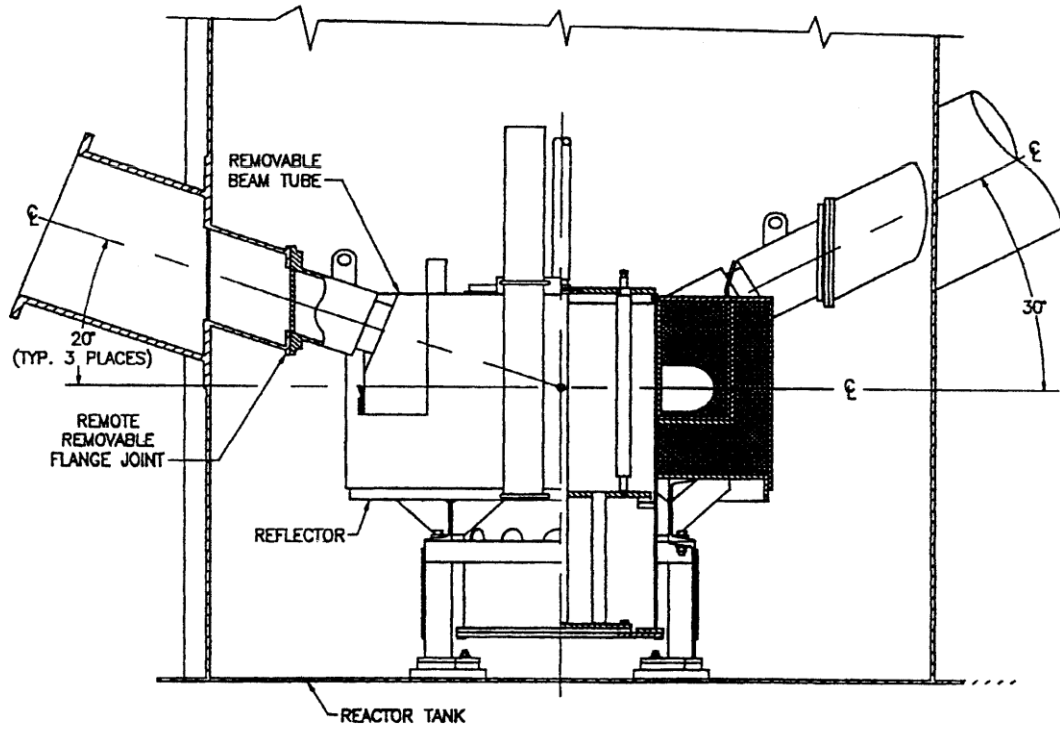


FIGURE 4.15 TYPICAL IN-TANK REACTOR CORE AND BEAM TUBE ASSEMBLY

TABLE 4-4 PARAMETERS FOR TRIGA® LEU FUELS

Type of Fuel	Weight Percent		Uranium-235 (g/element)	Uranium Enrichment (%)	$\alpha \times 10^5$ ( $\Delta k/k^\circ C$ )	Core lifetime (Mwd)	Uranium Volume (%)
	Uranium	Erbium					
Original LEU*	8.5	0.0	39	20	9.5	100	2.6
LEU*	12	0.0	57	20	10	600	3.8
LEU	20	0.5	99	20	10.5	1200	6.8
LEU	30	0.9	162	20	8	3000	11.2
LEU*	45	0.4-0.9	282	20	6-9	4000	19.5

\*Given for reference only.

LEU = low-enrichment uranium

The use of erbium burnable poison in conjunction with the higher  $^{235}\text{U}$  loadings permits longer core lifetimes than would be obtainable with the original TRIGA® fuel. It also permits maintaining a large prompt negative temperature coefficient of reactivity,  $\alpha$ , that is changed little from that of the original fuel through at least the 30-wt% LEU fuel. As shown in Table 4-4, the volume percent (v%) of uranium increases with the increasing uranium loading but remains a small value, increasing from 2.6 v% in the original fuel to 11.2 v% for the 30-wt% LEU fuel and to 19.5 v% for the 45 wt% fuel.

#### 4.5.1.2 Performance of Erbium Loaded Fuels

The primary intent of a GA Technologies Reactor Physics Qualification Program was to show that neutronically the 20-20 and 30-20 TRIGA® LEU fuels behave essentially the same as the TRIGA® Fuel Life Improvement Program (FLIP) fuel. The following was concluded (Reference 4.1):

- The power peaking factors in the LEU and FLIP fuels are very comparable. Any variations are due mainly to differences in the contained U-235 (not the total uranium loading).
- The prompt negative temperature coefficient, the reactivity worth, and the core lifetime of the TRIGA® LEU and FLIP fuels are comparable primarily because of the adjustment of the erbium poison concentration. Also, the reactor kinetics parameters most important to power/burst behavior, prompt neutron lifetime, and effective delayed neutron fraction are similar.

The data in Table 4-4 represent a single average estimate of  $\alpha$ . References 4.2 and 4.3 present plots of the effect of fuel temperature on the prompt coefficient for 20 wt% fuel. These sources show that, at low burnup, the feedback coefficient is a strong function of temperature, ranging from about  $-7 \times 10^{-5}$  at 200°C to about  $-15 \times 10^{-5}$  at 700°C. From the curve in Reference 4.2, an integrated average over the 23 to 750°C range is  $-10.9 \times 10^{-5}/^{\circ}\text{C}$ . Similarly, the curve from Reference 4.3 shows that for the ranges 23 - 800° and 23 - 1000°C, the averages are  $-11.05 \times 10^{-5}$  and  $-11.8 \times 10^{-5}/^{\circ}\text{C}$ , respectively. All of these values demonstrate that the prompt negative feedback characteristics are retained with the erbium additions to the 20 and 30 wt% fuel.

#### 4.5.1.3 Materials Properties

The materials properties of TRIGA<sup>®</sup> fuels with higher uranium contents were reviewed relative to those 8.5 wt% TRIGA<sup>®</sup> fuels (Reference 4.1) with the following conclusions.

Measurements were made of the thermal conductivity of 8.5-, 30-, and 45-wt% uranium-zirconium hydride fuels. The data from these measurements, in conjunction with density and specific heat data were used to determine the thermal conductivity of these materials. The thermal conductivity was found to be independent of uranium content within this range.

The specific heat of uranium-zirconium hydride was calculated as a function of uranium content using known specific heats for uranium and zirconium hydride and a linear interpolation. This method is a straightforward and acceptable approach, and the resulting values for heat capacity have been adequately factored into the analyses of kinetic behavior of the higher loaded LEU fuels.

The coefficient of thermal expansion was measured for 45-wt% uranium fuel and compared with that for 8- to 12-wt% fuel. For a maximum power density TRIGA<sup>®</sup> fuel element, the maximum radial expansion would be about 0.6% for 45-wt% fuel as compared with 0.5% for 8.5-wt% fuel, which is not a significant change.

The monitoring of hydrogen pressure during hydriding in the fabrication of high uranium content fuels showed that the equilibrium hydrogen dissociation pressure of the fuel depends only on the hydrogen/zirconium (H/Zr) ratio and the fuel temperature. It is independent of the uranium content.

Thermal cycling tests were performed on 45-wt% uranium fuel over the temperature range of 500 to 725°C, which includes the orthorhombic-to-tetragonal phase transformation at 653°C. Specimens were cycled 100 times out of pile and then 32 times in a neutron flux of  $4 \times 10^{12}$  n/cm<sup>2</sup>·s. There were no significant changes in dimensions in the out-of-pile tests, and a small decrease in weight was measured. The in-pile cycling test showed a small decrease in both length and diameter, which may be related to a loss of hydrogen. The dimensional stability of the high uranium content fuel is understandable considering the fine dispersion of the uranium in the zirconium hydride matrix. The dispersion of uranium in particles less than 5 µm in diameter evidently precludes anisotropic growth during cycling through the phase transformation because of accommodation by the matrix, which makes up 80% of the fuel volume in the case of 45-wt% uranium fuel.

Uranium and zirconium form eutectics with iron, nickel, and chromium, the principal constituents of the four alloys (304 or 304 L stainless steel, Incoloy 800, and Hastelloy-x) that are licensed for use for fuel rod cladding. The uranium eutectics have lower melting temperatures than those of zirconium, which is tied up as a hydride in any case. The melting points of the eutectics with uranium are: iron, 725°C; nickel, 740°C; and chromium, 859°C. As the uranium content of the fuel is increased, the potential for the formation of low-melting eutectics is enhanced. Localized fuel melting has been observed in 45-wt% uranium fuel in contact with Inconel 600 thermocouple sheathing at temperatures above 1050°C. The extent of potential eutectic melting due to fuel/cladding interaction should be less in the 20- and 30-wt% uranium fuels than in 45-wt% uranium fuel, but more than in the original 8.5 wt% uranium fuel. In all cases, the extent of eutectic melting would be limited by the relatively small volume fraction of uranium in the fuels (11.2 v% or less for the fuels under review). The temperature at which eutectic fuel melting has been observed (1050°C) is 100°C above the lowest temperature at which cladding failure by hydrogen overpressure is predicted under conditions in which the cladding is at approximately the fuel temperature. Therefore, eutectic fuel/cladding melting does not constitute a more severe limit for fuel rod integrity than does hydrogen overpressure. It does, however, have the potential to produce fuel melting at temperatures about 80°C lower than the uranium melting point. This mechanism could lead to somewhat higher releases of fission products from the fuel rod in the temperature range 1050 to 1130°C under some accident conditions (such as loss of coolant) or during film boiling; however, these temperatures are above the safety limit of 930°C.

During sustained irradiation, hydrogen tends to migrate from the hot radial center of the fuel to a cooler annulus near the pellet periphery. Hydrogen/zirconium (H/Zr) ratios can vary by ±10 to 15% of their initial values. The increased H/Zr ratio near the outer radius of the fuel, coupled with high peak fuel temperatures that occur at the outer radius during a pulse, can cause excessive hydrogen pressures in the fuel matrix, which can weaken and deform the fuel matrix and cause excessive swelling and fuel element deformation. Experience suggests that pulse sizes or maximum fuel temperatures should be limited in higher burnup cores to account for the effects of hydrogen redistribution. This effect, however, is independent of uranium content in the TRIGA<sup>®</sup> fuel, and the evidence suggests that an equilibrium hydrogen distribution is established within a moderate time scale.

A 45-wt% uranium LEU fuel rod that was instrumented for measuring temperature and pressure was subjected to a series of 30 power pulses in a TRIGA<sup>®</sup> reactor to maximum temperatures in the range of 1050 to 1100°C. Only very modest (generally less than 2 psi) pressure pulses were measured in the rod as a result of the pulsing, in agreement with previous data on negligible hydrogen release during the pulsing of 8.5-wt% uranium fuel to temperatures up to 1150°C. All surveillance examinations on rod deformation were satisfactory. Tests have shown that the pulse response of uranium-zirconium hydride TRIGA<sup>®</sup> fuel is independent of the uranium content of the fuel and is dominated by the behavior of the zirconium hydride, along with the prompt temperature coefficient of reactivity.

As mentioned earlier, pulse sizes or maximum fuel temperatures should be limited in higher burnup cores to account for the effects of hydrogen redistribution. This potential problem is adequately addressed by imposing limits on maximum operating temperatures in standard TRIGA<sup>®</sup> fuels. The effects of hydrogen migration will not lead to a fission product release if these restrictions are applied.

#### 4.5.2 Design Bases

The reactor design bases are established by the maximum operational capability for the fuel elements and configurations described in this report. The TRIGA<sup>®</sup> reactor system has three major areas that are used to define the reactor design basis:

- a. fuel temperature;
- b. prompt negative temperature coefficient;
- c. reactor power.

The ultimate safety limit is based on fuel temperature, while the negative temperature coefficient contributes to the inherent safety of the TRIGA<sup>®</sup> reactor. A limit on reactor power is set to ensure operation below the fuel temperature safety limit. A summary of the conclusions of the analyses that supports these limits is presented below.

##### Fuel Temperature

The fuel temperature is a limit in both steady-state and pulse mode operation. This limit stems from the out-gassing of hydrogen from U-ZrH fuel and the subsequent stress produced in the fuel element cladding material. The strength of the cladding as a function of temperature sets the upper limit on the fuel temperature. Fuel temperature limits of 1100°C (with clad <500°C) and 930°C (with clad >500°C) for U-ZrH with a H/Zr ratio less than 1.70 have been set to preclude the loss of clad integrity (Section 4.5.4.1.3). These temperature limits are less than the basic limits for TRIGA<sup>®</sup> fuel of 1150°C and 950°C as stated in Reference 4.1.

### Prompt Negative Temperature Coefficient

The basic parameter that provides the TRIGA<sup>®</sup> system with a large safety factor in steady-state operation and under transient conditions is the prompt negative temperature coefficient. This coefficient is a function of the fuel composition and core geometry. The value for the negative temperature coefficient in 8.5/20 fuels is rather constant with temperature and is 0.01 %/°C ( $1 \times 10^{-4} \Delta k/k/^\circ\text{C}$ ). For 20/20 and 30/20 fuels, the value is a strong function of temperature and the average value over temperatures of interest is at least as large as the value for 8.5/20 fuel, as described in Section 4.5.1.2.

### Reactor Power

Fuel and clad temperature define the safety limit. A power level limit is calculated that ensures that the fuel and clad temperature limits will not be exceeded. The design basis analysis indicates that operation at up to 2300 kW with an 100 element core (45°C inlet water temperature) natural convective flow will not allow film boiling, and therefore, high fuel and clad temperatures which could cause loss of clad integrity could not occur. Two MW reactor operation does not affect the fundamental aspects of the TRIGA<sup>®</sup> fuel, including the reactivity feedback coefficients, temperature safety limits, and fission product release rates (Section 4.5.4). The thermal-hydraulic performance is discussed in Section 4.6

#### 4.5.3 Design Criteria - Reference Cores

Two reference core loadings are defined for use in the safety calculations. The first case, 20E, is an all-20/20 fuel loading (except 8.5 wt% fuel followed control rods) having as much fuel as possible in Hex Rings D through G and some fuel in Hex Ring C (Figure 4.16). The second case, 30B, is much like 20E, but has seven fewer fuel elements in Row G and two more in Row C. Fresh 30/20 fuel is used in all rows except C, where fresh 20/20 fuel is used. The unfueled grid positions in Rows C and G contain graphite dummy elements (except 20/20 fuel followed control rods) (Figure 4.17). All initial reference core loadings require the central irradiation fixture-1 (CIF-1) as described in Sections 10.4.1.1 and 4.5.5.5 to be in place in the central cavity of the core, which occupies Hex Rings A and B.

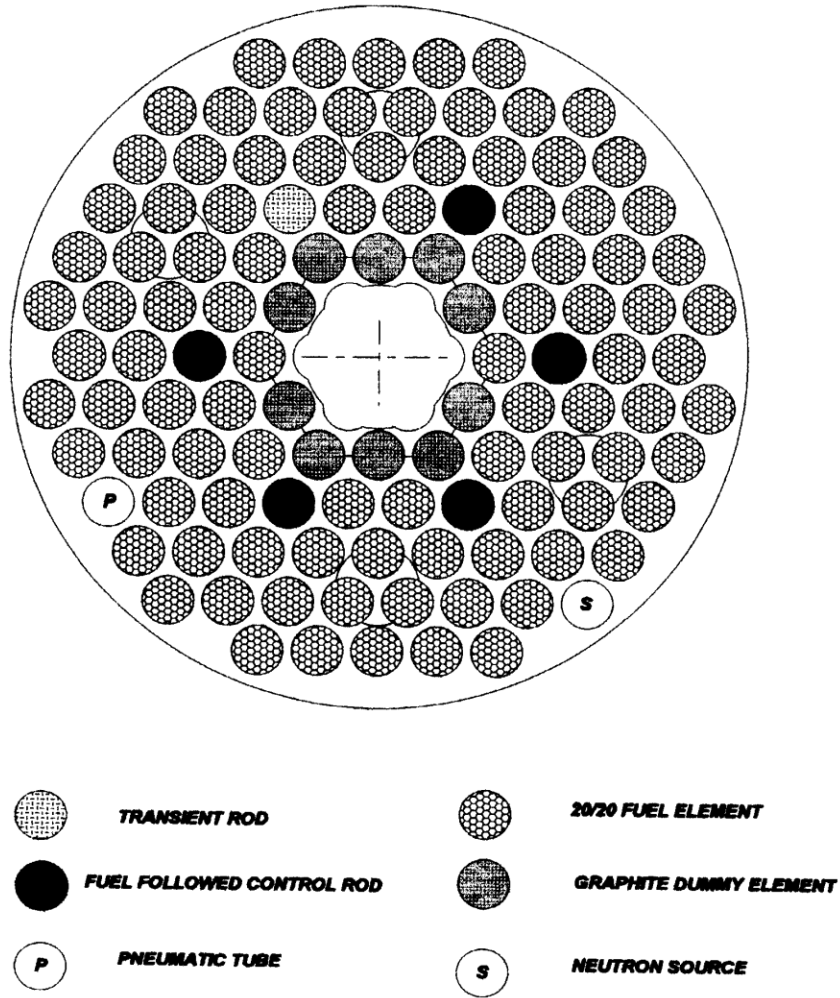
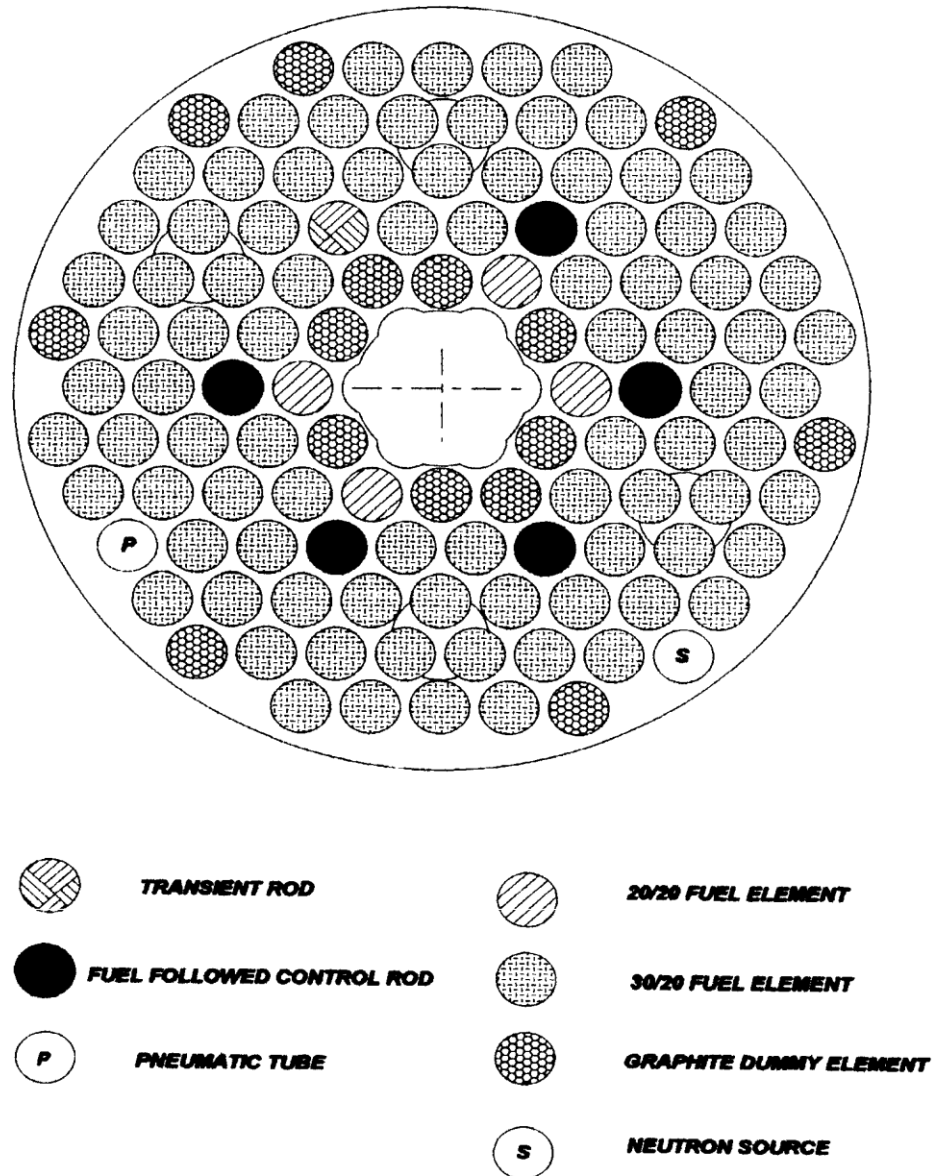


FIGURE 4.16: 20E REFERENCE CORE FUEL LOADING

Note: The initial load and test program for the 20E reference core requires the central irradiation fixture-1 (CIF-1) to be in place in the central cavity of the core.



**FIGURE 4.17: 30B REFERENCE CORE FUEL LOADING**

Note: The initial load and test program for the 30B reference core requires the central irradiation fixture-1 (CIF-1) to be in place in the central cavity of the core.

The fact that all the fuel used in the neutronics models was unburned makes the safety- related predictions conservative. This conservatism leads to overestimates of the power peaking compared to the expected situation where, within a fuel zone, the most burned fuel will be loaded in the innermost rows. The leakage-related performance parameters also tend to be underestimated by calculating all-fresh-fuel loadings. Furthermore, the flux in the central experiment facility is overestimated.

There are requirements and restrictions for loading 20E, and 30B cores regarding fuel types and their location in the core as follows:

#### 20E Core Loading

- No fuel will be loaded into Hex Ring A or B.
- FFCRs may contain either 20/20 or 8.5/20 fuel.
- A minimum of 100 fuel elements including FFCRs is required for operation at power levels above 0.5 MW.
- The initial load and test program to determine the excess reactivity of the 20E reference core shall be conducted with the central irradiation fixture-1 (CIF-1) in place in the central cavity.
- Variations to 20E having 20/20 fuel in Hex Ring C requires the 20/20 fuel to be loaded into corner positions only and graphite dummy elements in the flat positions. The recommendation regarding the performance of fuel temperature measurements also applies to these variations to the as-analyzed 20E configuration.

### 30B Core Loading

- No fuel will be loaded into Hex Ring A or B.
- The only fuel types allowed are 20/20 and 30/20.
- 20/20 fuel may be used in any position in Rings C through G.
- 30/20 fuel may be used in any positions in Rings D through G but not in Ring C.
- A minimum of 94 fuel elements, including FFCRs, is required for operation at power levels above 0.5 MW.
- The initial load and test program to determine the excess reactivity of the 30B reference core shall be conducted with the central irradiation fixture-1 (CIF-1) in place in the central cavity.

For the safety and performance analyses to be applicable, it is not necessary that the actual loadings precisely match 20E, 30B or a direct path between them. Reasonable variations on these loadings will have comparable safety and performance characteristics. Guidelines on what constitutes reasonable variations are discussed in detail in References 4.4 and 4.5.

### October 2017 Core Loading and Likely Future Core Loading

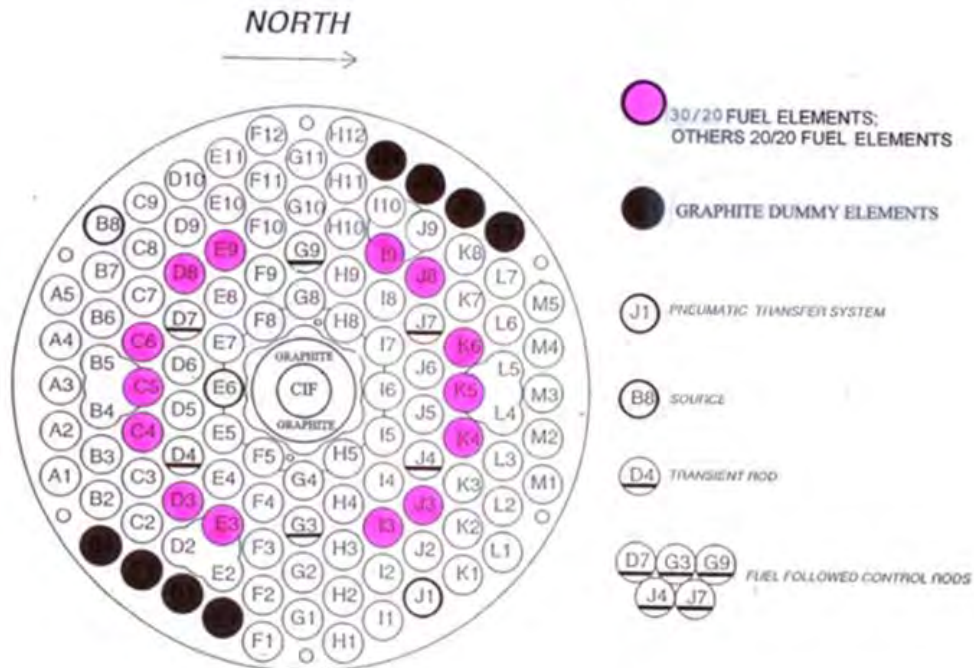


**FIGURE 4.18 OCTOBER 2017 CORE LOADING AND LIKELY FUTURE CORE LOADING**

The current core configuration can be seen figure 4.18. The core is technically a 30B with just over one half of the elements in the E ring being 30/20 elements, while all other elements are 20/20 element including fuel followed control rods. The clean excess reactivity is calculated to be \$5.42 using the MNRC MCNP core model, which is consistent with the measured value of \$5.41 in the startup of Monday morning on October 2, 2017. The MNRC core configuration is unlikely to change dramatically in the next several years. MNRC currently has no spare fuel elements and there is no source of new TRIGA fuel in the world. If new 20/20 elements were to become available these elements would likely replace the approximately 30 high burn up (>30% U-235 consumed) 20/20 elements in the core or replace graphite elements in the outer most ring. If new 30/20 elements were to become available these would likely replace 20/20 elements in the E ring. The displaced 20/20 elements would replace existing high burn up 20/20 elements elsewhere in the core or graphite elements in the outer most ring.

#### 4.5.4 Reactor Core Parameters

##### 4.5.4.1 Reactor Fuel Temperature

The basic safety limit for the TRIGA<sup>®</sup> reactor system is the fuel temperature. This applies for both the steady-state and pulsed mode of operation.

Limiting temperatures for the two modes of operation are of interest, depending on the type of TRIGA<sup>®</sup> fuel used. The UCD/MNRC reactor utilizes fuel with H/Zr ratios between 1.6 and 1.7. (i.e., greater than 1.5). This allows operation at a higher fuel temperature limit. Figure 4.19 indicates that the higher hydride compositions are single phase and are not subject to the large volume changes associated with the phase transformations at approximately 530°C in the lower hydrides. It has been noted in Reference 4.6 that the higher hydrides lack any significant thermal diffusion of hydrogen. These two facts preclude concomitant volume changes. The important properties of delta phase U-ZrH are given in Table 4-5.

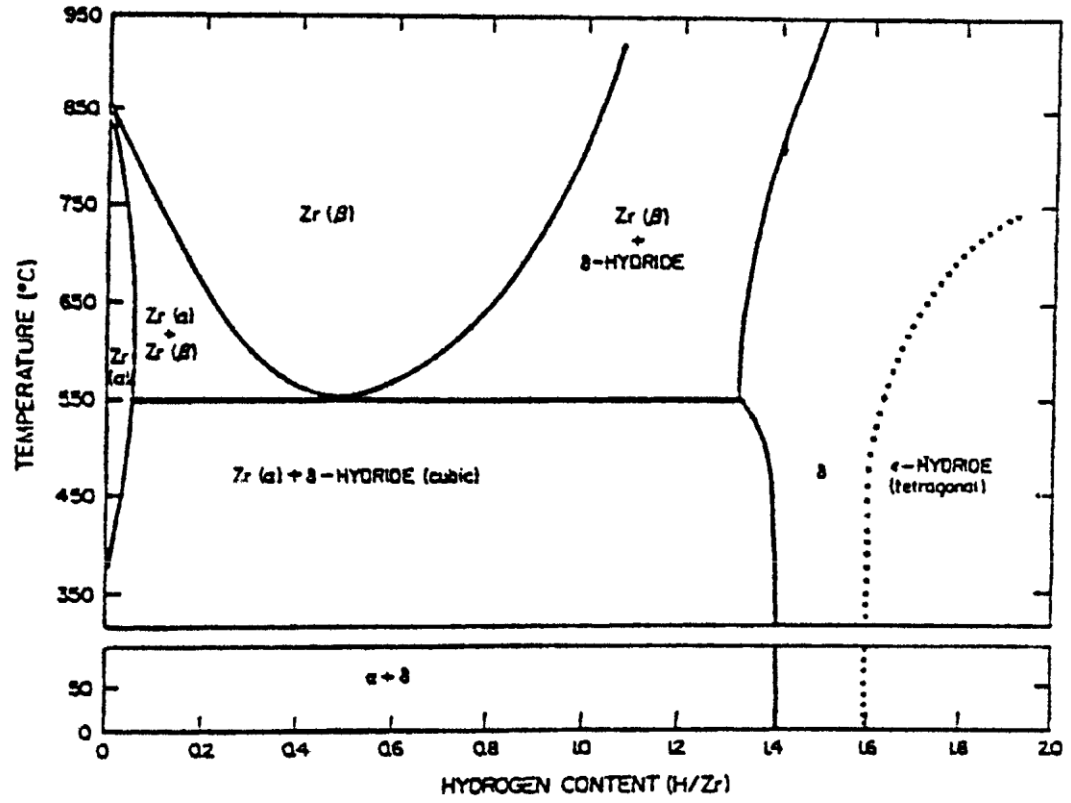


FIGURE 4. 19 PHASE DIAGRAM OF THE ZIRCONIUM-HYDROGEN SYSTEM

TABLE 4-5 PHYSICAL PROPERTIES OF DELTA PHASE U-ZrH

Thermal conductivity (93°C-650°C)	13 Btu/hr – ft <sup>2</sup> -°F
Elastic modulus: 20°C	9.1 x 10 <sup>6</sup> psi
650°C	6.0 x 10 <sup>6</sup> psi
Ultimate tensile strength (to 650°C)	24,000 psi
Compressive strength (20°C)	60,000 psi
Compressive yield (20°C)	35,000 psi
Heat of formation ( $\delta_{H_f}^\circ$ , 298°)	37.72 kcal/g-mole

Among the chemical properties of U-ZrH and ZrH, the reaction rate of the hydride with water is of particular interest. Since the hydriding reaction is exothermic, water will react more readily with zirconium than with zirconium hydride systems. Zirconium is frequently used in contact with water in reactors, and the zirconium-water reaction is not a safety hazard. Experiments carried out at GA Technologies show that the zirconium hydride systems have a relatively low chemical reactivity with respect to water and air. These tests (Reference 4.7), have involved the quenching with water of both powders and solid specimens of U-ZrH after heating to as high as 850°C, and of solid U-Zr alloy after heating to as high as 1200°C. Tests have also been made to determine the extent to which fission products are removed from the surfaces of the fuel elements at room temperature. Results prove that, because of the high resistance to leaching, a large fraction of the fission products are retained in even completely unclad U-ZrH fuel.

At room temperature, the hydride is like a ceramic and shows little ductility. However, at the elevated temperatures of interest for pulsing, the material is found to be more ductile. The effect of very large thermal stress on hydride fuel bodies has been observed in hot cell observations to cause relatively widely spaced cracks which tend to be either radial or normal to the central axis and do not interfere with radial heat flow (Reference 4.8). Since the segments tend to be orthogonal, their relative positions appear to be quite stable.

The limiting effect of fuel temperature is the hydrogen gas pressure causing cladding stress. Figure 4.20 relates equilibrium hydrogen pressure in a Zr/H mixture as a function of temperature for three different H/Zr ratios.

The main concern regarding hydrogen pressure is to ensure that the cladding ultimate strength is not exceeded by the stress caused by the pressure. The mechanisms in obtaining temperatures and pressures of concern are different in the pulsing and steady-state mode of operation, and each mechanism will be discussed separately.

The UCD/MNRC fuel consists of U-ZrH with a H/Zr ratio between 1.6 and 1.7 and with 20 or 30 wt% enriched in  $^{235}\text{U}$  to approximately 20%  $^{235}\text{U}$ . The cladding is 0.020 in. thick stainless steel and has an inside diameter of 1.43 in. The rest of the discussion on fuel temperatures will be concerned with fuel having H/Zr ratios greater than 1.5 (i.e., single phase and not subject to the large volume changes associated with phase transformation at approximately  $530^\circ\text{C}$  in the lower hydrides). Further, it will specifically address fuel with an H/Zr ratio of 1.7 since this is the highest ratio fuel to be used in the UCD/MNRC and will produce the highest clad pressure and stress for a given temperature. Figure 4.21 shows the characteristic of 304 stainless steel with regard to yield and ultimate strengths as a function of temperature.

The stress applied to the cladding from the internal hydrogen gas pressure is given by:

$$S = P r/t ; \quad (1)$$

where:

S = stress in psi;  
 P = internal pressure in psi;  
 r = radius of the stainless steel cylinder;  
 t = wall thickness of the stainless steel clad.

Using the parameters given above:

$$S = 36.7 P .$$

For safety considerations, it is necessary to relate the strength of the cladding material at its operating temperature to the stress applied to the cladding due to the internal gas pressure associated with the fuel temperature. Figure 4.22 gives the ultimate cladding strength and the stress applied to the cladding as a result of hydrogen dissociation for fuel having H/Zr ratios of 1.65 and 1.70, both as a function of temperature. This curve shows that the cladding will not fail for fuel with Zr/H<sub>1.7</sub> if both the clad and fuel temperatures are equal and below about  $930^\circ\text{C}$ . This is conservative since the cladding temperature will be below the fuel temperature. This establishes the safety limit on fuel temperature for steady-state operations. The actual steady-state peak fuel temperature at 2 MW is below the limiting maximum measured fuel temperature of  $750^\circ\text{C}$ . The remainder of this section deals with the safety limit for transient operation.

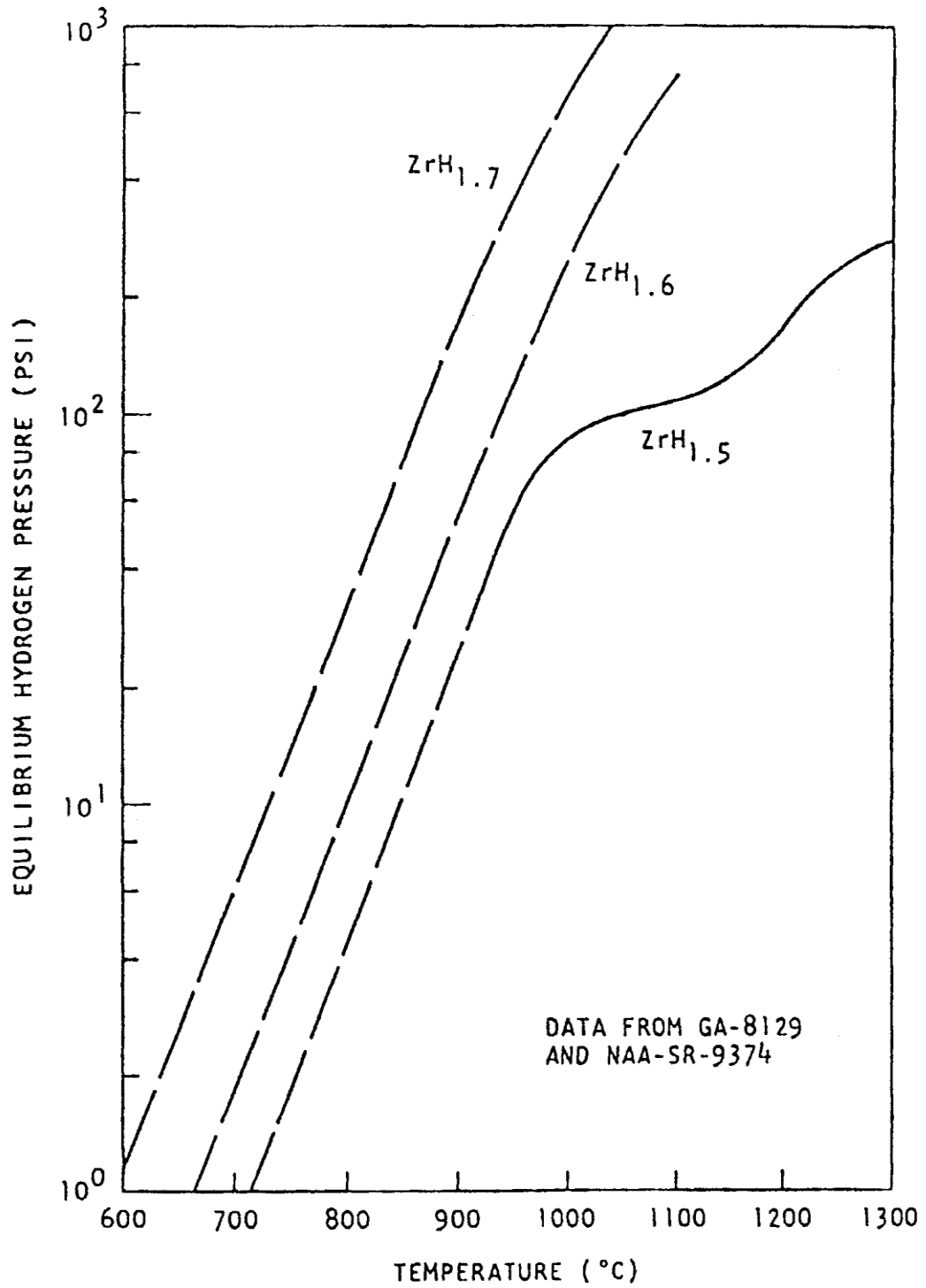


FIGURE 4.20 EQUILIBRIUM HYDROGEN PRESSURES OVER ZrH<sub>x</sub> VERSUS TEMPERATURE

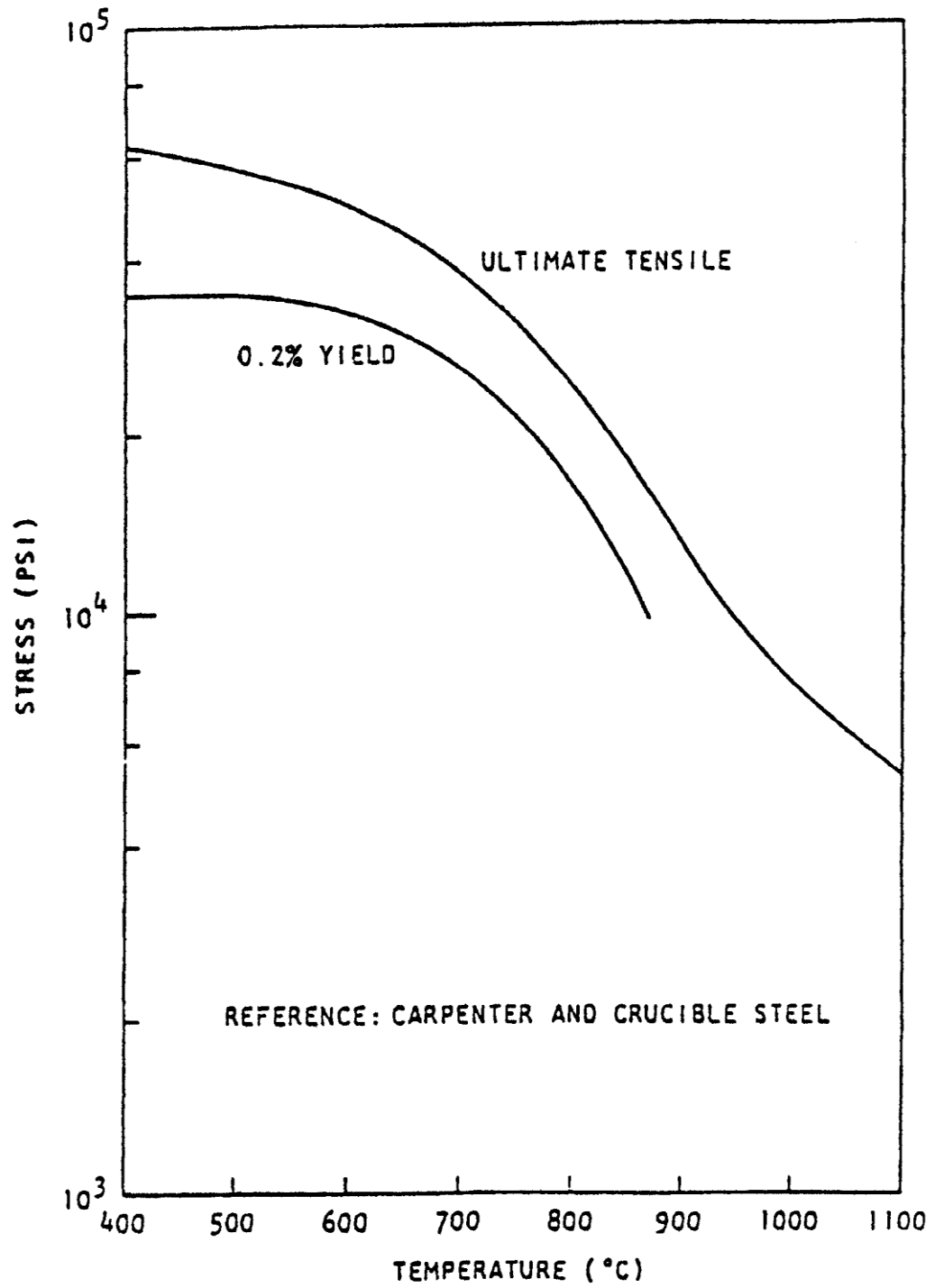


FIGURE 4.21 STRENGTH OF TYPE 304 STAINLESS STEEL AS A FUNCTION OF TEMPERATURE

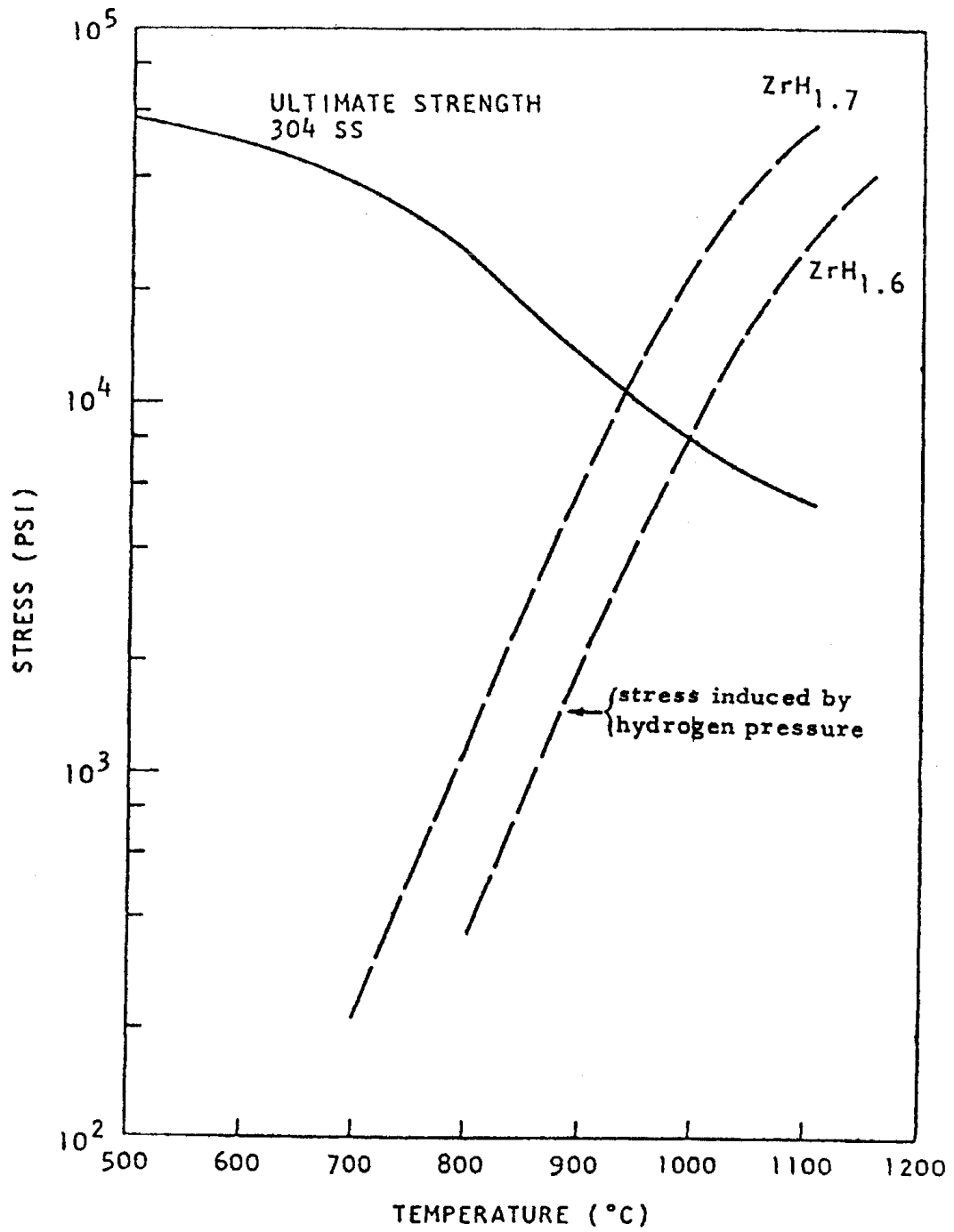


FIGURE 4.22: STRENGTH AND APPLIED STRESS AS A FUNCTION OF TEMPERATURE

In transient operation, it is necessary to account for the difference in fuel and cladding temperatures to establish a safety limit based on fuel temperature. Additionally, the diffusion of hydrogen reduces peak pressures from those predicted at equilibrium at the peak fuel temperatures. The net result of these two points is that a higher safety limit exists for transient operation. An analysis of the two points is given in the following two subsections.

#### 4.5.4.1.1 Fuel and Clad Temperature

For the steady-state safety limit, it was assumed that the cladding and fuel temperatures were the same. The following discussion shows that the cladding temperature is well below the maximum fuel temperature after a pulse. This allows a higher safety limit on fuel temperature. The radial temperature distribution in the fuel element immediately following a pulse is very similar to the power distribution shown in Figure 4.23. This initial steep thermal gradient at the fuel surface results in some heat transfer during the time of the pulse so that the true peak temperature does not quite reach the adiabatic peak temperature. A large temperature gradient is also impressed upon the clad which can result in a high heat flux from the clad into the water. If the heat flux is sufficiently high, film boiling may occur and form an insulating jacket of steam around the fuel elements permitting the clad temperature to approach the fuel temperature. Thermal transient calculations were made using the RAT computer code. RAT is a 2D transient heat transport code developed to account for fluid flow and temperature dependent material properties. Calculations show that if film boiling occurs after a pulse, it may take place either at the time of maximum heat flux from the clad, before the bulk temperature of the coolant has changed appreciably, or it may take place at a later time when the bulk temperature of the coolant has approached the saturation temperature, resulting in a reduced threshold for film boiling. Data obtained by Johnson et al., Reference 4.9, for transient heating of ribbons in 100°F water, showed burnout fluxes of 0.9 to 2.0 MBtu/ft<sup>2</sup>-hr for e-folding periods from 5 to 90 milliseconds. On the other hand, sufficient bulk heating of the coolant channel between fuel elements can take place in several tenths of a second to lower the departure from nucleate boiling (DNB) point to approximately 0.4 MBtu/ft<sup>2</sup>-hr. It is shown, on the basis of the following analysis, that the second mode is the most likely, i.e., when film boiling occurs, it takes place under essentially steady-state conditions at local water temperatures near saturation.

A value for the temperature that may be reached by the clad if film boiling occurs was obtained in the following manner. A transient thermal calculation was performed using the radial and axial power distributions in Figures 4.23 and 4.24, respectively. The thermal resistance at the fuel-clad interface was assumed to be zero.

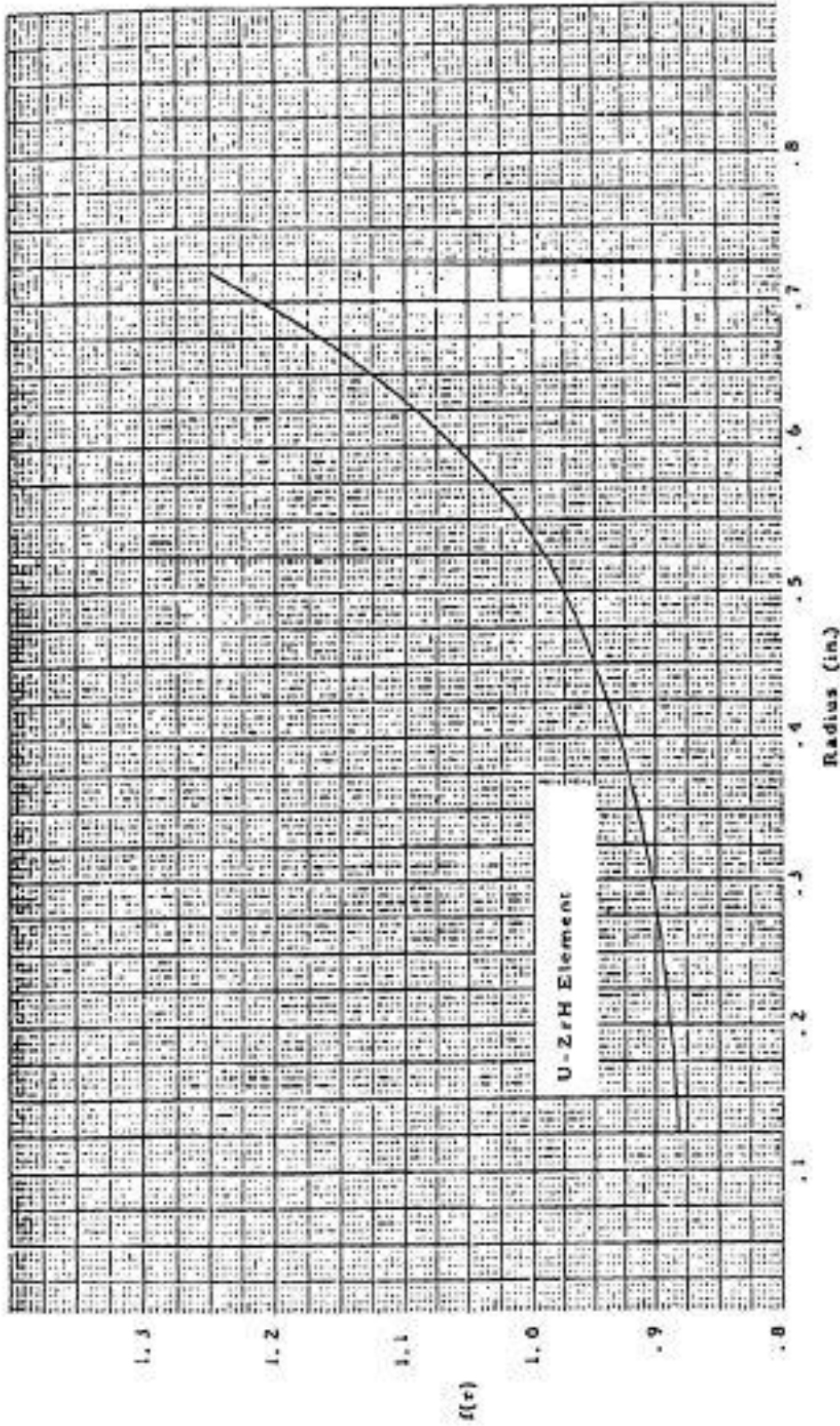
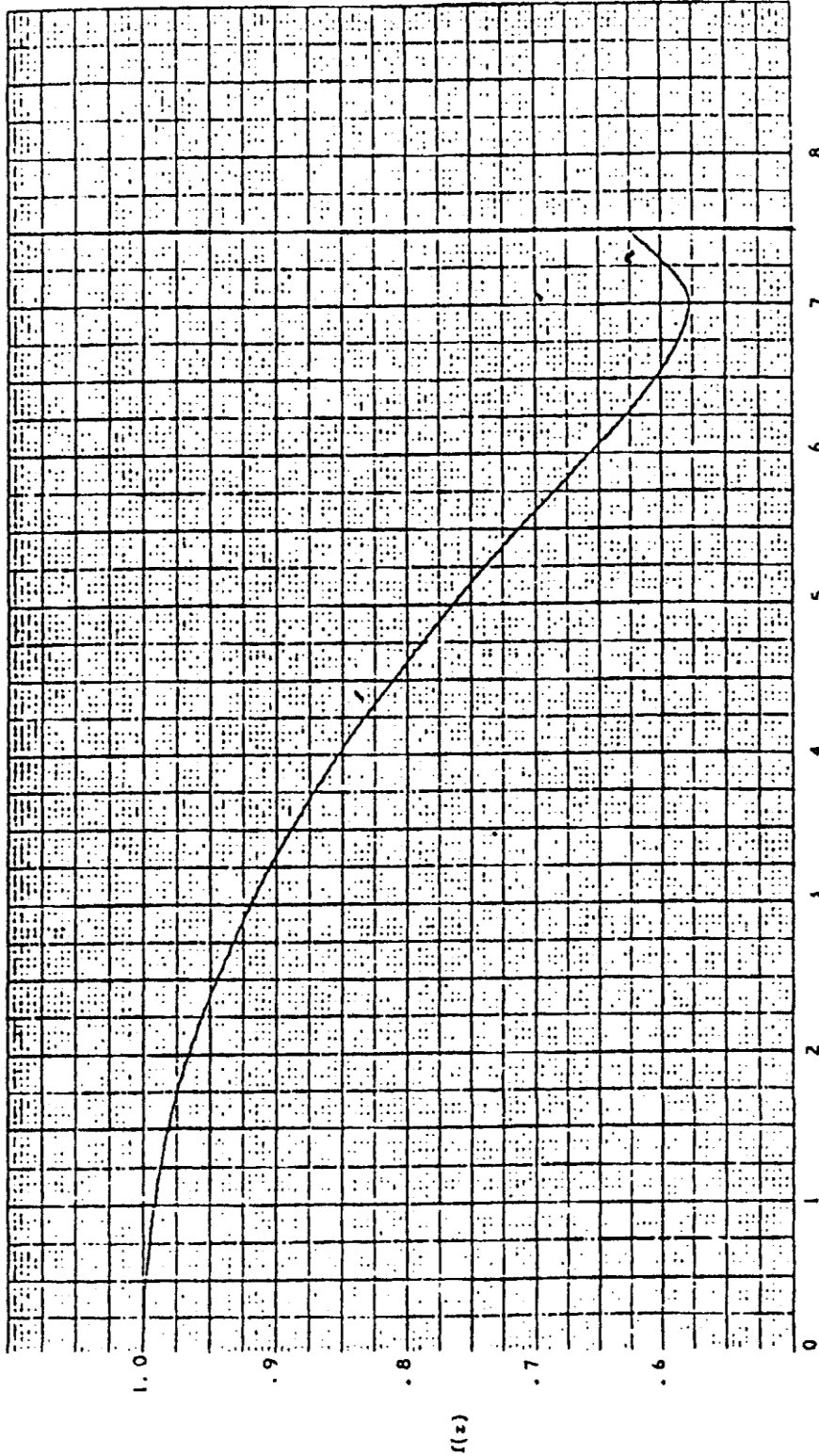


FIGURE 4.23 RADIAL POWER DISTRIBUTION IN U-ZrH FUEL ELEMENT



Axial Distance from Mid-Plane of Fuel Element (in.)

**FIGURE 4.24 AXIAL POWER DISTRIBUTION IN A FUEL ELEMENT ASSUMED FOR THERMAL ANALYSIS**

A boiling heat transfer model, as shown in Figure 4.25, was used in order to obtain an upper limit for the clad temperature rise. The model used the data of McAdams (Reference 4.10), for the subcooled boiling and the work of Sparrow and Cess (Reference 4.11), for the film boiling regime. A conservative estimate was obtained for the minimum heat flux in film boiling by using the correlations of Speigler et al. (Reference 4.12), Zuber (Reference 4.13), and Rohsenow and Choi (Reference 4.14), to find the minimum temperature point at which film boiling could occur. This calculation gave an upper limit of 760°C clad temperature for a peak initial fuel temperature of 1000°C, as shown in Figure 4.26. Fuel temperature distributions for this case are shown in Figure 4.27 and the heat flux into the water from the clad is shown in Figure 4.28. In this limiting case, DNB occurred only 13 milliseconds after the pulse, conservatively calculated assuming a steady-state DNB correlation. Subsequently, experimental transition and film boiling data were found to have been reported by Ellion (Reference 4.15), for water conditions similar to those for the TRIGA<sup>®</sup> system. The Ellion data show the minimum heat flux, used in the limiting calculation described above, was conservative by a factor of 5. An appropriate correction was made which resulted in a more realistic estimate of 470°C as the maximum clad temperature expected if film boiling occurs. This result is in agreement with experimental evidence obtained for clad temperatures of 400°C to 500°C for TRIGA<sup>®</sup> Mark F fuel elements which have been operated under film boiling conditions (Reference 4.16). Based on this analysis, the peak cladding temperature will be 470°C for a transient fuel temperature of 1000°C. Further analysis shows that this peak clad temperature is valid for a higher peak fuel temperature.

The preceding analysis assessing the maximum clad temperatures associated with film boiling assumed no thermal resistance at the fuel-clad interface. Measurements of fuel temperatures as a function of steady-state power level provide evidence that after operating at high fuel temperatures, a permanent gap is produced between the fuel body and the clad. This gap exists at all temperatures below the maximum operating temperature (for example, Figure 16 in Reference 4.16). The gap thickness varies with fuel temperature and clad temperature: cooling of the fuel or overheating of the clad tends to widen the gap and decrease the heat transfer rate. Additional thermal resistance due to oxide and other films on the fuel and clad surfaces is expected. Experimental and theoretical studies of thermal contact resistance have been reported, References 4.17-4.19, which provide insight into the mechanisms involved. They do not, however, permit quantitative prediction because the basic data required for input are presently not fully known. Instead, several transient thermal computations were made using the RAT code, varying the effective gap conductance, in order to determine the effective gap coefficient for which departure from nucleate boiling is incipient. These results were then compared with the incipient film boiling conditions of the 1000°C peak fuel temperature case.

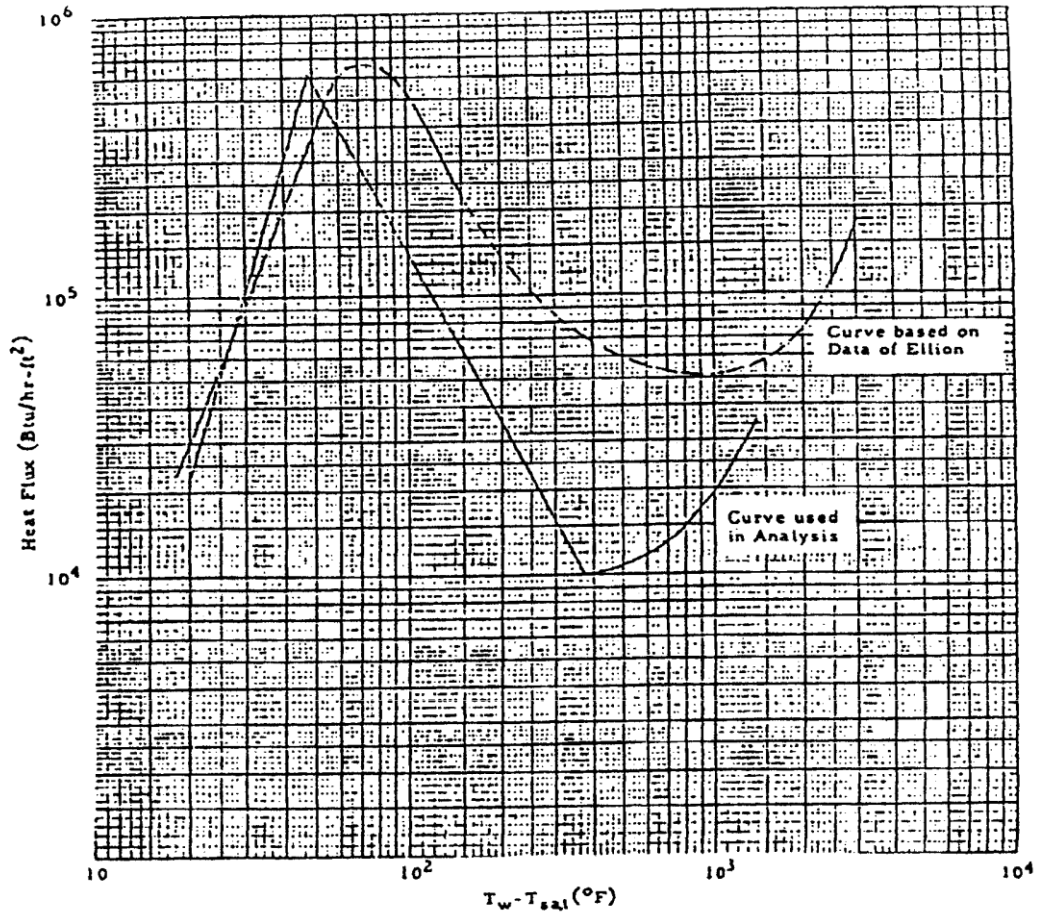


FIGURE 4.25 SUBCOOLED BOILING HEAT TRANSFER FOR WATER

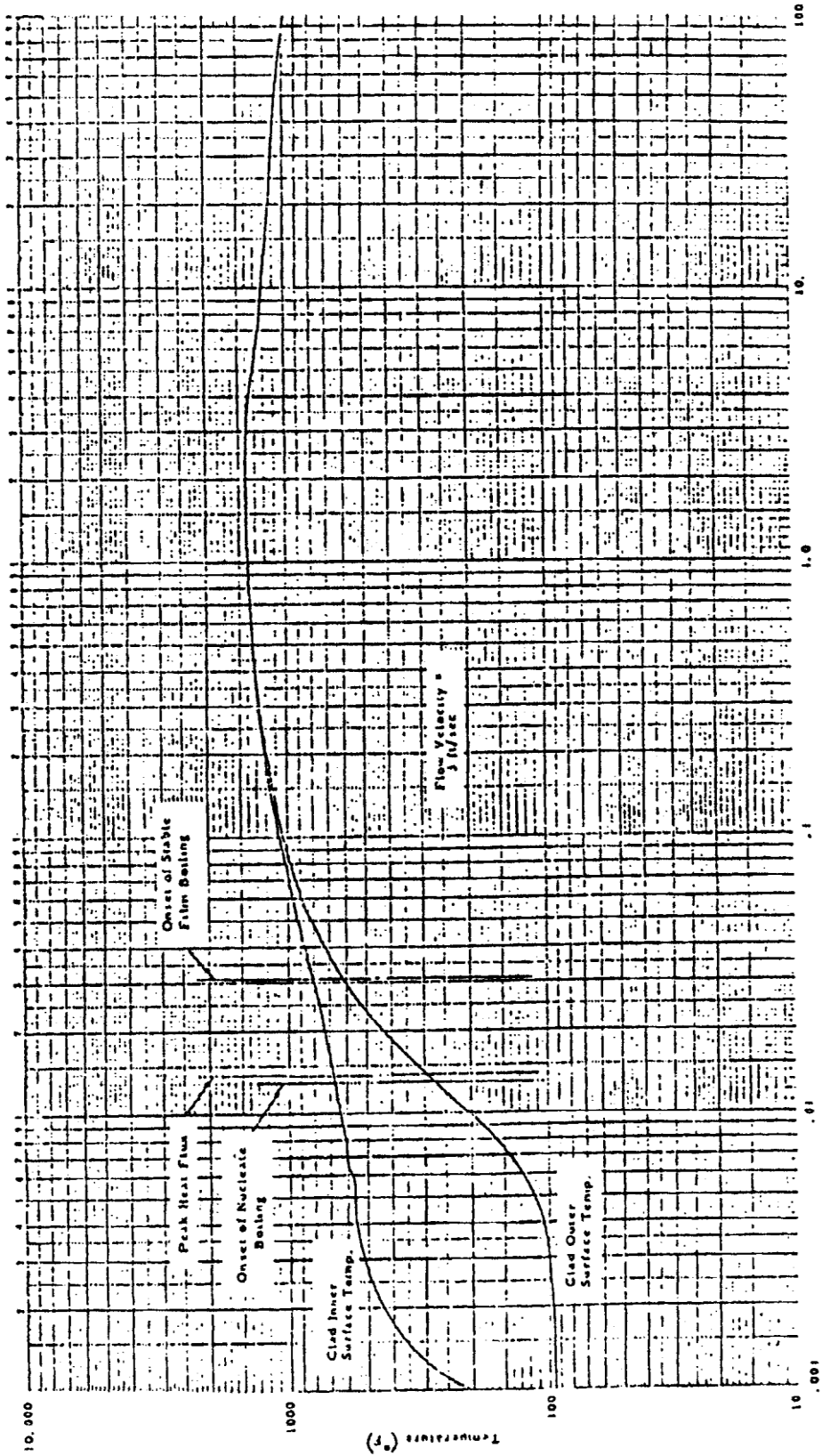


FIGURE 4. 26 CLAD TEMPERATURE AT MIDPOINT OF WELL BONDED FUEL ELEMENT

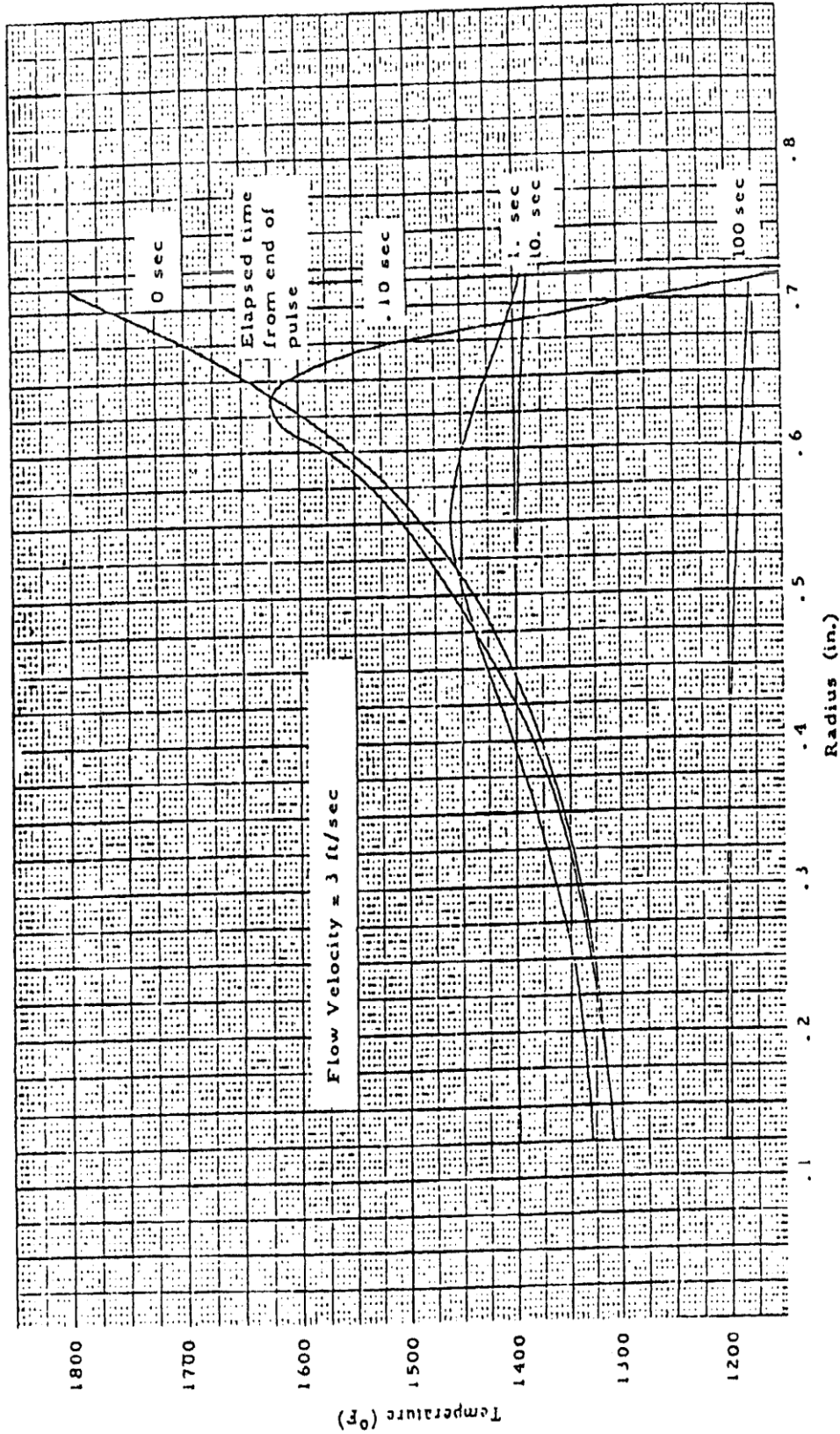


FIGURE 4. 27 FUEL BODY TEMPERATURES AT MIDPLANE OF WELL-BONDED U-Zr-H ELEMENT AFTER PULSE

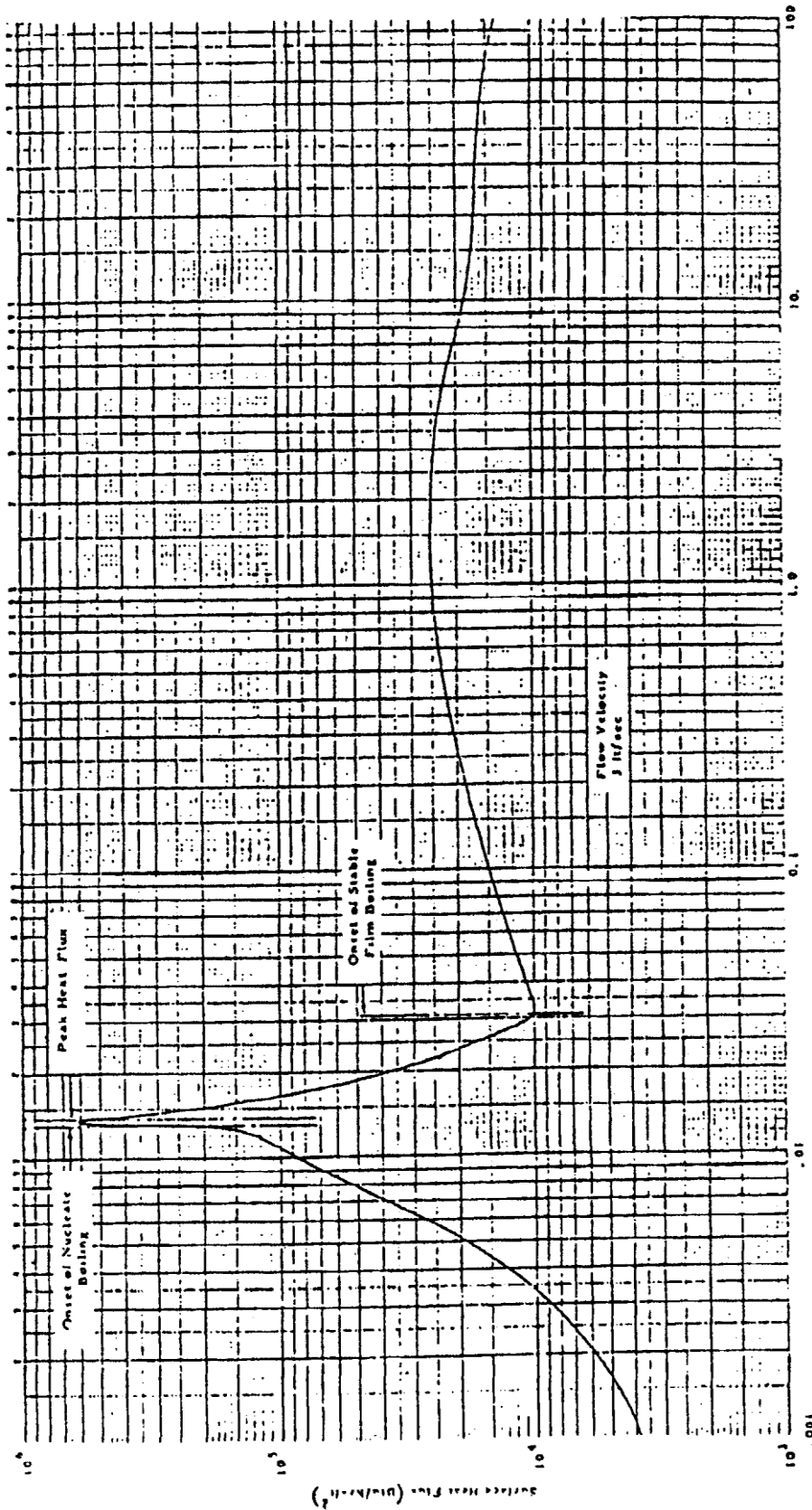


FIGURE 4.28 SURFACE HEAT FLUX AT MIDPLANE OF WELL BONDED U-Zr-H ELEMENT AFTER PULSE

For convenience, the calculations were made using the same initial temperature distribution as was used for the preceding calculations. The calculations assumed a coolant flow velocity of 1 ft per second, which is within the range of flow velocities computed for natural convection under various steady-state conditions for these reactors. The calculations did not use a complete boiling curve heat transfer model, but instead, included a convection cooled region (no boiling) and a subcooled nucleate boiling region without employing an upper DNB limit. The results were analyzed by inspection using the extended steady-state correlation of Bernath (Reference 4.20), which has been reported by Spano (Reference 4.21), to give agreement with SPERT II burnout results within the experimental uncertainties in flow rate.

The transient thermal calculations were performed using effective gap conductances of 500, 375, and 250 Btu/hr-ft<sup>2</sup>-°F. The resulting wall temperature distributions were inspected to determine the axial wall position and time after the pulse which gave the closest approach between the local computed surface heat flux and the DNB heat flux according to Bernath. The axial distribution of the computed and critical heat fluxes for each of the three cases at the time of closest approach is shown in Figures 4.29 through 4.31. If the minimum approach to DNB is corrected to TRIGA<sup>®</sup> Mark F conditions and cross-plotted, an estimate of the effective gap conductance of 450 Btu/hr-ft<sup>2</sup>-°F is obtained for incipient burnout so that the case using 500 is thought to be representative of standard TRIGA<sup>®</sup> fuel.

The surface heat flux at the midplane of the element is shown in Figure 4.32 with gap conductance as a parameter. It may be observed that the maximum heat flux is approximately proportional to the heat transfer coefficient of the gap, and the time lag after the pulse for which the peak occurs is also increased by about the same factor. The closest approach to DNB in these calculations did not necessarily occur at these times and places, however, as indicated on the curves of Figures 4.29 through 4.31. The initial DNB point occurred near the core outlet for a local heat flux of about 340 kBtu/hr-ft<sup>2</sup>-°F according to the more conservative Bernath correlations at a local water temperature approaching saturation.

From this analysis, a maximum temperature for the clad during a pulse which gives a peak adiabatic fuel temperature of 1000°C is estimated to be 470°C. This is conservative since it was obtained by assuming no thermal resistance between the fuel and the clad. As was shown above, a value of 500 Btu/hr-ft<sup>2</sup>-°F for the gap conduction is more realistic.

As can be seen from Figure 4.21, the ultimate strength of the cladding at a temperature of 470°C is 59,000 psi. If the stress produced by the hydrogen over pressure on the clad is less than 59,000 psi, the cladding will not be ruptured. Referring to Figure 4.22, and considering U-ZrH<sub>1.7</sub> fuel with a peak temperature of 1000°C, one finds the stress on the clad to be 24,000 psi. Analysis in the next section which considers diffusion will show that the actual hydrogen pressure produced in a pulse is less than the equilibrium pressure for the peak temperature. This allows a safe limit on fuel temperature to be 1100°C. TRIGA<sup>®</sup> fuel with a hydrogen to zirconium ratio of at least 1.6 has been pulsed to temperatures approaching 1150°C without damage to the clad (Reference 4.22).

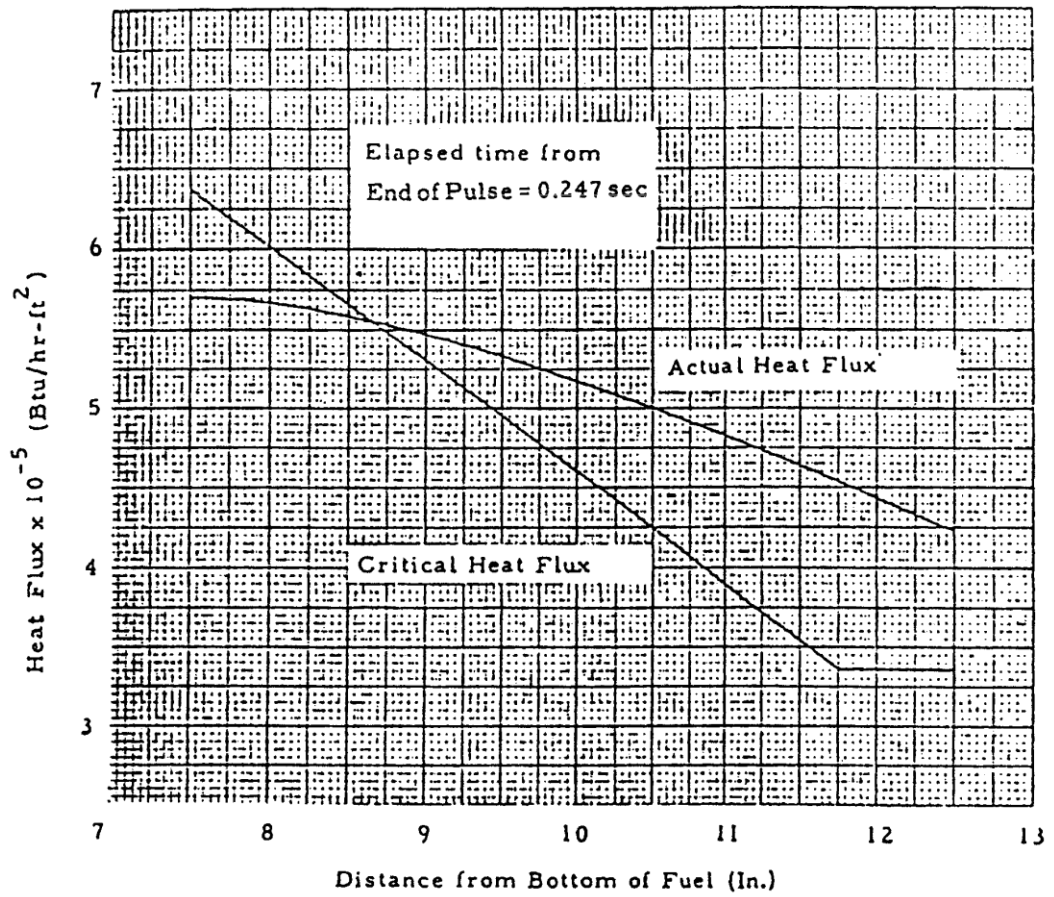


FIGURE 4.29 SURFACE HEAT FLUX DISTRIBUTION FOR STANDARD NON-GAPPED FUEL ELEMENT AFTER PULSE  
hgap = 500

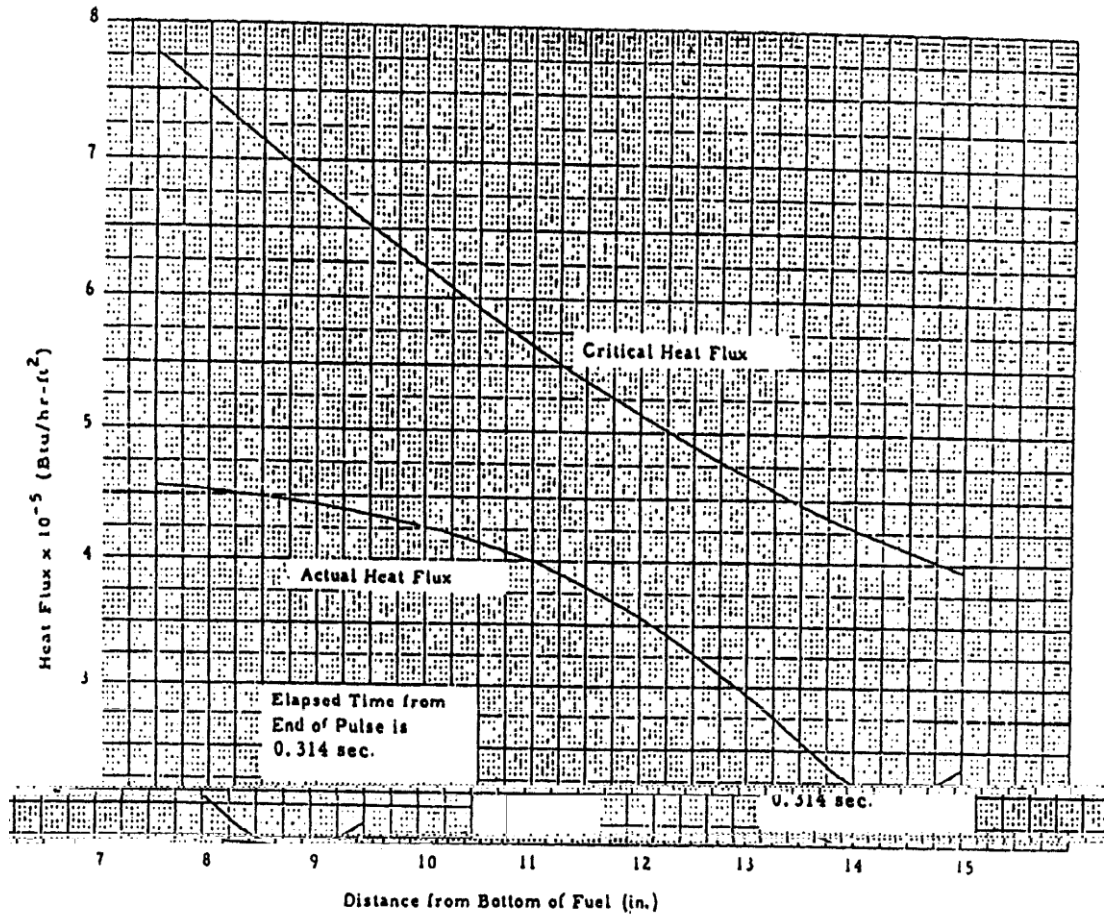


FIGURE 4.30 SURFACE HEAT FLUX DISTRIBUTION FOR STANDARD NON-GAPPED FUEL ELEMENT AFTER PULSE, hgap = 375

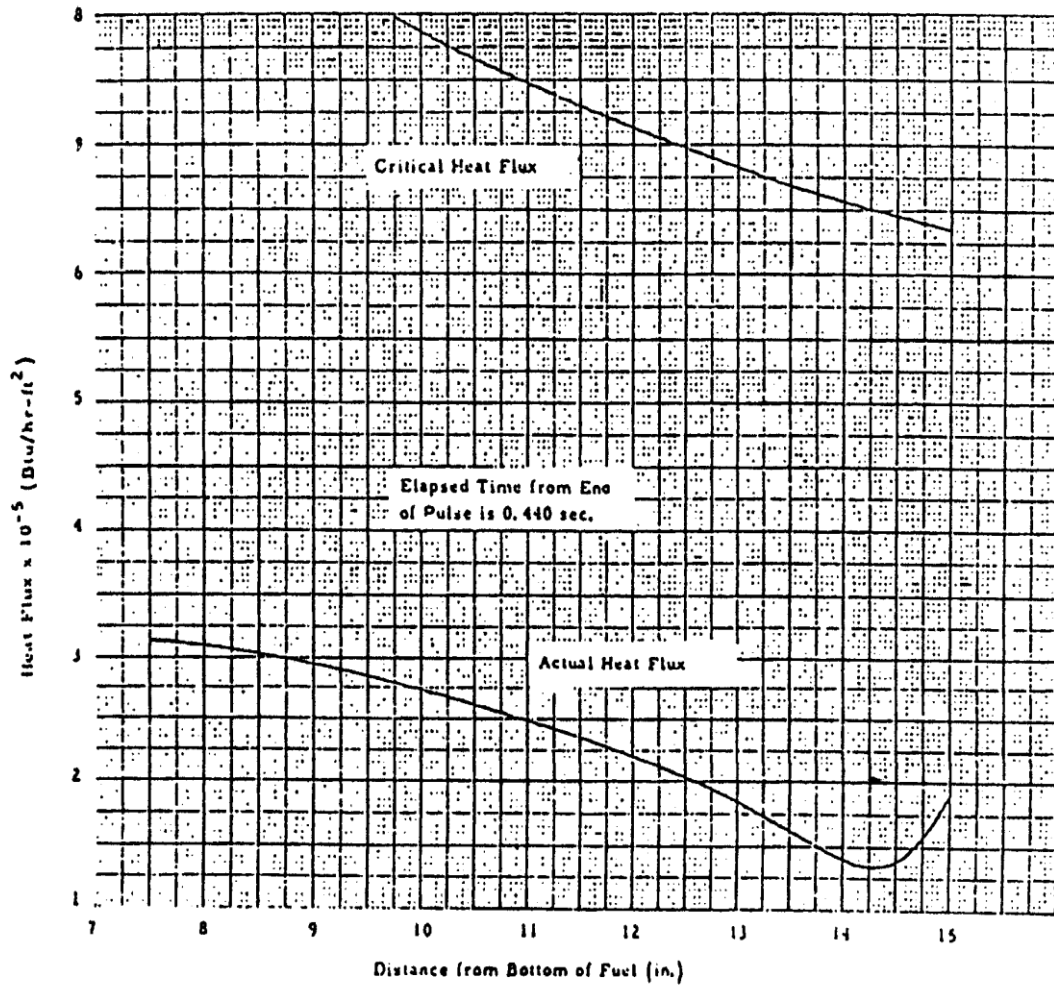


FIGURE 4.31 SURFACE HEAT FLUX DISTRIBUTION FOR STANDARD NON-GAPPED FUEL ELEMENT AFTER PULSE, hgap = 250

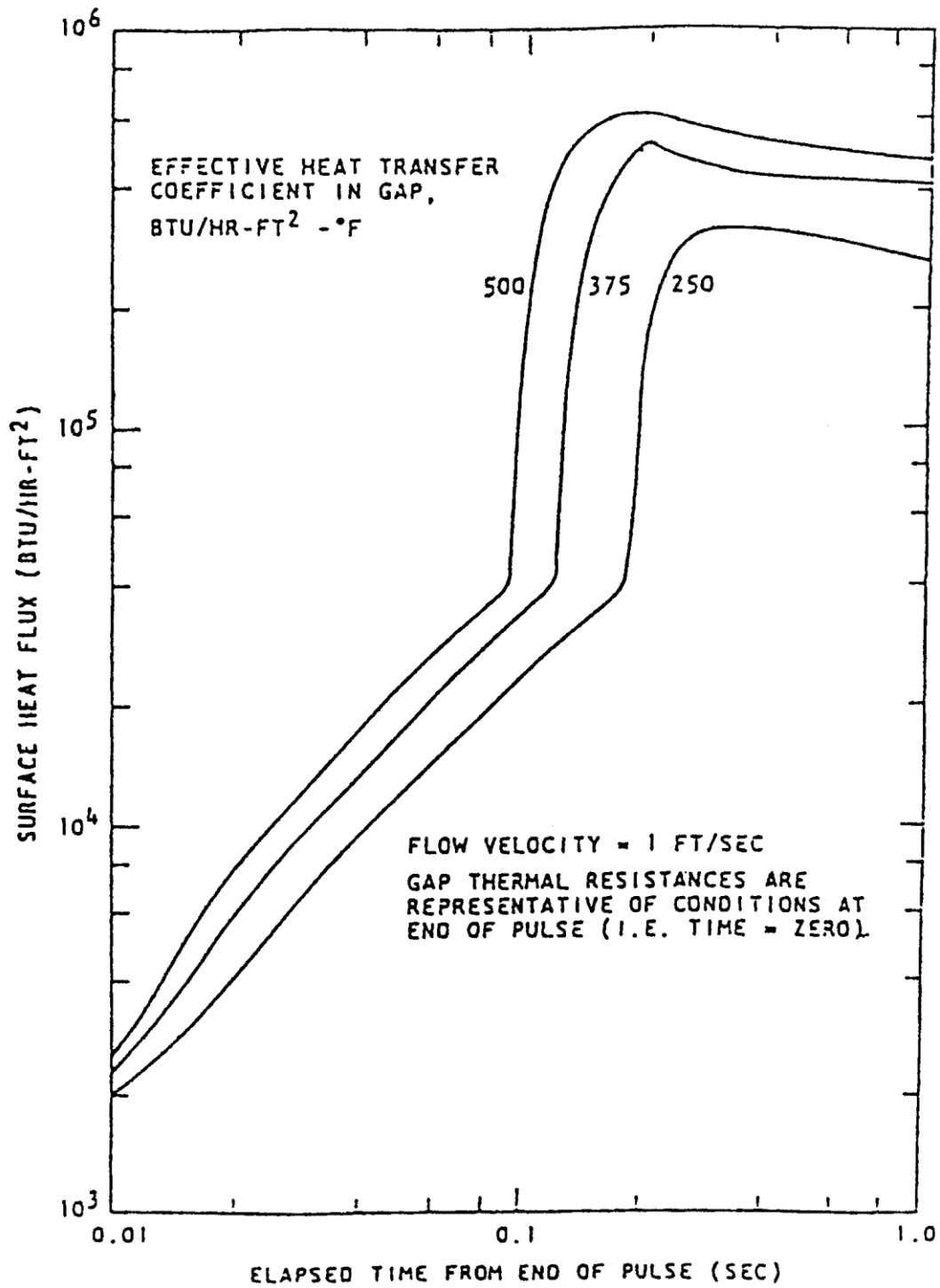


FIGURE 4.32 SURFACE HEAT FLUX AT MIDPOINT VERSUS TIME FOR STANDARD NON-GAPPED FUEL ELEMENT AFTER PULSE

## 4.5.4.1.2 Hydrogen Pressure in TRIGA® Fuel Elements

To assess the effect of the finite diffusion rate and the rehydriding at the cooler surfaces, the following analysis is presented.

As hydrogen is released from the hot fuel regions, it migrates to the cooler regions and the equilibrium pressure that is obtained is characteristic of some temperature lower than the maximum. To evaluate this reduced pressure, diffusion theory is used to calculate the rate at which hydrogen is evolved and reabsorbed at the fuel surface.

Ordinary diffusion theory provides an expression for describing the time dependent loss of gas from a cylinder:

$$\frac{\bar{c} - c_f}{c_i - c_f} = \sum_{n=1}^{\infty} \frac{4}{Z_n^2} \exp - \frac{Z_n^2 Dt}{r_0^2} ; \quad (3)$$

Where:

$\bar{c}, c_i, c_f$	=	the average, the initial, and the final gas concentration in the cylinder, respectively;
$Z_n$	=	the roots of the Equation $J_0(x) = 0$
$D$	=	the diffusion coefficient for the gas in the cylinder;
$r_0$	=	the radius of the cylinder;
$t$	=	time.

Setting the term on the right-hand side of Equation 3 equal to  $\kappa$ , one can rewrite Equation 3 as:

$$\bar{c}/c_i = c_f/c_i + (1 - c_f/c_i) \kappa \quad (4)$$

and the derivative in time is given by:

$$\frac{d(c/c_i)}{dt} = (1 - c_f/c_i) \frac{d\kappa}{dt} \quad (5)$$

This represents the fractional release rate of hydrogen from the cylinder,  $f(t)$ . The derivative of the series in the right-hand side of Equation 3 was approximated by:

$$\frac{d\kappa}{dt} = - (7.339e^{-8.34\epsilon} + 29.88e^{-249\epsilon}) \frac{d\epsilon}{dt} \quad (6)$$

Where  $\epsilon = Dt/r_0^2$

The diffusion coefficient for hydrogen in zirconium hydride in which the H/Zr ratio is between 1.56 and 1.86 is given by:

$$D = 0.25 e^{-17800/R(T+273)} \quad (7)$$

where:

R = the gas constant; and  
T = the zirconium hydride temperature in °C

Equation 3 describes the escape of gas from a cylinder through diffusion until some final concentration is achieved. Actually, in the closed system considered here, not only does the hydrogen diffuse into the fuel-clad gap, but also diffuses back into the fuel in the regions of lower fuel temperature. The gas diffuses through the clad at a rate dependent on the clad temperature. Although this tends to reduce the hydrogen pressure, it is not considered in this analysis. When the diffusion rates are equal, an equilibrium condition will exist. To account for this, Equation 5 was modified by replacing the concentration ratios by the ratio of the hydrogen pressure in the gap to the equilibrium hydrogen pressure,  $P_h/P_e$ . Thus:

$$f(t) = \frac{d(c/c_i)}{dt} = (1 - P_h(t)/P_e) \frac{d\kappa}{dt} \quad (8)$$

where:

$P_h(t)$  = the hydrogen pressure, as a function of time; and  
 $P_e$  = the equilibrium hydrogen pressure over the zirconium hydride which is a function of the fuel temperature and H/Zr ratios

The rate of change of the internal hydrogen pressure, in psi, inside the fuel element cladding is:

$$\frac{dP_h}{dt} = \frac{14.7 f(t) N_h}{6.02 \times 10^{23}} \frac{22.4}{V_g} \frac{T+273}{273} \quad (9)$$

where:

$N_h$  = the number of molecules of  $H_2$  in the fuel;

$T$  = the gas temperature ( $^{\circ}C$ );

$f(t)$  = the fractional loss rate from Equation 8;

$V_g$  = the free volume inside the fuel clad (liters).

For a fuel volume of  $24.4 \text{ in}^3$ , the moles of  $H_2$  available from fuel with  $ZrH_{1.65}$  and  $ZrH_{1.7}$  is 19.9 and 20.6 moles respectively. The free volume is assumed to consist of a cylindrical volume, at the top of the element, 0.125 in. high with a diameter of 1.43 in. for a total of  $0.2 \text{ in}^3$ . The temperature of the hydrogen in the gap was assumed to be the temperature of the clad. The effect of changing these two assumptions was tested by calculations in which the gap volume was decreased by 90% and the temperature of the hydrogen in the gap was set equal to the maximum fuel temperature. Neither of these changes resulted in maximum pressures different from those based on the original assumptions although the initial rate of pressure increase was greater. For these conditions:

$$P_h = A \times 10^3 (T+273) \int f(t) dt ; \quad (10)$$

where:

$A$  = 7.29 for  $ZrH_{1.65}$  and 7.53 for  $ZrH_{1.7}$ .

The fuel temperature used in Equation 7 to evaluate the diffusion coefficient is expressed as:

$$T(z) = T_0 ; t < 0;$$

$$T(z) = T_0 + (T_m - T_0) \cos [2.45(z-0.5)]; t \geq 0 ; \quad (11)$$

where:

$T_m$  = the peak fuel temperature ( $^{\circ}C$ );

$T_0$  = the clad temperature ( $^{\circ}C$ );

$z$  = the axial distance expressed as a fraction of the fuel length;

$t$  = the time after step increase in power.

It was assumed that the fuel temperature was invariant with radius. The hydrogen pressure over the zirconium hydride surface when equilibrium prevails is strongly temperature dependent as shown in Figure 4.20, and for ZrH, can be expressed by:

$$P_e = 2.07 \times 10^9 e^{-1.974 \times 10^4 / (T+273)} \quad (12)$$

The coefficients have been derived from data developed by Johnson (Reference 4.23). The rate at which hydrogen is released or reabsorbed takes the form:

$$g(t,z) = \frac{[P_e(z) - P_h(t)]}{P_e(z)} f(t,z); \quad (13)$$

where:

- $f(t,z)$  = the derivative given in Equation 8 with respect to time evaluated at the axial position  $z$ ;
- $P_h(t)$  = the hydrogen pressure in the gap at time  $t$ ;
- $P_e(z)$  = the equilibrium hydrogen pressure at the ZrH temperature at position  $z$ .

The internal hydrogen pressure is then:

$$P_h(t) = A \times 10^3 (T_0 + 273) \int_0^t \int_0^1 g(t, z) dz.$$

This equation was approximated by:

$$P_h(t_i) = A \times 10^3 (T_0 + 273) \times \sum_{i=1}^n \sum_{j=1}^m \left[ 1 - \frac{P_h(t_{i-1})}{P_e(z_j)} \right] \times f(t_i, z_j) \delta z \delta t; \quad (14)$$

where the inner summation is over the fuel element's length increments and the outer summation is over time.

For the cases where the maximum fuel temperature is 1150°C for ZrH<sub>1.65</sub> and 1100°C for ZrH<sub>1.7</sub>, the equilibrium hydrogen pressure in ZrH is 2000 psi, which leads to an internal stress of 72,000 psi. Using Equation 14, it is found that the internal pressure for both ZrH<sub>1.65</sub> and ZrH<sub>1.7</sub> increases to a peak at about 0.3 sec, at which time the pressure is about one-fifth of the equilibrium value or about 400 psi (a stress of 14,700 psi). After this time, the pressure slowly decreases as the hydrogen continues to be redistributed along the length of the element from the hot regions to the cooler regions.

Calculations have also been made for step increases in power to peak  $ZrH_{1.65}$  fuel temperatures greater than 1150°C. Over a 200°C range, the time to the peak pressure and the fraction of the equilibrium pressure value achieved were approximately the same as for the 1150°C case. Similar results were found for fuel with  $ZrH_{1.7}$ . Thus, if the clad remains below about 500°C, the internal pressure that would produce the yield stress in the clad (35,000 psi) is about 1000 psi and the corresponding equilibrium hydrogen pressure is 5000 psi. This corresponds to a maximum fuel temperature of about 1250°C in  $ZrH_{1.65}$  and 1180°C in  $ZrH_{1.7}$ . Similarly, an internal pressure of 1600 psi would produce a stress equal to the ultimate clad strength (over 59,000 psi). This corresponds to an equilibrium hydrogen pressure of 5 x 1600 or 8000 psi and a fuel temperature of about 1300°C in  $ZrH_{1.65}$  and 1240°C in  $ZrH_{1.7}$ .

Measurements of hydrogen pressure in TRIGA® fuel elements during steady-state operation have not been made. However, measurements have been made during transient operations and compared with the results of an analysis similar to that described here. These measurements indicated that in a pulse in which the maximum temperature in the fuel was greater than 1000°C the maximum pressure ( $ZrH_{1.65}$ ) was only about 6% of the equilibrium value evaluated at the peak temperature. Calculations of the pressure resulting from such a pulse using the methods described above gave calculated pressure values about three times greater than the measured values.

An instantaneous increase in fuel temperature will produce the most severe pressure conditions. When a peak fuel temperature is reached by increasing the power over a finite period of time, the resulting pressure will be no greater than that for the step change in power analyzed above. As the temperature rise times become long compared with the diffusion time of hydrogen, the pressure will become increasingly less than for the case of a step change in power. The reason for this is that the pressure in the clad element results from the hot fuel dehydrating faster than the cooler fuel rehydrides (takes up the excess hydrogen to reach an equilibrium with the hydrogen over pressure in the can). The slower the rise to peak temperature, the lower the pressure because of the additional time available for rehydriding.

#### 4.5.4.1.3 ZrH Fuel Temperature Limits

The foregoing analysis gives a strong indication that the cladding will not be ruptured if fuel temperatures are never greater than in the range of 1200°C to 1250°C, providing that the cladding temperature is less than about 500°C. However, for fuel with a  $ZrH_{1.7}$  a conservative safety limit of 1100°C has been chosen for this condition. As a result, at this safety limit temperature the pressure is about a factor of 4 lower than would be necessary for cladding failure. This factor of 4 is more than adequate to account for uncertainties in cladding strength and manufacturing tolerances. As a safety limit, the peak adiabatic fuel temperature to be allowed during transient conditions is considered to be 1100°C for U- ZrH fuel with ratios up to 1.70. Under any condition in which the cladding temperature increases above 500°C, the temperature safety limit must be decreased as the cladding material loses strength at elevated temperatures. To establish this limit, it is assumed that the fuel and the cladding are at the same temperature. There are no conceivable circumstances that could give rise to a situation in which the cladding temperatures are higher than the fuel temperature.

In Figure 4.22, the stress imposed on the clad by the equilibrium hydrogen pressure as a function of the fuel temperature is plotted. Also shown is the ultimate strength of 304 stainless steel at the same temperatures. The use of these data for establishing the safety limit for conditions in which the cladding temperature is greater than 500°C is justified as:

- a. the method used to measure ultimate strength requires the imposition of the stress over a longer time than would be imposed for accident conditions;
- b. the stress is not applied biaxially in the ultimate strength measurements as it is in the fuel clad

The point at which the two curves in Figure 4.22 intersect (for ZrH<sub>1.7</sub>) is the safety limit, that is, 930°C for conditions in which the cladding temperature is above 500°C. At that temperature, the equilibrium hydrogen pressure would impose a stress on the cladding equal to the ultimate strength of the clad.

The same argument about the redistribution of the hydrogen within the fuel presented earlier is valid for this case. In addition, at elevated temperatures the cladding becomes quite permeable to hydrogen. Thus, not only will hydrogen redistribute itself within the fuel to reduce the pressure, but some hydrogen will escape from the system entirely.

The use of the ultimate strength of the cladding material in the establishment of the safety limit under these conditions is justified because of the transient nature of accidents. Although the high cladding temperatures imply sharply reduced heat transfer rates to the surroundings (and consequently longer cooling times), only slight reductions in the fuel temperature are necessary to reduce the stress sharply. For a fuel with ZrH<sub>1.7</sub>, a 40°C decrease in temperature from 930°C to 890°C will reduce the stress by a factor of 2. The above analyses and limits are generic. They establish the bounds of the element's capability; the limits are not related to any specific fuel element power or fissionable material content. They relate to the temperatures in the element, to the properties of the fuel, and to the strength of and the stress on the cladding that can be allowed without cladding rupture.

These limits are thus reaffirmed; they continue to be fully applicable to operation of the UCD/MNRC at 2 MW.

#### 4.5.4.1.4 Performance of High Uranium wt% Fuels

A substantial review and evaluation of the performance of 20 and 30 wt% uranium fuel elements was conducted based on the information provided in References 4.1, 4.24 and 4.25. The basic conclusions are:

*The performance of these higher uranium content fuels is substantially independent of uranium content up to at least 45 wt%. The 20 and 30 wt% fuel are indistinguishable from the 8.5 wt% fuel. Fuel growth is as predicted; there is limited thermal migration of hydrogen; there is no pressure buildup inside the cladding as burnup proceeds; and the fission product release fractions from high-burnup elements is not significantly different from fresh fuel (Reference 4.24). From these studies, the release fractions of fission products were observed not to be related to uranium content; a single correlation serves to describe the gas release behavior over a broad temperature range (Reference 4.25). The basic release fraction for fuel temperatures less than 400°C remains as assessed previously ( $1.5 \times 10^{-5}$ ). These studies covered burnups up to 64% of the uranium-235 content.*

In summary, the prompt negative temperature coefficient, fuel properties, irradiation performance, behavior under pulse heating, and effect of hydrogen disassociation on the fuel element safety limits, for fuel containing up to 45 wt% uranium, were all found to mirror that of the reference 8.5 wt% fuel.

TRIGA® fuels of 20, 30, and 45 wt% uranium, 19.7% enriched, were irradiated in the Oak Ridge Research Reactor (ORR) and thoroughly examined (References 4.24 and 4.26), and evaluated (Reference 4.1). Table 4-6 presents a profile of the irradiation conditions of these elements.

The performance base for the higher wt% LEU fuels irradiated in ORR encompasses burnups to greater than 60% of the contained  $^{235}\text{U}$ , exposures as high as 919 full power days and fast neutron fluence of  $5 \times 10^{21}\text{n/cm}^2$ . The maximum linear power density during the ORR irradiations was comparable to the maximum predicted in Section 4.5 for the worst UCD/MNRC case.\*

TABLE 4-6 ORR IN-PILE IRRADIATION PARAMETERS

	20 Wt-%U	30 Wt-%U	45 Wt-%U
Contained U-235 per 22 in. fuel rod (g)	19	30	55
Vol-% U (19.7% Enriched)	7	11	20
Max Calc Rod Power Generation (kW)			
Initial Configuration		36	35
Full Cluster Configuration	41	43	48
45 Wt-% Only Configuration			55
Time at Power (FPD)			
Initial Configuration (Dec 79-Nov 80)	0	278	278
Full Cluster Config (May 81-Nov 82)	295	295	295
45 Wt-% Only Config (July 82-Nov 83)	0	0	328
45 Wt-% Only Config (Aug 84)	0	0	18
Target Burnup of U-235 (%)	35	40	50
Final Burnup Range (%)	45-57	47-57	60-66

It is stated in References 4.24 and 4.26 that the temperatures experienced by the LEU fuel during the ORR irradiations ranged from 25°C to 650°C. The upper end of this temperature range exceeds that for 2 MW operation in the UCD/MNRC. In addition, the performance of these fuels under extended thermal cycling and pulse heating has been reviewed and evaluated (Reference 4.1). The thermal cycling specimens were cycled 100 times out of pile and then 32 times in a neutron flux of  $4 \times 10^{12} \text{n/cm}^2 \text{ sec}$  over the temperature range of 500° to 725°C. The fuel displayed outstanding integrity and stability.

---

\*ORR maximum was  $1.26 \text{ max/avg} \times 55 \text{ kW}/55.9 \text{ cm} = 1.24 \text{ kW/cm}$ , UCD/MNRC maximum is  $1.33 \text{ max/avg} \times 33.2 \text{ kW}/38.1 \text{ cm} = 1.16 \text{ kW/cm}$

A 45 wt% uranium LEU fuel rod that was instrumented for measuring temperature and pressure was subjected to a series of 30 power pulses in a TRIGA<sup>®</sup> reactor to maximum temperatures in the range of 1050° to 1100°C. Only very modest (generally less than 2 psi) pressure pulses were measured in the rod as a result of the pulsing. This is in agreement with previous data showing negligible hydrogen release during the pulsing of 8.5 wt% uranium fuel to temperatures up to 1150°C. All surveillance examinations showed no rod deformation. Tests have shown that the pulse response of uranium-zirconium hydride TRIGA<sup>®</sup> fuel is independent of the uranium content of the fuel and is dominated by the behavior of the zirconium hydride, along with the prompt temperature coefficient of reactivity. Highly burned fuel does not necessarily have the benign response to power pulsing that was demonstrated in these tests. Hydrogen migrates to the fuel pellet periphery during burnup and a strong pulse under these conditions can produce excessive hydrogen pressure and cladding deformation. The pulse analysis in Section 13.2.2 predicts that highly irradiated fuel can be subjected to a reactivity pulse as large as \$1.92 without damage which justifies the \$1.75 limit specified in Section 4.7.

It was concluded in Reference 4.1:

*Tests of uranium-zirconium hydride fuels have shown that the limiting design basis for the operation of TRIGA<sup>®</sup> fuels is independent of uranium content up to at least 45 wt%.*

#### 4.5.4.2 Prompt Negative Temperature Coefficient

The basic parameter which provides the greatest degree of safety in the operation of a TRIGA<sup>®</sup> reactor system is the prompt negative temperature coefficient of reactivity. This temperature coefficient ( $\alpha$ ) allows great freedom in steady-state operation, since the effect of accidental reactivity changes occurring from experimental devices in the core is minimized.

The prompt negative temperature coefficient for the TRIGA<sup>®</sup>-LEU core is based on the same core spectrum hardening characteristics that occurs in a standard\* TRIGA<sup>®</sup> core. The spectrum hardening is caused by heating of the fuel-moderator elements. The rise in temperature of the hydride increases the probability that a thermal neutron in the fuel element will gain energy from an excited state of an oscillating hydrogen atom in the lattice. As the neutrons gain energy from the ZrH, the thermal neutron spectrum in the fuel element shifts to a higher average energy (the spectrum is hardened), and the mean free path for neutrons in the element is increased appreciably. For a standard TRIGA<sup>®</sup> element, the average chord length is comparable to a mean free path, and the probability of escape from the element before being captured is significantly increased as the fuel temperature is raised. In the water, the neutrons are rapidly rethermalized so that the capture and escape probabilities are relatively insensitive to the energy with which the neutron enters the water. The heating of the moderator mixed with the fuel in a standard TRIGA<sup>®</sup> element thus causes the spectrum to harden more in the fuel than in the water.

---

\*A standard TRIGA<sup>®</sup> core contains U-ZrH fuel with no erbium. The uranium is 8.5 wt-% with an enrichment of 20%, and the fuel element (rod) diameter is about 1.5 in. (3.8 cm) with a core water volume fraction of about 0.33.

As a result, there is a temperature-dependent disadvantage factor for the unit cell in which the ratio of absorptions in the fuel to total cell absorptions decreases as fuel element temperature is increased. This brings about a shift in the core neutron balance, giving a loss of reactivity.

In the TRIGA<sup>®</sup>-LEU fuel, the temperature-hardened spectrum is used to decrease reactivity through its interaction with a low-energy-resonance material. Thus, erbium, with its double resonance at  $\sim 0.5$  eV, is used in the TRIGA<sup>®</sup>-LEU fuel as both a burnable poison and a material to enhance the prompt negative temperature coefficient. The ratio of the absorption probability to the neutron leakage probability is increased for TRIGA<sup>®</sup>-LEU fuel relative to the standard TRIGA<sup>®</sup> fuel because the  $^{235}\text{U}$  density in the fuel rod is about 2.5 times greater and also because of the use of erbium. When the fuel-moderator material is heated, the neutron spectrum is hardened, and the neutrons have an increasing probability of being captured by the low-energy resonances in erbium. This increased parasitic absorption with temperature causes the reactivity to decrease as the fuel temperature increases. The neutron spectrum shift, pushing more of the thermal neutrons into the  $^{167}\text{Er}$  resonance as the fuel temperature increases, is illustrated in Figure 4.33, where cold and hot neutron spectra are plotted along with the energy-dependent absorption cross section for  $^{167}\text{Er}$ . As with a standard TRIGA<sup>®</sup> core, the temperature coefficient is prompt because the fuel is intimately mixed with a large portion of the moderator; thus, fuel and solid moderator temperatures rise simultaneously, producing the temperature-dependent spectrum shift.

For the reasons just discussed, more than 50% of the temperature coefficient for a standard TRIGA<sup>®</sup> core comes from the temperature-dependent disadvantage factor, or cell effect, and  $\sim 20\%$  each come from Doppler broadening of the  $^{238}\text{U}$  resonances and temperature-dependent leakage from the core. These effects produce a temperature coefficient of about  $9.5 \times 10^{-5}/^{\circ}\text{C}$ , which is essentially constant with temperature. On the other hand, for the TRIGA<sup>®</sup>-LEU core, the effect of cell structure on the temperature coefficient is smaller. Over the temperature range  $73^{\circ}$  to  $1292^{\circ}\text{F}$  ( $23^{\circ}$  to  $700^{\circ}\text{C}$ ), about 70% of the coefficient comes from temperature-dependent changes in  $\eta f$  within the core, and more than half of this effect is independent of the cell structure. Almost all the remaining part of the prompt negative temperature coefficient is contributed by Doppler broadening of the  $^{238}\text{U}$  resonances. Over the temperature range  $73^{\circ}$  to  $1292^{\circ}\text{F}$  ( $23^{\circ}$  to  $700^{\circ}\text{C}$ ), the temperature coefficient for the TRIGA<sup>®</sup>-LEU fuel is about  $1.07 \times 10^{-4}/^{\circ}\text{C}$ , thus being somewhat greater than the value for standard TRIGA<sup>®</sup> fuel. It is also temperature dependent.

The calculation of the temperature coefficient for standard TRIGA<sup>®</sup> and TRIGA<sup>®</sup>-LEU cores requires a knowledge of the differential slow neutron energy transfer cross section in water and ZrH, the energy dependence of the transport cross section of hydrogen as bound in water and ZrH, the energy dependence of the capture and fission cross sections of all relevant materials, and a multi-group transport theory reactor description which allows for the coupling of groups by speeding up as well as slowing down.

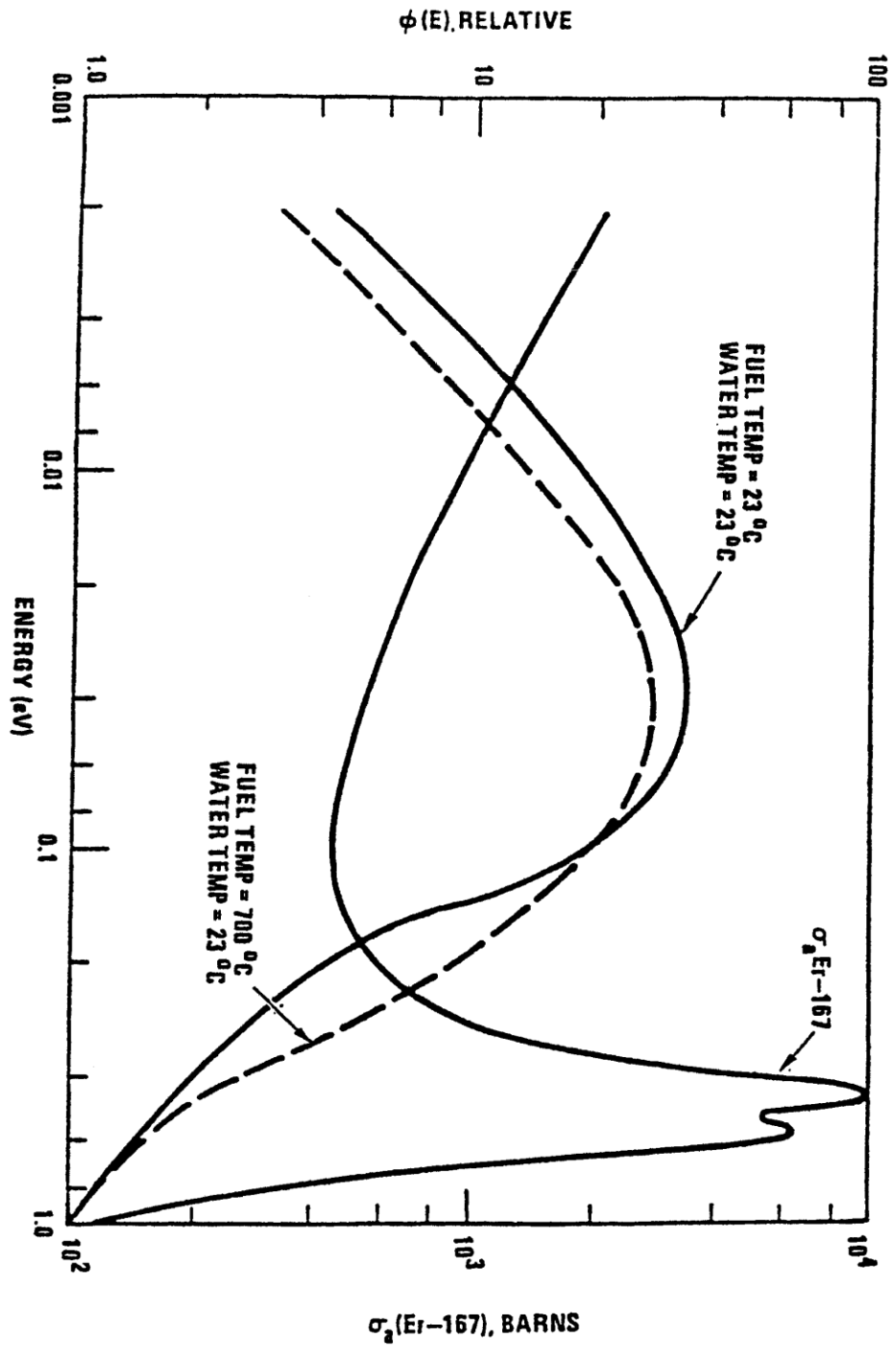


FIGURE 4.33 THERMAL NEUTRON SPECTRA VERSUS FUEL TEMPERATURE RELATIVE TO  $\sigma_a$  VERSUS ENERGY FOR Er-167

Qualitatively, the scattering of slow neutrons by ZrH can be described by a model in which the hydrogen atom motion is treated as an isotropic harmonic oscillator with energy transfer quantized in multiples of  $\sim 0.14$  eV. More precisely, the calculational model uses a frequency spectrum with two branches: one for the optical modes for energy transfer for the bound proton and the other for the acoustical modes for energy transfer with the lattice as a whole. The optical modes are represented as a broad frequency band centered at 0.14 eV and whose width is adjusted to fit measured cross-section data. The low-frequency acoustical modes are assumed to have a Debye spectrum with a cutoff of 0.02 eV and a weight determined by an effective mass of 360.

This structure then allows a neutron to thermalize by transition in energy units of  $\sim 0.14$  eV so long as its energy is above 0.14 eV. Below 0.14 eV, the neutron can still lose energy by the inefficient process of exciting acoustic Debye-type modes in which the hydrogen atoms move in phase with one another. These modes therefore correspond to the motion of a group of atoms whose mass is much greater than that of hydrogen, and indeed even greater than the mass of zirconium. Because of the large effective mass, these modes are very inefficient for thermalizing neutrons; but for neutron energies below 0.14 eV, they provide the only mechanism for slowing down the neutron. (In a TRIGA<sup>®</sup> core, the water provides for ample neutron thermalization below 0.14 eV.) In addition, in the ZrH it is possible for a neutron to gain one or more energy units of  $\sim 0.14$  eV in one or several scatterings from excited Einstein oscillators. Since the number of excited oscillators present in a ZrH lattice increases with temperature, this process of neutron acceleration is strongly temperature dependent and plays an important role in the behavior of ZrH-moderated reactors.

The temperature coefficient for the TRIGA<sup>®</sup>-LEU core increases as a function of fuel temperature because of the steadily increasing number of thermal neutrons being pushed into the  $^{167}\text{Er}$  resonance. This temperature-dependent character of the temperature coefficient of a TRIGA<sup>®</sup> core containing erbium is advantageous in that a minimum reactivity loss is incurred in reaching normal operating temperatures, but any sizable increase in the average core temperature results in a sizably increased prompt negative temperature coefficient to act as a shutdown mechanism. The temperature coefficients computed by GA Technologies (Reference 4.3) at beginning of life and 1000 and 2000 MWd of burnup are shown in Figure 4.34. After 1000 and 2000 MWd of burnup, the coefficient is less temperature dependent and smaller in magnitude than that for the initial clean core because of the sizable burnup of  $^{167}\text{Er}$  and the resulting increased transparency of the approximate 0.5-eV resonance region to thermal neutrons.

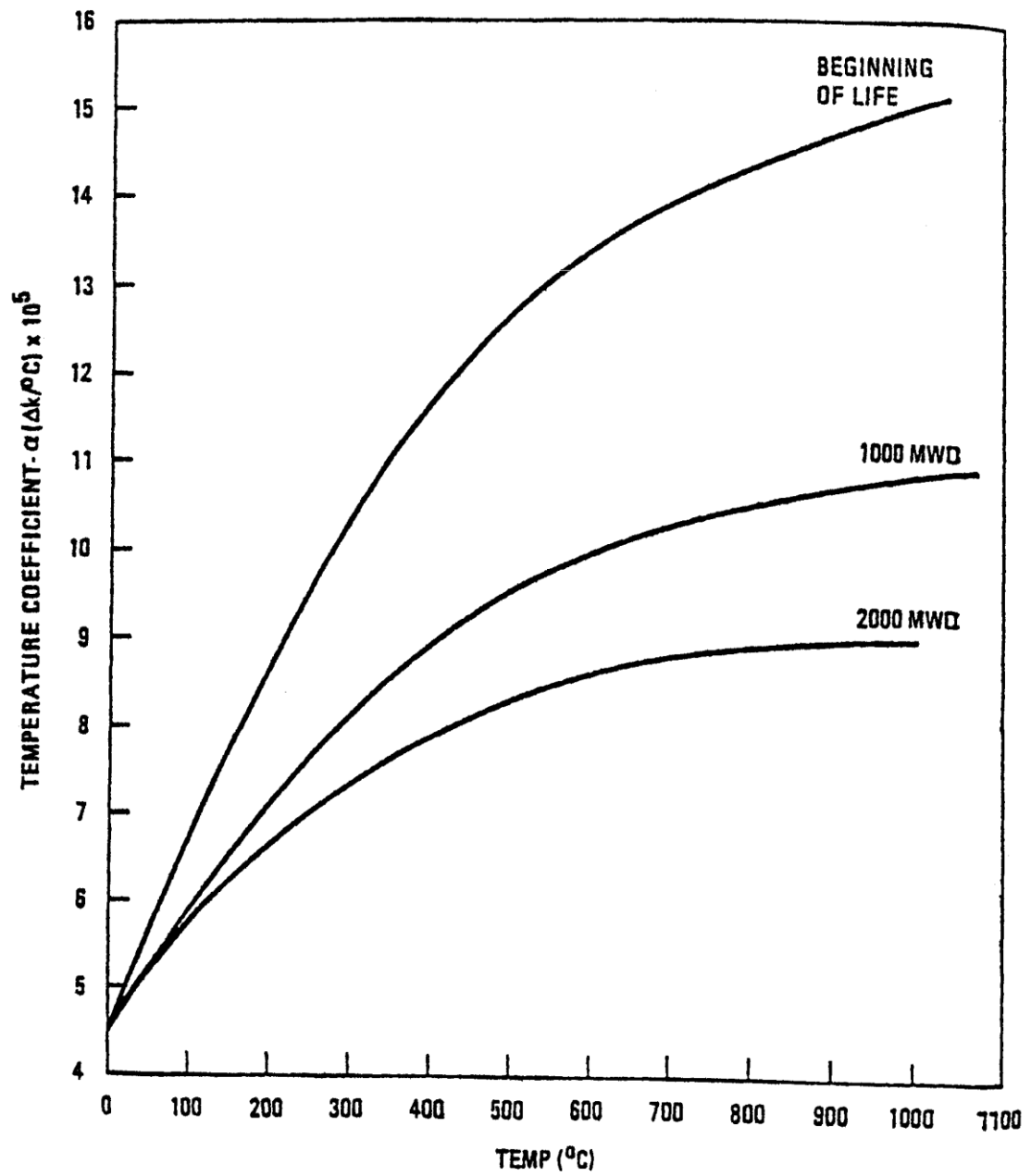


FIGURE 4.34 PROMPT NEGATIVE TEMPERATURE COEFFICIENT FOR TRIGA® LEU FUEL [20 wt-% URANIUM (19.7% ENRICHED), 0.47 wt-% ERBIUM]

The prompt negative temperature coefficient was computed for 20/20 and 30/20 fuel types at three burnups and several temperatures by Chen (Reference 4.28). The WIMS-D4 code and ENDF/B Version 5 cross section data base, which are described in Section 4.5.4.3 were used for these calculations. For a given burnup, a WIMS calculation of the eigenvalue was made for fuel at each of the discrete temperatures at which the scattering kernels for H and ZrH are available in WIMS. The scattering kernels in WIMS embody the energy transfer mechanisms described above. The fuel temperatures ranged for 300 °K to 1050 °K while the coolant temperature was kept at 300 °K. A simple finite difference approximation over 50° intervals was used to determine the temperature coefficient. For each fuel type and burnup, the data points from Chen's thesis were fit to a quadratic polynomial for use in the accident analyses in Chapter 13.

Evidence that this procedure yielded accurate prompt temperature coefficients is given in Figure 4.35. It shows the temperature coefficient for 20/20 fuel at approximately 13% <sup>235</sup>U burnup computed by two independent approaches, the procedure just described and a GA Technologies calculation. (The GA prediction is the 1000 MWD curve in Figure 4.34, which came from Reference 4.29, and the WIMS prediction is from Chen's 10 MWD/rod data.) The two predictions agree to within a few percent over the entire temperature range. When these two alternatives were used in Nordheim-Fuchs calculations of the peak temperature resulting from a \$2.20 step reactivity insertion, the resulting peak fuel temperature differed by only 4 °C.

The prompt negative temperature coefficient was computed for standard TRIGA<sup>®</sup> fuel (8.5/20) by GA Technologies (Reference 4.27). The temperature coefficient, which is essentially independent of temperature and burnup, is shown in Figure 4.18 of Reference 4.27 for a typical high-hydride TRIGA<sup>®</sup> core.

#### 4.5.4.3 Cross Section Generation

The WIMS-D4 code (Reference 4.30) and the ENDF/B Version 5 cross section data base were used to generate broad group cross sections for the steady state neutronic calculations. WIMS is a general lattice cell program that does a space and energy collapse of neutron cross sections using transport theory-based cell calculations. It has been used extensively for many light water reactor systems, including TRIGA<sup>®</sup> reactor calculations for the Reduced Enrichment Research and Test Reactor (RERTR) Program at Argonne National Laboratory (Reference 4.31).

Cross sections were produced for every cell type that could be anticipated for the 2 MW UCD/MNRC, about 20 in all. The dimensions and compositions used in the cell models were the latest information obtained from GA. The coolant area for the pin cells was based on the hex pitch of the new UCD/MNRC grid plate. Unlike the EPRI-CELL model, the central Zr rod in the fuel cells was not smeared throughout the fuel. For each of the four fuel cell types, an infinite lattice of that cell type was used. Non-fuel cells, e.g., the axial graphite reflector cell, were driven by a homogeneous core composition, with a water buffer region separating the core from the cell.

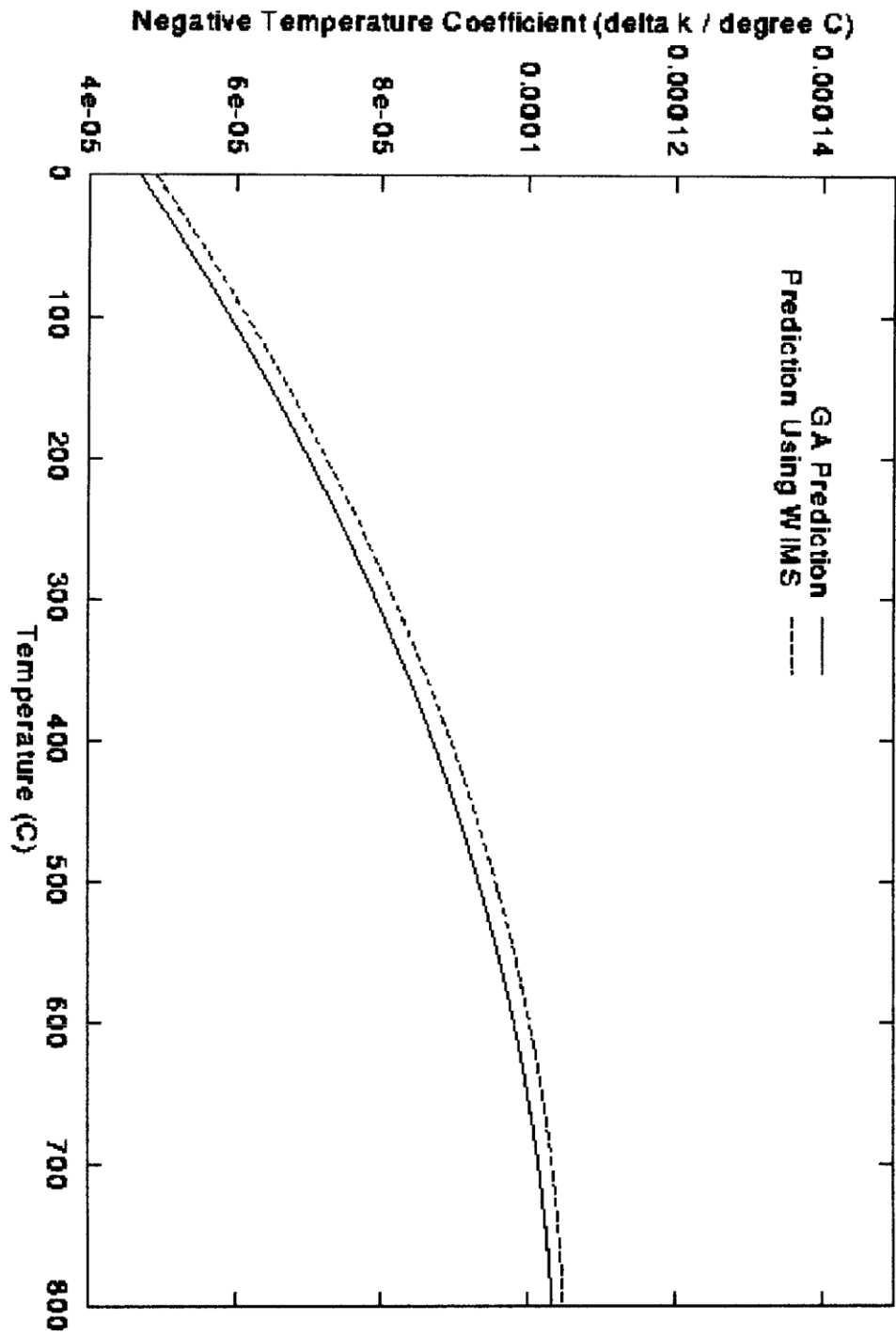


FIGURE 4.35 PROMPT NEGATIVE TEMPERATURE COEFFICIENT FOR 20/20 FUEL

Room temperature (300 K) was used, which implies that the cold-to-hot reactivity swing must be accounted for separately. The collapsing spectrum was generated with a near-critical buckling. The energy boundaries of the 7 broad groups were chosen to be as close to the standard 7-group GA structure as the WIMS based library's 69 fine group structure allowed.

Several tests of cross section accuracy were made, using continuous-energy Monte Carlo solutions produced with the VIM code as the standard (Reference 4.32). VIM provides essentially an approximation-free solution to the Boltzmann neutral particle transport equation limited only by statistical precision, the reactor description and the basic neutron cross section database. It has been used extensively in the analysis of critical experiment and for testing of deterministic methods (Reference 4.33). The cross sections produced with WIMS were supplied to a diffusion theory code (see DIF3D description in the next subsection) to obtain deterministic results. The results from one of these test problems, an infinite lattice of 20/20 fuel cells without leakage, are shown in Table 4-7. The deterministic eigenvalue is slightly low. The main contributor to this is under-prediction of  $^{235}\text{U}$  fission by 0.8%. Also, absorption in Zr in the hydride is over-predicted, probably because a WIMS problem made it necessary to use unbound Zr data. Overall, the agreement is quite good. For the next test, leakage was introduced by making the fuel cells 38.1 cm tall (and unreflected), while keeping the array infinite in the hex plane. The deterministic eigenvalue is within one standard deviation of the Monte Carlo value, 1.2480 compared to  $1.2472 \pm 0.0020$ . Next, axial reflector and steel end regions were added to the model. For this case, the deterministic eigenvalue is slightly low, 1.3034 compared to  $1.3056 \pm 0.0011$ . It was concluded from all these results that the accuracy of the fuel element cross sections generated with WIMS is more than adequate.

TABLE 4-7 CROSS SECTION ACCURACY TEST - INFINITE LATTICE OF 20/20 FUEL CELLS

Quantity		VIM Value	WIMS Value	WIMS Error
Eigenvalue		1.4200±.0011	1.4175	-0.0025
Balance				
absorption		1.0000±.0015	1.0000	0.0000
fission src		1.4190±.0025	1.4169	-0.0021
n, 2n		0.0005±.0000	0.0004	-0.0001
fission		0.5813±.0010	0.5804	-0.0009
capture		0.4187±.0005	0.4196	0.0009
Absorption				
U235		0.7036±.0012	0.6982	-0.0054
U238		0.0893±.0003	0.0889	-0.004
Er166		0.0042±.0000	0.0042	0.0000
Er167		0.0086±.0000	0.0085	-0.0001
Zr (rod)		0.0006±.0000	0.0008	0.0002
Zr (ZrH)		0.0228±.0001	0.0266	0.0038
H (ZrH)		0.0278±.0001	0.0277	-0.0001
U234		0.0031±.0000	0.0030	-0.0001
U236		0.0010±.0000	0.0010	0.0000
Fe		0.0202±.0001	0.0205	0.0003
H (H2O)		0.0303±.0001	0.0302	-0.0001
Fission				
U235		0.5786±.0010	0.5740	-0.0046
U238		0.0044±.0000	0.0046	0.0002
U234		0.0001±.0000	0.0001	0.0000
Spectrum				
Gr	Emax (ev)			
0	1.419E7	0.0005±0.0000	0	-0.0005

Quantity		VIM Value	WIMS Value	WIMS Error
1	1.000E7	0.3332±0.0005	0.3373	0.0041
2	5.000E5	0.2197±0.0002	0.2173	-0.0024
3	9.118E3	0.2643±0.0002	0.2643	0.0000
4	1.123E0	0.0273±0.0001	0.0272	-0.0001
5	4.000E-1	0.0341±0.0001	0.0336	-0.0005
6	1.400E-1	0.0722±0.0002	0.0721	-0.0001
7	5.000E-2	0.0486±0.0001	0.0483	-0.0003

A test of the cross sections generated for the boron poison region of control rods was also made. Self-shielding in the boron is extremely large, which made it difficult to get a well behaved solution from WIMS. A comparison of the effective cell average microscopic B-10 absorption cross section by group is shown in Table 4-8. The errors are statistically significant for most groups but they are not large. Thus, these cross sections should be adequate for computing rod worths.

**TABLE 4-8 TEST OF 10B CELL AVERAGE MICROSCOPIC ABSORPTION CROSS SECTIONS**

Group	VIM Value	WIMS Value	WIMS Error
1	0.352±0.4%	0.344	-2.3%
2	2.116±0.8%	2.190	3.5%
3	19.06±0.9%	19.82	4.0%
4	36.07±3.7%	32.98	-8.6%
5	31.62±3.1%	31.56	-0.2%
6	29.18±2.6%	28.90	-1.0%
7	24.69±2.9%	24.88	0.8%

#### 4.5.5 Reactor Physics Analysis - Reference Cores 1998 Analysis

##### 4.5.5.1 Original Hexagonal-Z Computational Model

An entirely new 2 MW calculational model of the UCD/MNRC was constructed for the 1998 license application. This analysis is left in this chapter to show it compares very well to the current October 2017 MCNP core model. A few assumptions had to be made about graphite components,\* but the new model rests on a reliable information base.

Descriptions of some of the more important cell types associated with elements are shown in Table 4-9. Here FFCR stands for fuel-followed control rods and TR stands for the transient rod. The outermost cell region in each element cell contains water and its outer boundary is a hexagon with a pitch of 1.714 in.. Material descriptions are given in Table 4-10. The elemental weight fractions for the two fuel types were obtained by averaging values from fabrication data sheets, a 31 element average for 20/20 fuel and a 4 element average for 8.5/20 fuel. The uranium isotopes were obtained as follows:  $^{235}\text{U}$  was from the fabrication data sheets,  $^{234}\text{U}$  and  $^{236}\text{U}$  were from an assay of 12 fuel samples, and  $^{238}\text{U}$  was the residual. Erbium isotopes for which no cross sections are available were ignored, not replaced by  $^{166}\text{Er}$ . The boron carbide description was taken from the previous UCD/MNRC model and it is nearly consistent with recently obtained manufacturing specifications.

A hex mesh with a 1.714 in. pitch was superimposed on the radial plane of the UCD/MNRC reactor. In the reactor grid region, this process is simple, since the mesh boundaries are natural, albeit artificial. At the edge of the grid and beyond, the volume fractions of materials within each hex mesh cell were determined using reasonable approximations. For cells at the inner and outer edges of the radial reflector, the approximation (good to a few percent) was to replace a hexagon divided by large-radius arcs, with an equivalent area circle divided by chords. For the reflector inserts, with their beam holes, the approximations were to shift some materials a fraction of a cell width and to replace circular hole cross sections with rectangles having nearly equivalent areas.

Aside from core loading variations, there are only a few unique radial (hex) plane layouts where this process had to be carried out. Examples of unique planes are the core, axial blanket and element end fixture levels. In the continuum, the slopes of the beam holes make the hex planes different throughout the height range of the beam holes. However, discretization into axial nodes leads naturally to the approximation of a small number of unique hex planes. Those planes differ only at the small fraction of hex cells where the slope causes the hole locations to step outward as the axial elevation increases. In order to reduce the model complexity further, all four beam holes were represented as having a 20° slope, even though one actually has a 30° slope.

---

\* All the graphite was assumed to have no impurities of neutronics significance and to have the typical density of reactor-grade graphite, 1.60 g/cc. The diameter of the graphite in dummy elements was assumed to be 1.435 in., which is larger than actual.

TABLE 4-9 DESCRIPTIONS OF SOME IMPORTANT ELEMENT CELL TYPES

Cell Type	Radial Regions From Center Outward (OD in inches)
Axial Reflector	graphite (1.353), void (1.438), 304SS (1.478), H2O
Fuel	Zr rod (0.225), void (0.250), fuel meat (1.435), void (1.438), 304SS (1.478), H2O H2O
FFCR Fuel	Zr rod (0.225), void (0.250), fuel meat (1.311), void (1.314), 304SS (1.354), H2O
FFCR B4C	B4C (1.300), void (1.314), 304SS (1.354), H2O
TR B4C	B4C (1.187), void (1.194), 6061A1 (1.250), H2O (1.399), 6061A1 (1.500), H2O
Dummy Graphite <sup>a</sup>	graphite (1.435), void (1.438), 6061A1 (1.478), H2O
Open Thimble	H2O (1.344), 6061A1 (1.500), H2O
Rabbit Tube	void (1.050), 6061A1 (1.158), void (1.330), 6061A1 (1.485), H2O

<sup>a</sup>After the analyses were completed it was determined that the clad wall thickness is actually 0.030 in., not 0.020 in.. Accordingly, the OD for the graphite and void shown here and used in the analyses are too large, but the effect on parameters of interest should be negligible.

TABLE 4-10 COMPOSITIONS USED IN THE HEX-Z UCD/MNRC MODEL

Material	g/cc	Element (Weight Fraction) <sup>a</sup>
30/20 Fuel Meat	7.1900	H (.01204), Zr(.67834), Er (.00889), U(.30072) [U234 (.00067), U235 (.05970), U236 (.00057), U238 (.23977)], impurities included in Zr
20/20 Fuel Meat	6.5474	H (.01337), Zr (.75411), Er (.00471), U (.19495) [U234 (.00044), U235 (.03859), U236 (.00037), U238 (.15555)], impurities (.03286) neglected
8.5/20 Fuel Meat	5.9643	H (.01597), Zr (.89067), U (.08325) [U234 (.00019), U235 (.01640), U236 (.00016), U238 (.06650)], impurities (.01012) neglected
Zr Rod	6.506	Zr (1.000)
304SS	8.032	Fe (.7012), Ni (.0925), Cr (.1900), Mn (.0100), Si (.0050)
6061A1	2.70	Al (.9720), Mg (.0100), Fe (.0035), Cr (.0020), Si (.0060), Cu (.0030) neglected
H2O	1.00	H (.1119), O (.8881)
B4C	2.49	C (.216), B (.784) [B10 (.156), B11 (.628)]
Graphite	1.60	C (1.000)

<sup>a</sup>Equivalent values of more common composition parameters are:

(net wt of fuel meat below is weight before hydriding, whereas weight fractions in the table are relative to gross weight, i.e., after hydriding)

*30/20 fuel meat* U-235 mass=165.5g, wt% U235 in U=19.85, wt% U in net wt=30.44, wt% Er in net wt=0.900, H/Zr atom ratio=1.606;

*20/20 fuel meat* U-235 mass=97.4g, wt% U235 in U=19.79, wt% U in net wt=19.76, wt% Er in net wt=0.478, H/Zr atom ratio=1.605;

*8.5/20 fuel meat* U-235 mass=37.7g, wt% U235 in U= 19.70, wt% U in net wt=8.46, wt% Er in net wt=0, H/Zr atom ratio=1.623;

*B4C* 19.9 wt% B10 in B.

The compositions used for positions of the UCD/MNRC hex plane model representing the reactor grid, the radial reflector, and positions touching the radial reflector or beyond are discussed in detail in Section 4.3.3 of Reference 4.4. The reactor grid is represented by 121 hex cell positions (Figure 4.10). The outer boundary of the model in the hex plane was specified so as to omit regions

of no significance to neutronics performance. There are 18 hex rings in the model but only the first 15 rings are complete. It was demonstrated with test calculations that completing these rings has no significant effect on any quantity of interest.

Many variations on this model were used in the analysis but they differ only in the reactor grid area. The meanings of reactor grid position symbols are given in the next section. Programs were written to easily modify the reactor grid loading and verify that the intended loading was as specified.

Although the use of diffusion theory is a source of error, the errors are acceptably small. The three-dimensional diffusion theory code used, DIF3D, employs modern nodal diffusion theory, which provides an accurate solution within the diffusion theory framework (Reference 4.35). It has been used successfully countless times for reactor design calculations and critical experiment analyses at Argonne National Laboratory and elsewhere. For leakage dominated performance quantities, such as beam tube flux, diffusion theory can be expected to indicate the relative merits of various loading options but not give accurate absolute performance levels. Diffusion theory should be acceptably accurate for the quantities of safety significance, such as excess reactivity, peak fuel element power and rod worths. When tested against a variational nodal transport solution, the DIF3D diffusion theory prediction of peak power was found to be in error by less than 1%.

Test calculation results indicate small errors from some other approximations: neglect of one of the fuel meat impurities (carbon), replacement of the Bi crystals in the beam tubes with stainless steel, and the spatial truncation error from using one node per hex in the radial plane. A calculation using  $^{166}\text{Er}$  as a substitute for the missing Er isotopes in 20/20 fuel, indicated that neglecting these isotopes could make the calculated excess reactivity for an all-20/20 loading too large by about \$0.7. The combined error from all sources, modeling, methods and data, is indicated by comparisons between calculations and measurements, described in the next section.

#### 4.5.5.1.1 Validation of Hexagonal - Z Model Analysis

Excess reactivity and rod worths measured in several loadings of two different TRIGA<sup>®</sup> reactors were compared to values computed with the new model and cross sections. In addition, the measured and calculated peak fuel temperature was compared in one case. A series of three loadings built during the initial startup of the Bangladesh reactor were modeled. These loadings had fresh 20/20 fuel in an hexagonal reactor grid. The hex equivalent of two previous UCD/MNRC loadings, the original Core B loading and the January 1995 mixed-fuel loading, were the other loadings used for the comparisons. Measurements in the Bangladesh reactor were made by GA during the commissioning of the reactor, and the measured data were supplied by W. L. Whittemore (Reference 4.35). For more detail of these modeled cores, see Section 4.3.3 of Reference 4.4.

While they give a reasonable indication of calculational accuracy, none of the comparisons below gives an unambiguous measure of the error in predictions of zero-power excess reactivity. Bang50 and Bang71 were essentially water reflected, which is unlike any loading of direct interest. The Bang100 model has the UCD/MNRC radial reflector with its inserts, rather than the Bangladesh reflector with its isotope production facility. That this difference can be significant is illustrated by the \$1.93 decrease in calculated excess reactivity when the reflector inserts were added to a previously clean model of the radial reflector. The Core B and Jan '95 loadings were actually in a circular grid but they were modeled in a hex grid. More importantly, all fuel is modeled as fresh, whereas, in reality, the Core B fuel was slightly burned and much of the Jan '95 fuel was quite burned.

The experimental and calculated results for zero-power excess reactivity are compared in Table 4-11. The errors are relatively small for the water-reflected cases, Bang50 and Bang71. The Jan '95 error is far larger than the others, probably because burnup was not accounted for in the calculation. As an attempt to generalize, it appears that calculated predictions are high by roughly  $\$1.0 \pm 0.2$  for graphite-reflected loadings with little burnup. Depending on how burned the fuel is, the prediction could be high by as much as another dollar or more.

**TABLE 4-11 COMPARISON OF MEASURED AND CALCULATED EXCESS REACTIVITY OF HEX-Z MODELED CORES**

<b>Zero-Power Excess Reactivity (\$)</b>			
<b>Loading</b>	<b>Measured</b>	<b>Calculated</b>	<b>Error</b>
Bang50	0.19	0.68	0.49
Bang71	8.94	8.89	-0.05
Bang100	10.27	11.40	1.13
Core B	6.75	7.62	0.87
Jan '95	6.95	8.78	1.83

The experimental and calculated results for rod worths are shown in Table 4-12. It appears that predictions of individual rod worths are generally accurate to within about 10%. Rod worths are measured one at a time, by moving the single rod against a bank of all the others. Correspondingly, the worth of each individual rod was calculated from the difference between a rod-up model and a rod-down model, where all other rods were banked at a constant, near-critical elevation. For the design scoping calculations in Section 4.3.3. of Reference 4.4, only the total rod worth was calculated and this was determined from the difference between all rods up and all rods down. Comparison of the calculated values in the last two rows of the table shows that this total rod worth is about 13% higher than the sum of individual rod worths.

**TABLE 4-12 COMPARISON OF MEASURED AND CALCULATED ROD WORTHS OF HEX-Z MODELED CORES**

<b>Rod Worth (\$)</b>			
	<b>Experimental</b>	<b>Calculated</b>	<b>C/E</b>
Core B			
Hex D10/Grid J04 FFCR	3.69	3.98	1.08
Bang100			
Hex D01/Grid D07 TR	2.24	2.32	1.04
Hex D04/Grid G10 FFCR	2.82	2.81	1.00
Hex D07/Grid J07 FFCR	2.73	2.70	0.99
Hex D10/Grid J04 FFCR	2.78	2.73	0.98
Hex D13/Grid G03 FFCR	3.06	2.80	0.91
Hex D16/Grid D04 FFCR	3.12	2.75	0.88
sum individual	16.75	16.11	0.96
all simultaneously		18.20	

A test of peak temperature predictions was made using a measurement performed in the Bang100 loading operating at 1.2 MW in the natural circulation mode. A neutronics calculation of the core power distribution was made and then these data were input to a thermal-hydraulic calculation. The accuracy of the prediction cannot be determined precisely, because the thermocouple was in a steep thermal gradient, although near the center of the fuel. Still, the agreement seems to be reasonable. The measured temperature was 415°C, the calculated centerline temperature is 440°C and the calculated temperature at the estimated thermocouple location is 425°C. These results constitute evidence that the neutronics calculations of power distributions are reasonably accurate.

#### 4.5.5<sup>2</sup> Reference Core 20E

The grid loading for the 20/20-fuel reference, 20E, is shown in Figure 4.36. It is a nearly-symmetric, single-fuel-zone, annular core design. As many grid positions as possible in Rows D through G are filled with fuel. There are only two fuel elements in Row C, with the rest of that row being filled with graphite dummy elements. The central cavity contains the central irradiation fixture-1 (CIF-1).

The calculated 20E zero-power excess reactivity is \$9.35 with all fresh fuel. If more fuel elements need to be added because of burnup losses, dummy elements could be replaced by fuel at corners of Row C. Calculations have confirmed that this does not produce a higher peak power. Substitutions of dummy elements for fuel in any row could be made to reduce the excess reactivity, although Rows C and G would probably be the best places. The

approximate reactivity change produced by a fuel-dummy substitution as a function of grid row is shown in Table 4-13. Again, the exact worth depends on the specific grid position.

**TABLE 4-13 FUEL-DUMMY SUBSTITUTION WORTH IN 20E**

<b>Position</b>	<b>Worth (\$)</b>
Hex C09/Grid G04	0.68
Hex D12/Grid H04	0.49
Hex E15/Grid I03	0.25
Hex F18/Grid J02	0.21
Hex G21/Grid K01	0.20

The peak element power in 20E is 34.8 kW (in Hex C07/Grid I05) with all fresh fuel and control rods fully up. The fueling of all available positions in Rows D through G was done to minimize the peak power. This step has only a weak effect on the peak power, since, for a given overall fuel distribution and total power, the peak is inversely proportional to the number of elements. There almost certainly would be no motivation to take this step if partially burned fuel were used in Row C. Thus, it should be acceptable to have some dummy elements in Row G, for example, if burned fuel is used in Row C.

The calculated control rod worths in 20E are shown in Table 4-14. The transient rod full-travel worth is \$1.95. Four of the FFCRs shown here have 8.5/20 fuel. These 8.5/20 rods will eventually reach their end of life and be replaced by 20/20 FFCRs. But this substitution has very little effect in an all-20/20 core. When this change was made in the model, the excess reactivity went up 8¢, the peak element power went down 1 kW and the worth of inserting all rods simultaneously was virtually unchanged. There are large rod interaction effects, which perturb the shutdown margin. Interaction is the cause of the large difference between the two predictions of total rod worth in the table. The individual worths in the table were computed with the other rods fully up. The worth of Rod Hex D07/Grid J07 was also computed with the other rods fully down. The result, \$4.51, is about twice as large as the value in the table. To estimate the effect on shutdown reactivity, the worth of dropping all rods from the full-up position but Rod Hex D07/Grid J07 not moving was modeled explicitly and was found to be worth \$12.83.

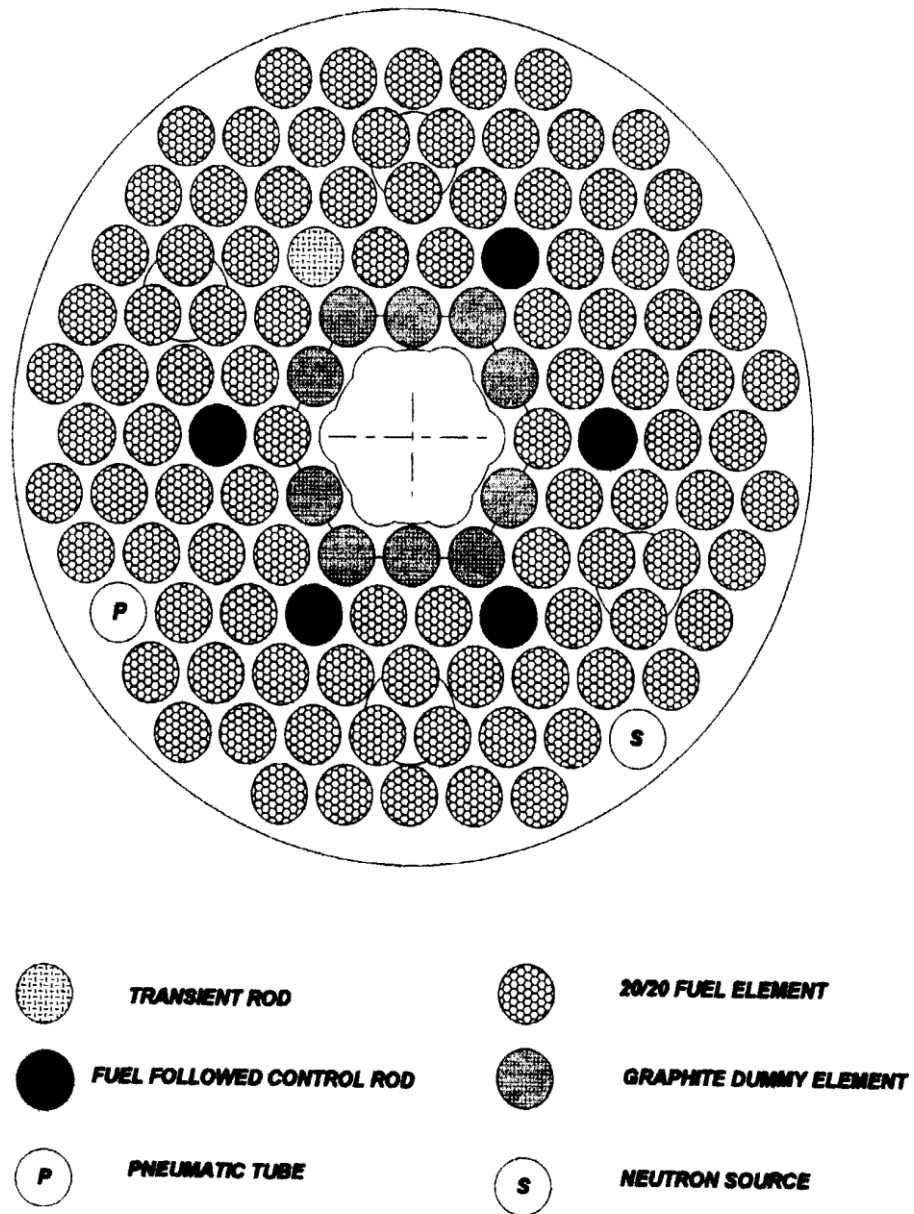


FIGURE 4.36 REFERENCE CORE 20E FUEL LOADING

Note: The initial load and test program for the 20E reference core requires the central irradiation fixture-1 (CIF-1) to be in place in the central cavity of the core.

**TABLE 4-14 CALCULATED ROD WORTHS IN 20E**

Rod(s)	Worth (\$)
Hex D01/Grid D07 8.5/20 FFCR	2.11
Hex D04/Grid G10 TR	1.95
Hex D07/Grid J07 20/20 FFCR	2.36
Hex D10/Grid J04 8.5/20 FFCR	2.31
Hex D13/Grid G03 8.5/20 FFCR	2.18
Hex D16/Grid D04 8.5/20 FFCR	2.12
sum individual	13.03
all simultaneously	17.34

This value is bracketed by two estimates that do not account properly for rod interactions: 1) omitting Hex D07/Grid J07 from the summation of individual rod worths in Table 4-14 yields \$10.67, and 2) subtracting the Hex D07/Grid J07 worth from the Table 4-14 worth of moving all rods simultaneously yields \$14.96.

The result is a shutdown margin of \$0.32. This is less than the required \$0.50 margin by \$0.18, indicating that the excess reactivity is required to be less than the assumed value by at least this much. According to Table 4-13, removal of a single fuel element from Row G would be sufficient to accomplish this. It is relevant to recognize two mitigating factors. One is that the assumed excess reactivity is an overestimate as demonstrated in Table 4-11. The other factor is that neglect of the rod interaction effect on this shutdown margin caused this estimate to be too small; based on values from the previous paragraph, this error is  $\$12.83 - \$10.67 = \$2.16$ .

Two alternatives to the central irradiation fixture-1 (CIF-1) were computed. Operation at full power with 20/20 fuel in Row C and the central facility filled with water was calculated to quantify the consequences. The excess reactivity decreased \$2.08. There is a 4% (1.5 kW) decrease in peak element power and a 3% increase in power peaking across the element. These results do not indicate that the power peaking is unacceptable when Row C 20/20 fuel is restricted to corner positions. However, because the separability assumptions used in the analysis are approximations, fuel temperature measurements at the anticipated hot spot should be made if this mode of operation is attempted. Replacing the central irradiation fixture-1 (CIF-1) with silicon results in a small drop in excess reactivity, \$0.07, and a small decrease in peak element power, 1.8 kW.

#### 4.5.5.3 Reference Core 30B

The grid loading for the 30/20-fuel reference, 30B, is shown in Figure 4.37. It is a nearly-symmetric, annular core design much like the 20/20-fuel reference (20E). Relative to 20E, it has seven fewer fuel elements in Ring G and two more in Ring C. There is a total of 96 fueled elements, including FFCRs. Fresh 30/20 fuel is used in all Rings except C, where fresh 20/20 fuel is used. The unfueled grid positions in Rings C and G contain graphite dummy elements. The central region contains the central irradiation fixture-1 (CIF-1).

The calculated 30B zero-power excess reactivity is \$8.20 with all fresh fuel. If more fuel elements need to be added because of burnup losses, these could replace any dummy elements in any position, even ones on the flats of Ring C. Calculations have shown that the peak element-integrated power would increase less than 1 kW and remain below the value in 20E for any such substitution. The approximate reactivity change produced by a fuel-dummy substitution as a function of grid ring is shown in Table 4-15. Element integrated power of fuel at the substitution position is also shown there.

The peak element-integrated power for the 30B loading with all fresh fuel and control rods fully up is 32.3 kW. Interestingly, the peak is not in Ring C (which has a maximum of 32.0 kW in Hex C07/Grid I05) but rather in Hex D05/Grid H09, which is next to the withdrawn transient rod (TR). This rod position provides another location (besides the neighboring Ring C dummy elements) where neutrons can slow down past the  $^{167}\text{Er}$  0.5 eV absorption resonance and then enter the uranium-rich 30/20 fuel element in Hex D05/Grid H09. It is this phenomenon of increased fissioning caused by escape of the Er poisoning effect that leads to use of 20/20 fuel, rather than 30/20 fuel, in Ring C of this reference design. This phenomenon is also the reason for the seemingly strange trend of substitution worths in Table 4-15.\*

---

\*The substitution of the dummy element causes the power to go up in neighboring fuel elements because neutrons slow down below the  $^{167}\text{Er}$  0.5 eV resonance in the dummy element. This increases the reactivity associated with the neighbors and partially offsets the reactivity loss from removing the fuel element. This partial compensation is less significant in Ring G than in interior rings because in Ring G the reflector already provides a means of escaping the Er poisoning effect.

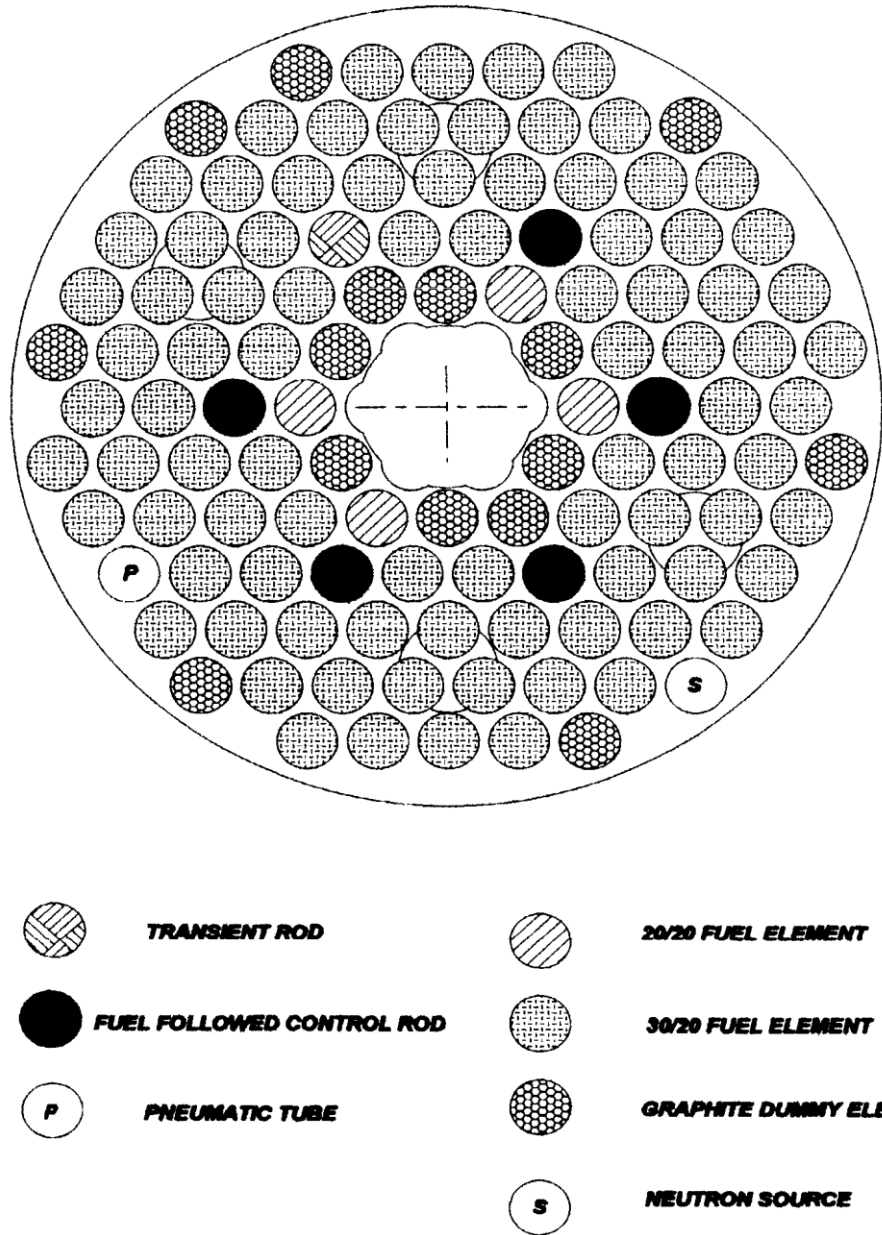


FIGURE 4.37 REFERENCE CORE 30B FUEL LOADING

Note: The initial load and test program for the 30B reference core requires the central irradiation fixture-1 (CIF-1) to be in place in the central cavity of the core.

**TABLE 4- 15 FUEL-DUMMY SUBSTITUTION WORTH IN 30B**

Position	Worth (\$)
Hex C04/Grid H08	0.60
Hex C09/Grid G04	0.56
Hex C10/Grid F05	0.61
Hex D12/Grid H04	0.40
Hex E15/Grid I03	0.19
Hex F18/Grid J02	0.15
Hex G21/Grid K01	0.20

**TABLE 4- 16 CALCULATED ROD WORTHS IN 30B**

Rod(s)	Worth(\$)
Hex D01/Grid D07	1.99
Hex D04/Grid G10	1.81
Hex D07/Grid J07	2.16
Hex D10/Grid J04	2.21
Hex D13/Grid G03	2.19
Hex D16/Grid D04	2.05
sum individual	12.41
all simultaneously	16.66

The calculated control rod worths in 30B are shown in Table 4-16. There are large rod interaction effects, as evidenced by the \$4 difference between moving all rods down simultaneously and summing the worths of lowering each rod computed with all other rods fully up. The prescription for determining the shutdown margin is to add \$1 to the excess, assume the highest worth rod (Hex D10/Grid J04 in this case) is stuck in the full up position and sum the individually measured rod worths. Following this prescription, using calculated rod worth values, yields a shutdown margin of \$1.00 for 30B. In contrast, the calculated value that includes rod interaction effects is \$3.24.

Two alternatives to the central irradiation fixture-1 (CIF-1) were computed. With the aluminum/graphite central plugs removed and the experiment facility filled with water, the excess reactivity decreased \$2.20, which probably does not leave enough reactivity for full power operation once Xe poisons build in. There is a 3% (1.1kW) decrease in peak element power in Hex D05/Grid H09 and a similar (0.9 kW) decrease at Hex C07/Grid I05, the hottest Ring C element. The 3% increase in predicted power peaking across the Ring C element for this condition in 20E should apply here to Hex C07/Grid I05 and the increase should be less in Hex D05/Grid H09. Thus, no excessive power peaking is predicted with the central water hole in the 30B loading. Replacing the central irradiation fixture-1 (CIF- with silicon results in a small loss of excess reactivity (\$0.21) and a small decrease in peak element power (0.7 kW). As in the other reference loadings, the silicon substitution presents no safety problem.

The performance results for 30B and the performance changes relative to 20E are presented in Reference 4.5. As might be expected, the two loadings have quite similar performance. The only difference of any consequence is that the flux is approximately 5% lower in 30B.

#### 4.5.5.4 Reference Core Considerations

Three configurations of the central region were computed. The central core irradiation facility has a boundary defined by a 4 in. OD Al tube with a 0.100 in. wall. The reference loading calculations had the central irradiation fixture-1 (CIF-1) in place in the central cavity. A radial slice through the central irradiation fixture-1 (CIF-1) is shown in Figure 4.38. The fixture has two plugs, a central aluminum rod, 2 in. in diameter, and an aluminum-clad graphite annulus. One or both of these plugs could be replaced by an experiment but no specific replacements have been calculated. A second configuration that was calculated for the reference cores is with the plugs removed and the central irradiation fixture-1 (CIF-1) filled with water. The results for peaking factors are shown in Table 4-17.

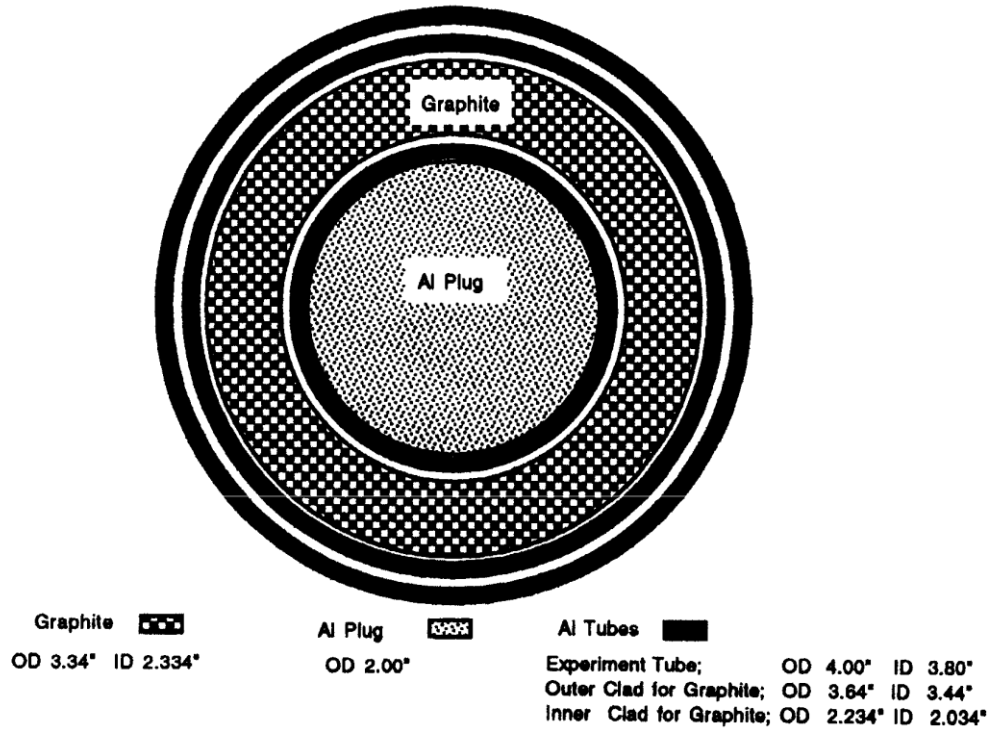


FIGURE 4.38 CROSS SECTION OF CENTRAL IRRADIATION FIXTURE-1 (CIF-1)

The final calculated configuration has the central irradiation fixture-1 (CIF-1) replaced by a 4 in. diameter column of silicon supported by aluminum rails that occupy 10% of the remaining water gap volume in Row B. This approximates the anticipated configuration for silicon doping irradiations in the central cavity. These results were stated earlier for the 20E, and 30B reference cores.

The neutron kinetics parameters used are the effective delayed neutron fraction,  $\beta_{\text{eff}}$ , and the effective prompt neutron lifetime. The  $\beta_{\text{eff}}$  is essentially 0.007 for all the variations in fuel type and loading arrangement.  $\beta_{\text{eff}}$  was used in this chapter to convert from calculated  $\Delta k/k$  to dollars. The prompt neutron lifetime is 32  $\mu\text{s}$  for an all-20/20 loading. To be conservative, the smaller value was used in the accident analysis in Chapter 13.

#### 4.5.5.5 Power Peaking Factor Analysis

..5 The thermal-hydraulic calculations of peak steady-state temperatures in Section 4.6 and the accident calculations of peak fuel temperatures in Chapter 13 require power peaking factors as input. The required peaking factors were obtained from steady-state neutronics calculations. Since the predicted temperatures determine safety limits, a reasonable amount of conservatism was built into the peaking factors. A conservative condition that runs through all the peaking factors is that fresh (unirradiated) fuel was used in all the neutronics calculations. Other conservative conditions are noted below.

As many as four factors contribute to the total power peaking factor, which is the ratio of the highest power density to the average power density in the fuel. The computed factors are displayed in Table 4-17 for several variations of the 20E reference loadings. The core radial factor is the ratio of the peak to average values of the element-integrated powers. It depends strongly on the core loading but weakly on the contents of the central cavity and the control rod bank position. The axial peaking factor depends strongly on the control rod bank position but weakly on the core loading and the contents of the central cavity. Based on these considerations, the conditions chosen for the temperature analyses are the 20E loading with control rods down 1/3 of their travel. (A constraint on the excess reactivity is that the rods will not have to be inserted more than 1/3 of their travel during 2 MW operation).

For the full-power steady-state temperature prediction, the axial and core radial peaking factors from Case 5 were used (i.e., the total peaking factor is 2.23). The central irradiation fixture-1 (CIF-1) has slightly higher peaking factors, so that condition is used.

The third and fourth factors account for the power distribution across the cross sectional area of the fuel element. The power density increases with radial distance from the center of the element because the population of neutrons that were thermalized in the coolant water increases with radius.

**TABLE 4-17 POWER PEAKING FACTORS**

Case	1	2	3	4	5	6	7
Loading	MixJ*	MixJ*	MixJ*	20E	20E	20E	20E
Center Contents	Al/C	Al/C	H2O	Al/C	Al/C	H2O	H2O
Rod Elevation	up	d 1/3	up	up	d 1/3	up	d 1/3
Peaking Factors							
core radial	1.37	1.36	1.35	1.76	1.68	1.68	1.60
axial	1.25	1.32	1.27	1.23	1.33	1.25	1.35
pin radial				1.33	1.33	1.33	1.33
pin tilt	1.32		1.50	1.64	1.63	1.69	1.68
Combined Factors							
first two	1.71	1.80	1.71	2.16	2.23	2.10	2.16
third and fourth				2.18	2.17	2.25	2.23
all four				4.72	4.84	4.72	4.86

\*Note: While the MixJ loading configuration is no longer used, the MixJ Power Peaking Factors (cases 1 through 3) are still listed here for reference in analyzing fuel loading errors (See Chapter 13 Section 13.2.5.2.2.1 1998 Fuel Loading Error).

The peaking factor that accounts for this (pin radial) was computed with the VIM Monte Carlo code for an infinite lattice of 20/20 fuel elements. The fact that the fuel element is in a non-uniform core, rather than in a uniform infinite lattice, alters the power distribution across the element. The peaking factor that captures this effect (pin tilt) was computed for the highest power fuel element using the RCT code (Reference 4.36), which reconstructs the flux within the homogenized node using the DIF3D nodal diffusion theory flux solution.

The peak-power element is in Row C and its pin tilt peaking factor is influenced primarily by thermalized neutrons coming from the central cavity. The water filled central irradiation facility is more effective at thermalizing neutrons than is the Al/C plug of the central irradiation fixture-1 (CIF-1), making the pin tilt factor larger with the water hole. A much stronger influence from water than Al/C was observed in node-average detector fission rates in the 20E loadings but it is not apparent in the 20E pin tilt factors.

For the pulse accident analysis, the four factors from Case 7 were used, (i.e., the total peaking factor is 4.86). The third and fourth factors were included here because the power peaking at the outer radius of the fuel element raises the peak fuel temperature under the adiabatic heating assumption of the analysis. Case 7 represents the worst-case conditions.

#### 4.5.5.6 The Future of the 30 B Core and the 2017 Core Model

It is not obvious from the original 1998 core modeling (describe in section 4.5.5 up to this point) of the 20E and 30B cores that the core radial peaking in section 4.6.2 is the maximum of all potential allowed core configurations described in section 4.5.3.

Axial peaking is most strongly a function of rod height position and is always maximized for low/no burn up cores because the control rods will be at their lowest position for given power level. As core excess reactivity is depleted control rods will be further withdrawn and the axial peaking factor will gradually decrease. The substitution of 30/20 elements for 20/20 elements in fuel rings D through G for cases 4-7 in section table 4-17 would have no negative effect on axial peaking (would not increase it to a value beyond 1.33) as the peaking in the 20E core is known to be the most severe (ref 4.5).

Pin radial peaking is a function of the fuel unit cell and is not altered by fuel loading patterns so long as fuel spacing and fuel type remain fixed. Due to the fact fuel spacing is fixed and that the 20E core is known to have the most severe pin radial and tilt peaking, using the maximum values in case 7 for accident analysis purposes is conservative (ref 4.5).

Core radial peaking is the peaking factor that varies the greatest with core loading. A discussion of how core radial peaking will be calculated in future variations (in order to ensure radial peaking is kept below the maximum value in table 4-12) of the 30B core is given below. While core radial peaking was originally found to be satisfactorily low in the reference 30B core it was known that placing 30/20 elements in a 20/20 environment increased power output (i.e. axial peaking) by approximately 15% relative to the original 20/20 element (ref 4.5). This axial peaking of 30/20 elements in a 20/20 environment is addressed in detail below.

In the past 25 years it has become increasingly common to model core neutronics with a 3 dimensional Monte Carlo simulation. Since the granting of the 1998 license to MNRC the facility has developed and benchmarked a detailed model of the reactor in MCNP5 (reference 4.44 ). This model is most commonly used to accurately estimate neutron energy profiles, estimate fuel burn up rate on a per element basis, and estimate changes to excess reactivity for fuel shuffles. In this section the model is described and compared to the original 1998 core model. This model is used to accurately predict radial peaking on a per element basis. The data that results from this analysis is in the form of averaged per element heat output at 2 MW steady state operation. This data is used to support that

the axial peaking factors calculated using the original 1998 core model are, in fact, the worst case scenario and therefore the thermal hydraulics analysis in section 4.6 is still bounding.

A study was performed to evaluate the current and future 30B core loading as described in the original 1998 SAR and core modeling. The main purpose is to make a direct comparison with the reference core loading 20E, which is stated as the worst case scenario for the thermo-hydraulic study in section 4.6. If the current and future 30B reactor core is conservatively operated in more favorable conditions (i.e. having lower peaking factors and thus having an additional safety margin than the worst case scenario), the thermo-hydraulic study (section 4.6) will remain valid and give reasonable assurance of safe reactor operations at the UCD/ MNRC for the term of the license renewal. The MNRC shifted to the 30B core in 2010. The current core has sufficient excess reactivity to support the expected utilization rate for an additional 6-10 years (from 2018). MNRC has petitioned the Department of Energy (fuel owner) to supply the MNRC with either 20/20 or 30/20 stainless steel clad elements when they become available to continue reactor operation indefinitely. Therefore, the 30B is the only foreseeable core configuration at the MNRC. If MNRC intends to utilize any fuel type other than 20/20 or 30/20 stainless steel clad fuel a new neutronics analysis must be performed and submitted to the NRC for approval.

Monte Carlo (MCNP) code, version 5, with ENDF/ B-VI continuous neutron and photon cross-section data, has been used to evaluate the 30B core loading with both the 20/20 and 30/20 type TRIGA fuel elements (FEs), together with five control rods having 20/20 type fuel as follows. This base case is our reactor core configuration on October 2, 2017, which is the most recent core configuration for reporting and completing our fuel depletion and inventory. To evaluate the clean reactor core excess reactivity compared to the reactor operational data for a benchmark, all six control rods, including five fuel followed control rods (FFCRs) and one transient rod, are completely out of the core, or in full up position. The clean excess reactivity is calculated to be \$5.42, which is consistent with the measured value of \$5.41 in the startup of Monday morning on October 2, 2017.

After the benchmark calculation was found to be satisfactory, two more MCNP runs were performed. Both of the following MCNP runs have the same central irradiation fixture-1 (CIF-1) in place in the central facility to make a direct comparison to the worst case scenario in the original 1998 calculation. The initial 20E reference core was run with all fresh 20/20 type fuel elements and all control rods lowered 1/3 of their travel from the full up position. The total heat released in G4 and G8 positions in the C-hex, after a normalization of 2.0 MW for the total reactor output, are 32.4 kW and 33.3 kW, respectively. These values are consistent with the hottest fuel rod value, 33.2 kW, which is stated in section 4.5.5.4 and was used as the basis for the thermo-hydraulic analysis in section 4.6.

The second calculation was performed for the current and future 30B core configuration with all control rods lowered 1/3 of their travel from the full up position as well. The

hottest fuel rod among 30/20 type FEs is 28.9 kW at K5 position in the E-hex, after a normalization of 2.0 MW for the total reactor output. The hottest fuel rods among 20/20 type FEs are 28.6 kW and 28.8 kW at F8 and H5 positions in the C-hex, respectively. These values are consistent with our previous studies to guide fuel deployment or shuffling at the MNRC that the total heat for each in-core fuel element shall be less than 32.0 kW, after a normalization of 2.0 MW for the total reactor output, as our routine evaluation guideline.

The primary reasons leading to the worst case scenario in the initial 20E reference core can be realized by examining the surroundings of fuel elements at G4 and G8 positions in the C-hex. Instead of neutron competing fuel elements in the C-hex as in our current and future 30B core configuration, graphite dummy elements are placed next to the fuel elements at G4 and G8 positions. Neutron fluxes, or the total heat, are enhanced by firstly, graphite as a neutron reflector compared to uranium-zirconium-hydride as a neutron absorber, and secondly, aluminum as the cladding for the dummy elements compared to stainless steel, a neutron absorber, as the cladding for the fuel elements. Thirdly, fresh 20/20 type fuel elements are used in the initial 20E reference core loading. Therefore, the total heat of the hottest fuel rods are more than 10% higher than that of any hottest fuel rod in our current and future 30B core loading.

In addition, all of the current neutron applications at the MNRC do not require any extended 2.0 MW operation power. As a matter of fact, MNRC has been operating up to 1.0 MW and on rare occasion up to 1.5 MW, since April 2007 for all of its neutron application activities. In the case of 1.5 MW operating power, the total heat of the hottest fuel rod in our current and future 30B reactor core will be <22.0 kW.

From the above calculations and evaluations, we are confident to conclude that the total heat of each in-core fuel element in our current and future 30B core will stay 10% below the hottest value of 33.2 kW which was the worst case scenario of the initial reference core loading 20E. Since this unique value was used, and scaled up by a factor of 1.15 to make the temperature calculations for the maximum analyzed power of 2.3 MW, we are even more confident that our current and future operation conditions will be conservative, safely covered by the original thermo-hydraulic study for steady state operation at the MNRC.

Axial peaking and radial peaking factors will decrease in magnitude as the core burnup is increased. Thus the thermal hydraulic analysis in section 4.6 becomes more conservative as core burnup increased. It is unknown at this time if new TRIGA fuel will be available to the MNRC before the MNRC's eventual decommissioning. If suitable fuel does become available it will be slowly introduced to the core replacing the approximately 1/3 of the core which contains high burnup elements (>30% U-235 consumption). It is very unlikely an entirely fresh 30B core will be loaded into the MNRC reactor. In this unlikely event it is highly recommended the entire core is modeled in detail to ensure the peaking analysis in the chapter and the resulting thermal hydraulic analysis are bounding.

In order to maintain a high degree of confidence that the thermal hydraulic analysis in section 4.6 is bounding for all 30 B core configurations maximum fuel element heat output shall be limited to 32 kW at 2.0 MW steady state operation. This restriction is put in place to limit the amount of radial peaking in the core which represents an additional safety margin in an already conservative analysis. This will likely preclude the placement of 30/20 elements in the D ring, which would not impact any planned operations.

#### 4.5.5.7 Neutron Flux Analysis

The rates of production of the radioactive gases Ar-41 and N-16 in the core are computed in Appendix A. These computations require values of core-average fluxes as input. The thermal flux is needed for the Ar-41 calculation and the flux above 0.6 eV is needed for the N-16 calculation. These fluxes were obtained from steady-state neutronics calculations.

The core-average fluxes over energy ranges of interest are given in Table 4-18 for five different core loadings. The thermal flux boundary used here is 1.1 eV. It is apparent from these data that the thermal flux level depends strongly on the proportions of 8.5/20 and 20/20 fuel types in the core. This is because the erbium and the high concentration of uranium in the 20/20 fuel depress the thermal flux. These results are for fresh fuel and the thermal flux depression would decrease as the erbium and uranium are depleted. The flux above 0.6 eV has a relatively weak dependence on the fuel mix.

Since the flux values decrease with increasing 20/20 and 30/20 content, it is conservative to use values at the all-8.5/20 fuel limit. Accordingly, the recommended values to use in Appendix A are  $2.0 \times 10^{13}$  thermal flux for Ar-41 production and  $4.2 \times 10^{13}$  flux above 0.6 eV for N-16 production.

TABLE 4-18 CORE AVERAGE NEUTRON FLUXES

Loading	Fueled Elements			Core-Average Flux ( $10^{13}$ n/cm <sup>2</sup> s)		
	8.5/20	20/20	30/20	Thermal	Above 0.6 eV	Total
@ 1 MW						
Core B	89	0	0	0.98	2.09	3.02
Jan '95	63	30	0	0.75	1.96	2.66
@ 2 MW						
Core B	89	0	0	1.97	4.18	6.04
Jan '95	63	30	0	1.50	3.92	5.33
MixA	48	48	0	1.38	3.70	4.99
MixJ	50	49	0	1.36	3.71	4.97
20E	4	97	0	0.87	3.57	4.35
30B	0	9	87	0.60	3.68	4.20

## 4.5.5.8 Fission Product Release Fraction

Considerable effort has been expended to measure and define the fission product release fractions for TRIGA® LEU fuels. Data on this aspect of fuel performance are reported in References 4.24, 4.25 and 4.26 and evaluated in Reference 4.1.

Using these data, GA developed a conservative correlation for fission gas release:

$$\text{Release Fraction} = 1.5 \times 10^{-5} + 3600e^{-13400/T};$$

where:

T = fuel temperature in degrees Kelvin.

In characterizing the conservatism, it is stated on page 35 of Reference 4.25, "At normal TRIGA® operating temperatures (<750°C), there is a safety factor of approximately four between predicted values by the above equation and experimentally deduced values." The same observation is reported in Reference 4.37. This correlation was adopted to predict the release of the inert gases and semi-volatile halogen fission products to the fuel-clad gap.

It is generally accepted that the solid fission products (those having low volatility, such as Cs and Sr) are released at significantly lower rates.

The appropriate temperature to use in the GA correlation is the fuel temperature averaged over the irradiation history. The fuel can be characterized as having two separate temperature histories: the average temperature the fuel experienced during its steady state irradiation and the temperature the fuel may experience during the accident that is presumed to lead to a cladding rupture. To induce rupture, the fuel temperatures must equal or exceed the safety limits. The basis for defining the appropriate fuel temperature, and thus the release fraction, is given in Chapter 5 of Reference 4.8, as follows:

“The release fraction for accident conditions is characteristic of the normal operating temperature, not the temperature during accident conditions. This is because the fission products released as a result of a fuel clad failure are those that have been collected in the fuel-clad gap during normal operation.”

The fuel temperatures used to compute the release fraction are those predicted for the worst-case normal operating conditions. Of all the projected normal operating conditions, the highest element power occurs at position C7 of the 20E (all-20/20 fuel reference) loading when the control rods are banked 1/3 down from the full up position. This element's power was used in the thermal-hydraulic model of the 20E loading to predict the radial and axial fuel temperature distribution in the hottest channel (Section 4.6).

The gaseous fission product release fraction was determined by integrating over this hottest element's fuel. The release fraction at a given fuel node was found by evaluating the correlation function at the node-average fuel temperature. Weighting by the volume fraction of the node and summing over all fuel nodes yielded  $7.7 \times 10^{-5}$ , the fraction of gaseous fission products released to the fuel-clad gap. This is the value recommended for use in the accident analyses.

#### 4.6 Thermal and Hydraulic Design

The thermal and hydraulic required analysis has been performed for operation of the UCD/MNRC at a nominal 2 MW and maximum 2.3 MW power using the RELAP5/MOD3 computer program (Reference 4.37). The RELAP5 code was developed for the USNRC by the Idaho National Engineering Laboratory (INEL) to analyze transients and accidents in light water reactors. The RELAP5 code is highly generic and can be used to analyze a wide variety of hydraulic and thermal transients involving almost any user defined nuclear or non-nuclear system.

The MOD3 version of RELAP5 has been developed jointly by the NRC and a consortium of several countries and domestic organizations that are members of the International Code Assessment and Applications Program (ICAP). The RELAP5/MOD3 development program included many improvements based on the results of assessments against small-break LOCAs and operational transient test data.

A RELAP5 model consists of a system of control volumes connected by flow junctions. The fluid mass, momentum, and energy equations along with the appropriate equation of state are solved for the user defined geometry. The RELAP5/MOD3 code uses a full non-homogeneous, non-equilibrium, six-equation, two-fluid model for transient simulation of two-phase system behavior. User defined heat structures are used to simulate the reactor fuel rods. Heat transfer coefficients are computed as appropriate for the channel flow and fluid state. A space independent reactor kinetics model is available for reactivity transients.

Some of the RELAP5/MOD3 features important for simulating a natural circulation reactor like UCD/MNRC include:

- ability to compute the system density distribution and the gravity force terms in the momentum equation;
- ability to compute implicitly the local pool or convective sub-cooled boiling, which is known to occur in TRIGA<sup>®</sup> reactors;
- a new critical heat flux correlation for rod bundles based upon an extensive tabular set of experimental data;
- temperature dependent material properties;
- special cross flow models that allow simulation of the two dimensional flow due to radial power differences in the core.

Analyses of many different systems have been reported in the open literature using RELAP5. Many of the system transients analyzed were at low pressure and with natural circulation flow. The RELAP5 code selects the heat transfer correlation to be used based upon the wall temperature and local flow and fluid state. The critical heat flux correlation also uses local conditions and implicitly accounts for axial power distribution. The critical heat flux correlation is further corrected for potential errors if the correlation is entered with flow and fluid conditions which are not in the dominant regions of the data base. The RELAP5 code can thus be used for analysis of the UCD/MNRC thermal and hydraulic performance.

#### 4.6.1 Thermal and Hydraulic Analysis

As power in the UCD/MNRC core is increased, nucleation begins to occur on the fuel rod surfaces and fully developed nucleate boiling occurs. If the surface heat flux remains below the critical heat flux (CHF) it is possible to increase the heat flux without an appreciable increase in fuel rod surface temperature. If the CHF is exceeded, film boiling occurs and the surface temperature increases almost immediately to a much higher value and fuel rod damage will occur. The safe operation of the reactor is dependent upon the operating heat flux in relation to the critical heat flux. The ratio of the critical heat flux to the peak core heat flux is a measure of the safety margin.

The RELAP5 model used in the UCD/MNRC analyses is shown in Figure 4.39. The model specifies pipe, branch, or single volume components for all major regions of water between the lower grid plate and the upper water surface. These components are connected by junctions as required. Heat structures are defined to simulate the fuel in the average core and hot channel. The hot fluid channel is conservatively assumed to be connected only to rods with the hottest fuel rod power. Pipe components are divided into a user specified number of volumes. In the core region where the axial distribution is important, pipe components with 9 axially distributed volumes were used for the average and hot channel regions. Branch components contain a single volume with a user specified number of junctions connecting to other components. Branches were used to model the unfueled rod regions directly above and below the active core. Single volume or pipe components and single junction components were used for the balance of the system.

The primary loop, including the N-16 diffuser, was also modeled. Time dependent junctions were used to model the flow from the upper reactor tank and the return flow to the diffuser and lower tank. The diffuser flow was assumed to be 20% of the total primary flow. A time dependent volume was used to reference the entire model to atmospheric pressure.

The net driving force for flow within the UCD/MNRC tank is the difference between the net buoyancy of the water heated in the core and the friction within the flow paths. Both are computed implicitly by the RELAP5 code. The friction losses consist mainly of the wall friction within the fuel pin flow channels and form losses in the upper and lower grid regions. Friction in other flow paths are computed but are small due to the low velocities. The wall friction is computed directly within RELAP5.

The form loss coefficients for the upper and lower grid regions are supplied as input to the code. Values were computed from data presented in handbooks for similar geometries. These calculated loss coefficients are significantly larger than those used by General Atomics (Reference 4.38) in their analyses. The set of loss coefficients selected for a given calculation was the one that yielded the more conservative result for the quantity of interest. The computed values were used for the reactor thermal and hydraulic analyses in this section since they yield higher temperatures. A separate calculation was performed using the General Atomics loss coefficients to provide a higher flow rate for use in the fission gas transport calculations in Appendix A of this addendum.

The steady state fuel temperature depends strongly upon the thermal resistance at the fuel cladding interface. The resistance was assumed to be zero as in prior SAR analyses (Reference 4.39).

The buoyancy of the water in the core hot channel can be influenced by the cross flow between the hot and average channels. Traditionally the hot and average channels have been assumed to be completely separate (no cross flow) because of the very narrow spacing between the fuel rods. The RELAP5 code provides a means for estimating the effects of cross flow between the hot and average flow channels. The cross flow effect is expected to be very small, and it is impossible to assess the accuracy of computed cross flows. Scoping calculations with RELAP5 showed cross flow to have no effect on fuel temperature and to slightly increase the critical heat flux ratio. Thus, cross flow is conservatively neglected in this analysis.

**RELAP5Components**

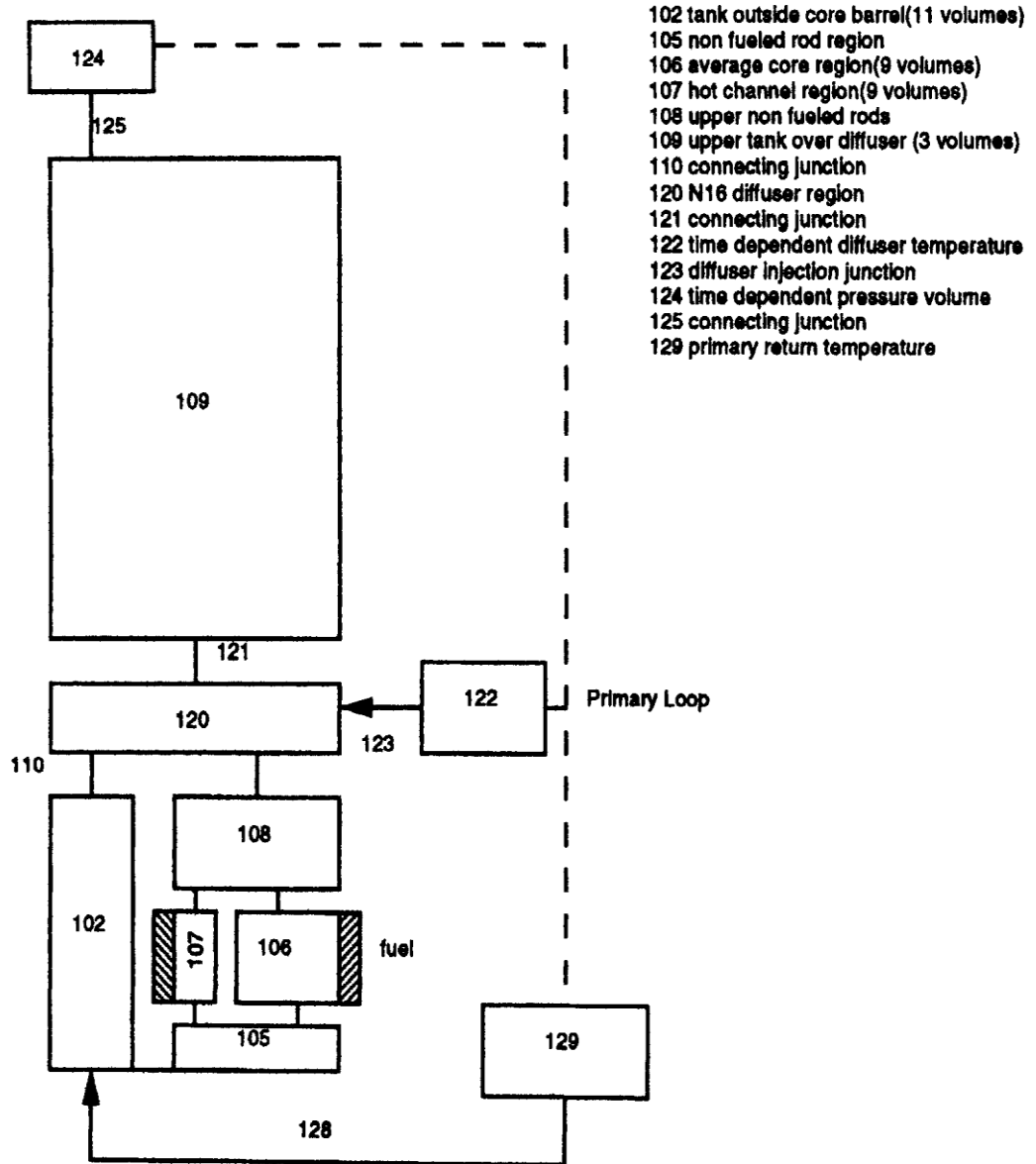


FIGURE 4.39 UCD/MNRC RELAP5 MODEL

#### 4.6.2 Steady State Results

The RELAP5 model described above was used to evaluate the thermal and hydraulic performance of the UCD/MNRC during steady state operation. The power distribution in the model corresponds to worst case conditions as described in Section 4.5.5.4. This is referred to as Case 5, the 20E reference loading with the control rods lowered 1/3 of their travel from the full up position. The axial power shape from the 3-D neutronics calculation, shown in Figure 4.40, was used. The axial peaking factor was 1.33. The core was assumed to have 101 fuel elements with the hot fuel rod operating at 33.2 kW for a radial peaking factor of 1.68. This fuel rod power comes from a normalization of 2 MW for the total reactor output. It is less than the value of 34.8 kW in Section 4.5.5.2 because lowering the control rods reduces the neutron flux in the central region of the reactor core, which results in more power being produced in the outer region of the core. The 33.2 kW value was scaled up by a factor of 1.15 to make the temperature calculations for the maximum analyzed power of 2.3 MW. The total peaking factor (axial × radial) was 2.23, which is higher than the 2.0 assumed in prior SAR analyses. The radial power distribution in the fuel was conservatively assumed to be uniform. The temperature dependent fuel thermal properties were obtained from Reference 4.8. Two calculations were performed. The power level and core inlet temperature were assumed to be at the maximum analyzed limits of 2.3 MW and 45°C, respectively, for the first case (Reference 4.40) and at nominal operating conditions with power of 2.0 MW and 32.2°C inlet temperature for the second case (Reference 4.4).

The steady state results are presented in Table 4-19.

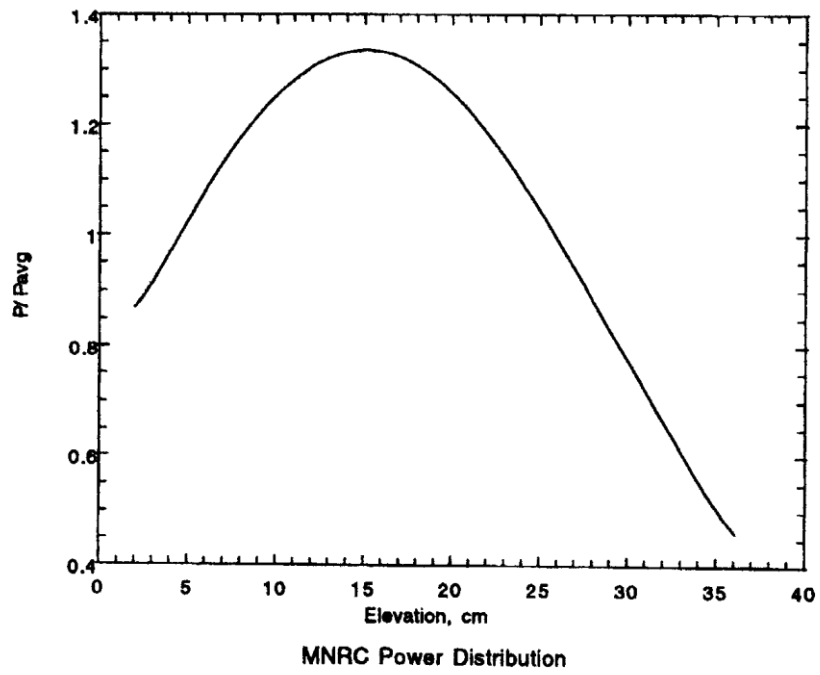


FIGURE 4.40 UCD/MNRC POWER DISTRIBUTION

**TABLE 4-19 HEAT TRANSFER AND HYDRAULIC PARAMETERS FOR OPERATION WITH 101 FUEL ELEMENTS**

<b>Parameter</b>	<b>At Limiting Inlet Temperature (45°C) and 2.3 MW</b>	<b>At Nominal Inlet Temperature (32.2°C) and 2.0 MW</b>
Diameter of Fuel Element	3.75 cm	3.75 cm
Length of Fuel Element	38.1 cm	38.1 cm
Flow Area	546 cm <sup>2</sup>	546 cm <sup>2</sup>
Hydraulic Diameter	1.86 cm	1.86 cm
Heat Transfer Surface Area	4.53 m <sup>2</sup>	4.53 m <sup>2</sup>
Inlet Coolant Temperature	45.0°C	32.2°C
Exit Coolant Temperature	109.3°C	103°C
Upper Pool Temperature	73.8°C	57°C
Coolant Mass Flow	8.5 kg/sec	6.7 kg/sec
Avg Fuel Temperature	365°C (hot pin) 269°C (average pin)	341°C (hot pin) 254°C (average pin)
Maximum Clad Surface Temperature	180°C	144°C
Maximum Fuel Temperature	705°C	631°C
Avg Heat Flux	50.8 w/cm <sup>2</sup>	44.2 w/cm <sup>2</sup>
Max Heat Flux	113 w/cm <sup>2</sup>	98 w/cm <sup>2</sup>
Hot Channel Outlet Void	6.6 %	2.0%
Core Outlet Subcooling	5.3 °C	11°C
Minimum CHF Ratio	2.40	2.94

The minimum critical heat flux ratio of 2.40 is much higher than the values calculated in prior safety analyses because of the very conservative correlations used in the past. The current value indicates that a significant margin exists between the maximum operating power (2 MW<sub>t</sub>) and the power that would result in exceeding the critical heat flux. The magnitude of the critical heat flux is dependent upon local fluid conditions as well as channel inlet conditions and power. The change in magnitude as power increases is, thus, not linear with power and the critical heat flux correlation cannot be used directly to determine the CHF. It is not practical to perform numerous RELAP5 analyses to determine the power level at which the CHF would exactly equal 1.0.

All other reactor parameters in Table 4-19 are also acceptable. The predicted fuel temperature is well below 750°C. The calculated coolant temperature and void distributions in the hot channel for both the nominal and limiting cases are shown in Figure 4.41. The liquid subcooling and low channel voids are expected to result in condensation of the vapor immediately after detaching from the fuel rod surface, thus the process of heat removal by natural convection is assured and fuel temperatures will be well below the safety limit. Chugging and the resultant power fluctuations are, therefore, not expected to occur (Reference 4.41). If chugging were to occur, it would be detectable below the level of any safety concern and the power could be reduced to eliminate it. Experiments conducted by GA demonstrated that there was no fuel damage from deliberately induced chugging although associated power fluctuations could be readily observed (References 4.42 and 4.43).

## 4.7 Operating Limits

### 4.7.1 Operating Parameters

The main safety consideration is to maintain the fuel temperatures below the value that would result in fuel damage. The fuel temperature is controlled by setting limits on other operating parameters (i.e., limiting safety system settings). The operating parameters established for the UCD/MNRC reactor are:

- a. Steady-state power level;
- b. Fuel temperature measured by thermocouple;
- c. Maximum step reactivity insertion of transient rod;
- d. Maximum core inlet coolant water temperature.

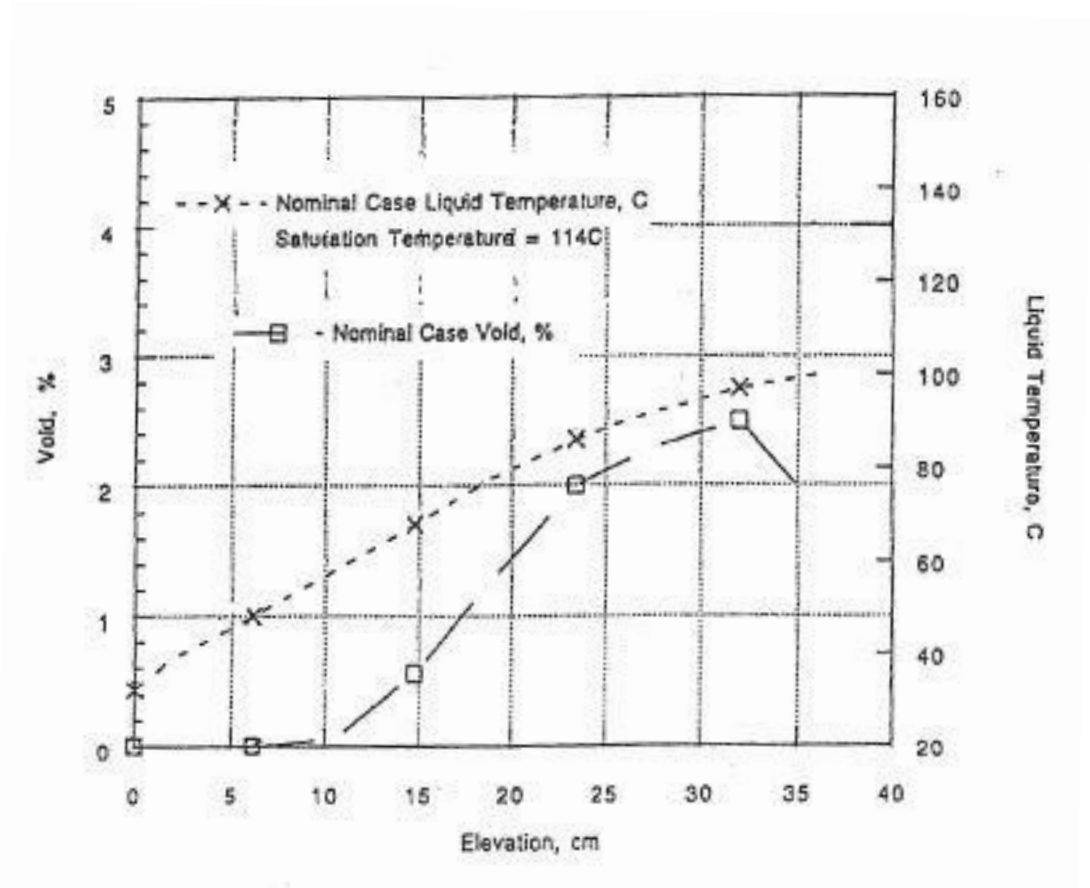


FIGURE 4.41 CALCULATED COOLANT TEMPERATURE AND VOID DISTRIBUTION

#### 4.7.2 Limiting Safety System Settings

The limiting safety system settings given in Table 4-20 are defined to assure that the safety limits in the design basis will not be exceeded for normal and abnormal operations.

**TABLE 4-20 LIMITING SAFETY SYSTEM SETTINGS**

Parameter Limited	Safety Setting	Function
Power level at steady-state	2.2 MW <sub>t</sub>	Reactor Scram
Measured fuel temperature	750°C	Reactor Scram

In addition, Technical Specification limits are imposed for the transient rod and coolant water temperatures as follows:

- Maximum worth of transient rod step insertion of less than \$1.75;
- Reactor tank inlet water temperature of less than 45°C.
- No fuel elements will be placed in the core such that the total rod output is expected to exceed 32.0 kW during 2.0 MW<sub>t</sub> steady state reactor operations.

The \$1.75 reactivity insertion limit is justified by the analysis in Section 13.2.2, which shows that there will be no damage if insertions are less than \$1.92. These safety settings are conservative in the sense that if they are adhered to the consequence of normal or abnormal operation would be fuel or cladding temperatures well below the safety limits indicated in the reactor design basis.

**CHAPTER 5**

**REACTOR COOLANT SYSTEMS**

Chapter 5 - Valid Pages Rev.  
Rev. 5 04/26/18

i	Rev. 5	04/26/18
ii	Rev. 5	04/26/18
5-1	Rev. 5	04/26/18
5-2	Rev. 5	04/26/18
5-3	Rev. 5	04/26/18
5-4	Rev. 5	04/26/18
5-5	Rev. 5	04/26/18
5-6	Rev. 5	04/26/18
5-7	Rev. 5	04/26/18
5-8	Rev. 5	04/26/18

TABLE OF CONTENTS

5.0 REACTOR COOLANT SYSTEMS .....5-1

5.1. Summary Description ..... 5-1

5.2. Reactor Tank..... 5-1

5.3. Primary Coolant System ..... 5-3

5.4. Secondary Coolant System ..... 5-5

5.5. Reactor Water Purification Systems..... 5-5

5.6. Primary Coolant Makeup Water System ..... 5-8

5.7. Nitrogen-16 Control System ..... 5-8

5.8. Fuel Storage Pit Water System ..... 5-8

LIST OF FIGURES

5.1	Reactor Tank.....	5-2
5.2	Primary Cooling System.....	5-4
5.3	Secondary Cooling System.....	5-6
5.4	Reactor Water Purification And Makeup System.....	5-7

## 5.0 REACTOR COOLANT SYSTEMS

### 5.1. Summary Description

### 5.2. Reactor Tank

The reactor core is positioned near the bottom of an open 1/4 in. thick aluminum tank 7-1/2 ft in diameter by 24-1/2 ft high (Figure 5.1). The tank contains approximately 7,000 gallons of high-purity water so the core is clearly visible from the top. About 20 ft of water over the top of the reactor core provides biological shielding for personnel in the reactor room. The tank is imbedded in a massive concrete structure which provides biological shielding for personnel in surrounding areas.

Pipe assemblies welded to both the inside and outside of the tank wall (the tank wall is continuous), slightly above the reactor core, form one part of the beam tubes. Flanges have been welded to the pipe stubs on the inside of the tank and are used to attach the in-tank section of the beam tube (Section 9.2). Clearance has been provided between the pipe stubs outside the tank and the reactor bulk shielding to prevent structural loading of the tank wall from thermal expansion. An aluminum angle used for support of fuel storage racks, underwater lights, and other equipment is located around the tank top.

The exterior surface of the tank is coated with epoxy and tar-saturated roofing felt to prevent corrosion. The felt is applied in a double thickness using a bituminous material. In addition, a corrugated liner, approximately 1 in. in thickness, is located between the tank exterior and the concrete shield. The corrugated liner provides a path for water to drain to a collection point under the tank should the tank overflow or leak. A drain around the base of the tank is designed to collect any water from the corrugated section. The drain is installed so that it can be routinely monitored for evidence of leakage.

A bridge assembly provides support for the control rod drives and the tank covers. It is located above the top (8 feet above) of the reactor tank directly over the reactor core. The assembly consists of structural channels covered with plates.

The top of the reactor tank is closed by aluminum grating covers that are hinged. Lucite plastic is attached to the bottom of each grating section to prevent foreign matter from entering the tank while still permitting visual observation.

Tank materials, welding procedures, and welder qualifications were in accordance with the ASME code. The integrity of tank weld joints has been verified by radiography, dye penetrant checking, leak and hydrostatic testing.

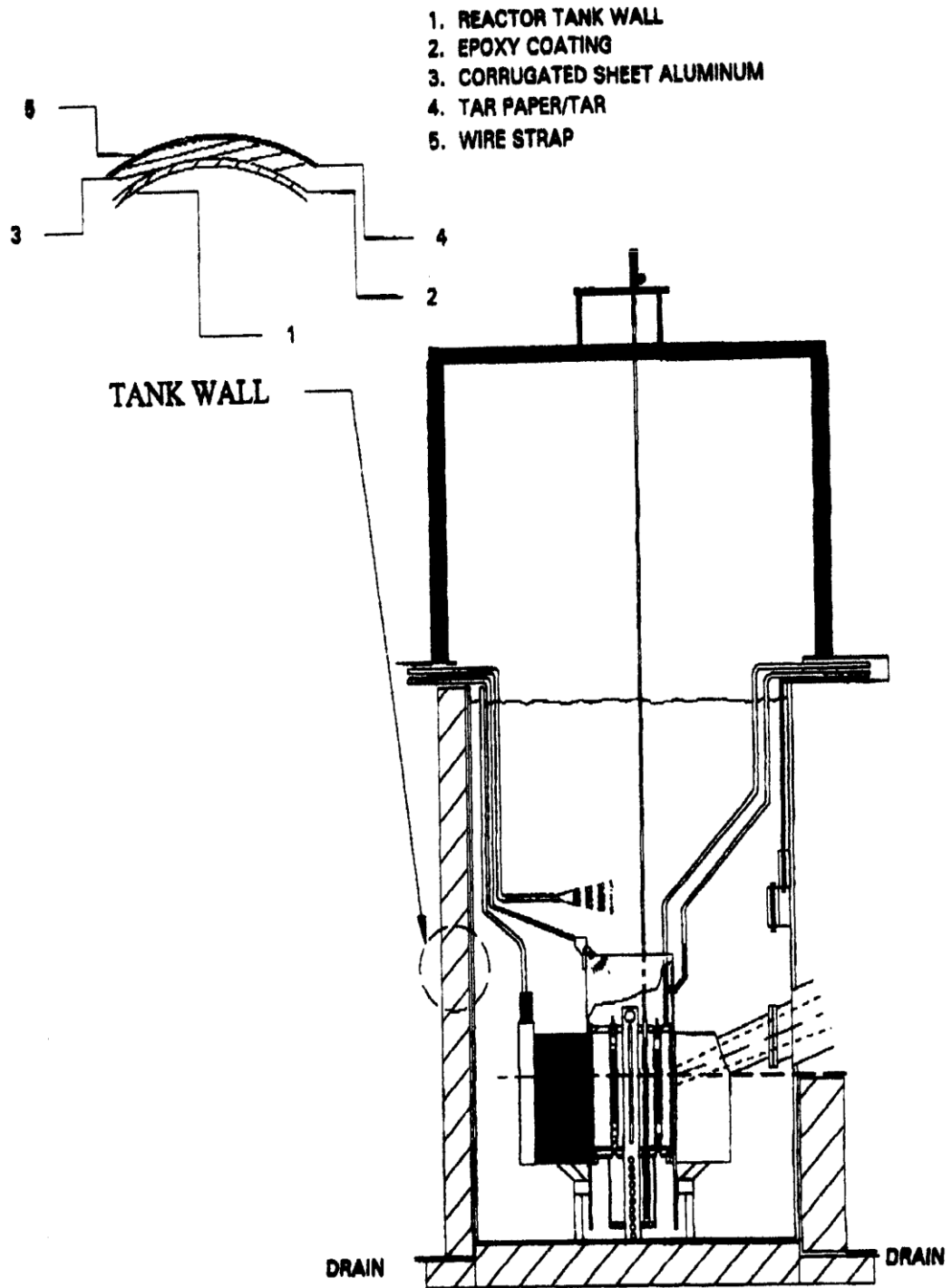


FIGURE 5.1 REACTOR TANK

### 5.3. Primary Coolant System

The reactor core is cooled by natural circulation of the reactor tank water. The tank water temperature is maintained at approximately 90-110°F by the primary cooling system.

The primary cooling system, Figure 5.2, is designed to continually remove 2 MW of heat from the reactor tank. It contains the necessary equipment and controls to circulate up to 1000 gpm of tank water and maintain the temperature of the water returning to the tank at about 32.2°C (90°F). Instrumentation is provided to monitor the system operation, water temperatures, pressure, flow, and tank level. Tank bulk water outlet and inlet temperatures are continuously recorded on the DAC.

This system is operated and monitored from the reactor control room. The remote controls and monitoring instrumentation are located in the reactor room.

The system is regulated to maintain the primary water system pressure lower than the secondary system pressure. This pressure differential will prevent radioactivity from entering the secondary system, especially the cooling tower, should a leak develop between the two systems.

With the exception of pressure, system parameters are read out in the reactor control room. Alarms are provided on the reactor control console, if flow, tank bulk temperature, or tank water level exceeds preset limits. System pressure gages have local readouts. Tank water level can be monitored visually (via video camera) from the reactor room.

All system components that contact the primary water are normally made from either aluminum or stainless steel. The heat exchanger is a plate-type with the primary water flowing within the plates.

The entrance to the pump suction line is less than 3 ft below the normal tank water level. In addition the line is perforated from about 8 in. below the normal tank water level to the entrance. Should a primary system component fail downstream of the pump, the tank water level would lower to the first perforation, about 8 in. At this point the pump should lose suction and quit pumping. However, in no case can the pump lower the water level beyond the entrance to the pump suction line, less than 3 ft. Even if the water level lowers to the entrance to the pump suction line there will be approximately 16-1/2 ft of water above fuel elements in the core. This feature prevents the loss of a significant amount of tank water should a leak develop in any of the primary system components when the pump is operating.

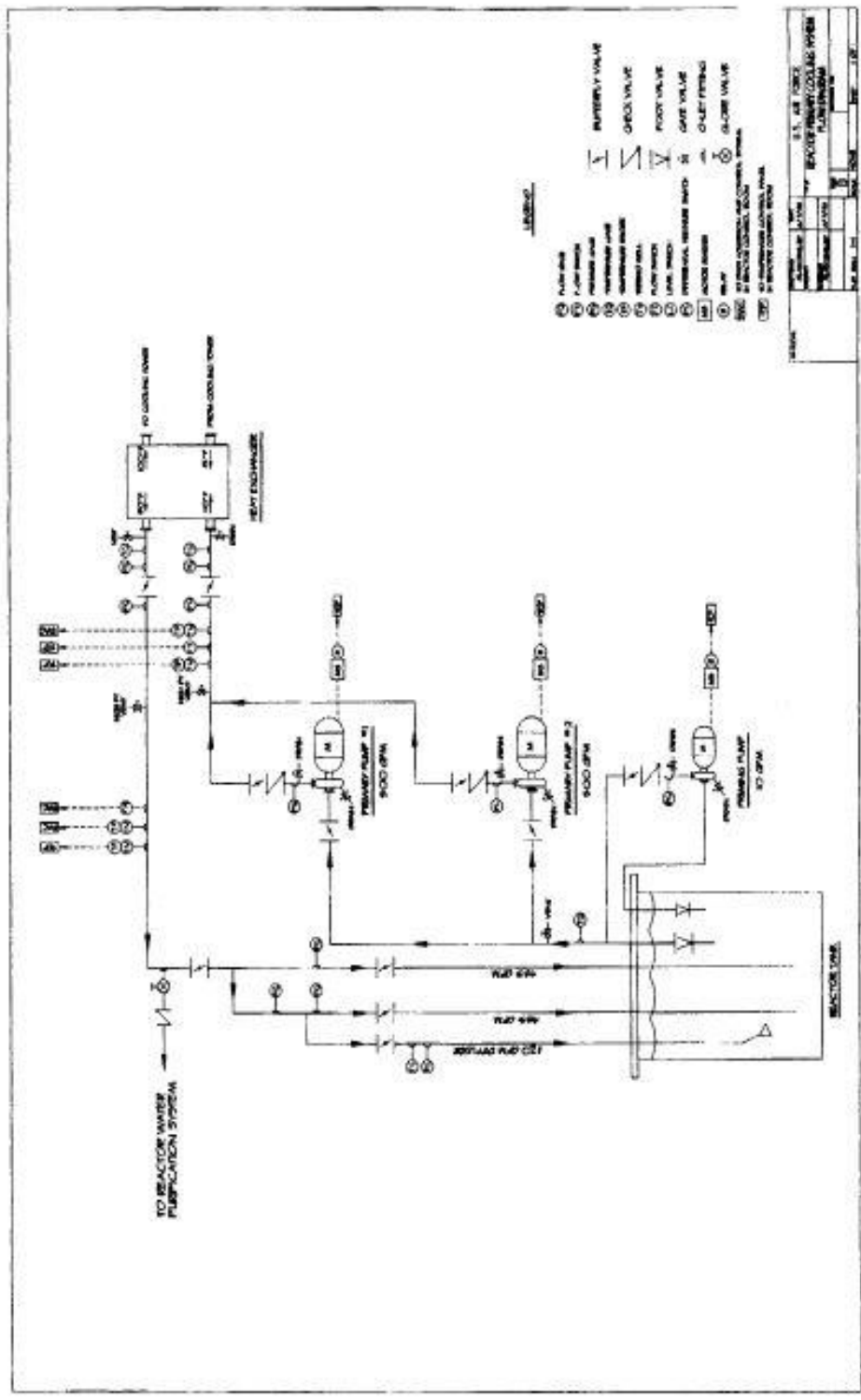


FIGURE 5.2 PRIMARY COOLING SYSTEM

#### 5.4. Secondary Coolant System

The secondary cooling system is capable of continually removing 2 MW of heat from the primary system during normal weather conditions. The system circulates approximately 1000 gpm of water from a cooling tower through the primary-to-secondary heat exchanger and back to the cooling tower (Figure 5.3). The pressure of the secondary system is maintained higher than the primary system to prevent cross contamination of secondary water should a leak develop in the heat exchanger.

Water chemistry, conductivity, and pH are monitored and maintained by an automatic water conditioning system that adds chemicals as required.

#### 5.5. Reactor Water Purification Systems

The reactor water purification systems maintain the primary water purity and optical clarity (Figure 5.4). There are two separate systems that can be operated independently or can be cross-connected to operate as one unit. One system is used to filter particulate matter from the surface of the reactor tank and the other system deionizes the water to maintain the purity.

The filtration system uses a drum surface skimmer that floats near the surface of the water in the reactor tank. A pump moves water from the surface skimmer to fiber cartridge filter elements. These filter elements remove any dirt or debris from the reactor tank water by mechanically filtering them from the water before returning the water to the reactor tank. The system can be used to return the filtered water directly to the reactor tank or, through a series of valve manipulations, it can send the filtered water through the deionizers (resin columns) and then back to the reactor tank. The system is used to supply the deionizing resin bed during extended shutdown periods when the primary cooling system is not operational.

A set of deionizing resin beds (four) are supplied from the primary cooling system (outlet of the heat exchanger) at a nominal flow rate of fifteen gallons per minute (15 gpm). The resin bed consists of four fiberglass canisters of mixed-bed resin. Two of the canisters are normally on-line and the other two canisters are in a stand-by condition. Two conductivity cells are used to measure the conductivity of water entering the resin beds and the conductivity of the water exiting the resin beds subsequent to entering the reactor tank. There are local readouts of the conductivity near the resin tanks and remote readouts and alarm functions located on the reactor console.

Pressure gauges are located within the systems to monitor the overall performance of the systems.



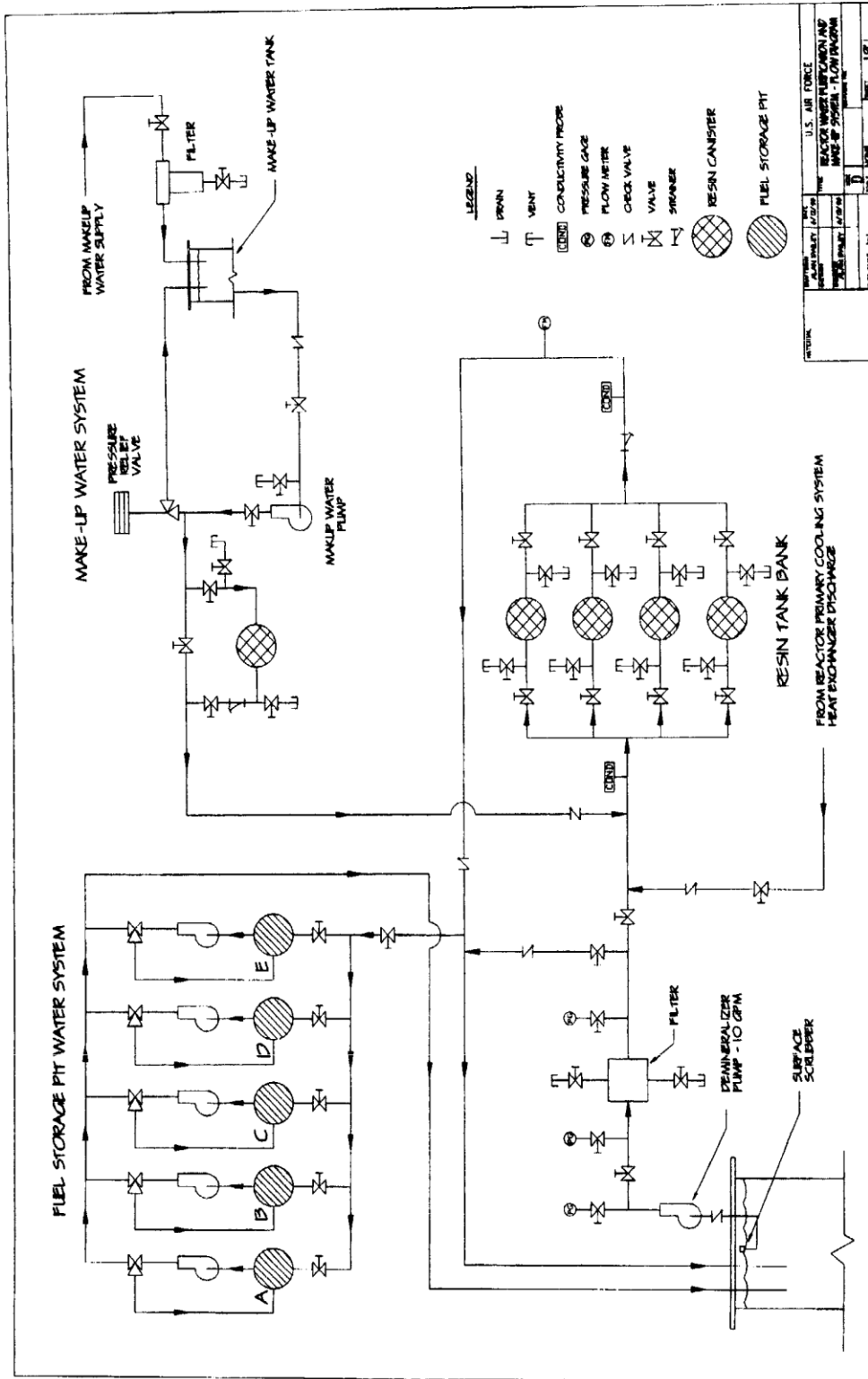


FIGURE 5.4 REACTOR WATER PURIFICATION AND MAKEUP SYSTEM

#### 5.6. Primary Coolant Makeup Water System

A 300 gallon plastic tank of demineralized water is available to make up any primary cooling system water lost by evaporation or other means. The makeup system is equipped with a positive displacement pump and resin canister of the same type that are used in the purification system. The outlet flow of the makeup system discharges to the purification system.

#### 5.7. Nitrogen-16 Control System

A diffuser has been incorporated into the system to reduce the N-16 at the tank top. The diffuser discharge is located about 2 ft above the reactor and directs about 120 gpm through two nozzles designed to produce a laminar flow sheet across the entire top of the reactor (Figure 5.2). The diffuser operates anytime the primary pump is running.

#### 5.8. Fuel Storage Pit Water System

The fuel storage pit water system is used when shielding of stored fuel elements is required (Figure 5.4). The system's water supply is from the demineralized system outlet and pit water level is controlled by a float actuated water supply valve. Each pit subsystem contains a pump and a three-way valve in the pump discharge line. This configuration allows for once-through, recirculation, or feed-and-bleed operation depending on fuel element shielding requirements. When operating in the once-through or feed-and-bleed modes, excess water is returned to the reactor tank.

## **CHAPTER 6**

### **ENGINEERED SAFETY FEATURES**

Chapter 6 - Valid Pages  
Rev. 5 04/27/18

i Rev. 5 04/27/18  
6-1 Rev. 5 04/27/18  
6-2 Rev. 5 04/27/18

TABLE OF CONTENTS

6.0 ENGINEERED SAFETY FEATURES.....6-1  
6.2 Introduction.....6-1  
6.3 Emergency Core Cooling System (ECCS).....6-1

LIST OF FIGURES

6.1 Emergency Core Cooling System (ECCS) .....6-2

REFERENCES

6.1 Emergency Core Cooling System Requirements for the McClellan Nuclear Radiation Center 2 MW TRIGA<sup>®</sup> Reactor, GEN-52, General Atomics, January 1997.

## 6.0 ENGINEERED SAFETY FEATURES

### 6.1 Introduction

During the design of the UCD/MNRC and subsequent analysis for safety considerations for the UCD/MNRC, the only requirement identified for an Engineered Safety Feature was for an Emergency Core Cooling System (ECCS). This feature is required for operation of the UCD/MNRC at >1.5 MW. Previous analysis has shown that an ECCS was not required for the UCD/MNRC, since at 1 MW even an instantaneous loss of the entire tank water would not have resulted in fuel temperatures which would have threatened the fuel clad.

An operational history since the issuing of the MNRC license in 1998 is given in chapter 4. Since 2007 the MNRC has essential operated at 1.0 MW steady state for only one shift. This mode of operation will continue for the foreseeable future. Even though MNRC will likely never return to an operational mode that will require the ECCS, the system is required and will be maintained.

### 6.2 Emergency Core Cooling System (ECCS)

The Emergency Core Cooling System (ECCS) supplies water to the reactor core in the event the reactor core becomes uncovered. The water is supplied from the domestic water supply.

Water is supplied to the reactor core by hooking up a hose between the domestic water supply and the aluminum piping to the reactor core area. The domestic water supply and hose are located on the roof area outside the reactor room. All hose connections are quick-connectors and require no tools to attach. The aluminum piping that goes to the reactor core area has a nozzle that is positioned approximately two feet above the reactor core so water will be dispersed over the reactor core (Reference 6.1). The nozzle rests on a two foot high aluminum chimney that surrounds the upper grid plate.

The system is actuated by the reactor operator using some or all of the following indications, as appropriate, that water is leaking from the reactor tank:

1. Reactor tank low level alarm;
2. Primary system low flow alarm;
3. Demineralizer low flow alarm;
4. Reactor room radiation area monitor alarm;
5. Reactor room radiation criticality alarm and evacuation alarm;
6. Reactor room and stack continuous air monitor alarms;
7. Visual indication of water loss with the remote television camera.

The ECCS contains pressure and flow gauges to verify sufficient water flow is maintained for the duration of its use (Section 13.2.3.2.2).

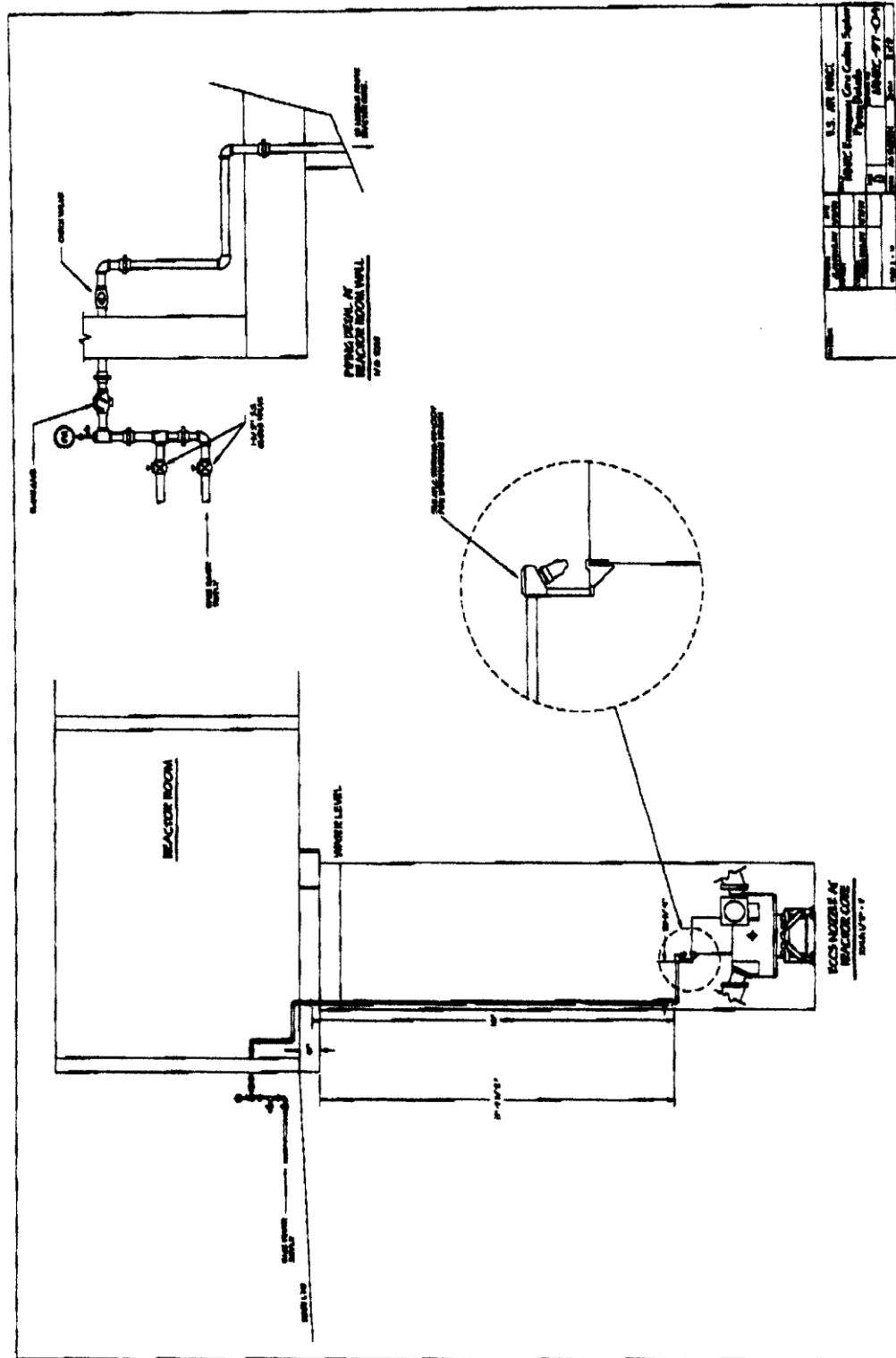


FIGURE 6.1 EMERGENCY CORE COOLING SYSTEM (ECCS)

**CHAPTER 7**

**INSTRUMENTATION AND CONTROL**

Chapter 7 - Valid Pages  
Rev. 5 05/01/18

i	Rev. 5	05/01/18
ii	Rev. 5	05/01/18
7-1	Rev. 5	05/01/18
7-2	Rev. 5	05/01/18
7-3	Rev. 5	05/01/18
7-4	Rev. 5	05/01/18
7-5	Rev. 5	05/01/18
7-6	Rev. 5	05/01/18
7-7	Rev. 5	05/01/18
7-8	Rev. 5	05/01/18
7-9	Rev. 5	05/01/18
7-10	Rev. 5	05/01/18
7-11	Rev. 5	05/01/18
7-12	Rev. 5	05/01/18
7-13	Rev. 5	05/01/18
7-14	Rev. 5	05/01/18
7-15	Rev. 5	05/01/18
7-16	Rev. 5	05/01/18
7-17	Rev. 5	05/01/18
7-18	Rev. 5	05/01/18
7-19	Rev. 5	05/01/18
7-20	Rev. 5	05/01/18
7-21	Rev. 5	05/01/18
7-22	Rev. 5	05/01/18
7-23	Rev. 5	05/01/18
7-24	Rev. 5	05/01/18
7-25	Rev. 5	05/01/18
7-26	Rev. 5	05/01/18

TABLE OF CONTENTS

7.0	INSTRUMENTATION AND CONTROL.....	7-1
7.1	Introduction.....	7-1
7.1.1	Design Basis.....	7-3
7.1.2	Instrumentation and Control System Design.....	7-3
7.1.2.1	NM-1000 Safety and Neutron Monitoring Channel.....	7-3
7.1.2.2	NPP-1000 Safety Channel.....	7-4
7.1.2.3	Data Acquisition Computer.....	7-6
7.1.2.4	Control System Computer/Printer.....	7-6
7.1.2.5	Reactor Operating Controls.....	7-7
7.1.2.6	Reactor and Facility Display Equipment.....	7-12
7.2	Reactor Protective System.....	7-15
7.3	Rod Control System.....	7-19
7.3.1	Control Rods.....	7-19
7.3.2	Control Rod Drive Assemblies.....	7-20
7.3.3	Transient Rod Drive Assembly.....	7-23

LIST OF TABLES

7-1	Typical CRT Window Display.....	7-15
7-2	Typical CRT Warning Window Display.....	7-18
7-3	Typical CRT Status Window Display.....	7-19

LIST OF FIGURES

7.1	Block Diagram Of Instrumentation And Control System.....	7-2
7.2	Typical Neutron Channel Operating Ranges.....	7-5
7.3	UCD/MNRC Reactor Control Console.....	7-8
7.4	Typical Mode Control Panel.....	7-9
7.5	Typical Rod Control Panel.....	7-10
7.6	Typical CRT Display Of Reactor Operational Information.....	7-13
7.7	Indicator Panel.....	7-14
7.8	Typical Protective System Scram Logic.....	7-16
7.9	External Scram Inputs.....	7-17
7.10	Typical Fuel Follower Control Rod Shown Withdrawn And Inserted.....	7-21
7.11	Rack-And-Pinion Control Rod Drive (Typical).....	7-22
7.12	Adjustable Fast Transient Rod Drive Assembly (Typical).....	7-24

REFERENCES

- 7.1 "Microprocessor Based Research Reactor Instrumentation and Control System,"  
INS-24, GA Technologies, Inc., May, 1986.

## 7.0 INSTRUMENTATION AND CONTROL

### 7.1 Introduction

The Instrumentation and Control System (ICS) for the UCD/MNRC TRIGA<sup>®</sup> reactor is a computer-based system incorporating the use of a GA-developed, multifunction, NM-1000 microprocessor-based neutron monitoring channel and a NPP-1000 analog-type neutron monitoring channel (Figure 7.1). The NM-1000 system provides a safety channel (percent power with scram), a wide-range log percent power channel (below source level to full power), period indication, and a multirange linear power channel (source level to full power) (Reference 7.1). The NPP-1000 system provides a second safety channel for redundancy (percent power with scram). In the pulse mode of operation, the Data Acquisition Computer (DAC) makes a gain change in the NPP-1000 safety channel to provide NV and NVT indication along with a peak pulse power scram. The NM-1000 is essentially bypassed once a pulse has been initiated.

The NM-1000 digital neutron monitor system was developed for the nuclear power industry. The system is based on a special, GA-designed, fission chamber and low-noise ultra-fast pulse amplifier. The NPP-1000 safety channel was designed to the same high performance criteria as the NM-1000 channels.

The control system logic is contained in a separate Control System Computer (CSC) with a color graphics display. While information from the NM-1000, NPP-1000, and fuel temperature channels is processed and displayed by the CSC, each is direct wired to its own output display, and the safety channel connects directly to the protective system scram circuit. That is, signals to the scram circuits are not processed by the Data Acquisition Computer or the control computer. The nuclear information goes directly from the detectors to either the NM-1000 or NPP-1000 where it is processed. The processed signals connect directly to the scram circuit switches. Fuel temperature information goes directly to "action pack modules" for amplification and then to the scram circuit switches. The ability of this configuration to meet the intent of protection system requirements for reliability, redundancy, and independence for TRIGA<sup>®</sup>-type reactors has been accepted by the NRC.

The CSC manages all control rod movements, accounting for such things as interlocks and choice of particular operating modes. It processes and displays information on control rod positions, power level, fuel and water temperature, and pulse characteristics. The CSC performs many other functions, such as monitoring reactor usage and facility radiation instruments, and storing historical operating data for replay at a later time. A computer-based control system has many advantages over an analog system: speed, accuracy, reliability, the ability for self-calibration, improved diagnostics, graphic displays, and the logging of vital information.

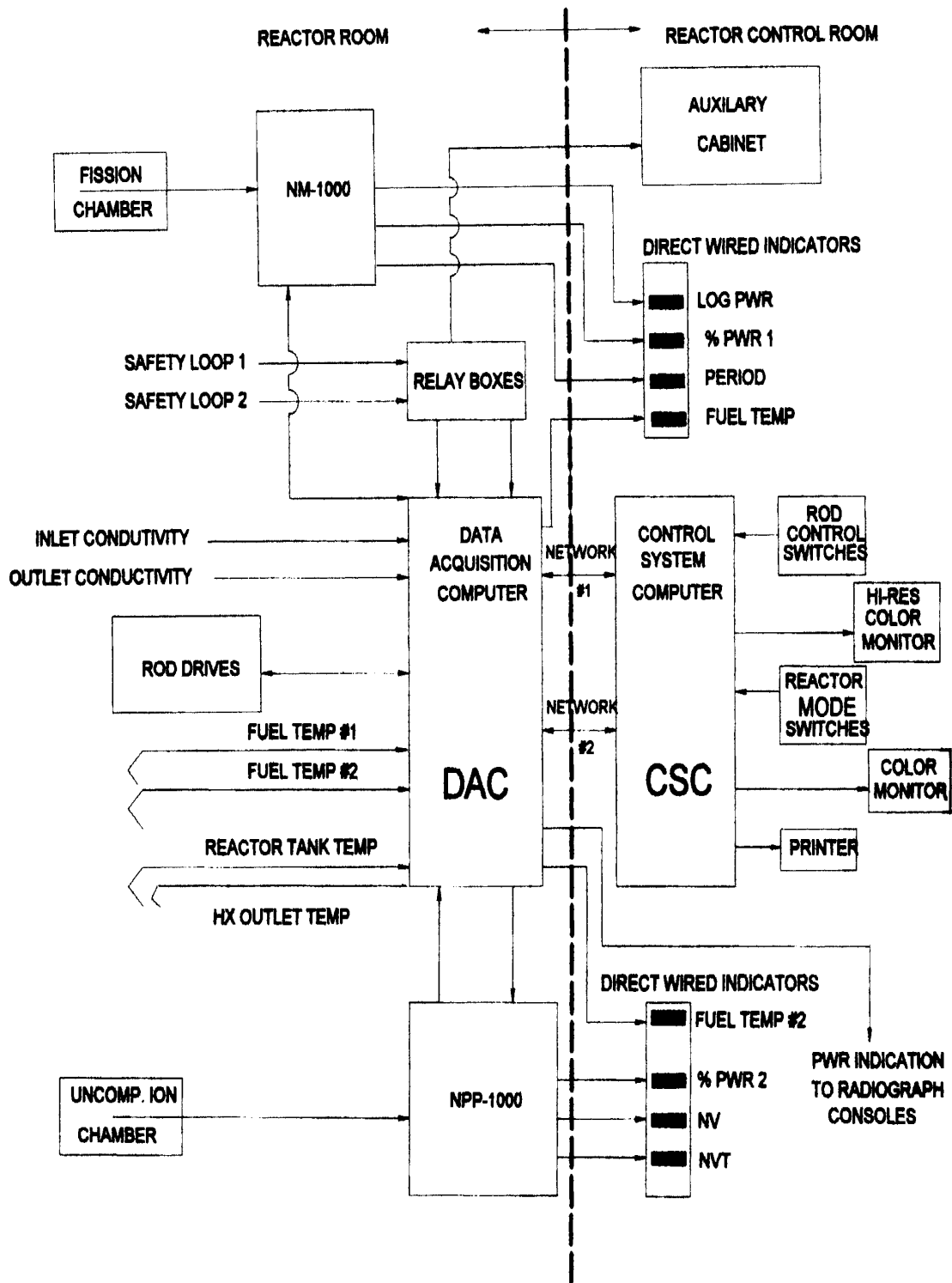


FIGURE 7.1 BLOCK DIAGRAM OF INSTRUMENTATION AND CONTROL SYSTEM

### 7.1.1 Design Basis

The ICS for the UCD/MNRC reactor is designed to perform the following functions:

- Provide the operator with information on the status of the reactor and facility;
- Provide the means for insertion or withdrawal of control rods;
- Provide for automatic control of the reactor power level;
- Provide for detecting overpower conditions and automatically scram the control rods to terminate the overpower condition;
- Provide for the storage of data for later retrieval.

A scram system is included as part of the instrumentation and control system. The scram system is designed to meet the single-failure criterion applied to power reactors and is independent of the normal reactivity-control system.

### 7.1.2 Instrumentation and Control System Design

#### 7.1.2.1 NM-1000 Safety and Neutron Monitoring Channel

The NM-1000 nuclear channel has the multifunction capability to provide safety (scram) action as well as neutron monitoring over a wide power range from a single detector. The functions are the following:

1. Percent power with scram;
2. Wide-range log power;
3. Power rate of change;
4. Multirange linear power.

For the UCD/MNRC ICS, the NM-1000 system is designated to provide the wide-range log power function and the percent power safety channel with scram (linear power level from 1% to 120%). The wide-range log power function is a digital version of the patented GA 10-decade log power system to cover the reactor power range from below source level to 150% power and provide a period signal. For the log power function, the chamber signal from startup (pulse counting) range through the Campbelling [root mean square (RMS) signal processing] range covers in excess of 10-decades of power level. The self-contained microprocessor combines these signals and derives the power rate of change (period) through the full range of power. The microprocessor automatically tests the system to ensure that the upper decades are operable while the reactor is operating in the lower decades and vice versa when the reactor is at high power. The output signal from the microprocessor goes directly to the scram circuit switches and the direct reading bar graphs on the console.

For the multirange function, the NM-1000 uses the same signal source as for the log function. However, instead of the microprocessor converting the signal into a log function, it converts it into 10 linear power ranges. This feature provides for a more precise reading of linear power level over the entire range of reactor power. The same self-checking features are included as for the log function. The multirange function is auto-ranging.

The NM-1000 system is contained in two National Electrical Manufacturers Association (NEMA) enclosures located in the reactor room. The amplifier assembly contains modular plug-in subassemblies for pulse preamplifier electronics, bandpass filter and RMS electronics, signal conditioning circuits, low-voltage power supplies, detector high-voltage power supply, digital diagnostics, and communication electronics. The processor assembly is made up of modular plug-in subassemblies for communication electronics (between amplifier and processor), the microprocessor, a control/display module, low-voltage power supplies, isolated 4 to 20 mA outputs, and isolated alarm outputs. Outputs are Class IE as specified by IEEE 323-1974. Communication between the amplifier and processor assemblies is via twisted-pair shielded cables. The amplifier/microprocessor circuit design employs automatic on-line self-diagnostics and calibration verification. Detection of unacceptable circuit performance is automatically alarmed. The system can be automatically calibrated and checked (including the testing of trip levels) prior to operation. The checkout data is recorded for future use. The accuracy of the channels is equal to or better than  $\pm 3\%$  of full scale, and trip settings are repeatable within 1% of full-scale input.

The neutron detector uses the standard 0.2 counts/s per nv fission chamber that has provided reliable service in the past. It has, however, been improved by additional shielding to provide a greater signal-to-noise ratio. The low noise construction of the chamber assembly allows the system to respond to a low reactor shutdown level which is subject to being masked by noise. An illustration of the neutron channel operating ranges is shown in Figure 7.2.

#### 7.1.2.2 NPP-1000 Safety Channel

The NPP-1000 system provides the redundant percent power safety channel with scram. The amplified signal from this channel goes directly to the direct wired % power indicator and the scram circuit switches. In the pulse mode of operation, the DAC makes a gain change in the NPP-1000 safety channel to provide NV and NVT indication along with a peak pulse power scram. The NPP-1000 system is an upgrade of GA systems which have been in use in TRIGA<sup>®</sup> installations world-wide for many years. The nuclear detector for the NPP-1000 is an uncompensated ionization chamber. NPP-1000 systems are utilized at the Sandia National Laboratory, the AFRRRI reactor at Bethesda, MD, the University of Texas, and at GA's facility at San Diego, CA.

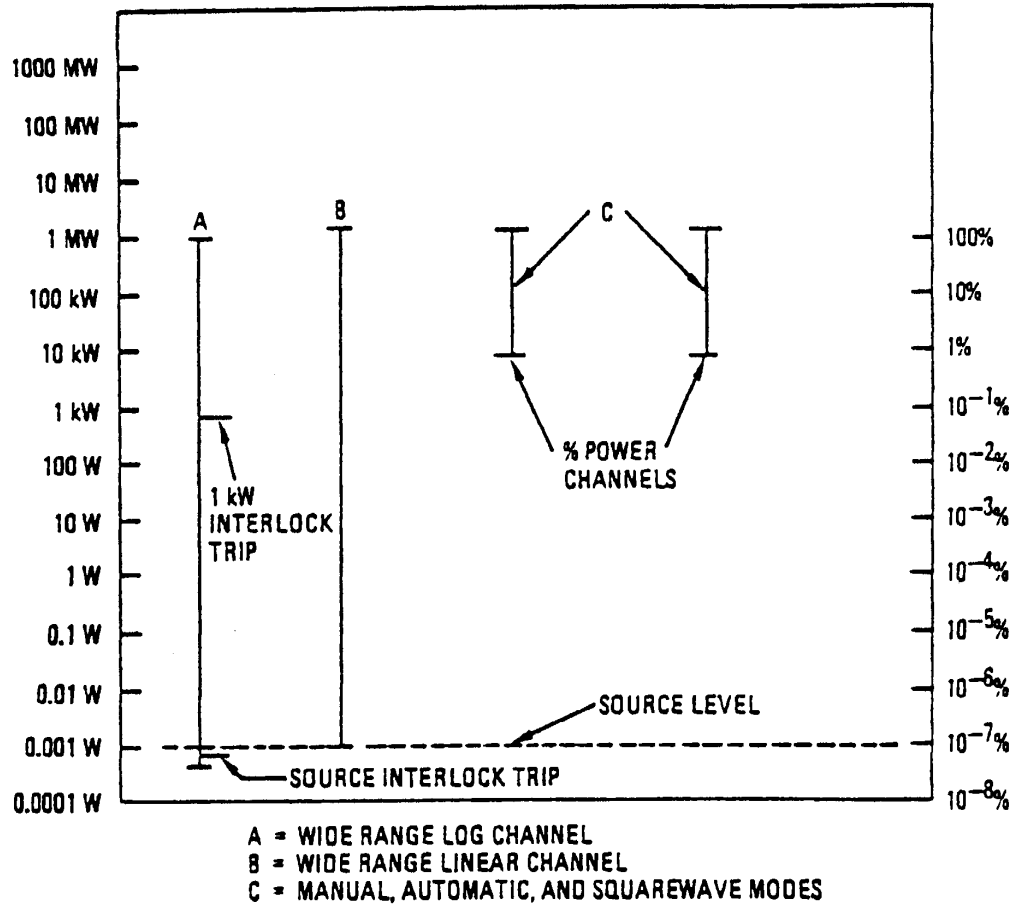


FIGURE 7.2 TYPICAL NEUTRON CHANNEL OPERATING RANGES

The NPP-1000 is located in the reactor room in the DAC assembly cabinet. The cabinet that houses the NPP-1000 has a heat detection and a halon fire suppression system. If the heat detector is activated, a "DAC HALON RELEASE" warning appears on the reactor control room console. After a short time delay, the electric power to the cabinet is turned off. The time delay is long enough for the operator to confirm reactor shutdown.

#### 7.1.2.3 Data Acquisition Computer

As indicated in Figure 7.1, the Data Acquisition Computer (DAC) receives and processes, converts from analog-to-digital form or digital-to-analog form, information from the NM-1000 and NPP-1000 as well as from numerous other instruments associated with reactor and facility operations. The processed information is then transmitted, as appropriate, to the Control System Computer (CSC), the NM-1000, or the NPP-1000. Information transfer between the DAC and CSC is by high speed data transmitter.

In the pulse mode of operation, the DAC makes a gain change in the NPP-1000 channel to provide NV and NVT information along with a peak pulse power scram.

The control and transient rod drive control signals produced by the CSC are processed by the DAC prior to being sent to the devices.

The DAC is located in the reactor room and is housed in the same enclosure as the NPP-1000.

#### 7.1.2.4 Control System Computer/Printer

The Control System Computer (CSC) provides all of the logic functions needed to control the reactor and augments the safety system by monitoring operating characteristics. Information from this computer is displayed on monitors for ease of comprehension. Essentially, all of the control system logic contained in previous TRIGA<sup>®</sup> reactor control systems is incorporated into the CSC.

However, instead of using electronic circuits and electrical relay circuits, the logic is programmed into the computer. The availability of the computer allows great versatility and flexibility in operationally-related activities aside from the direct control of rod movements. Many other functions are performed by the CSC, such as monitoring reactor usage, monitoring radiation instruments, storing data, and logging operator identity. A rod-drop timing circuit and a display, capable of time measurements in the 10 ms range, are provided within the CSC and displays.

The computer samples all operational data in the steady-state mode every 30 seconds and stores this data. The memory can hold 9,000 such samples or 75 hrs of operational data. In the pulse mode, there is enough storage for 10 pulses with all parameters.

Operational data can be printed in the same format as displayed on the console CRTs. This includes all real time and archival data. The displays can be reproduced in graphic and print form only.

The computer is located in the reactor control console (Figure 7.3). The reactor control console and the reactor control room both contain halon fire suppression systems. While the reactor control console system is activated by a thermal detector, the reactor control room system located under the false floor is activated by a signal from at least two smoke detectors.

#### 7.1.2.5 Reactor Operating Controls

The UCD/MNRC reactor can be operated in four modes: manual, automatic, square wave, and pulse. The operations are controlled from the mode control panel (Figure 7.4) and the rod control panel (Figure 7.5).

The manual and automatic modes are steady-state reactor conditions; the square-wave and pulse modes are the conditions implied by their names and require the use of the pulse rod.

The manual and automatic reactor control modes are used for reactor operation from source level to 100% power. These two modes are used for manual reactor startup, change in power level, and steady-state operation.

A captive keyswitch located on the rod control panel controls the current to the control and transient rod magnets. This keyswitch must be in the "ON" position for any rod movement actions. Anytime the magnet current has been removed, this switch must be turned to the "RESET" position and then back to the "ON" position for the magnet current to be restored. This keyswitch causes "REACTOR ON" lights to be illuminated throughout the UCD/MNRC.

Manual rod control is accomplished through the use of pushbuttons on the rod control panel. The top row of pushbuttons (magnet) is used to interrupt the current to the rod drive magnet. If the rod is above the down limit, it will fall back into the core and the magnet will automatically drive to the down limit, where it will again contact the armature.

The middle row of pushbuttons (up) and the bottom row (down) are used to position the control rods. Depressing the pushbuttons causes the control rod to move in the direction indicated. Interlocks prevent the movement of the rods in the up direction under the following conditions:

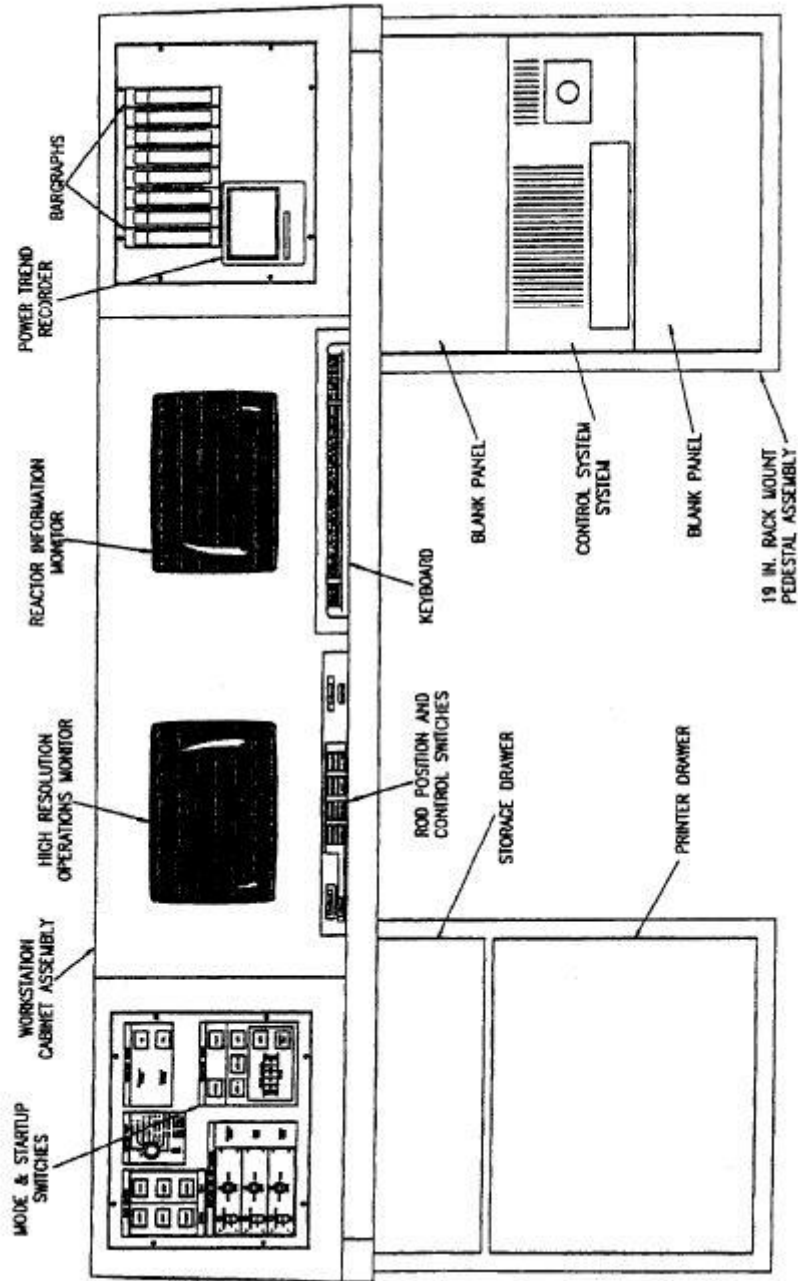


FIGURE 7.3 UCD/MNRC REACTOR CONTROL CONSOLE

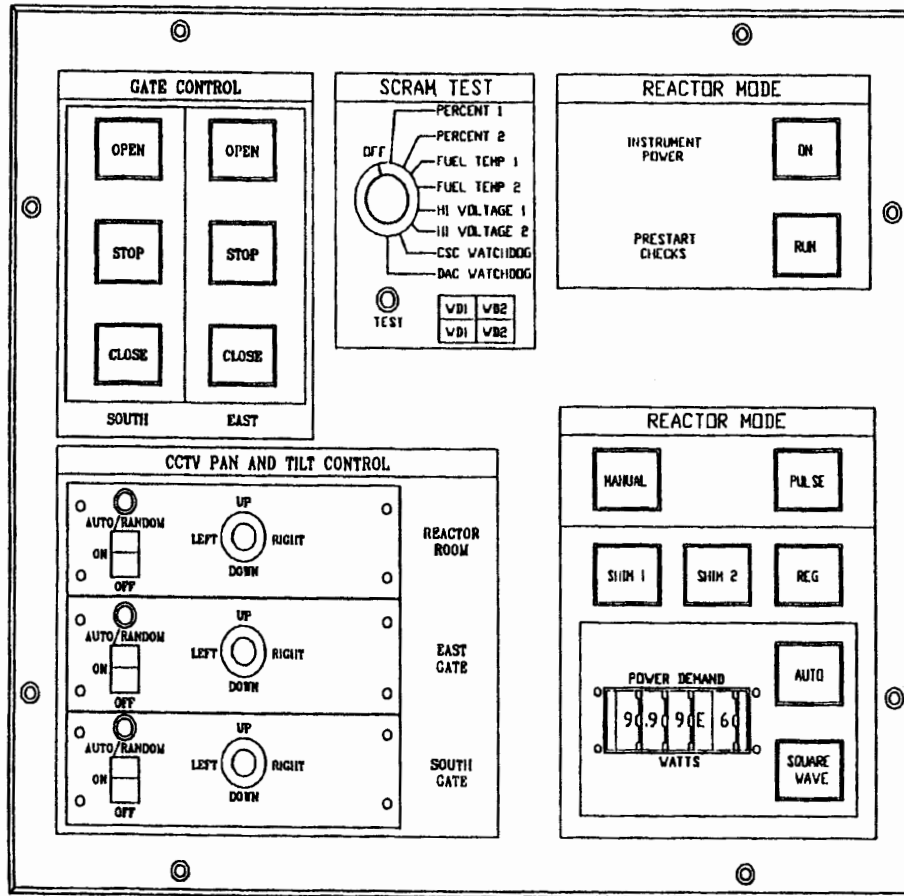


FIGURE 7.4 TYPICAL MODE CONTROL PANEL

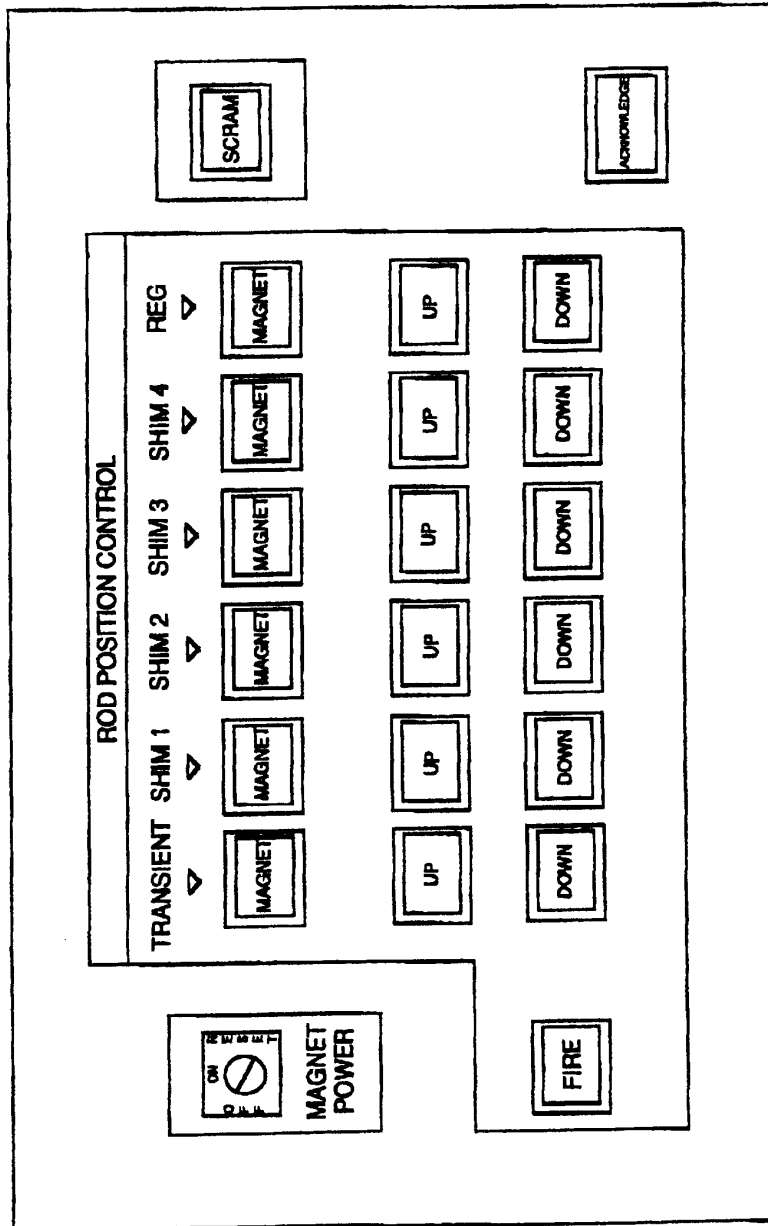


FIGURE 7.5 TYPICAL ROD CONTROL PANEL

1. Scrams not reset;
2. Source level below minimum count;
3. Two UP switches depressed at the same time;
4. Mode switch in the PULSE position;
5. Mode switch in the AUTOMATIC position [servocontrolled rod(s) only];
6. Square wave mode - switch depressed or lighted.

There is no interlock inhibiting the down direction of the control rods except in the case of the servocontrolled rod(s) while in the automatic mode.

Automatic power control can be obtained by switching from manual operation to automatic operation on the mode control panel. All the instrumentation, safety, and interlock circuitry described above applies in the operation of this mode. However, the servocontrolled rod(s) is (are) controlled automatically to a power level and period signal. The reactor power level is compared with the demand level set by the operator, on the mode control panel, and used to bring the reactor power to the demand level on a fixed preset period. The purpose of this feature is to maintain automatically the preset power level during long-term power runs.

The square-wave mode allows the reactor power to be quickly raised to a desired power level. In a square-wave operation, the reactor is first brought to criticality below one kW in the manual mode, leaving the transient rod partially in the core. The desired power level is set by the reactor operator using the power demand selector located on the mode control panel. All of the steady-state instrumentation is in operation. The transient rod is ejected from the core by means of the transient rod FIRE pushbutton located on the rod control panel. When the power level reaches the demand level, it is maintained in the automatic mode.

Reactor control in the pulsing mode consists of manually establishing criticality at a flux level below one kW in the steady-state mode. This is accomplished by the use of the control rods, leaving the transient rod either fully or partially inserted. The pulse mode selector switch located on the mode control panel is then depressed. The MODE SELECTOR switch automatically causes the DAC to make a gain change in the NPP-1000 safety channel to monitor and record peak flux (NV), energy release (NVT), and to provide a peak pulse power scram. The pulse is initiated by activating the FIRE pushbutton. Once a pulse has been initiated and it is detected by the DAC, the NM-1000 safety scram is bypassed. Pulsing can be initiated from either the critical or subcritical reactor state.

The rod control panel contains a manual scram switch and a switch to acknowledge warning information that appears on one of the reactor control room displays.

The mode control panel contains controls for instrument power, prestart checks, and reactor scram test. Controls for the UCD/MNRC entrance gates and the CCTV cameras for the reactor room are located on this panel.

### 7.1.2.6 Reactor and Facility Display Equipment

Reactor and facility operating and monitoring information is displayed on two color monitors and a bar graph indicator located on the reactor control console.

The high resolution monitor displays important reactor operating information (Figure 7.6). This monitor has a scram/warning window which indicates the cause of the scram/warning when a scram occurs or a predetermined limit is reached. This window is normally black, but changes to red when under a scram/warning condition. An audible alarm is sounded when a scram/warning condition exists. Tables 7-1 and 7-2 list the parameters that can appear on the window, one at a time. If more than one limit is reached, the first-in will be displayed. Once acknowledged and cleared, the next parameter will appear. The date, time of day, operating mode, and demanded power are also displayed. The reactor operating information, generated by the Control System Computer, is displayed on this monitor as follows:

- Linear power;
- Log power;
- Percent power from both safety channels;
- Rod position (resolution of  $\leq 0.1$  in.);
- Fuel temperature;
- Tank water temperature.

The second monitor is used to display reactor and facility information.

Three types of information are made available for reactor operator use: scram, warning, and status. The information available for display for each of these three categories is shown in Tables 7-1, 7-2, and 7-3, respectively. The console keyboard is used to select the category to be displayed. If the scram category is selected, the parameters in Table 7-1 that have exceeded the scram setpoints will be displayed in the order in which the setpoints were exceeded, first-in. As noted above, the first parameter to cause the scram is indicated in the scram/warning window on the high resolution monitor. The scram indication will remain on the display until it has been cleared.

If the warning category is selected, the parameters in Table 7-2 that have exceeded the warning setpoint will be displayed. The display on the high resolution monitor, the order, and clearing is the same as for the scram category.

The third category that may be selected is System Status. The parameters listed in Table 7-3, with the current reading, will be displayed.

The bar graph indicator panel displays information important to reactor operations. The information displayed on this panel is shown in Figure 7.7. The reactor power and period information displayed on this panel comes directly from the NM-1000 and NPP-1000 safety channels. It is hard-wired and does not come through the Control System Computer.

Included on the indicator panel is a single-pen recorder for wide-range-linear power.

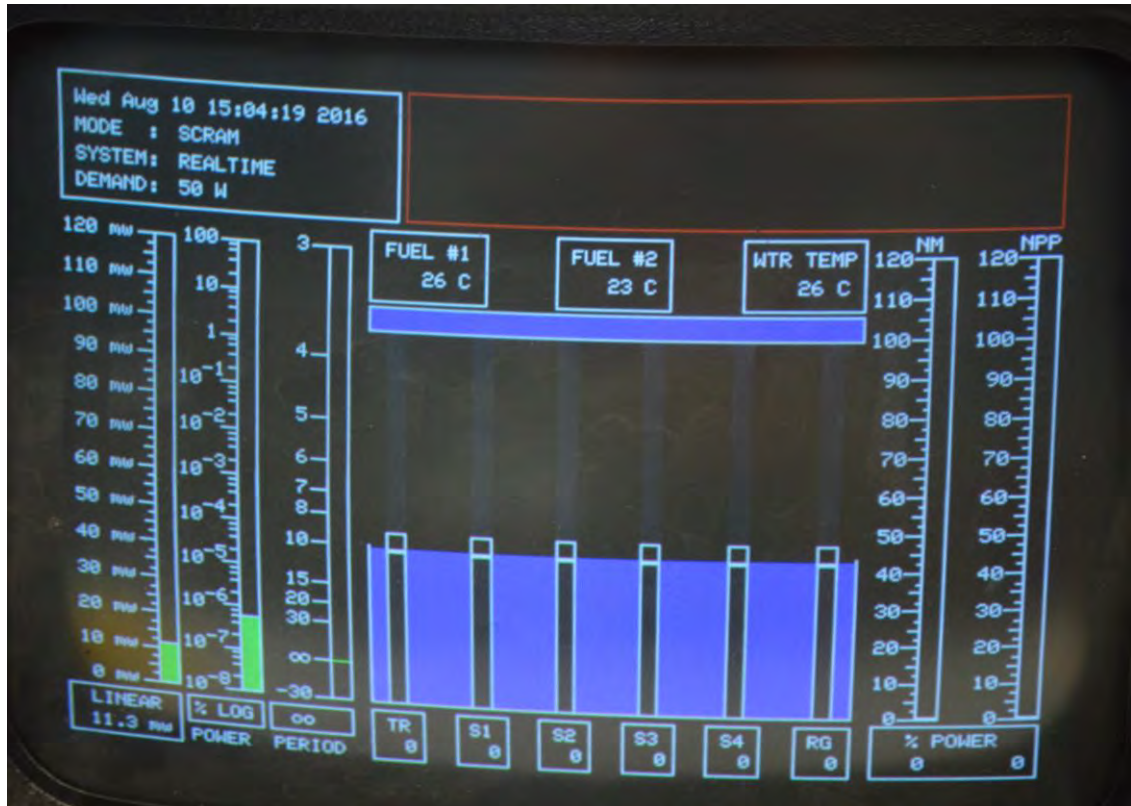


FIGURE 7.6 TYPICAL CRT DISPLAY OF REACTOR OPERATIONAL INFORMATION

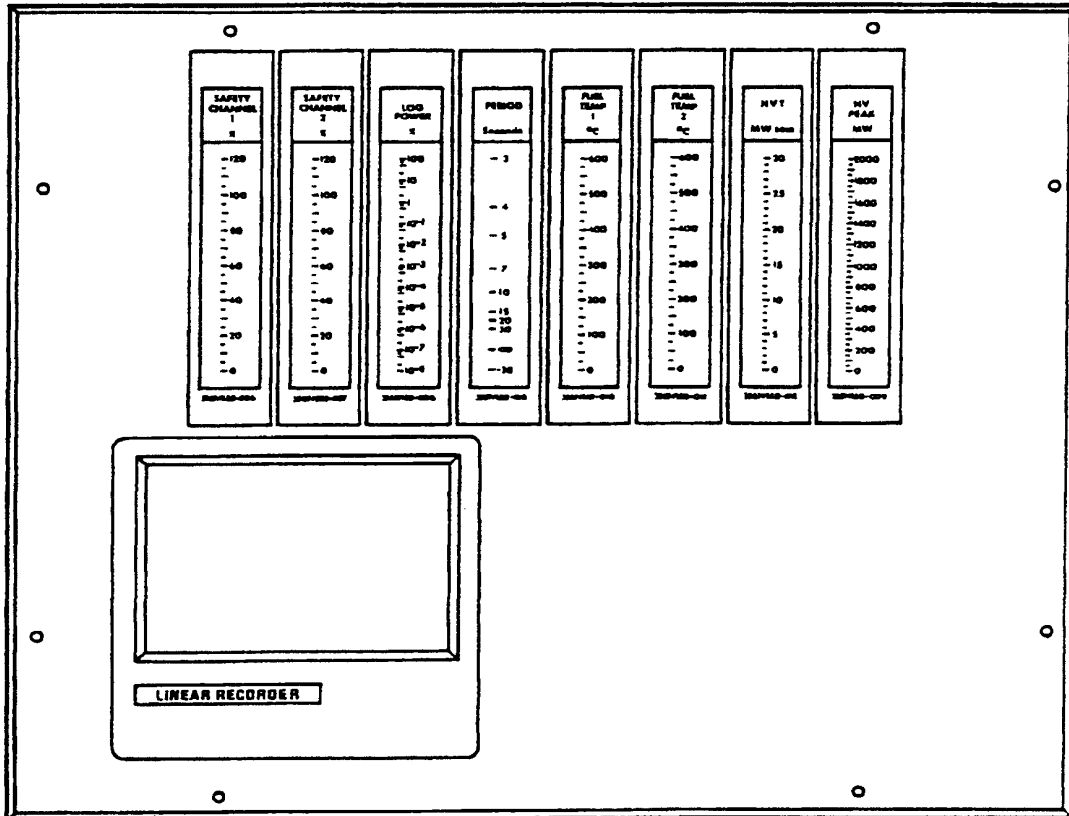


FIGURE 7.7 INDICATOR PANEL

## 7.2 Reactor Protective System

The reactor protective system scram logic is shown in Figure 7.8. A reactor protective action interrupts the rod magnet current and results in the immediate insertion of all rods if the setpoints of any of the parameters shown in Table 7-1 are exceeded. The external scram inputs are shown in Figure 7.9.

**TABLE 7-1 TYPICAL CRT WINDOW DISPLAY**

1. Scram - Console Manual	14. Scram -NPP-1000 Power Hi
2. Scram - Reactor Room Manual	15. Scram - NM-1000 Power Hi
3. Scram - Bay Rip Cord	16. Scram - NM-1000 Hi Voltage Lo
4. Scram - Fuel Temp #1 Hi	17. Scram - NPP-1000 Hi Voltage Lo
5. Scram - Fuel Temp #2 Hi	18. Scram - Keyswitch Off
6. Scram - External #1	19. Scram - Please Log In
7. Scram - External #2	20. Scram - Net Fault, Please Reboot
8. Scram - CSC DIS64 Timeout	21. Scram - Database Timeout
9. Scram - DAC DIS64 Timeout	22. Scram - NM-1000 Comm Fault
10. Scram - CSC Watchdog Fault	23. Scram - NM-1000 Data Error
11. Scram - CSC Watchdog Timeout	24. Scram - DOM32 Fault
12. Scram - DAC Watchdog Fault	25. Scram - A1016 #1 Fault
13. Scram - DAC Watchdog Timeout	26. Scram - A1016 #2 Fault

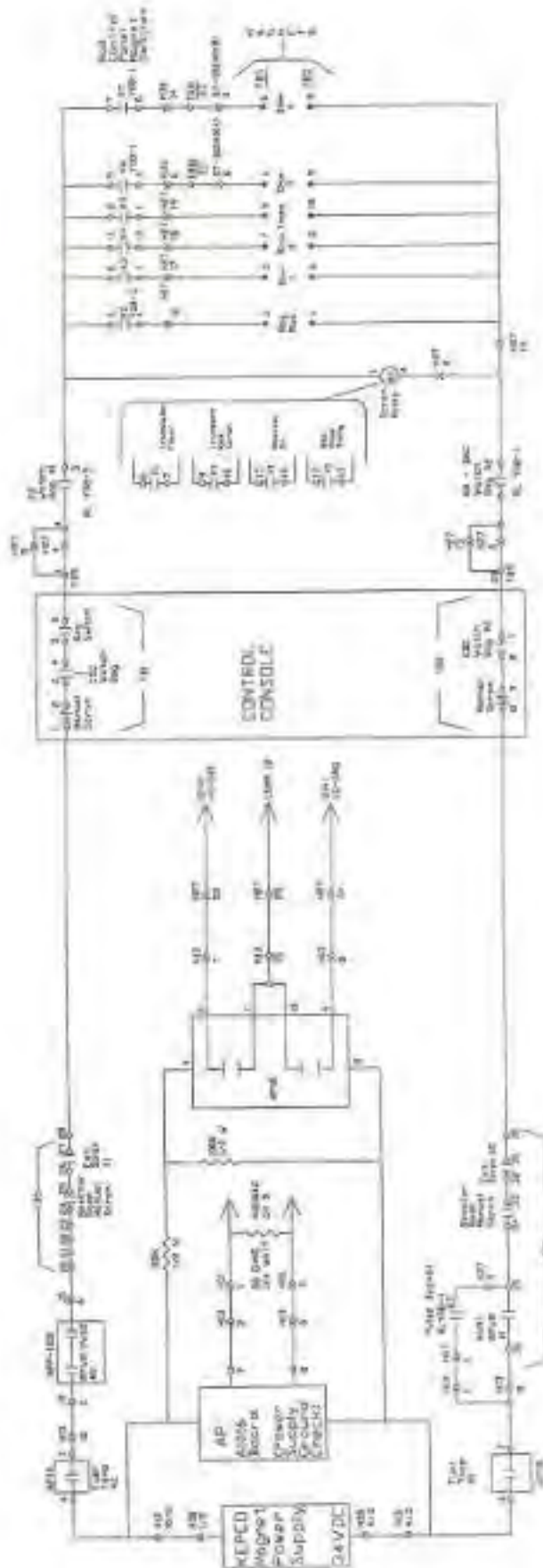
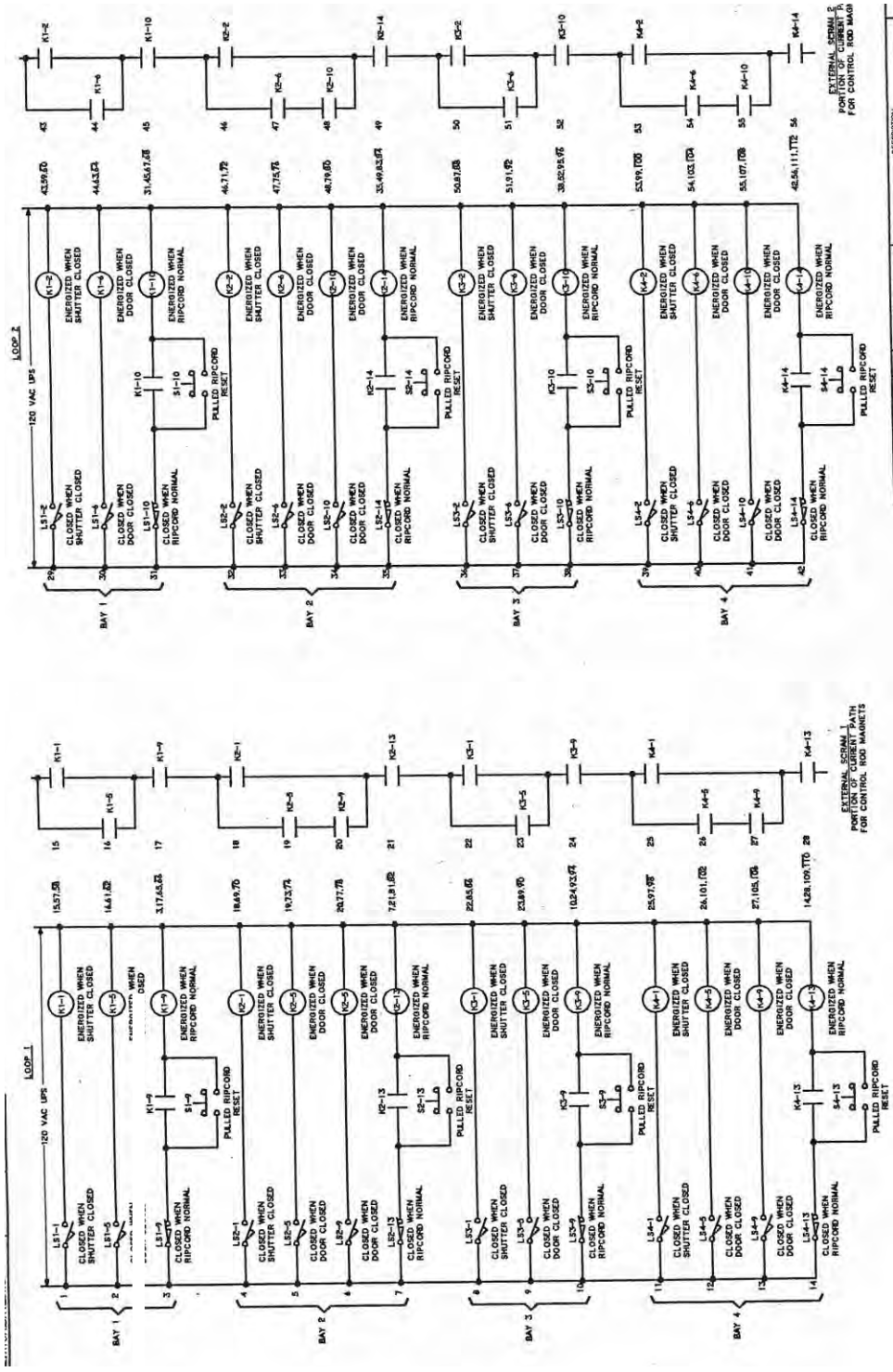


FIGURE 7.8 TYPICAL PROTECTIVE SYSTEM SCRAM LOGIC

FIGURE 7.9 EXTERNAL SCRAM INPUTS



**TABLE 7-2 TYPICAL CRT WARNING WINDOW DISPLAY**

1.	Pulse Not Detected	22.	Rx Room RAM
2.	Demand Power Not Reached	23.	Demineralizer RAM
3.	High IC-Net Comm Fault	24.	Equipment Area RAM
4.	Low IC-Net Comm Fault	25.	Staging Area #1 RAM
5.	Power Too Hi to Pulse	26.	Staging Area #2 RAM
6.	Trans Rod Air Must Be Off	27.	Staging Area #4 RAM
7.	Period Too Short to Pulse	28.	Rx Rm Particulate
8.	Line Printer Not On Line	29.	Rx Rm Noble Gas
9.	Rod Withdrawal Prohibit	30.	Rx Rm Iodine
10.	Rx Tank Return Temp Hi	31.	Bay Particulate
11.	Magnet Supply Voltage Grounded-Hi Side	32.	Stack Particulate
12.	Magnet Supply Voltage Grounded - Low Side	33.	Stack Noble Gas
13.	Primary System Flow	34.	Stack Argon
14.	Demin System Flow	35.	Bay Argon
15.	Secondary System Flow	36.	Rx Rm CAM Fault
16.	Demin Inlet Condtvty	37.	Stack CAM Fault
17.	Demin Outlet Condtvty	38.	Bay CAM Fault
18.	Rx Tank Water Level Hi	39.	Rx Rm CAM Alert
19.	Rx Tank Water Level Lo	40.	Stack CAM Alert
20.	Cooling Tower Water Level Hi	41.	Rx Rm CAM Alarm
21.	Cooling Tower Water Level Lo	42.	Stack CAM Alarm
		43.	Fire in DAC

TABLE 7-3 TYPICAL CRT STATUS WINDOW DISPLAY

Primary System Flow	000.0 gpm	Staging Area #1 RAM	000 mR/hr
Secondary System Flow	000.0 gpm	Staging Area #2 RAM	000 mR/hr
Demin System Flow	00.0 gpm	Staging Area #4 RAM	000 mR/hr
Demin Inlet Condtvty	0.0 uMHOS	Rx Rm Particulate	0.0e+0 cpm
Demin Outlet Condtvty	0.0 uMHOS	Rx Rm Noble Gas	0.0e+0 cpm
Rx Tank Temp	00.0 C	Rx Rm Iodine	0.0e+0 cpm
Hx Outlet Temp	00.0 C	Stack Particulate	0.0e+0 cpm
Hx Inlet Temp	00.0 C	Stack Noble Gas	0.0e+0 cpm
Rod Drop Timer	0.00 sec		
Reactor Room RAM	000 mR/hr	Stack Argon	0.0e+0 cpm
Demineralizer RAM	000 mR/hr	Bay Particulate	0.0e+0 cpm
Equipment Area RAM	000 mR/hr	Bay Argon	0.0e+0 cpm
One Kilowatt Interlock	Yes		
Rod Withdrawal Prohibit	No		

The majority of the parameters listed in Table 7-1 initiate scram action in two ways. First, the in-series relays shown in Figure 7.8 will interrupt the rod drive magnet current causing a scram if the parameter setpoint is exceeded. Second, the SCRAM signal is detected by the computer and the computer generates a redundant scram signal that opens the four parallel relays (RLY08-3 K2, K3, K4, and RLY08-1 K5, K6, K7) interrupting rod magnet current. These same parallel relays are opened by a computer generated signal whenever the setpoints of the parameters listed in Figure 7.8 as "Computer Generated" exceed their setpoints.

Scram conditions are automatically indicated on the monitors and there is an audible annunciator. A manual scram may be used for a normal fast shutdown of the reactor.

### 7.3 Rod Control System

The reactivity of the UCD/MNRC reactor is controlled by six control rods. The control and transient rod drives are mounted on a bridge at the top of the reactor tank. The drives are connected to the control and transient rods through a connecting rod assembly. The following sections describe the control and transient rods and their respective drive assemblies.

#### 7.3.1 Control Rods

Reactor core loadings utilize fuel-followed control rods, i.e., control rods that have a fuel section below the absorber section. The uppermost section is 6.5 inch-long air-filled void and the next 15 inches is a solid boron carbide neutron absorber section. Immediately below the absorber is the fuel section consisting of 15 inches of U-ZrH<sub>1.7</sub> whose uranium is enriched in <sup>235</sup>U to less than 19.7%. The weight percent of uranium in the fuel is either 8.5, 12.5, or 20, depending on the core loading (currently 20 with 30B core).

The bottom section of the rod has an air-filled void approximately 6.5 inches long. The fuel and absorber sections are sealed in a Type 304 stainless steel tube approximately 43 inches long by 1.35 inches in diameter.

The fuel-followed control rods pass through and are guided by 1.5 in. diameter holes in the top and bottom grid plates. A typical control rod with fuel follower is shown in the withdrawn and inserted positions in Figure 7.10.

The transient rod is a sealed, 44.25 in. long by 1.25 in. diameter tube containing solid boron carbide as a neutron absorber and air as a follower. The absorber section is 21 in. long and the follower is approximately 23 in. long. The transient rod passes through the core in a perforated aluminum guide tube. The tube receives its support from the safety plate and its lateral positioning from both grid plates. It extends above the top grid plate. Water passage through the tube is provided by a large number of holes distributed evenly over its length.

### 7.3.2 Control Rod Drive Assemblies (For Transient Rod Assembly see Section 7.3.3)

The control rods are positioned by five standard TRIGA<sup>®</sup> electrically powered rack and pinion drives (Figure 7.11). One rod is designated as a regulating rod and used in conjunction with an automatic power control. All rods and rod drives are exactly the same and operate at a nominal rate of approximately 24 in. per minute.

The rod drives are connected to the control rods through a connecting rod assembly. These assemblies contain a bolted connection at each end to accept the control rod at one end and the control rod drive at the other. The grid plates provide guidance for all control rods during operation of the reactor. No control rods can be inserted or removed by their drives a sufficient distance to allow disengagement from the grid plates.

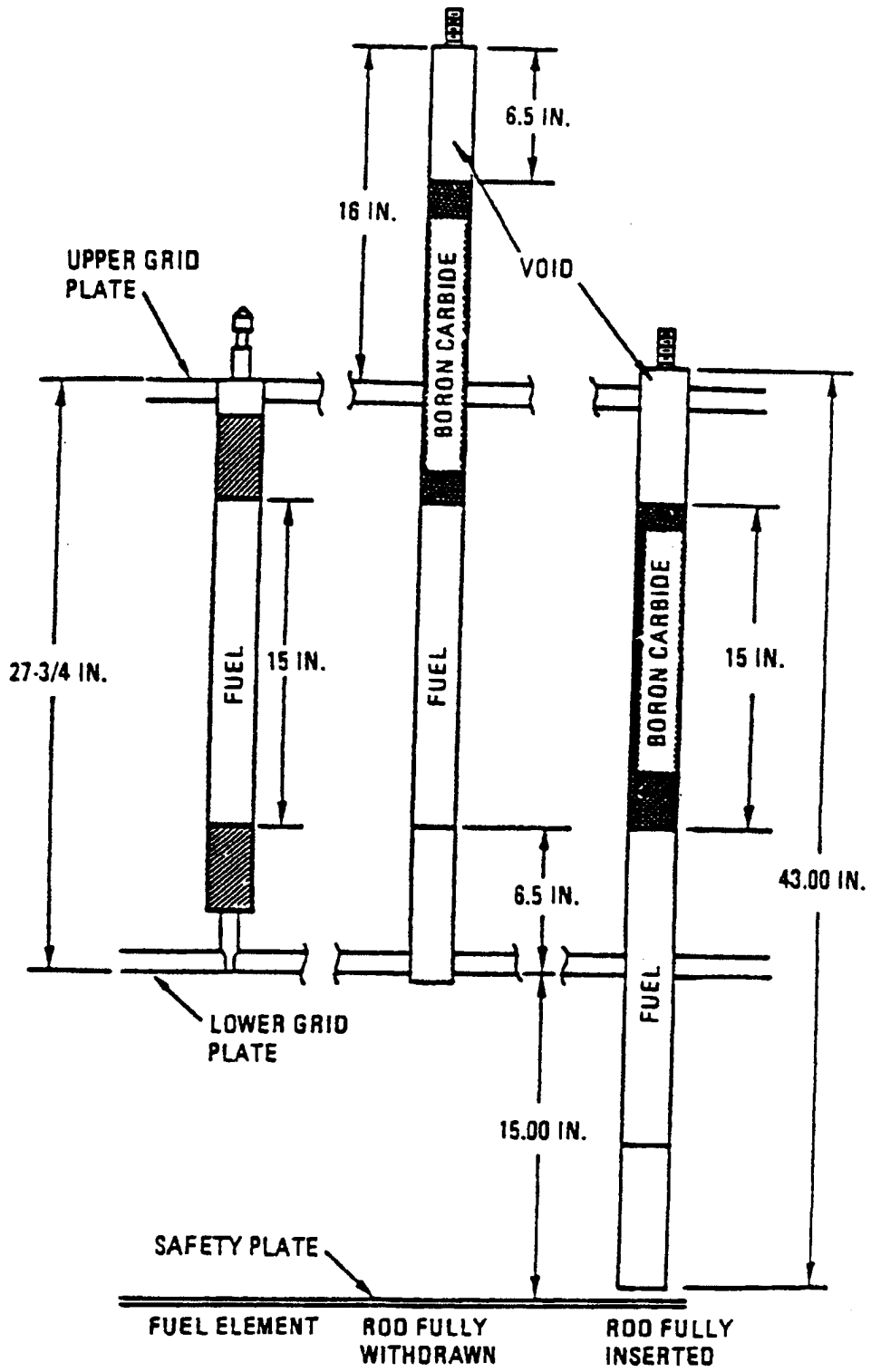


FIGURE 7.10 TYPICAL FUEL FOLLOWER CONTROL ROD SHOWN WITHDRAWN AND INSERTED

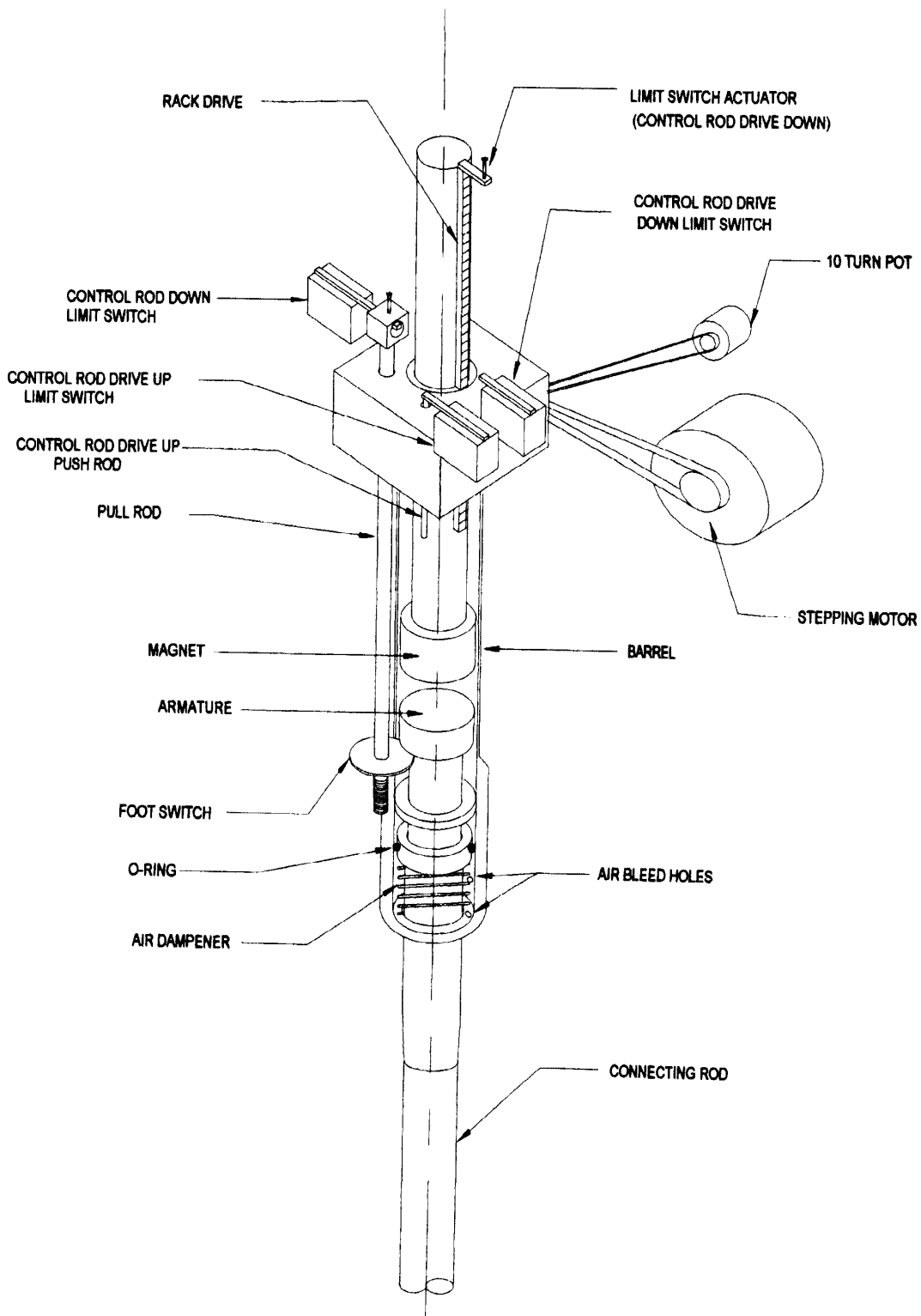


FIGURE 7.11 RACK-AND-PINION CONTROL ROD DRIVE (TYPICAL)

Each drive consists of a stepping motor, a magnet rod-coupler, a rack and pinion gear system, and a ten-turn potentiometer used to provide an indication of rod position. The pinion gear engages a rack attached to a draw tube which supports an electromagnet. The magnet engages a chrome-plated armature to the end of a connecting rod that fits into the connecting tube. The connecting tube extends down to the control rod. The magnet, its draw tube, the armature, and the upper portion of the connecting rod are housed in a tubular barrel. The barrel extends below the control rod drive mounting plate with the lower end of the barrel serving as a mechanical stop to limit the downward travel of the control rod drive assembly. The lower section of the barrel contains an air snubber to dampen the shock of the scrambled rod. In the snubber section, the control rods are decelerated through a length of 3 in. During this length, air is compressed under a piston attached to the connecting rod by the weight of the control rod and is slowly bled to atmosphere through an adjustable needle valve. The control rod can be withdrawn from the reactor core when the electromagnet is energized. When the reactor is scrambled, the electromagnet is de-energized and the armature is released.

The rod drive motors are stepping motors driven by a translator. The speed of the rods is adjustable and is normally set to insert or withdraw the control rods at a nominal rate of 24 in./min. The unique characteristics of a stepping motor/translator system are used to provide fast stops and to limit coasting or overtravel. The control rod drive speeds are administratively controlled. Access to the control rod drives is restricted to authorized personnel and the physical location is in a restricted area.

These rod drives have the capability of withdrawing the rods at a maximum rate of 42 in./min.. The system is fail-safe, that is, multiple system failures are required to get uncontrolled withdrawal of the rods at this maximum speed. In addition, reactivity insertion accident analyses, Chapter 13, have shown no significant effects.

Limit switches mounted on each drive assembly stop the rod drive motor at the top and bottom of travel and provide switching for console indication which shows:

1. When the magnet is in the up position;
2. When the magnet (and thus the control rod) is in the down position;
3. When the control rod is in the down position.

A key-locked switch on the reactor console power supply prevents unauthorized operation of all control rod drives.

These rod drives were first developed in 1959, and have been modified and improved a number of times. The design has proven to be reliable and has been used in more than 60 TRIGA<sup>®</sup> reactors containing more than 160 rod drives.

### 7.3.3 Transient Rod Drive Assembly

The UCD/MNRC adjustable fast transient rod drive (Figure 7.12) consists of a combination of a standard TRIGA<sup>®</sup> rack-and-pinion control drive, described in Section 7.3.2, and a

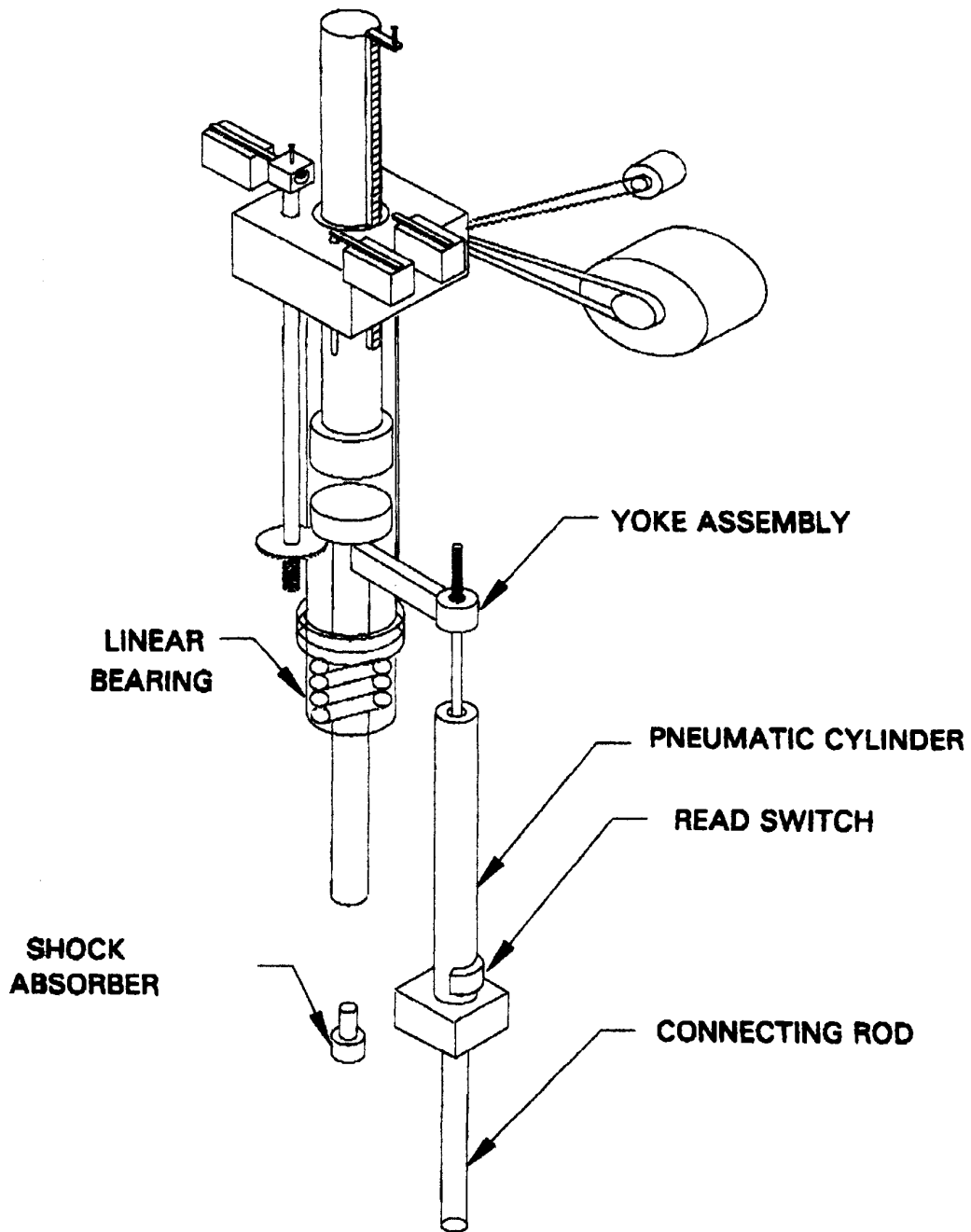


FIGURE 7.12 ADJUSTABLE FAST TRANSIENT ROD DRIVE ASSEMBLY (TYPICAL)

standard TRIGA<sup>®</sup> fast transient control rod drive, both of which have been modified. This combination transient rod drive can be used to fire low-level pulses and keep the pulse rod totally out of the core during the pulse. This combination drive unit was chosen to take advantage of the extensive operating experience gained on both the standard rack-and-pinion drive and on the standard fast transient rod drive. This combination drive unit has extensive operating experience at the Japan Atomic Energy Institute (JAERI) and Sandia National Laboratory.

The standard fast transient rod drive portion of the assembly consists of a pneumatic cylinder to drive the transient rod out of the core and a dashpot to decelerate the transient rod and drive system at the end of the stroke. The total length of the transient rod travel is 21 in. including a 6 in. deceleration length.

The pneumatic cylinder is single-acting and has a maximum stroke of 22 in. Clearance is provided to ensure that the dashpot will bottom out before the upper limit of the pneumatic cylinder. The cylinder is equipped with low friction seals so that the rod will drop freely back into the core after the transient. A piston position switch is provided to indicate when the piston, and therefore the control rod, is in the full down position. The dashpot is at the lower end of the cylinder assembly. This assembly has its own piston and bleed ports and is designed to decelerate the transient rod and eliminate any hard stops.

The standard fast transient rod drive is provided with its own pneumatic cylinder, accumulator tank, pressure regulator, and solenoid valve. The solenoid valve actuates the cylinder from the accumulator tank which may be pressurized up to 150 psi. Aluminum tubing 7/8 in. diameter is used as a connecting rod between the pneumatic cylinder, which is mounted on the rod drive bridge, and the transient rod.

The standard fast transient rod drive is thoroughly developed and tested. These drives have been installed on the TRIGA<sup>®</sup> reactors at GA Technologies Facility, University of California at Irvine, Sandia National Laboratory, University of Illinois, Japan Atomic Energy Institute (JAERI), and the dual-core TRIGA<sup>®</sup> research reactor in Romania.

The basic concept used in the UCD/MNRC drive is to modify the standard fast transient rod drive to have a portion of the piston assembly extend through the top of the drive. This extension of the transient rod piston engages a yoke mounted below the armature. The rack-and-pinion drive is mounted slightly above and to one side of the transient rod drive. When the rack-and-pinion drive is driven up, the yoke moves under the transient rod drive piston extension and moves the piston assembly, and therefore the transient rod upward with it. The rack-and-pinion drive position is read out on the console and the drive can be stopped at any position of its travel by the reactor console operator. Upon initiating a pulse, the transient rod will move until it is completely out of the reactor core. During this portion of travel, the piston rod extension will slide freely in the yoke mounted to the rack-and-pinion drive and no movement of the rack-and-pinion drive will be required.

Upon completion of a transient, both of the coupled drives will scram and the transient rod will fall completely back into the reactor core. The yoke mounted on the armature will fall about the same speed as the piston rod assembly attached to the transient drive. The rack-and-pinion drive is capable of moving and holding the transient rod at any position between full out and full in. The rack-and-pinion rod drive is capable of moving the rod approximately 15 inches of travel, the same as the travel of a standard control rod drive, and of scrambling and dropping the transient rod from any position.

In order to combine the operation of the rack-and-pinion drive and the transient rod drive, the rack-and-pinion rod drive has been modified. The drive uses the same rack-and-pinion assembly, magnet and armature connection, and modified version of the lower barrel assembly as the standard control rod drive. The lower barrel assembly is shorter and contains a slot on one side for the yoke assembly. The lower barrel assembly, as modified, terminates in a large heavy flange. A bearing housing with a double set of ball bearings is bolted to the bottom of the lower barrel and an actuator shaft passes through the bearing housing. The top end of the actuator shaft contains the magnet armature, and the yoke assembly is bolted to the actuator shaft just below the magnet armature. The bearing housing provides a rigid and accurate parallel path for the entire rack-and-pinion rod drive assembly.

The entire assembly consisting of the standard control rod drive assembly, the modified lower barrel, and the bearing housing are rigidly bolted to a support which runs parallel to the transient rod air cylinder.

CHAPTER 8

ELECTRICAL DISTRIBUTION

Chapter 8 - Valid Pages  
Rev. 7 05/01/18

i	Rev. 7	05/01/18
8-1	Rev. 7	05/01/18
8-2	Rev. 7	05/01/18
8-3	Rev. 7	05/01/18

---

TABLE OF CONTENTS

8.0	ELECTRICAL POWER .....	8-2
8.1	Introduction.....	8-2
8.2	UCD/MNRC Electrical Power System.....	8-2
8.3	UCD/MNRC Raceway System.....	8-3

LIST OF FIGURES

8.1	UCD/MNRC Electrical Distribution System - Single Line Diagram.....	4
-----	--	---

## 8.0 ELECTRICAL POWER

### 8.1 Introduction

The electrical power for the UCD/MNRC is supplied from a transformer located to the south of the facility. The interconnections between the transformer and the UCD/MNRC are designed in accordance with the following codes and standards:

National Electrical Code - NFPA-70;  
National Electrical Safety Code;  
NEMA Standards.

The design of the UCD/MNRC reactor does not require electrical power to safely shut down the reactor, nor does it require electrical power to maintain acceptable shutdown conditions.

### 8.2 UCD/MNRC Electrical Power System

The UCD/MNRC receives its electrical power through an underground primary 480/277 V, 3-phase, 3-wire distribution system from the nearby transformer.

As shown in Figure 8.1, the UCD/MNRC electrical power is channeled through a 480/277 V, 800 A, 4-wire, main breaker which incorporates a "UFER" ground system. This breaker feeds the facility main distribution panel, HD. The reactor system receives electrical power through the 50 kVA, 480 V, 3 $\phi$  input 208/120 V transformer through panel 2A.

A Uninterruptible Power Supply (UPS) feeds the reactor instrumentation and control system and radiation monitoring equipment. This system is designed to provide power to the reactor console and the translator rack for approximately 15 minutes after loss of normal electrical power.

The UCD/MNRC UPS also provides power to the stack continuous air monitor (CAM), and the six facility remote area monitors (RAMs), for a minimum of four (4) hours after loss of normal electrical power.

The UCD/MNRC UPS is not needed for safe reactor shutdown or maintenance of safe shutdown conditions. It does, however, supply the necessary instrumentation so that the operator can initiate and affirm complete reactor shutdown, rod positions, and power level. More importantly, it supplies radiation monitoring equipment with power so that radiation levels are known.

The electrical power for the UCD/MNRC reactor's primary, makeup, and purification water systems, as well as the pool and reactor "on" lights, is supplied from panel 2B.

The facility air handling and exhaust systems are fed through panels 2AC and 2A.

A propane generator provides backup power to the reactor room ventilation system (Chapter 9).

Two other UCD/MNRC systems, fire alarm and security, are equipped with their own UPSs. The battery packs for both of these systems are capable of maintaining normal operations for 24 hours after loss of normal power.

The reactor/radiation instruments receive their power from a regulated power supply that meets a commercial grade standard.

### 8.3 UCD/MNRC Raceway System

The UCD/MNRC raceway system consists of the conduit runs, cable trays, pull boxes, and fittings that contain all power, instrumentation, and control wiring associated with the reactor. Cabling originating in (detectors) or above the tank (control rod drives) is routed either along the tank wall or under the bridge to the reactor room cable trench. A raceway contains the cables between the cable trench and the NM-1000 and the NPP-1000 (Chapter 7). Separate conduit runs have been provided between the reactor room and the control room for reactor control and instrumentation wiring. The routing is such that there are two independent paths giving physical isolation. That is, the reactor-instrumentation wiring is designed so that one control and one safety-instrumentation channel takes one path. Additionally, the other control and safety-instrumentation channel is contained in the other path. The control wiring for control-rod drives is split in the same manner.

Since controls are not required for safe shutdown, no special fire-protection system is required for the raceway system.

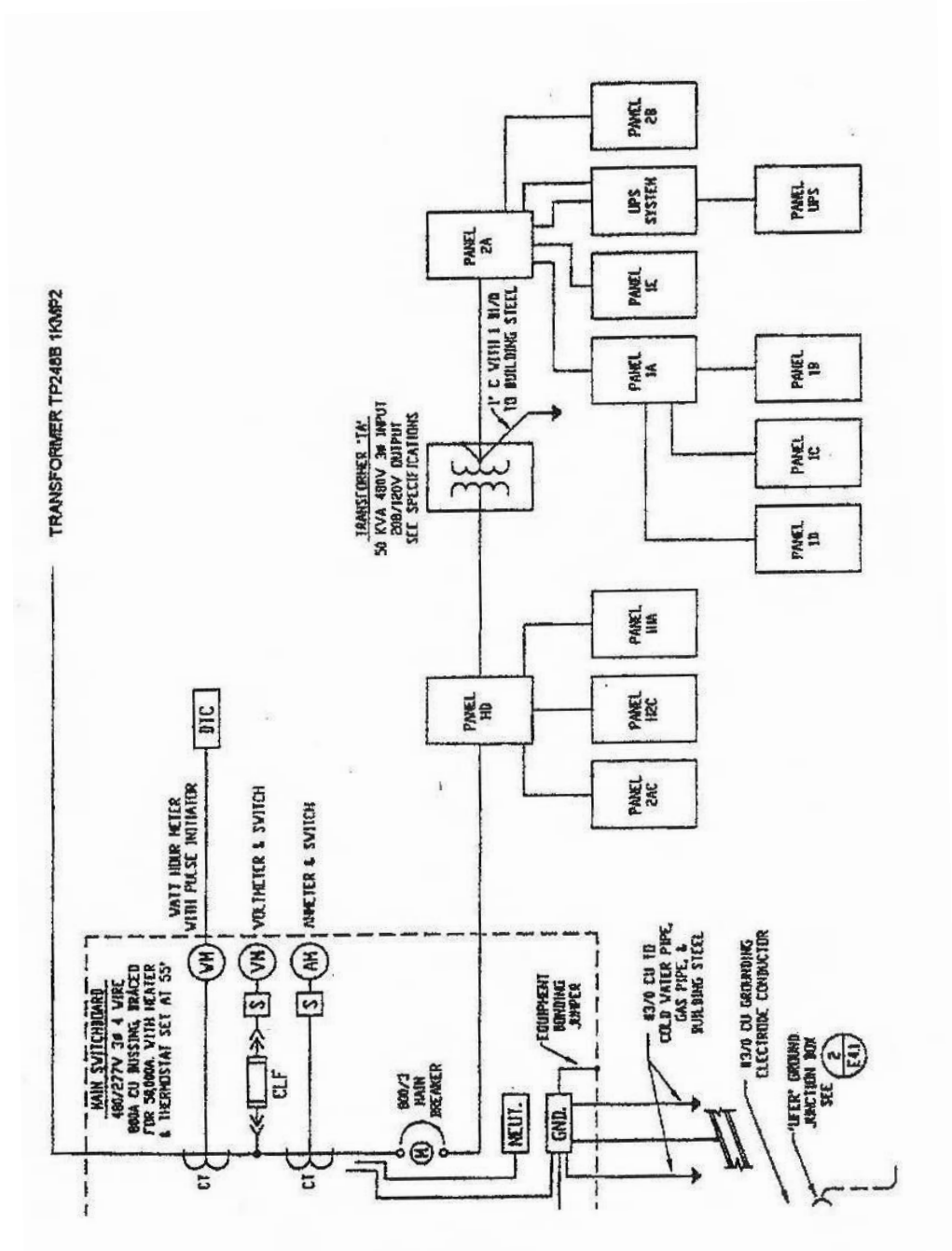


FIGURE 8.1 UCD/MNRC ELECTRICAL DISTRIBUTION SYSTEM - SINGLE LINE DIAGRAM

CHAPTER 9

AUXILIARY SYSTEMS

Chapter 9 Valid Pages

Rev. 5 05/02/18

i	Rev. 5	05/02/18	9-21	Rev. 5	05/02/18
ii	Rev. 5	05/02/18	9-22	Rev. 5	05/02/18
iii	Rev. 5	05/02/18	9-23	Rev. 5	05/02/18
9-1	Rev. 5	05/02/18	9-24	Rev. 5	05/02/18
9-2	Rev. 5	05/02/18	9-25	Rev. 5	05/02/18
9-3	Rev. 5	05/02/18	9-26	Rev. 5	05/02/18
9-4	Rev. 5	05/02/18	9-27	Rev. 5	05/02/18
9-5	Rev. 5	05/02/18	9-28	Rev. 5	05/02/18
9-6	Rev. 5	05/02/18	9-29	Rev. 5	05/02/18
9-7	Rev. 5	05/02/18	9-30	Rev. 5	05/02/18
9-8	Rev. 5	05/02/18	9-31	Rev. 5	05/02/18
9-9	Rev. 5	05/02/18	9-32	Rev. 5	05/02/18
9-10	Rev. 5	05/02/18	9-33	Rev. 5	05/02/18
9-11	Rev. 5	05/02/18	9-34	Rev. 5	05/02/18
9-12	Rev. 5	05/02/18	9-35	Rev. 5	05/02/18
9-13	Rev. 5	05/02/18	9-36	Rev. 5	05/02/18
9-14	Rev. 5	05/02/18	9-37	Rev. 5	05/02/18
9-15	Rev. 5	05/02/18	9-38	Rev. 5	05/02/18
9-16	Rev. 5	05/02/18	9-39	Rev. 5	05/02/18
9-17	Rev. 5	05/02/18	9-40	Rev. 5	05/02/18
9-18	Rev. 5	05/02/18	9-41	Rev. 5	05/02/18
9-19	Rev. 5	05/02/18			
_____ 9-20	Rev. 5	05/02/18			

TABLE OF CONTENTS

9.0	AUXILIARY SYSTEMS.....	9-1
9.1	Fuel Storage and Handling.....	9-1
9.1.1	Bay 2 Fuel Storage Area.....	9-1
9.1.1.1	Design Basis .....	9-1
9.1.1.2	Facility Description .....	9-1
9.1.1.3	Safety Evaluation .....	9-2
9.1.2	In-Tank Fuel Storage.....	9-2
9.1.2.1	Design Basis .....	9-2
9.1.2.2	Facilities Description.....	9-2
9.1.2.3	Safety Evaluation .....	9-2
9.1.2.4	Inspection and Testing .....	9-3
9.1.3	Spent Fuel Storage.....	9-6
9.1.3.1	Design Basis .....	9-6
9.1.3.2	Facilities Description .....	9-6
9.1.3.3	Safety Evaluation.....	9-9
9.1.4	Fuel Handling System .....	9-9
9.1.4.1	Design Basis .....	9-9
9.1.4.2	Equipment Description .....	9-10
9.1.4.2.1	Fuel Handling Tools .....	9-10
9.1.4.2.2	Overhead Handling Systems.....	9-10
9.1.4.2.3	Fuel Transfer Cask.....	9-10
9.1.4.2.4	Cask Positioning Plate.....	9-13
9.1.4.3	Description of Fuel Transfer .....	9-13
9.1.4.4	Safety Evaluation .....	9-14
9.2	Helium Supply System.....	9-14
9.3	Building Water Systems.....	9-16
9.3.1	Auxiliary Make-Up Water System (AMUWS) .....	9-16
9.4	Fire Protection .....	9-18
9.4.1	Design Basis .....	9-18
9.4.2	Description.....	9-18
9.4.3	Evaluation .....	9-19
9.5	Air Handling System .....	9-19
9.5.1	Design Basis.....	9-19

9.5.2	Description .....	9-22
9.5.3	Evaluation.....	9-24
9.6	Interlocks/Controls - Bay Shutters/Doors .....	9-24
9.6.1	Shutter (Bulk Shield) Control/Interlocks .....	9-24
9.6.2	Bay Door Controls/Interlocks .....	9-31
9.6.3	ReactorInterlocks .....	9-34
9.7	Communication and CCTV Systems.....	9-34
9.8	Security System .....	9-41

LIST OF FIGURES

9.1	Typical In-Tank Fuel Storage Rack .....	9-4
9.2	Typical In-Tank Fuel Storage Rack Locations .....	9-5
9.3	Fuel Storage Location .....	9-7
9.4	Fuel Storage Pit/Rack.....	9-8
9.5	Fuel Element Handling Tool.....	9-11
9.6	Fuel Element Transfer Cask .....	9-12
9.7	Typical Helium Supply.....	9-15
9.8	Auxiliary Makeup Water System (AMUWS) .....	9-17
9.9	UCD/MNRC Fire Suppression System, Main Floor .....	9-20
9.10	UCD/MNRC Fire Suppression System, Second Floor.....	9-21
9.11	UCD/MNRC Air Handling System.....	9-23
9.12	UCD/MNRC Shutter Control Schematic (Bay 2).....	9-26
9.13	UCD/MNRC Shutter Bay Door And Rip Cord Limit Switches .....	9-27
9.14	UCD/MNRC Shutter Control Logic (Radiography Control Room) .....	9-28
9.15	UCD/MNRC Shutter Control Logic (Inside Bay) .....	9-29
9.16	UCD/MNRC Bay Door Control Schematic (Bay 2).....	9-32
9.17	UCD/MNRC Bay Door Control Logic .....	9-33
9.18	UCD/MNRC Bay Door, Shutter, And Rip Cord Control Schematic – Reactor Scram Chain Input (Loop No. 1) .....	9-35
9.19	Rip Cord Location – Bays 1 And 2 .....	9-36
9.20	Rip Cord Location – Bays 3 And 4 .....	9-37
9.21	Rip Cord Location – Plan View .....	9-38
9.22	Typical UCD/MNRC Closed Circuit Television – Main Floor .....	9-39
9.23	Typical UCD/MNRC Closed Circuit Television – Second Floor .....	9-40

#### REFERENCES

- 9.1 G. A. Letter, D. B. Hagmann to Wade Richards, USAR Information, June 15, 1988.
- 9.2 Brinkley, Anthony L., Seismic Analysis on Fuel Element Storage Racks, June 1997.
- 9.3 G. A. Letter, D. B. Hagmann to Wade Richards, Fuel Storage Pits, July 25, 1988.
- 9.4 G. A. memo, F. C. Foushee to D. B. Hagmann, SNRS Fuel Storage Pits - Energy Deposition and Removal, August 13, 1987.
- 9.5 GA Report, Criticality Calculations of MNRC Reactor Fuel Storage Pits, September 30, 1996.
- 9.6 ANL memo, J.C. Courtney to R. D. Phipps, Shielding Analysis of the McClellan Air Force Base Fuel Transfer Cask, MP-N2282, June 24, 1988.
- 9.7 ANL memo, J. G. Gale to E. K. Sherman, TRIGA® Fuel Cask, Cart, and Adapter Plate Stress Analysis for McClellan Air Force Base, April 19, 1988.

## 9.0 AUXILIARY SYSTEMS

This chapter discusses the auxiliary systems that support the UCD/MNRC operation.

### 9.1 Fuel Storage and Handling

The fuel loading for the UCD/MNRC reactor will consist of approximately 100 fuel elements, including up to five control rods, one transient rod, and graphite elements. Fuel elements can be stored in the reactor tank and/or storage pits [REDACTED] to facilitate burn-up management or, when spent, until such time that they can be shipped to a repository facility.

Basically, the fuel handling cycle within the UCD/MNRC consists of (1) receiving fresh fuel packaged in accordance with DOT transport requirements, (2) storing fuel in one or more of the three authorized fuel storage locations, (3) transferring the fuel elements into in-tank storage racks by use of the fuel element handling tool, (4) unloading spent fuel elements from the reactor grid into the in-tank storage racks, (5) loading the fuel elements from the in-tank storage racks into the reactor grid, (6) repositioning fuel elements within the reactor grid, (7) interchanging fuel elements between the reactor grid and the in-tank storage racks, (8) transferring irradiated fuel elements from the reactor in-tank storage rack by use of the fuel storage pits [REDACTED] and (9) transferring fuel from either the storage pits or in-tank storage racks to a shipping cask for removal.

#### 9.1.1 Bay 2 Fuel Storage Area

##### 9.1.1.1 Design Basis

- a. All SNM stored in the Bay 2 Fuel Storage Area shall be in NRC/DOT shipping containers approved at the time of receipt for the contained SNM. All SNM stored in the Bay 2 Fuel Storage Area shall have a K-effective value less than 0.9 for any stored configuration.
- b. The Bay 2 Fuel Storage Area shall comply with the applicable NRC security requirements.

##### 9.1.1.2 Facility Description

The Bay 2 Fuel Storage Area shall be located in the lower portion of the Bay 2 escape trunk. Normal entry into Bay 2 is through one of two massive shield doors. In order to reduce the scattered thermal neutron flux in the Bay 2 fuel storage area, a one-inch thick borated polyethylene shield has been placed across the front of the storage area.

### 9.1.1.3 Safety Evaluation

All SNM stored in the Bay 2 Fuel Storage Area shall be in NRC/DOT shipping containers – approved at the time of receipt for the contained SNM. The design basis 9.1.1.1 (a) may be derived from either an approved NRC/DOT certificate of compliance, an established transportation index, or calculation.

### 9.1.2 In-Tank Fuel Storage

#### 9.1.2.1 Design Basis

- a. The in-tank fuel storage racks are designed with sufficient spacing between fuel elements to ensure that the array, when fully loaded, will be substantially subcritical.
- b. The in-tank fuel storage racks have a combined capacity for storage of nearly an entire core of irradiated fuel elements with one fuel element per storage hole.
- c. The in-tank fuel storage racks are mounted on the inside of the reactor tank and deep enough below the water surface to provide adequate radiation shielding.
- d. The in-tank fuel storage racks are designed and arranged to permit efficient handling of fuel elements during insertion, removal, or interchange of fuel elements.

#### 9.1.2.2 Facilities Description

Five in-tank aluminum fuel storage racks, with a combined capacity to accommodate 100 irradiated fuel elements are provided (Figure 9.1). The in-tank fuel storage racks are located at the outer edge of the reactor tank (Figure 9.2). Each rack has two levels with storage space to accommodate 20 fuel elements.

The fuel elements are loaded into the in-tank fuel storage racks from above. Each storage hole has adequate clearance for inserting or withdrawing a fuel element without interference. The weight of the fuel elements is supported by the lower plates of the racks.

Each in-tank fuel storage rack is securely hung from the top of the reactor tank by two 3/4- in. diameter aluminum rods. These rods are secured to the tank flange and the rack by threaded fasteners. This mounting arrangement prevents the racks from tipping or being laterally displaced.

#### 9.1.2.3 Safety Evaluation

Within a fuel storage rack, control of spacing is not actually required to limit the effective multiplication factor of the array (keff). The in-tank fuel storage racks are configured such that criticality is not possible (Reference 9.1).

Based on the fact that the storage racks are limited to 20 elements, there should be no effect on the criticality conditions, since even with the heaviest elements (i.e., all 30/20), 60 elements are required to go critical.

Furthermore, Reference 9.1 shows that 2 racks of 8.5 wt% fuel stored back to back are subcritical (i.e.,  $k_{\text{eff}} = 0.74$  for twice the  $^{235}\text{U}$  mass). While the 30/20 fuel increases the  $^{235}\text{U}$  mass by  $\sim 4.00$ , it contains erbium, causing the 30/20 fuel to have a reactivity more similar to an 8.5 wt % fuel element. Therefore, there should be no effect on the criticality of the system. In the unlikely event of loss of reactor tank coolant water, the loss of the water moderator would increase the safety margin by reducing the  $K_{\text{eff}}$ . The in-tank fuel storage racks are made of aluminum and are designed to withstand a UBC Zone 3 earthquake with importance factor 1.5, when fully loaded.

The in-tank storage racks are bolted to the upper tank flange and will resist a limited pull-up force in the event that the fuel element or handling equipment becomes fouled during handling operations.

Seismic analysis performed on the in-tank storage racks could not substantiate conclusively the survival of the racks post a design basis seismic event. Therefore, analysis was performed to ascertain the survival of a fuel element dropped from the fuel rack location and impacting on the bottom of the tank (Reference 9.2). This analysis predicts survival of a fuel element under all impact conditions. Clumping of fuel elements into a critical matrix after falling to the tank bottom is considered incredible.

#### 9.1.2.4 Inspection and Testing

The in-tank fuel storage racks will be visually inspected during installation to check that they are not deformed and that all fasteners are tight and in place.



**FIGURE 9.1 TYPICAL IN-TANK FUEL STORAGE RACK**

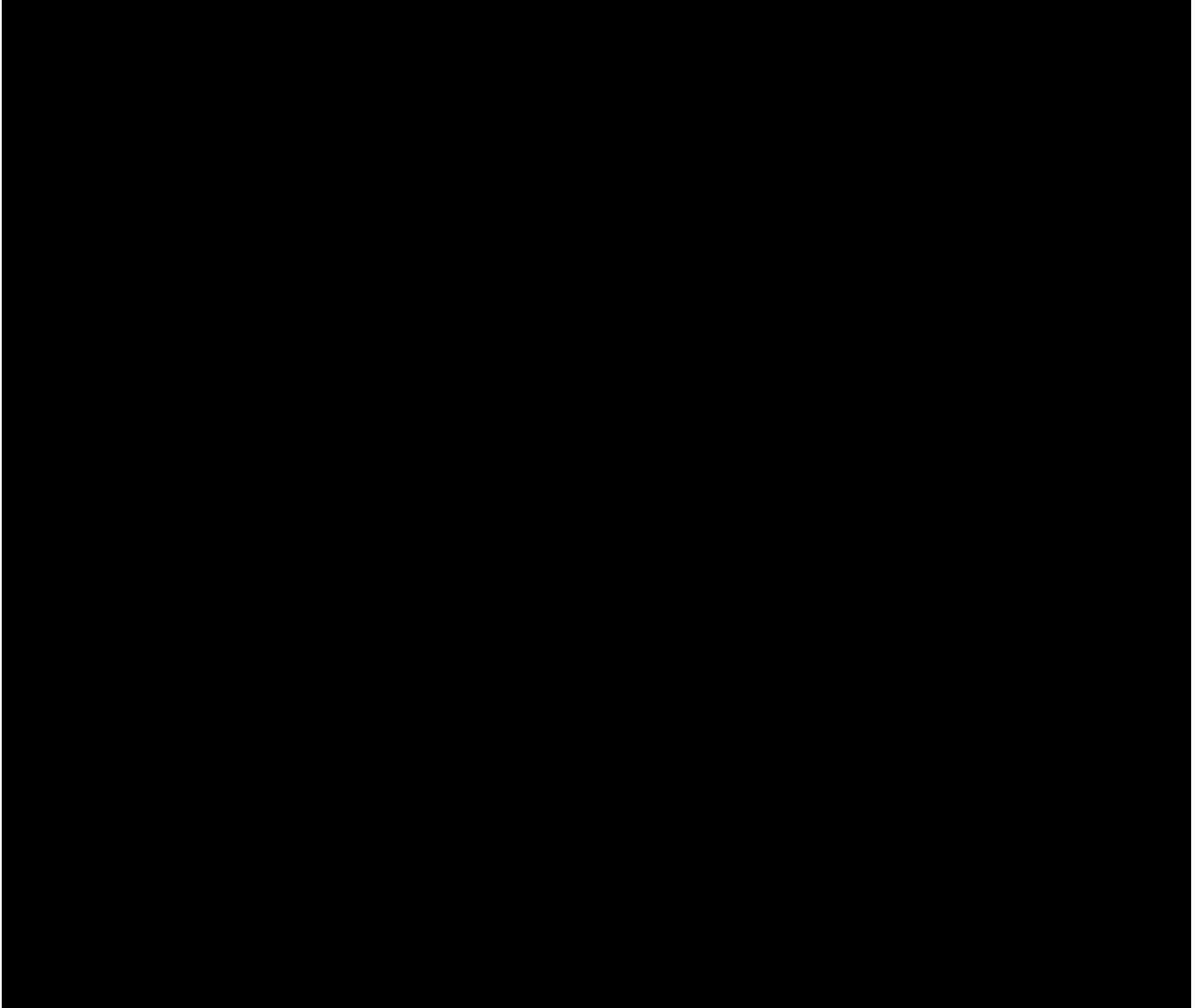


**FIGURE 9.2 TYPICAL IN-TANK FUEL STORAGE RACK LOCATIONS**

### 9.1.3 Spent Fuel Storage

#### 9.1.3.1 Design Basis

The spent fuel storage pits are designed with sufficient spacing to ensure that the array, when fully loaded, will be substantially subcritical.

The spent fuel storage pits are designed to withstand earthquake loading to prevent damage and distortion of the pit arrangement.

The spent fuel storage pits have a combined capacity for storage of 190 irradiated fuel elements with 38 fuel elements per storage pit (Reference 9.5).

The spent fuel storage pits are fabricated from materials compatible with the fuel elements and provide adequate personnel shielding.

The spent fuel storage pits are designed and arranged to permit efficient handling of fuel elements during insertion or removal of fuel elements.

The spent fuel storage pits have shield plugs that can be locked in place.

#### 9.1.3.2 Facilities Description

Five spent fuel storage pits, with a combined capacity to accommodate 190 (38 each) irradiated fuel elements, [REDACTED] Each pit has a liner and a lead-filled shield plug that will be locked in place when fuel is not being moved into or out of the pits. The pits have racks with holes for holding fuel elements (Figure 9.4). Each hole in the rack can only hold one fuel element. All storage pit material (liners, racks, plug casing, and pipes) that may contact either the fuel elements or the pit water are fabricated from aluminum or 304 stainless steel. This is the same type of material as used for the fuel element cladding and end fittings.

The fuel elements are loaded into the racks from above. Each hole in the rack has adequate clearance for inserting or withdrawing a fuel element without interference. However, with a fuel element in place in a hole, additional fuel elements cannot be inserted into the same hole. The weight of the fuel elements is supported by the lower plates of the racks which are, in turn, supported by the pit liners.

Each rack is designed so that it is constrained by the pit liner and cannot tip or become laterally displaced.

The storage pits are equipped with a cooling water system that will be used if required by the stored fuel elements. This system is described in Chapter 5.



**FIGURE 9.3 FUEL STORAGE LOCATION**

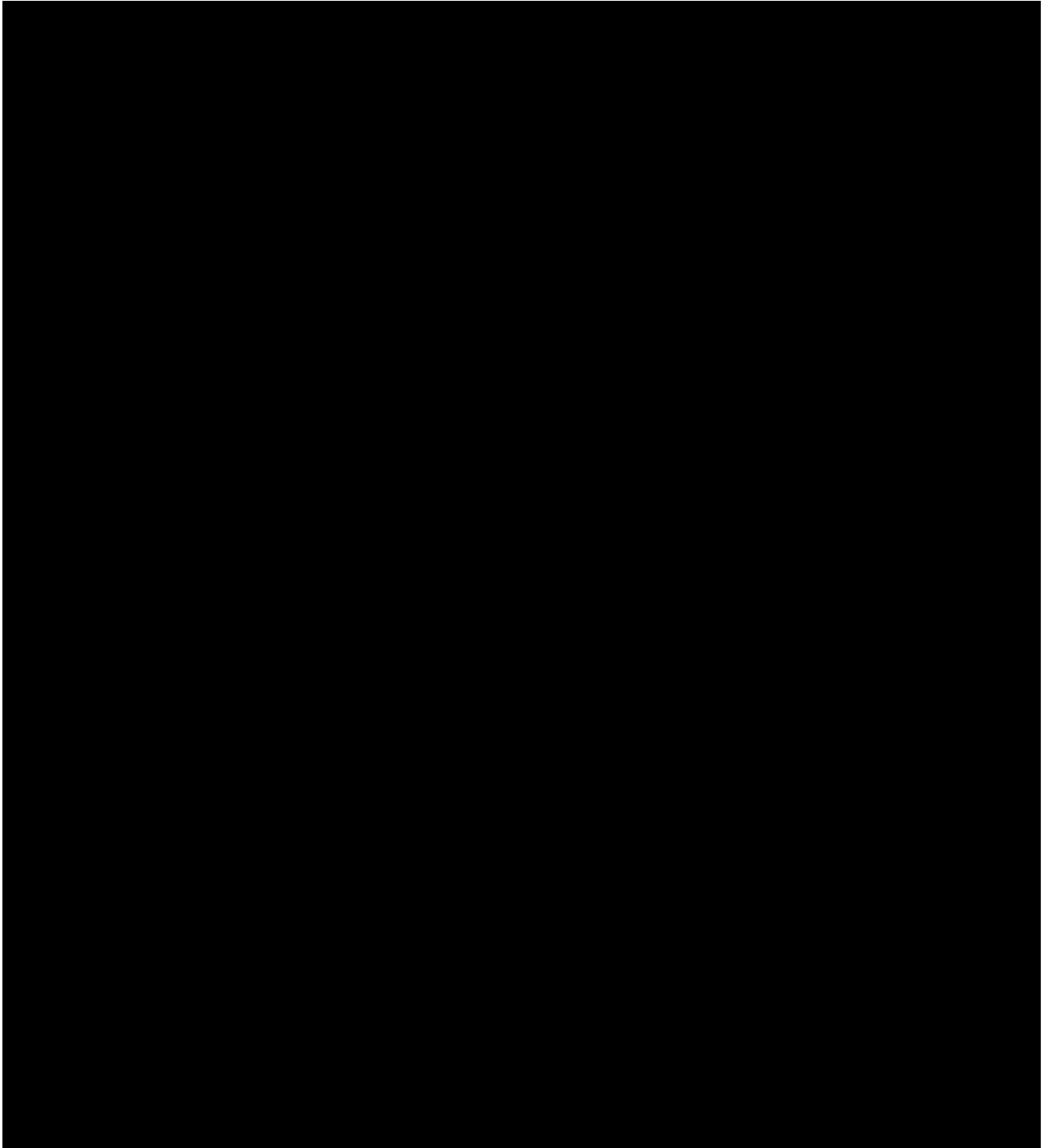


**FIGURE 9.4 FUEL STORAGE PIT/RACK**

Analysis shows that 19 fuel elements that have been in the core operating at 200 kW (one-tenth of the core power) can be removed from the reactor tank after one day and can be safely stored in a single fuel storage pit either with or without water (dry) (References 9.3 and 9.4). Since in a core operating at 2 MW power, the initial residual heat generation will be significantly higher, at least 10 days of decay must be allowed prior to transferring 19 fuel elements from the pool to the storage pit. This will allow for the residual thermal load to decrease to a level equivalent to that associated with the prior analysis conducted for a core operating at 200 kW and provides a margin of safety so that temperatures remain within analyzed safety limits. Elements are typically decayed in tank for months to years before moved to dry storage.

Reference 9.4 shows the expected radiation levels at the floor level with 38 irradiated elements in a single storage pit that have been in the core operating indefinitely at 1 MW, cooled for 24 hours, will be below one (1)  $\mu\text{R/hr}$  if the pit is filled with water or the lead shield plug is in place. Without water or the lead plug, the radiation level at floor level is predicted to be 15 rem/hr. For 2 MW operation, the estimated radiation levels will at most double (i.e., less than 2  $\mu\text{R/hr}$  with water or lead, and - 30 rem/hr with no shielding).

#### 9.1.3.3 Safety Evaluation

Within a fuel storage pit filled with water, control of spacing is not required to limit the effective multiplication factor of the array ( $K_{\text{eff}}$ ). An analysis shows the largest  $K_{\text{eff}}$  for a pit is approximately 0.93 when all five pits are loaded to capacity with 8.5 wt% fuel elements (38 each) and are full of water (0.45 when dry) (Reference 9.5). Since both 20/20 and 30/20 fuel contains erbium, they are similar in reactivity to 8.5 wt % , and there should be no significant changes to the criticality of the storage pits. Besides, 38 elements is  $\frac{2}{3}$  the number required for criticality. Also, radiation levels at the reactor room floor level with either water in the storage pits or the lead plug in place are below two (2)  $\mu\text{r/hr}$ , (see above). Exposures during fuel handling are discussed in Section 9.1.4.

The spent fuel storage pits are designed to withstand horizontal and vertical accelerations due to earthquakes. Stresses in a fully loaded storage pit will not exceed stresses specified by the UBC Zone 3, importance factor 1.5, seismic criteria.

#### 9.1.4 Fuel Handling System

##### 9.1.4.1 Design Basis

The fuel handling system provides a safe, effective, and reliable means of transporting and handling reactor fuel from the time it enters the UCD/MNRC facility until it leaves.

#### 9.1.4.2 Equipment Description

##### 9.1.4.2.1 Fuel Handling Tools

Tools are provided for handling individual fuel elements and for manipulating other core components. Individual fuel elements are handled with a flexible or rigid handling tool (Figure 9.5). The fuel element handling tool utilizes a locking ball-detent grapple to attach to the top end fitting of a fuel element. No special tool is provided for the fuel-followed control rods, as they are handled by the segmented connecting rod extending above the pool water surface to the control rod drive mechanism.

##### 9.1.4.2.2 Overhead Handling Systems

The reactor room has an electrically driven 5-ton overhead bridge crane. The crane is dual speed and pendant controlled and has provisions for locking the controls when it is not in use. The preparation area has an electrically driven 5-ton overhead monorail hoisting system. The monorail system is positioned directly above the preparation room floor access doors. These hoisting devices have been designed, fabricated, installed, and initially load tested in accordance with OSHA 1910.184.

The reactor room crane and the preparation room monorail system are operated in accordance with the ANSI B30.11, Monorail Systems and Underhung Cranes, prior to fuel cask handling. In addition, any slings required to transfer the fuel cask will be used in accordance with 29 CFR Part 1910.184, Slings.

##### 9.1.4.2.3 Fuel Transfer Cask

A shielded fuel transfer cask is used to transfer irradiated fuel elements from the reactor tank to the spent fuel storage pits or to a shipping cask. The fuel transfer cask is both top and bottom loading and will hold either one fuel element, an instrumented fuel element, or a fuel-followed control rod (Figure 9.6). The structural components are fabricated from stainless steel with a lead filler. The radiation exposure to operating personnel is about 5 mr/hr (gamma) at the outer surface of the transfer cask when it is loaded with an irradiated fuel element that has been allowed a six-month cooling time after operating in the highest flux region of the core for one year at one megawatt power (Reference 9.6). For fuel operated at 2 MW, the exposure should be 10mr/hr for the same period of decay. The cask internals that contact the fuel are fabricated from stainless steel. Cask-lifting lugs have been designed using the ASME code for analysis guidelines. This analysis shows that the maximum load on the lifting lug to cask weld is less than 1000 lb/in. of weld when the entire weight of the cask is on one lug (Reference 9.7). The allowable load for this weld is 6360 lb/in. of weld, a margin of greater than six even with the conservative assumption that all weight is on one lug. The cask lugs have been load tested in accordance with NE F8-6T.

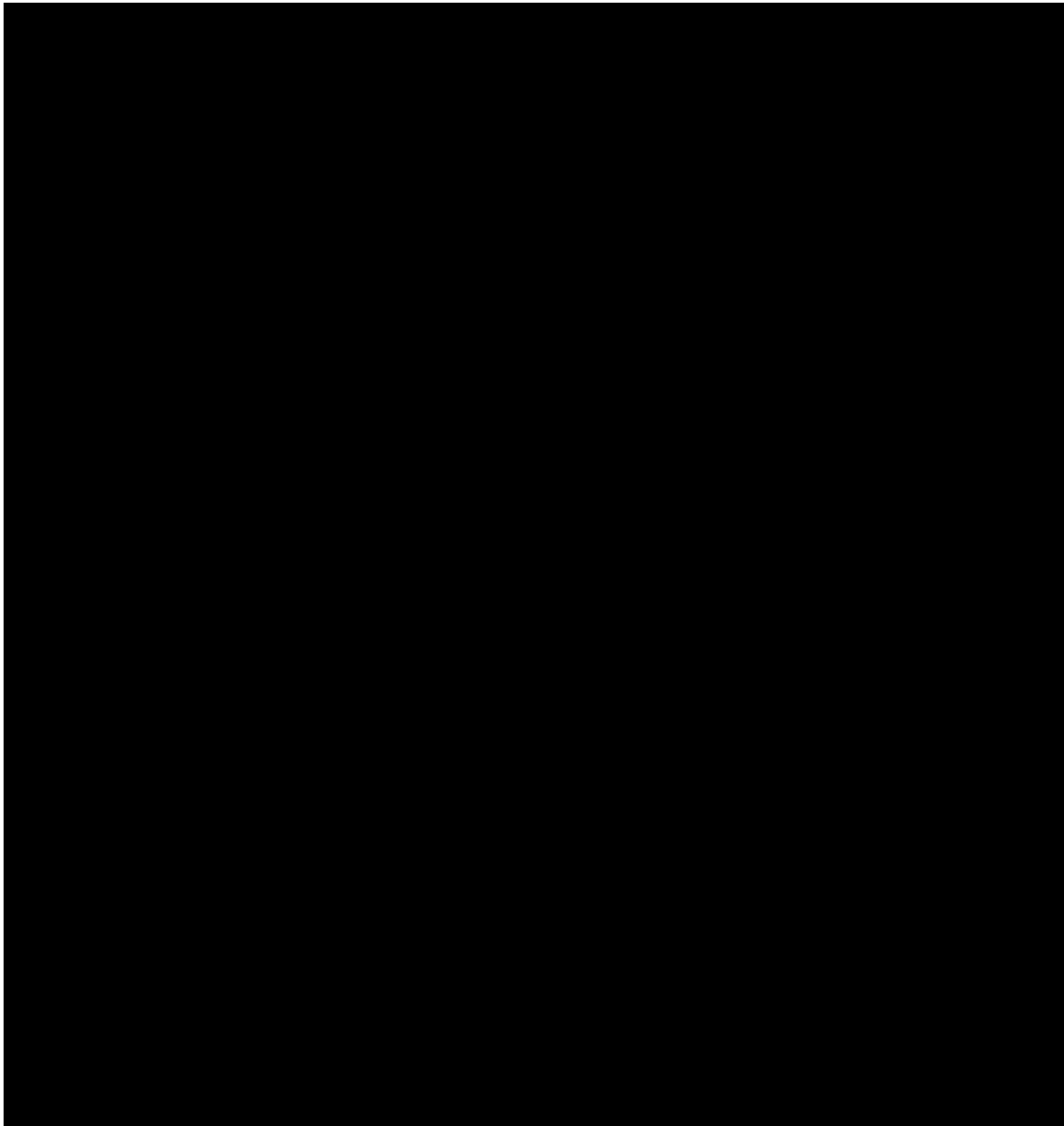


**FIGURE 9.5 FUEL ELEMENT HANDLING TOOL**

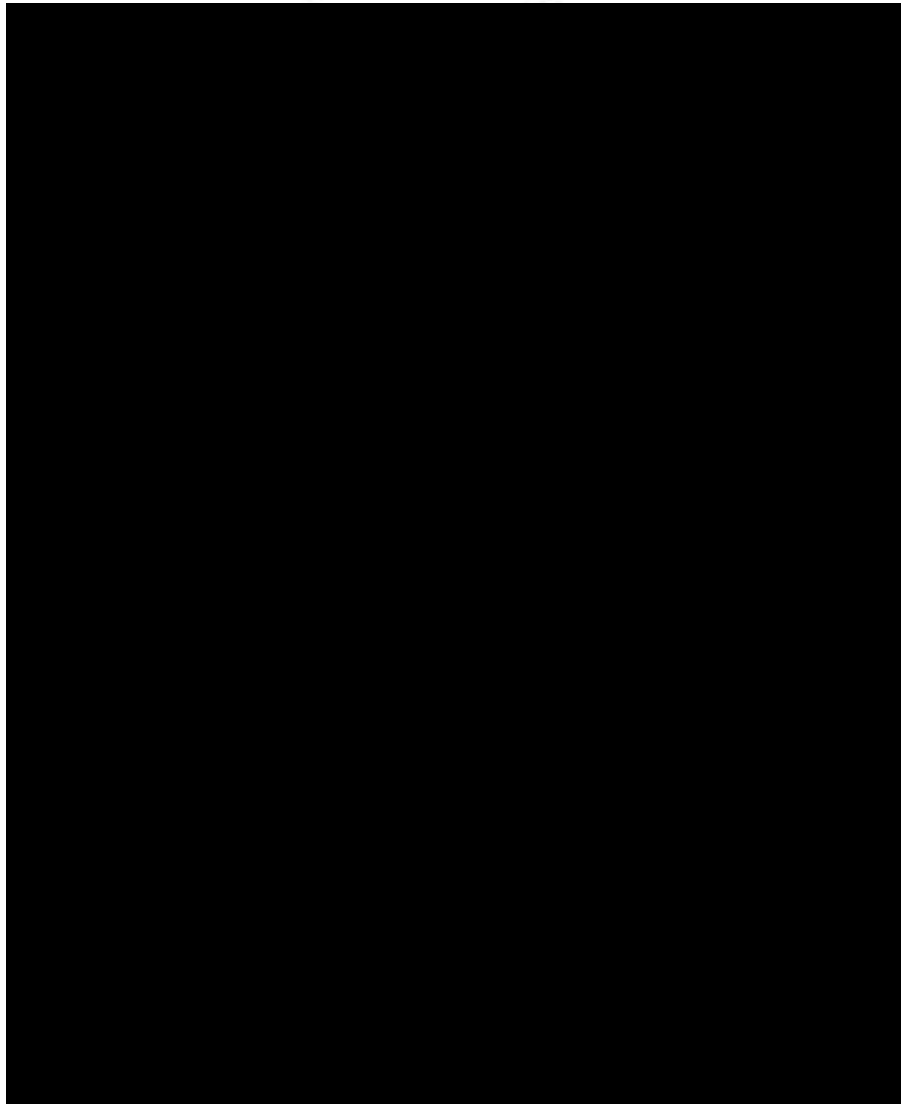


**FIGURE 9.6 FUEL ELEMENT TRANSFER CASK**

#### 9.1.4.2.4 Cask Positioning Plate

The cask positioning adapter supports and locates the transfer cask above the fuel storage pit. This adapter can be indexed so that the center bore of the cask can be located directly above the hole in the fuel storage rack designated to receive the fuel element being transferred.

A closed circuit television camera and light are located on the lower side of the adapter plate. A television monitor is used to observe the lowering, or retrieval, of an element either into or from the storage pit rack.

#### 9.1.4.3 Description of Fuel Transfer

The fuel handling system provides a safe and effective means for transporting and handling the reactor fuel from the time it enters the boundaries of the UCD/MNRC facility until it leaves.

Previous sections described and listed the major pieces of equipment and the methods that are used in fuel handling. The following paragraphs describe the steps during fuel handling.

Unirradiated fuel arrives at the facility in Nuclear Regulatory Commission/Department of Transportation approved shipping containers. The fresh fuel, ~7 lbs per element, is removed from the shipping containers by hand and stored until needed.

All handling of fuel within the reactor tank is accomplished by use of the fuel element handling tool, with the exception of the fuel-followed control rods and the instrumented fuel elements, which are handled by their components that extend above the water level.

The reactor room overhead crane and the fuel transfer cask are used to transfer irradiated fuel elements between the in-tank storage racks and the fuel storage pits.

The reactor room overhead crane is used to position the fuel transfer cask in the reactor tank such that the cask top is approximately 9 ft below the water level. With the lead plug removed, the fuel element handling tool is used to lift an irradiated fuel element from an in-tank fuel storage rack and place it into the cask. The reactor room crane is used to raise the cask out of the tank and transport it to a position over a fuel storage pit. Using the fuel element handling tool, the fuel element is raised from the bottom door of the transfer cask, allowing the bottom door to be opened. The fuel element is lowered out of the cask into its storage location. The TV camera is used to monitor the lowering operation and to confirm that the element has been placed in the proper rack location. The reverse operation is used to remove an irradiated element from the storage pits and place it in the fuel transfer cask. Appropriate radiation monitoring by health physics personnel will be conducted during the preceding operation in order to assure that doses are kept as low as reasonably achievable.

An approved shipping cask will be used to transport irradiated fuel elements from the UCD/MNRC to a reprocessing or long term storage location. Much of the same equipment, described above, used to transfer an irradiated fuel element from the in-tank storage racks to the UCD/MNRC storage pits, will be used to place an irradiated fuel element in the shipping cask.

The first step in this operation is to load an irradiated fuel element into the fuel transfer cask, as described above, from the storage pits or in-tank storage racks. The reactor room crane is used to move the cask to an area near the reactor room/preparation room door. The fuel transfer cask is then loaded on a pallet truck, rated capacity of 6,500 lbs. This pallet truck is pushed from the reactor room into the preparation room. The preparation room monorail system is used to position the cask over the opened preparation room floor access doors. The fuel element transfer cask is lowered through the access doors and mated to the top of the shipping cask. The shipping cask, mounted on a trailer, will be positioned in the staging area directly below the preparation room floor access doors.

The transfer of the irradiated fuel element from the fuel element transfer cask to the shipping cask is the same for the transfer of a fuel element from the transfer cask to the storage pits.

#### 9.1.4.4 Safety Evaluation

All parts of the cask and crane system are rigorously maintained, including load tests and radiographic or dye penetrant inspections as appropriate. Therefore, the dropping of the transfer cask during fuel transfers is considered a highly unlikely event.

If, however, a cask drop accident should occur, the event is considered enveloped by the evaluation presented for the single fuel element dropped in air accident (MHA), since that evaluation conservatively assumed a ground level release of material.

## 9.2 Helium Supply System

A system to inert the beam tube sections with helium has been provided. Replacing the air with helium reduces the neutron beam attenuation, i.e., scattering, resulting in a more intense and purer beam for radiography.

The helium system is essentially a static system, i.e., once a helium environment is established, helium is only added to or exhausted from the system to compensate for temperature and barometric related pressure changes or to make-up helium lost by leakage (Figure 9.7).

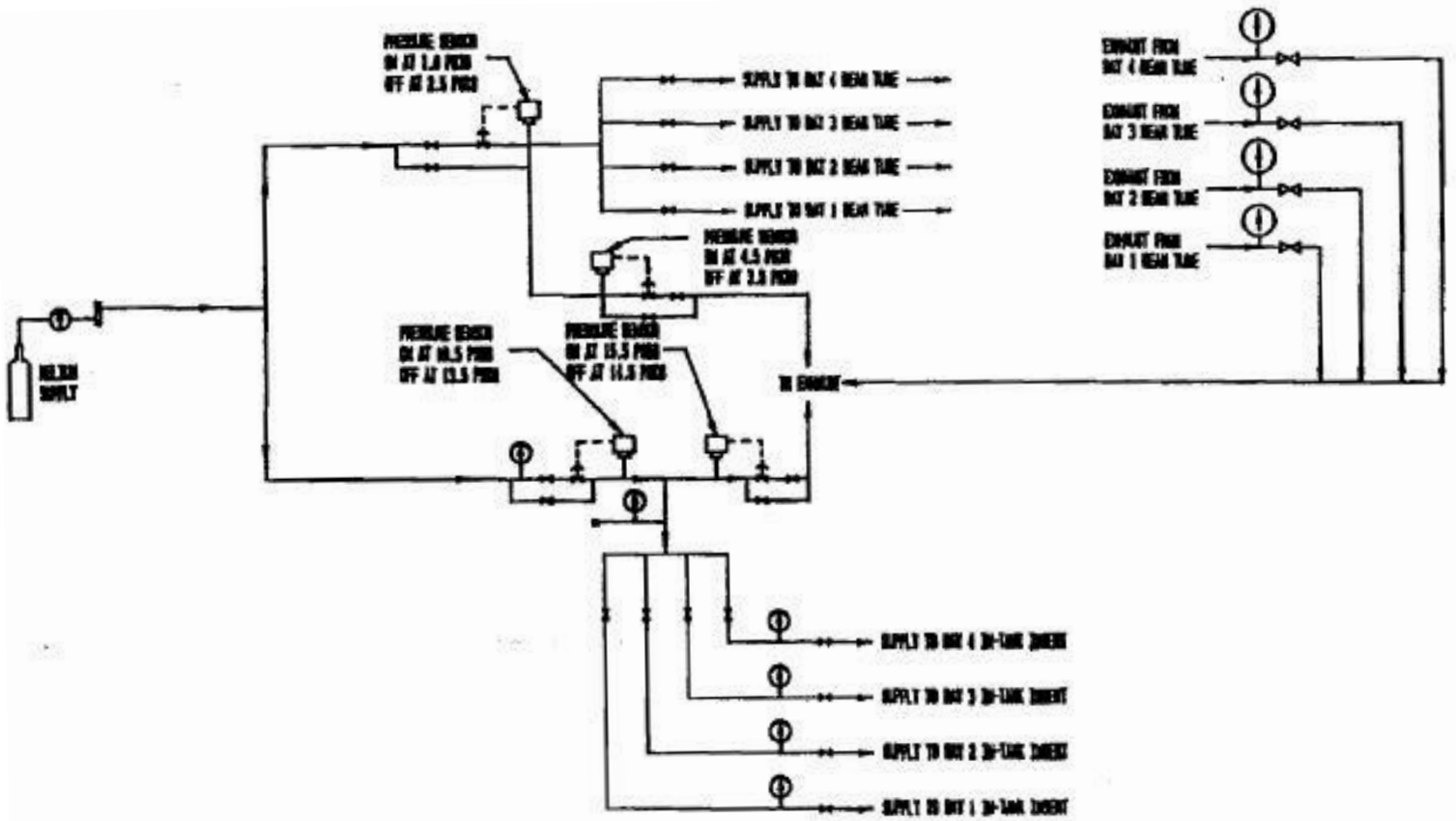


FIGURE 9.7 TYPICAL HELIUM SUPPLY

The supply for this system is from one standard helium bottle and regulator. Downstream of the regulator the system splits into two subsystems. One of these subsystems controls the pressure in the bulk shielding sections of the beam tubes. The other subsystem controls the pressure in the in-tank and tank wall sections of the beam tubes to prevent entrance of water. The venting from these subsystems is to the pneumatic transfer system exhaust duct.

The method of pressure control for both subsystems is identical. Both subsystems contain helium makeup and vent valves that are activated by pressure sensors. The valves are sequenced to maintain a positive pressure within the subsystems.

There must be multiple equipment failures to overpressure the system. To overpressure the in-tank and tank-wall sections, both the pressure regulator and supply valves must fail open so that the supply capacity exceeds the vent capacity. For the in-tank and tank-wall sections, both the supply valve and pressure relief valve must fail.

### 9.3 Building Water Systems

The water supply for the UCD/MNRC is connected to the on-site 12 in. combination fire and domestic water main. The UCD/MNRC water supply system consists of a water meter, main shutoff valve, and facility distribution piping.

The potable water requirements for the UCD/MNRC are minimum. The main users are the wash/change rooms, heating and ventilating units, and the cooling tower.

Water from the radiography bays and the decontamination shower and sink is pumped to a 2000 gallon tank. Water collected in the tank will be sampled for radioactivity and disposed of in accordance with 10 CFR 20.

#### 9.3.1 Auxiliary Make-Up Water System (AMUWS)

The auxiliary make-up water system (AMUWS) can supply water to the reactor core from a source external to the domestic water supply (Figure 9.8). Water is supplied from two storage tanks located below the secondary cooling tower. Each tank contains approximately twenty-three hundred (2300) gallons of deionized water. The water storage tanks have enough capacity, if needed, to supply water to the reactor core area for approximately four hours at twenty gallons per minute as a backup supply to the ECCS. Water purity is maintained by a set of resin columns located next to the storage tanks.

A control switch, located on the temperature control panel (TCP), enables the reactor operator to start a three horsepower pump from the reactor control room. The pump can supply water to the reactor tank at a flow rate of twenty gallons per minute. A flow proof light illuminates on the TCP when flow has been initiated through the AMUWS.

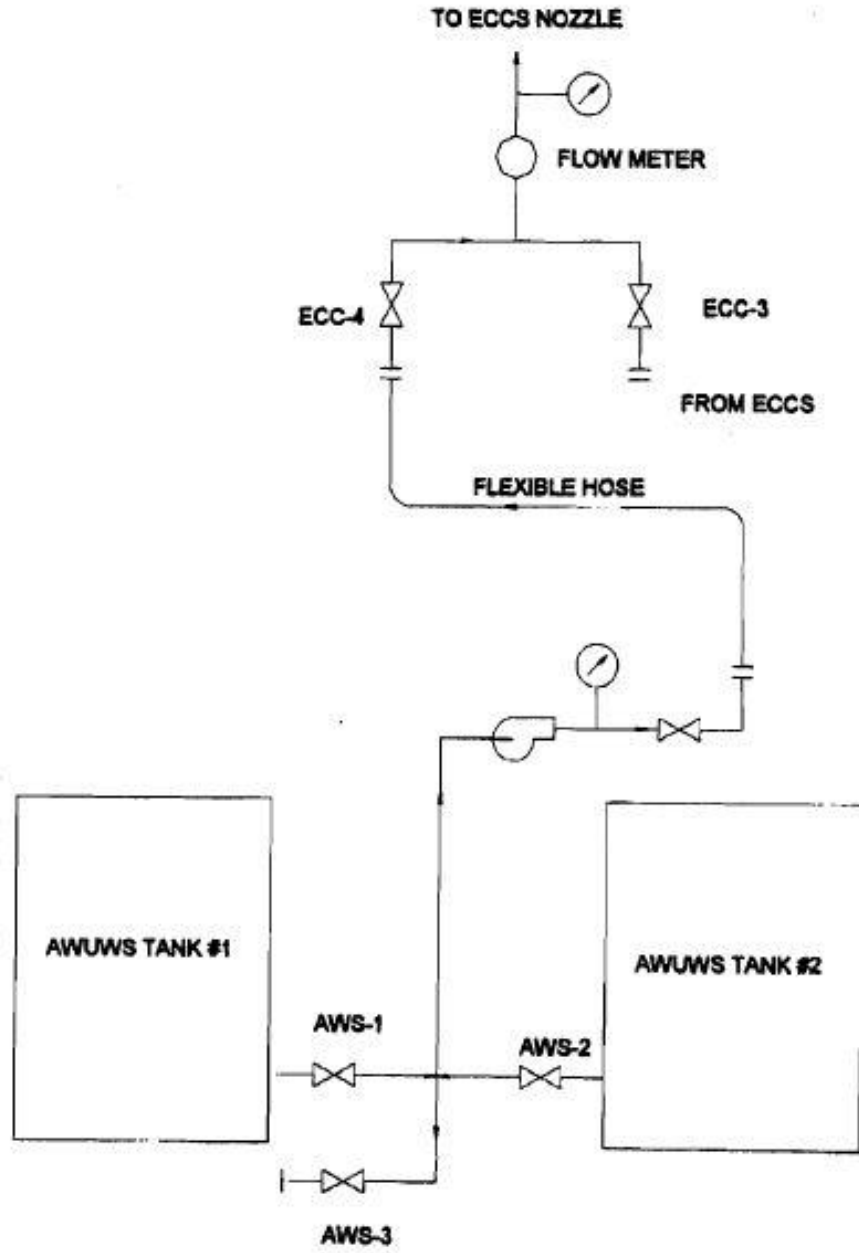


FIGURE 9.8 AUXILIARY MAKEUP WATER SYSTEM (AMUWS)

Normally the AMUWS piping is dry and will only be filled with water when the pump is started by the reactor operator from the control room. Check valves located in the reactor room prevent water from siphoning from the reactor tank back into the storage tanks when the system is in the stand-by mode of operation.

A propane electrical generator supplies back-up electrical power to the AMUWS pump, the TCP, the reactor room ventilation fan (EF-1), and the damper controls for the reactor room in the event that normal electrical power is lost. A light on the TCP indicates if the generator is operational.

The AMUWS contains pressure and flow gauges to verify sufficient water flow is maintained for the duration of its use (Section 13.2.3.2.2).

## 9.4 Fire Protection

### 9.4.1 Design Basis

The design basis for the UCD/MNRC fire protection system is to provide a detection and suppression capability which will mitigate any losses to property should a fire develop. It should be noted that fire protection is not required to accomplish a safe shutdown of the reactor or to maintain a safe shutdown condition.

### 9.4.2 Description

Both detection and suppression systems installed in accordance with National Fire Protection Code are utilized in the UCD/MNRC.

A dry-pipe, pre-action fire sprinkler system provides fire suppression for the UCD/MNRC as shown in Figures 9.9 and 9.10. This system receives its water supply from the existing on-site 12-in. combination fire and domestic water main. Also, a fire hydrant is located approximately 150 ft from the UCD/MNRC.

In addition to the dry-pipe system, the DAC in the reactor room, and the instrument cabinets and control consoles in the reactor and radiography control rooms contain fire detection and halon suppression systems, i.e., units located within the enclosures.

The entire UCD/MNRC has either thermal or ionization-type fire detection devices as well as manual pull boxes. Thermal detectors located in select air handling system ducts shut down the system when activated (Section 9.5).

The UCD/MNRC fire detection/suppression system is automatic, zoned, and is supervised with hardwired signal connections. The system has a self-contained 24-hr battery backup. There are two master panels: one is located in the control room; the other panel is outside near the vehicle gate. The master panel provides local alarm information and transmits signals to a 24-hour monitored location.

Whenever one of the fire detection devices activates, visual and audible warning devices alarm throughout the facility.

#### 9.4.3 Evaluation

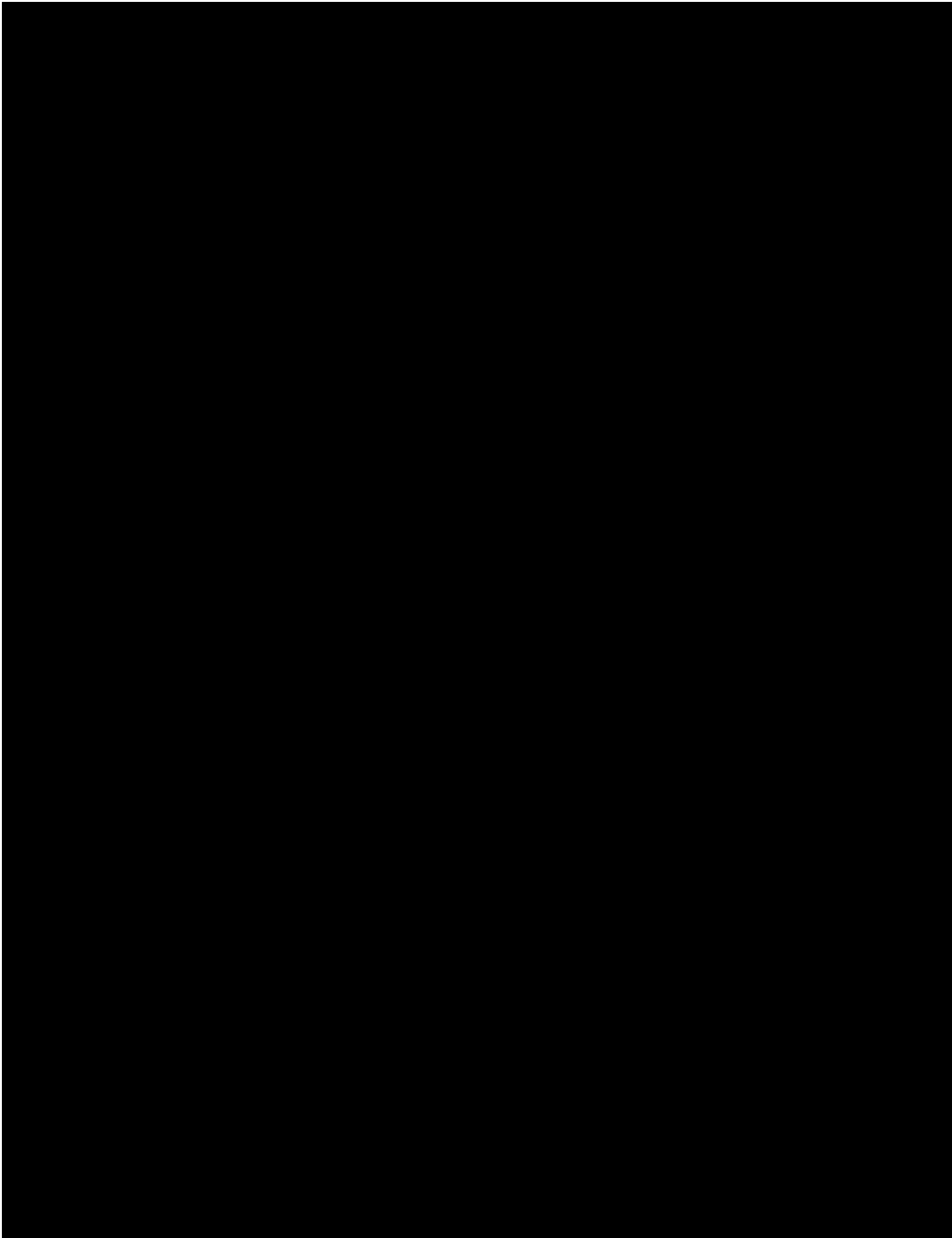
The UCD/MNRC fire protection system has been designed to meet the design basis. The dry-pipe suppression provides coverage of the critical areas and the detection system covers the entire structure. Special halon systems have been provided to protect instrumentation and control cabinets/consoles.

### 9.5 Air Handling System

#### 9.5.1 Design Basis

The UCD/MNRC air handling system provides heating and cooling for personnel comfort and serves several important roles for radiological control. These roles are as follows:

- Provide air changes in the reactor room and in other areas throughout the facility to maintain Ar-41 and N-16 concentrations within the limits in of 10CFR Part 20;
- Maintain pressure differentials throughout the facility to limit spread of radioactive contamination;
- Provide a means to isolate, recirculate, and filter the air in the reactor room should there be a release of fission products or other abnormal airborne radionuclides.



DATE  
5/2/18

FIGURE 9.9 UCD/MNRC FIRE SUPPRESSION SYSTEM, MAIN FLOOR

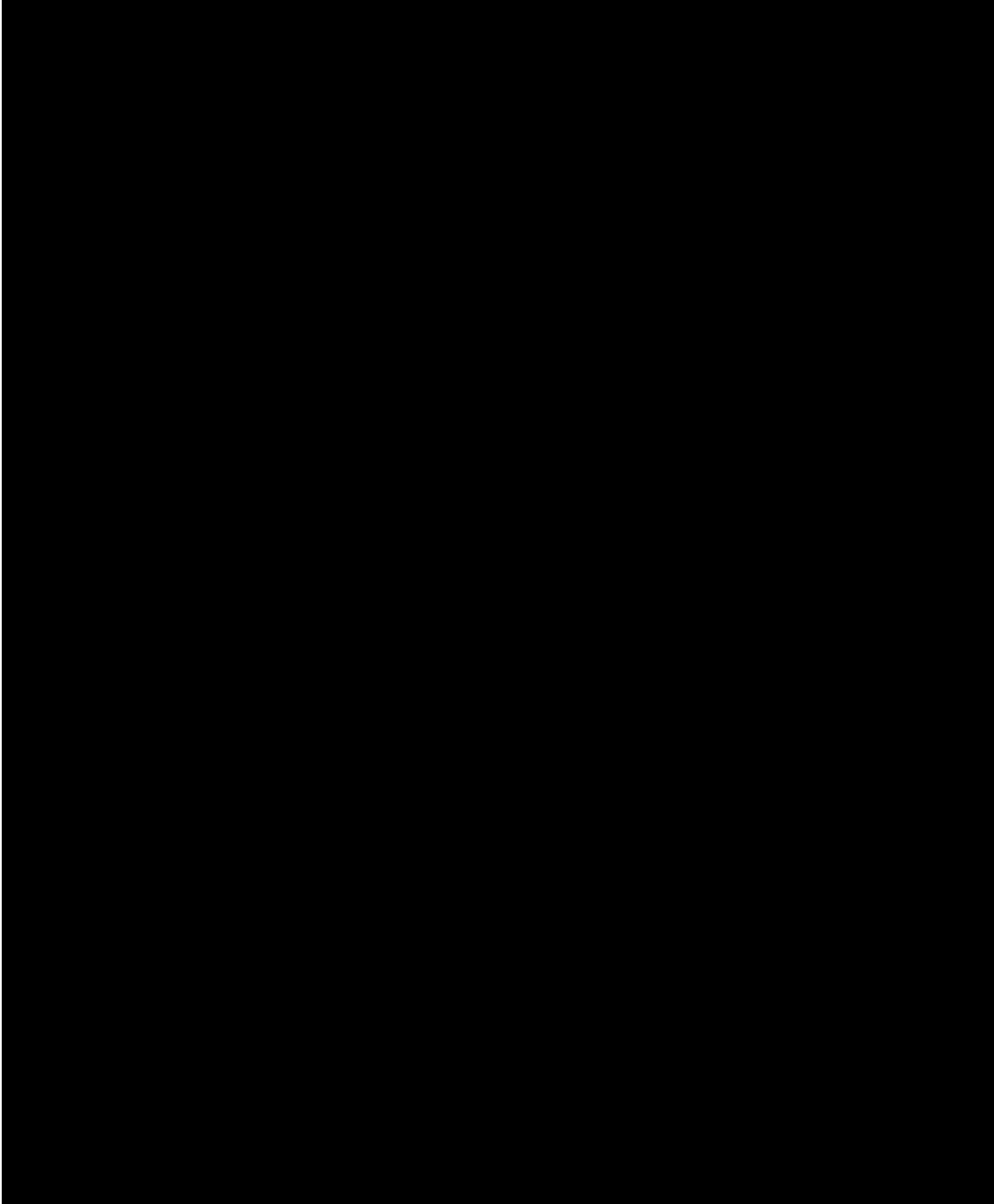


**FIGURE 9. 10 UCD/MNRC FIRE SUPPRESSION SYSTEM, SECOND FLOOR**

### 9.5.2 Description

The UCD/MNRC air handling system is served by 14 different heating and air conditioning systems and two exhaust systems (Figure 9.11). All of these systems provide normal heating, cooling, and ventilation functions for personnel comfort and equipment cooling. In addition to the normal functions, many of these systems serve important roles in minimizing Ar-41 and N-16 concentrations, and help with contamination control.

All of these systems are functionally similar. They recirculate and condition a significant portion of the air from the areas they serve and receive makeup air from outside the facility. These systems are refrigeration-type except those in the staging areas. The units for these areas are equipped with evaporator-type coolers.

The flows throughout the UCD/MNRC have been designed and balanced so that the reactor room, and other areas within the facility are at a slightly negative pressure with respect to the surrounding areas. The flow rates throughout the facility, and the expected negative pressure differential in the reactor room, the preparation area and equipment room, and the radiography bays are as shown in Figure 9.11. The pressure differentials are monitored by manometers.

The radiography bay air handling (ventilation) system will normally operate whenever the reactor is operating. However, it is permissible to operate the reactor without operating this part of the air handling system. The impact of not operating this ventilation system while the reactor is operating is not significant relative to occupational or offsite doses and is discussed in detail in Chapter 11 (Sections 11.1.1.1.1 through 11.1.1.1.4) and Appendix A.

The reactor room exhaust passes through a pre-filter and a HEPA filter prior to being discharged through the 60-ft high stack. The exhaust from the radiography bays passes through a standard particulate filter prior to being discharged through the stack. It should be noted that the exhaust from the fume hood located in the preparation area outside the reactor room passes through a HEPA filter prior to discharge into the radiography bay exhaust system. Each radiography bay exhaust contains a damper that can be closed for isolation.

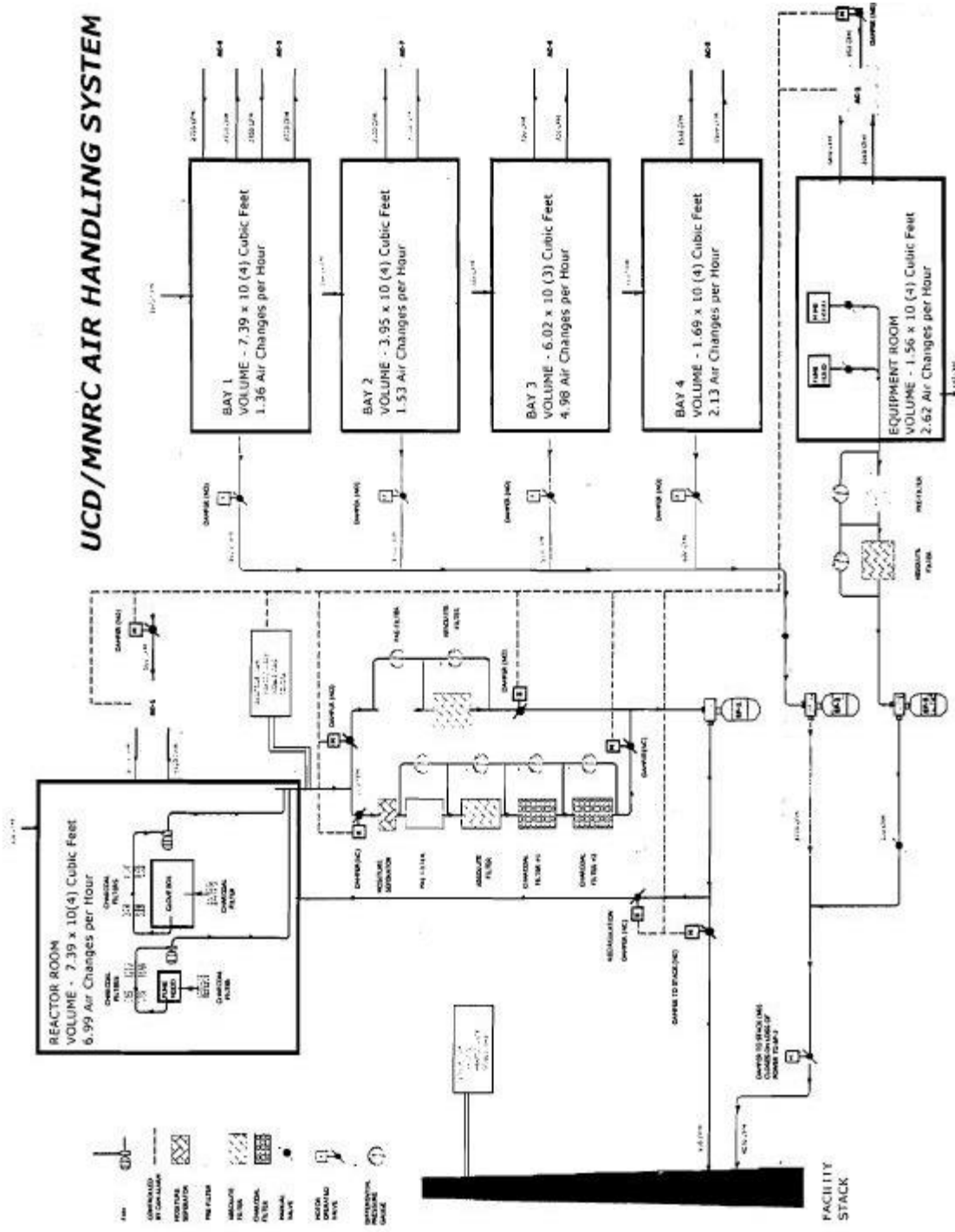


FIGURE 9.11 UCD/MNRC AIR HANDLING SYSTEM

The reactor room ventilation system normally by-passes the particulate-charcoal filter system and the normal exhaust path is through a pre-filter, a HEPA filter and then out the stack. However, during a LOCA, the radiation levels in the reactor room could cause the reactor room CAM to alarm. This would automatically redirect the reactor room exhaust path through a moisture separator, a pre-filter, HEPA filter, two charcoal filters and then back to the reactor room. A ventilation damper control switch located on the temperature control panel in the reactor control room enables the reactor operator to override the damper controls for recirculation and continue exhausting air from the reactor room through the normal exhaust path. (Section 13.2.3.2.2.)

### 9.5.3 Evaluation

The UCD/MNRC air handling system has been designed to maintain the reactor room consistently negative with respect to air pressure in the surrounding areas. It provides the necessary air changes in the reactor room to maintain routine radioactive gas concentrations at a level where the 10 CFR Part 20 dose limits will be easily met. It also provides a means for isolating the reactor room and recirculating the room air through HEPA and activated charcoal filters should there be a release of fission products or other abnormal airborne radionuclides.

The air handling system will also maintain the radiography bays at a negative pressure relative to surrounding areas when the radiography bays ventilation system is operating, which is the normal operating mode for the UCD/MNRC facility.

## 9.6 Interlocks/Controls - Bay Shutters/Doors

Each of the UCD/MNRC radiography bay shutters (bulk shield) and the bay doors are equipped with controls incorporating interlocks to prevent personnel from entering the bays anytime the reactor is on and shutters are not closed. In addition to the shutter and door interlocks, there are reactor shutdown devices that will either scram the reactor or prevent it from being operated if an unsafe condition exists. The following sections describe the controls, interlocks, and reactor shutdown devices in detail.

### 9.6.1 Shutter (Bulk Shield) Control/Interlocks

Figure 9.12 is the Bay 2 shutter control/interlock schematic and Figure 9.13 shows the corresponding limit switches. The controls/interlocks for all four shutters are identical except for the number of bay doors. Bays 1, 3, and 4 have one door each while Bay 2 has two doors.

The shutter can be controlled from three locations, the radiography control room and two locations in the bay. One of the bay shutter control stations is located on the parapet next to the shutter, and the other is on the bay floor in the area of the motor control center.

The logic diagrams for shutter operation from the radiography control room and from the bay are shown in Figures 9.14 and 9.15, respectively.

The key features of this control/interlock system are as follows:

1. The shutter movement can be stopped at any time from any of the three shutter control stations;
2. The shutter can be closed at any time (except when a "stop" switch is depressed) from either of the two control stations located in the radiography bay;
3. There is a keyswitch associated with the radiography control room and the bay floor control stations. These keyswitches use the same key. The key must be removed from one location and taken to the other location before the controls can be activated;
4. The shutter cannot be closed from the radiography control room without the keyswitch being activated. This prevents closing of the shutter from the radiography control room if personnel are on the parapet;
5. The shutter can only be opened from the radiography control room if the keyswitch (S2-2) is in place and the bay doors (K2-7X and K2-11X) are closed;
6. The shutter can only be opened from the bay floor station if the keyswitch (S2-1) is activated and the reactor is scrammed (K2-SR).

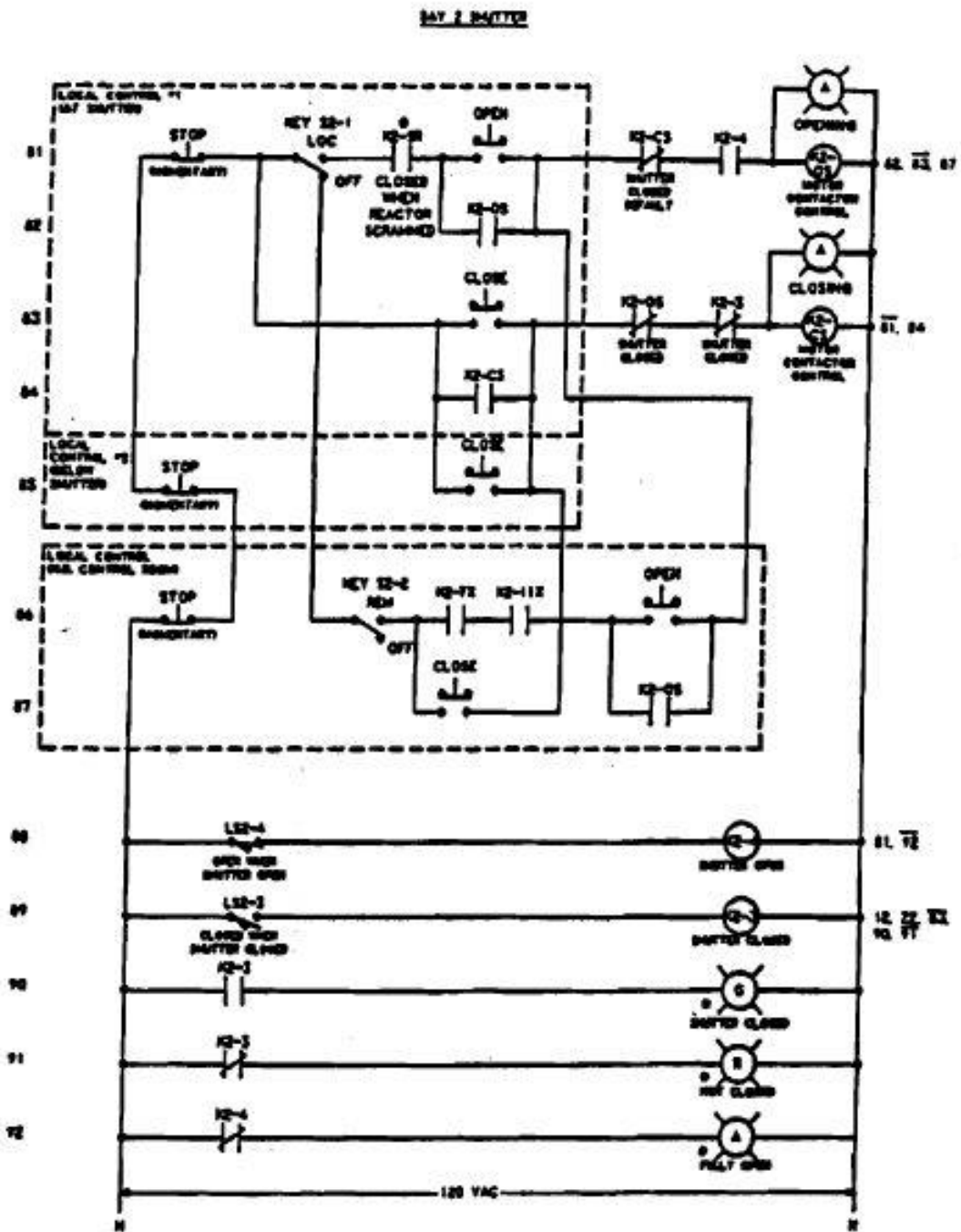


FIGURE 9.12 UCD/MNRC SHUTTER CONTROL SCHEMATIC (BAY 2)

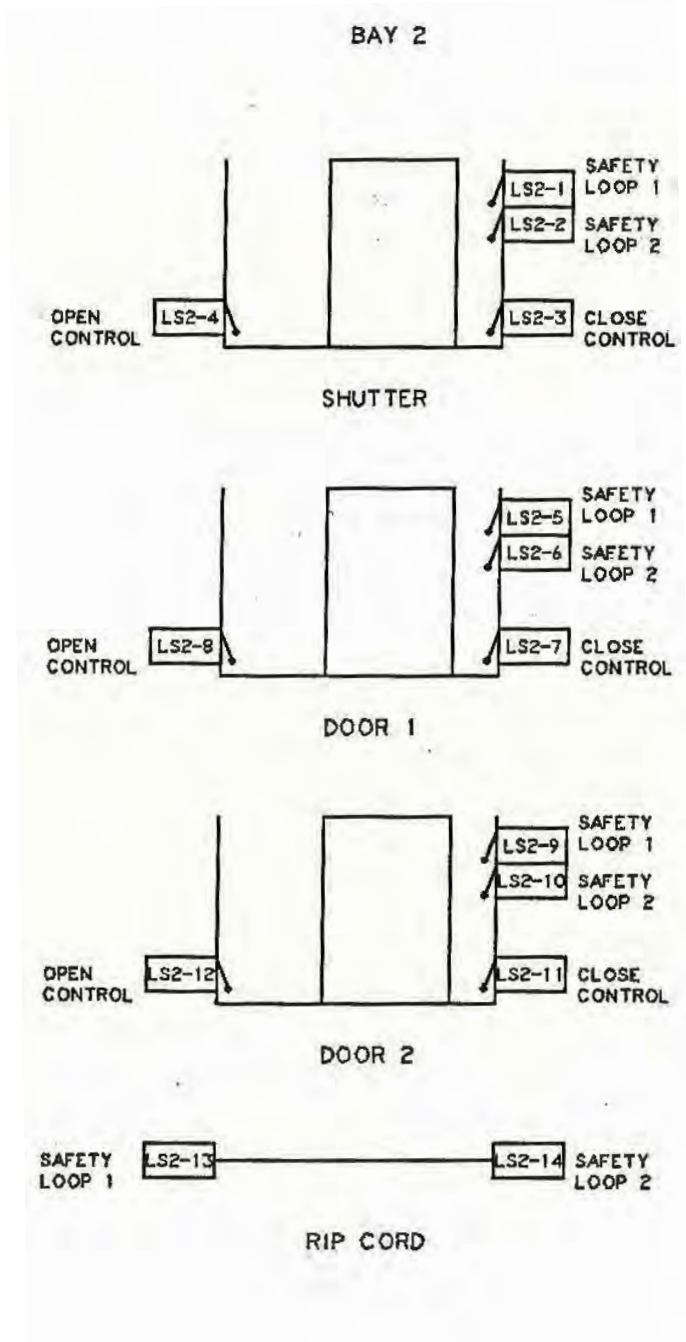


FIGURE 9.13 UCD/MNRC SHUTTER BAY DOOR AND RIP CORD LIMIT SWITCHES

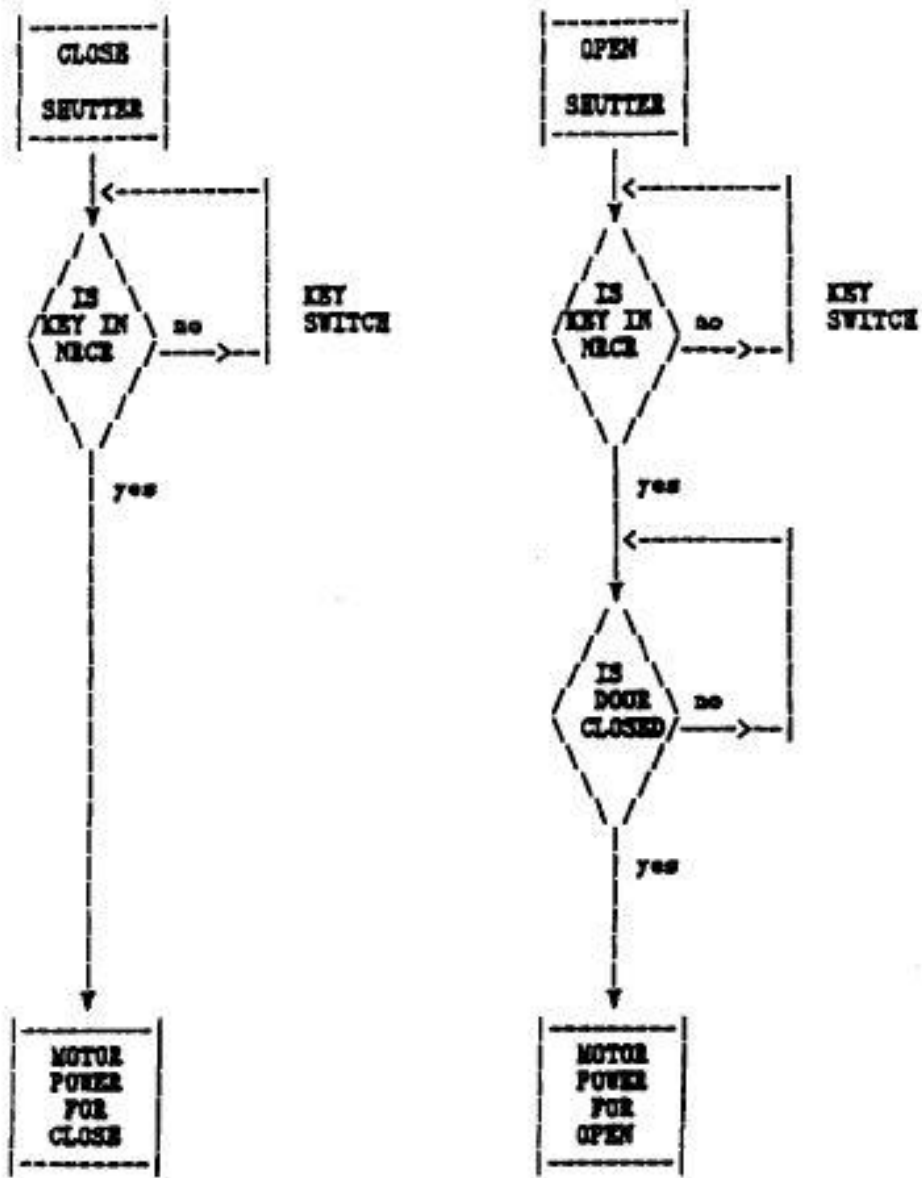


FIGURE 9.14 UCD/MNRC SHUTTER CONTROL LOGIC (RADIOGRAPHY CONTROL ROOM)

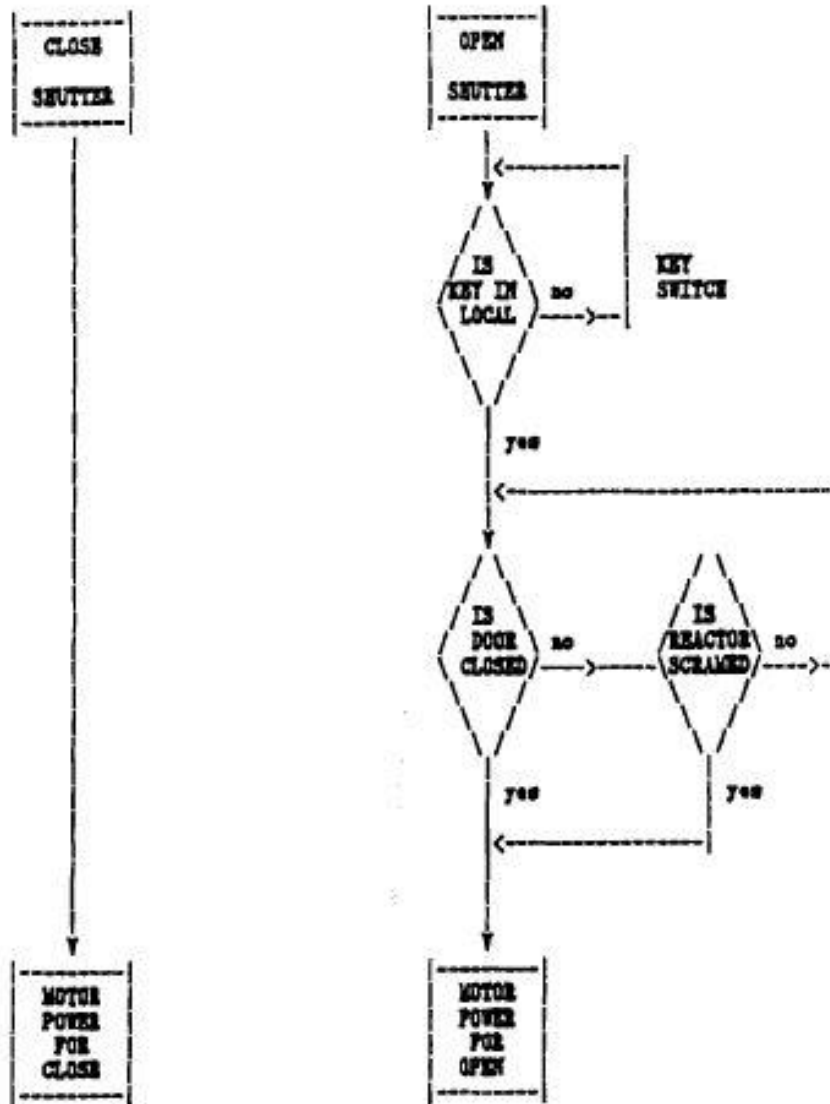


FIGURE 9.15 UCD/MNRC SHUTTER CONTROL LOGIC (INSIDE BAY)

The controls and indicator lights at each of the three control stations are as follows:

Radiography Control Room	
Controls	Indicator Lights
Keyswitch	Shutter closed - green
Closed	Shutter not closed - red
	Shutter fully open – amber & red
Stop	Shutter travelling open - red
Open	Shutter travelling closed - green

Control Station on Parapet	
Controls	Indicator Lights
Close	n/a
Stop	n/a

Control Station – Bay Floor	
Controls	Indicator Lights
Keyswitch	None
Closed	None
Stop	None
Open	None

Reactor Control Room	
Controls	Indicator Lights
None	Shutter closed - green
None	Shutter not closed - red

### 9.6.2 Bay Door Controls/Interlocks

Figure 9.16 is the Bay 2 door/interlock schematic and Figure 9.13 shows the corresponding limit switches. The controls/interlocks for the doors in all four bays are functionally the same. However, there are two doors in Bay 2 and only one door each in Bays 1, 3, and 4.

The open-closed controls for the bay doors are mounted on the bay door. Both switches are momentary contact-type (deadman) and must be held in position to move the door.

In series with the door control power is a multiple keyswitch (11 captive keys). The door cannot be operated unless all 11 keys are in place. Whenever a person enters the bay, they will be required (administrative control) to remove a key and keep this key in their possession while in the bay. Upon leaving the bay, the key is reinserted and the controls can be activated. This key device is intended to prevent the bay doors from being closed with personnel in the bay.

The door position indicator lights are as follows:

Radiography Control Room	Reactor Control Room
Door closed - green	Door closed - green
Door not closed - red	Door not closed - red

The control/interlock logic for the bay doors is shown in Figure 9.17.

The key features of this control/interlock system are:

- All keys must be in the multiple keyswitch before power can be applied to the door;
- The control switches are the momentary contact-type so personnel must be in attendance anytime the door is operated;
- The door can be closed anytime all of the keys are in place;
- The door can only be opened if the shutter is closed (K2-3) or the reactor is scrammed

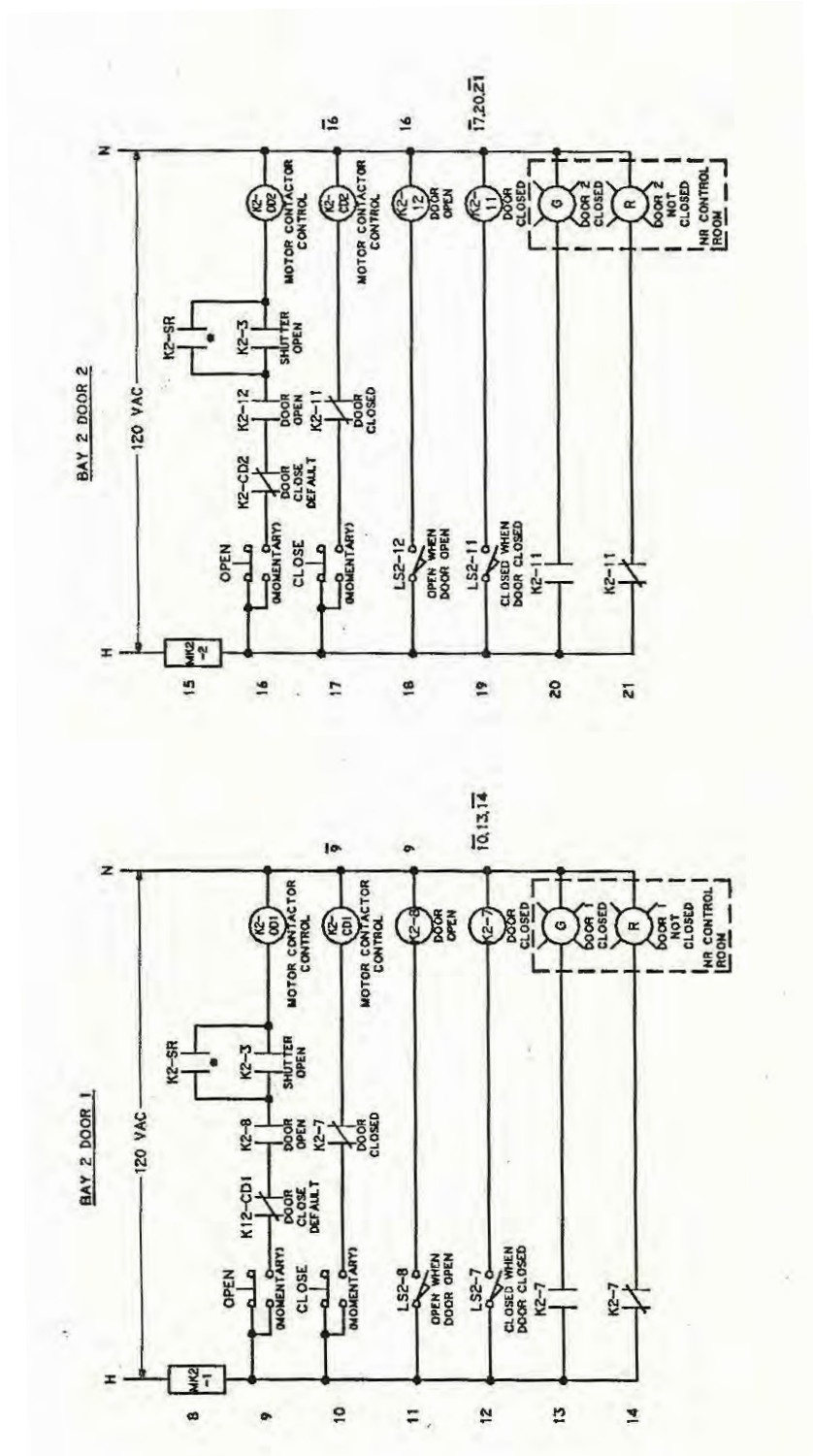


FIGURE 9.16 UCD/MNRC BAY DOOR CONTROL SCHEMATIC (BAY 2)

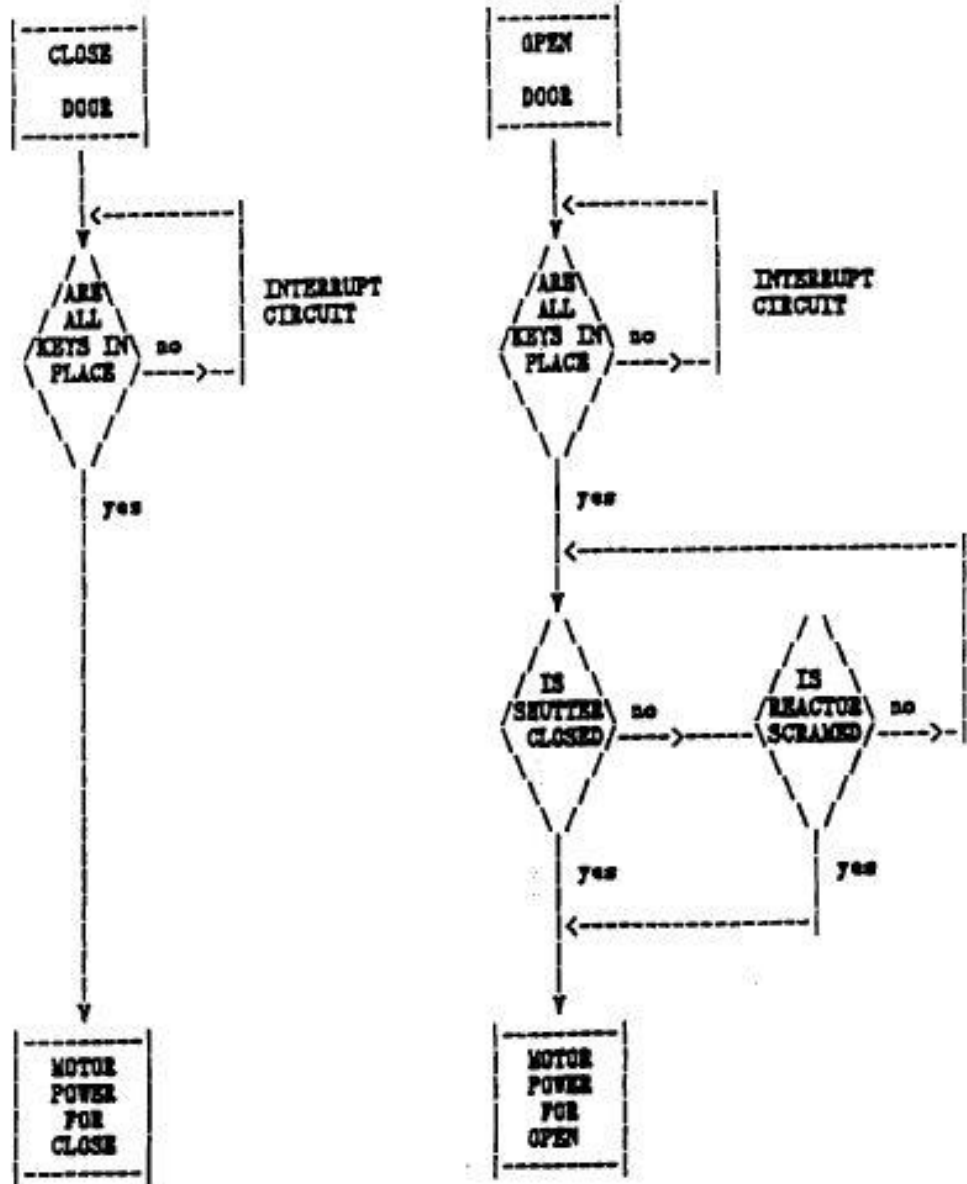


FIGURE 9.17 UCD/MNRC BAY DOOR CONTROL LOGIC

### 9.6.3 Reactor Interlocks

In addition to the interlocks described above that prevent access to the bays when radiation levels are high (i.e., reactor on and bay shutters not closed), there are three types of inputs from bay safety devices to the reactor scram chain. Figure 9.18 shows the schematic and Figure 9.16 shows the limit switches for the corresponding relays in the Bay 2 circuitry. All other bays are the same except for the number of doors.

The three types of scram chain inputs are from limit switches located on the shutters, the bay doors, and from switches located at the ends of rip cords located in each bay. The rip cord locations are as shown in Figures 9.19, 9.20, and 9.21. As shown in Figure 9.13, each shutter, door, and rip cord have two independent signal devices. These devices provide independent input signals to the reactor's external scram inputs. These devices and their installation is in accordance with requirements of the reactor safety system.

The key features of these reactor scram devices are as follows:

- The reactor is either scrammed or cannot be operated if the shutter and the bay door are open;
- The reactor is either scrammed or cannot be operated when the rip cord circuits have been activated;
- Once activated, the rip cord circuit can only be reset from inside the bay.

### 9.7 Communication and CCTV Systems

The UCD/MNRC contains telephone, intercom and closed circuit TV (CCTV) systems. The telephone system has been extended to a terminal board in the UCD/MNRC. Distribution within the UCD/MNRC is from this terminal board.

An intercom system has been provided between the reactor room, reactor control room, radiography control rooms, radiography bays, and equipment room. The master intercom stations are located in the reactor and radiography control rooms.

An emergency evacuation system has been installed in the UCD/MNRC. This system can be activated from the reactor control room and the reactor room. When energized, a number of evacuation horns in the facility are sounded.

There are CCTV cameras located in the UCD/MNRC facility. These cameras are positioned so that key areas can be monitored. The typical locations and types of cameras are shown in Figures 9.22 and 9.23. Monitors for the TV cameras are located in both the reactor control room and the radiography control rooms.

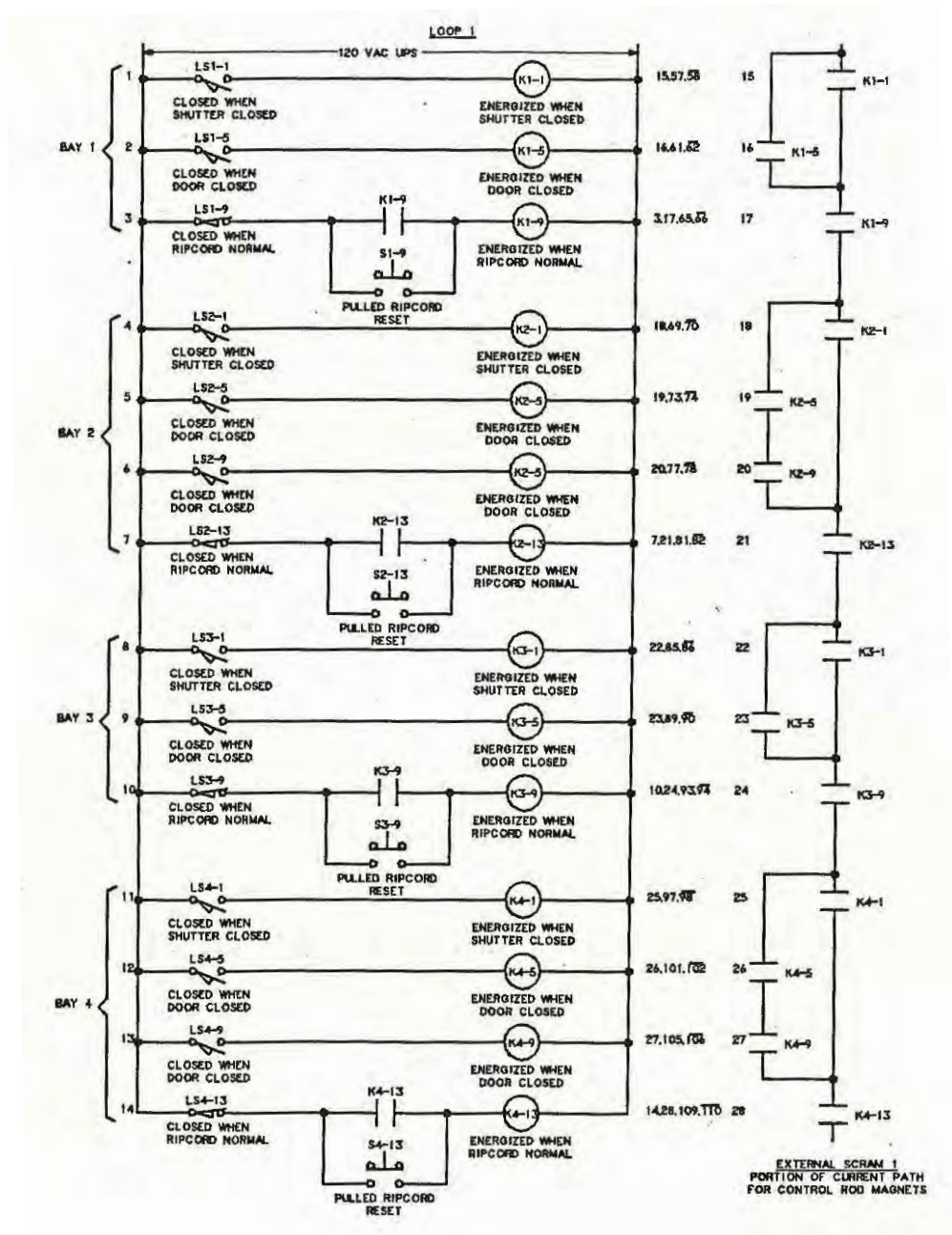
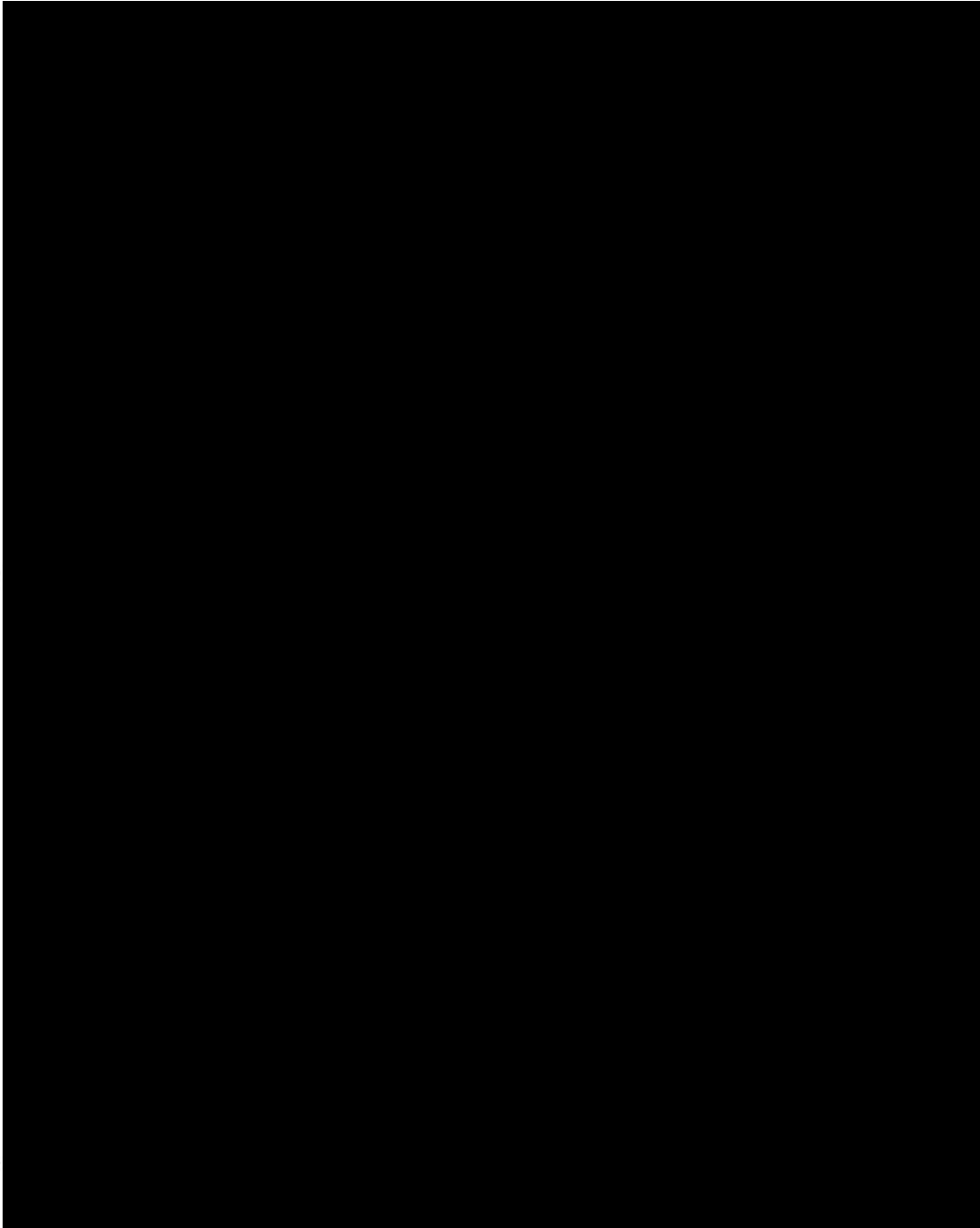
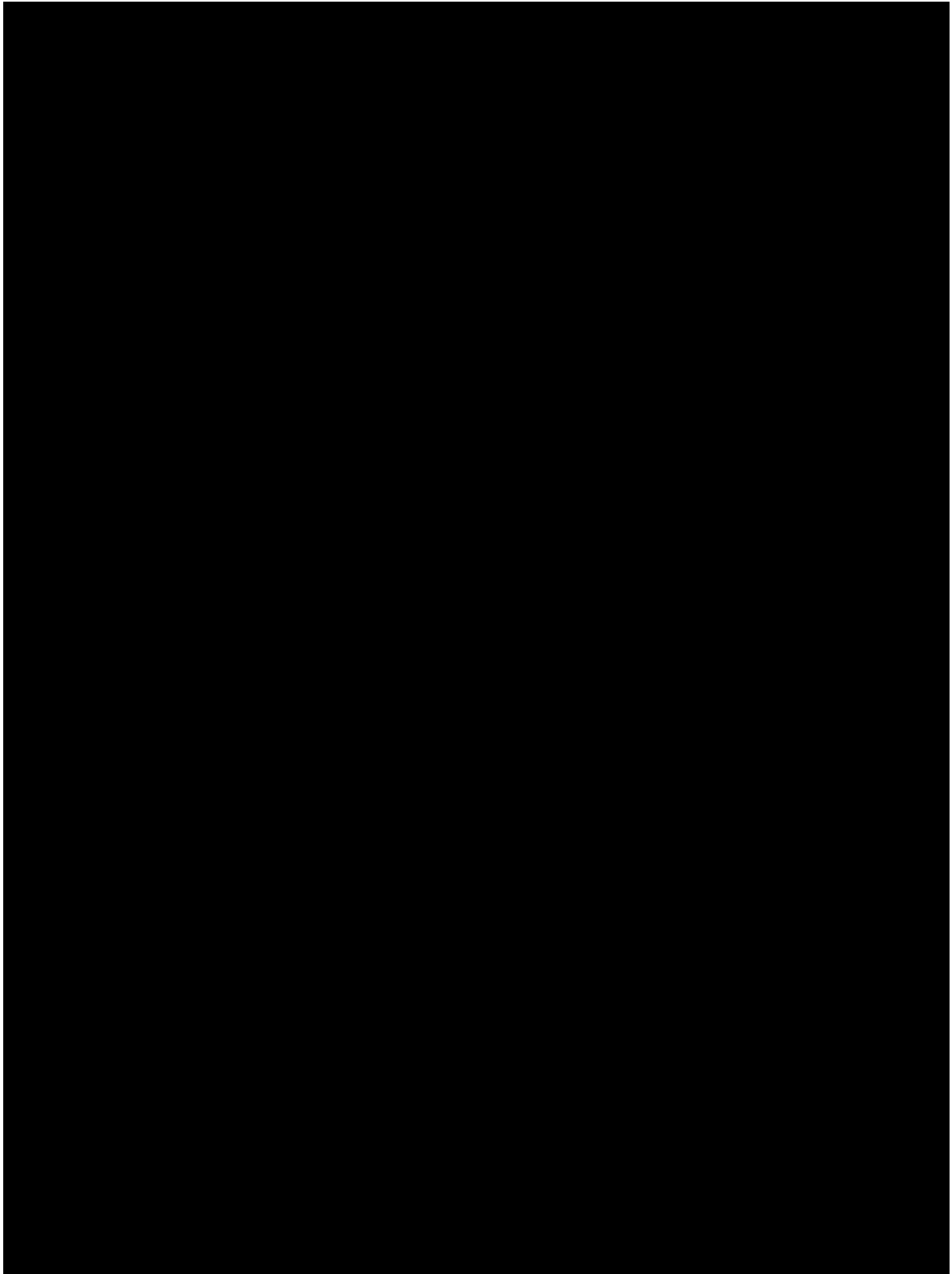


FIGURE 9.18 UCD/MNRC BAY DOOR, SHUTTER, AND RIP CORD CONTROL SCHEMATIC – REACTOR SCRAM CHAIN INPUT (LOOP NO. 1)



**FIGURE 9. 19 RIP CORD LOCATION – BAYS 1 AND 2**



**FIGURE 9. 20 RIP CORD LOCATION – BAYS 3 AND 4**

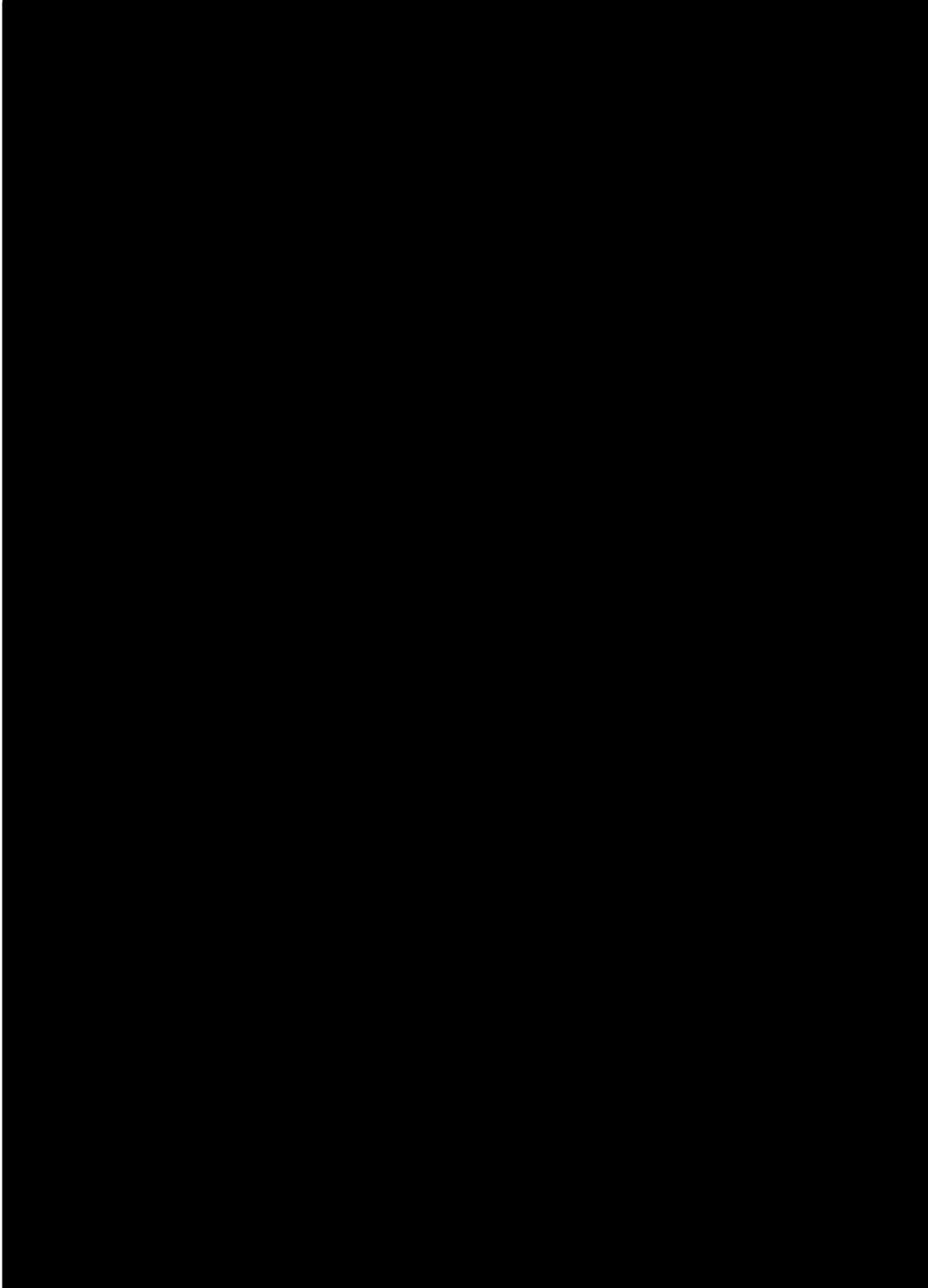


**FIGURE 9.21 RIP CORD LOCATION – PLAN VIEW**

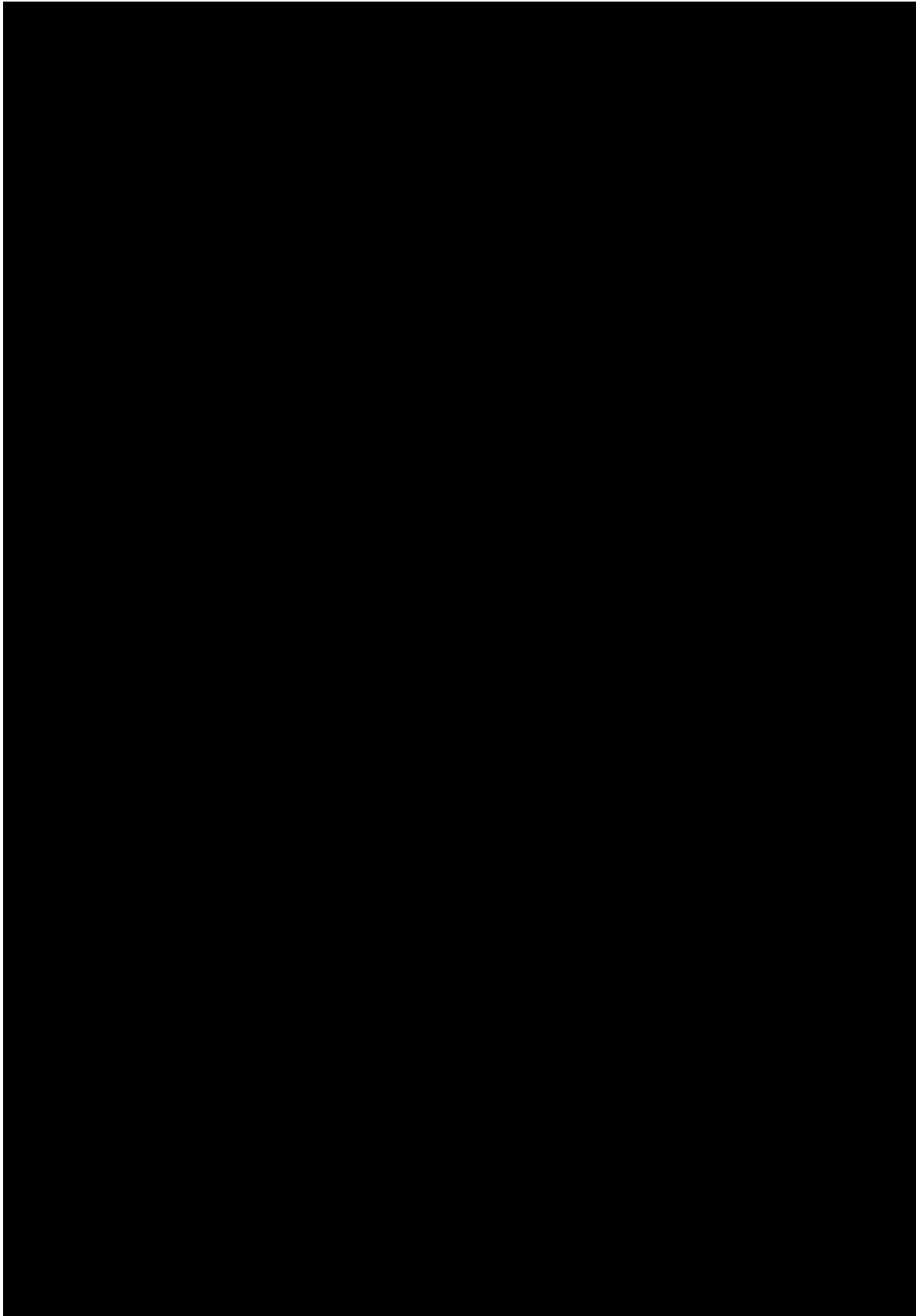


**FIGURE 9.22 TYPICAL UCD/MNRC CLOSED CIRCUIT TELEVISION – MAIN FLOOR**

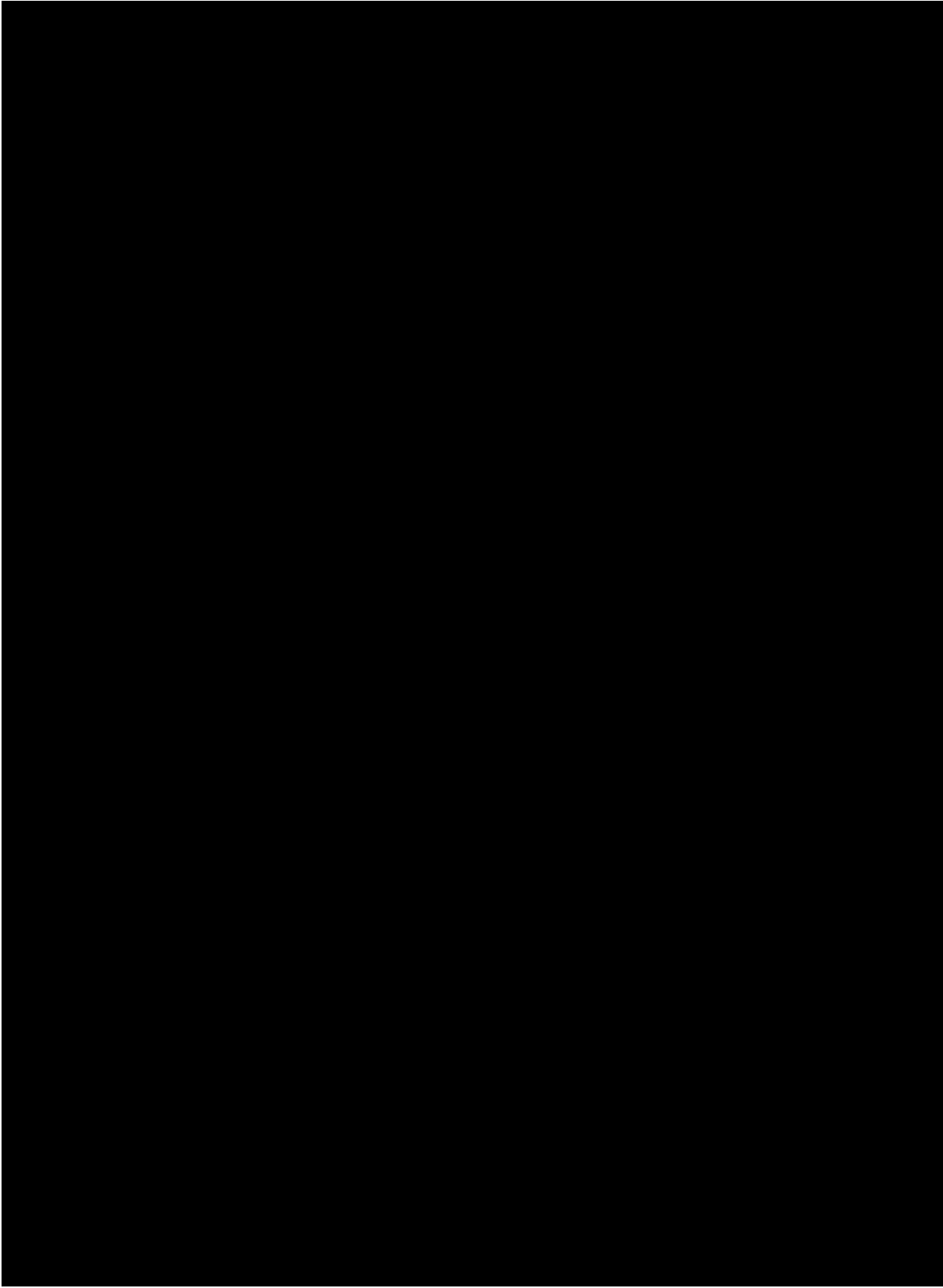
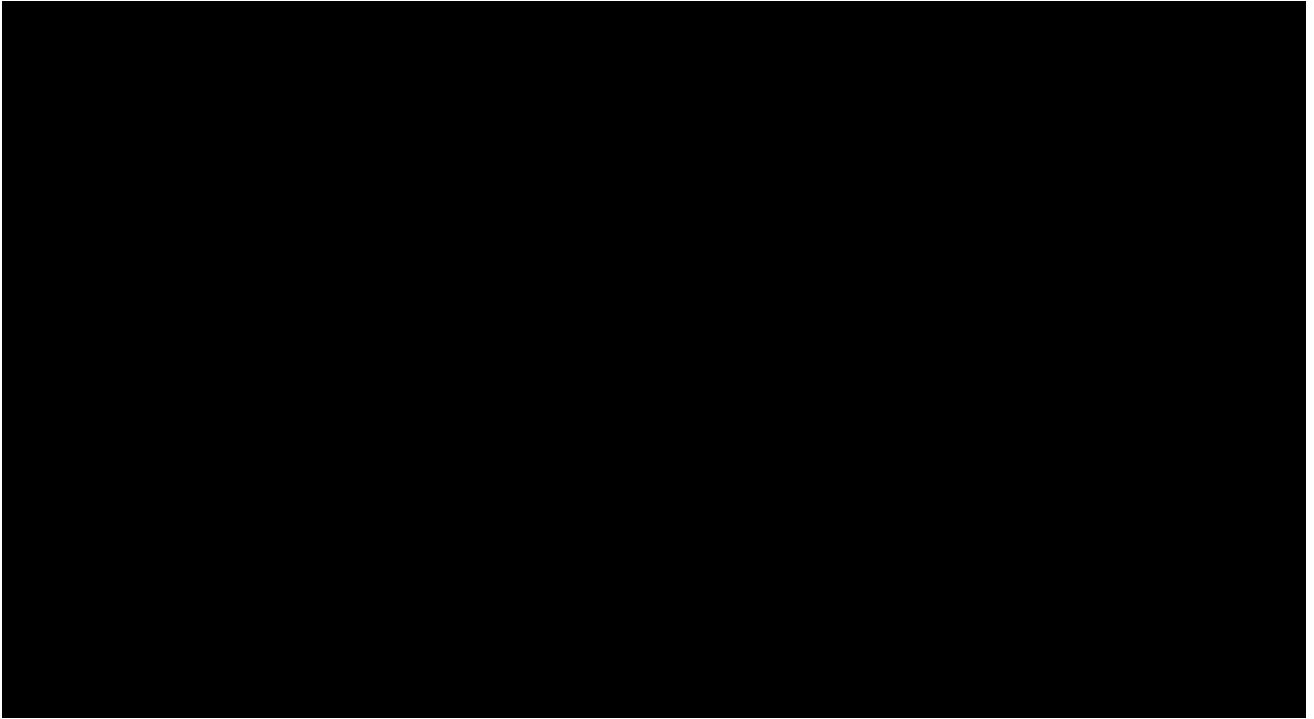


**FIGURE 9. 23 TYPICAL UCD/MNRC CLOSED CIRCUIT TELEVISION – SECOND FLOOR**



#### 9.8 Security System

The UCD/MNRC security system consists of personnel access control, detection and assessment equipment as described in the UCD/MNRC Physical Security Plan.



\*\* Each radiography console has a dedicated monitor for the corresponding Bay.  
For Bays 1 and 2, either one of the camera outputs can be selected for monitoring.

**CHAPTER 10**

**EXPERIMENTAL FACILITIES  
AND  
UTILIZATION**

Valid Pages

Rev. 9 05/03/18

i	Rev. 9 05/03/18
ii	Rev. 9 05/03/18
10-1	Rev. 9 05/03/18
10-2	Rev. 9 05/03/18
10-3	Rev. 9 05/03/18
10-4	Rev. 9 05/03/18
10-5	Rev. 9 05/03/18
10-6	Rev. 9 05/03/18
10-7	Rev. 9 05/03/18
10-8	Rev. 9 05/03/18
10-9	Rev. 9 05/03/18
10-10	Rev. 9 05/03/18
10-11	Rev. 9 05/03/18
10-12	Rev. 9 05/03/18
10-13	Rev. 9 05/03/18
10-14	Rev. 9 05/03/18
10-15	Rev. 9 05/03/18
10-16	Rev. 9 05/03/18
10-17	Rev. 9 05/03/18
10-18	Rev. 9 05/03/18
10-19	Rev. 9 05/03/18
10-20	Rev. 9 05/03/18
10-21	Rev. 9 05/03/18
10-22	Rev. 9 05/03/18
10-23	Rev. 9 05/03/18
10-24	Rev. 9 05/03/18
10-25	Rev. 9 05/03/18
10-26	Rev. 9 05/03/18
10-27	Rev. 9 05/03/18

## TABLE OF CONTENTS

10.0	EXPERIMENTAL FACILITIES AND UTILIZATION.....	10-1
10.1	Summary Description .....	10-1
10.2	Beam Tubes and Beam Tube Shutter/Bulk Shield.....	10-1
10.2.1	Beam Tubes .....	10-1
10.2.1.1	Design Basis .....	10-1
10.2.1.2	Description .....	10-1
10.2.1.3	Evaluation.....	10-7
10.2.2	Beam Tube Shutter/Bulk Shield.....	10-7
10.2.2.1	Design Basis.....	10-7
10.2.2.2	Description .....	10-8
10.2.2.3	Evaluation.....	10-8
10.3	Component Positioning Equipment .....	10-9
10.3.1	Bay 1 Component Handling System .....	10-9
10.3.2	Bay 2 Component Handling System .....	10-9
10.3.3	Bay 3 Component Handling System .....	10-9
10.4	In-core Irradiation Facilities.....	10-12
10.4.1	Central Irradiation Facility .....	10-12
10.4.1.1	Central Irradiation Facility (CIF-1) .....	10-12
10.4.2	Experiment Tubes in Upper Grid Plate Cutout Positions.....	10-15
10.4.3	Pneumatic Transfer System .....	10-15
10.4.4	Individual Grid Plate Fuel Element Positions.....	10-18
10.5	Ex-Core In-Tank Facilities.....	10-18
10.5.1	Neutron Irradiator Facility .....	10-18
10.5.1.1	Conditioning Well .....	10-22
10.5.1.2	Exposure Vessel.....	10-22
10.5.2	Silicon Doping Facility (Neutron Transmutation Doping) .....	10-22
10.5.3	Argon Production Facility .....	10-24
10.6	Experiment Review.....	10-26
10.6.1	UCD/MNRC Experiment Coordinator (EC).....	10-27
10.6.2	UCD/MNRC Director .....	10-27
10.6.3	Experiment Review Board .....	10-27
10.6.4	Nuclear Safety Committee (NSC).....	10-28

LIST OF FIGURES

10.1	Reflector Beam Tube Location .....	10-2
10.2	MNRC In-Tank Experimental Facilities And Beamlines Inserts .....	10-3
10.3	In-Tank Beam Tube.....	10-4
10.4	UCD/MNRC Beam Tube And Biological Shield .....	10-5
10.5	Bays 1 And 2 Component Positioning System .....	10-10
10.6	Bay 3 Component Positioning System.....	10-11
10.7	UCD/MNRC Typical In-Core Facilities .....	10-13
10.8	UCD/MNRC Central Irradiation Facility (Thimble) And Central Irradiation Fixture-1 (CIF-1) .....	10-14
10.9	UCD/MNRC Pneumatic Transfer System .....	10-16
10.10	UCD/MNRC In-Core And Ex-Core In-Tank Facilities.....	10-19
10.11	Neutron Irradiator Facility - Plan View .....	10-20
10.12	Neutron Irradiator - Vertical View.....	10-21
10.13	Silicon Irradiation Facility – Vertical View .....	10-23
10.14	Floor Lay-Out For Argon-41 Production Facility .....	10-25

## 10.0 EXPERIMENTAL FACILITIES AND UTILIZATION

### 10.1 Summary Description

The UCD/MNRC provides a broad range of radiographic and irradiation services to the military and non-military sector. The facility presently provides four radiography bays and consequently four beams of neutrons for radiography purposes. In addition to the radiography bays, the UCD/MNRC reactor core and associated experiment facilities are completely accessible for the irradiation of material. These irradiation services include: silicon doping, isotope production (both medical and industrial) and neutron activation analysis (e.g., geological samples). Although all four radiography bays are capable of using radiography film techniques, Bays 1, 2, and 3 are equipped with electronic imaging devices. All bays contain the equipment required to position parts for inspection as well as the radiography equipment. To meet facility use requirements, the reactor system and associated experiment facilities are designed to operate three shifts per day.

### 10.2 Beam Tubes and Beam Tube Shutter/Bulk Shield

#### 10.2.1 Beam Tubes

##### 10.2.1.1 Design Basis

The design basis for the beam tubes is to provide a path for primary neutrons with minimum scattering and attenuation between the reflector and the radiography bays.

##### 10.2.1.2 Description

Four beam tubes spaced at 90° intervals around the base of the reactor tank penetrate the reactor graphite reflector and provide a direct path for neutrons to each of the radiography bays. The beam tubes are positioned tangentially with respect to the reactor core and are inclined (20° and 30°) with respect to the horizontal plane (Figures 10.1, 10.2 , 10.3, and 10.4).

Each of the four beam tubes is made up of three major sections: the in-tank section, the tank wall section, and the reactor bulk shielding section.

The in-tank section of the beam tube (a replaceable aperture, made from neutron absorbing material and graphite housed in a water-tight aluminum container) is shown in Figure 10.4. This section is the most important part of the beam tube since it is part of the reactor core reflector, provides a source of neutrons, and purifies and shapes the beam. It consists of a large graphite block with a 6 in. diameter hole bored along the beam centerline. The key elements within the bore are a graphite end plug which serves as a source of neutrons, a bismuth crystal which attenuates gamma rays and a boron-carbide aperture which shapes the beam. An aluminum spacer and lead-cadmium sleeve and shield are also located in the bore.

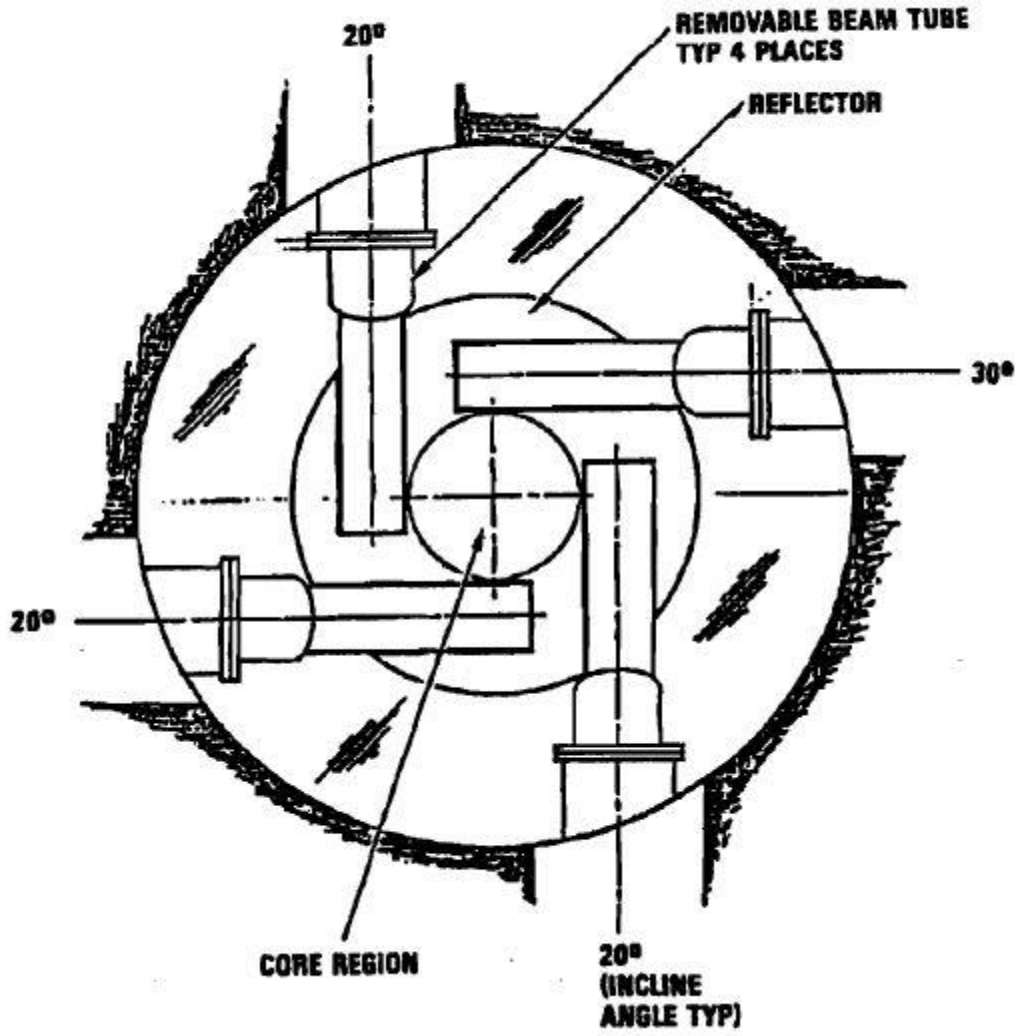


FIGURE 10.1 REFLECTOR BEAM TUBE LOCATION

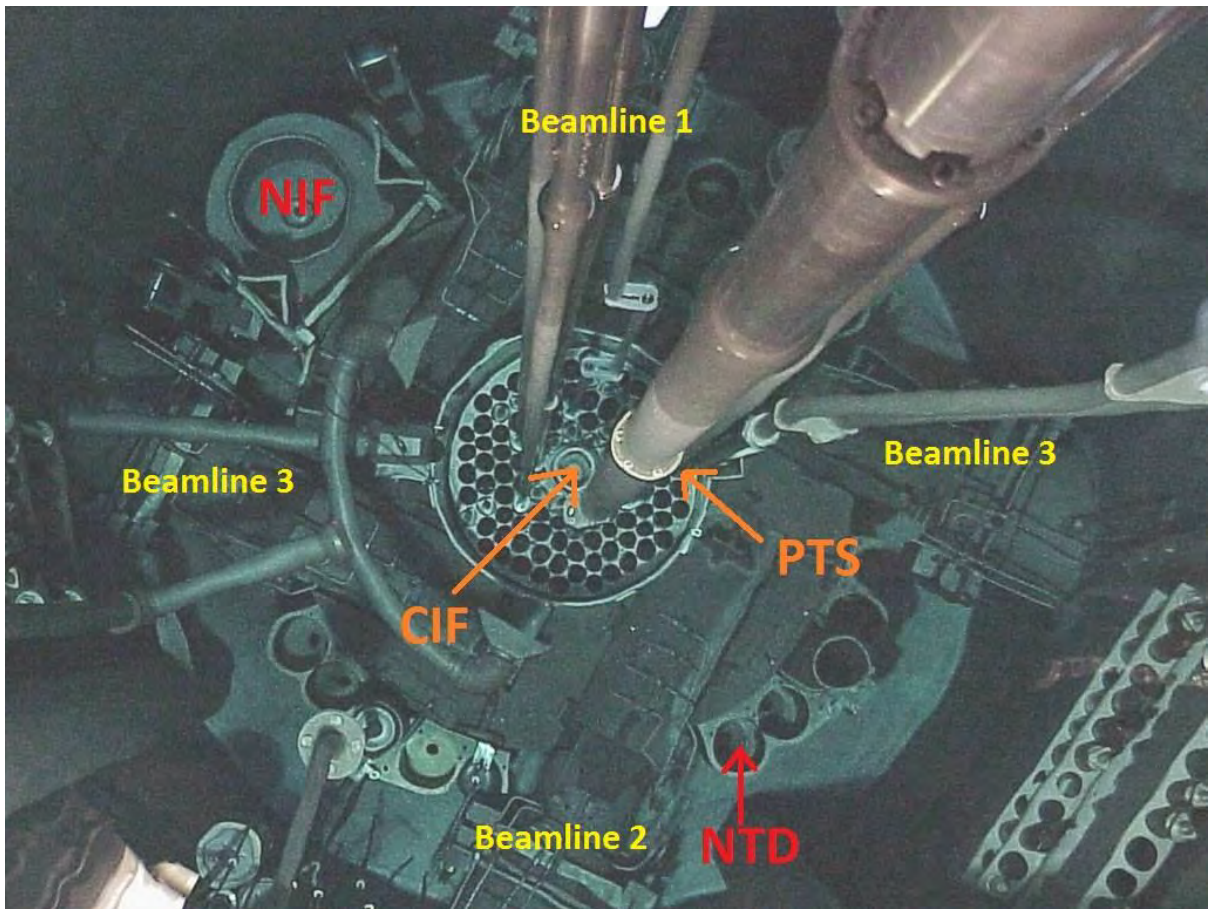


FIGURE 10.2 MNRC IN-TANK EXPERIMENTAL FACILITIES AND BEAMLINES INSERTS

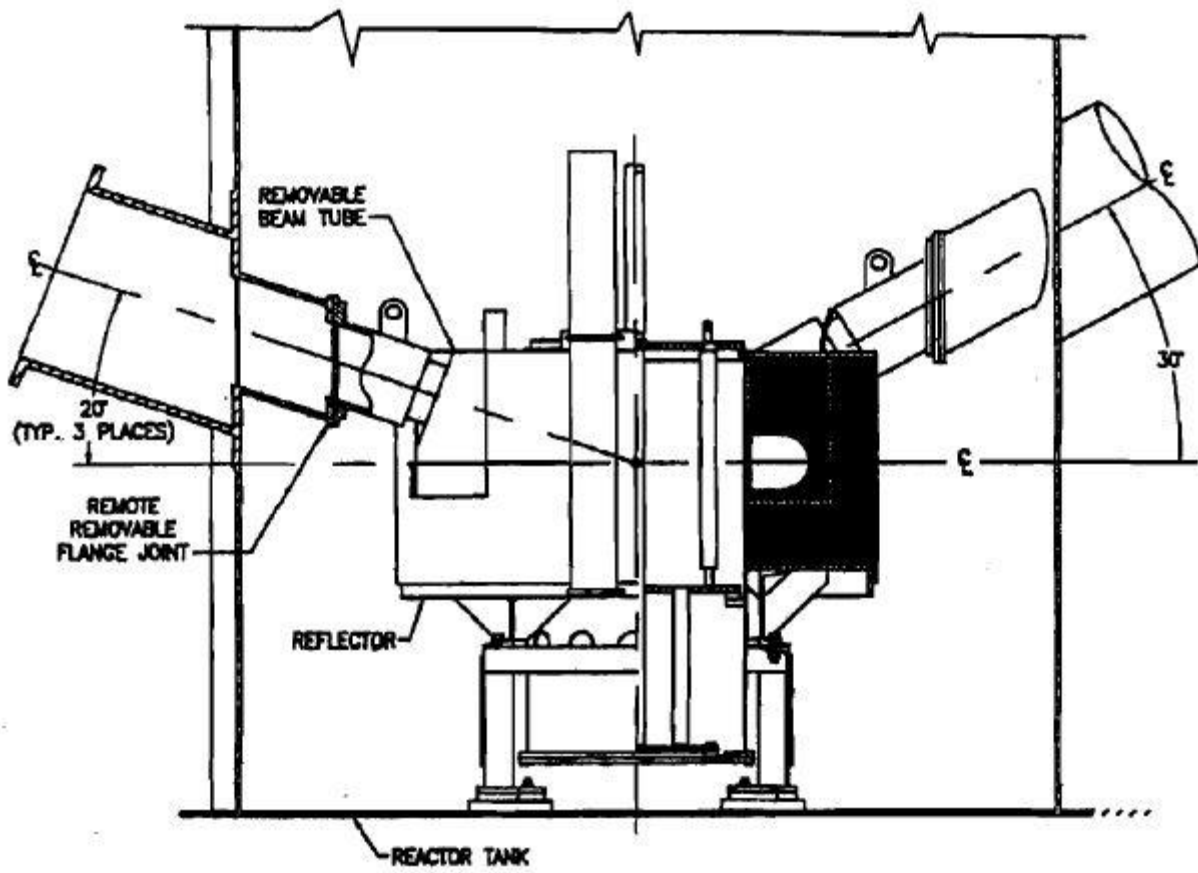


FIGURE 10.3 IN-TANK BEAM TUBE

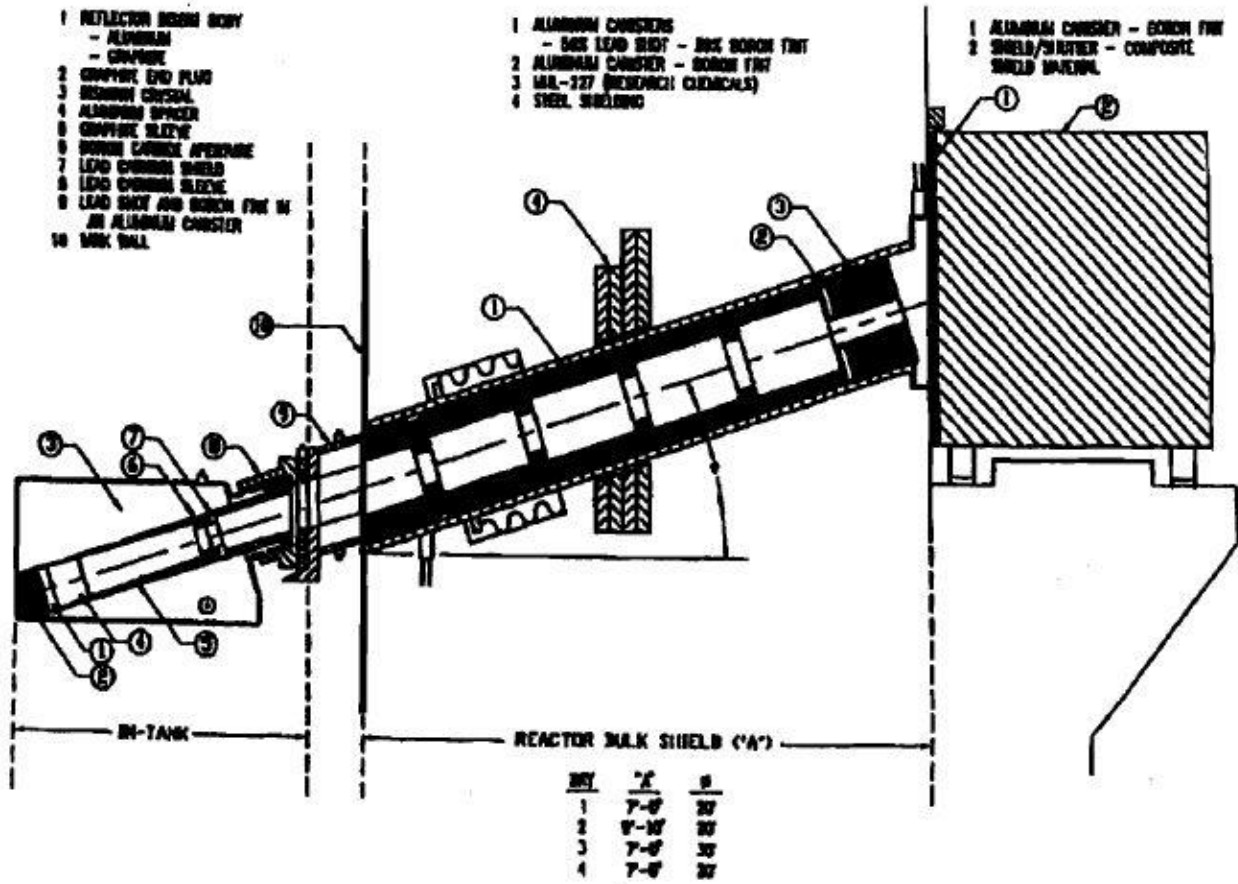


FIGURE 10.4 UCD/MNRC BEAM TUBE AND BIOLOGICAL SHIELD

The sleeve and shield serve as neutron and gamma ray shields. All of these components are contained in an aluminum housing that transitions into a 12-1/2 in. diameter circular cross section with a bellows assembly and flange with a bolt-on faceplate. A lead coated metal O- ring forms the seal between the flange and the faceplate. The faceplate and the in-tank assembly have two tube fittings that connect to a helium supply or vacuum system. The entire unit is watertight and can be remotely removed and replaced from the tank top. The assembly mates with the tank-wall section of the beam tube to provide a water free path within the reactor tank for the neutron beam. Removal and replacement of the in-tank section of the beam tube has a small effect on the reactor core reactivity. Although the entire in-tank section of the beam tube is watertight, none of the components will react with water nor will they degrade should water enter the assembly.

The tank-wall section of the beam tube consists of a 12-1/2 in. diameter pipe welded to the tank wall and a special flange welded to the core end (Figure 10.4). An aluminum container filled with 50 vol % boron frit and 50 vol % #9 lead shot by volume is located within the pipe section. The internal surface of the aluminum container is coated with gadolinium. The tank wall section does not penetrate the tank wall and serves as a watertight container when assembled as well as both a neutron and gamma shield. The gadolinium helps prevent scattered neutrons from reentering the beam. This section contains tube fittings that are attached to a helium supply or evacuation system.

The in-tank and tank-wall section flanges are held together by a two-piece bolted clamp. The clamp bolts can be remotely removed and replaced from the tank top.

The bulk shielding section of the beam tube extends from the outside of the tank wall to the radiography bays (Figure 10.4). The housing for this section is a 20 in. diameter steel pipe and bellows assembly imbedded into the concrete. The bellows assembly provides flexibility for expansion and contraction. The pipe is in close proximity, but is not physically attached to the tank wall. Within the housing are a number of annular shaped aluminum containers filled with 50 vol % boron frit and 50 vol % #9 lead shot. The primary function of these materials and their design is to provide neutron and gamma ray shielding, help shape the beam, and prevent scattered neutrons from reentering the beam. The annular section next to the tank wall is permanently installed. The remaining boron/lead filler sections can be removed and replaced with units of different internal diameters if the beam size (cross section) needs to be changed. The two annular containers at the exit of the beam tube into the radiography bay contain 100% boron frit and a Research Chemicals MHL-277, respectively. These elements are the final beam shapers and both are excellent neutron shields. Both assemblies can be replaced from the radiography bay. The inner surfaces of all containers in this section are also coated with gadolinium.

The ends of the beam tubes are closed with aluminum plates. These plates are 0.60 inches for the beam tubes in radiography Bays 1, 2, and 4, and 0.75 inches for the beam tube in radiography Bay 3.

The amount of explosive material allowed in radiography Bays 1, 2, 3, and 4 is 3 pounds of TNT equivalent per bay. This explosives limit is supported by safety analyses performed by Southwest Research Institute (Reference 13.11) and by the UCD/MNRC (Reference 13.10). Actual results of these analyses show that the four radiography bays could each safely contain up to ■ pounds of TNT

equivalent, provided the door tracks and suspension on Bays 2 and 3 were strengthened. However, by establishing a limit of 3 pounds of TNT equivalent for each bay, only the beam tube cover plates specified in the previous paragraph are required.

All three sections of the beam tube are equipped with gas lines. These lines are attached to the helium supply or evacuation system and can be used to either evacuate or fill the tubes with helium to prevent degradation of the neutron beam. The helium supply and vacuum system has venting and/or pressure controls to prevent over-pressurization of the beam tube (Section 9.2). There is very little, if any, Ar-41 formed in these beam tubes because of the absence of air.

#### 10.2.1.3 Evaluation

The beam tubes, by use of shaped rings and being sealed and void of air, provide a neutron path with minimum neutron scattering.

The beam tubes do not penetrate the reactor tank wall, and therefore, do not increase the probability of tank leakage.

The beam tube cover plates on the ends of the beam tubes, where they exit into the bays, provide closure and prevent pressure waves from reaching the reactor core and damaging the fuel should the maximum allowable amount of explosives being radiographed detonate.

It should be noted that supplemental shielding has been placed in the reactor bulk shield to compensate for the void volumes created by the beam tubes.

### 10.2.2 Beam Tube Shutter/Bulk Shield

#### 10.2.2.1 Design Basis

The design basis for the beam tube shutter/shield is:

- (a) To attenuate the neutron radiation beam at the location where it exits into the radiography bay such that radiation levels in the radiography bay are as-low-as-reasonably-achievable;
- (b) To provide a fast-acting thermal neutron shutter so that radiography film exposure times and real-time imaging can be controlled.

### 10.2.2.2 Description

Each of the beam tubes has a bulk shield and shutter. These units are located adjacent to the radiography bay end of the beam tubes as shown in Figure 10.4, and serve two basic functions. First, they provide the biological shielding from reactor core neutrons and gamma rays when the beam is not being used and the radiography bays are occupied. Second, they provide a means to start and stop the flow of thermal neutrons during radiography operations.

The shield/shutter unit is motor-driven and can be positioned so that the bulk shield covers the beam tube or so that only the thermal neutron shutter is in the beam path. The bulk shield is a massive composite structure containing materials to thermalize fast neutrons, capture thermal neutrons, and shield against both direct and capture gamma rays.

The bulk shield has an average density of 4.7 gm/cm<sup>3</sup> and is made up of cement, boron carbide, limonite, and steel shot. Boron frit, approximately 1 in. thick contained in aluminum, is placed in front of the composite shield to attenuate thermal neutrons. This shield has been designed so that the surface radiation level on the radiography bay side where personnel will be working during reactor operation at 2 MW will be less than 1 mr/hr. The motor drive on the shield is controlled from the radiography control room or in the radiography bay. Indicator lights in the radiography and reactor control room show the shutter position. There is an interlock system that prevents the shield from being moved from the closed position any time the radiography bay door is opened and the reactor is operating. Sections 9.6 and 11.1.5.1 contain a complete description of the shield, shield controls and interlocks.

The thermal neutron shutter is a rectangular aluminum can approximately 1 in. thick filled with boron frit. The shutter is air actuator-driven, and remotely controlled from the radiography control room. As far as radiation protection is concerned, it is not considered an integral part of the bulk shield.

### 10.2.2.3 Evaluation

The beam tube shutter/shield provides the necessary biological shielding to protect personnel working in the radiography bay from the intense source of neutrons in the radiography beams. These shields limit the radiation levels, within the radiography bays, to less than 1 mr/hr at 2 MW (Chapter 11).

The boron frit shutter provides an effective means of controlling the flow of thermal neutrons.

### 10.3 Component Positioning Equipment

The UCD/MNRC has three automated component positioning systems. The automated systems are located in Bays 1, 2 and 3. Bay 4 is provided with an inspection table and fixtures.

#### 10.3.1 Bay 1 Component Handling System

Following are specific design features which have been included in the component handling system of Bay 1. Figure 10.5 shows an elevation layout of the component handling system. This system is used to position large components. The maximum size component which can be inspected measures 32.5 ft long x 12.5 ft high and weighs 3800 lbs.

The system consists of one cart with fixtures to hold the components. The cart is latched to the positioning system which provides five axes of motion. Large components are held with special fixtures which provide positive location of the component on the cart. This fixturing has been designed to hold the components at each end to eliminate support structures at the center of the component which would interfere with the radiograph.

#### 10.3.2 Bay 2 Component Handling System

Following are specific design features which have been included in the component handling system of Bay 2. Figure 10.5 shows an elevation layout of this system. The system is sized to handle parts weighing up to 1500 lbs and measuring up to 18 x 9 ft.

The system in Bay 2 includes two carts which hold the components to be inspected. The carts have been designed to accept large part fixturing which is used on the Bay 1 cart. The carts are also equipped with adjustable fixturing to hold smaller parts. This fixture can accommodate four components at one time. This system provides the same degrees of freedom as provided in Bay 1.

#### 10.3.3 Bay 3 Component Handling System

Following are specific design features which are included in the component handling system of Bay 3. Figure 10.6 shows an elevation layout of this system. This system is sized to handle small parts up to 5 ft x 5 ft and curved parts with curvatures up to 160 deg. For inspecting curved parts, more yaw motion is required in this bay than in the other bays. For this reason, this positioner is designed differently than the ones in Bays 1 and 2.

This system does not use a cart. Instead, operators load the components onto the positioner in the inspection bay. To facilitate this, an adjustable frame has been provided which can be adjusted to support small parts. After the fixture is loaded, the system will position the component in the beam path.

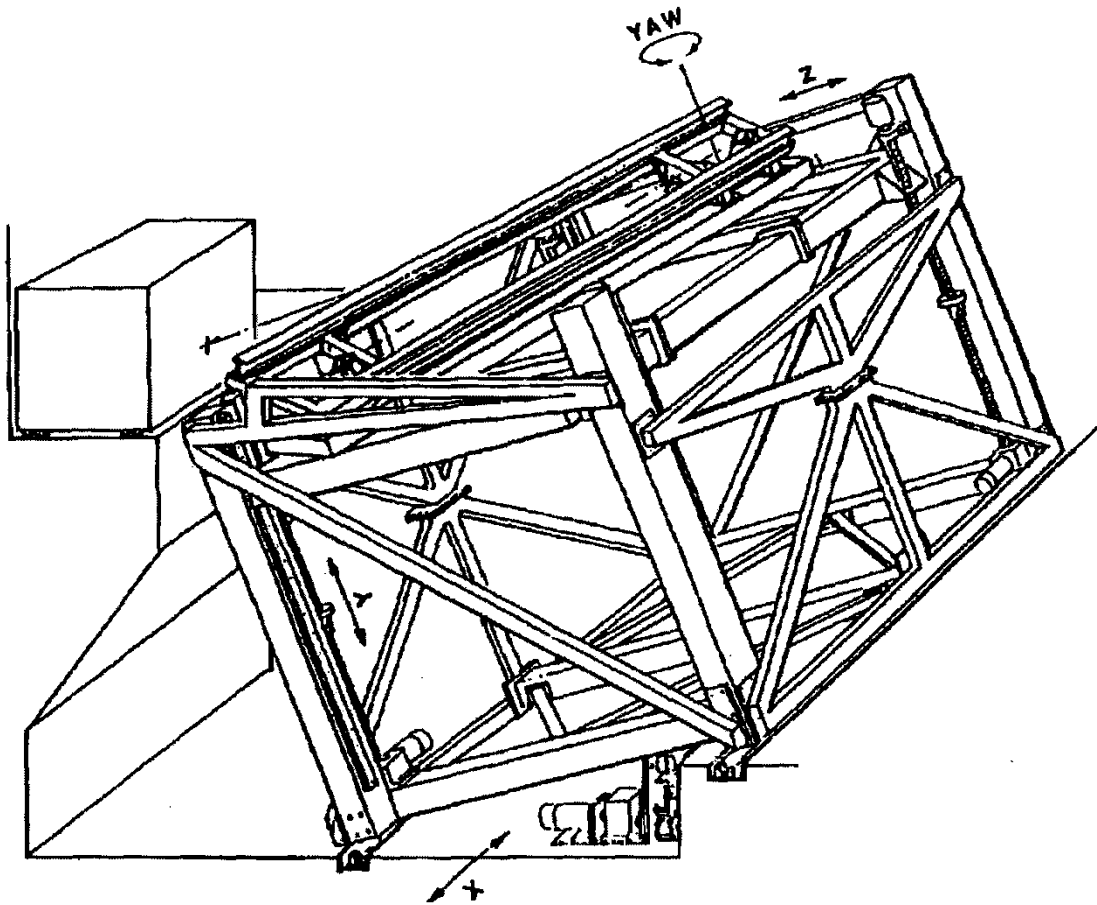


FIGURE 10.5 BAYS 1 AND 2 COMPONENT POSITIONING SYSTEM

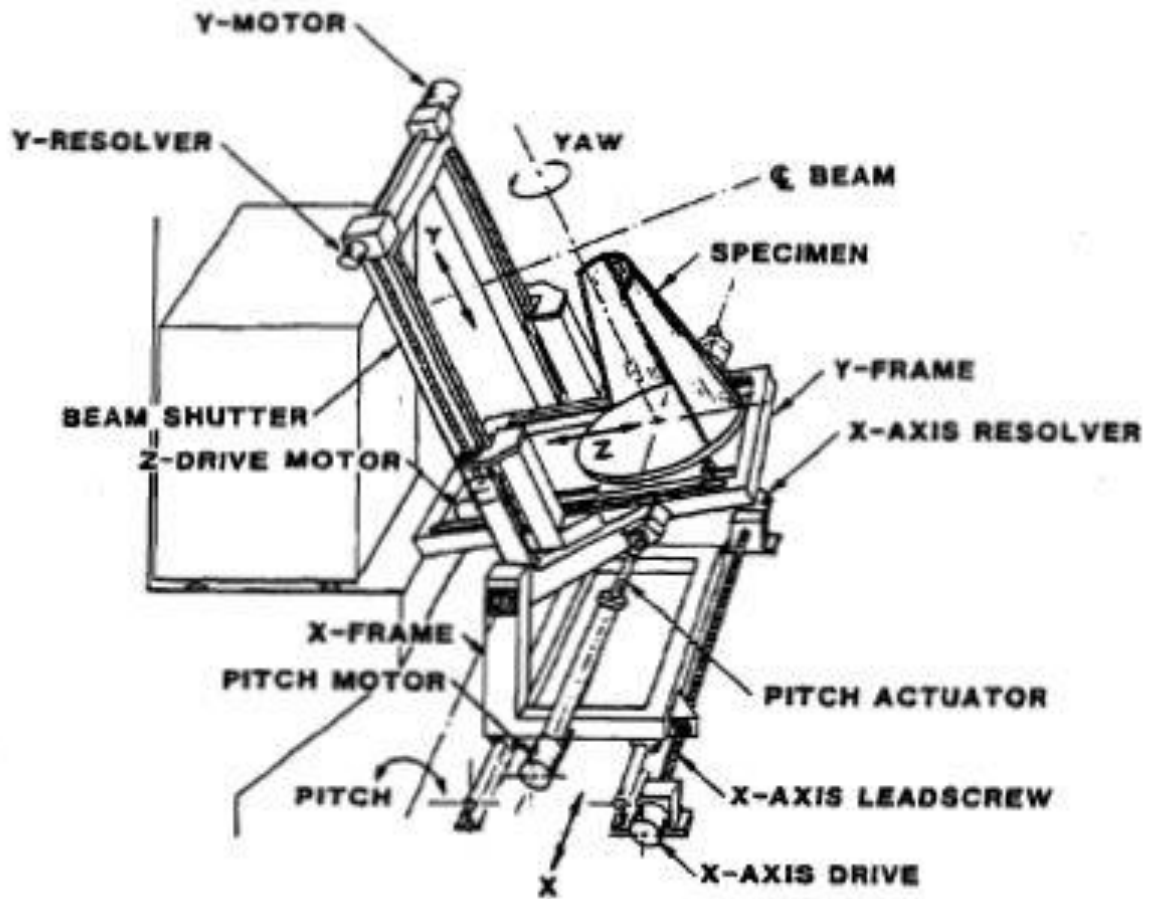


FIGURE 10.6 BAY 3 COMPONENT POSITIONING SYSTEM

## 10.4 In-core Irradiation Facilities

The UCD/MNRC reactor is designed with several locations for in-core irradiation facilities. These in-core locations are indicated in Figure 10.7 and include a central cavity, four experiment tube locations, a location for a pneumatic transfer tube, and individual fuel element locations. The irradiation facilities which may be installed in these in-core locations are described below.

### 10.4.1 Central Irradiation Facility

The central irradiation facility is formed by the installation of a central thimble (Figure 10.8) into the central cavity in the reactor core. Once installed in the central cavity, the central thimble shall not be removed from the reactor core unless it is to be replaced with another facility of similar dimensions that has been analyzed to show how it affects the overall operation of the reactor (See Section 10.4.1.1).

The central thimble is approximately 55 inches in length and 4.22 inches in diameter with an inside dimension of approximately 4.0 inches. The central thimble once in place passes through the upper grid plate, the lower grid plate and the safety plate. The bottom of the central thimble sits on the bottom of the reactor tank. An aluminum ring located approximately 24.5 inches from the bottom of the central thimble aligns with the bottom grid plate and prevents samples or fixtures from dropping below the lower grid plate. There is a 1.5 inch hole in the center of the aluminum ring and twenty-four 1.0 inch holes in the lower 24 inches to allow cooling flow throughout the central thimble. Aluminum shims have been added to the outer periphery of the central thimble in the fuel region. These shims align the central thimble and displace the water from the scallops of the fuel element locations in the B hex ring 4.25 inch hole. Samples or fixtures can be inserted into or removed from the central irradiation facility using underwater tools.

#### 10.4.1.1 Central Irradiation Facility (CIF-1)

The central irradiation fixture (CIF-1) consists of a graphite thimble plug and associated removable aluminum thimble plug insert positioned in the central irradiation facility (Figure 10.8).

The graphite thimble plug is a graphite-filled sealed aluminum can having dimensions of 26.88 inches long and 3.95 inches in diameter with a central through hole of 2.25 inch. A 6 inch long aluminum pipe welded to the top of the graphite thimble plug allows the removal or installation into the central thimble of this plug.

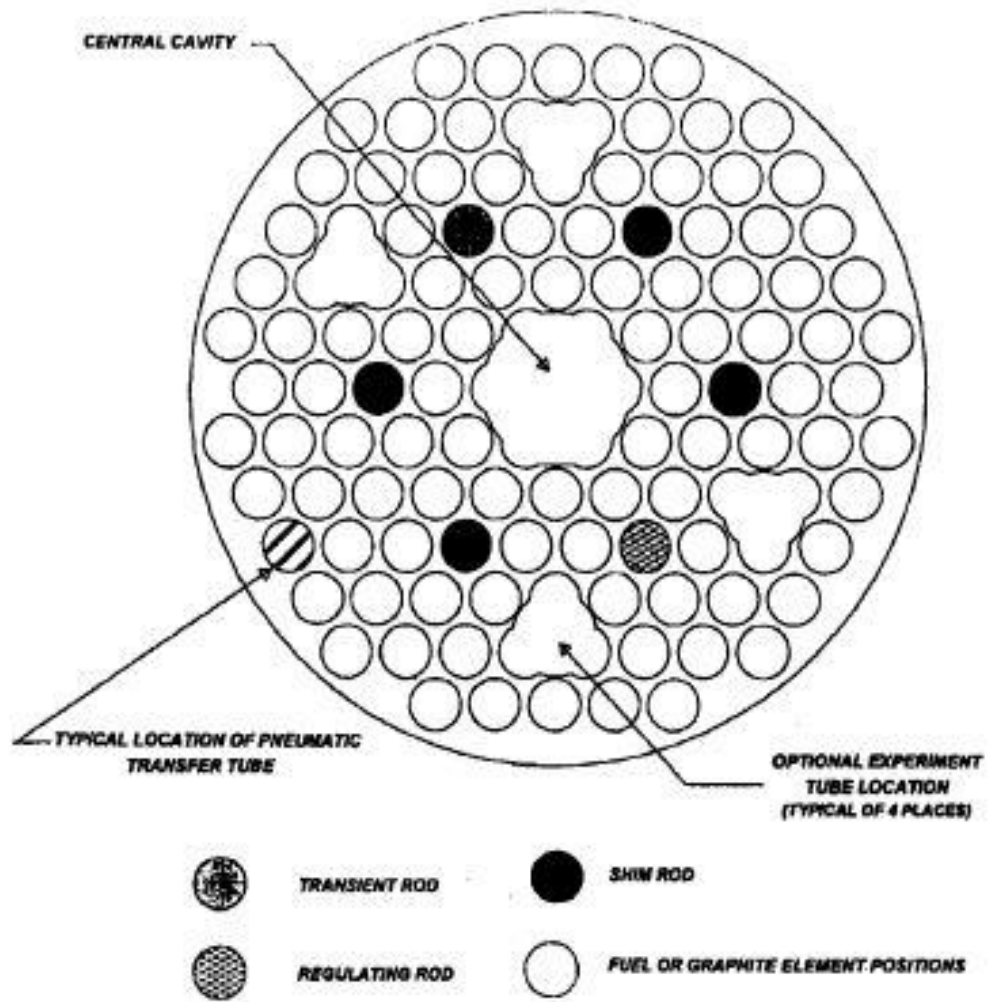


FIGURE 10.7 UCD/MNRC TYPICAL IN-CORE FACILITIES

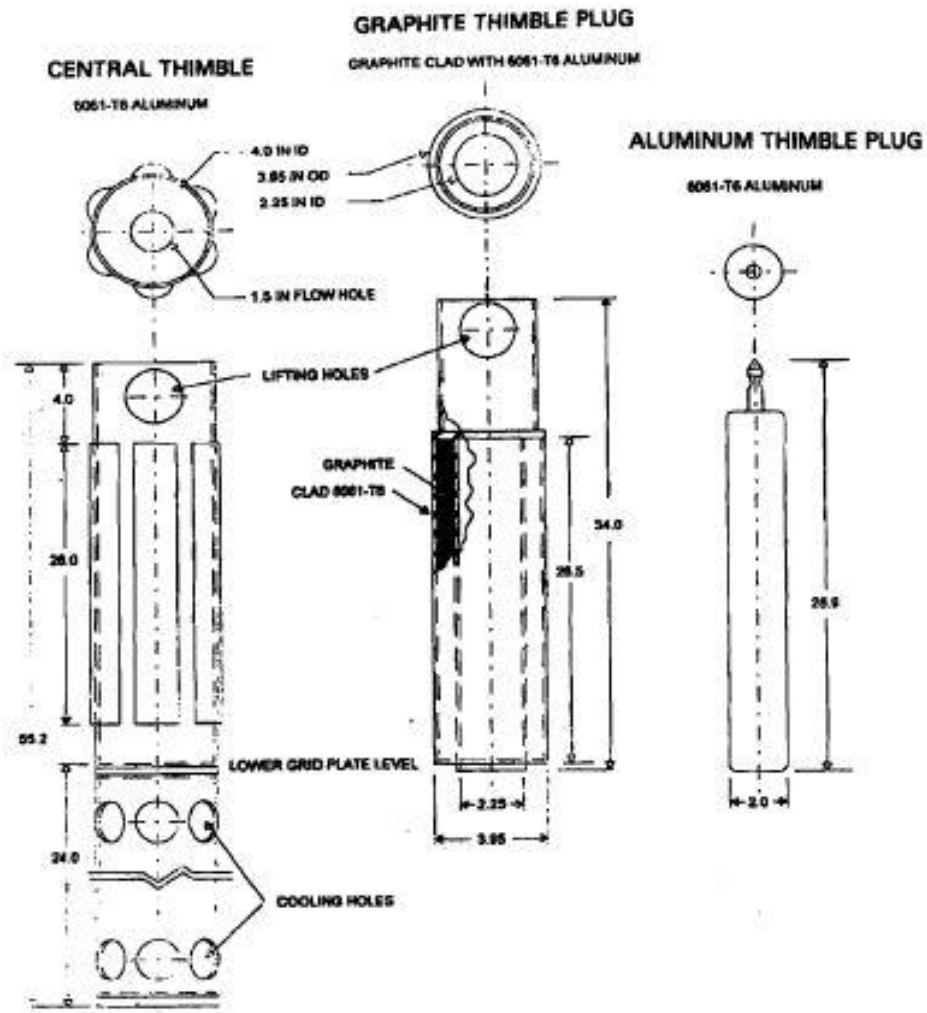


FIGURE 10.8 UCD/MNRC CENTRAL IRRADIATION FACILITY (THIMBLE) AND CENTRAL IRRADIATION FIXTURE-1 (CIF-1)

The removable aluminum thimble plug is a 2 inch aluminum bar approximately 29 inches in length. The upper end of the plug has been machined so the fuel element handling tool can be used to insert or remove the plug. Removal of the aluminum thimble plug provides a water filled region for the irradiation of experiments.

#### 10.4.2 Experiment Tubes in Upper Grid Plate Cutout Positions

Four triangular shaped cutout sections, described in Section 4.2.3, have been provided in the upper grid plate to allow for removal of groupings of three fuel elements and the insertion of tubes up to 2.4 in. outside diameter for experiment placement.

#### 10.4.3 Pneumatic Transfer System

The UCD/MNRC Pneumatic Transfer System, shown in Figure 10.9, is designed to quickly transfer individual specimens into and out of the reactor core. The specimens are placed in a small polyethylene holder, "rabbit," which in turn is placed into the receiver. The rabbit travels through aluminum tubing to the terminus at reactor core centerline, then returns along the same path to the receiver. Directional air flow moves the rabbit between receiver and terminus. A blower assembly moves air through the system, and a solenoid valve directs air flow. Controls to operate the blower and solenoid valve are wall-mounted adjacent to a hood which contains the receiver. The air flow design is such that the rabbit is never pushed but rather pulled from place to place, minimizing the possibility of fragments from a shattered rabbit becoming trapped in the terminus. The key system elements and their functions are described below.

The "rabbit" is an enclosed polyethylene holder. Experiments are inserted into the rabbit and contained by a screw cap on one end. Available space inside the rabbit is approximately 0.625 in. in diameter and 4.5 in. in length.

The receiver positions the rabbit for transfer to the terminus and receives the rabbit after irradiation. An aluminum door retains the rabbit in the receiver during transfer operations. Two transfer lines connect the receiver to the terminus: one allows the rabbit to travel between the receiver and terminus, the other controls the air flow direction.

The receiver is located in a stainless steel hood which encloses the area around the receiver and prevents uncontrolled release of airborne radioactivity. The hood's exhaust fan maintains the hood at a negative pressure with respect to the surrounding room and maintains a hood face air velocity of approximately 100 ft/min when the sash is open. The air to the fan passes through a prefilter, an absolute filter and exhausts to the facility stack. The hood is located in the preparation area and provides working space around the receiver for handling rabbits before and after irradiation.

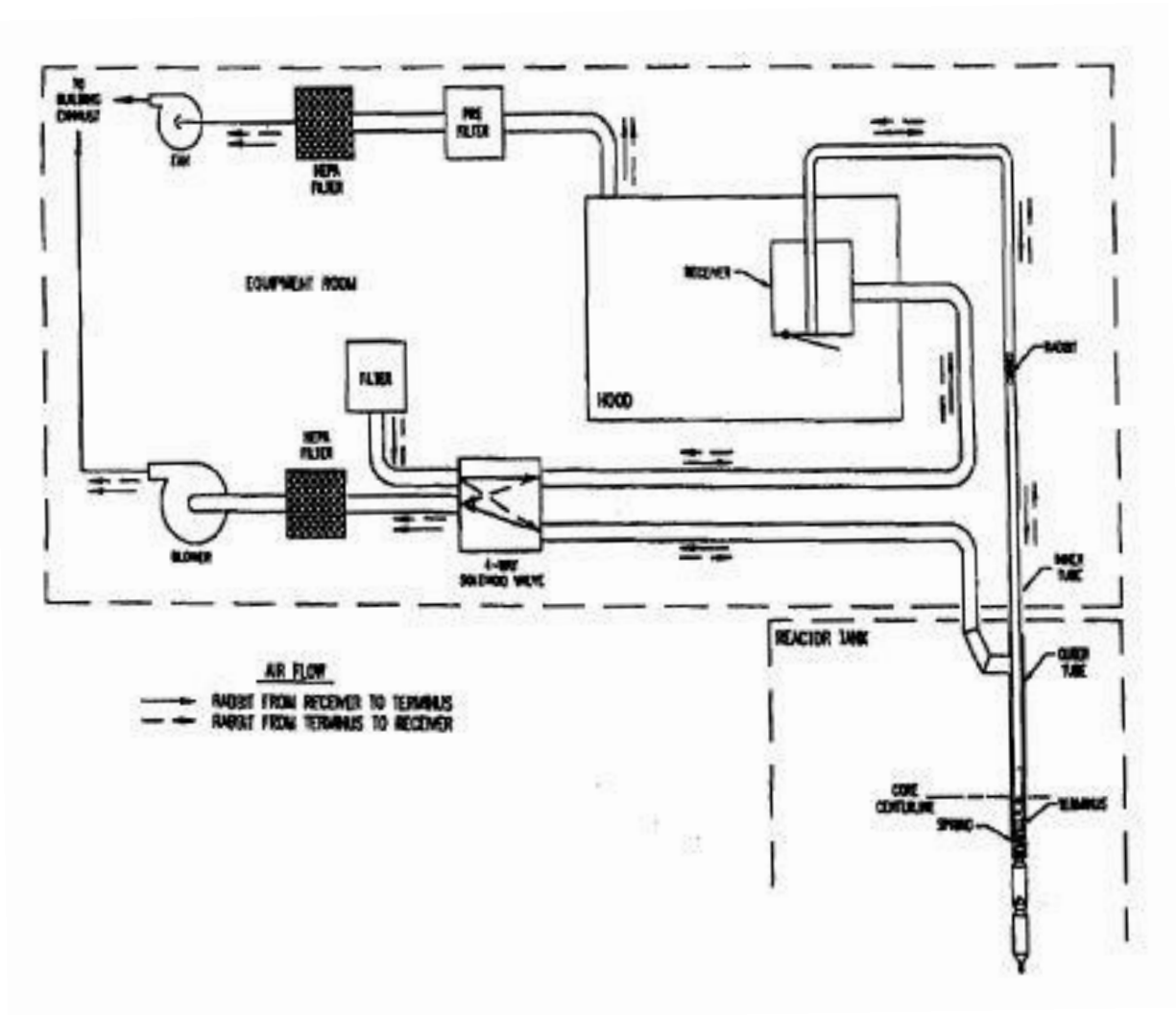


FIGURE 10.9 UCD/MNRC PNEUMATIC TRANSFER SYSTEM

The terminus consists of two concentric tubes which extend into the reactor core. The inner tube is perforated with holes (which are smaller than the rabbit diameter). The bottom of the inner tube contains an aluminum spring shock absorber to lessen the impact of the rabbit when it reaches this end of the transfer line, which is approximately at the mid-plane of the core. When air flows to the terminus, the capsule rests in the bottom of the inner tube; when air flows to the receiver, the capsule moves out of the inner tube by air flowing through the tube's holes. The outer tube supports the inner tube and provides a path for the air to flow through.

The outer tube bottom support is shaped like the bottom of a fuel element and can fit into any fuel location in the core lattice. Both tubes, which extend to the top of the reactor tank, are offset to reduce radiation streaming. A weight has been installed to counteract the buoyancy of the air-filled tubes and keep the terminus firmly positioned in the core. The terminus can be removed from the core by releasing two couplings.

Two 1.25 in. aluminum transfer lines form a loop with receiver and terminus. The "rabbit" transfer line provides a path for rabbit travel between the receiver and terminus while the "air" transfer line directs air flow between receiver and terminus. Tubing bends are a minimum 2 ft radius, allowing clearance for the rabbit.

A solenoid valve directs flow through the transfer-line-loop sending the rabbit either to the terminus or to the receiver depending on valve position. When the solenoid valve is deenergized, rabbit transfer line air flows from terminus to receiver; when the solenoid valve is energized, rabbit transfer line air flows from receiver to terminus. Solenoid status (energized or deenergized) is indicated by red markings on the solenoid alignment rod.

A two horsepower blower circulates air through the transfer lines. The blower draws filtered room air through the solenoid valve, transfer lines, and a High Efficiency Particulate Air (HEPA) filter. The blower outlet goes to the facility exhaust system.

The transfer systems' controls allow operations in either manual or automatic modes. In manual mode, the solenoid valve is activated by the operator; in the automatic mode, the solenoid valve is activated by the timer mechanism, sending the rabbit into the core-when the timer starts and retrieving the rabbit after a predetermined time period. The blower is manually operated in either mode. The controls for the system are located in a box next to the hood.

An interlock switch in the reactor control room provides the reactor operator with overall control of operation. The switch is interlocked to the power supply for the blower such that the switch must be "ON" for the blower to operate.

#### 10.4.4 Individual Grid Plate Fuel Element Positions

Reactor grid positions vacant of fuel elements may be utilized for the irradiation of materials. These in-core irradiation facilities involve placement of an experiment in a fuel element grid position and use of these locations shall meet all the applicable requirements of the UCD/MNRC Technical Specifications.

#### 10.5 Ex-Core In-Tank Facilities

Ex-core in-tank facilities have been established as shown in Figure 10.10. These facilities include the neutron irradiator facility, multiple silicon doping fixtures, and the Argon-41 production facility.

##### 10.5.1 Neutron Irradiator Facility

The Neutron Irradiator Facility is used to expose experiments to a high energy neutron environment with minimal thermal neutron and gamma radiation (Figures 10.11 and 10.12). The Neutron Irradiator has four main components: a Conditioning Well, an Exposure Vessel, a Motor Drive Unit, and a Computer. The Conditioning Well is installed inside the reactor tank adjacent to the reflector and consists of boron nitride and lead (for shielding thermal neutrons and gammas respectively) encased in aluminum. The Exposure Vessel (EV) is lowered into the Conditioning Well for irradiation. The EV houses the experiment(s) and contains temperature probes for monitoring the EV internal temperature during irradiation. A 5-piece lead and boron nitride shield assembly placed on top of an assembled EV completes the shielding around the experiment(s). The Motor Drive Unit is mounted at the top of the reactor tank and rotates the exposure vessel to provide a uniform neutron flux distribution. The Computer is connected to the EV and the Motor Drive Unit to monitor temperature and control rotation respectively. The Conditioning Well and Exposure Vessel are described in further detail below.

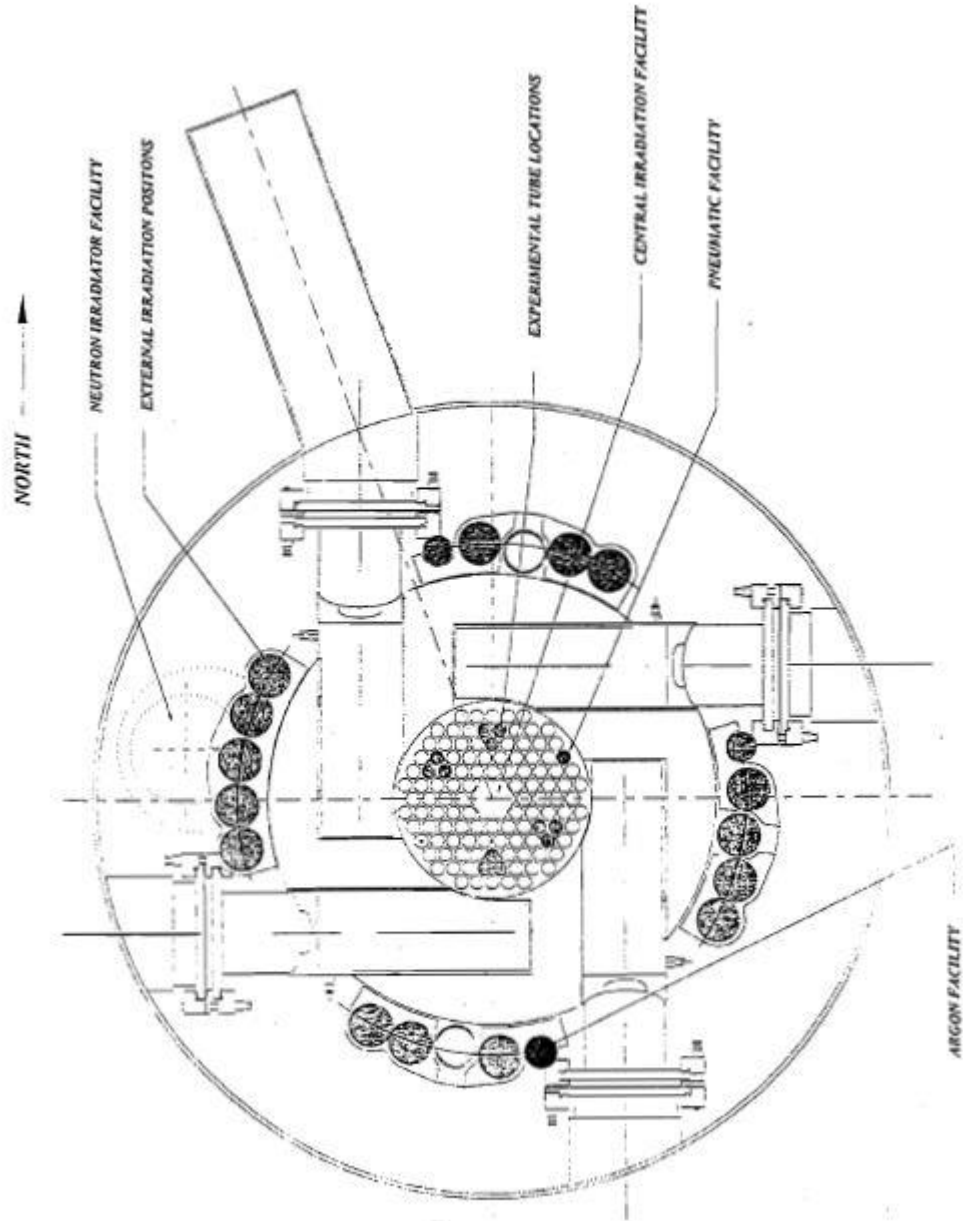
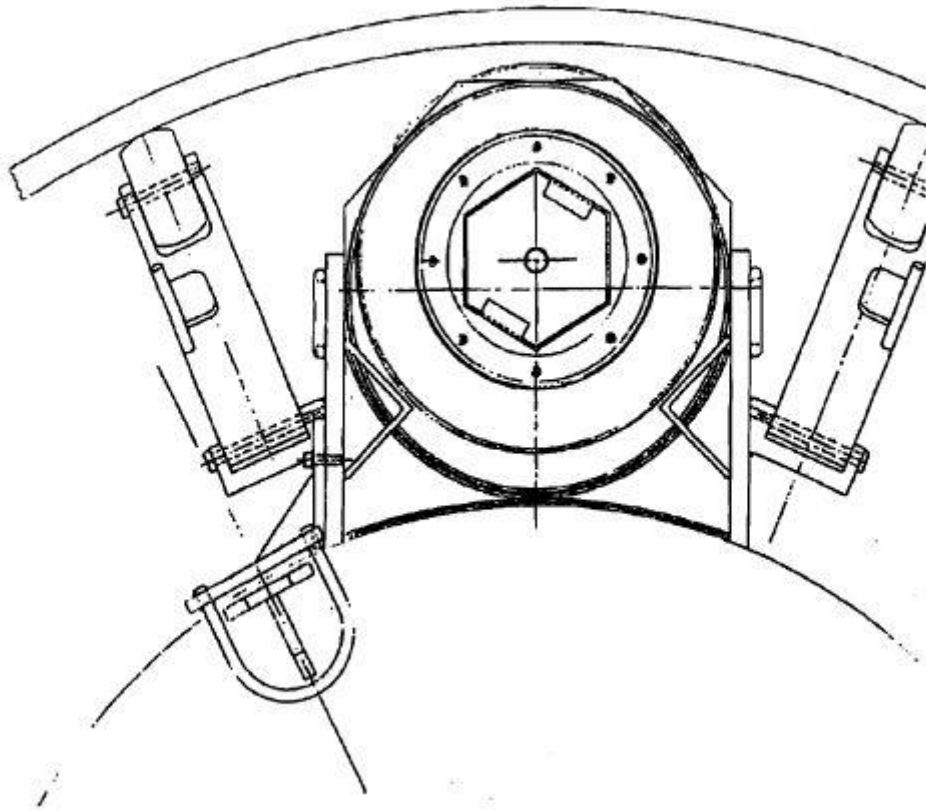


FIGURE 10.10 UCD/MNRC IN-CORE AND EX-CORE IN-TANK FACILITIES



**FIGURE 10.11 NEUTRON IRRADIATOR FACILITY - PLAN VIEW**

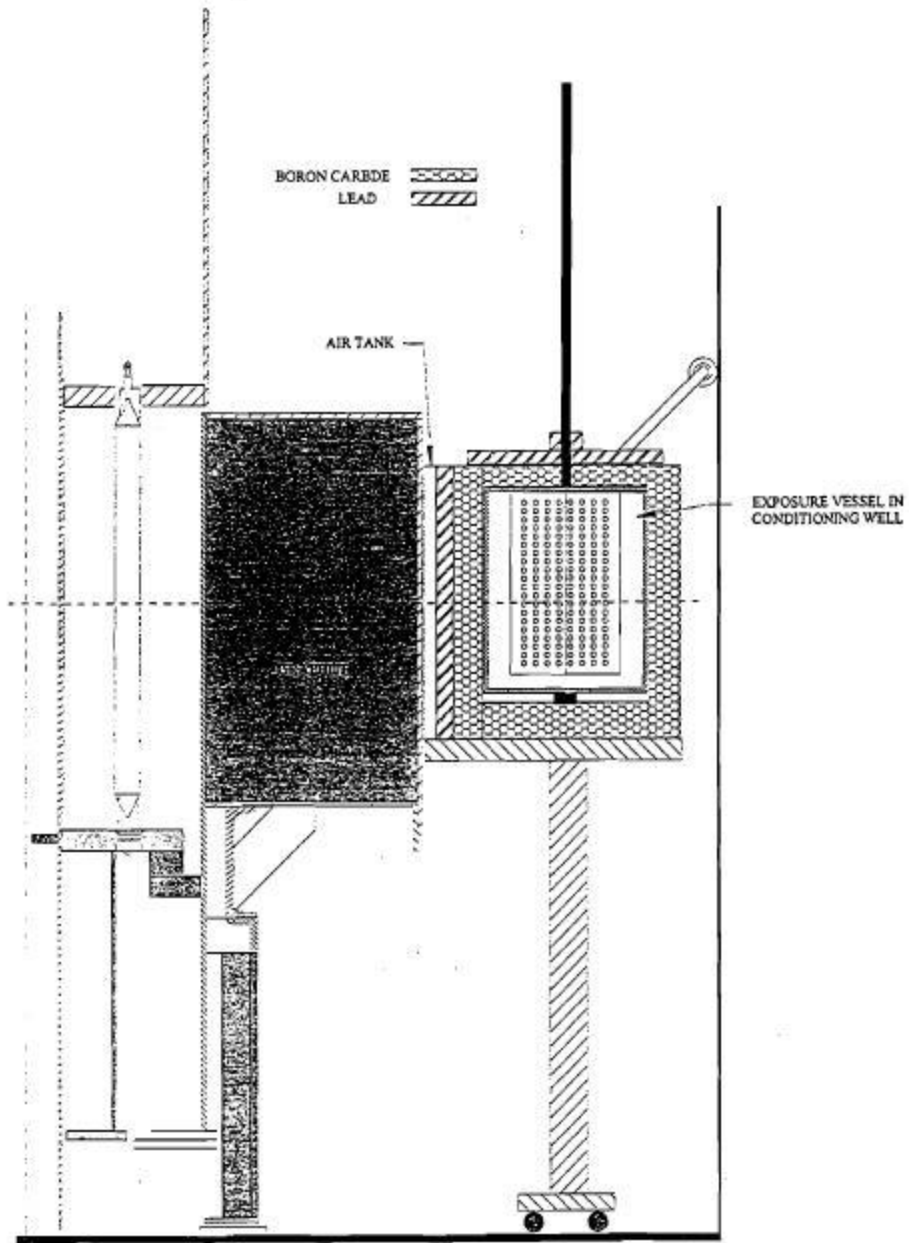


FIGURE 10.12 NEUTRON IRRADIATOR - VERTICAL VIEW

### 10.5.1.1 Conditioning Well

The Conditioning Well is installed adjacent to the core's graphite reflector in the reactor tank and is held vertically in place by a three wheeled stand which rests on the bottom of the tank. It is held laterally by the levering action of two arms with steel rollers lightly pressing against the reactor tank wall. No fasteners, nuts, or bolts are required to secure the well in place. The inner sleeve is approximately 9.5 in. in diameter and 12 in. deep and both the inner sleeve and outer casing are made of aluminum. The lead and boron nitride are completely enclosed between the inner sleeve and the outer casing.

### 10.5.1.2 Exposure Vessel

The Exposure Vessel (EV) consists of three major components: the Main Body, the Cylindrical Cup, and the 5-piece Detachable Upper Shield. The Main Body consists of a titanium top plate welded to a 48 in. titanium tube with a multi-pin electrical connector at the top. Attached to the bottom of the top plate are six titanium plates arranged in a hexagon; each plate is approximately 4 in. high and 3.5 in. wide with threaded holes for attaching experiments using aluminum screws and straps. The Cylindrical Cup is constructed of aluminum and covers the hexagonal plates enclosing and sealing the experiments. The cup is approximately 9 in. in diameter and 10 in. high. The cup's inside surface is lined with a gadolinium coating to absorb thermal neutrons. A thin sheet of aluminum protects the gadolinium coating and shields secondary radiation resulting from the neutron absorption in the gadolinium. The 5-piece Detachable Upper Shield is constructed using lead and boron nitride for shielding and is completely encased in aluminum. The shield assembly is placed on top of an assembled EV ensuring the seams are overlapping by at least 45° and then anchored in place by a collar to completely enclose the EV.

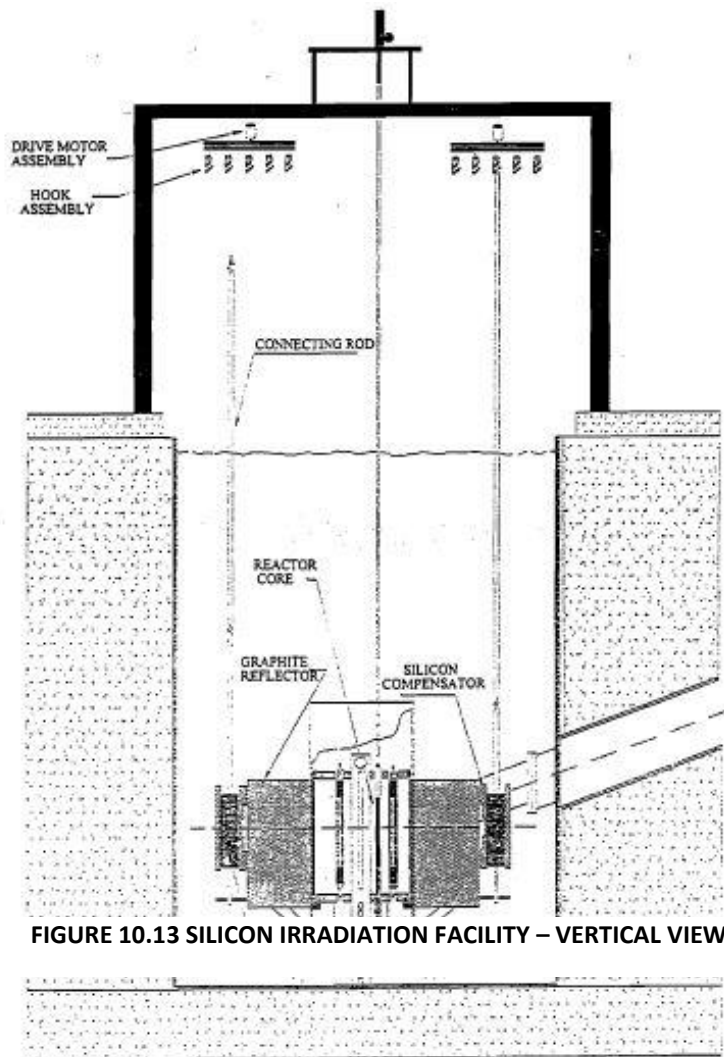
## 10.5.2 Silicon Doping Facility (Neutron Transmutation Doping)

A typical silicon doping facility consists of 5 individual motor drive assemblies mounted as a group to the tank top and positioned over an assembly at the bottom of the tank that positions irradiation canisters in locations adjacent to the reflector (Figure 10.10). The irradiation canisters containing silicon ingots have a recessed bottom section that fit over bayonets for positioning and have drive shafts extending vertically to the motor drives. The shaft assembly has a cross pin that is positioned in a yoke attached to the motor shaft. The weight of the drive shaft and irradiation canister is carried by the yoke assembly.

Each gear reduction motor and drive shaft assembly rotates the irradiation canister at a slow rotational speed for uniform irradiation of the silicon ingot. The motor drive and shaft assembly is protected from damage by a clutch mechanism in the event the shaft or irradiation canister binds or locks in position. A vertical view of the silicon irradiation facility installation is shown in Figure 10.13.

The silicon irradiation canisters provide a water environment for the silicon ingot and are designed to accommodate the removal underwater of an irradiated ingot. This handling procedure reduces irradiation exposures to individuals handling the ingots in the interest of the ALARA program. An underwater table having an adjustable work platform for vertical positioning in the tank is also utilized in the handling and loading of the irradiation canisters.

It should be noted that these silicon doping positions have not been used for silicon doping in over 10 years and are now used most often for neutron activation analysis and radiation hardness testing of electronics.



### 10.5.3 Argon Production Facility

The Argon-41 Production Facility can produce up to 4 curies of  $^{41}\text{Ar}$ , but normally will only produce 1-2 curies of  $^{41}\text{Ar}$  for research and commercial use. The  $^{41}\text{Ar}$  will be produced by introducing argon gas into a 6061-T aluminum container located on one of the silicon irradiation positions (adjacent to the graphite reflector and external to the reactor core - Figure 10.14). All the components containing activated  $^{41}\text{Ar}$  are located in the reactor room. Argon gas from a commercial argon gas cylinder will supply the irradiation container. After the irradiation container is pressurized (approximately 500 psig) to the desired level, the gas cylinder will be isolated from the irradiation container. To produce the desired activity level of  $^{41}\text{Ar}$  the sample will be irradiated for approximately 24 hours.

After irradiation, liquid nitrogen is added to a Dewar. A motor operated valve is opened to pressurize the cooling coils above the liquid nitrogen bath. The Dewar is then raised to cover the cooling coils and  $^{41}\text{Ar}$  is cryogenically extricated from the irradiation container. After extrication is completed, the valve from the irradiation container is shut and another motor operated valve is opened. This allows diffusion of  $^{41}\text{Ar}$  gas to the sample containers. The liquid nitrogen Dewar is lowered thus exposing the cooling coils. Remote heaters are energized to raise the cooling coil temperature. When that portion of the system between the cooling coils and the sample containers has reached equilibrium, the sample containers will be isolated and removed from the system. The coil is surrounded with a lead shield to minimize the radiation exposure to personnel.

A catch tank surrounds the Dewar to contain any liquid nitrogen escaping from the Dewar or in the unlikely event of a total failure of the Dewar.

Over pressure protection of the overall system is provided by several relief valves that vent to an over pressure tank. The over pressure tank is protected by its own relief valve which vents to the reactor room. The tank is located as high as possible in the reactor room.

All piping and valves in the system are stainless steel. Compression fittings or double-ended shut-off quick connectors are used for all connections normally in contact with the  $^{41}\text{Ar}$ .

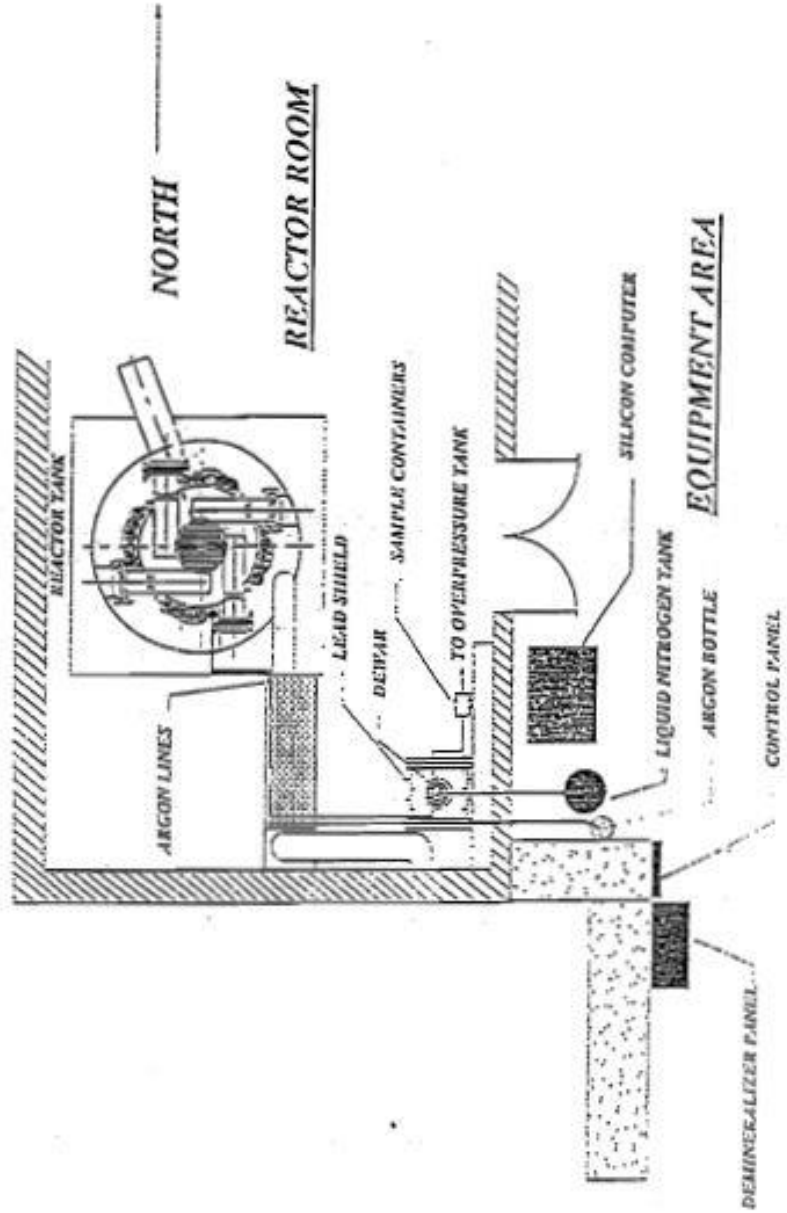


FIGURE 10.14 FLOOR LAY-OUT FOR ARGON-41 PRODUCTION FACILITY

The Argon-41 Production Facility consists of several different components with the major components listed below:

<b>COMPONENT</b>	<b>MATERIAL</b>	<b>DESCRIPTION</b>
<i>Irradiation Chamber</i>	6061-T aluminum	The irradiation container is a 1000-ml sample cylinder. The container is constructed of 6061-T aluminum with a working pressure of 600 psig and a maximum rated pressure of 1000 psig. It conforms to the "Shipping Container Specifications" from the U.S. Code of Federal Regulations, Title 49 or Bureau of Explosives Tariff No. BOE 6000
<i>Over Pressure Relief Valves</i>	304 stainless steel	The adjustable proportional pressure relief valves have a working pressure up to 6000 psig. When upstream pressure overcomes the force exerted by the spring, the popper opens, allowing flow through the valve. As the upstream pressure increases, flow through the valve increases proportionately. Cracking pressure is only sensitive to inlet pressure and is not affected by outlet pressure
<i>Over Pressure Relief Tank</i>	Carbon steel	30 gallon tank
<i>Valves</i>	304 Stainless steel	Bellows sealed valves
<i>Tubing</i>	304 Stainless steel	1/4-inch and 1/2-inch

#### 10.6 Experiment Review

The UCD/MNRC experiment review and authorization process is described in MNRC-0027- DOC, "Utilization of the University of California- Davis/McClellan Nuclear Research Center Research Facility," and in more detail in MNRC-0033-DOC, "University of California- Davis/McClellan Nuclear Research Center Reactor Facility Experiment Review and Authorization Process." This process requires that any individual wishing to utilize the UCD/MNRC reactor experiment facilities submit an Experimenter Approval Request Form to the UCD/MNRC Director's Office, where it will be reviewed and processed according to procedures in the above documents.

### 10.6.1 UCD/MNRC Experiment Coordinator (EC)

The UCD/MNRC Experiment Coordinator (EC) is the primary point of contact between the experimenter and the use of the UCD/MNRC experimental facilities. The EC reviews all forms submitted and ensures that all required information has been supplied and validated. The EC then forwards completed requests to the UCD/MNRC Director.

### 10.6.2 UCD/MNRC Director

The UCD/MNRC Director reviews new submitted experiment requests and takes one of the following actions:

- If the newly proposed experiment, in the judgment of the UCD/MNRC Director falls within the scope of a currently approved Facility Use Authorization and poses no controversial or unreviewed safety questions based on NRC regulations in 10 CFR Part 50.59, or based on facility experience or similar experiments, then the UCD/MNRC Director may approve the proposed experiment; or
- If the proposed experiment does not fall within the scope of one of the currently approved Facility Use Authorizations, the UCD/MNRC Director shall, after any necessary consultation and review by the Experiment Review Board (ERB), submit the experiment and a new or amended Facility Use Authorization to the Nuclear Safety Committee (NSC). The UCD/MNRC Director shall not approve the experiment until an appropriate Facility Use Authorization is approved by the NSC that will allow performance of the newly proposed experiment.
- If the proposed experiment, in the judgment of the UCD/MNRC Director, requires a change to the license or the Technical Specifications, or introduces an unreviewed safety question, the UCD/MNRC Director shall, after any necessary consultation and review by the Experiment Review Board (ERB), submit the proposed change to the license and/or the Technical Specifications and an applicable safety analysis to the NSC for approval prior to submission to the Nuclear Regulatory Commission (NRC). The UCD/MNRC Director shall not approve the experiment until licensing authorization is received from the NRC and an appropriate Facility Use Authorization has been approved by the NSC.

### 10.6.3 Experiment Review Board

The Reactor Supervisor serves as the ERB Chairman and conducts the ERB meetings in accordance with a written charter. The ERB is assembled as a working group that performs a technical evaluation of proposed UCD/MNRC experiments sent to them by the UCD/MNRC Director. As a result of their technical evaluation, the ERB Chairman makes a recommendation to the UCD/MNRC Director concerning the approval or disapproval of the experiment.

#### 10.6.4 Nuclear Safety Committee (NSC)

The Nuclear Safety Committee (NSC) is responsible for oversight of radiation safety and nuclear operations at the UCD/MNRC facility and operates in accordance with a written charter. Once the UCD/MNRC Director submits a new or amended Facility Use

Authorization for approval, the NSC reviews the new or amended Facility Use Authorization and takes one of the following actions:

- The NSC may approve the new or amended Facility Use Authorization and return it to the UCD/MNRC Director for implementation, or
- The NSC may disapprove the new or amended Facility Use Authorization and send it back to the UCD/MNRC Director for resolution of NSC concerns.

**CHAPTER 11**

**RADIATION PROTECTION AND  
WASTE MANAGEMENT PROGRAM**

Chapter 11 - Valid Pages  
Rev. 8 05/04/18

i	Rev. 8	05/04/18	11-38	Rev. 8	05/04/18
ii	Rev. 8	05/04/18	11-39	Rev. 8	05/04/18
iii	Rev. 8	05/04/18	11-40	Rev. 8	05/04/18
iv	Rev. 8	05/04/18	11-41	Rev. 8	05/04/18
v	Rev. 8	05/04/18	11-42	Rev. 8	05/04/18
11-1	Rev. 8	05/04/18	11-43	Rev. 8	05/04/18
11-2	Rev. 8	05/04/18	11-44	Rev. 8	05/04/18
11-3	Rev. 8	05/04/18	11-45	Rev. 8	05/04/18
11-4	Rev. 8	05/04/18	11-46	Rev. 8	05/04/18
11-5	Rev. 8	05/04/18	11-47	Rev. 8	05/04/18
11-6	Rev. 8	05/04/18	11-48	Rev. 8	05/04/18
11-7	Rev. 8	05/04/18	11-49	Rev. 8	05/04/18
11-8	Rev. 8	05/04/18	11-50	Rev. 8	05/04/18
11-9	Rev. 8	05/04/18	11-51	Rev. 8	05/04/18
11-10	Rev. 8	05/04/18	11-52	Rev. 8	05/04/18
11-11	Rev. 8	05/04/18	11-53	Rev. 8	05/04/18
11-12	Rev. 8	05/04/18	11-54	Rev. 8	05/04/18
11-13	Rev. 8	05/04/18	11-55	Rev. 8	05/04/18
11-14	Rev. 8	05/04/18	11-56	Rev. 8	05/04/18
11-15	Rev. 8	05/04/18	11-57	Rev. 8	05/04/18
11-16	Rev. 8	05/04/18	11-58	Rev. 8	05/04/18
11-17	Rev. 8	05/04/18	11-59	Rev. 8	05/04/18
11-18	Rev. 8	05/04/18	11-60	Rev. 8	05/04/18
11-19	Rev. 8	05/04/18			
11-20	Rev. 8	05/04/18			
11-21	Rev. 8	05/04/18			
11-22	Rev. 8	05/04/18			
11-23	Rev. 8	05/04/18			
11-24	Rev. 8	05/04/18			
11-25	Rev. 8	05/04/18			
11-26	Rev. 8	05/04/18			
11-27	Rev. 8	05/04/18			
11-28	Rev. 8	05/04/18			
11-29	Rev. 8	05/04/18			
11-30	Rev. 8	05/04/18			
11-31	Rev. 8	05/04/18			
11-32	Rev. 8	05/04/18			
11-33	Rev. 8	05/04/18			
11-34	Rev. 8	05/04/18			
11-35	Rev. 8	05/04/18			
11-36	Rev. 8	05/04/18			
11-37	Rev. 8	05/04/18			

TABLE OF CONTENTS

11.0	RADIATION PROTECTION AND WASTE MANAGEMENT .....	11-1
11.1	Radiation Protection .....	11-1
11.1.1	Historical Health Physics Data from MNRC .....	11-1
11.1.2	Radiation Sources .....	11-4
11.1.2.1	Airborne Radiation Sources .....	11-5
11.1.2.1.1	Argon-41 in the Radiography Bays .....	11-5
11.1.2.1.2	Production and Evolution of Ar-41 in the Reactor Room .....	11-7
11.1.2.1.3	Ar-41 from the Pneumatic Transfer System .....	11-8
11.1.2.1.4	Ar-41 Release to the Unrestricted Area.....	11-8
11.1.2.1.5	Production and Evolution of N-16 in the Reactor Room .....	11-10
11.1.2.1.6	Ar-41 from the Ar-41 Production Facility .....	11-11
11.1.2.2	Liquid Radioactive Sources .....	11-11
11.1.2.2.1	Radioactivity in the Primary Coolant .....	11-12
11.1.2.2.2	N-16 Radiation Dose Rates from Primary Cooling System Components .....	11-13
11.1.2.3	Solid Radioactive Sources .....	11-13
11.1.2.3.1	Shielding Logic .....	11-16
11.1.3	Radiation Protection Program .....	11-16
11.1.3.1	Organization of the Health Physics Branch.....	11-16
11.1.3.2	Working Interface Between Health Physics and Reactor Operations.....	11-19
11.1.3.3	Health Physics Procedures.....	11-19
11.1.3.4	Radiation Protection Training .....	11-22
11.1.3.5	Audits of the Health Physics Program.....	11-23
11.1.3.6	Health Physics Records and Record Keeping.....	11-24
11.1.4	ALARA Program.....	11-25
11.1.5	Radiation Monitoring and Surveying .....	11-26
11.1.5.1	Monitoring for Radiation Levels and Contamination.....	11-26
11.1.5.2	Radiation Monitoring Equipment .....	11-28
11.1.5.3	Instrument Calibration.....	11-32
11.1.6	Radiation Exposure Control and Dosimetry .....	11-32
11.1.6.1	Shielding .....	11-33
11.1.6.2	Ventilation System.....	11-45
11.1.6.3	Containment.....	11-47
11.1.6.4	Entry Control - Radiography Bays and Demineralizer Cubicle .....	11-47

11.1.6.4.1	Entry Control for Radiography Bays .....	11-47
11.1.6.4.2	Entry Control for the Demineralizer Cubicle .....	11-48
11.1.6.5	Protective Equipment.....	11-48
11.1.6.5.1	Respiratory Protection Equipment.....	11-49
11.1.6.5.2	Personnel Dosimetry Devices.....	11-49
11.1.6.6	Estimated Annual Radiation Exposure.....	11-50
11.1.6.6.1	Estimated Annual Doses in the Restricted Area.....	11-50
11.1.6.6.2	Estimated Annual Dose in the Unrestricted Area.....	11-53
11.1.7	Contamination Control.....	11-53
11.1.8	Environmental Monitoring .....	11-55
11.2	Radioactive Waste Management .....	11-57
11.2.1	Radioactive Waste Management Program.....	11-57
11.2.2	Radioactive Waste Controls .....	11-58
11.2.2.1	Gaseous Waste.....	11-58
11.2.2.2	Liquid Waste .....	11-58
11.2.2.3	Solid Waste.....	11-59
11.2.3	Release of Radioactive Waste .....	11-60

LIST OF FIGURES

11.1	Historical Mnrc Work Dose Data .....	11-2
11.2	Maximum Exposed Individual Dose From MNRC Ar-41 Effluence .....	11-3
11.3	Annual Dose At MNRC Facility Boundary .....	11-4
11.4	Reactor Bulk Shield Direct Dose Rate - 1 MW Operation .....	11-17
11.5	Organizational Structure Of The Mnrc Radiation Protection Program .....	11-18
11.6	Organizational Structure Showing The Radiation Protection Program Within The UCD/MNRC .....	11-18
11.7	Radiation Monitoring Equipment - Main Floor Figure .....	11-30
11.8	Radiation Monitoring Equipment - Second Floor .....	11-31
11.9	Reactor Bulk Shield .....	11-34
11.10	MNRC Beam Tube And Biological Shield .....	11-36
11.11	MNRC Shielding - Bays 1 And 2 .....	11-38
11.12	MNRC Shielding - Bays 3 And 4 .....	11-39
11.13	Projected Radiation Dose Rates - Bays 1 And 2 At 1 MW And 2 MW .....	11-42
11.14	Projected Radiation Dose Rates - Bays 3 And 4 At 1 MW And 2 MW .....	11-43
11.15	Projected Radiation Dose Rates - Plan View At 1 MW And 2 MW .....	11-44
11.16	Shielding For Demineralizer Resins And Radiation Monitoring Equipment - Second Floor .....	11-46

LIST OF TABLES

11-1	Argon-41 Concentrations In Radiography Bays During Film Radiography .....	11-6
11-2	Argon-41 Concentrations In Radiography Bays With Electronic Imaging Devices In Bays 1, 2, And 3 And Film Radiography In Bay 4 .....	11-6
11-3	Concentrations Of Ar-41 Released From The MNRC Stack Under Different Atmospheric Conditions .....	11-9
11-4	Predominant Radionuclides And Their Projected Equilibrium Concentrations In The MNRC Reactor Primary Coolant At 2 Mw .....	11-12
11-5	Representative Radioactive Sources For The Mnrc 2 MW Reactor Program .....	11-14
11-6	Radiation Monitoring And Related Equipment Used In The MNRC Radiation Protection Program .....	11-29
11-7	Radiation Levels (Millirem/Hr) .....	11-35
11-8	Composite Shield Makeup .....	11-37
11-9	Composition Of B6ac Stainless Steel .....	11-40
11-10	Summary Of Typical Protective Equipment Used In The MNRC Radiation Protection Program .....	11-49
11-11	Typical Personnel Monitoring Devices Used At The UCD/MNRC .....	11-50
11-12	Environmental Monitoring And Sampling Program .....	11-56

REFERENCES

- 11.1 United States Nuclear Regulatory Commission, Title 10, Rules and Regulations, Part 20, Standards for Protection Against Radiation, Washington, D.C.
- 11.2 Kocher, D. C., "Dose-Rate Conversion Factors for External Exposure to Photons and Electrons," Health Physics 45, pp. 665-686, 1983.
- 11.3 CAP88-PC, Clean Air Act Assessment Package-1988, Version 1.0, United States Environmental Protection Agency, 1988.
- 11.4 ANSI/ANS-15.11, "Radiation Protection at Research Reactor Facilities," 1995.
- 11.5 Emmett, M. B., "The MORSE Monte Carlo Radiation Transport Code System," ORNL-4972 (February 1975), Department of Energy, Oak Ridge National Laboratory.
- 11.6 Engle, W. W., Jr., "ANISN, A One-Dimensional Discrete Ordinates Transport Code with Anisotropic Scattering," K-1693 (March 1967), Department of Energy, Oak Ridge National Laboratory.
- 11.7 Nuclear Engineering Handbook, Harold Etherington, McGraw Hill Publishers, 1958.
- 11.8 Utilization of the University of California - Davis/McClellan Nuclear Radiation Center (UCD/MNRC) Research Reactor Facility, MNRC-0027-DOC, March 1999.
- 11.9 United States Nuclear Regulatory Commission, Regulatory Guide 8.20, "Application of Bioassay for Iodine-125 and Iodine-131," Revision 1, September 1979.
- 11.10 UCD/MNRC RSO Memorandum – "Changes to the Health Physics Program" dated 20 Jan 2005

## 11.0 RADIATION PROTECTION AND WASTE MANAGEMENT

This chapter deals with the overall MNRC radiation protection program and the corresponding program for management of radioactive waste. The chapter is focused on identifying the radiation sources which will be present during normal operation of the reactor and upon the many different types of facility radiation protection programs carried out to monitor and control these sources. This chapter also identifies expected radiation exposures due to normal operation and use of the reactor. Many of the detailed calculations supporting this chapter are contained in Appendix A.

### 11.1 Radiation Protection

The purpose of the MNRC radiation protection program is to allow the maximum beneficial use of radiation sources with minimum radiation exposure to personnel. Requirements and procedures set forth in this program are designed to meet the following fundamental principles of radiation protection:

- Justification - No practice shall be adopted unless its introduction produces a net positive benefit;
- Optimization - All exposures shall be kept as low as reasonably achievable, economic and social factors being taken into account;
- Limitation - The dose equivalent to individuals shall not exceed limits established by appropriate state and federal agencies. These limits shall include, but not be limited to, those set forth in Title 10, Code of Federal Regulations, Part 20 (10 CFR 20) (Reference 11.1).

The radiation protection measures used at the MNRC are patterned after other TRIGA<sup>®</sup> reactor facilities where the radiation sources are much the same as well as the ANSI 15.11 standard. Facility organization charts, actual radiation measurements and operating data from around the MNRC, and a description of radiation protection program components will be used to characterize the features of the different programs used to maintain occupational doses and releases of radioactivity to the unrestricted environment as low as reasonably achievable (ALARA).

#### 11.1.1 Historical Health Physics Data from MNRC

This section is provided to give quantitative data on the relevant health physics information for the MNRC from the year 2000 to the year 2016. It is important to note data from the year 2004 could not be located at MNRC or on the NRC database. It is reasonable to assume that based on the relatively high number of MW hours that year, all health physics data was near the highest annual values recorded (2002, 2003, 2005, and 2006).

The most significant historical trend that can be observed is the reduction in all health physics doses and effluence beginning in the year 2006. This drop in doses and effluence can be directly attributed to the facility moving from two-shift to one-shift operation. Further reduction in doses and effluence in subsequent years can be explained by the fact the reactor was operated less often above 1.0 MW.

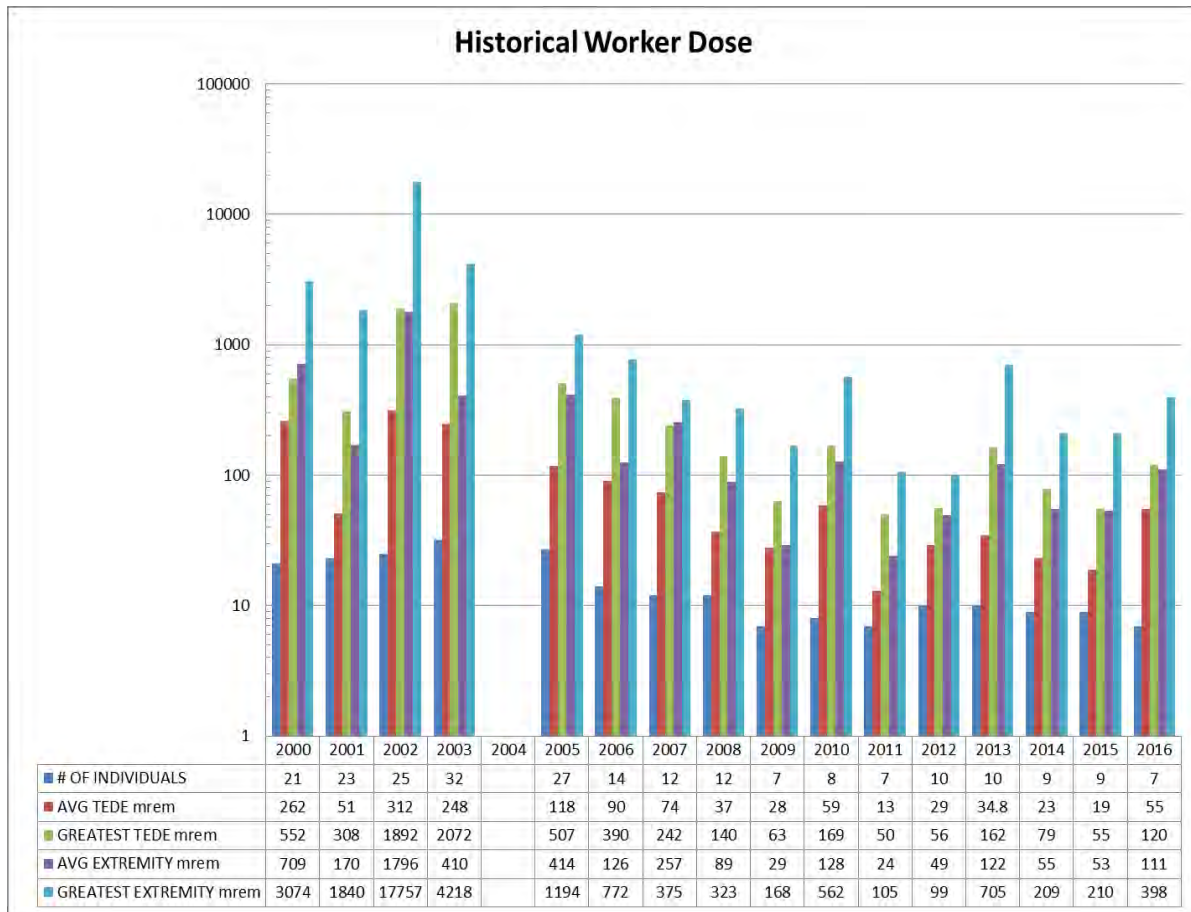


**FIGURE 11.1 HISTORICAL MNRC WORK DOSE DATA.**

Personnel doses, as seen in figure 11.1, have been well below 10 CFR 20 limits. Since the year 2008 average radiation work TEDE have been approximately 1% of the 10 CFR 20 limits.

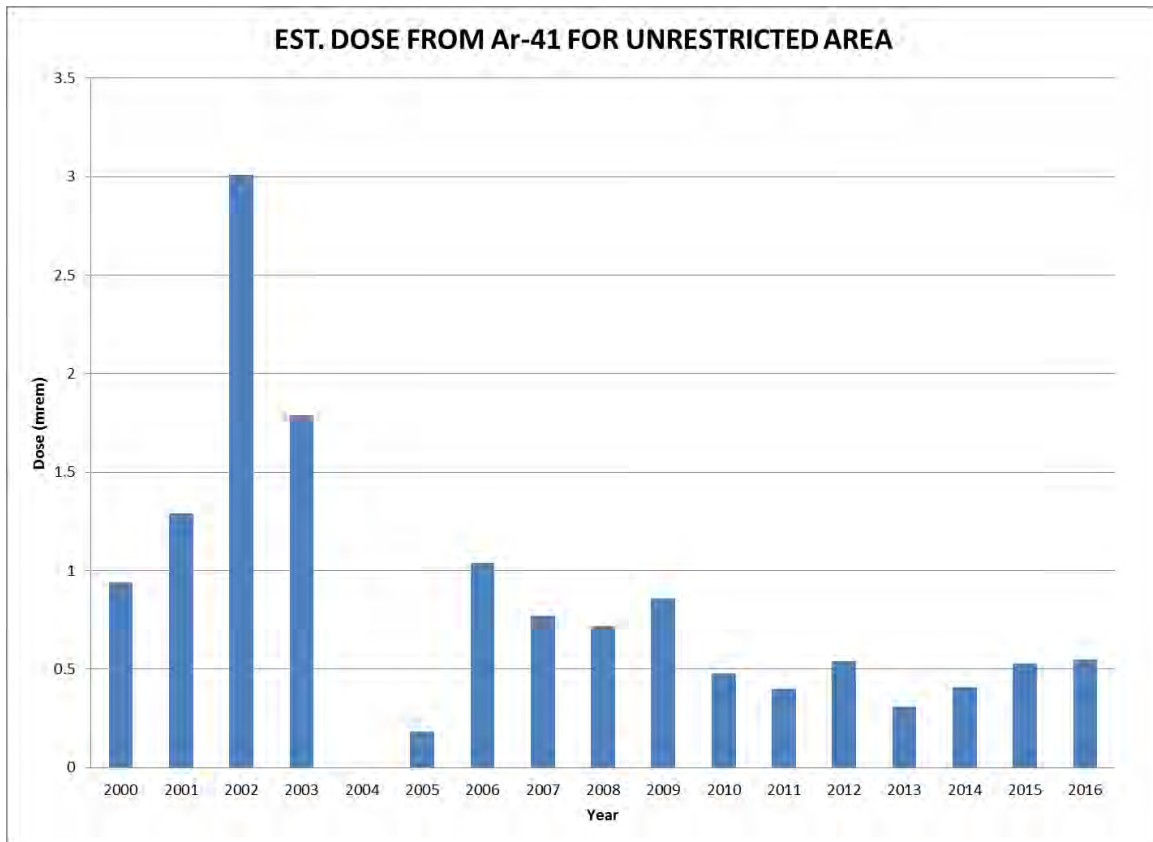


**FIGURE 11.2 MAXIMUM EXPOSED INDIVIDUAL DOSE FROM MNRC AR-41 EFFLUENCE**

All doses in unrestricted areas from Ar-41 effluences, as seen in figure 11.2, are below the 10 CFR 20 limits. Just as with radiation worker doses a decrease in unrestricted area doses can be seen in 2006 and again in 2010. This can be explained by the fact that the facility moved to single-shift operation in 2006 and rarely operated above 1.0 MW after 2009. These doses are for the maximum exposed individual standing at the highest dose rate position caused by Ar-41 effluence for the entire year. The CAP88 model provides a much more realistic estimation of public dose from radioactive effluence. These CAP88 values are significantly lower than the values given in figure 11.2.

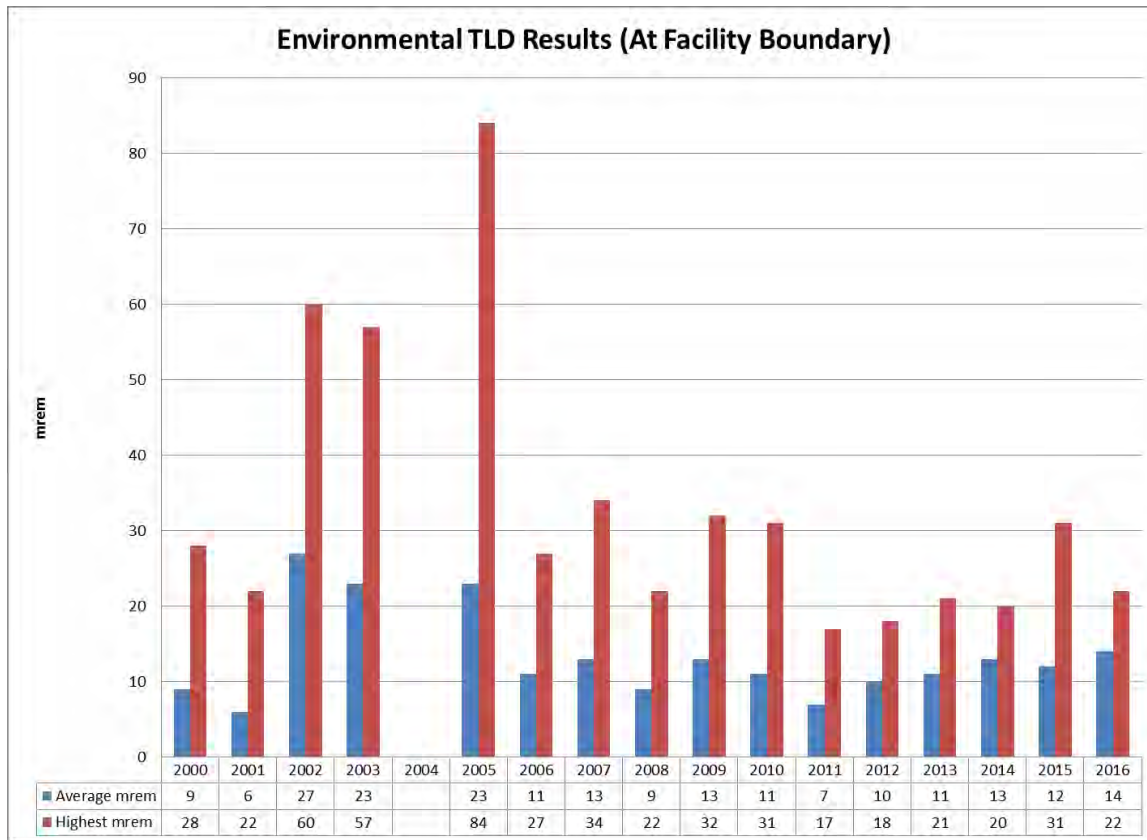


**FIGURE 11.3 ANNUAL DOSE AT MNRC FACILITY BOUNDARY**

Elevated radiation levels from reactor operations have been measured at the MNRC’s boundaries. These values have been below the applicable 10 CFR 20 limits. As with personnel dose and Ar-41 effluence, facility boundary dose has fallen as annual reactor MW hours have decreased.

As MNRC continues its mission of neutron radiography, in-tank irradiations, education, and outreach it is likely these objectives can be completed during single-shift 1 MW operation. Therefore, during the foreseeable future all doses and effluences should be very comparable to the historical values observed from approximately 2006 until 2016. Any new experiments or operation that may cause a change in doses or effluence shall be evaluated as part of the MNRC’s ALARA program.

**11.1.2 Radiation Sources**

The radiation sources present at the MNRC can be categorized as airborne, liquid, or solid. While each of these categories will be discussed individually in Sections 11.1.2.1 through 11.1.2.3, the major contributors to each category can be summarized as follows: Airborne sources consist mainly of Argon-41 (Ar-41, half-life 1.8 hrs.), due largely to neutron activation of air in the radiography bays and air dissolved in the reactor’s primary coolant, and Nitrogen-16 (N-16, half-life 7.1 sec.), due to neutron interactions with oxygen in the primary coolant.

Liquid sources are quite limited at the MNRC and include mainly the reactor primary coolant. No routine liquid effluent or liquid waste is anticipated. Any non-routine liquid effluent or liquid waste will be discharged in accordance with 10 CFR 20.2003 requirements. Solid sources are a bit more diverse, but for the most part are very typical of a TRIGA<sup>®</sup> reactor facility. Such sources include the fuel in use in the current 2 MW core, irradiated fuel from the former 1 MW core, and unirradiated fuel. In addition, other solid sources are present such as the neutron startup source, small fission chambers for use with nuclear instrumentation, irradiated components subjected to neutron radiography, other items irradiated as part of normal reactor use, and small instrument check and calibration sources. Solid waste is yet another solid source, but is expected to be very limited in volume and curie content.

#### 11.1.2.1 Airborne Radiation Sources

During normal operation of the MNRC reactor, there are two sources of airborne radioactivity, namely Ar-41 and N-16. The assumptions and calculations used to assess the production and radiological impact of these airborne sources during normal operations are detailed in Appendix A. Therefore, that information will only be summarized in this section.

Fuel element failure, although not expected, could occur while the reactor is operating normally. Such a failure would usually occur due to a manufacturing defect or corrosion of the cladding and would result in a small penetration of the cladding through which fission products would be slowly released into the primary coolant. Some of these fission products, primarily the noble gases, would migrate from the cooling water into the air of the reactor room. Although this type of failure could occur during normal operation, its occurrence is not normal and no normal operation would take place after such an event until the situation had been eliminated (i.e., the failed element located and removed from the core). As a result, the failure of a single element (for any reason) is evaluated in Appendix B as an abnormal situation or an accident, and is discussed further in Chapter 13.

##### 11.1.2.1.1 Argon-41 in the Radiography Bays

Occupational exposure to Ar-41 during normal operation of the MNRC reactor can occur in the radiography bays and in the reactor room. Ar-41 concentrations in the radiography bays (Table 11-1 and Table 11-2) will be low compared to 10 CFR 20 limits even when film radiography is being conducted in all bays and the radiography bays exhaust system is turned off. However, operation with the radiography bays exhaust system turned off will not be a normal operational mode even though it is permissible. Furthermore, Ar-41 production in the radiography bays is virtually insignificant when considering the release of this radionuclide from the facility into the unrestricted areas.

**TABLE 11-1 ARGON-41 CONCENTRATIONS IN RADIOGRAPHY BAYS DURING FILM RADIOGRAPHY**

Location	Ar-41 Concentration (Radiography Bay Exhaust System On)	Ar-41 Concentration (Radiography Bay Exhaust System Off)
Bay 1	$5.0 \times 10^{-9} \mu\text{Ci/ml}$	$2.2 \times 10^{-8} \mu\text{Ci/ml}$
Bay 2	$7.0 \times 10^{-9} \mu\text{Ci/ml}$	$3.1 \times 10^{-8} \mu\text{Ci/ml}$
Bay 3	$1.2 \times 10^{-8} \mu\text{Ci/ml}$	$1.7 \times 10^{-7} \mu\text{Ci/ml}$
Bay 4	$1.1 \times 10^{-8} \mu\text{Ci/ml}$	$7.6 \times 10^{-8} \mu\text{Ci/ml}$

**TABLE 11- 2 ARGON-41 CONCENTRATIONS IN RADIOGRAPHY BAYS WITH ELECTRONIC IMAGING DEVICES IN BAYS 1, 2, AND 3 AND FILM RADIOGRAPHY IN BAY 4**

Location	Ar-41 Concentration (Radiography Bay Exhaust System On)	Ar-41 Concentration (Radiography Bay Exhaust System Off)
Bay 1	$9.0 \times 10^{-10} \mu\text{Ci/ml}$	$4.0 \times 10^{-9} \mu\text{Ci/ml}$
Bay 2	$1.0 \times 10^{-9} \mu\text{Ci/ml}$	$6.0 \times 10^{-9} \mu\text{Ci/ml}$
Bay 3	$2.0 \times 10^{-9} \mu\text{Ci/ml}$	$3.2 \times 10^{-8} \mu\text{Ci/ml}$
Bay 4	$1.1 \times 10^{-8} \mu\text{Ci/ml}$	$7.6 \times 10^{-8} \mu\text{Ci/ml}$

As shown in Table 11-1, if film radiography is used in all bays and the radiography bays exhaust system is operating, the highest Ar-41 concentration is in Bay 3 and is 250 times lower than the 10 CFR Part 20 occupational concentration limit (for a 2000 hour/year occupancy) of  $3 \times 10^{-6} \mu\text{Ci/ml}$ . Under the same conditions of ventilation, when electronic imaging devices are used in Bays 1, 2, and 3, Ar-41 concentrations are about three orders of magnitude below the 10 CFR Part 20 limit. When the radiography bays exhaust system is not operational, Ar-41 concentrations in the bays are obviously higher, but still easily below the applicable 10 CFR Part 20 limit. The assumption of even distribution throughout the enclosure volume is, of course, only an approximation. Some regions will have higher concentrations and some will have lower values. Occupancy factors will be combined with actual survey meter readings of radiation levels inside the radiography bays when establishing safe operating procedures.

The external dose equivalent rate from Ar-41 for an occupationally exposed individual in a radiography bay can be estimated by assuming that the room is a hemisphere with the equivalent volume of the room, and the individual is immersed in the Ar-41 cloud at the center of the hemisphere. Because none of the radiography bays have dimensions large enough to equal the volume of a semi-infinite cloud for Ar-41, immersion of an individual at the center of a hemispherical cloud based on the volume of the largest radiography bay will still give a total effective dose equivalent (TEDE) after 2000 hours of occupational exposure that is well below the NRC Part 20 limit of 5000 mrem.

The calculations supporting this conclusion are shown in Appendix A. Furthermore, these calculations indicate that the TEDE for a worker in the radiography bay with the highest Ar-41 concentration, assuming the radiography bay exhaust system is on, will be approximately 0.5 millirem following 2000 hours of annual exposure. However, if this individual worked the 2000 hours with the radiography bays exhaust system off, the annual TEDE would still be only about 7.0 millirem. While this latter situation would not be a “normal” operational mode, especially for a period of one year, it is included at this point to show the low exposure potential of Ar-41 in the radiography bays with or without the radiography bays exhaust system being operational.

#### 11.1.2.1.2 Production and Evolution of Ar-41 in the Reactor Room

Argon-41 in the reactor room occurs as the irradiated argon evolves from the primary coolant into the air of the room. This evolution results from the reduced solubility of argon in water as the water temperature increases. Considering the expected temperature rise of the water passing through the core, an immediate release of about 29% of the Ar-41 produced could be expected during passage. Some of this Ar-41 will be redissolved as it is transported into cooler water but, since the cooler water is in equilibrium with the air above, it is nearly saturated with argon and will not absorb all of the argon released by water passing through the core. However, it is expected that approximately 60% of the released Ar-41 will be reabsorbed. Detailed calculations addressing the production and evolution of Ar-41 from the primary coolant are contained in Appendix A.

Assuming complete mixing of the Ar-41 with reactor room air, the equilibrium Ar-41 concentration in the reactor room with the room exhaust system on will be approximately  $7.55 \times 10^{-6} \mu\text{Ci/ml}$ . Should the reactor be operated without the room's exhaust system in operation, the equilibrium concentration would increase to  $1.36 \times 10^{-4} \mu\text{Ci/ml}$ , but this will not be a permissible mode of normal operation and therefore will not occur for a sufficient period of time to allow this concentration to develop in the room.

The 10 CFR Part 20 Derived Air Concentration (DAC) for a semi-infinite cloud of Ar-41 is  $3.0 \times 10^{-6} \mu\text{Ci/ml}$ . Therefore, the  $7.55 \times 10^{-6} \mu\text{Ci/ml}$  calculated Ar-41 concentration for the reactor room under 2 MW steady state with the reactor room exhaust system operating, is about 2.52 times the NRC occupational concentration limit. However, even 2000 hours of annual occupancy at this concentration will still result in a TEDE which is well below NRC regulatory limits, as shown below. With the reactor room exhaust system off, the  $1.36 \times 10^{-4} \mu\text{Ci/ml}$  calculated Ar-41 concentration for the room is about 45 times the DAC in Part 20, but this is not a normal mode of operation for the reactor since license requirements will mandate that the reactor room exhaust system be fully operational when the reactor is operating.

Actual measurements of Ar-41 in the reactor room after the reactor had operated for about 9.0 hours at 1 MW (reactor room exhaust system on) showed Ar-41 concentrations averaging about  $1.5 \times 10^{-6} \mu\text{Ci/ml}$  for areas which are occupied during normal work in the room. This would then correlate to about  $3.0 \times 10^{-6} \mu\text{Ci/ml}$  at 2 MW.

Using the same calculational method employed for estimating the Ar-41 dose to personnel in the radiography bays, and recognizing that the dimensions of the reactor room do not provide a cloud volume large enough to create a semi-infinite cloud for Ar-41, the total effective dose equivalent (TEDE) after 2000 hours of immersion in an Ar-41 concentration of  $7.55 \times 10^{-6} \mu\text{Ci/ml}$  is about 318 millirem, and for 2000 hours in a concentration of  $3.0 \times 10^{-6} \mu\text{Ci/ml}$  the TEDE is about 126 millirem. Obviously, both of these doses are well within NRC occupational dose limits.

#### 11.1.2.1.3 Ar-41 from the Pneumatic Transfer System

Ar-41 will also be produced in the section of the pneumatic transfer system that is located in the reactor core. During operation of the transfer system, air containing very small amounts of Ar-41 is exhausted from the system through a HEPA filter to the facility stack. There has not been a significant increase in Ar-41 releases, as measured by the stack monitor, from numerous operations of this system. Therefore, the Ar-41 from the pneumatic transfer system is not considered to be a measurable contributor to the Ar-41 doses associated with MNRC operations.

#### 11.1.2.1.4 Ar-41 Release to the Unrestricted Area

The Ar-41 from the reactor room and the radiography bays will be discharged from the MNRC through the facility's exhaust stack, which is 60 feet above ground level. Dilution with other building ventilation air and atmospheric dilution will reduce the Ar-41 concentration considerably before the exhaust plume returns to ground level locations which could be occupied by personnel. Utilization of this dilution credit is allowed by the NRC. The detailed calculations relating to the dispersion of Ar-41 released from the stack are contained in Appendix A.

It is important to note that only a modest amount of dilution is required to reduce the Ar-41 concentration to a level that is well below the 10 CFR Part 20 limit of  $1 \times 10^{-8} \mu\text{Ci/ml}$  for unrestricted areas. This is due in part to the fact that the Ar-41 concentration leaving the stack is not expected to exceed about  $1.0 \times 10^{-6} \mu\text{Ci/ml}$  when the ventilation flow from the radiography bays air handling system is available (i.e., the system is on), and this flow is mixed with the other building ventilation flow. If the radiography bay air handling system is not operational, then the projected Ar-41 concentration leaving the stack will increase slightly to about  $3.0 \times 10^{-6} \mu\text{Ci/ml}$ , and this will occur only while the radiography bays ventilation is turned off. Since the normal mode of operation for the reactor will be with the radiography bays ventilation system turned on, it should also be noted that the concentration of Ar-41 leaving the stack may actually be closer to  $4.0 \times 10^{-7} \mu\text{Ci/ml}$  if one chooses the 1 MW measured concentration for Ar-41 in the reactor room and extrapolates that value to 2 MW ( $3.0 \times 10^{-6} \mu\text{Ci/ml}$ ).

Results of the plume dispersion calculations for the discharge of Ar-41 out of the facility stack are shown for various atmospheric conditions in Table 11-3. Additional information is provided in Appendix A.

**TABLE 11-3 CONCENTRATIONS OF AR-41 RELEASED FROM THE MNRC STACK UNDER DIFFERENT ATMOSPHERIC CONDITIONS**

Atmospheric Stability Classification	Ar-41 Concentration* ( $\mu\text{Ci}/\text{ml}$ )	Distance From Stack (meters)
Extremely Unstable (A)	$1.5 \times 10^{-10}$	92
Slightly Unstable (C)	$2.3 \times 10^{-10}$	240
Slightly Stable (E)	$9.4 \times 10^{-11}$	720
Extremely Stable (G)	$7.0 \times 10^{-11}$	4200

\*Concentrations are based on a maximum projected Ar-41 release concentration at the stack of  $1.0 \times 10^{-6} \mu\text{Ci}/\text{ml}$

Using Ar-41 concentrations from the preceding table and Ar-41 dose conversion factors for immersion in a semi-infinite cloud (Reference 11.2), calculations show that a person immersed for a full year in a semi-infinite cloud of Ar-41 at the maximum projected concentration in the unrestricted area ( $2.3 \times 10^{-10} \mu\text{Ci}/\text{ml}$ ) would receive a total effective dose equivalent of approximately 1.4 mrem. This dose is well within all applicable limits in 10 CFR Part 20.

Determination of radiation dose to the general public from airborne effluents may also be carried out using several other computer codes recognized by regulatory authorities. One such method involves use of the Clean Air Assessment Package - 1988 (CAP88-PC) (Reference 11.3). Application of this code (V1.0) to the projected Ar-41 releases from the MNRC predicts a dose to the general public of less than 0.1 mrem per year.

#### 11.1.2.1.5 Production and Evolution of N-16 in the Reactor Room

In addition to Ar-41, the other source of airborne radioactivity during normal operation of the MNRC reactor is Nitrogen-16 (N-16). N-16 is generated by the reaction of fast neutrons with Oxygen-16 (O-16) in water passing through the core. The amount of oxygen present in air, either in a beam path or entrained in the water near the reactor core, is insignificant compared to the amount of oxygen in the water molecule in the liquid state. Production of N-16 resulting from neutron interactions with the oxygen in air and air entrained in the cooling water can therefore be neglected.

The cross-section energy threshold for the O-16 (n,p) N-16 reaction is 9.4 MeV; however, the minimum energy of the incident neutrons must be about 10 MeV because of center of mass corrections. This high energy threshold limits the production of N-16, since only about 0.1% of all fission neutrons have an energy in excess of 10 MeV. Moreover, a single hydrogen scattering event will reduce the energy of these high-energy neutrons to below the necessary threshold.

After N-16 is produced in the core region, it rises to the tank surface and forms a disc source which creates a direct radiation field near the top of the tank. Some of the N-16 is subsequently released into the reactor room. Calculations for the production and mixing of N-16 in the primary coolant and for the evolution of N-16 from the reactor tank into the reactor room air are presented in Appendix A. Radiation levels associated with the N-16 in the tank and in the reactor room air are also addressed as part of Appendix A. Without exception, the calculated N-16 concentrations and dose rates are very conservative because they do not assume use of the conventional in-tank N-16 diffuser system, which is present in the MNRC primary water circulation system. Since this diffuser system is used during all normal operation of the reactor, and is designed to significantly delay the N-16 transit time to the upper regions of the tank, the 7.14 second N-16 half-life brings about considerable decay and a corresponding reduction in N-16 radiation levels at the tank surface and in the reactor room itself.

Recognizing the conservatisms involved in the N-16 calculations, and assuming the diffuser system is off, it is possible to predict the dose rate from N-16 at the tank water surface at a 2 MW power level. Using the technique shown in Appendix A, this value turns out to be approximately 1350 millirem per hour. This value agrees very well with the "diffuser off" N-16 dose rate measured at the surface of the tank water at the MNRC reactor and with N-16 dose rates measured at several other comparable 1 MW TRIGA<sup>®</sup> reactors, after the 1 MW values were extrapolated to 2 MW (Section 11.1.6.1, Table 11-7).

Since operation with the diffuser off is not a normal mode of operation, it is more realistic to estimate N-16 dose rates over the reactor tank with the diffuser on. Calculation of these dose rates would be difficult without knowing the actual effect of the diffuser in the presence of the new 2 MW coolant flow rates. Therefore, estimates of N-16 dose rates are based on extrapolations of actual dose rate measurements at about 1 foot and 3 feet over the UCD/MNRC reactor tank at 1 MW with the diffuser on.

Using this approach, the predicted 2 MW N-16 dose rate at 1 foot over the tank water surface will be about of 60 millirem per hour and at 3 feet about 10 millirem per hour. This predictive model corresponds well to actual radiation measurements taken above the reactor tank at 2 MW.

The escape of N-16 into the reactor room air will also deliver a radiation dose to workers in the room based on the N-16 concentration, which will be influenced by dilution in room air, by decay of this short-lived radionuclide and by room ventilation. Once again assuming the diffuser is off, by referring to the calculations in Appendix A and by using the volume of the reactor room with its current 800 cubic feet per minute ventilation rate, a conservative reactor room N-16 concentration of  $1.4 \times 10^{-4}$   $\mu\text{Ci/ml}$  is predicted. As with Ar-41, the reactor room volume is not large enough to create a semi-infinite cloud geometry for N-16, and therefore the calculated dose rate from the preceding N-16 concentration, when it is distributed uniformly throughout the room, is about 7.7 millirem per hour near the center of the room. Because of its short half-life and the reactor room ventilation pattern, even given the fact that the N-16 diffuser is assumed to be off, it is very unlikely that N-16 will ever reach a uniform concentration of  $1.4 \times 10^{-4}$   $\mu\text{Ci/ml}$  in the room. Therefore, the actual dose rate from N-16 in the reactor room is expected to be considerably lower than this worst case estimate. Although some N-16 may be removed from the reactor room by the ventilation system, the N-16 contribution to dose rates in the unrestricted area is negligible because of its rapid decay.

#### 11.1.2.1.6 Ar-41 from the Ar-41 Production Facility

Ar-41 will be produced by the Ar-41 Production Facility (see Chapter 10) as needed. The Ar-41 that is produced by the Ar-41 Production Facility will be contained in the system so there should be no increase in the Ar-41 levels in the reactor room or the Ar-41 that is released to the unrestricted area. Catastrophic failure of the system will not result in any 10 CFR 20 limit being exceeded and is further discussed in Chapter 13.

#### 11.1.2.2 Liquid Radioactive Sources

Liquid radioactive material routinely produced as part of the normal operation of the UCD/MNRC will be miscellaneous neutron activation product impurities in the primary coolant, most of which are deposited in the mechanical filter and the demineralizer resins. Therefore, these materials are dealt with as solid waste (Section 11.1.2.3, Table 11-5). Non-routine liquid radioactive waste could result from decontamination or maintenance activities (i.e., filter or resin changes). The amount of this type of liquid waste is expected to remain small, especially based on past experience. Because of this, the liquid will be processed to a solid waste form on site and will be disposed of with other solid wastes.

## 11.1.2.2.1 Radioactivity in the Primary Coolant

As mentioned above, the only significant liquid radioactive source at the MNRC is the reactor primary coolant. Radioactivity in this liquid source occurs due to neutron activation of Argon-40 in entrained air (creating Ar-41); neutron interactions with oxygen in the water molecule (creating N-16); and neutron interactions with tank and structural components with subsequent transfer of the radioactivity into the primary coolant. Radionuclides such as Manganese-56 and Sodium-24 are common examples of waterborne radioactivity created in this manner. Tritium is also present in the primary coolant due to activation of natural deuterium in water and from tritium migrating out of the fuel from the fission process.

As noted, other sources of liquid radioactivity are not currently projected for the MNRC reactor operations.

Radionuclides and their concentrations in the primary coolant vary depending on reactor power, reactor operating time and time since reactor shutdown, assuming that other variables (e.g., the effectiveness of the water purification system) remain constant. The typical primary coolant radionuclide concentrations are given below (~25-30 MW hours per week of operation) along with the projected equilibrium concentrations at 2 MW. Due to the fact the MNRC has not conducted 2.0 MW 24/7 operations, projected values of the equilibrium concentration of primary coolant radionuclides are given below instead of measured readings at 2MW operations.

**TABLE 11-4 Predominant Radionuclides and Their Projected Equilibrium Concentrations in the MNRC Reactor Primary Coolant at 2 MW**

Radionuclide	Half Life	Projected Equilibrium Concentration at 2 MW ( $\mu\text{Ci/ml}$ )	Typical Concentration at 1MW ( $\mu\text{Ci/mL}$ )
Aluminum-28	2.3 min	$6.0 \times 10^{-3}$	$3.0 \times 10^{-3}$
Argon-41	1.8 hr	$3.0 \times 10^{-3}$	$1.0 \times 10^{-3}$
Hydrogen-3	12 yr	$6.5 \times 10^{-3*}$	$2.0 \times 10^{-2}$
Magnesium-27	9.46 min	$4.0 \times 10^{-4}$	$2.0 \times 10^{-4}$
Manganese-56	2.58 hr	$4.7 \times 10^{-4}$	$1.0 \times 10^{-4}$
Nitrogen-16	7.14 sec	131**	65**
Sodium-24	14.96 hr	$2.6 \times 10^{-3}$	$2.0 \times 10^{-4}$

\*maximum buildup in 20 years without any water addition;

\*\*calculated approximation based on water leaving the core - not a uniform concentration)

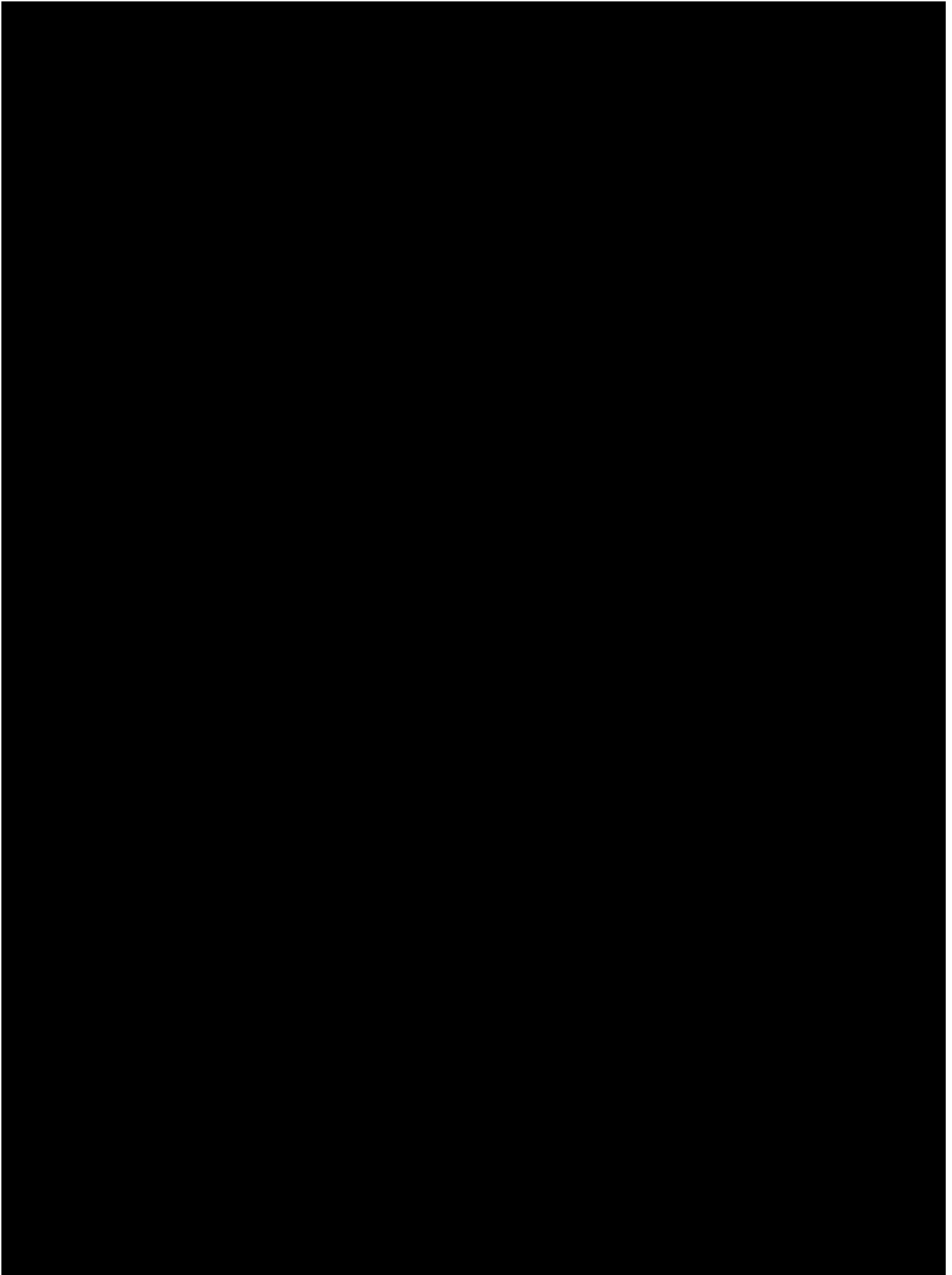
As mentioned, it is MNRC policy not to release liquid radioactivity as an effluent or as liquid waste. Therefore, the primary coolant does not represent a source of exposure to the general public during normal operations. Furthermore, occupational exposure from liquid sources is also limited because there are few operations which require contact with the primary coolant. In cases where contact is a potential, such as in certain maintenance operations, the primary coolant could be allowed to decay for several days or more to significantly reduce radioactivity concentrations. Because of the short half-lives of most of the predominant radionuclides in the primary coolant, five radionuclides would be essentially gone after 48 hours, sodium-24 would be reduced by about a factor of 10, and experience at other TRIGA<sup>®</sup> reactors indicates that Hydrogen-3 would not be a source of significant occupational dose.

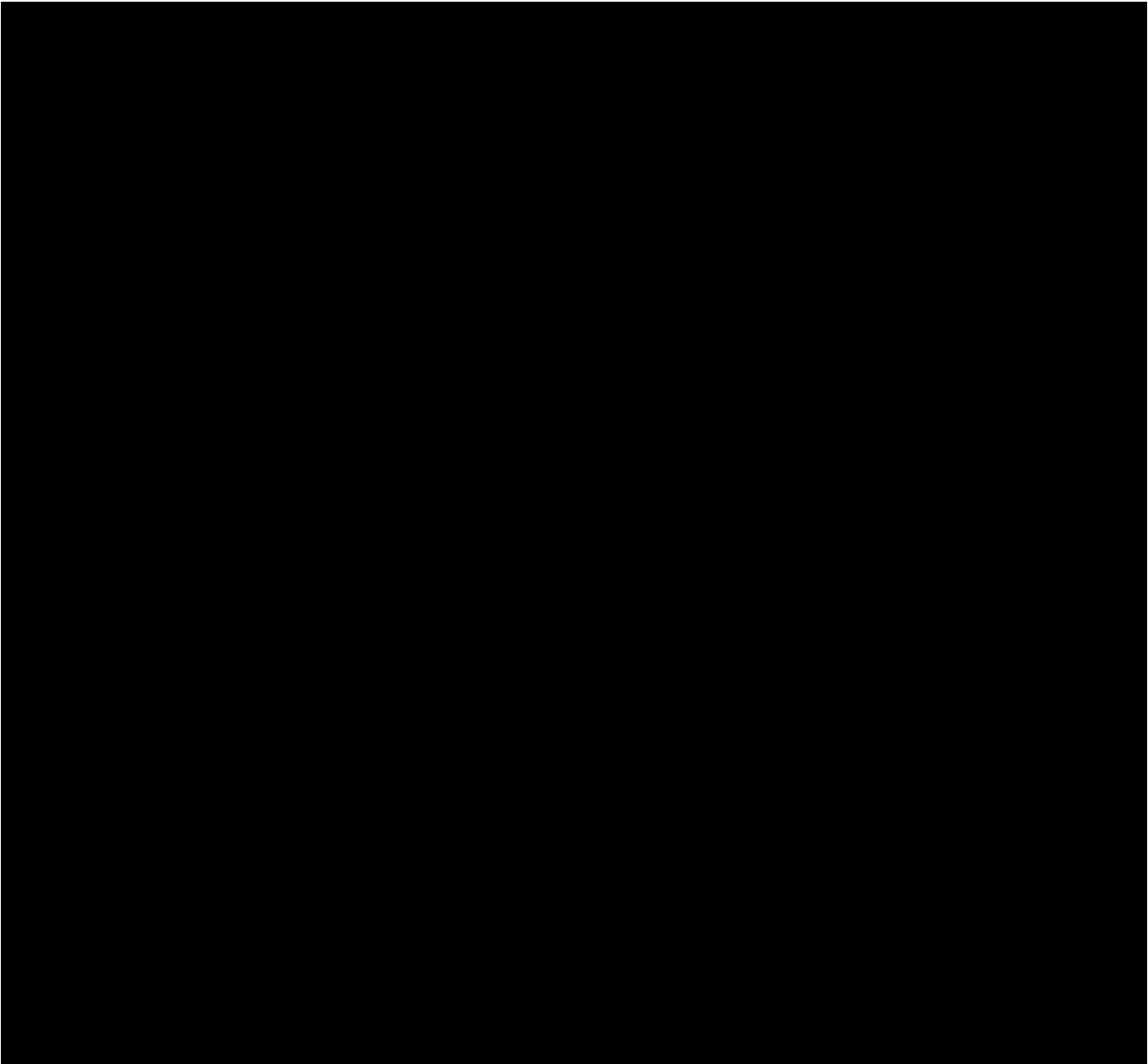
#### 11.1.2.2.2 N-16 Radiation Dose Rates from Primary Cooling System Components

N-16 has been addressed previously in Section 11.1.2.1, however, the potential for N-16 radiation dose rates from primary coolant piping and from the heat exchanger were not included in that discussion. Measurements of gamma dose rates at contact with these cooling system components after extended operation at 1 MW is 1 to 2 millirem per hour. Dose rates for from these sources during 2 MW operation is 2 to 6 millirem per hour. These radiation levels are not considered abnormal and do not represent a radiation protection problem since they were expected and they occur inside the posted radiation area on the second floor of the reactor building.

#### 11.1.2.3 Solid Radioactive Sources

The solid radioactive sources associated with the MNRC program are summarized in Table 11-5. Because the actual inventory of reactor fuel and other radioactive sources continuously changes as part of the normal operation, the information in Table 11-5 is to be considered representative rather than an exact inventory.





Although solid waste is included in the preceding table, more information on waste classification, storage, packaging and shipment is included in Section 11.2. In an effort to elaborate somewhat on the waste entry in Table 11-5, it can be stated that routinely produced solid waste includes water purification system demineralizer resin bottles, mechanical filters, rags, paper towels, plastic bags, rubber gloves, and other materials used for contamination control or decontamination. The radioactivity level of this material is normally in the microcurie range, and it is anticipated that approximately one (or two) regular 55 gallon drums of this type of material and 2 resin bottles will be generated each year. Typically only one "B-25" box of radioactive waste is shipped from the facility every 5 years.

#### 11.1.2.3.1 Shielding Logic

Although not a solid source of radioactivity itself, shielding is involved in reducing radiation levels from many solid sources and therefore the basic logic used for the 2 MW shielding is included here. The logic and bases used for the MNRC 2 MW shielding design is directly related to that employed for the original 1 MW design and includes the following: (NOTE: There is a much more detailed discussion of shielding in Section 11.1.6.1)

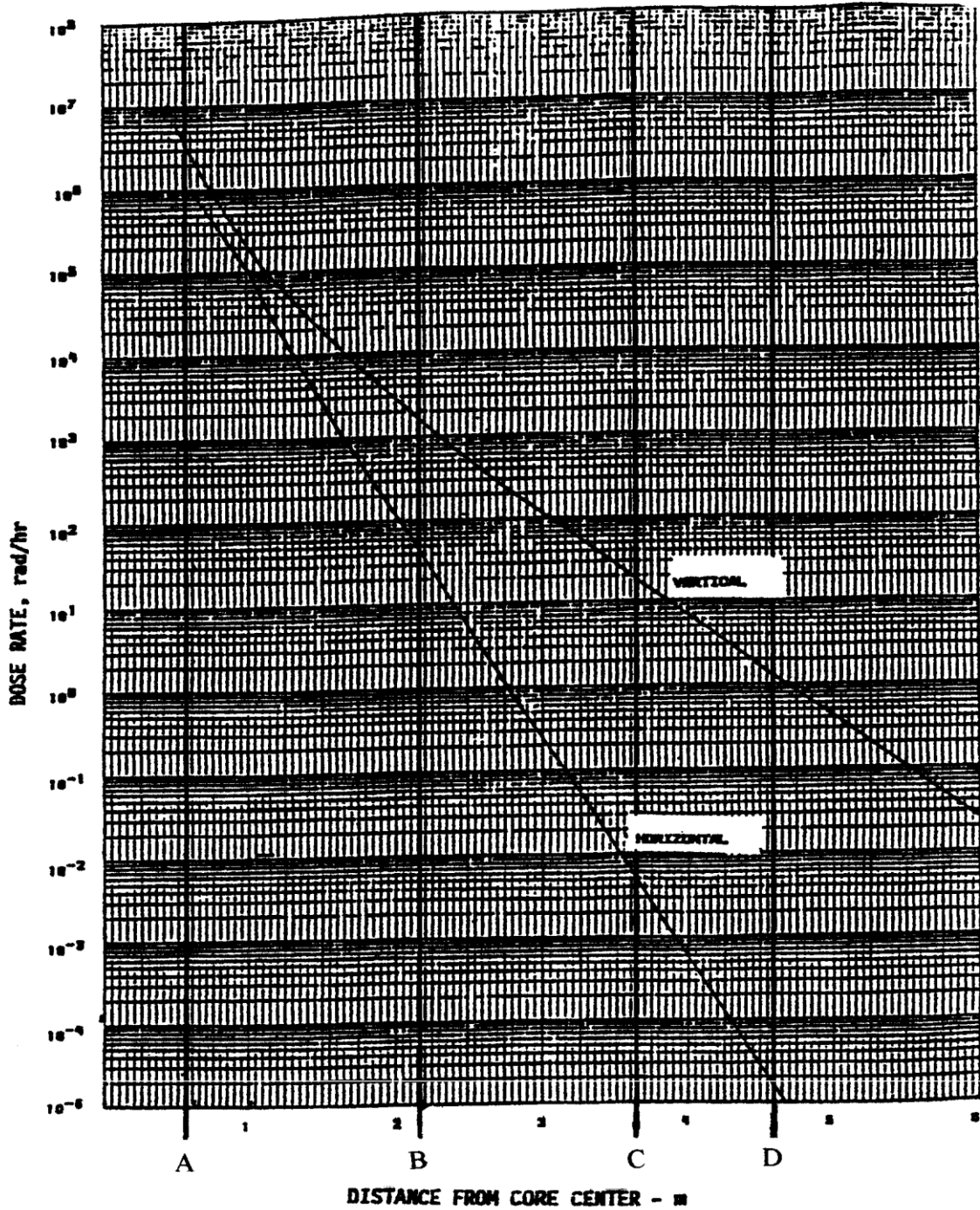
- General Atomic has developed source terms to serve as a basis for reactor shielding design analysis. Radiation levels for a 1 MW TRIGA<sup>®</sup> shield based on these analyses are shown in Figure 11.4. For 2 MW operations, dose rates approximately twice the values in Figure 11.4 can be expected and have been observed;
- Reactor shields for 1 MW TRIGA<sup>®</sup> reactors have been built and proven based on the preceding design analysis. Actual radiation measurements at the surface of this type of shielding at 1 MW have shown radiation levels to about one millirem/hr or less. For 2 MW operation, most radiation levels are in the one to two millirem/hr range, which is still quite low;
- The MNRC reactor bulk shield is very similar, in material type and thickness, to other proven TRIGA<sup>®</sup> shields. Two significant differences are the beam tube penetrations. Where the basic shielding configuration has been penetrated by beam tubes, supplemental shielding was added. This supplemental shielding has been designed to provide the same attenuation to both neutrons and gammas as the basic unpenetrated shield. The second is the Bay 5 cavity described in Section 1.2.1. The radiation levels at the surface of the biological shield as a result of the cavity cut are 0.35 mR/hr  $\gamma$  and < 1 mrem/hr neutron on contact.

#### 11.1.3 Radiation Protection Program

The health physics program for the UCD/MNRC reactor is located organizationally within the UCD/MNRC. The organizational structure and reporting pathways relating to the UCD/MNRC radiation protection program are shown in Figures 11.5 and 11.6.

##### 11.1.3.1 Organization of the Health Physics Branch

The Health Physics Branch within UCD/MNRC is the organization that administers the radiation protection program for the reactor.



A: Core Boundary

B: Tank Boundary

C&D: Biological Shield

FIGURE 11.4 REACTOR BULK SHIELD DIRECT DOSE RATE - 1 MW OPERATION

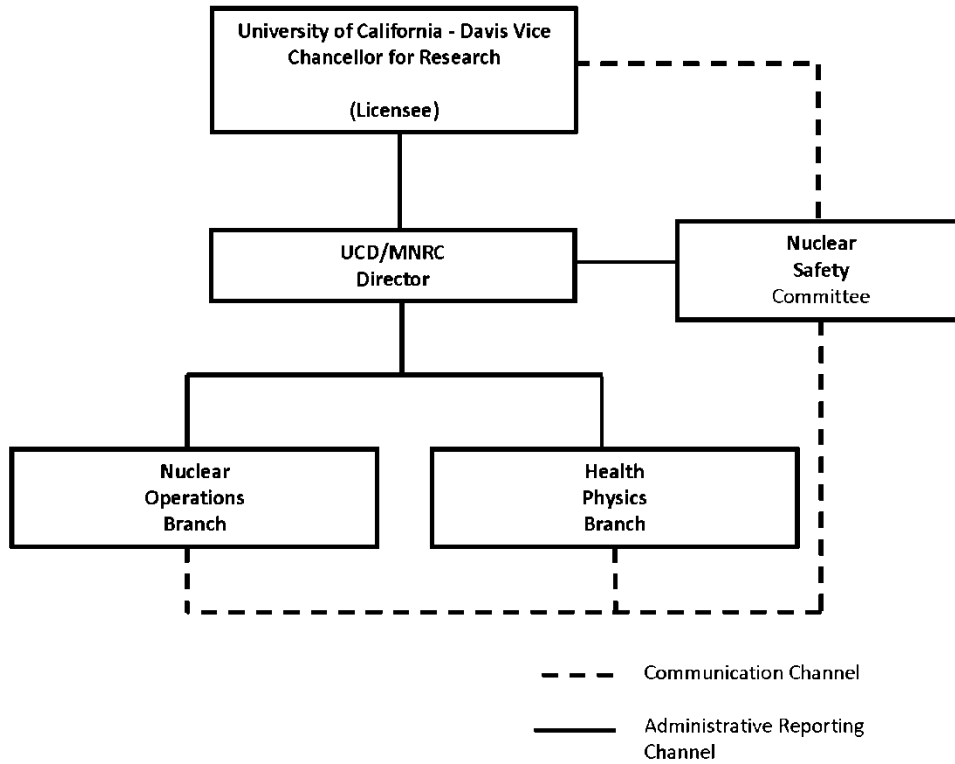


FIGURE 11.5 ORGANIZATIONAL STRUCTURE OF THE MNRC RADIATION PROTECTION PROGRAM

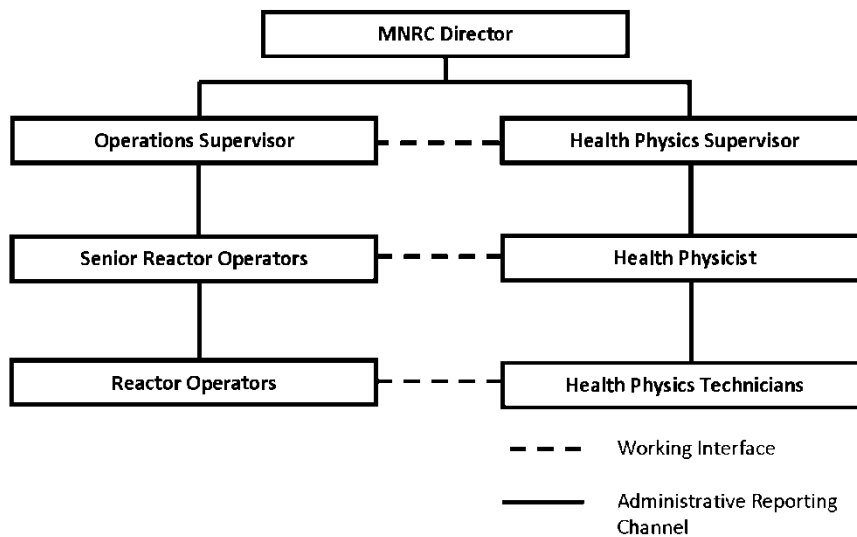


FIGURE 11.6 ORGANIZATIONAL STRUCTURE SHOWING THE RADIATION PROTECTION PROGRAM WITHIN THE UCD/MNRC

The positions of authority and responsibility within the Health Physics Branch are as follows:

- Health Physics Supervisor (Radiation Safety Officer) - The Health Physics Supervisor reports directly to the MNRC Facility Director. The Health Physics Supervisor is responsible for directing the activities of the Health Physics Branch including the development and implementation of the MNRC Radiation Protection Program;
- Health Physicist - Health Physicists report to the Health Physics Supervisor. Health Physicists are responsible for implementing the MNRC Radiation Protection Program policies and procedures, and directing the activities of the Health Physics Technicians.
- Health Physics Technicians - Health Physics Technicians report directly to the Health Physicist on-duty. Health Physics Technicians are responsible for providing radiological control during reactor operations and maintenance. This includes radiological monitoring, surveillance checks on radiological monitoring equipment and radiological control oversight of operations involving radiation and/or contamination. The position description for the health physics technician specifies the authority to interdict perceived unsafe practices. Typically ROs and SROs are trained to perform some of the tasks described here. ROs and SROs trained in this manner are to report health physics issue to the RSO and other operational issue to the reactor supervisor.

The qualifications for the preceding positions are as follows:

- Health Physics Supervisor (Radiation Safety Officer)- The Health Physics Supervisor shall have a minimum of six years of health physics experience. The individual shall have a recognized baccalaureate or higher degree in health physics or related scientific field. The degree may fulfill four of the six years of the health physics experience requirement on a one-for-one basis;
- Health Physicist – The Health Physicist shall have a recognized baccalaureate or higher degree in health physics or related scientific field (work experience may be substituted for a degree on a case by case basis). At least two years of health physics experience is desired;
- Health Physics Technician - The Health Physics Technician shall have received sufficient training at the facility or elsewhere to satisfy the job requirements. Individuals shall have a high school diploma or have successfully completed the General Education Development (GED) test. Previous job-related experience or education shall be considered highly desirable.

#### 11.1.3.2 Working Interface Between Health Physics and Reactor Operations

The working relationship of the health physics program relative to reactor operations is shown in Figure 11.6. As shown in this figure, there is a clear separation of responsibilities for the two groups, each with a clear reporting line to the Facility Director.

#### 11.1.3.3 Health Physics Procedures

Operation of the health physics program is carried out under the direction of the Health Physics Supervisor using written health physics procedures. These procedures are reviewed for adequacy by

the Health Physics Supervisor and the operations supervisor (reactor manager), and are approved by the UCD/MNRC Director. They are also audited, normally on an annual basis, by the Nuclear Safety Committee. The health physics procedures are reviewed annually by the MNRC staff and changes are made as necessary.

While not intended to be all inclusive, the following list provides an indication of typical radiation protection procedures used in the MNRC program:

- a) Testing and calibration of area radiation monitors, facility air monitors, laboratory radiation detection systems, and portable radiation monitoring instrumentation;
- b) Working in laboratories and other areas where radioactive materials are used;
- c) Facility radiation monitoring program including routine and special surveys, personnel monitoring, monitoring and handling of radioactive waste, and sampling and analysis of solid and liquid waste and gaseous effluents released from the facility;
- d) Monitoring radioactivity in the environment surrounding the facility;
- e) Administrative guidelines for the facility radiation protection program to include personnel orientation and training;
- f) Receipt of radioactive materials at the facility, and unrestricted release of materials and items from the facility;
- g) Leak testing of sealed sources containing radioactive materials;
- h) Special nuclear material accountability;
- i) Transportation of radioactive materials;
- j) General decontamination procedures;
- k) Personnel decontamination procedures;
- l) Personnel exposure investigation procedures;
- m) Personnel access procedures for radiography bays and the reactor room;
- n) Spill procedures;
- o) Radiation work permit procedures;
- p) Pneumatic transfer system procedures;
- q) In-core and in-tank irradiation facility procedures;
- r) ALARA procedures.

#### 11.1.3.4 Radiation Protection Training

The radiation protection training is conducted by the Health Physics Branch. It is structured at different levels in order to meet the needs of different categories of facility staff and researchers using the reactor. All personnel and visitors entering the MNRC facility shall receive training in radiation protection sufficient for the work/visit, or shall be escorted by an individual who has received such training. The general levels of training are as follows:

- Initial Training - All personnel permitted unescorted access in the MNRC facility shall receive training in radiation protection as required by 10 CFR19.12. Initial training shall cover the following areas in sufficient depth for the work being done:
  - a) Storage, transfer, and use of radiation and/or radioactive material in portions of the restricted area, including radioactive waste management and disposal;
  - b) Health protection problems and health risks (including prenatal risks) associated with exposure to radiation and/or radioactive materials
  - c) Precautions and procedures to minimize radiation exposure (ALARA);
  - d) Purposes and functions of protective devices;
  - e) Applicable regulations and license requirements for the protection of personnel from exposure to radiation and/or radioactive materials;
  - f) Responsibility to report potential regulatory and license violations or unnecessary exposure to radiation or radioactive materials;
  - g) Appropriate response to warnings in the event of an unusual occurrence or malfunction that involves radiation or radioactive materials;
  - h) Radiation exposure reports which workers will receive or may request.

- Specialized Training - Certain personnel (e.g., reactor operators) require more in-depth training than that described above. Such individuals shall successfully complete training over the following outlined topics in sufficient depth for the work being done and pass a written examination with a minimum grade of 70%:
  - a) Principles of Atomic Structure;
  - b) Radiation Characteristics;
  - c) Sources of Radiation;
  - d) Interaction of Radiation with Matter;
  - e) Radiation Measurements;
  - f) Biological Effects of Radiation;
  - g) Radiation Detection;
  - h) Radiation Protection Practices;
  - i) ALARA;
  - j) Radioactive Waste Management and Disposal.
  
- Annual Refresher Training - All personnel permitted unescorted access in the MNRC facility shall receive annual radiation safety refresher training. The annual training shall cover the following areas in sufficient depth for the work being done:
  - a) Review of proper radiation safety practices, including radioactive waste management and disposal;
  - b) Occurrences at the MNRC facility over the past year;
  - c) ALARA summary;
  - d) Notable changes in procedures, equipment, facility, etc.

#### 11.1.3.5 Audits of the Health Physics Program

The Nuclear Safety Committee (NSC) provides timely, objective, and independent reviews, audits, recommendations and approvals on matters affecting nuclear safety at the UCD/MNRC. The NSC charter requires that membership shall consist of individuals who have the extensive experience necessary to evaluate the safety of the UCD/MNRC.

The chairman of the NSC is appointed by the UCD/MNRC license holder. Voting membership on the NSC is specified in the NSC Charter. The independent members are voting members and are selected based on their technical qualifications.

NSC meetings are held at least semi-annually (the period between meetings cannot exceed 7.5 months).

The NSC is chartered to conduct an annual on-site audit/inspection of the UCD/MNRC health physics and reactor operations programs and associated records. The annual health physics inspection is performed by an independent member of the NSC and normally covers all aspects of the radiation protection program.

The audit typically covers areas such as actions on NSC recommendations from previous audits, health physics staffing, the interface between health physics and reactor operations, health physics training for MNRC staff and MNRC users, health physics procedures, personnel monitoring, environmental monitoring, effluent monitoring, operational radiological surveys, instrument calibration, radioactive waste management and disposal, radioactive material transportation, SNM accountability, and a review of unusual occurrences.

The audit reports are sent to the chairman of the NSC, who in turn presents a report of the audit findings to the full NSC at the next NSC meeting. Copies of the audit findings are provided to the MNRC Facility Director who is responsible for ensuring that corrective actions are taken.

#### 11.1.3.6 Health Physics Records and Record Keeping

Radiation protection program records such as radiological survey data sheets, personnel exposure reports, training records, inventories of radioactive materials, environmental monitoring results, waste disposal records, instrument calibration records and many more, are maintained by the Health Physics Branch. The records will be retained for the life of the facility either in hard copy, or on photographic or electronic storage media. Records for the current and previous year are retained in the health physicist's office in binders or file cabinets. Other records are retained in long-term storage. Radiation protection records are required to be reviewed and signed by a health physicist prior to filing.

Radiation protection records are used for developing trend analysis, particularly in the personnel dosimetry area, for keeping management informed regarding radiation protection matters, and for reporting to regulatory agencies, e.g., the ALARA dose trend analysis charts. In addition, they are also used for planning radiation-protection-related actions, e.g., radiological surveys to preplan work or to evaluate the effectiveness of decontamination or temporary shielding efforts.

#### 11.1.4 ALARA Program

An ALARA program for the MNRC has been established in accordance with 10 CFR 20.1101. The bases for this program are the guidelines found in ANSI/ANS 15.11 (Reference 11.4). The licensee (UCD) has the ultimate responsibility for the ALARA program, but has delegated this responsibility to the Health Physics Supervisor. The ALARA program incorporates a review of all MNRC operations with emphasis on operational procedures and practices that might reduce MNRC staff exposures to radiation and lower potential radioactive effluent releases to unrestricted areas.

Personnel radiation doses at the MNRC are minimized by considering use of the following ALARA actions when performing work with radiation or radioactive materials:

- Reviewing records of similar work previously performed;
- Eliminating unnecessary work;
- Preparing written procedures;
- Using special tools;
- Installing temporary shielding;
- Performing as much work as possible outside of radiation areas;
- Performing mockup training;
- Conducting prework briefings and postwork critiques;
- Keeping unnecessary personnel out of areas where radiation exposure may occur.

In addition to the above actions, the MNRC ALARA program also contains the following elements which are designed to enhance the effectiveness of the overall program:

- Exposure investigations are conducted when an individual receives greater than 100 millirem in one month or 300 millirem in one quarter. The investigation is focused on determining the cause of the exposure so that appropriate ALARA actions, if any, can be applied;
- ALARA dose trend analysis charts are prepared quarterly and posted for review by all MNRC personnel;
- An annual inspection of the UCD/MNRC ALARA program; and
- A health physicist is required to be involved during planning, design approval, and construction of new MNRC facilities; during planning and implementation of new MNRC reactor use; during maintenance activities; and during the management and disposal of radioactive waste. In addition, written procedures pertaining to the preceding operational facilities are required to be reviewed by the Health Physics Supervisor for ALARA considerations prior to implementation.

### 11.1.5 Radiation Monitoring and Surveying

The radiation monitoring program for the MNRC reactor is structured to ensure that all three categories of radiation sources (air, liquid and solid) are detected and assessed in a timely manner. To achieve this, the monitoring program is organized such that two major types of radiation surveys are carried out: namely, routine radiation level and contamination level surveys of specific areas and activities within the facility, and special radiation surveys necessary to support non-routine facility operations.

#### 11.1.5.1 Monitoring for Radiation Levels and Contamination

The routine monitoring program is structured to make sure that adequate radiation measurements of both radiation fields and contamination are made on a regular basis. This program includes but is not limited to the following:

Typical surveys for radiation fields as follows:

1. Surveys whenever operations are performed that might significantly change radiation levels in occupied areas;
2. Daily surveys at temporary boundaries (e.g., rope barriers);
3. Weekly surveys in accessible radiation areas and high radiation areas, and in all other occupied areas of the MNRC facility;
4. Quarterly surveys outside of the MNRC facility, but within the facility fence;
5. Quarterly surveys in radioactive material storage areas;
6. Quarterly surveys of potentially contaminated ventilation ducting outside of the MNRC facility;
7. Surveys upon initial entry into a radiography bay after the shutter is closed or upon entry into the demineralizer cubicle;
8. Surveys in surrounding areas where personnel could potentially be exposed when radioactive material is moved;
9. Surveys when performing operations that could result in personnel being exposed to small intense beams of radiation (e.g., when transferring irradiated fuel, when removing shielding, or when opening shipping/storage containers);

10. Surveys of packages received from another organization;
11. Surveys when irradiated parts or equipment are removed from a radiography bay, or from the reactor core, from a fuel storage pit, from the pneumatic transfer system terminal, or from the reactor room;
12. Surveys as necessary to control personnel exposure. Such surveys may include the following:
  - a) Gamma surveys of potentially contaminated exhaust ventilation filters when work is performed on these filters;
  - b) Gamma and neutron surveys on loaded irradiated fuel containers;
  - c) Gamma and neutron surveys when handling an unshielded neutron source.

Typical surveys for contamination as follows:

1. Surveys at the exits to the MNRC facility once per shift;
2. Daily surveys in accessible contaminated areas and occupied areas surrounding contaminated areas;
3. Weekly surveys in occupied non-contaminated areas of the MNRC;
4. Quarterly surveys in areas outside of the MNRC facility, but within the facility fence;
5. Quarterly surveys in radioactive material storage areas;
6. Surveys as necessary to control the spread of contamination whenever operations are performed that are known to result in, or expected to result in, the spread of contamination;
7. Surveys prior to removal of paint from areas where contaminated paint is possible;

8. Surveys as part of the following operations:
  - a) Decontamination of equipment;
  - b) Removal of irradiated parts or equipment from a radiography bay, from the reactor core, from a fuel storage pit, from the pneumatic transfer system terminal, from the reactor room, or from the MNRC facility;
  - c) Inspection, maintenance, or repair of the primary cooling system;
  - d) Initial opening of the secondary cooling system (heat exchanger) for inspection, maintenance, or repair;
  - e) When working in or entering areas where radioactive leaks or airborne radioactivity has occurred previously;
  - f) Upon initial entry into potentially contaminated exhaust ventilation ducting;
  - g) Prior to replacing filters or ducting in potentially contaminated exhaust ventilation systems.

#### 11.1.5.2 Radiation Monitoring Equipment

Radiation monitoring equipment used in the MNRC reactor program is summarized in Table 11-6. The locations of many of the pieces of equipment are shown in Figures 11.7 and 11.8. Because equipment is updated and replaced as technology and performance requires, the equipment in Table 11-6 should be considered representative rather than an exact listing. The function this equipment performs will remain the same.

**TABLE 11-6 RADIATION MONITORING AND RELATED EQUIPMENT USED IN THE MNRC RADIATION PROTECTION PROGRAM**

<u>ITEM</u>	<u>LOCATION</u>	<u>FUNCTION</u>
Continuous Air Monitors (3) <ul style="list-style-type: none"> <li>• Stack Effluent Monitor</li> <li>• Reactor Room Air</li> <li>• Radiography Bays Air</li> </ul>	CAM Room CAM Room Sample Preparation Area	Measure radioactivity in stack effluent Measure reactor room airborne radioactivity Measure radiography bay airborne radioactivity (All monitors measure particulate)
Radiation Area Monitors (6)	Staging Area No. 1 Staging Area No. 2 Staging Area No. 4 Equipment Room Demineralizer Area Reactor Room	Measure gamma radiation fields in occupied or accessible areas of the MNRC facility
Portable Ionization Chamber Survey Meters (3)	Staging Area No. 1 Staging Area No. 4 Sample Preparation Area	Measure beta-gamma radiation dose rates
Portable Neutron Survey Meters (2)	Staging Area No. 1 Sample Preparation Area	Measure neutron radiation dose rates
Portable MicroR Survey Meters (2)	Staging Area No. 1	Measure low level and environmental gamma radiation dose rates
Portable G-M Survey Meters (4)	Staging Area No. 1 Staging Area No. 4 Sample Preparation Area Health Physics Lab	Measure beta/gamma contamination levels
Portable Alpha Survey Meters (2)	Staging Area No. 1	Measure alpha contamination levels
Lab Swipe Counter (1)	Health Physics Lab	Measure alpha/beta contamination on swipes
Gamma Spectroscopy Systems (HPGe) (4)	Health Physics Lab	Gamma Spectroscopy
Hand and Foot Monitor (1)	Equipment Room Exit	Measure potential contamination on hands and feet prior to leaving radiation restricted areas
Direct Reading Pocket Dosimeters (20)	Staging Area No. 1	Measure personnel gamma dose
Environmental TLDs	Various on-site, on-base, and off-base locations	Measure environmental gamma radiation doses
Portable Air Sampler (1)	Staging Area No. 1	Collect grab air samples
Air Flow Velometer (1)	Sample Preparation Area	Measure ventilation flow rates
Air Flow Calibrator (1)	Health Physics Lab	Calibrate CAM air flows

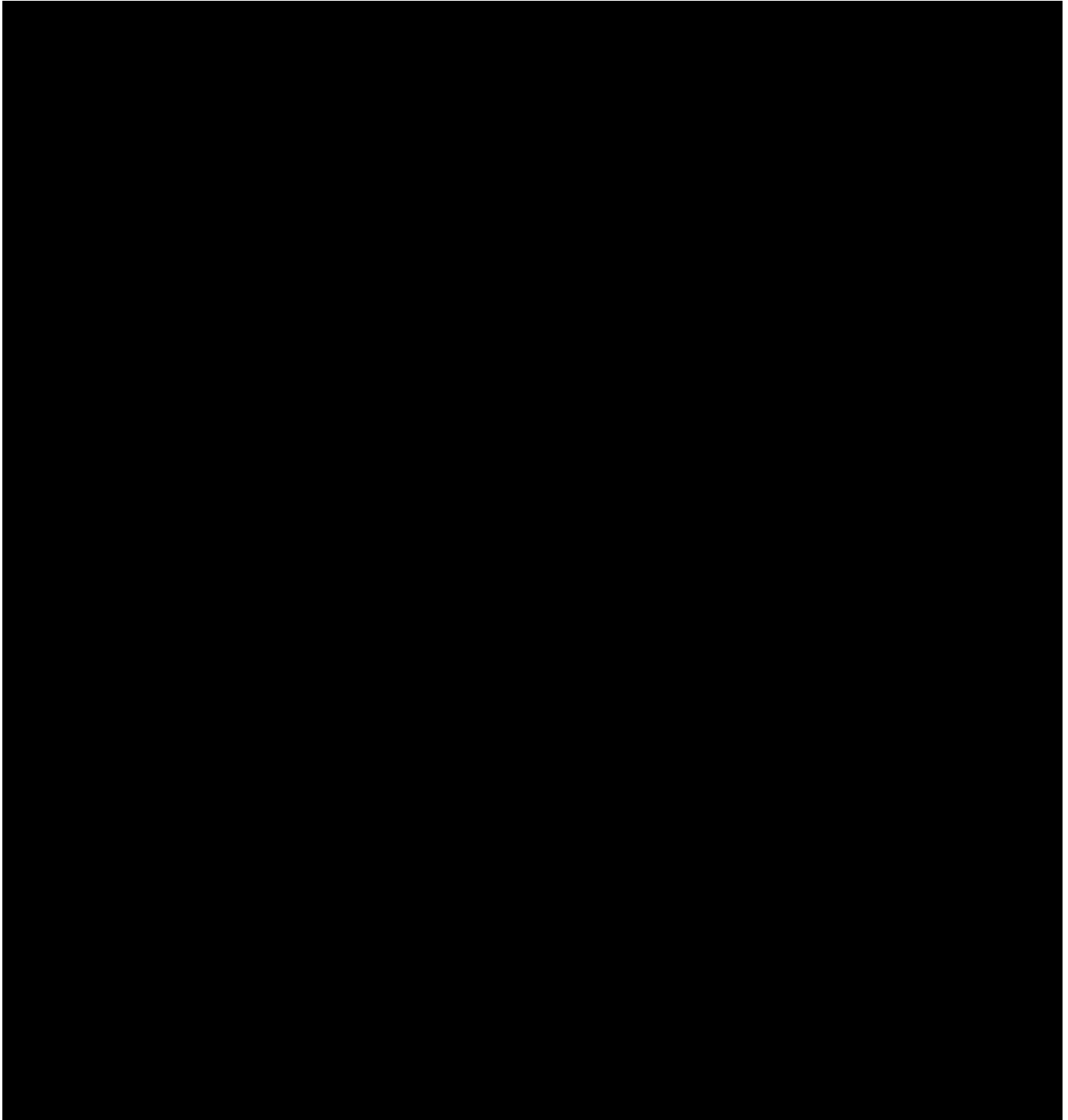


**FIGURE 11.7 RADIATION MONITORING EQUIPMENT - MAIN FLOOR FIGURE**

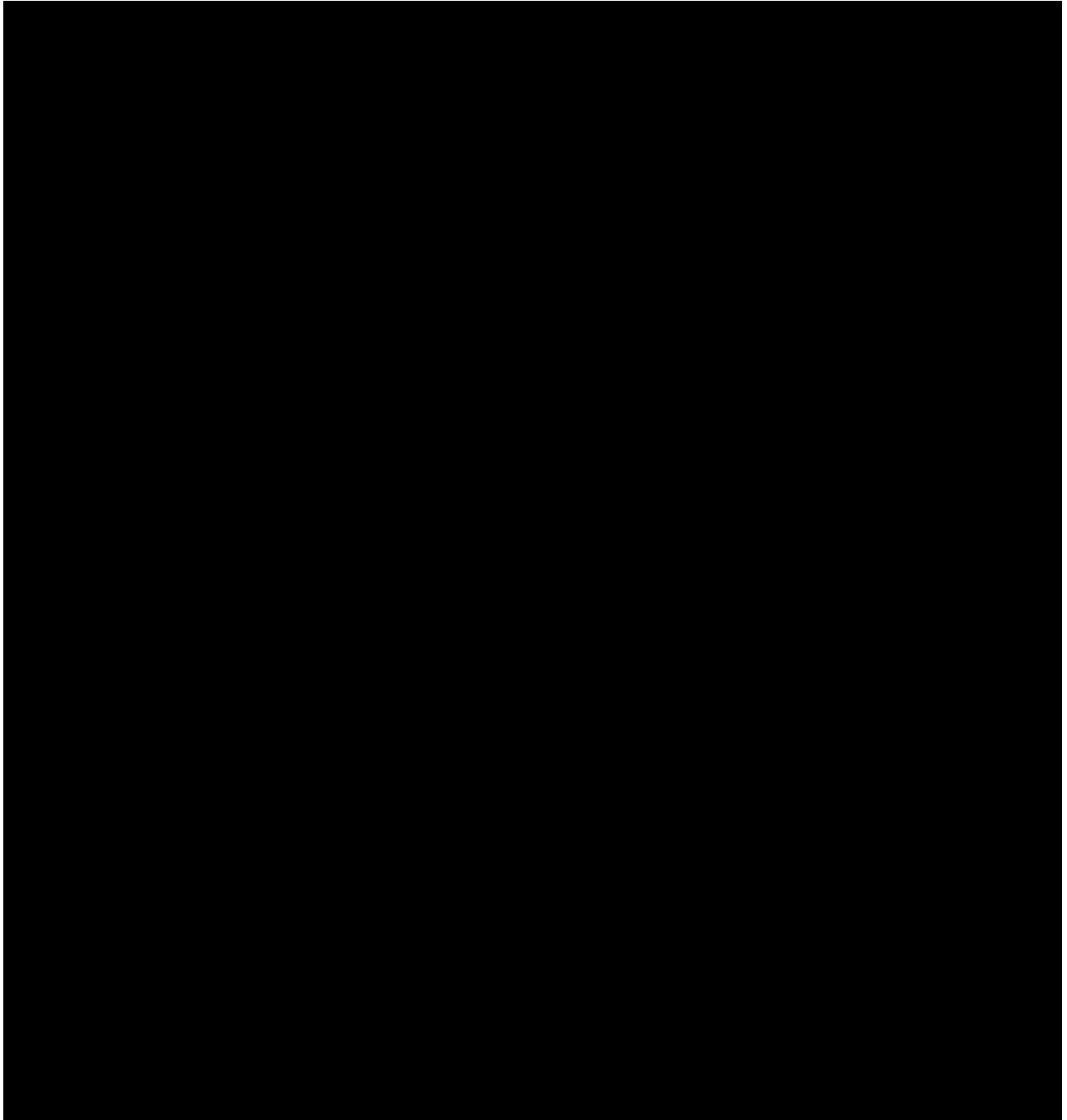


**FIGURE 11.8 RADIATION MONITORING EQUIPMENT - SECOND FLOOR**

### 11.1.5.3 Instrument Calibration

Radiation monitoring instrumentation is calibrated according to written procedures. It is the policy of the MNRC to use NIST traceable sources for instrument calibrations whenever possible. The following instrumentation is normally calibrated at the MNRC by health physics personnel:

- Continuous Air Monitors;
- Radiation Area Monitors;
- Swipe Counter;
- Gamma Spectroscopy Systems;
- Portable G-M Survey Meters;
- Hand and Foot Monitor;
- Portable Air Sampler.

The following instrumentation is normally calibrated at a contractor calibration facility:

- Portable Ionization Chamber Survey Meters;
- Alpha Survey Meters;
- Direct Reading Dosimeters;
- Air Flow Velometer;
- MicroR Survey Meters;
- Portable Neutron Survey Meters;
- Air Flow Calibrator.

Instrument calibrations are tracked by a computer-based tracking system. Instrument calibration records are maintained by the Health Physics Branch and calibration stickers showing pertinent calibration information (e.g., counting efficiency, the most recent calibration date, and the date the next calibration is due) is attached to all instruments.

### 11.1.6 Radiation Exposure Control and Dosimetry

Radiation exposure control depends on many different factors including facility design features, operating procedures, training, proper equipment, etc. Training and procedures have been discussed previously under the section dealing with the MNRC's radiation protection program (Section 11.1.3). Therefore, this section will focus on design features such as shielding, ventilation, containment and entry control devices for high radiation areas, and will also include protective equipment, personnel dosimetry, and estimates of annual radiation exposure for specific locations within the facility. A description of the dosimetry records used to document facility exposures and a summary of exposure trends at the MNRC will also be presented.

### 11.1.6.1 Shielding

The biological shielding around the MNRC reactor is the single biggest design feature in controlling radiation exposure during operation of the facility. The shielding is based on TRIGA® shield designs used successfully at many other similar reactors, but has been modified to accommodate the beam tubes and radiography bays unique to this reactor.

The logic and bases used for the MNRC's 2 MW shielding design is directly related to that employed for the original 1 MW design and includes the following:

- General Atomic (GA) has developed source terms to serve as a basis for reactor shielding design analysis. Radiation levels for designing a 1 MW TRIGA® shield based on GA analyses are shown in Figure 11.4. For 2 MW operation, the values in Figure 11.4 can be doubled;
- Reactor shields for 1 MW TRIGA® reactors have been built and proven based on the preceding design analyses. Actual radiation measurements at the surface of this type of shielding at 1 MW reactors have shown radiation levels of about one millirem/hr or less. For 2 MW, most radiation levels around the reactor shield are in the one to two millirem/hr range, which is still quite low;
- The MNRC Reactor bulk shield is very similar, in material type and thickness, to other proven TRIGA® shields. The one significant difference is the beam tube penetrations. Where the basic shielding configuration has been penetrated by beam tubes, supplemental shielding has been added. This supplemental shielding has been designed to provide the same attenuation to both neutrons and gammas as the basic unpenetrated shield.

The MNRC has eight areas with specially designed shielding: the reactor bulk shield, the four radiography bays, the demineralizer resin cubicle, the CAM room, and the second floor hand and foot monitor. Included in the radiography bays' shielding are the shutter biological shields, the beam stops, and the walls and roof of the individual bays. Shielding has been designed so that radiation levels in areas occupied by personnel are as-low-as- reasonably-achievable.

- Reactor Bulk Shield The reactor shield is essentially the same as that which has been used for other above ground TRIGA® reactors. The shield consists of approximately 20 ft of water above the core to protect personnel in the reactor room (Figure 11.9). The radial shielding, which protects personnel in the adjoining radiography bays, is provided by the graphite reflector and pool water to a radius of 3.5 ft and by standard reinforced concrete extending to a radius of 10.5 ft (7 ft thick in Bay 1). This basic shield has been augmented in the areas of beam tube penetration with shadow shields of steel. Actual measured radiation levels at the surface of this shield at 1 MW show 1 millirem per hour or less or 2 millirem per hour for 2 MW operations. The reinforced concrete pad below the tank is approximately 10 ft thick and prevents soil and ground water activation.

The 20 ft of water above the core provides the bulk shielding for personnel in the reactor room. The results of surveys of two similar 1 MW TRIGA® facilities and of the MNRC reactor operating at 1 MW showed the following radiation levels above the center of the reactor tank. (NOTE: These levels drop off rapidly at the edge of the tank).

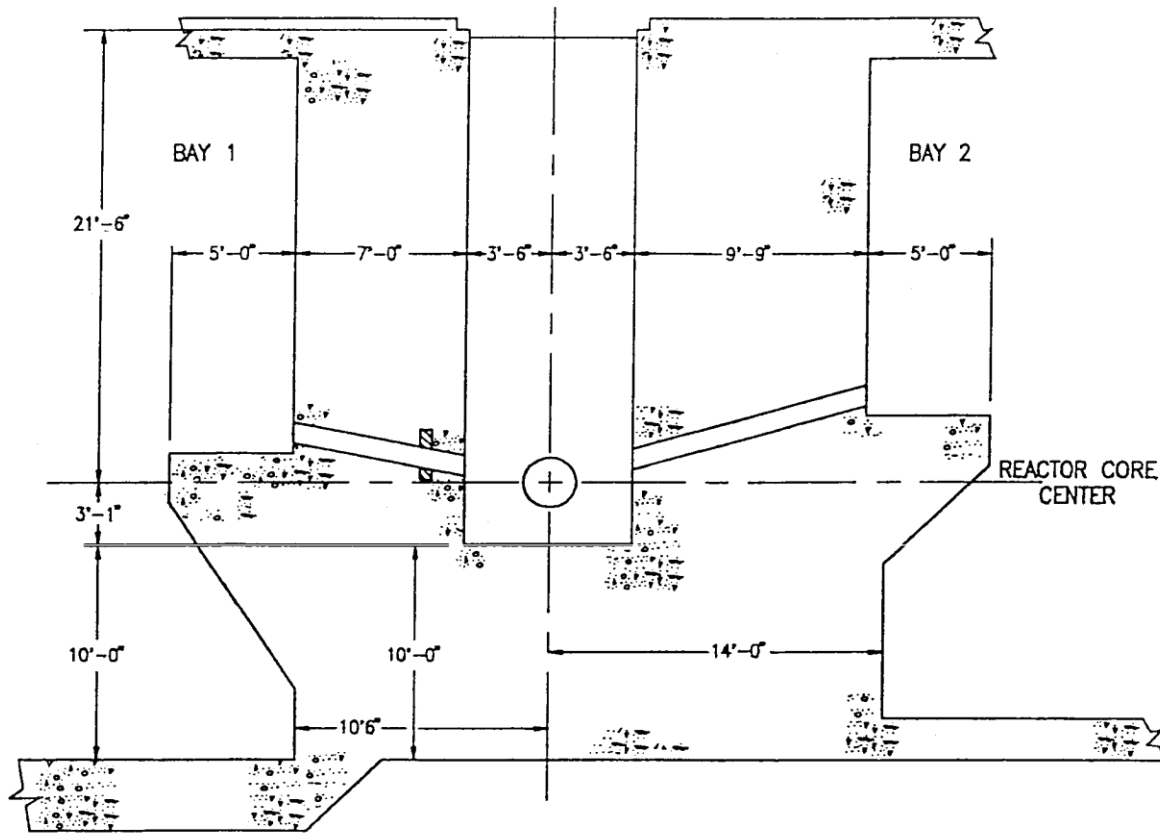


FIGURE 11.9 REACTOR BULK SHIELD

TABLE 11-7 Radiation Levels (Millirem/Hr)

Reactor	Tank Size		millirem/hr Diffuser "ON"	millirem/hr Diffuser "OFF"
	Dia. (Ft)	Height (Ft)	Water Surface	Water Surface
USGS	8.0	24.8	16	600
Malaysia	6.5	20.7	240	750
MNRC	7.5	24.5	80	600

- Neutron Beam Shutter, Biological Shield, Beam Stops, Radiography Bay Walls, and Roof The neutron beam shutter/biological shield, the beam stop, and the radiography bay walls and roof must protect personnel from both gamma and neutron radiation contained in the radiography beam. The beam tube shutter/biological shield and the radiography bay interior walls were designed to reduce radiation levels to less than 5 millirem/hr in areas in the radiography bays that are routinely occupied when the reactor is operating. The actual radiation levels were less than 5 millirem/hr for 1 MW and 2 MW operations.

Two sources of radiation were considered when designing the radiography bay shields. First, the direct beam which is attenuated by the shutter/biological shield. Second, the neutrons that scatter from adjoining radiography bays and are attenuated by the interior walls of the radiography bays. The shutter shield orientation is shown in Figure 11.7. The face of the shield contains a section filled with boron frit approximately 1 in. thick to attenuate thermal neutrons. The remaining shield is a composite made up of the materials shown in Table 11-8.

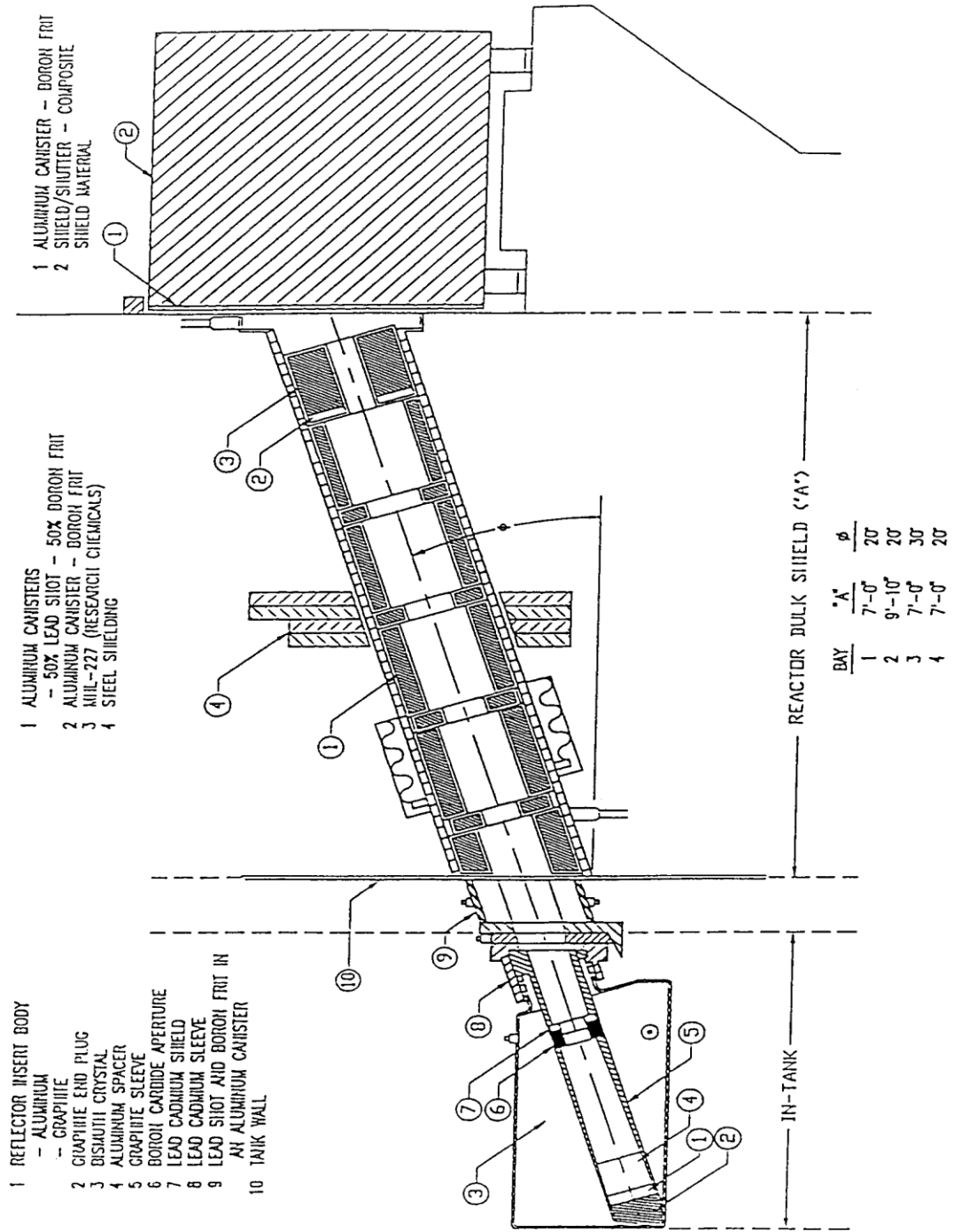


FIGURE 11.10 MNRC BEAM TUBE AND BIOLOGICAL SHIELD

**TABLE 11-8 Composite Shield Makeup**

Material	Wt %
Cement	11.7
Water	3.4
Boron Carbide	0.5
Limonite	18.7
Steel Shot	65.8

The shutter shield is designed to thermalize fast neutrons, to capture thermal neutrons, and to attenuate direct gamma radiation from the core as well as the capture gammas produced in the shield. A MORSE and ANISN analysis (References 11.5 and 11.6, respectively) predicted radiation levels on the bay side of this shield of approximately 0.1 millirem/hr. The actual measured radiation level on the bay side of the shield with the reactor operating at 1 MW was 0.3 millirem/hr. At 2 MW the radiation level is still below 1.0 millirem/hr.

The interior walls of the radiography bays are made from 2 ft thick standard reinforced concrete. Calculations, similar to those discussed below for the exterior walls and roofs, predict maximum radiation levels of less than 5 millirem/hr at the closest point on the wall of an adjacent bay when the maximum scattering target is directly in the beam. Survey results indicate these calculations were overestimates.

The exterior walls and doors of the radiography bays, shown in Figures 11.11 and 11.12, are made of standard reinforced concrete with thicknesses that range from 2 to 3 ft. They have been designed to reduce the radiation levels from scattered gammas and neutrons, especially in the staging and preparation areas. Beam stops have been incorporated into the bay walls to attenuate the direct neutron and gamma radiation. These stops not only reduce the direct radiation levels but also reduce scattering.

The roofs of the radiography bays are constructed from standard reinforced concrete 2 ft. thick at the outer edge of the building. The thickness of the roofs increases at approximately 0.25 in./ft so they are about 32 in. thick at the building center.

To determine the required thickness of the walls and roofs of the radiography bays, it was assumed that a typical aircraft component placed in the beam represented a point source of neutrons arising from scattering collisions in the target.

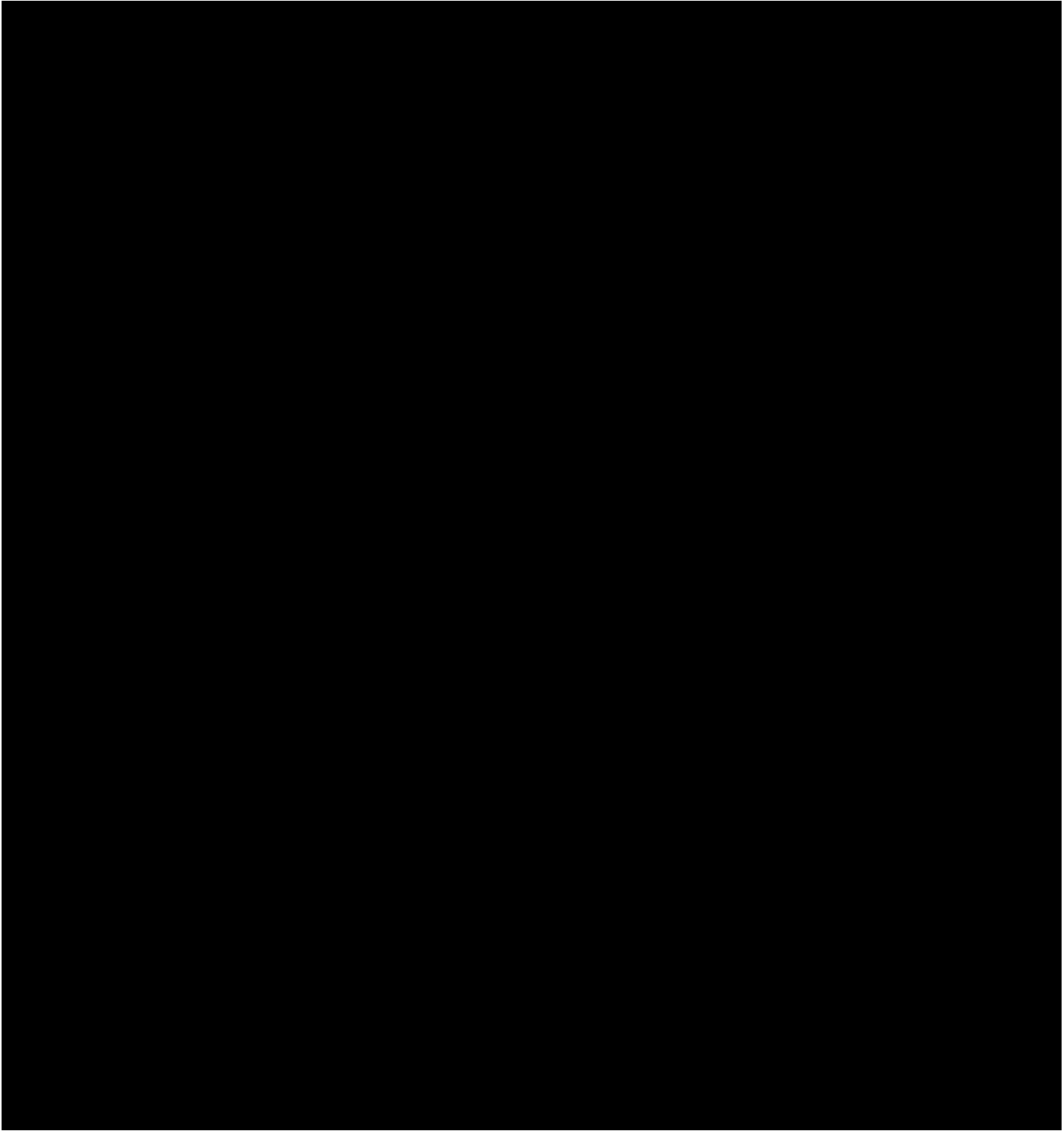


**FIGURE 11.11 MNRC SHIELDING - BAYS 1 AND 2**

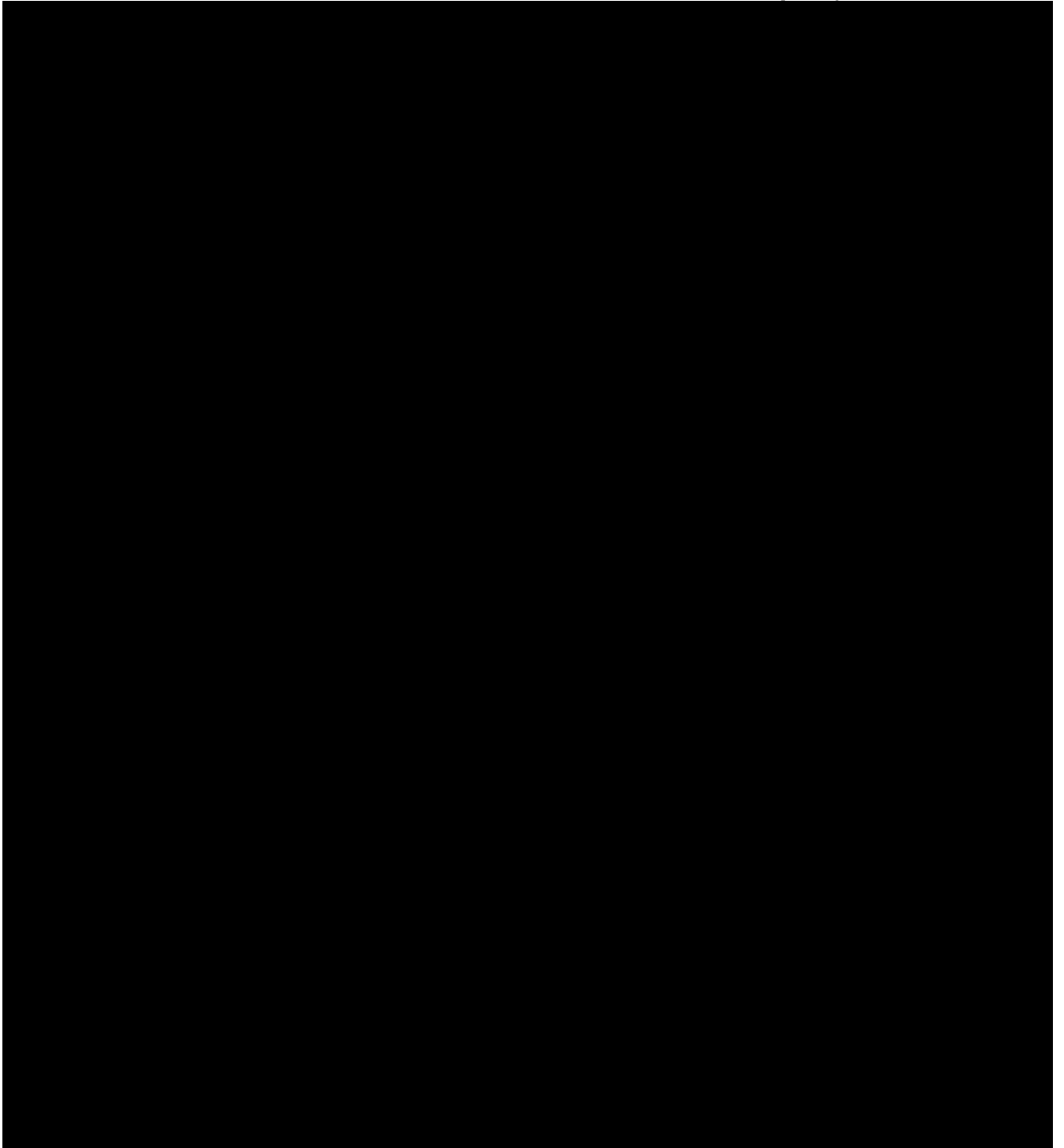


**FIGURE 11.12 MNRC SHIELDING - BAYS 3 AND 4**

For these calculations a neutron beam consisting of one-half thermal and one-half fast neutrons was used. The largest components are handled in Bay 1, so the target was assumed to be a 38.5 kg piece of B6AC stainless steel plate with a surface area, normal to the beam, of 0.223 m<sup>2</sup>. The 38.5 kg piece of material is representative of an aircraft wing hinge and has a composition as shown in Table 11-9. The size of targets for the other bays were somewhat smaller and representative of the components being examined.

**TABLE 11-9 Composition Of B6AC Stainless Steel**

Element	Wt-%
Carbon	0.47
Manganese	0.75
Sulfur	0.22
Chromium	1.05
Nickel	0.55
Molybdenum	1.00
Vanadium	0.11
Iron	95.80

Macroscopic thermal capture cross sections, and thermal and fast scattering cross- sections were calculated from cross-sections given in Etherington (Reference 11.7). By this method it was found that about 19% of all the neutrons were captured and about 75% were scattered when the beam was one-half thermal and one-half fast neutrons. A Monte Carlo calculation also indicated that about 26% of the source neutrons are captured in the target and 68% are scattered out of the beam. In this calculation a 7-energy group distribution was used. The Monte Carlo calculation also showed that neutron scattering is essentially isotropic as would be expected.

A FORTRAN program using removal cross-sections was written to calculate either the concrete thickness for a given dose rate or the dose rate for a given concrete thickness, where the inside dimensions of the room, the target location and composition, and the beam strength and horizontal angle are specified as input. The last was included to account for any anisotropy in neutron scattering.

It was assumed that all fast neutrons that were scattered were available to penetrate the walls, and that all thermal neutrons that were not captured in the target would be captured ultimately within the room.

In each of the four radiography bays the wall calculations were done in a horizontal plane containing the target and a vertical plane containing the beam.

Additional calculations were made to assess the contribution to the dose rate outside the room from capture gammas in the room or in the walls themselves. Three different assumptions were made:

1. Every neutron entering a spherical room was captured uniformly in the room (The room volume was that of radiography Bay 3);
2. Every neutron entering the room was captured uniformly over the inside surface of the room;
3. Every neutron entering the room was subject to removal (using a removal cross-section for concrete) and that removal produced a 1.5 MeV photon.

Only the third assumption yielded dose rates of any significance and these were only about 3% of the neutron dose rates from the detailed calculations and are comparable to the gamma doses in those calculations.

The results of this analysis were used to establish the concrete thickness shown in Figures 11.11 and 11.12. With these thicknesses, the predicted radiation dose rates at 1 MW are shown in Figures 11.13, 11.14, and 11.15. Actual measured dose rates at 1 MW and projected dose rates at 2 MW outside the radiography bays and on the roofs are also shown in these three figures. It is of interest to note that the projected (and subsequently measured) dose rates at 2 MW are lower than the 1 MW values. The reason for this is that the beam intensities were reduced by a factor of 4 compared to the 1 MW intensities by reducing the size of the aperture in the beam tube.

Because of a conservative shielding design for the 1 MW operation, essentially all of the existing shielding will provide adequate radiation protection factors when the reactor is operated at 2 MW.

- Auxiliary Systems Shielding In addition to the primary biological shielding for the reactor and radiography bays, certain auxiliary systems require shielding. An additional 1 foot of concrete was installed around the demineralizer system in order to keep the radiation levels on the second floor of the reactor building as low as reasonably achievable during 2 MW operations, and to maintain an acceptable radiation background for health physics instrumentation in the general area. In order to achieve a background reduction sufficient to maintain adequate counting sensitivity, in addition to the demineralizer resins, the east wall of the CAM room (containing the reactor room and the stack CAMs) is also shielded with one foot of concrete in an "L" configuration. Figure 11.16 shows the locations of the shielding for the demineralizer and radiation monitoring systems.
- Bay 4 Structural Modification Shielding (Bay 5) The lower level in Bay 4 has a large cavity cut up to the reactor tank wall for planned neutron cancer therapy (NCT) research. The cavity is approximately 10' x 10' x 10' and is currently filled with concrete blocks stacked in overlapping layers (to prevent radiation streaming). The radiation levels at 2 MW are less than 0.5 mR/hr gamma and less than 0.1 mrem/hr neutron on the outside of the concrete blocks.

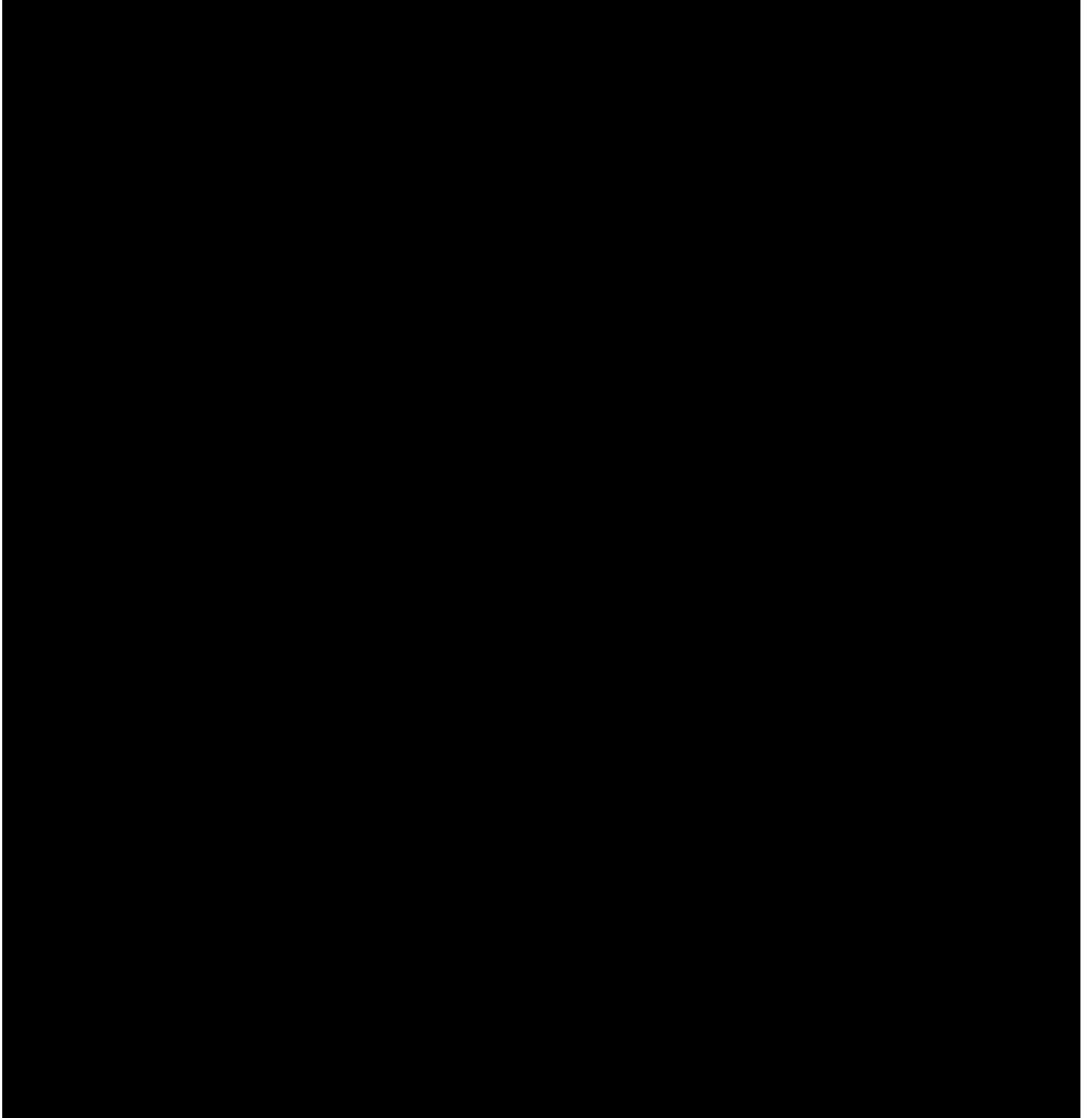


**FIGURE 11.13 PROJECTED RADIATION DOSE RATES - BAYS 1 AND 2 AT 1 MW AND 2 MW**

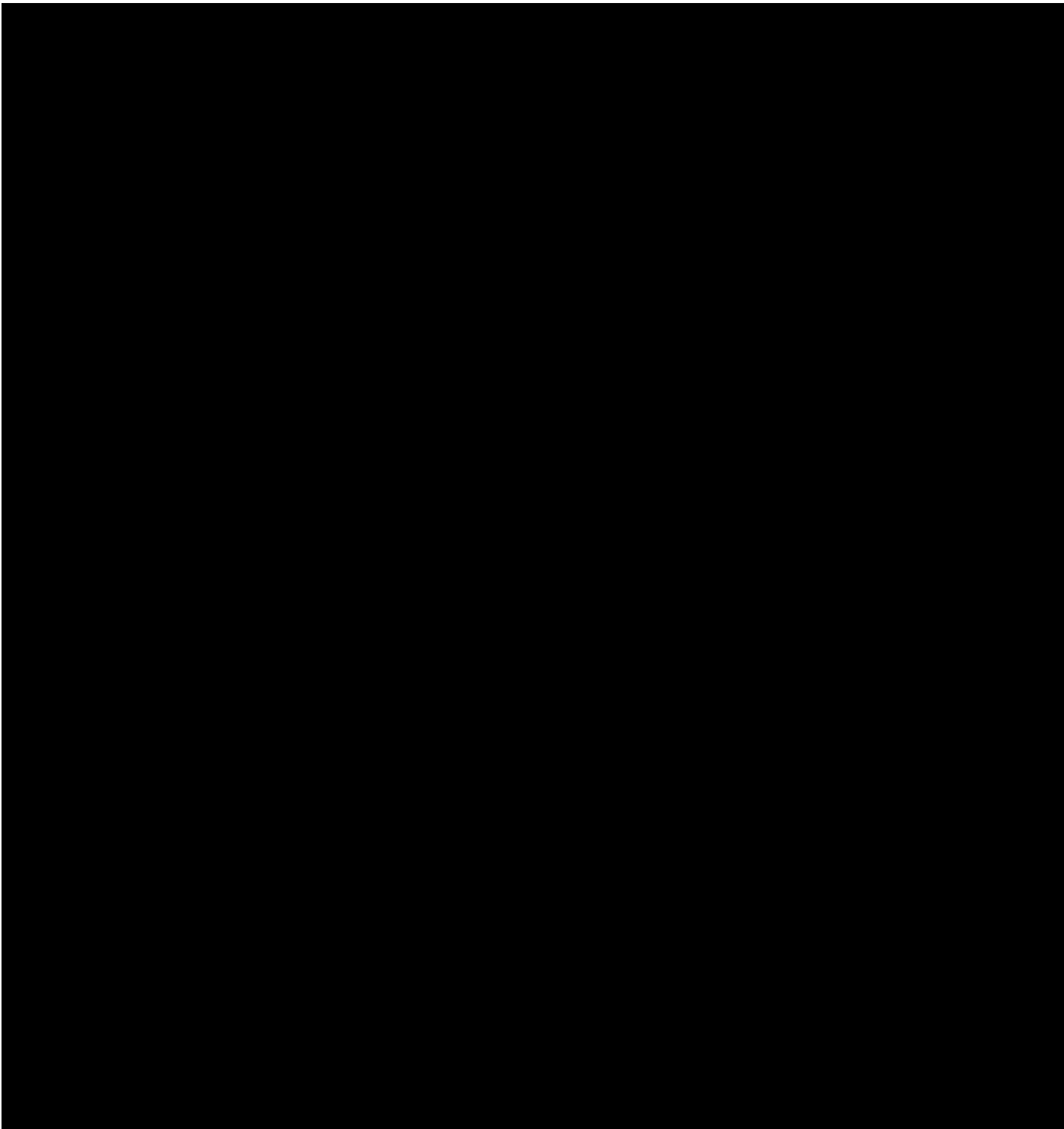


**FIGURE 11.14 PROJECTED RADIATION DOSE RATES - BAYS 3 AND 4 AT 1 MW AND 2 MW**

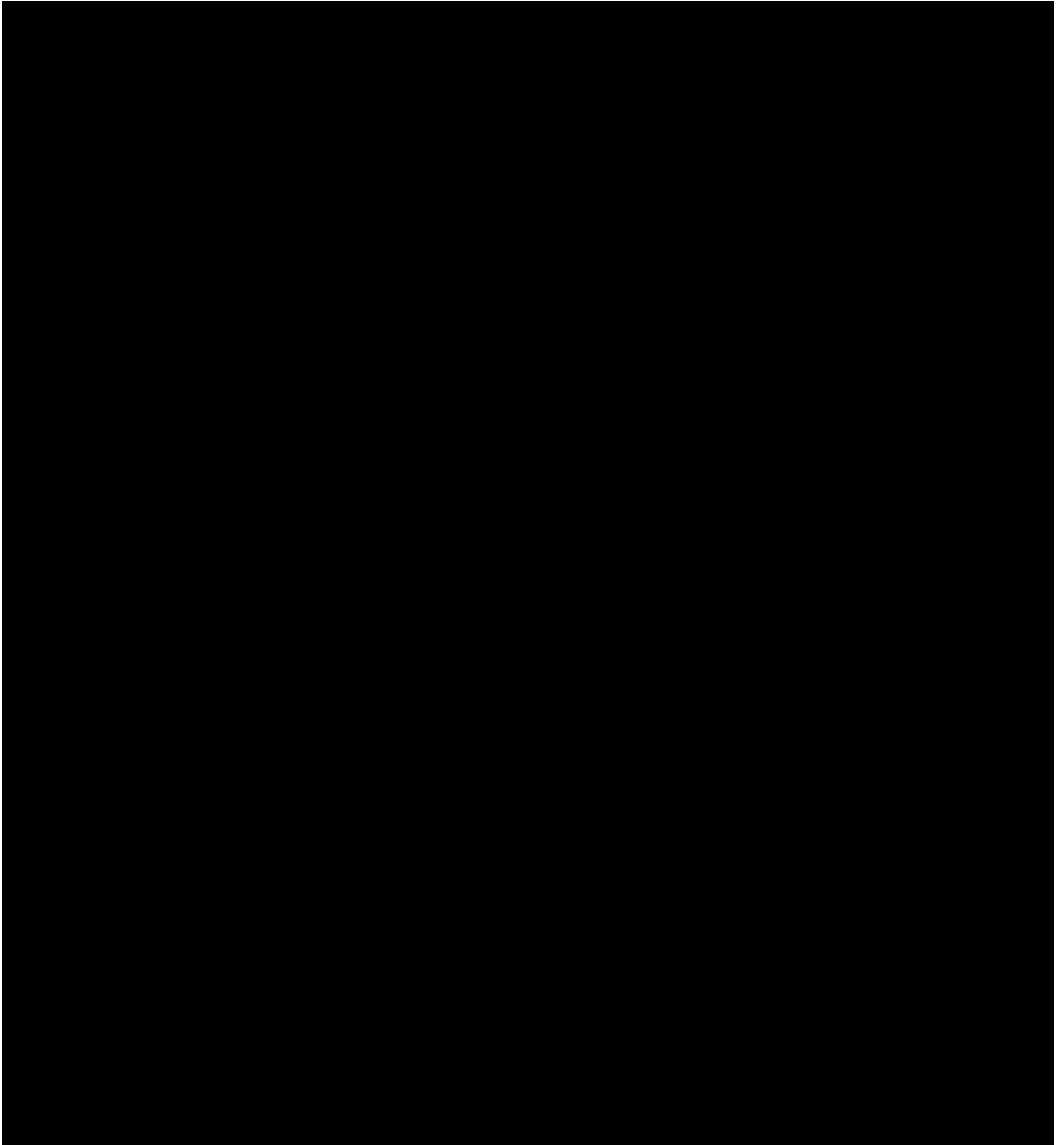


**FIGURE 11.15 PROJECTED RADIATION DOSE RATES - PLAN VIEW AT 1 MW AND 2 MW**

### 11.1.6.2 Ventilation System

Control of radiation exposure due to airborne sources is discussed in Section 11.1.2.1 and in Appendix A. In addition, details of the ventilation system (an integral part of the control process for airborne emitters) are provided in Section 9.5. This section discusses only those ventilation design features that have been incorporated for radiation protection.

- First and most important, the design of the radiography bays and reactor room exhaust systems will maintain Ar-41 and N-16 levels in the reactor room and Ar-41 levels in the radiography bays at concentrations consistent with keeping occupational doses well below the limits in 10 CFR Part 20. However, even when the radiography bays exhaust system is not operational, Ar-41 concentrations in the bays and subsequent occupational doses will still be below 10 CFR Part 20 limits) (See Section 11.1.2.1.1).
- Second, the ventilation systems are balanced so that the differential air pressure in the reactor room, the equipment room and the sample preparation area is negative with respect to surrounding areas. The radiography bays will also have a negative air pressure relative to surrounding areas when the radiography bays exhaust system is operative, which will be the normal mode of operation.
- Third, the reactor room exhaust system contains a high efficiency filter (99.95% for 0.3 micron sized particles) to remove any radioactive particulates.
- Fourth, the reactor room exhaust system recirculates the air exhaust back into the reactor room should the reactor room CAM exceed preset limits. (Reactor room air can then be recirculated through HEPA and charcoal filters to remove radionuclides.)
- In this mode, no reactor room air is exhausted through the stack.
- Fifth, the hood in the sample preparation/pneumatic transfer area exhausts through a HEPA filter. It also maintains an in-flow of air through the hood to prevent the release of radioactivity into the surrounding area.

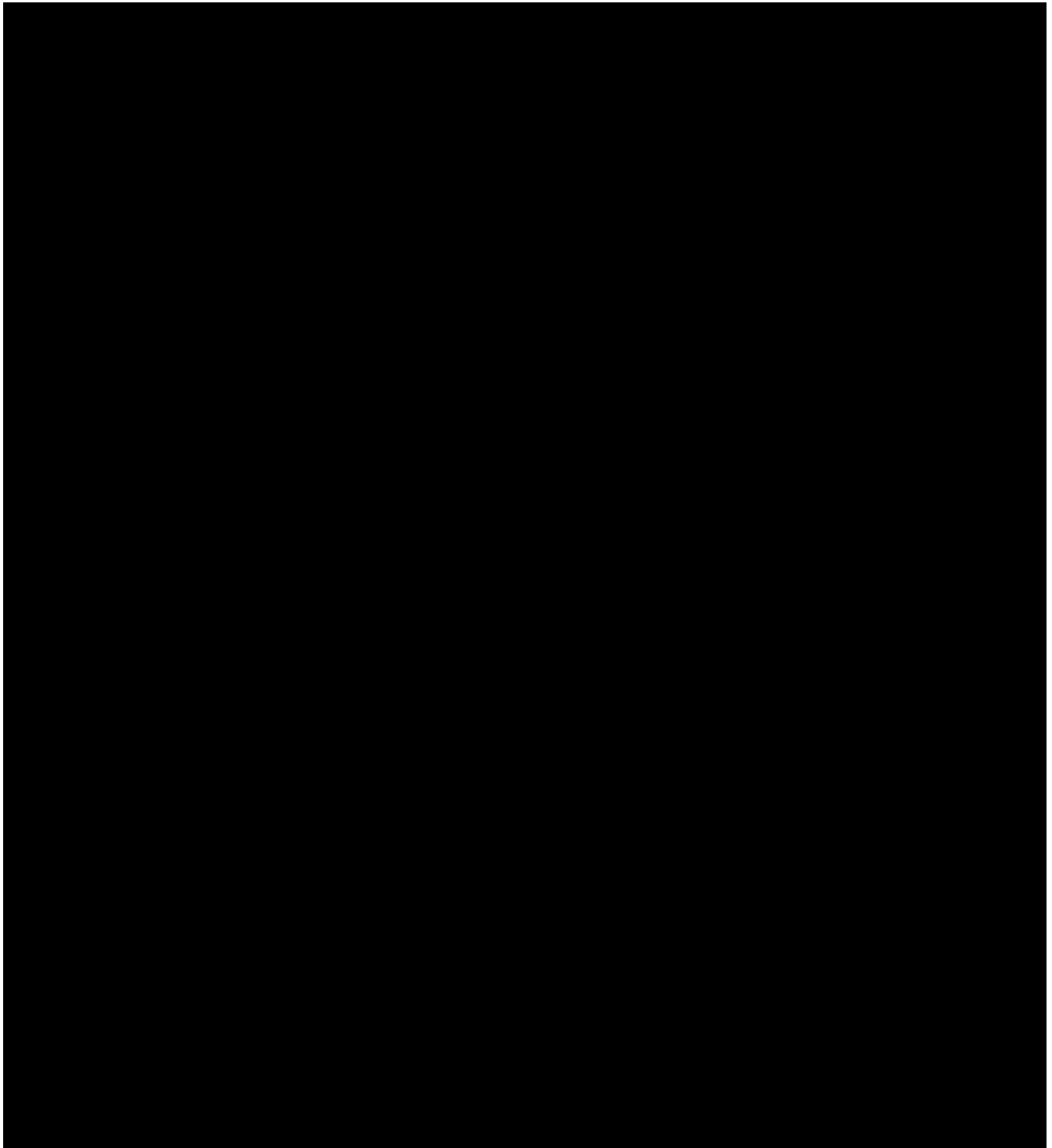


**FIGURE 11.16 SHIELDING FOR DEMINERALIZER RESINS AND RADIATION MONITORING EQUIPMENT -  
SECOND FLOOR**

### 11.1.6.3 Containment

Containment of radioactivity within the MNRC is primarily a concern with respect to experiments being irradiated in the various irradiation facilities and with the reactor fuel. Containment of fission products within the fuel elements is achieved by maintaining the integrity of the fuel's stainless steel cladding, which is accomplished by maintaining the fuel and cladding temperatures below specified levels. This matter is discussed in detail in Chapter 4. Containment of other radionuclides generated during use of the irradiation facilities is achieved through strict encapsulation procedures for samples and strict limits on what materials will be irradiated, as specified in "Utilization of the McClellan Nuclear Research Center Reactor Facility" (Reference 11.8) and in Chapter 10.

To further improve containment and minimize the potential release of radioactivity from experiments irradiated in the in-core pneumatic transfer system, the terminal where samples are loaded and unloaded is located inside a fume hood. The hood, which exhausts through a HEPA filter, maintains an in-flow of air to prevent the release of radioactivity to the surrounding area (Figure 9.10).

### 11.1.6.4 Entry Control - Radiography Bays and Demineralizer Cubicle

There are five main areas within the MNRC facility which will require entry control in order to meet the 10 CFR 20 requirements for limiting access into high radiation areas. Specifically, these are presently the four radiography bays and the small cubicle containing the demineralizer resins.

#### 11.1.6.4.1 Entry Control for Radiography Bays

Access into the radiography bays is controlled by a system of interlocks and warning devices incorporated into the facility design and described in Section 9.6.

Operation of the neutron beam shutters within the radiography bays is normally controlled remotely from the respective radiography bay control room; however, during maintenance activities, etc., these shutters can be controlled from within the respective bays. The bay doors are locally operated only by "dead man" switches mounted to the door. An interlock and warning system has been incorporated into each beam shutter control and bay door control to do the following:

- Prevent the radiography bay doors from opening when the beam shutter is open and the reactor is operating;
- Scram the reactor if both the beam shutter and the bay door are open;
- Sound an audible alarm and activate a red flashing light within the bay when the beam shutter starts to open;
- Show the operational status of the reactor throughout the facility.

The logic for this interlock system is shown in Figures 9.13 and 9.14.

Another feature of the interlock system is a series key-lock subsystem. A key box mounted near the closure side of each radiography bay shield door contains 10 captive keys and a master key that is controlled by a qualified UCD/MNRC staff member. When any one of the radiography bay keys is removed, electrical power cannot be applied to the respective bay door drive mechanism. Use of the master key assures the required attendance of a qualified UCD/MNRC during opening and closing of radiography bay doors. Each individual entering a radiography bay is required to remove one of the ten keys and to maintain the key in his or her possession while in the bay. When an individual leaves the bay, that person's key is reinserted into the key box. When all 10 individual keys and the master key have been inserted and are captive in the key box, the bay door can be closed. Following the door closure, the master key is removed returning the control and interlock system to its secured mode.

Rip cords have also been located in each of the radiography bays. Figures 9.18, 9.19, and 9.20 show their locations in the different bays. Activation of any rip cord will scram the reactor or will not allow it to start if shutdown. To reset a tripped rip cord, personnel must enter the bay and depress the reset button (i.e., determine if personnel in the bay activated the system). In addition, a scram button is located in the reactor room and can be used to shut the reactor down.

Reactor "ON" lights are located throughout the facility. These lights illuminate any time the control rod drive magnets have power. Also, anytime a radiography bay shutter "open" command is given an audible horn is sounded for 15 sec and a red flashing light is illuminated in the bay. Figures 9.21 and 9.22 show the locations of reactor "ON" lights and the shutter "opening" warning lights.

#### 11.1.6.4.2 Entry Control for the Demineralizer Cubicle

Access control for the demineralizer cubicle will be based on the fact that it is a high radiation area when the reactor is operating at 2 MW. This is due primarily to the expected buildup of primary coolant activation products (mainly Na-24) in the resins. Additional radiation shielding around the cubicle is in place, and the access is controlled by a locked barrier at the point of entry into the area. The locked barrier will be opened only under controlled conditions commensurate with the fact that the area is considered a high radiation area. Entry procedures will incorporate all 10 CFR 20 access requirements for entering a high radiation area.

#### 11.1.6.5 Protective Equipment

Typical protective equipment and related materials used in the MNRC radiation protection program are summarized in Table 11-10.

**TABLE 11-10 SUMMARY OF TYPICAL PROTECTIVE EQUIPMENT USED IN THE MNRC RADIATION PROTECTION PROGRAM**

Item	Use - Routine (R) - Emergency (E)
Lab Coat	R & E
Rubber Gloves	R & E
Latex Examination Gloves	R & E
Safety Glasses	R & E
Face Shields	R & E
Coveralls	R & E
Hoods/Caps	R & E
Plastic Shoe Covers	R & E
Rubber Over Shoes	E
Small Spill Kits	E
Large Spill Kits	E
Decontamination Locker	E
Decontamination Shower	E
Decontamination Sink	E

#### 11.1.6.5.1 Respiratory Protection Equipment

Other than Ar-41 and N-16, no airborne radioactivity is expected to occur at the MNRC as part of normal operations. Consequently, respiratory protection equipment is not part of the protective equipment typically used at the MNRC. Should the situation change and respiratory protection become necessary in order to meet ALARA objectives, the MNRC will implement a respiratory protection program in accordance with Subpart H of 10 CFR 20.

#### 11.1.6.5.2 Personnel Dosimetry Devices

Personnel dosimetry devices in use at the MNRC have been selected to provide monitoring of all radiation categories likely to be encountered. Table 11-11 summarizes the devices typically used. Personnel dosimeters are changed monthly. An administrative action level of 100 millirem in one month or 300 millirem in one quarter has been established. An exposure investigation is required if any action level is exceeded in order to determine the source of the exposure. This is part of the MNRC ALARA program described previously (Section 11.1.4).

There are no routine operations at the UCD/MNRC which present a potential for internal deposition of radionuclides. The requirement for annual whole body counting was eliminated in 2005 when I-125 production was terminated. (per UCD/MNRC RSO memo dated 20Jan2005 "Changes to the Health Physics Program")

Personnel exposure reports are maintained by the Health Physics Branch and are retained for the life of the facility. In addition, radiological survey data sheets which document worksite radiological conditions are maintained by the Health Physics Branch and are retained for the life of the facility.

**TABLE 11-11 TYPICAL PERSONNEL MONITORING DEVICES USED AT THE UCD/MNRC**

Type	Dose	Radiation Measured
OSL	Deep Dose Equivalent Eye Dose Equivalent Shallow Dose Equivalent	Beta, Gamma
Albedo OSL	Deep Dose Equivalent	Thermal Neutrons
OSL Finger Ring	Extremity Dose Equivalent	Beta, Gamma
CR-39 Track Etch	Deep Dose Equivalent	Fast Neutrons

The average annual occupational whole body exposure (Deep Dose Equivalent) for 2 MW operations for 1998 was 217 millirem. The average annual extremity and eye dose for 2 MW operations for 1998 was 181 and 195 millirem, respectively. In contrast the average annual whole body, extremity, and eye exposure for more recent single shift 1 MW operation has been approximately 25, 50, and 50 millirem respectively. These doses are not expected to change significantly in the future and are well below 10 CFR 20 limits.

#### 11.1.6.6 Estimated Annual Radiation Exposure

The guidelines for radiation doses and for airborne concentrations of radionuclides during normal operations of the MNRC are contained in 10 CFR 20. These guidelines establish levels for both “restricted” and “unrestricted” areas. With respect to the MNRC, the “restricted” area is considered to be all locations within the operations boundary (within the UCD/MNRC perimeter fence). The “unrestricted” area includes all locations and the personnel outside the operations boundary. The following sections contain an estimate of annual radiation exposure in these two areas.

##### 11.1.6.6.1 Estimated Annual Doses in the Restricted Area

It is assumed that an individual working at the UCD/MNRC will be in the facility only one shift/day (40 hrs/wk). Further, it is assumed that an occupationally exposed individual will only spend a fraction of the time in areas where there is a potential for significant radiation levels (within the radiography bays, the demineralizer cubicle, or in the reactor room). Therefore, the predicted occupational doses are based on an estimate of the actual time an individual will spend in areas where there are measurable radiation levels.

Radiation levels outside the radiography bays in the staging areas are typically less than 0.2 millirem/hr with the reactor operating at 2 MW. If personnel were exposed to these levels for 20 hr/wk for 50 weeks during the year the annual Total Effective Dose Equivalent (TEDE) would be 200 millirem, which is well below the 10 CFR 20 annual occupational dose limit. Radiation levels are higher (1-3 millirem/hr) immediately outside the radiography bay walls which contain the beam stops. However, personnel doses from these areas are still expected to be very low (less than 2 millirem/wk) because personnel spend less than 1 hr/wk in these areas. Historical worker dosimetry show these estimates to be conservative.

Radiation levels are high in the radiography bays when the neutron shutters and gamma shields are open and the reactor is operating. However, personnel are restricted from these areas anytime the shutters are open and the reactor is operating. Radiation levels in bays adjacent to an operating bay are approximately 1 millirem/hr during 2 MW operations.

A prediction of the dose rates from typical aircraft materials activated in the neutron beams was made in Appendix A. The predicted dose rate from an aluminum plate being radiographed using film techniques or from an entire wing scanned for 8 hrs using electronic imaging devices is less than 1 millirem/hr at five feet if a 5-10 min period is allowed for the aluminum to decay. The radiation levels from these components when compared to those discussed above will be insignificant since exposure times will be short. These components may need to be stored in an isolated area for a few days for all activity to decay.

The radiation exposures from activation products in the shutter bulk shield will be less than 1 mrem since nearly all of the activity is in the first 12 inches of the shield leaving 36 inches of high density material for attenuation. However, during decommissioning, the shield will have to be handled as low-level radioactive waste due to induced gamma emitting radionuclides, and more importantly, due to the long-lived non-gamma emitters, such as <sup>55</sup>Fe, which has a 2.7 year half-life.

The total effective dose equivalent from Ar-41 in the radiography bays was predicted in Appendix A. Using the highest Ar-41 concentration for 2000 hours of annual exposure will result in an annual TEDE of only 0.5 millirem. Nevertheless, the exposure of personnel working in radiography bays will be closely monitored so that guideline levels are not exceeded and exposure to all individuals is kept as-low-as-reasonably-achievable.

The radiation level (due primarily to N-16) is approximately 60 millirem per hour at one foot over the tank and about 10 millirem per hour at 3 feet above the tank, but these levels drop rapidly at the tank's edge.

Radiation doses in the reactor room away from the tank will be mainly from airborne N-16 and Ar-41. The predicted 2 MW concentrations of N-16 and Ar-41 with the reactor room exhaust system operating but with the diffuser system OFF are  $1.4 \times 10^{-4}$   $\mu\text{Ci/ml}$  and  $5.22 \times 10^{-6}$   $\mu\text{Ci/ml}$ , respectively (Appendix A and Section 11.1.2). The predicted whole body (immersion) dose rate from these two isotopes is 7.8 millirem per hour, with N-16 contributing nearly all of the dose rate (7.7 millirem per hour). In actual practice, however, the radiation levels from these two radionuclides will be considerably less than predicted, since the diffuser will be operating and the N-16 contribution will therefore be lower by about one order of magnitude. The radiation level from all sources about 3 feet above floor level (not over the tank) is approximately 1.0 millirem per hour at 1 MW and 2.0 millirem per hour at 2 MW. Although these are relatively low radiation levels, access to the reactor room will still be controlled and personnel exposures closely monitored.

Maintenance of equipment located in the reactor room, such as control rod drives, instrumentation, and primary water system components, will not be allowed when the reactor is operating. Therefore, it is estimated that personnel exposures from this type of activity will be insignificant.

Handling and inspection of MNRC fuel is accomplished in the reactor tank (with the reactor shut down). Removing or replacing fuel elements, either in the core or in the in-tank storage racks, requires that the element be raised in the vertical direction far enough to clear the grid plate/reflector or storage racks. However, with the fuel element at its highest point, it is still covered by about 15 ft of water and the radiation level at the tank surface is insignificant.

Should it be necessary to remove a fuel element from the tank after operation, it will normally be moved from the core and placed in the in-tank storage rack. It is anticipated that removal of most irradiated fuel elements from the tank will be carried out using the fuel element transfer cask. Therefore, the next step will normally be to lower the transfer cask into the tank, remove the element from the storage rack and then place it in the transfer cask. For this operation, there will be about 6-1/2 ft of water between the operator and the fuel element. Although the radiation level could be as much as 50 millirem per hour, the radiation dose to the operator will be insignificant since the time required for the operation is estimated to be less than one minute.

As discussed in Section 13.2.5, fission products would be released into the tank water should the cladding on a fuel element fail. Although not expected, if such a failure did occur, the noble gases, krypton and xenon, would escape from the water and into the reactor room. Most of the halogens, bromine and iodine, would be retained in the primary cooling water and would eventually end up in the water purification system resins or mechanical filter.

A prediction of the radiation doses in the reactor room due to a single fuel element failure is provided in Appendix B and in Section 13.2.5.

Other categories of individuals who might receive exposure at the MNRC include research and service personnel and visitors. Past exposure history on these two groups shows little or no recorded dose and there does not appear to be any reason to expect this situation to change. In addition, the MNRC has an administrative dose limit of 50 millirem per year TEDE for embryos, fetuses, declared pregnant women, minors and students, although the occupational exposure history at the facility would certainly indicate that it is very unlikely that this exposure would be received by anyone in these groups. Most visitors to MNRC receive a reactor room tour that is typically 30 minutes in duration. Most of the visitors only visit the MNRC once for a one-time dose of approximately 1.0 mrem.

#### 11.1.6.6.2 Estimated Annual Dose in the Unrestricted Area

A detailed discussion of the expected annual TEDE in the unrestricted area from Ar-41 production during normal operation of the MNRC reactor is contained in Section 11.1.2.1.4 and in Appendix A. The annual dose values for the unrestricted area shown in both of the preceding parts of this SAR indicate a maximum TEDE (primarily from Ar-41) ranging between 0.1 and 1.4 millirem per year, depending upon which atmospheric dispersion model is used. The maximum historical TEDE measured at the MNRC fence line has been 61 millirem gross, 45 millirem background, and 26 millirem net.

#### 11.1.7 Contamination Control

Radioactive contamination is controlled at the MNRC by using written procedures for radioactive material handling, by using trained personnel, and by operating a monitoring program designed to detect contamination in a timely manner. The program for routine monitoring to detect and identify fixed and loose contamination is described in Section 11.1.5.1. In addition to this monitoring program, the following items are also part of the program for contamination control at the MNRC:

- Two areas are known to be contaminated in the MNRC facility. These are the reactor tank and the pneumatic transfer system (PTS) hood. The MNRC Health Physics Procedures, MNRC-0029-DOC, contains specific procedures for working with radioactive material and for working with experiments that originate from in- tank or from the PTS hood. For other work where contamination is considered likely, a detailed written procedure or a radiation work permit (RWP) will provide the necessary contamination controls. All such work requires coverage by a qualified health physics technician and all material which must be removed from a contaminated area with suspected loose contamination is appropriately monitored and contained to minimize potential spread, or is decontaminated;
- After working in contaminated areas, personnel are required to perform surveys to ensure that no contamination is present on clothing, shoes, etc., before leaving the work location. Additionally, personnel exiting controlled areas surrounding a contaminated area are required to use a hand and foot monitor located at the exit. MNRC personnel are not exposed to sources of radioactivity likely to result in internal exposure.
- Anti-contamination (Anti-C) clothing designed to protect personnel against contamination is used as appropriate. Normally, Anti-C clothing will be specified in a written procedure or in an RWP. Anti-C clothing is monitored after each use;
- The MNRC Health Physics Procedures, MNRC-0029-DOC, contains procedures for monitoring and handling contaminated equipment and components;
- Procedures for classifying contaminated material, equipment and working areas and managing, controlling, storing, and disposing of identified contaminated material are contained in the MNRC Health Physics Procedures, MNRC-029- DOC.
- Staff and visitors are trained on the risks of contamination and on the techniques for avoiding, limiting, and controlling contamination as specified in the MNRC Health Physics Procedures, MNRC-0029-DOC;
- Contamination events are documented in a radiological investigation report (RIP). These reports help avoid repeating events which caused unplanned contamination. RIPs are maintained by the Health Physics Branch and are retained for the life of the facility;
- Encapsulation requirements for items likely to cause contamination during or after irradiation are contained in the document entitled, Utilization of the University of California - Davis/McClellan Nuclear Radiation Center (UCD/MNRC) Research Reactor Facility, MNRC-0027-DOC (Reference 11.8).

### 11.1.8 Environmental Monitoring

The MNRC has carried out an environmental radiation monitoring program since 1988. For about two years, the program collected preoperational data, but since 1990 the program has monitored the facility during operation. While many different types of samples have been collected and analyzed, to date there has been no indication that MNRC operations have impacted the environment except at the facility fenceline which shows a slight increase in ambient radiation levels above background at several specific locations, and there are no trends in environmental data which indicate that additional impacts will occur. This result is consistent with expectations for a facility of this type.

On an annual basis, the Nuclear Safety Committee audits the MNRC environmental monitoring program and the environmental data generated by the program. As a result of these audits, modifications have been made to improve the quality of the program.

The procedures for carrying out the environmental monitoring program are contained in the MNRC Health Physics Procedures (MNRC-0029-DOC). The procedures are focused on ensuring a comprehensive monitoring program which incorporates an adequate number of sample types, collected at the appropriate frequencies, analyzed with sufficient sensitivity, and reported in a timely manner to provide an early indication of any environmental impacts. Document Control measures for these procedures have already been described in Section 11.1.3.3.

With the exception of Ar-41, which has been thoroughly discussed in Section 11.1.2.1.4 and Appendix A, and in view of the MNRC policy of not discharging liquid radioactive materials down the sewer or as liquid effluents, there are virtually no pathways for radioactive materials from the MNRC to enter the unrestricted environment during normal facility operations. However, the MNRC environmental monitoring program has been structured to provide surveillance over a broad range of environmental media even though there is no credible way the facility could be impacting these portions of the environment.

The current environmental monitoring program consists of the following basic components which may change from time to time to meet program objectives; environmental monitoring locations and the types of measurements made or samples collected are summarized in Table 11-12:

- Integrated gamma dose measurements using optically stimulated luminescent dosimeters (OSL) which are exchanged quarterly. Currently OSLs are located at 37 on- industrial park sites (Sites 1-20, 50-62, and 64-71) and 7 off-industrial park sites (Sites 27, 28, 31, 38-40, and 42) (Typical sensitivity ~ 1 mrem/quarter);
- Water sample obtained quarterly. Currently this water sample is obtained at Well 54 (Site 42) (Typical sensitivity based on average minimum detectable activity for gamma emitters ~ 7 pCi/l).

- Water samples are submitted to a contractor's laboratory for analysis. Water samples are normally analyzed for gross alpha, gross beta, and tritium, and also normally undergo gamma spectroscopy. Soil and vegetation samples are normally analyzed for gross beta and normally undergo gamma spectroscopy. OSLs are processed by a contractor. All of the results are returned to the Health Physics Branch for review and compilation.
- Environmental procedures for direct radiation measurements, airborne, soil and vegetation sampling eliminated per UCD/MNRC RSO memo dated 20Jan2005 "Changes to the Health Physics Program". Memo also changed location of well water sample location.

**TABLE 11-12 ENVIRONMENTAL MONITORING AND SAMPLING PROGRAM**

	<u>SITE</u>	<u>LOCATION</u>	<u>TYPE</u>
ON-IP:	1	Control Tower Access Rd. / by control tower	O
	2	Control Tower Access Rd. / by Bldg. 1020 on fence	O
	3	A St. / by Bldg. 514	O
	4	A St./end of dorm parking lot	O
	5	Price Ave. / by Bldg. 1028	O
	6	Price Ave. / north end by perimeter fence	O
	7	Patrol Rd. / by creek	O
	8	Patrol Rd. / by red & white radar tower	O
	9	Patrol Rd. / by shooting range	O
	10	Patrol Rd. / by Magpie Creek monitoring site	O
	11	North of fire station / near Bldg. 721	O
	12	Dudley & Kilzer/ E. side Bldg. 663	O
	13	Perimeter Fence / N.E. of Bldg. 475A	O
	14	Perimeter Fence / CE yard	O
	15	Parking Lot / E. of Bldg. 10	O
	16	Palm St. / across from Air Museum	O
	17	Main Water Tower / underneath tower on N.W. side	O
	18	Well #10 / by Gate 3	O
	19	Grass Area / west of Bldg. 258	O
	20	Price Ave. / Bldg. 878 roof	O
OFF-IP:	27	Rio Linda Well / Elkhorn Blvd. & 24th St. (N.W. of Base)	O
	28	Rio Linda Well / 20th St. by Vineland School (N.W. of	O
	31	Capehart Water Tower / south side of fence (N.E.	O
	38	City Well / Orange Grove Rd. (S. of Base)	O
	39	City Well / Elkhorn Blvd. & Butterball (N.E. of Base)	O
	40	City Well / Walnut Ave. water tower (E. of Base)	O
	42	City Well / Dry Creek & Ascot Ave. ( W. of Base )	O, W
50-61	MNRC Facility perimeter fence	O	
62	MNRC Staging Area (facility area monitor)	O	
ON-IP:	64	Bldg. 243G / roof (west end)	O
	65-69	MNRC Facility perimeter fence	O
	71	MNRC Facility perimeter fence	O

Legend: O = OSL; W = Water Sample; IP = Industrial Park

## 11.2 Radioactive Waste Management

The MNRC reactor program generates very modest quantities of radioactive waste, as previously noted in Sections 11.1.2.2 and 11.1.2.3. This is due to the type of program carried out at the facility and to the fact that a conscious effort is made to keep waste volumes to a minimum.

### 11.2.1 Radioactive Waste Management Program

The objective of the radioactive waste management program is to ensure that radioactive waste is minimized, and that it is properly handled, stored and disposed of.

The Health Physics Branch is responsible for administering the radioactive waste management program. The organization and staffing levels, the authorities and responsibilities, and the position descriptions for the Health Physics Branch are discussed in Section 11.1.3.1. The working relationships between the health physics staff and the operations staff are discussed in Section 11.1.3.2.

The MNRC Health Physics Procedures, MNRC-0029-DOC, addresses the specific procedures for handling, storing and disposing of radioactive waste. Document control measures relating to these procedures and to other waste management documents are described in Section 11.1.3.3.

The radioactive waste management program is audited as part of the oversight function of the Nuclear Safety Committee (NSC). The NSC charter, responsibilities, meeting frequency, audit and review responsibilities, scope of audits and reviews, and qualifications and requirements for committee members are described in Section 11.1.3.5.

Waste management training is part of both the initial radiation protection training and the specialized training. It is also included in the annual refresher training. This training program and the topics covered were previously described in Section 11.1.3.4.

Radioactive waste management records are maintained by the Health Physics Branch. Radioactive waste packages in storage are tracked by a computer based radioactive material accountability system until shipment for disposal or transfer to an authorized broker. Radioactive material shipment and transfer records are also maintained by the Health Physics Branch. All records are retained for the life of the facility.

### 11.2.2 Radioactive Waste Controls

At the MNRC, radioactive waste is generally considered to be any item or substance which is no longer of use to the facility and which contains, or is suspected of containing, radioactivity above the established natural background radioactivity. Because MNRC waste volumes are small and the nature of the waste items is limited and reasonably repetitive, there is usually little question about what is or is not radioactive waste. Equipment and components are categorized as waste by the reactor operations staff, while standard consumable supplies like plastic bags, gloves, absorbent material, disposable lab coats, etc., automatically become radioactive waste if detectable radioactivity above background is found to be present.

When possible, radioactive waste is initially segregated at the point of origin from items that will not be considered waste. Screening is based on the presence of detectable radioactivity using appropriate monitoring and detection techniques and on the projected future need for the items and materials involved. All items and materials initially categorized as radioactive waste are monitored a second time before packaging for disposal to confirm data needed for waste records, and to provide a final opportunity for decontamination/reclamation of an item. This helps reduce the volume of radioactive waste by eliminating disposal of items that can still be used.

#### 11.2.2.1 Gaseous Waste

Although Ar-41 is released from the MNRC stack in the facility ventilation exhaust, this release is not considered to be waste in the same sense as the solid waste which is collected and disposed of by the facility. The Ar-41 is usually classified as an effluent which is a routine part of the normal operation of the MNRC reactor. In the MNRC facility, as in many non-power reactors, there are no special off-gas collection systems for the Ar-41. Typically, this gas simply mixes with reactor room and other facility air and is discharged along with the normal ventilation exhaust.

A complete description of Ar-41 production, evolution from the reactor tank and discharge into the unrestricted environment is contained in Sections 11.1.2.1.1 through 11.1.2.1.4 and in Appendix A. Furthermore, a description of MNRC ventilation system features which minimize releases of airborne radioactivity is contained in Section 11.1.6.2.

#### 11.2.2.2 Liquid Waste

It is MNRC policy to minimize the release of radioactive liquid waste. Because normal MNRC operations create only small volumes of liquid which contain radioactivity, it has been possible to convert the liquids to a solid waste form and thus adhere to facility policy. In special cases, the MNRC may generate a large volume of radioactive liquid waste which cannot be converted to a solid waste. In these cases, disposal by the sanitary sewer in accordance with 10 CFR 20 may be required.

Section 11.1.2.2 describes the liquid radioactive sources associated with the MNRC reactor program . As indicated in Section 11.1.2.2, the reactor primary coolant is the only significant source. Since the primary coolant is by design contained to the maximum extent possible, there are no routine releases of this liquid and thus no significant volumes of liquid which require management as liquid waste. Certain maintenance operations, such as replacement of demineralizer resin bottles, result in very small amounts of primary coolant being drained from the water purification loop, but this liquid is easily collected at the point of origin and converted into an approved solid waste form. Other liquid radioactive waste sources such as laboratory wastes, decontamination solutions, and liquid spills have been very rare and easily within the capability of the health physics staff to convert to a solid.

Certain maintenance operations may generate a large volume of liquid waste, e.g., heat exchanger cleaning or activated concrete removal. In these cases, sewer disposal in accordance with 10 CFR 20 may be the only viable option for disposal. These cases are rare and still are not considered the norm.

#### 11.2.2.3 Solid Waste

The procedures for managing solid waste are specified in Section 11.2.1. As with most non-power reactors, solid waste is generated from reactor maintenance operations and irradiations of various experiments. A general idea of where solid waste enters the waste control program can be obtained from the preceding information. No solid radioactive waste is intended to be retained or permanently stored on site.

Appropriate radiation monitoring instrumentation will be used for identifying and segregating solid radioactive waste. Radioactive waste is packaged in metal drums or boxes within the restricted area of the MNRC and is temporarily stored in a weatherproof enclosure within the MNRC site boundary until shipment for disposal or transfer to a waste broker. Typically a single routine "B-25 box" shipment is made every 5 years.

As stated previously, minimization of radioactive waste is a policy of the MNRC. Although there are no numerical volume goals set due to the small volume of waste generated at the MNRC, the health physics supervisor and the reactor operations supervisor periodically assess operations for the purpose of identifying opportunities or new technologies that will reduce or eliminate the generation of radioactive waste. The NSC also conducts an annual audit of the waste minimization programs as described in Section 11.1.3.5.

### 11.2.3 Release of Radioactive Waste

The MNRC releases Ar-41 in the ventilation exhaust as a radioactive effluent. All of the details relating to the release and potential impact of Ar-41 have been discussed previously in Sections 11.1.2.1.1 through 11.1.2.1.4 and in Appendix A. Aside from the release of this radionuclide, which may or may not qualify as a “controlled release of radioactive waste,” and infrequent releases of liquid waste as described in Section 11.2.2.2, the MNRC does not plan any routine controlled releases of radioactive waste to the environment.

Normally, the only transfer of solid radioactive waste is to an authorized solid waste broker. However, the MNRC may opt to ship solid radioactive waste directly to a low-level radioactive waste disposal site without using a broker.

## **CHAPTER 12**

### **CONDUCT OF OPERATIONS**

Chapter 12 – Valid Pages  
Rev. 11 05/10/18

i	Rev. 11	05/10/18
ii	Rev. 11	05/10/18
iii	Rev. 11	05/10/18
12-1	Rev. 11	05/10/18
12-2	Rev. 11	05/10/18
12-3	Rev. 11	05/10/18
12-4	Rev. 11	05/10/18
12-5	Rev. 11	05/10/18
12-6	Rev. 11	05/10/18
12-7	Rev. 11	05/10/18
12-8	Rev. 11	05/10/18
12-9	Rev. 11	05/10/18
12-10	Rev. 11	05/10/18
12-11	Rev. 11	05/10/18
12-12	Rev. 11	05/10/18
12-13	Rev. 11	05/10/18
12-14	Rev. 11	05/10/18
12-15	Rev. 11	05/10/18
12-16	Rev. 11	05/10/18
12-17	Rev. 11	05/10/18
12-18	Rev. 11	05/10/18

## TABLE OF CONTENTS

12.0	CONDUCT OF OPERATIONS .....	12-1
12.1	Organization .....	12-1
12.1.1	Structure .....	12-1
12.1.2	Responsibility.....	12-4
12.1.3	Staffing.....	12-5
12.1.4	Selection and Training of Personnel.....	12-5
12.1.5	Radiation Safety.....	12-6
12.2	Review and Audit Activities .....	12-6
12.2.1	Composition and Qualifications .....	12-7
12.2.2	Charter and Rules .....	12-7
12.2.3	Review Function .....	12-8
12.2.4	Audit/Inspection Function.....	12-9
12.3	Procedures.....	12-9
12.3.1	Reactor Operations: .....	12-9
12.3.2	Health Physics.....	12-10
12.4	Required Action.....	12-11
12.4.1	Reportable Events .....	12-11
12.4.1.1	Safety Limit Violation.....	12-11
12.4.1.2	Release of Radioactivity.....	12-11
12.4.1.3	Special Reports .....	12-11
12.4.1.4	Other Reports .....	12-12
12.4.1.5	Annual Report.....	12-13
12.5	Records .....	12-14
12.5.1	Lifetime Records.....	12-14
12.5.2	Five Year Records .....	12-14
12.6	Emergency Planning .....	12-14
12.7	Security Planning .....	12-15
12.8	Quality Assurance.....	12-15
12.9	Operator Training and Requalification Program .....	12-16
12.10	Startup Plan .....	12-18
12.11	Environmental Reports.....	12-18

LIST OF FIGURES

12.1 UCD/MNRC ORGANIZATION ..... 12-2  
12.2 UCD/MNRC INTERNAL ORGANIZATION ..... 12-3

LIST OF REFERENCES

12.1 American National Standards Institute/American Nuclear Society, ANSI/ANS 15.1, "Development of Technical Specifications for Research Reactors," ANS, La Grange Park, Illinois, 1990.

12.2 American National Standards Institute/American Nuclear Society, ANSI/ANS 15.4, "Selection and Training of Personnel for Research Reactors," ANS, La Grange Park, Illinois, 1988.

12.3 American National Standards Institute/American Nuclear Society, ANSI/ANS 15.1 1, "Radiological Protection of Research Reactor Facilities," ANS, La Grange Park, Illinois, 1993.

12.4 American National Standards Institute/American Nuclear Society, ANSI/ANS 15.16, "Emergency Planning for Research Reactors," ANS, La Grange Park, Illinois, 1978.

12.5 American National Standards Institute/American Nuclear Society, ANSI/ANS, 15.8, "Quality Assurance Program Requirements for Research Reactors," ANS, La Grange Park, Illinois, 1996.

12.6 Environmental Assessment for the McClellan Nuclear Radiation Center Reactor Operation at 2 MW, July 1995.

## 12.0 CONDUCT OF OPERATIONS

This chapter describes and discusses the Conduct of Operations at the University of California-Davis/McClellan Nuclear Research Center (UCD/MNRC). The Conduct of Operations involves the administrative aspects of facility operations, the facility emergency plan, the security plan, the quality assurance plan, the reactor operator selection and re-qualification plan, the startup plan, and environmental reports. This chapter of the Safety Analysis Report (SAR) forms the basis of Section 6 of the Technical Specifications (Reference 12.1).

### 12.1 Organization

The UCD/MNRC Director reports directly to the UCD Vice Chancellor for Research. The UCD/MNRC is organized and administratively controlled as shown in Figures 12.1 and 12.2.

#### 12.1.1 Structure

The organizational structures in Figures 12.1 and 12.2 show the UCD/MNRC licensee as the UCD Vice Chancellor for Research. The UCD/MNRC facility is under the direct control of the UCD/MNRC Director. The Director reports to the UCD Vice Chancellor for Research for all nuclear safety and licensing issues.

Both the Reactor Supervisor and Radiation Safety Officer report to the UCD/MNRC Director. Both the Reactor Supervisor and the Radiation Safety Officer can go directly to the Nuclear Safety Committee (NSC) with nuclear or radiation safety concerns if they cannot resolve the issue with the UCD/MNRC Director.

The UCD/MNRC license to operate is issued by the United States Nuclear Regulatory Commission (USNRC). Licensing and reporting information goes from the UCD/MNRC Director through the UCD Vice Chancellor for Research to the USNRC.

The Vice Chancellor for Research has a Nuclear Safety Committee (NSC) that meets at least semi-annually. This committee performs the review and audit of nuclear operations for the Vice Chancellor and Director, and in some cases issues approvals of various specified activities. The committee also issues an annual audit report to the UCD/MNRC Director concerning the regulatory compliance and operation of the UCD/MNRC. The UCD/MNRC Director shall review the annual audit report with the licensee once each year.

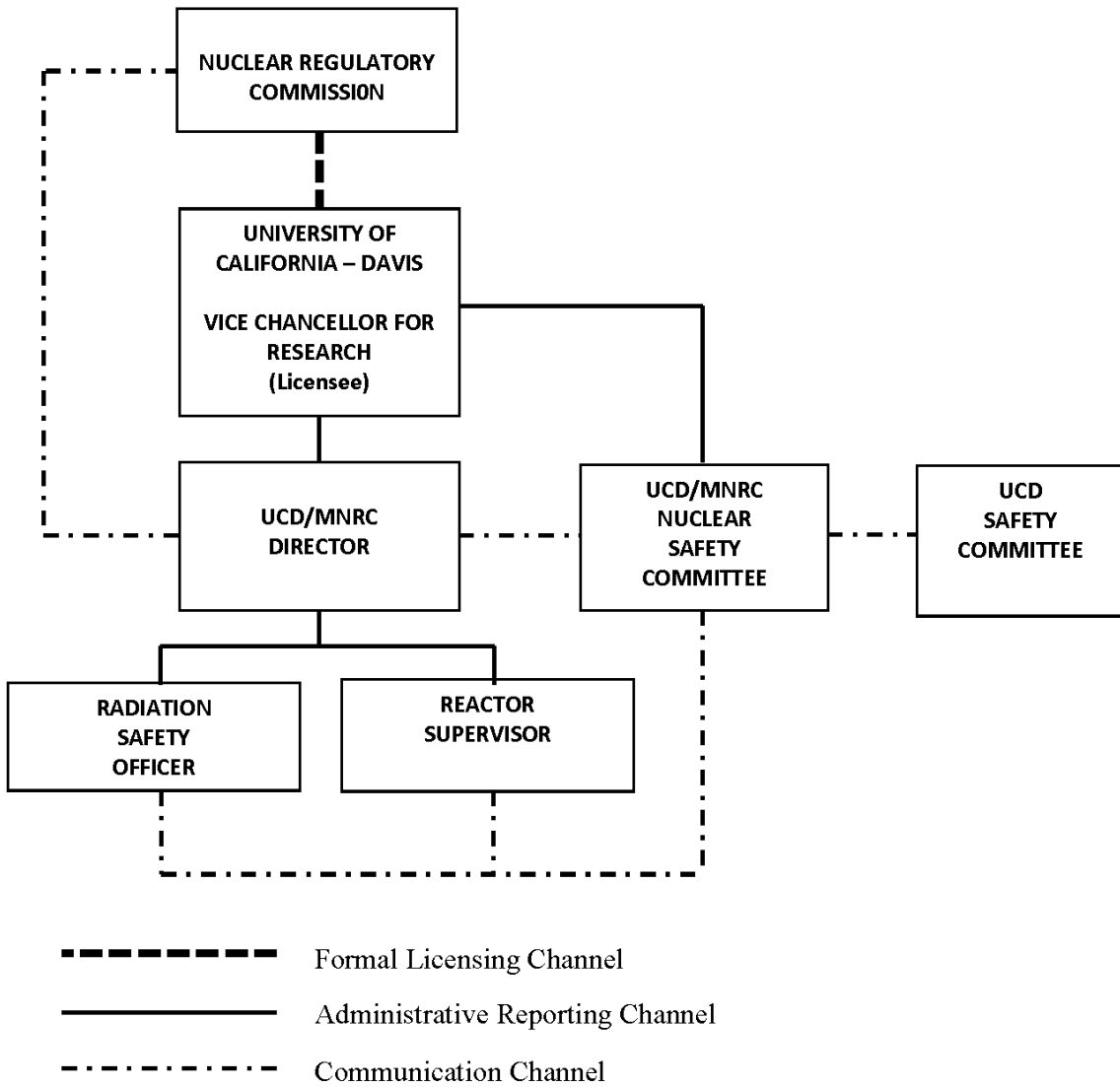


**FIGURE 12.1 UCD/MNRC ORGANIZATION**

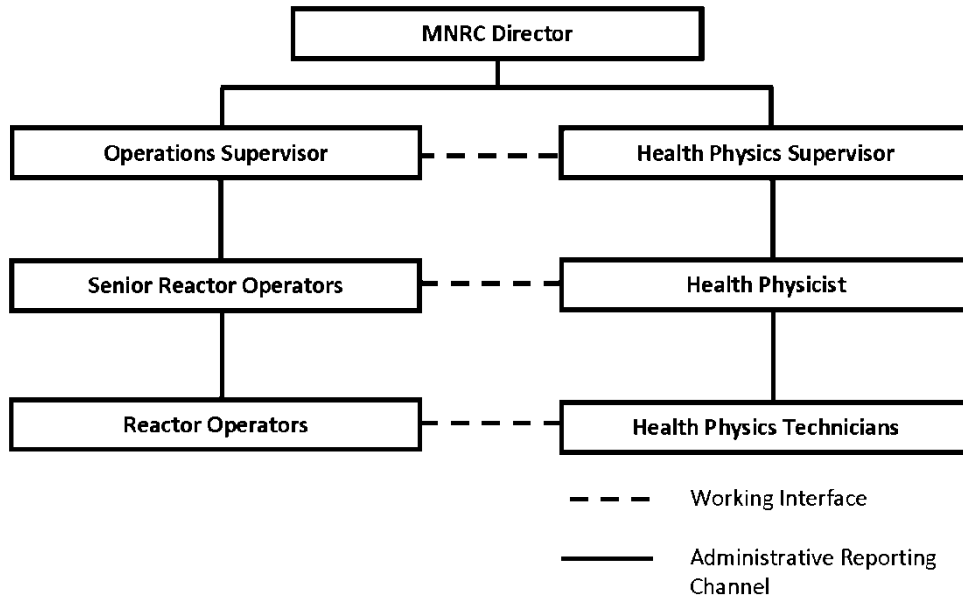


**FIGURE 12.2 UCD/MNRC INTERNAL ORGANIZATION**

### 12.1.2 Responsibility

- a. UCD Vice Chancellor for Research – The UCD Vice Chancellor for Research is accountable for ensuring compliance with all licensing requirements in accordance with the USNRC codes and guides. The UCD Vice Chancellor for Research has delegated the implementation and enforcement authority for these requirements to the UCD/MNRC Director.
- b. UCD/MNRC Director - The UCD/MNRC Director reports directly to the UCD Vice Chancellor for Research.
- c. Operations Supervisor (Reactor Supervisor) – The Reactor Supervisor is responsible to the UCD/MNRC Director. The Reactor Supervisor reports directly to the UCD/MNRC Director on all matters concerning the reactor. The Reactor Supervisor is responsible for directing the activities of Senior Reactor Operators and Reactor Operators, and for the day-to-day operation and maintenance of the reactor. The Reactor Supervisor shall be licensed as a Senior Reactor Operator.
- d. Health Physics Supervisor (Radiation Safety Officer) – The Radiation Safety Officer reports directly to the UCD/MNRC Director. The Radiation Safety Officer is responsible to the UCD/MNRC Director for directing the activities of Health Physics personnel, including development and implementation of the Radiation Safety Program.
- e. Senior Reactor Operator – Senior Reactor Operators report to the Reactor Supervisor. Senior Reactor Operators are responsible for directing the activities of Reactor Operators on their assigned shift. Senior Reactor Operators shall be licensed at the Senior Reactor Operator level.
- f. Health Physicist – The Health Physicist report to the Health Physics Supervisor. The Health Physicist is responsible for implementation of the Radiation Safety Program and for directing activities of the Health Physics Technicians.
- g. Reactor Operator – Reactor Operators report to the Senior Reactor Operator on their assigned shift. Reactor Operators are primarily involved in the manipulation of reactor controls, monitoring of instrumentation and operation and maintenance of reactor related equipment. Reactor Operators shall be licensed at the Reactor Operator level.
- h. Health Physics Technicians – Health Physics Technicians report to the Radiation Safety Officer. Health Physics Technicians are responsible for radiological monitoring, performing surveillance checks on radiological monitoring equipment throughout the UCD/MNRC facility, as well as taking environmental samples and providing radiological control oversight of operations involving radiation and/or contamination. Health Physics Technicians have the authority to interdict perceived unsafe practices.

### 12.1.3 Staffing

- a. A list of reactor facility personnel by name and telephone number is available in the reactor control room for use by the Reactor Operator whenever needed. The call list shall include:
  - (1) Management personnel
  - (2) Health Physics personnel; and
  - (3) Reactor Operations personnel
- b. Reactor operator trainees shall be permitted to manipulate the controls of the reactor under the direct supervision of Licensed Reactor Operators
- c. The minimum staffing when the reactor is not secured shall be:
  - (1) A reactor operator in the control room
  - (2) A second person in the facility area who can perform prescribed instructions
  - (3) A Senior Reactor Operator readily available. The available senior reactor operator should be within thirty (30) minutes of the facility and reachable by telephone and;
  - (4) A Senior Reactor Operator shall be present whenever a reactor startup is done, fuel is being moved or experiments are being placed in the reactor tank.

### 12.1.4 Selection and Training of Personnel

The UCD/MNRC Selection and Training Plan for Reactor Personnel (MNRC-009-DOC) contains the detailed information concerning the selection, training, licensing and re-qualification of reactor personnel. This plan addresses the qualifications, initial training, licensee responsibilities, and requalification of UCD/MNRC reactor operations personnel.

The UCD/MNRC training program complies with ANSI/ANS 15.4-1988 (Reference 12.2). The program's objective is to train, qualify, and re-qualify individuals for operation and maintenance of the reactor. The content of the training program covers the as-built and existing facility, significant facility modifications, current procedures, and administrative rules and regulations.

In addition to actual personnel training, Reactor Operators and Senior Reactor Operators are required to meet specific medical qualifications. The physical condition and the general health of UCD/MNRC reactor operations personnel shall be such that they are capable of properly operating under normal, abnormal and emergency conditions. The primary responsibility for assuring that medically qualified personnel are on duty rests with the UCD/MNRC Director. The health requirements set forth in the UCD/MNRC Selection and Training Plan for Reactor Personnel (MNRC-009-DOC) shall be used to determine the physical condition and general health of the individual. The designated medical examiner should be conversant with the medical requirements of this program.

In addition to the selection and training of reactor operations personnel, the UCD/MNRC provides formal annual training for all facility personnel in radiation protection topics, in items required by 10 CFR Part 19, in the As Low as Reasonably Achievable (ALARA) concept and in other related areas. The training is structured at different levels in order to meet the needs of different categories of facility staff and facility users. For more details in this aspect of UCD/MNRC personnel training, see Chapter 11, Section 11.1.3.4.

#### 12.1.5 Radiation Safety

The purpose of the Radiation Safety Program is to allow the maximum beneficial use of radiation sources with minimum radiation exposure to personnel. Requirements and procedures set forth in this program are designed to meet the following fundamental principles of radiation protection:

- Justification - No practice shall be adopted unless its introduction produces a net positive benefit
- Optimization - All exposures shall be kept as low as reasonably achievable
- Limitation – the dose equivalent to individuals shall not exceed limits established by appropriate state and federal agencies. These limits shall include, but not be limited to those set forth in the Federal Regulations

All personnel using radiation sources shall become familiar with the requirements of the Radiation Safety Program and conduct their operations in accordance with them.

The Radiation Safety Program uses Reference 12.3 as a guide.

The details of the Radiation Safety Program can be found in Chapter 11

#### 12.2 Review and Audit Activities

General Policy. It is the policy that nuclear facilities shall be designed, constructed, operated, and maintained in such a manner that facility personnel, the general public, and both university and non-university property are not exposed to undue risk. These activities shall be conducted in accordance with applicable government regulatory requirements.

The UCD Vice Chancellor for Research as the facility licensee has ultimate responsibility for assuring that the above policy is followed. The Nuclear Safety Committee (NSC) has been chartered to assist in meeting this responsibility by providing timely, objective, and independent reviews, audits, recommendations and approvals on matters affecting nuclear safety. The NSC is established in accordance with the guidance of Reference 12.1. The following describes the procedures, which govern the composition and conduct of the NSC.

### 12.2.1 Composition and Qualifications

The UCD/MNRC Vice Chancellor for Research shall appoint the chairman of the NSC. The NSC Chairman shall appoint a Nuclear Safety Committee of at least seven (7) members knowledgeable in fields which relate to nuclear safety.

### 12.2.2 Charter and Rules

The NSC shall conduct its review and audit/inspection functions in accordance with a written charter. This charter shall include provisions for:

- a. Meeting frequency (the committee shall meet at least semiannually);
- b. Voting rules
- c. Quorums
- d. A committee review function and an audit/inspection function;
- e. Use of subcommittees; and;
- f. Review, approval and dissemination for meeting minutes.

### 12.2.3 Review Function

The responsibilities of the NSC, or a designated subcommittee thereof, shall include but are not limited to the following:

- a. Review approved experiments utilizing UCD/MNRC nuclear facilities;
- b. Review and approve all proposed changes to the facility license, the Technical Specifications and the Safety Analysis Report, and any new or changed Facility Use Authorizations and proposed Class I modifications, prior to implementing (Class I) modifications, prior to taking action under the preceding documents or prior to forwarding any of these documents to the Nuclear Regulatory Commission for approval.
- c. Review and determine whether a proposed change, test, or experiment would constitute an un-reviewed safety question or require a change to the license, to a Facility Use Authorization, or to the Technical Specifications. This determination may be in the form of verifying a decision already made by the UCD/MNRC Director;
- d. Review reactor operations and operational maintenance, Class I modification records, and the health physics program and associated records for all UCD/MNRC nuclear facilities
- e. Review the periodic updates of the Emergency Plan and Physical Security Plan for UCD/MNRC nuclear facilities
- f. Review and update the NSC Charter every two (2) years;
- g. Review abnormal performance of facility equipment and operating anomalies;
- h. Review all reportable occurrences and all written reports of such occurrences prior to forwarding the final written report to the Nuclear Regulatory Commission; and
- i. Review the NSC annual audit/inspection of the UCD/MNRC nuclear facilities and any other inspections of these facilities conducted by other agencies.

#### 12.2.4 Audit/Inspection Function

The NSC, or a subcommittee thereof, shall audit/inspect reactor operations and health physics annually. The annual audit/inspection shall include, but not be limited to the following:

- a. Inspection of the reactor operations and operational maintenance, Class I modification records, and the health physics program and associated records, including the ALARA program, for all UCD/MNRC nuclear facilities;
- b. Inspection of the physical facilities at the UCD/MNRC;
- c. Examination of reportable events at the UCD/MNRC;
- d. Determination of the adequacy of UCD/MNRC standard operating procedures;
- e. Assessment of the effectiveness of the training and retraining programs at the UCD/MNRC;
- f. Determination of the conformance of operations at the UCD/MNRC with the facility's license and Technical Specifications, and applicable regulations;
- g. Assessment of the results of actions taken to correct deficiencies that have occurred in nuclear safety related equipment, structures, systems, or methods of operation;
- h. Inspection of the currently active Facility Use Authorizations and associated experiments;
- i. Inspection of future plans for facility modifications or facility utilization;
- j. Assessment of operating abnormalities; and
- k. Determination of the status of previous NSC recommendations.

#### 12.3 Procedures

Written procedures shall be prepared and approved prior to initiating any of the activities listed in this section. The procedures shall be approved by the UCD/MNRC Director. A periodic review of procedures will be performed and documented in a timely manner to assure they are current. Procedures shall be adequate to assure the safe operation of the reactor, but will not preclude the use of independent judgment and action should the situation require. The following sections list UCD/MNRC programs that will typically require reviewed written procedures.

##### 12.3.1 Reactor Operations:

- a. Startup, operation, and shutdown of the reactor;
- b. Fuel loading, unloading, and movement within the reactor;

- c. Control rod removal or replacement;
- d. Routine maintenance of the control rod drives and reactor safety and interlock systems or other routine maintenance that could have an effect on reactor safety;
- e. Testing and calibration of reactor instrumentation and controls, control rods and control rod drives;
- f. Administrative controls for operations, maintenance, and conduct of irradiations and experiments that could affect reactor safety or core reactivity.
- g. Implementation of required plans such as emergency or security plans; and
- h. Actions to be taken to correct specific and foreseen potential malfunctions of systems, including responses to alarms and abnormal reactivity changes.

#### 12.3.2 Health Physics

- a. Testing and calibration of area radiation monitors, facility air monitors, laboratory radiation detection systems, and portable radiation monitoring instrumentation;
- b. Working in laboratories and other areas where radioactive materials are used;
- c. Facility radiation monitoring program including routine and special surveys, personnel monitoring, monitoring and handling of radioactive waste, and sampling and analysis of solid and liquid waste, and gaseous effluents released from the facility;
- d. Monitoring radioactivity in the environment surrounding the facility;
- e. Administrative guidelines for the facility radiation protection program to include personnel orientation and training;
- f. Receipt of radioactive materials at the facility, and unrestricted release of materials and items from the facility, which may contain induced radioactivity or radioactive contamination;
- g. Leak testing of sealed sources containing radioactive materials;
- h. Special nuclear material accountability; and
- i. Transportation of radioactive materials.

Changes to the written procedures of the above programs shall require approval of the UCD/MNRC Director. All such changes shall be documented.

## 12.4 Required Action

### 12.4.1 Reportable Events

#### 12.4.1.1 Safety Limit Violation

Actions to be taken in the case of a safety limit violation shall include cessation of reactor operations until resumption is authorized by the licensing authority, a prompt report of the violation to the licensing authorities and to the licensee, and a subsequent follow-up report which shall be reviewed by the NSC and then submitted to the licensing authority.

The follow-up report shall describe applicable circumstances leading to the violation, including causes and contributing factors that are known, effect of the violation upon reactor facility components, systems or structures, health and safety of personnel and the public, and corrective actions to prevent recurrence. Prompt reporting of the event shall be by telephone and confirmed by written correspondence within 24 hours. A written report is to be submitted within 14 days.

#### 12.4.1.2 Release of Radioactivity

Actions to be taken in the event of a release of radioactivity from the operations boundary above allowable limits shall include returning the reactor to normal operating conditions or, if necessary to correct the occurrence, a reactor shutdown and no return to normal operation until authorized by the UCD/MNRC Director. There will also be a report to the licensee and licensing authority, and a review of the event and applicable reports by the NSC prior to submission of the required reports. Prompt reporting of the event shall be by telephone or similar conveyance within 24 hours to the NRC Operations Center. A written report is to be submitted to the NRC Document Control Desk, Washington, D.C. within 14 days.

#### 12.4.1.3 Special Reports

Other events that will be considered reportable events are listed in this section. Appropriate reports shall be submitted to licensing authorities and such reports shall be reviewed by the NSC prior to submission. (Note: Where components or systems are provided in addition to those required by the Technical Specifications, the failure of these components or systems is not considered reportable provided that the minimum number of components or systems specified or required perform their intended reactor safety function.)

Special reports are used to report unplanned events as well as planned major facility and administrative changes. The following classifications shall be used to determine the appropriate reporting schedule:

- a. A report within 24 hours by telephone or similar conveyance to the NRC operations center of:
  - (1) Any accidental release of radioactivity into unrestricted areas above applicable unrestricted area concentration limits, whether or not the release resulted in property damage, personal injury, or exposure;
  - (2) Any violation of a safety limit;

- (3) Operation with a limiting safety system setting less conservative than specified;
  - (4) Operation in violation of a Limiting Condition for Operation;
  - (5) Failure of a required reactor or experiment safety system component which could render the system incapable of performing its intended safety function unless the failure is discovered during maintenance tests or a period of reactor shutdown;
  - (6) Any unanticipated or uncontrolled change in reactivity greater than \$1.00;
  - (7) An observed inadequacy in the implementation of either administrative or procedural controls, such that the inadequacy could have caused the existence or development of a condition which could have resulted in operation of the reactor outside the specified safety limits and;
  - (8) A measureable release of fission products from a fuel element.
- b. A report within 14 days in writing to the NRC, Document Control Desk, Washington DC:
- (1) Those events reported as required by Sections a. (1) through a. (8) above; and
  - (2) The written report (and, to the extent possible, the preliminary telephone report or report by similar conveyance) shall describe, analyze, and evaluate safety implications, and outline the corrective measures taken or planned to prevent recurrence of the event.

#### 12.4.1.4 Other Reports

A written report shall be submitted within thirty (30) days to the NRC, Document Control Desk, Washington DC as a result of the following conditions:

- a. Any significant variation of measured values from a corresponding predicted or previously measured value of safety-connected operating characteristics occurring during operation of the reactor;
- b. Any significant change in the transient or accident analysis as described in the Safety Analysis Report (SAR);
- c. A personnel change involving the positions of UCD/MNRC Director or UCD Vice Chancellor for Research; and
- d. Any observed inadequacies in the implementation of administrative or procedural controls such that the inadequacy causes or could have caused an existence or development of an unsafe condition with regard to reactor operations.

#### 12.4.1.5 Annual Report

An annual report covering the activities of the reactor facility during the previous calendar year shall be submitted within six months following the end of each calendar year. Each annual report shall include the following information:

- a. A brief summary of operating experiences including experiments performed, changes in facility design, performance characteristics and operating procedures related to reactor safety occurring during the reporting period, and results of surveillance tests and inspections;
- b. A tabulation showing the energy generated by the reactor (in megawatt hours), hours the reactor was critical, and the cumulative total energy output since initial criticality;
- c. The number of emergency shutdowns and inadvertent scrams, including reasons for the shutdowns or scrams;
- d. Discussion of the major maintenance operations performed during the period, including the effect, if any, on the safety of the operation of the reactor and the reasons for any corrective maintenance required;
- e. A brief description, including a summary of the safety evaluations, of changes in the facility or in procedures, and of tests and experiments carried out pursuant to Section 50.59 of 10 CFR Part 50;
- f. A summary of the nature and amount of radioactive effluents released or discharged to the environment beyond the effective control of the licensee as measured at or prior to the point of such release or discharge;
- g. An annual summary of the radiation exposure received by facility operations personnel, by facility users, and by visitors in terms of the average radiation exposure per individual and the greatest exposure per individual in each group;
- h. An annual summary of the radiation levels and levels of contamination observed during routine surveys performed at the facility in terms of average and highest levels; and
- i. An annual summary of any environmental surveys performed outside the facility.

## 12.5 Records

Records of the following activities shall be maintained and retained for the periods specified below. The records may be in the form of logs, data sheets, or other suitable forms. The required information may be contained in single or multiple records, or a combination thereof.

### 12.5.1 Lifetime Records

Lifetime records are records to be retained for the lifetime of the reactor facility. (Note: Applicable annual reports, if they contain all of the required information, may be used as records in this section.) The following are examples of lifetime records:

- a. Offsite environmental monitoring surveys;
- b. Fuel inventories and transfers;
- c. Facility radiation and contamination surveys;
- e. Radiations exposures for all personnel and;
- f. Update, corrected and as-built drawings of the facility

### 12.5.2 Five Year Records

Records which are to be retained for a period of at least five years or for the life of the component involved whichever is shorter are as follows:

- a. Normal reactor operation;
- b. Principal maintenance activities
- c. Those events reported as required by Section 12.4.1
- d. Equipment and component surveillance activities required by the Technical Specifications;
- e. Experiments performed with the reactor; and
- f. Airborne and liquid radioactive effluents released to the environments and solid radioactive waste shipped off site.

## 12.6 Emergency Planning

The UCD/MNRC Emergency Plan (MNRC-001-DOC) contains detailed information concerning the UCD/MNRC response to emergency situations. The UCD/MNRC Emergency Plan is written to be in accordance with Reference 12.4. The information below will give a general overview of the emergency plan.

The UCD/MNRC Emergency Plan is designed to provide response capabilities to emergency situations involving the UCD/MNRC. The plan deals with the UCD/MNRC Facility, the spectrum of emergency situations and accident conditions that could arise within the facility, and the associated

emergency responses that are required due to the unique nature of the reactor facility. Detailed emergency implementing procedures referenced in this plan. This approach provides the UCD/MNRC facility emergency staff the flexibility to cope with a wide range of emergency situations without requiring frequent revisions to the plan.

The responsibility for the plan rests with the UCD/MNRC Director who is also responsible for response to and recovery from emergencies. Implementation of the UCD/MNRC Emergency Plan on a day-to-day basis is the responsibility of the Senior Reactor Operator (SRO) on duty.

Provisions for reviewing, modifying, and approving emergency implementation procedures are defined in the UCD/MNRC Emergency Plan to assure that adequate measures to protect the staff and the general public are in effect at all times.

#### 12.7 Security Planning

The UCD/MNRC Physical Security Plan (MNRC-003-DOC) contains detailed information concerning the UCD/MNRC security measures. The information below will give a general overview of this plan.

The UCD/MNRC Physical Security Plan provides the criteria and actions for protecting the facility from acts of intrusion, theft, civil disorder and bomb threats.

Overall responsibility for facility security rests with the UCD/MNRC Director, who is responsible for implementation of the plan. Implementation of the security plan on a day-to-day basis during hours of operation is the responsibility of the Senior Reactor Operator (SRO) on duty.

#### 12.8 Quality Assurance

The UCD/MNRC Quality Assurance (QA) Program (MNRC-0045-DOC) contains detailed information concerning the UCD/MNRC QA Program elements and their implementation.

The UCD/MNRC QA Program provides criteria for design, construction, operation, and decommissioning of the UCD/MNRC reactor facility. The level of QA effort applied to UCD/MNRC reactor activities is consistent with the importance of these activities to safety. The activities included in the UCD/MNRC QA Program are those related to reactor safety and applicable radiation monitoring systems. The specific elements of the UCD/MNRC QA Program are the same as those listed in Reference 12.5.

## 12.9 Operator Training and Requalification Program

The UCD/MNRC Selection and Training Plan for Reactor Personnel (MNRC-009-DOC) has been established to train, qualify, and re-qualify individuals for operation and maintenance of the reactor. The content of the training shall cover the as-built and existing facility, significant facility modifications, current procedures, and administrative rules and regulations (Reference 12.2).

The program shall carry the trainee through documented stages of academic training and on-the-job training. The intended results shall be a candidate who anticipates conditions, who communicates well and who can accomplish required tasks during normal and abnormal operational situations. Licensing of a candidate is achieved after successful completion of the training and the following examinations. Written examinations covering the following categories shall be passed:

- a. Nuclear Theory and Principles of Operation;
- b. Facility Design and Operating Characteristics;
- c. Facility Instrumentation and Control Systems;
- d. Normal, Abnormal and Emergency Procedures;
- e. Radiological Control and Safety;
- g. Technical Specifications, to include bases for Senior Reactor Operator candidates;
- h. Fuel Handling; and
- i. Administrative Controls, Procedures and Regulations.

The minimum acceptance score in any category shall be established. Failures in no more than two categories can be made up by re-examination in only those categories. Failure in more than two categories requires repeating the entire examination. Regardless of the test results, if the individual's test record indicates a deficiency in a critical area that affects safety, security or operational functions, a remedial training program shall be administered to promptly correct the critical deficiency.

The objective of the re-qualification program is to refresh reactor operator's knowledge in areas of infrequent operation, to review facility and procedural changes, to address subject matter not reinforced by direct use, and to improve performance weaknesses. The program shall be designed to evaluate an operator's knowledge and proficiency for his duties. The program shall take into account the specialized nature and mode of operation of the UCD/MNRC reactor, and the background, skill, degree of responsibility, and participation of UCD/MNRC reactor operations personnel in activities related to reactor operations.

The requalification program shall consist of the following items:

- Schedule: The requalification program shall be conducted over a period not to exceed 24 months to be followed by successive two-year programs;
- Content: To formulate the basis for determining the contents of the re-qualification program, changes in jobs, tasks, and participation in related activities should be periodically reviewed. The following shall be adhered to:

1. Lectures: The re-qualification program shall include preplanned lectures in the categories listed in 12.9;
2. On the Job Training: To maintain active status, each licensed reactor operator shall manipulate the reactor controls and each licensed senior reactor operator shall either manipulate the reactor controls or direct the activities of individuals during reactor control manipulations for a minimum of four hours per calendar quarter;
3. Comprehensive Written Examination: A comprehensive written examination covering the categories listed in 12.9 shall be administered biennially to determine whether weaknesses exist and to identify categories for which retraining and retesting may be required;
4. Annual Operating Examination: An operational examination shall be given annually that requires the Senior Reactor Operator and the Reactor Operator to demonstrate an understanding of, and the ability to perform, the actions necessary to accomplish a comprehensive sample of the items listed below:
  - a. Perform pre-startup procedures for the facility;
  - b. Manipulate the console controls as required to operate the facility during normal, abnormal and emergency conditions;
  - c. Identify annunciators and condition indicating signals and perform appropriate remedial actions;
  - d. Identify the instrumentation systems and their significance;
  - e. Describe the function of the facility's radiation monitoring system as it pertains to reactor operations;
  - f. Demonstrate knowledge of significant radiation hazards and the steps taken to reduce personnel exposure;
  - g. Demonstrate knowledge of the facility emergency plan including, as appropriate, the Senior Reactor Operator's or Reactor Operator's responsibility to decide whether the plan should be executed and the duties under the plan
  - h. Demonstrate that the Senior Reactor Operator or Reactor Operator can function in the control room in such a way that the facility licensee's procedures are adhered to and that the limitations in its license and amendments are not violated;

5. Licensed operators shall be trained on changes to the facility and facility documentation, including Technical Specifications and procedures, before performing licensed duties that are affected by the changes; and
  6. All licensed operators shall review the contents of all normal, abnormal, and emergency procedures on an annual basis
- Absence from Licensed Functions: An individual who has not actively performed licensed functions for four (4) hours per calendar quarter shall demonstrate to the Reactor Supervisor or the UCD/MNRC Director that his/her knowledge and understanding of the operation and administration of the UCD/MNRC facility are satisfactory before returning to licensed duties. This shall be accomplished through an interview and evaluation or a written or operational examination or a combination thereof. The individual shall be required to perform a minimum of six (6) hours of shift functions under the direction of a Senior Reactor Operator before returning to licensed duties.

Re-qualification examinations shall be administered by individuals knowledgeable of the UCD/MNRC operation.

#### 12.10 Startup Plan

A start up plan is not required as this is not a new facility nor does this license renewal application request authorization of modifications that require verification of operability before normal operations are resumed.

#### 12.11 Environmental Reports

An Environmental Assessment (EA) for the UCD/MNRC reactor operating license renewal application was prepared and was provided to the NRC staff separately.

**CHAPTER 13**

**ACCIDENT ANALYSIS**

Chapter 13 - Valid Pages  
Rev. 10 05/11/18

i	Rev. 10	05/11/18	13-38	Rev. 10	05/11/18
ii	Rev. 10	05/11/18	13-39	Rev. 10	05/11/18
iii	Rev. 10	05/11/18	13-40	Rev. 10	05/11/18
iv	Rev. 10	05/11/18	13-41	Rev. 10	05/11/18
v	Rev. 10	05/11/18	13-42	Rev. 10	05/11/18
13-1	Rev. 10	05/11/18	13-43	Rev. 10	05/11/18
13-2	Rev. 10	05/11/18	13-44	Rev. 10	05/11/18
13-3	Rev. 10	05/11/18	13-45	Rev. 10	05/11/18
13-4	Rev. 10	05/11/18	13-46	Rev. 10	05/11/18
13-5	Rev. 10	05/11/18			
13-6	Rev. 10	05/11/18			
13-7	Rev. 10	05/11/18			
13-8	Rev. 10	05/11/18			
13-9	Rev. 10	05/11/18			
13-10	Rev. 10	05/11/18			
13-11	Rev. 10	05/11/18			
13-12	Rev. 10	05/11/18			
13-13	Rev. 10	05/11/18			
13-14	Rev. 10	05/11/18			
13-15	Rev. 10	05/11/18			
13-16	Rev. 10	05/11/18			
13-17	Rev. 10	05/11/18			
13-18	Rev. 10	05/11/18			
13-19	Rev. 10	05/11/18			
13-20	Rev. 10	05/11/18			
13-21	Rev. 10	05/11/18			
13-22	Rev. 10	05/11/18			
13-23	Rev. 10	05/11/18			
13-24	Rev. 10	05/11/18			
13-25	Rev. 10	05/11/18			
13-26	Rev. 10	05/11/18			
13-27	Rev. 10	05/11/18			
13-28	Rev. 10	05/11/18			
13-29	Rev. 10	05/11/18			
13-30	Rev. 10	05/11/18			
13-31	Rev. 10	05/11/18			
13-32	Rev. 10	05/11/18			
13-33	Rev. 10	05/11/18			
13-34	Rev. 10	05/11/18			
13-35	Rev. 10	05/11/18			
13-36	Rev. 10	05/11/18			
13-37	Rev. 10	05/11/18			

TABLE OF CONTENTS

13.0	ACCIDENT ANALYSIS .....	13-13-1
13.1	Introduction.....	13-13-1
13.2	Accident Initiating Events and Scenarios, Accident Analysis, and Determination of Consequences .....	13-13-2
13.2.1	Maximum Hypothetical Accident.....	13-13-2
13.2.1.1	Accident Initiating Events and Scenario.....	13-13-2
13.2.1.2	Accident Analysis and Determination of Consequences.....	13-13-3
13.2.2	Insertion of Excess Reactivity.....	13-13-5
13.2.2.1	Accident Initiating Events and Scenarios .....	13-13-5
13.2.2.2	Accident Analysis and Determination of Consequences.....	13-13-6
13.2.2.2.1	Maximum Reactivity Insertion.....	13-13-6
13.2.2.2.2	Uncontrolled Withdrawal of a Control Rod .....	13-13-9
13.2.2.2.3	Uncontrolled Withdrawal of All Control Rods .....	13-13-10
13.2.2.2.4	Beam Tube Flooding or Removal.....	13-13-11
13.2.2.2.5	Metal-water Reactions .....	13-13-11
13.2.3	Loss of Coolant Accident (LOCA).....	13-13-12
13.2.3.1	Accident Initiating Events and Scenarios .....	13-13-12
13.2.3.2	Accident Analysis and Determination of Consequences.....	13-13-12
13.2.3.2.1	Pumping of Water from the Reactor Tank.....	13-13-12
13.2.3.2.2	Reactor Tank Failure .....	13-13-12
13.2.3.2.2.1	Description of ECCS and Assumptions .....	13-13-14
13.2.3.2.2.2	Spray Cooling.....	13-13-15
13.2.3.2.2.3	Air Cooling .....	13-13-15
13.2.3.2.2.4	Assumptions Made for ECCS Operation .....	13-13-16
13.2.3.2.2.5	Performance of the ECCS.....	13-13-16
13.2.3.2.2.6	Thermal Model for Natural Convection Air Cooling .....	13-13-17
13.2.3.2.2.7	Reactor Core for LOCA.....	13-13-18
13.2.3.2.2.8	Mixed Air Temperature in the Reactor Room.....	13-13-18
13.2.3.2.2.9	Results of ECCS Calculations .....	13-13-20
13.2.3.2.2.10	Cladding Stress Analysis .....	13-13-24
13.2.3.2.2.11	Ground Water Contamination.....	13-13-24
13.2.3.2.2.12	Radiation Levels from the Uncovered Core .....	13-13-29
13.2.4	Loss of Coolant Flow .....	13-13-31

13.2.4.1	Accident Initiating Events and Scenarios .....	13-13-31
13.2.4.2	Accident Analysis and Determination of Consequences .....	13-13-32
13.2.4.2.1	Loss of Coolant Flow Without Immediate Operator Action .....	13-13-32
13.2.5	Mishandling or Malfunction of Fuel .....	13-13-32
13.2.5.1	Accident Initiating Events and Scenarios .....	13-13-32
13.2.5.2	Accident Analysis and Determination of Consequences .....	13-13-33
13.2.5.2.1	Single Element Failure in Water .....	13-13-33
13.2.5.2.2	Fuel Loading Error .....	13-13-36
13.2.5.2.2.1	1998 Fuel Loading Error .....	13-13-36
13.2.5.2.2.2	Current 30B Fuel Loading Error .....	13-13-37
13.2.6	Experiment Malfunction .....	13-13-38
13.2.6.1	Accident Initiating Events and Scenario .....	13-13-38
13.2.6.2	Accident Analysis and Determination of Consequences .....	13-13-38
13.2.7	Loss of Normal Electrical Power .....	13-13-45
13.2.7.1	Accident Initiating Events and Scenarios .....	13-13-45
13.2.7.2	Accident Analysis and Determination of Consequences .....	13-13-45
13.2.8	External Events .....	13-13-47
13.2.8.1	Accident Initiating Events and Scenarios .....	13-13-47
13.2.8.2	Accident Analysis and Determination of Consequences .....	13-13-47
13.2.9	Mishandling of Malfunction of Equipment .....	13-13-47
13.2.9.1	Accident Initiating Events and Scenarios .....	13-13-47
13.3	Summary and Conclusions .....	13-13-48

#### LIST OF FIGURES

13.1	Prompt Negative Temperature Coefficient For TRIGA® Fuels .....	13-13-8
13.2	Axial Power Distribution For Fuel In Core 20E .....	13-13-19
13.3	Maximum And Average Fuel Temperature During Air Cooling Cycle For Various Spray Cooling Times .....	13-13-21
13.4	Maximum And Average Fuel Temperatures For The Hottest Fuel Element As Functions Of Time After End Of Spray Cooling For Three Hours .....	13-13-22
13.5	Clad Strength And Applied Stress Resulting From Equilibrium Hydrogen Dissociation Pressure as a Function Of Temperature .....	13-13-25
13.6	Maximum And Average Fuel Temperatures For The Hottest Fuel Element as Functions Of Time After End Of Spray Cooling For 3.7 Hours .....	13-13-26

LIST OF TABLES

13-1	Occupational Radiation Doses In The UCD/MNRC Reactor Room Following The Maximum Hypothetical Accident. ....	13-4
13-2	Radiation Doses To Members Of The General Public Under The Most Conservative Atmospheric Conditions (Pasquill F) At Different Distances From The UCD/MNRC Following A Fuel Element Cladding Failure In Air With No Decay (The MHA). ....	13-5
13-3	Maximum Reactivity Insertion And Related Quantities For Various Fuels And Burnups.....	13-7
13-4	Maximum Fuel Temperatures With Various Chimney Heights .....	13-23
13-5	Comparison Of Cooling Results With 2 Ft. And 3 Ft. Chimneys .....	13-23
13-6	Predominant Radionuclides In Primary Coolant At Equilibrium And Upon Reaching Ground Water.....	13-28
13-7	Dose Rates On The UCD/MNRC Reactor Top After A Loss Of Pool Water Accident Following 2 MW Operations.....	13-29
13-8	Scattered Radiation Dose Rates In The UCD/MNRC Reactor Room After A Loss Of Pool Water Accident Following 2 MW Operations.....	13-30
13-9	Scattered Radiation Dose Rates At The UCD/MNRC Facility Fence After A Loss Of Pool Water Accident Following 2 MW Operations .....	13-30
13-10	Occupational Radiation Doses In The UCD/MNRC Reactor Room Following A Single Element Failure In Water.....	13-35
13-11	Radiation Doses To Members Of The General Public Under Different Atmospheric Conditions And At Different Distances From The UCD/MNRC Following A Cladding Failure In Water 48 Hours After Reactor Shutdown. ....	13-36
13-12	Material Strengths.....	13-40
13-13	Container Diameter To Thickness Ratio .....	13-41
13-14	Changes To Beam Tube Cover Plates .....	13-43

REFERENCES

- 13.1 Credible Accident Analyses for TRIGA<sup>®</sup> and TRIGA<sup>®</sup>-Fueled Reactors. NUREG/CR-2387, PNL-4028, April 1982.
- 13.2 Guidelines for Preparing and Reviewing Applications for the Licensing of Non-Power Reactors, Format and Content, NUREG-1537, Part 1, February 1996.
- 13.3 SRA (Shonka Research Associates, Inc.), Software Verification and Validation Report for the WINCO RSAC-5 Code, Marietta, GA, 1993.
- 13.4 ANSI/ANS 10.4, "American National Standard Guidelines for the Verification and Validation of Scientific and Engineering Programs for the Nuclear Industry," 1987.
- 13.5 Research Reactor Core Conversion Guidebook, IAEA-TECDOC-643, April 1992; reprinted as UZR-27 by General Atomics.
- 13.6 Saphier, D., "The Simulation Language of DSNP," ANL-CT-77-20, Rev. 02, Argonne National Laboratory, 1978.
- 13.7 GA Report, "Low Enriched TRIGA<sup>®</sup> Fuel-Water Quench Safety Test," GA-A15413.
- 13.8 Larsen, G. G., "An Analysis of Heat Transfer Data for Spray-Cooled Rods," Nuclear Safety 9, No. 1 (Jan.-Feb. 1968), and Hideo, Uchida, "Experimental Investigation of Core Spray," Nuclear Safety 7, No. 3 (Spring 1966).
- 13.9 Jensen, R. T., "Experimental Evaluation of Emergency Core Spray Cooling Performance," USAEC Report IDO-17249, Phillips Petroleum Co., March 1968.
- 13.10 Sharp, R., "TRIGA<sup>®</sup> Emergency Spray Cooling Experiment," Gulf Energy & Environmental System Report GA-10521, March 31, 1971.
- 13.11 Razvi, J., Sorrento Electronics, Personal Communication to W. Richards, "Additional Information related to ECCS," April 4, 1997.
- 13.12 Boonstra, R. H., "TAC2D, A General Purpose Two-Dimensional Heat Transfer Computer Code - User's Manual," General Atomics Report GA-A 14032 (15 July 1976).
- 13.13 Schaefer, Bob (ANL-West) to Dan Newell (MNRC), "Power by Element in 20E with AL/C Plug," e-mail communications (Dec. 11 & 12, 1996).

- 13.14 Engineering Science, 1983, "Final Report Installation Restoration Program, Phase II, ...Confirmation," Vol. 1, June, Prepared for the U.S. Air Force, McClellan Air Force Base, Sacramento, CA.
- 13.15 Safety Analysis Report, TRIGA<sup>®</sup> Reactor Facility, University of Texas at Austin, May 1991.
- 13.16 10 CFR 50.59 Safety Analysis of Explosive Limits for Radiography Bays 1, 2, 3, and 4, McClellan Nuclear Radiation Center, Sacramento, CA., 1996.
- 13.17 Southwest Research Institute, "Safety Analysis To Determine Limiting Criteria for Explosives in Bay 3 of the McClellan Nuclear Radiation Center," September 1995.
- 13.18 Liu, H. Ben, "Safety Analysis for the Central Irradiation Facility (CIF) at the MNRC," Memorandum to Wade J. Richards, September 22, 1998.
- 13.19 Strohmayer, W.H., and M.G. Stamatelatos, "Probabilistic Assessment of the Airplane Crash Risk for the McClellan Air Force Base TRIGA<sup>®</sup> Reactor," G.A. Technologies, March 1986.

## 13.0 ACCIDENT ANALYSIS

### 13.1 Introduction

In about 1980, the U.S. Nuclear Regulatory Commission requested an independent and fresh overview analysis of credible accidents for TRIGA<sup>®</sup> and TRIGA<sup>®</sup>-fueled reactors. Such an analysis was considered desirable since safety and licensing concepts had changed over the years. The study resulted in NUREG/CR-2387, Credible Accident Analysis for TRIGA<sup>®</sup> and TRIGA<sup>®</sup>-fueled Reactors (Reference 13.1). The information developed by the TRIGA<sup>®</sup> experience base and appropriate information from NUREG/CR-2387 serve as a basis for some of the information presented in this chapter of the UCD/MNRC Safety Analysis Report.

The reactor physics and thermal-hydraulic conditions in the UCD/MNRC TRIGA<sup>®</sup> reactor at a power level of 2 MW are established in Chapter 4. The core physics analysis demonstrates that the fundamental physical conditions in the UCD/MNRC reactor are preserved by an appropriate choice of the composition of mixed TRIGA<sup>®</sup> fueled cores.

The fuel temperature is a limit in both steady-state and pulse mode operation. This limit stems from the out-gassing of hydrogen from U-ZrH fuel and the subsequent stress produced in the fuel element cladding material. The strength of the cladding as a function of temperature sets the upper limit on the fuel temperature. Fuel temperature limits of 1100°C (with clad <500°C) and 930°C (with clad >500°C) for U-ZrH with a H/Zr ratio less than 1.70 have been set to preclude the loss of clad integrity (Section 4.5.4.1.3).

Nine credible accidents for research reactors were identified in NUREG-1537 (Reference 13.2) as follows:

- the maximum hypothetical accident (MHA);
- insertion of excess reactivity;
- loss of coolant accident (LOCA);
- loss of coolant flow;
- mishandling or malfunction of fuel;
- experiment malfunction;
- loss of normal electrical power;
- external events;
- mishandling or malfunction of equipment.

This chapter contains analyses of postulated accidents that have been categorized into one of the above nine groups. Some categories do not contain accidents which appeared applicable or credible for the UCD/MNRC TRIGA® reactor, but this was acknowledged in a brief discussion of the category. Some categories contain an analysis of more than one accident even though one is usually limiting in terms of impact. Any accident having significant radiological consequences was included.

For those events that do result in the release of radioactive materials from fuel, only a qualitative evaluation of the event is presented. Events leading to the release of radioactive material from a fuel element were analyzed to the point where it was possible to reach the conclusion that a particular event was, or was not, the limiting event in that accident category. The maximum hypothetical accident (MHA) for TRIGA® reactors is the cladding failure of a single irradiated element in air with no radioactive decay of contained fission products. Calculations supporting the analysis of this accident and several of the other accidents discussed in this chapter are contained in Appendix B.

## 13.2 Accident Initiating Events and Scenarios, Accident Analysis, and Determination of Consequences

### 13.2.1 Maximum Hypothetical Accident

#### 13.2.1.1 Accident Initiating Events and Scenario

A single fuel element could fail at any time during normal reactor operation or while the reactor was shutdown, owing to a manufacturing defect, corrosion, or handling damage. This type of failure is infrequent, based on many years of operating experience with TRIGA® fuel, and such a failure would not normally incorporate all the necessary operating assumptions required to obtain a worst case fuel failure scenario.

For the UCD/MNRC TRIGA® reactor, the MHA has been defined as a cladding rupture of one highly irradiated fuel element with no decay followed by instantaneous release of fission products into the air. The failed fuel element was assumed to have been operated at the highest core power density for a continuous period of 1 year at 2 MW. This is the most severe accident for a TRIGA® and is analyzed to determine the limiting or bounding potential radiation doses to the reactor staff and to the general public in the unrestricted area.

A realistic scenario for the MHA is difficult to establish since fuel handling, the activity frequently associated with this accident, would be unlikely to occur immediately after reactor shutdown, and fuel elements would not be moved out of the reactor tank into air with no time to decay. Nevertheless, the accident has been analyzed for the UCD/MNRC TRIGA® in Appendix B and the results are summarized in this section.

### 13.2.1.2 Accident Analysis and Determination of Consequences

The fission product inventory used in the MHA is listed in Table B-1 of Appendix B. These data are based on compilations from Reference B.1 and have been adjusted for 2 MW operation. The data are for the volatile fission products present at shutdown in a fuel element run to saturation at the highest core power density.

A fission product release fraction of  $7.7 \times 10^{-5}$  is assumed for the release of noble gases and halogens from the fuel to the cladding gap. This release fraction is developed in Section 4.5.5.8, and is based on a RELAP5/3.1 calculation of fuel temperature in the hottest core element. In addition, it is assumed that 100% of the noble gases ultimately reach the unrestricted environment outside the reactor building and that 25% of the halogens released to the cladding gap are eventually available for release from the reactor room to the outside environment. This value for the halogens is based on historical usage and recommendations from Appendix B References B.2, B.3, B.4, B.5, and B.6, where Reference B.2 recommends a 50% release of the halogens. References B.3 and B.4 apply a natural reduction factor of 50% due to plateout in the building. This latter 50% applied to the 50% of the inventory released from the fuel element cladding gap results in 25% of the available halogen inventory reaching the outside environment. It should be noted, however, that this value appears to be quite conservative based on the 1.7% gap release fraction for halogens quoted in References B.7 and B.8.

Radiological consequence calculations were done using the Radiological Safety Analysis Computer Program (RSAC-5), Version 5.2, 02/22/94 (Reference B.9). RSAC-5 calculates the consequences of the release of radionuclides to the atmosphere and it can generate a fission product inventory; decay and ingrow the inventory with time; model the downwind dispersion of the activity; and calculate doses to downwind individuals. RSAC-5 has been subjected to extensive independent verification and validation for use in performing safety-related dose calculations to support safety analysis reports. Shonka Research Associates, Inc. (Reference 13.3) conducted this verification and validation in accordance with the guidelines presented in ANSI/ANS-10.4, "American National Standard Guidelines for the Verification and Validation of Scientific and Engineering Programs for the Nuclear Industry" (Reference 13.4).

For the MHA at the UCD/MNRC, dispersion coefficients ( $\chi/Q$  values) for locations in the unrestricted area, 10 m (the UCD/MNRC perimeter fence line nearest the facility which defines the interface of the restricted and unrestricted area) out to 100 m, were input directly into the code and were calculated using Regulatory Guide 1.145 methodology (Reference B.11). Calculations were performed for Pasquill weather classifications A through F. Diffusion coefficients were taken from Reference B.12 and are presented in Table B-2. Calculations were performed assuming a ground level release at an 800 cfm reactor room release rate without any credit for stack height or building wake effects, which would only improve mixing and lower projected doses. Furthermore, it was assumed that all of the fission products were released to the unrestricted area by a single reactor room air change, which maximizes the dose rate to persons exposed to the plume during the accident and minimizes the exposure time to receive the highest estimated dose from this accident.

These latter assumptions regarding release are very, very conservative since the reactor room is not at ground level and, rather than 10 meters, is approximately 30 meters from the perimeter fence. Furthermore, there are no normal or direct flow pathways to support an 800 cfm ground level flow from the reactor room to the unrestricted area.

The results of the RSAC-5 calculations for the MHA are shown in Tables B-4 and B-5. Shown are doses inside the reactor room and doses at several locations in the unrestricted area outside the UCD/MNRC (10 to 100 m from the building) as a function of weather class. Results are reported for the Committed Dose Equivalent (CDE) to the thyroid, the Committed Effective Dose Equivalent (CEDE) due to inhalation, the Deep Dose Equivalent (DDE) due to air immersion, and the Total Effective Dose Equivalent (TEDE) resulting from adding the CEDE and the DDE.

As indicated by the results in Table 13-1, the occupational dose to workers who evacuate the reactor room within 5 minutes following the MHA should be approximately 454 millirem Total Effective Dose Equivalent and 11,500 millirem Committed Dose Equivalent to the Thyroid. If evacuation were to occur within 2 minutes, as it no doubt would because the reactor room is small and easy to exit, the doses drop to 180 millirem TEDE and 4,640 millirem CDE. All of these doses are well within the NRC limits for occupational exposure as stated in 10 CFR 20.1201.

**TABLE 13-1 OCCUPATIONAL RADIATION DOSES IN THE UCD/MNRC REACTOR ROOM FOLLOWING THE MAXIMUM HYPOTHETICAL ACCIDENT.**

<b>Accident: Cladding Failure in Air (MHA)</b>				
	<b>CDE Thyroid (millirem)</b>	<b>CEDE (millirem)</b>	<b>DDE (millirem)</b>	<b>TEDE (millirem)</b>
2 minute room occupancy	4,640	140	40	180
5 minute room occupancy	11,500	360	94	454

Projected doses to the general public in the unrestricted area around the UCD/MNRC following the MHA are shown in Table 13-2. To receive the indicated dose, a person must be exposed to the airborne plume from the reactor room for the entire 9.2 minute period it is being vented. Even using this exposure requirement at the closest distance to the UCD/MNRC building (10 meters), and assuming the most unfavorable atmospheric conditions (Category F), the maximum TEDE to a member of the general public would be 66 millirem.

Although this accident and the corresponding radiation doses are never expected to occur, the maximum estimated dose of 66 millirem to the general public is still within the 100 millirem TEDE limit for the general public published in the NRC's most recent revision to 10 CFR 20 (Reference 10 CFR 20.1301). Furthermore, the above analysis clearly shows that the UCD/MNRC can be subjected to current MHA criteria and remain within dose limits established by the NRC for occupational radiation exposure and exposure of the general public. As a point of interest, should the MHA occur after 48 hours of decay, the maximum TEDE to the public drops to approximately 34 millirem.

**TABLE 13-2 RADIATION DOSES TO MEMBERS OF THE GENERAL PUBLIC UNDER THE MOST CONSERVATIVE ATMOSPHERIC CONDITIONS (PASQUILL F) AT DIFFERENT DISTANCES FROM THE UCD/MNRC FOLLOWING A FUEL ELEMENT CLADDING FAILURE IN AIR WITH NO DECAY (THE MHA).**

Distance (Meters)	CDE Thyroid (millirem)	CEDE (millirem)	DDE (millirem)	TEDE (millirem)
10	1,694	53	13	66
20	1,330	42	9.9	52
40	90	2.9	6.7	0.6
80	52	1.7	3.7	5.4
100	42	1.3	3.0	4.3

- CDE - Committed Dose Equivalent
- CEDE - Committed Effective Dose Equivalent
- DDE - Deep Dose Equivalent
- TEDE - Total Effective Dose Equivalent

### 13.2.2 Insertion of Excess Reactivity

#### 13.2.2.1 Accident Initiating Events and Scenarios

The most credible generic accident is the inadvertent rapid insertion of positive reactivity which could, if large enough, produce a transient resulting in fuel overheating and a possible breach of cladding integrity. Operator error or failure of the automatic power level control system could cause such an event to occur due to the uncontrolled withdrawal of a single control rod. Flooding or removal of beam tube inserts could also have a positive effect on reactivity but not as severe as removal of a control rod. In a separate scenario, a large reactivity insertion was postulated to create fuel cladding temperatures which might cause a metal-water reaction, but for many reasons this accident is not considered to be a safety risk in TRIGA<sup>®</sup> reactors.

### 13.2.2.2 Accident Analysis and Determination of Consequences

#### 13.2.2.2.1 Maximum Reactivity Insertion

Raising the temperature of TRIGA® fuel has a strong, prompt negative reactivity effect, which can overcome a rapid reactivity insertion such as that produced by the firing of the transient rod. The quantity that captures this effect is the prompt negative temperature coefficient discussed in Section 4.5.4.2. There is a limit to the protection provided by this feedback, since the peak fuel temperature attained before the feedback terminates the transient increases with the magnitude of the inserted reactivity. The Nordheim-Fuchs model was used to compute the maximum reactivity pulse that can occur without exceeding the safety limit of 1100°C established in Section 4.5.4.1.3.

In the Nordheim-Fuchs model it is assumed the transient is so rapid that 1) the temperature rise is adiabatic and 2) delayed neutrons can be neglected. Thus, the model is given by the following set of coupled differential equations:

$$\frac{dn}{dt} = \frac{\rho - \beta}{l} \times n ;$$

$$\rho(T) = \rho_o - \alpha(T) \times T ;$$

$$\frac{dT}{t} = \frac{n}{C_p(T)}$$

Where  $n$  is the reactor power,  $\rho$  is the time-dependent reactivity,  $l$  is the neutron lifetime,  $\beta$  is the effective delayed neutron fraction,  $T$  is the core-average temperature,  $\rho_o$  is the reactivity insertion,  $\alpha$  is the temperature feedback reactivity coefficient, and  $C_p$  is the whole-core heat capacity. Given values of  $\beta$ ,  $l$ , and  $\rho_o$ , and expressions for  $\alpha$  and  $C_p$ , this set of equations was solved numerically using simple finite difference techniques. The quantity of interest in the solution is  $\Delta T$ , the difference between the maximum and initial values of the core-average fuel temperature. From the solution  $\Delta T$ , the peak fuel temperature was found using the simple expression:

$$T_{peak} = T_o + PF \times \Delta T ;$$

where  $T_o$  is the initial temperature and PF is the total peaking factor. In the equation just described,  $\rho_o$  is an input parameter and  $T_{peak}$  is the output, yet what is needed is the reverse; the object was to find the value of  $\rho_o$  that yields  $T_{peak} = 1100^\circ\text{C}$ . The object was attained by an iterative search. The search converged in no more than 3 iterations (estimates of  $\rho_o$ ) because  $T_{peak}$  varies essentially linearly with  $\rho_o$  over a wide range.

The following input values were used for all the results displayed here:

$\beta = 0.007$ ;  
 $l = 32 \mu\text{s}$ ;  
 $T_o = 20^\circ\text{C}$ ;  
 $\text{PF} = 4.86$ .

Although some quantities, such as the peak reactor power, depend on the value of  $l$ ,  $T_{peak}$  was found not to change with reasonable variations in  $l$ . The value of  $\beta$  is well known. The value used for  $T_o$  is the nominal zero-power temperature. The value of PF is the largest total peaking factor in Table 4-17 (Section 4.5.5.5). This value was determined for the 20E reference core with all fresh fuel and control rods raised 2/3 of full travel. It is a conservative value for any other permissible core loading and rod bank position.

The reactivity insertion limit is shown for seven cases in Table 13-3. Each case has a different combination of fuel type and core-average burnup. The expressions for heat capacity,  $C_p$ , as a function of temperature correspond to a minimum core size, 94 elements, and they were derived using the prescription in Reference 13.5. The insertion limit was found to be independent of  $C_p$ . The insertion limit is sensitive to the prompt negative temperature coefficient,  $\alpha$ . The curves in Figure 13.1 show that this coefficient varies with temperature, fuel type and fuel burnup. The different expressions for  $\alpha$  are directly responsible for the differences in the reactivity insertion limit among the seven cases in Table 13-3.

**TABLE 13-3 MAXIMUM REACTIVITY INSERTION AND RELATED QUANTITIES FOR VARIOUS FUELS AND BURNUPS**

<u>Fuel Type</u>	<u>Burnup (%)(MWD/rod)</u>		<u>Heat Capacity <math>C_p</math> (watt-sec/<math>^\circ\text{C}</math>)</u>	<u>Prompt Negative Temperature Coefficient <math>\alpha</math> (<math>\Delta\text{k}/\text{k}^\circ\text{C}</math>)</u>	<u>Reactivity <math>\rho_o</math> (<math>\\$</math>)</u>
8.5/30	independent		$7.31 \times 10^4 + 150T$	$7.16 \times 10^{-5} + 2.33 \times 10^{-7}T - 4.35 \times 10^{-10}T^2 + 2.09 \times 10^{-13}T^3$	2.66
20/20	0	0	$7.12 \times 10^4 + 143T$	$4.91 \times 10^{-5} + 1.93 \times 10^{-7}T - 9.73 \times 10^{-11}T^2$	2.33
20/20	13	10	$7.12 \times 10^4 + 143T$	$4.90 \times 10^{-5} + 1.32 \times 10^{-7}T - 7.82 \times 10^{-11}T^2$	2.16
20/20	33	27	$7.12 \times 10^4 + 143T$	$5.24 \times 10^{-5} + 7.45 \times 10^{-8}T - 6.13 \times 10^{-11}T^2$	2.06
30/20	0	0	$7.39 \times 10^4 + 145T$	$4.84 \times 10^{-5} + 1.59 \times 10^{-7}T - 7.3 \times 10^{-11}T^2$	2.23
30/20	15	20	$7.39 \times 10^4 + 145T$	$4.71 \times 10^{-5} + 9.13 \times 10^{-8}T - 4.63 \times 10^{-11}T^2$	2.03
30/20	39	54	$7.39 \times 10^4 + 145T$	$5.02 \times 10^{-5} + 3.10 \times 10^{-8}T - 2.24 \times 10^{-11}T^2$	1.92

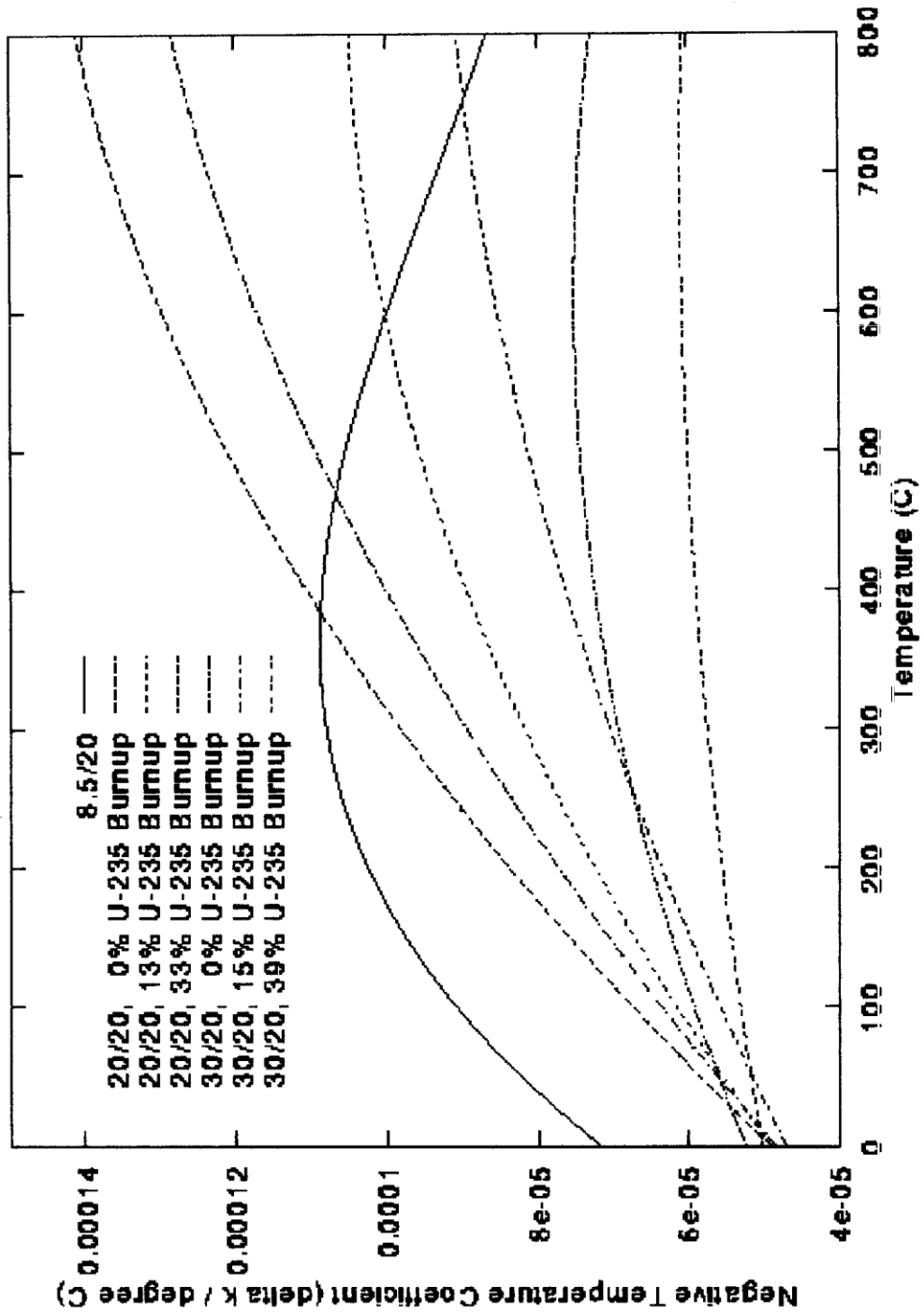


FIGURE 13.1 PROMPT NEGATIVE TEMPERATURE COEFFICIENT FOR TRIGA® FUELS

The worst-case result in Table 13-3, \$1.92, was chosen as the maximum reactivity insertion allowed for the UCD/MNRC reactor. There are at least two reasons why this is a conservative bound. One is that the core-average burnup, 39% <sup>235</sup>U, is greater than is likely to be achieved, which means that there will be more prompt feedback reactivity than was used for this case. The other reason is that the peaking factor is significantly larger than would be the actual case for a highly burned 30/20 loading.

#### 13.2.2.2.2 Uncontrolled Withdrawal of a Control Rod

Operator error or failure of the automatic power level control system could cause one of the control rods to be driven out, starting at either high or low power levels. The maximum speed of a control rod is 1.78 cm/sec (42. in./min). The maximum single rod worth for the reference loadings of Section 4.5.5 is \$2.65, but a rod worth of \$3.50 was used here to allow for reasonable variations about the reference loadings. These values were combined with a measured rod worth profile to calculate the inserted reactivity as a function of time.

The initial reactor power levels of 100 W or 2 MW were analyzed using the Dynamic Simulator for Nuclear Power Plants (DSNP) code to solve the one group point kinetics equation with a delayed neutron fraction of 0.007 and the one group decay constant equal to 0.405 sec<sup>-1</sup> (Reference 13.6). The one group decay constant was chosen to match solutions near prompt critical. The feedback reactivity was assumed to be:

$$\alpha (T) = 5.018 \times 10^{-5} + 3.097 \times 10^{-8}T - 2.244 \times 10^{-11}T^2 \quad \Delta k/k/^{\circ}C.$$

This corresponds to worst-case (weakest feedback) conditions (i.e., 30/20 fuel at end-of-life).

The heat capacity of the core was assumed to be:

$$C_p = 7.39 \times 10^4 + 145.0 T \text{ watt-second/}^\circ\text{C}.$$

Again, this corresponds to worst-case conditions for all 30/20 fuel loadings with 94 fueled elements. The most unfavorable initial control rod position was assumed to be 32% inserted. The insertion rate at this position is \$0.23/sec.

The amount of shutdown reactivity at the time of scram is based on the following: four control rods are capable of providing a total of \$0.50 of shutdown reactivity (conservative assumption) and the rod that is adding reactivity for the “uncontrolled withdrawal of a control rod” is available as shutdown reactivity. Thus the total shutdown reactivity is \$0.50 plus reactivity of the moving rod at the time of scram. Rod fall time of 2 seconds is assumed. The rod fall time includes the power channel delay time.

For the case with an initial reactor power at 100 watts, an average fuel temperature of 35°C, and a worst case trip level setpoint of 2.3 MW, the reactor power was calculated to reach the trip point at 4.26 seconds. Assuming it takes 0.5 seconds for the signal to cause actual release of the rods, the peak reactivity inserted would be \$1.18. As shown in Section 13.2.2.2.1, this amount of reactivity could be inserted instantaneously with no adverse safety effects.

For the case with initial power at 2 MW, an average fuel temperature of 257.2°C, and a worst case trip level setpoint of 2.3 MW, the reactor power was calculated to reach the trip point in 0.54 seconds. The scram signal causing actual release of the rods occurs 0.5 seconds later. Reactivity inserted at the time all of the rods are released is \$0.25. This reactivity insertion is much less than the limiting reactivity insertion derived in Section 13.2.2.2.1 for the pulse accident.

#### 13.2.2.2.3 Uncontrolled Withdrawal of All Control Rods

This accident has been analyzed using a measured rod worth profile and a total control rod worth for five rods of \$17.50. Using the DSNP model with feedback described above, initial power of 100 W, and the rods at an assumed initial position of 32% insertion, with a normal rod withdrawal rate of 1.02 cm/sec. (24 in./min.) for all five rods, an initial reactivity insertion rate of \$0.66/sec. is obtained. The worst case trip level setpoint of 2.3 MW is reached at 1.73 seconds with the scram occurring at 2.23 seconds. Reactivity inserted at the time all of the rods are released is \$1.52. This reactivity insertion is less than the limiting reactivity insertion derived in Section 13.2.2.2.1 for the pulse accident. For five rods to add reactivity simultaneously, there must be multiple failures in the control system. Therefore, this accident is not considered to be credible.

Since three control rods can be banked for reactor control, uncontrolled withdrawal of three control rods could be considered credible, but is bounded by the accidents analyzed.

#### 13.2.2.2.4 Beam Tube Flooding or Removal

In the event of flooding of one or more beam tubes, air or inert gas would be substituted with water. This will constitute a positive reactivity addition. It has been estimated that the worth of one flooded beam tube is about \$0.25. This amount of excess reactivity is well below the limits discussed in Section 13.2.2.2.1; therefore, it does not represent a safety significant event.

During the removal of the in-tank section of a beam tube, air and graphite will be replaced by water because a portion of the graphite reflector is removed with this section of the beam tube. Again, replacement of the air/gas with water results in a positive increase in reactivity. On the other hand, replacement of graphite with water results in a negative effect on reactivity. The net result will be a smaller reactivity addition than for beam tube flooding so this action is of even less overall consequence.

#### 13.2.2.2.5 Metal-water Reactions

Although metal-water reactions have occurred in some reactor accidents or destructive tests, the evidence from these events and laboratory experiments shows that a dispersed liquid metal is required for a violent chemical reaction to occur (References 13.1 and 13.7). The conditions for a solid metal-water reaction are not readily achievable in a reactor system such as the UCD/MNRC.

Water quench tests on TRIGA<sup>®</sup> fuel have been conducted to fuel temperatures as high as 1200°C without significant effect. Since the operating temperatures at 2 MW do not approach this temperature, this effect does not represent a safety risk. The only credible way in which temperatures high enough to allow metal-water reactions to be created in a TRIGA<sup>®</sup> reactor is through a large reactivity excursion. The limits set on excess reactivity preclude this.

### 13.2.3 Loss of Coolant Accident (LOCA)

#### 13.2.3.1 Accident Initiating Events and Scenarios

Loss of coolant from the UCD/MNRC reactor could occur primarily through one of two scenarios, pumping water from the reactor tank or reactor tank failure. These scenarios are analyzed as part of this section.

#### 13.2.3.2 Accident Analysis and Determination of Consequences.

##### 13.2.3.2.1 Pumping of Water from the Reactor Tank

The intake for the primary-cooling-system pump is located about 3 ft below the normal tank water level. In addition, the line is perforated from about 8 in. below the normal tank water level to the intake line entrance. The intake for the purification-system pump is through a short flexible line attached to a skimmer that floats on the surface of the tank water. However, the length of the flexible line is such as to cause loss of pump suction if the tank water level is lowered about 4 ft. Thus, the reactor tank cannot be accidentally pumped dry by either the primary pump or the purification-system pump. Also, it is not possible for other cooling system or water cleanup system components to fail and syphon water from the tank since all of the primary-water-system and purification-system piping and components are located above the normal tank water level.

The tank could be pumped out with a portable pump, but this would require deliberate action on the part of the operators and it is inconceivable that such an action would take place while the reactor was operating or at any other time without removing the fuel and taking numerous other precautions. However, if the reactor were somehow pumped dry while the reactor was shut down, the fuel temperature obtained would be considerably lower than for a loss of water while the reactor was operating, and this unlikely error would not cause damage to the fuel elements. Similarly, the dose rate from the uncovered core and the water radioactivity concentration would be less than that shown in Sections 13.2.3.2.11 and 13.2.3.2.12.

##### 13.2.3.2.2 Reactor Tank Failure

A hole in or near the bottom of the reactor tank could cause the water level to drop below the top of the fuel elements. This event could occur either during reactor operation or while the reactor was shut down and unattended. There are no nozzles or other penetrations in the reactor tank below the normal water level, so the only mechanisms that could cause tank failure are corrosion of the tank or a mechanical failure. Leaks caused by corrosion would unquestionably be small leaks, which would be detected before the water level had lowered significantly. In such a case, makeup water could be supplied by the auxiliary make-up water system (AMUWS) until the leak is repaired.

Provisions to monitor for and collect tank leakage have been incorporated into the facility design. First, the tank is surrounded by corrugated metal. The corrugations provide a path to the bottom of the tank for any water leakage from the walls. Second, a drain, see Chapter 5, within the bulk shield surrounds the bottom of the tank. This drain will collect any water that may leak from the tank walls or bottom. Third, a duct leads from the drain to Radiography Bay 1 and the exit of this duct is periodically monitored for water leakage. If leakage is detected, the water could be easily collected at this point or diverted to the liquid holdup tank outside the building.

Consequences of a slow tank leak would be minimal and would require collection and containment of the water which leaked from the tank. This would be easily accomplished by using the existing liquid effluent control system described above. Small tank leaks due to corrosion are normally repairable using conventional techniques for patching aluminum, and thus it is expected that a leak could be located and fixed before there would be any significant loss of water from the tank.

An earthquake of much greater intensity than the Uniform Building Code Zone 3 earthquake appears to be the only credible mechanism for causing a large rupture in the tank, since the tank when supported by its associated biological shield structure was designed (with an importance factor of 1.5) to withstand this magnitude of earthquake. Even if such an event is assumed to cause very rapid loss of water while the reactor is operating at peak power; a reactor shutdown would be caused by voiding of water from the core, even if there were no scram.

A large rupture of the tank would obviously result in a more rapid loss of water than a leak due to corrosion or a minor mechanical failure in the tank wall. The UCD/MNRC reactor tank has no breaks in its structural integrity (i.e., there are no beam tube protrusions or other discontinuities in the reactor tank surface). In addition, the reactor core is below ground level. Thus the potential for most types of leaks is minimized.

Part of the 2 MW upgrade to the reactor included a new cavity (Bay 5) cut into the biological shield. This cut exposes the reactor tank wall below the reactor core level, and this introduces an increased possibility of draining water from the core area. While steps have been taken to minimize the probability of a tank rupture in this location, and it is believed that the likelihood of such a rupture is very low, an unplanned occurrence could nevertheless initiate such an event. Therefore, an Emergency Core Cooling System (ECCS) was installed to cool the core until the fuel has decayed to a level where air cooling is adequate to maintain fuel temperatures below the design basis limit (see Chapter 6 for details of the ECCS design and operation).

An analysis detailing the cooling capabilities of the ECCS is described in the sections which follow. This analysis does not postulate the occurrence of a particular initiating sequence of events leading to all fuel elements in the core being uncovered. Instead, it simply assumes that the tank has ruptured and all the water is lost. Such an event has several different consequences.

First there is the possibility of fuel clad rupture should the fuel temperature exceed design basis values. This event is covered in the analysis that follows, and focuses on the action of the ECCS to prevent fuel temperatures from reaching safety limits. Second, there is a possibility of personnel exposure to radiation from the uncovered reactor core due to the direct beam from the core or from radiation scattered from the reactor room walls and ceiling. Finally, there is a chance that the lost water could cause ground water contamination. Both of these latter events are also analyzed as part of the LOCA evaluation.

#### 13.2.3.2.2.1 Description of ECCS and Assumptions

A loss-of-coolant accident (LOCA) is postulated for the UCD/MNRC in which the reactor tank is rapidly drained of water during operation at 2 MW (it is assumed that the reactor has been running at 2 MW for an infinitely long time). Because the LOCA uncovers the core quickly, the fuel clad temperature in some of the centrally located fuel elements could exceed the design basis temperature limit of 930°C after a period of at least 20 minutes.

When the reactor tank water level drops below the normal operating range (typically a loss of approximately six (6) inches of water) a tank low-level alarm sounds. This alerts the operator that action must be taken. Depending upon the rate of water loss, the suspected cause of the loss, and other considerations, several different actions may be taken by the operator in response to a reduction in the tank water level. One such action could be activation of the ECCS.

Upon activation of the ECCS, cooling water from the domestic water supply will be introduced into the reactor tank and maintained until the fuel no longer contains sufficient decay heat to present a threat to the fuel cladding or water is restored to a level above the core. If the tank water level has dropped to less than about two (2) feet above the core, water from the ECCS will be sprayed onto the top of the remaining water column above the core; however, if the tank water has dropped below or partially below core level, the ECCS water will be sprayed directly onto the core. During this time, the decay heat will be removed by the remaining tank water or by the water spray and the maximum fuel temperature will be reduced rapidly from an elevated operating temperature down to about 200°C and then gradually to 100°C with continued spray cooling.

At the end of spray cooling, natural air convection will be established in the core. During this cooling phase, the temperature of the fuel will rise slowly over several hours to a maximum and then decrease with continued air cooling. The maximum fuel and cladding temperature is controlled by the length of spray cooling and by the natural air cooling. Under the preceding conditions, no fuel cladding will be ruptured.

The detailed components of the emergency core cooling system to be used to maintain fuel temperatures below the design basis limit are described in Chapter 6. Basically the system consists of a quick connect system for coupling to the domestic water supply, sensing devices to indicate the need to initiate emergency cooling water flow, a nozzle to distribute the coolant flow over the core, a chimney mounted above the core structure to provide a sufficient channel length for maintaining sufficient air flow through the core, and a ventilation system to provide air circulation through the reactor room.

It should be noted that in a TRIGA® reactor, loss of reactor coolant water will automatically cause a complete reactor shutdown even without a control rod scram. Experiments with the GA subcritical assembly have indicated that the reactivity worth of the water in the core is on the order of 10% (more than 13 dollars). As a result, were the reactor to be operating during a catastrophic event in which the cooling water were completely lost, the reactor would automatically shutdown (even without insertion of control rods) once the water level dropped a few centimeters below the upper grid plate.

#### 13.2.3.2.2.2 Spray Cooling

A considerable amount of experimental data has been gathered on the efficacy of spray cooling for a system of heated cylindrical rods in bundles. These data indicate that the amount of heat that can be removed by a water spray without the rod's wall temperature exceeding about 100°C is simply the amount of heat that would increase the enthalpy of the sprayed water from its inlet enthalpy to the saturated liquid enthalpy (Reference 13.8). The experiments were conducted for heat fluxes up to about 4 W/cm<sup>2</sup>, which is larger than the maximum heating rate in the hottest fuel element during the loss-of-coolant accident. Even if the initial surface temperatures were very high (~900°C) before the spray is initiated, the surface temperature would be very quickly reduced to about 100°C if sufficient water is provided to remove the heat without increasing the coolant temperature to the saturation point (Reference 13.9). The spray flow rate required to cool the fuel to 100°C from 2 MW operation corresponds to 12.3 gpm through the TRIGA® core, including the consideration of peak power in the core.

Measurements have been made to determine the actual flow rate required to fulfill the 12.3 gpm flow requirement through a TRIGA® core (Reference 13.10). These tests indicated that both the nozzle type as well as its location and orientation are important in order to provide the required cooling spray. Results also showed that a total spray flow of 20 gpm from the nozzle, as specified in Reference 13.10, located approximately 2 ft. above the top grid plate will assure that adequate core spray cooling is available to meet the requirements above. Provisions have been established to ensure that sufficient spray cooling water can be supplied to the reactor core when needed from the building domestic water supply.

#### 13.2.3.2.2.3 Air Cooling

The relatively small size (~7500 cu. ft.) of the reactor room can affect the convective air cooling of the reactor core after spray cooling ceases. In the small reactor room, hot air from the core is expected to overload the air conditioning system and raise the ambient air temperature. Since this is the air that is available for cooling the core, this situation was analyzed in detail.

The air flow in the reactor room during normal operation is the following: an exhaust flow of 800 cfm passes through absolute filters on the way to the stack, 500 cfm of which comes from the air conditioning system (1100 cfm outgoing, 1600 cfm returned) and 300 cfm comes from leaks into the reactor room from around doors or other leaks in the reactor room enclosure. Appendix D provides schematics of the reactor room and the exhaust and supply air ducts.

Although 1100 cfm is withdrawn from the room by the HVAC, and is refrigerated, and returned with an additional 500 cfm of air at ambient temperature, it will be assumed that during the LOCA event, this air flow continues but that the refrigeration fails due to an excessive heat load. (Note: If the HVAC fails, the reactor room exhaust fan will still be able to draw at least 500 cfm of ambient air in through the open HVAC damper.) Thus, 500 cfm (from the air conditioning) plus 300 cfm (from in-leakage into the reactor room) are continuously supplied to the reactor room at an ambient air temperature (~80°F) to match the 800 cfm exhaust that continues during the accident. To ensure a continuous air supply to and from the reactor room a backup power supply has been provided for the reactor room exhaust fan (EF-1).

#### 13.2.3.2.2.4 Assumptions Made for ECCS Operation

The following assumptions are necessary to initiate and evaluate ECCS operation:

1. The ECCS will be initiated by the reactor operator if the water level drops to a level that requires the system to be turned on. Operator action and manual operation of the ECCS is considered sufficient since at least 20 minutes is available for initiation after an instantaneous loss of the tank water during operations at peak power before sufficient heat will build up in the fuel to threaten the safety limit (Reference 13.11);
2. If the reactor room continuous air monitor (CAM) actuates the recirculation mode of ventilation for the reactor room due to elevated radiation levels following tank water loss, the reactor operator will assess the situation and then switch the room ventilation from recirculation back to the manual ventilation mode (Chapter 9);
3. Based on assumption number 2, the reactor room exhaust fan will continue to extract 800 cfm from the reactor room (typically 500 cfm from the top of the reactor and 300 cfm from near the ceiling).

#### 13.2.3.2.2.5 Performance of the ECCS

Because of the relatively small reactor room, it is necessary to consider for any air cooling portion of the loss-of-coolant accident that the initial conditions consist of an air filled reactor tank containing a hot core near its bottom and surmounted by a small reactor room (7500 cu ft.). Hot air rises (~227 cfm) from the core in a plume, part of which is removed into the 500 cfm exhaust duct at the top of the reactor tank. The remainder of the hot air plume rises into the reactor room, mixing with the room air. Near the top of the reactor room 300 cfm of mixed air is exhausted. Ambient air at 80°F comes into the reactor room at 800 cfm.

At quasi equilibrium, the mixed air in the reactor room, including that near the top of the reactor tank, is warmer than the 80°F ambient air from the outside. This mixed air flows in a near annulus down the reactor tank adjacent to the tank wall as the hot plume from the reactor core flows upward in the center of the tank. The downflow air partially mixes with the hot air plume rising from the core and increases in temperature. This downflow air then enters the bottom of the reactor core.

An estimate of this air mixing using boundary layer analysis for the mixing region indicates that the temperature increase of the downflow air is approximately 10% of the difference between the downflow air temperature and the upflow average plume temperature.

#### 13.2.3.2.2.6 Thermal Model for Natural Convection Air Cooling

A thermal model was constructed to assess the fuel temperatures for the LOCA event after the termination of spray cooling and with subsequent natural convection air flow through the core. The TAC2D general purpose thermal analysis code was used to calculate the maximum and average fuel temperatures for typical fueled channels representing hot, average and cold regions of the core (Reference 13.12).

Four flow channels were used to represent the natural convective flow past these three (3) fueled regions and one (1) unfueled region. No cross flow was considered between the various flow channels. One flow channel represented all the flow channels in the cooler F and G rings and one flow channel represented all the flow channels in the average powered D and E rings. Individual flow channels were modeled to represent the locally different flow channels surrounding the hottest fuel element. To complete the surface boundary conditions for these latter two flow channels, it was necessary to include in the thermal model a fifth flow channel. This channel was used to represent the temperature response of two adjacent unheated graphite elements in the C-ring and the adjacent central in-core experiment facility.

Decay heat is removed from the reactor by radial conduction to the surface of the fuel elements where it is removed by convective air currents driven by buoyant forces generated by the reactor natural convection loop. The resulting peak and average fuel temperatures were calculated for the hottest element as a function of time. The natural convection flow rate is dependent on the pressure balance in the system. The buoyancy driving head for the natural convection flow is the difference between the density head of the cooler downflow and the density head of the hot upflow. The subsequent analysis shows that a chimney two (2) feet high provides adequate buoyant driving head.

#### 13.2.3.2.2.7 Reactor Core for LOCA

The 20E Core with the central experiment facility containing the aluminum and graphite plugs in place, all control rods fully up, and 101 fuel elements was chosen as the LOCA core configuration (Chapter 4). The axial power distribution with rearrangement required for the TAC2D code, was used for power density calculations (Reference 13.13). The results are shown in Figure 13.2.

Account was taken of the five fuel followers on the control rods. For the LOCA event, the control rods are fully inserted into the core. This means that the five fuel followers are suspended below the bottom grid plate. Each of these fueled sections is located within a guide tube that has 12 openings in the surface. The 12 individual openings provide 24 In<sup>2</sup> of surface area and are situated symmetrically around the device to provide adequate cooling air for each element.

#### 13.2.3.2.2.8 Mixed Air Temperature in the Reactor Room

For the design case (3.7 hours of spray cooling, 2-ft chimney) the highest average temperature in the hot air plume from the core is approximately 1360°F. At this value the plume density is very low and, consequently, the mass flow rate is low relative to the other air streams in the room. The volume of air flow in this plume is 227 cfm. It is assumed, on average, that about 100 cfm of this plume is swept into the 500 cfm duct at the top of the reactor tank and that about 127 cfm of hot air rises into the reactor room. (See Appendix D for details.) It is assumed that 800 cfm of air at 80°F is continuously supplied to the reactor room and that the duct near the top of the reactor room exhausts 300 cfm of mixed air. It is further assumed that the reactor room is small enough and the air cooling time is long enough (several hours) that a quasi steady state condition exists. That is, the temperature of the mixed air in the reactor room is simply the mixed mean temperature of the plume from the core and the incoming air streams on a mass flow basis, and further that constant specific heat and ideal gas behavior for the air streams can be assumed.

For 80°F air inlet to the room and an average plume temperature of 1364°F, the mean temperature of the mixed air is about 138°F. Even if all the hot air in the plume were to rise into the reactor room rather than a portion being drawn off at the top of the reactor tank, the mixed air temperature would only rise to 180°F, a value that does not alter significantly the cooling conditions of the reactor fuel.

In addition to the above consideration of the mixed mean air temperature in the reactor room, there is the additional consideration that the 800 cfm rate of room air exhaust will provide about 6.6 changes of room air per hour. During the two hours during which the peak fuel temperature exceeds 900°C and the average plume temperature exceeds 1290°F, the ventilation system changes the reactor room air more than 12 times while bringing into the room 80°F air at 800 cfm. This fact provides additional rationale for a quasi equilibrium condition with mixed room air at relatively low temperature.

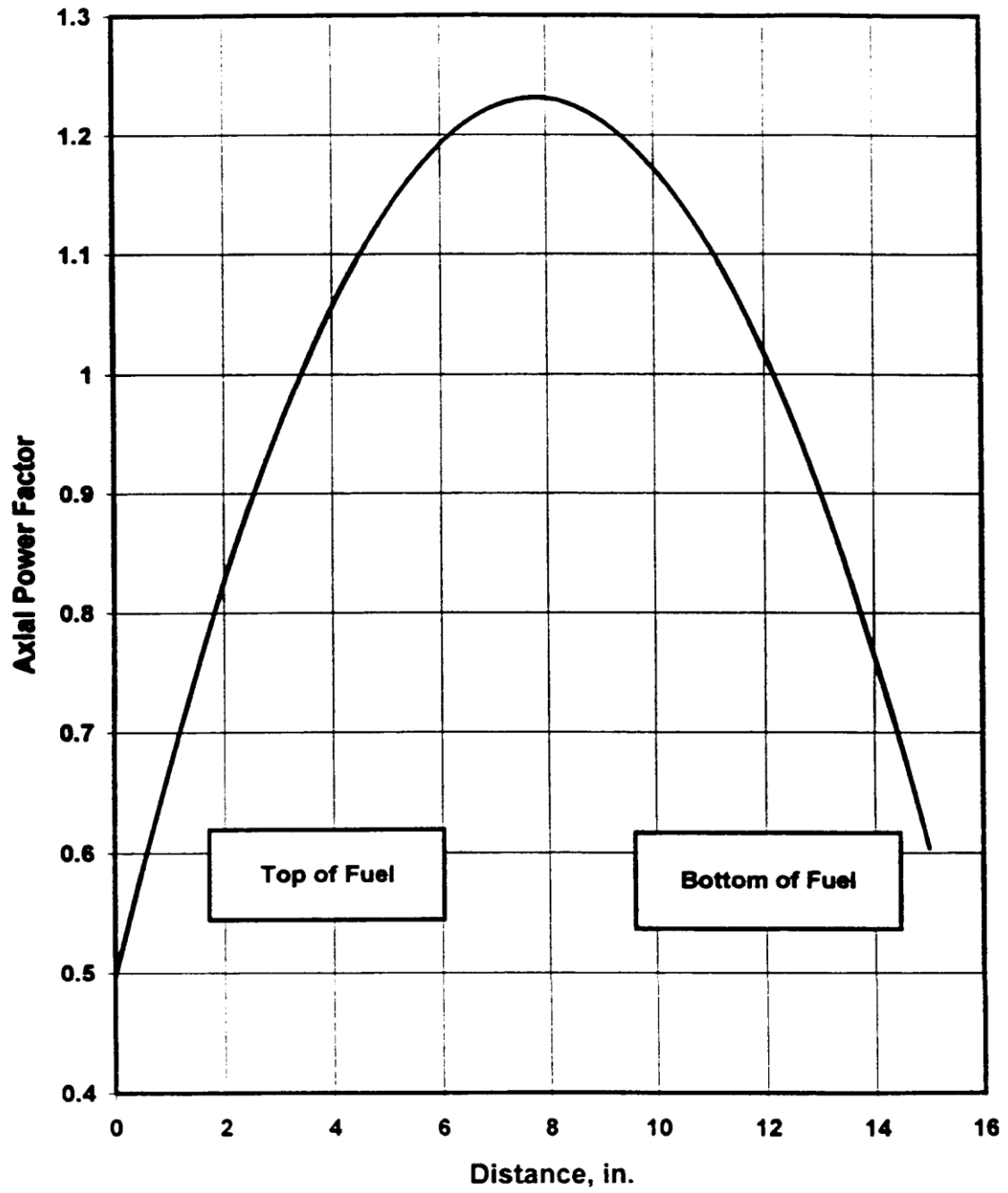


FIGURE 13.2 AXIAL POWER DISTRIBUTION FOR FUEL IN CORE 20E

The calculation of the mixed air temperature in the reactor room is conservative. It is assumed that the hot air plume has its maximum temperature even at the start of the air cooling cycle. Actually, the plume temperature starts at 212°F, reaches 580°F in a half hour and is below 1000°F for the first hour of cooling. Under these circumstances, the reactor fuel would be cooled more efficiently since the inlet air at the bottom of the core would be lower. However, to be conservative, it is assumed that the hot air plume has its maximum temperature during the entire air cooling cycle.

#### 13.2.3.2.2.9 Results of ECCS Calculations

Although it is recognized that the ECCS system when hooked to the domestic water supply should be able to deliver an infinite supply of water, should the domestic water supply not be available, the ECCS function will be supplied by the backup system, the auxiliary make-up water system (AMUWS). Since this system has a limited water supply, considerations of a finite water supply with transition to air cooling were utilized in this calculation.

Using the preceding assumptions for the reactor core and for the temperature of the cooling air available in the reactor room, the TAC2D code was used to evaluate the cooling requirements in order to maintain fuel temperatures below safety limits. Figure 13.3 presents the peak and average fuel temperatures in the hottest fuel element during the air cooling cycle after spray cooling for time varying from zero to four hours (with a chimney height of two feet). From Figure 13.3 it may be noted that spray cooling for three hours will lower the resulting average temperature in the hottest fuel element to 886°C, well below the safety limit of 930°C. From the discussion in the following sections, it will become clear that to maintain cladding integrity it is really only necessary for the average temperature to be below the safety limit, since the colder sections of the fuel will act as a sink for any free hydrogen released from the hotter sections. Figure 13.3 also illustrates that with a two foot chimney and slightly more than 3.5 hours of spray cooling, the peak fuel temperature in the hottest fuel element will not exceed the safety limit of 930°C.

Figure 13.4 demonstrates the time dependent fuel temperatures (peak to average) during the air cooling cycle with a two foot chimney after spray cooling for three hours. This graph shows that the peak and average fuel temperatures reach a maximum at about 4.1 hours. While not shown in this graph, it is also clear that the six inches of the fuel in the hottest fuel element which is cooler than the average fuel temperature (886°C) has temperatures that are far below the applicable safety limit. The UCD/MNRC has elected to spray cool the fuel for at least 3.7 hours. The resulting UCD/MNRC fuel temperatures during the air cooling cycle with a 2 foot chimney are presented in Table 13-4, and the resulting cladding stresses are presented in Section 13.2.3.2.2.10.

TAC2D calculations were also made to illustrate the effect of chimney height on maximum and average fuel temperatures assuming three hours of spray cooling (or more in the absence of any chimney). These results are shown in Table 13-4. Table 13-5 shows the spray cooling requirements if the chimney height were three feet rather than two feet. As expected, the performance of a three foot chimney is better than that for a two foot chimney. However, the specifications for the location of the spray cooling nozzle suggests that the nozzle should be 26 inches above the top of the core (Reference 13.10). This height is compatible with a two foot chimney, but could be a problem with a three foot chimney.

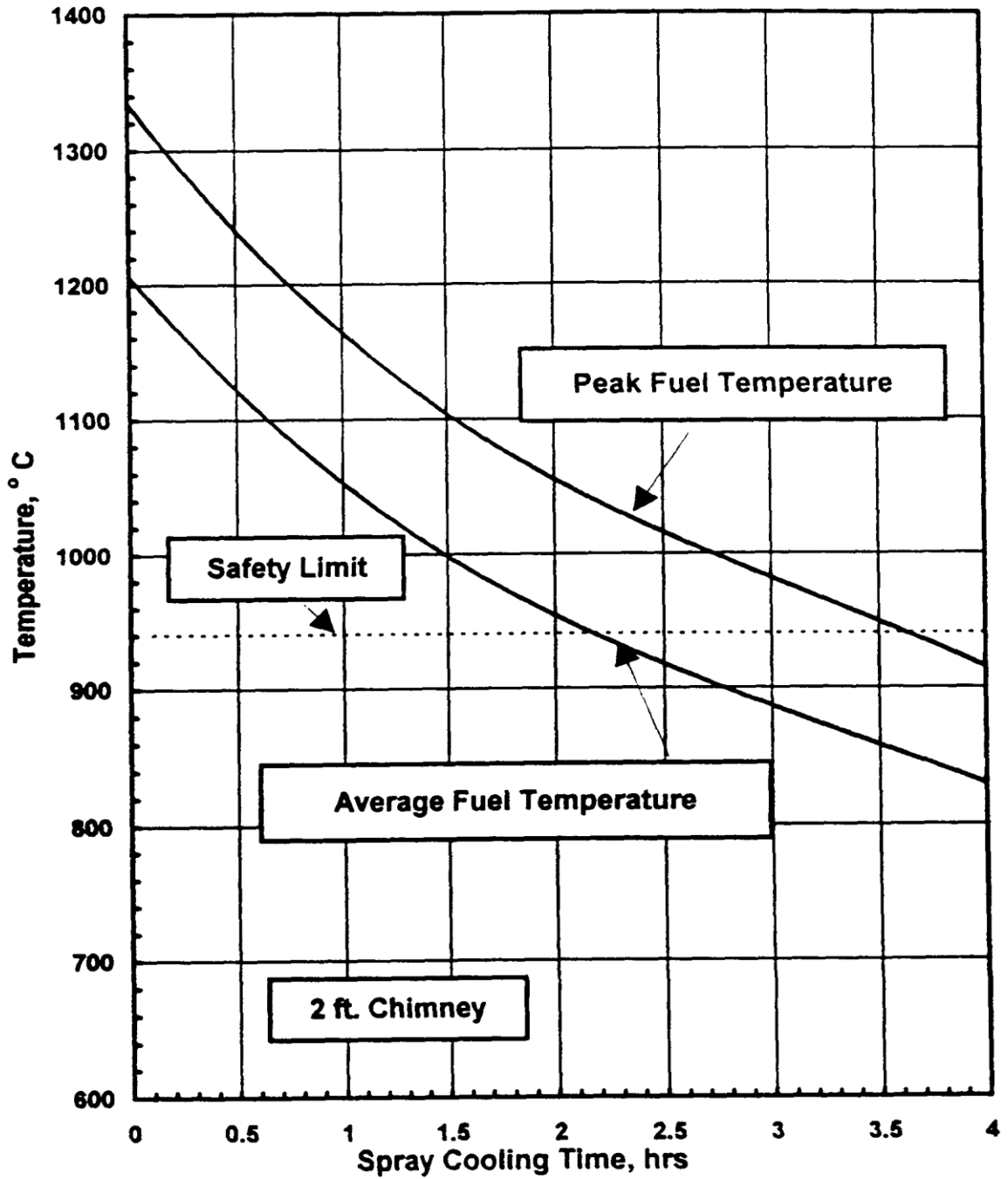


FIGURE 13.3 MAXIMUM AND AVERAGE FUEL TEMPERATURE DURING AIR COOLING CYCLE FOR VARIOUS SPRAY COOLING TIMES

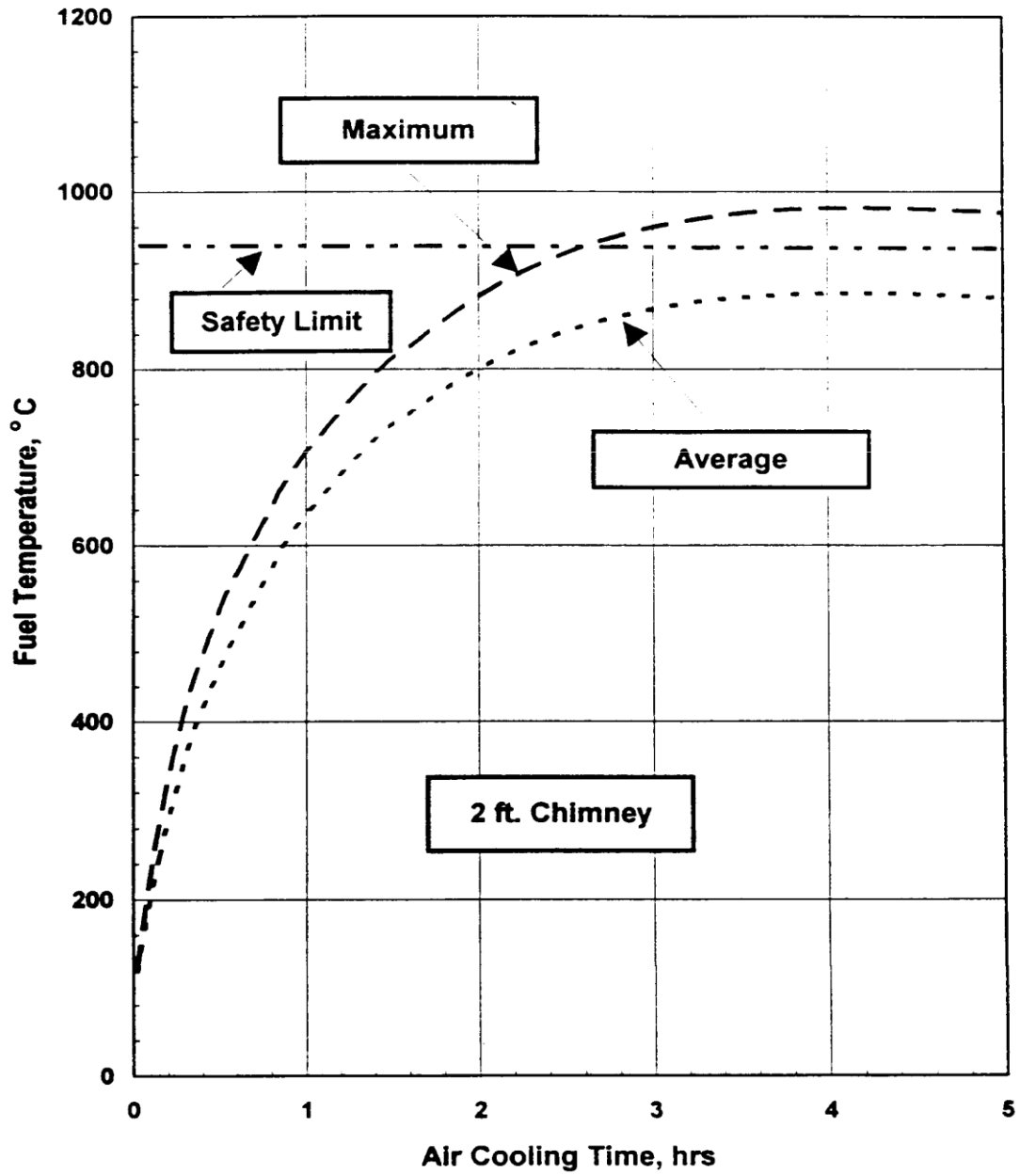


FIGURE 13.4 MAXIMUM AND AVERAGE FUEL TEMPERATURES FOR THE HOTTEST FUEL ELEMENT AS FUNCTIONS OF TIME AFTER END OF SPRAY COOLING FOR THREE HOURS

TABLE 13-4 MAXIMUM FUEL TEMPERATURES WITH VARIOUS CHIMNEY HEIGHTS

T (hr) spray cooling	Chimney (ft)	T <sub>peak</sub> (°C)	T <sub>avg</sub> (°C)
3	3	900	813
3	2	982	886
(UCD/MNRC) 3.7	2	930*	845*
3	1	>1220**	>1112**
3	0	>1451**	>1355**
10	0	>1209**	>1122**
48	0	953***	873***
* fuel temperatures taken from Figure 13.3			
** temperature still rising after 5 hours of air cooling			
*** temperature peaks at about 13 hours and then decreases			

TABLE 13-5 Comparison of Cooling Results with 2 ft. and 3 ft. Chimneys

T (hr) spray cooling	Chimney (ft)	T <sub>peak</sub> (°C)	T <sub>avg</sub> (°C)
2	3	941	850
3	3	900	813
3	2	982	886

Finally, additional elements of conservatism not mentioned earlier in this analysis provide further assurance that the cooling of the fuel will be at least as effective as described above. For instance, no account was taken of the added cooling provided by the conduction of heat from the fuel elements to the cooler portions of the fuel assembly. Similarly, the radiation of heat (especially when the fuel temperatures have reached the higher values) to the cooler parts of the system outside the core was not included in the transient heat flow considerations. Furthermore, the TAC2D calculations reported herein assumed that the temperature of the inlet air at the bottom of the core was 300°F. This is somewhat higher than would result from the considerations in Sections 13.2.3.2.2.6 and 13.2.3.2.2.8. With those earlier results, the core inlet air temperature would be about 260°F (138°F [mixed air in the reactor room] plus 122°F [ $\Delta T$  from additional mixing in the tank]). If all the hot plume were to rise into the reactor room, the mixed air temperature in the room would be about 180°F. In this unlikely case, the core inlet air temperature would then be about 298°F (180°F [mixed air in the reactor room] plus 118°F [ $\Delta T$  from additional mixing in the tank]). Both of these estimates of the core inlet air temperature are less than the more conservative value of 300°F used for the TAC2D calculations performed here.

#### 13.2.3.2.2.10 Cladding Stress Analysis

In Figures 13.3 and 13.4, it is shown that spray cooling for only three hours with a two foot chimney will assure that the average fuel temperature in the hottest fuel element will not exceed 886°C, although the corresponding peak fuel temperature will reach 982°C. Figure 13.5 presents clad strength and applied stress from equilibrium hydrogen dissociation pressure plus any other gas present within the clad as a function of fuel temperature. Early in the fuel life, there is residual air backfilling but relatively little fission gas. Both the nitrogen and oxygen form metal compounds after the fuel has been operated at full power for a period of time. Early in the effective fuel life, the air disappears as a gas leaving only hydrogen and fission gas.

For Figure 13.5 to be valid, all the fuel within the clad must have the same temperature and be at the same temperature as the clad. In this case, the Safety Limit is the crossover of the Clad Strength Curve and Gas Pressure Curve. Except for a time duration very early in the fuel element life before the air has been absorbed, the Safety Limit is about 930°C. In a real fuel element during a LOCA much of the fuel has a temperature lower than the peak temperature. For this case, the excess hydrogen gas from the hotter portions of the fuel element will disappear into the sink created by the cooler portions of the curve.

In the current example using three hours of spray cooling and a two foot chimney, the hottest fuel element ranges in temperature from 603°C at the bottom to a peak temperature of 982°C near the top. The average fuel temperature is 886°C with the bottom six (6) inches of the 15- inch fuel having fuel temperatures considerably less than the average fuel temperature. The clad temperature is a few degrees (6-8°C) cooler than the adjacent fuel temperature. There is thus a small area along the clad in which the clad temperature reaches 975°C. The curve in Figure 13.5 shows that the resulting clad strength in this region of the clad is about 35 Mpa. The peak temperature of the fuel slowly rises (over a 4-hour period) from 100°C to 980°C. Consequently, the excess hydrogen gas due to dissociation has time to be absorbed in the cooler fuel sections without raising the pressure substantially above that characteristic of the cooler section (603°C-700°C) of the fuel element. The resulting gas pressure will be less than 0.8 Mpa (700°C) which is considerably less than the 35 Mpa strength of the hot clad. There is thus no danger of clad rupture during the air cooling portion of the LOCA scenario when the fuel is previously spray cooled for only three hours. However, as a further conservatism, the UCD/MNRC will spray cool the fuel for a least 3.7 hours and will therefore experience an average fuel temperature in the hottest element of approximately 845°C and a maximum fuel temperature of 930°C during the air cooling phase (Figure 13.6). Since these temperatures are lower than those used in the preceding example, it is clear that at the UCD/MNRC there is even less danger of clad rupture during the air cooling portion of a LOCA

#### 13.2.3.2.2.11 Ground Water Contamination

As a result of activation of impurities in the primary cooling water, the water will contain small amounts of radionuclides depending on reactor power, reactor operating time and time since reactor shutdown. To characterize the radioactivity expected to be present in the UCD/MNRC primary coolant at 2 MW, measured values for the predominant radionuclides were adjusted to reflect estimated equilibrium concentrations at 2 MW (Table 11-4, Section 11.1.1.2.1).

€ R

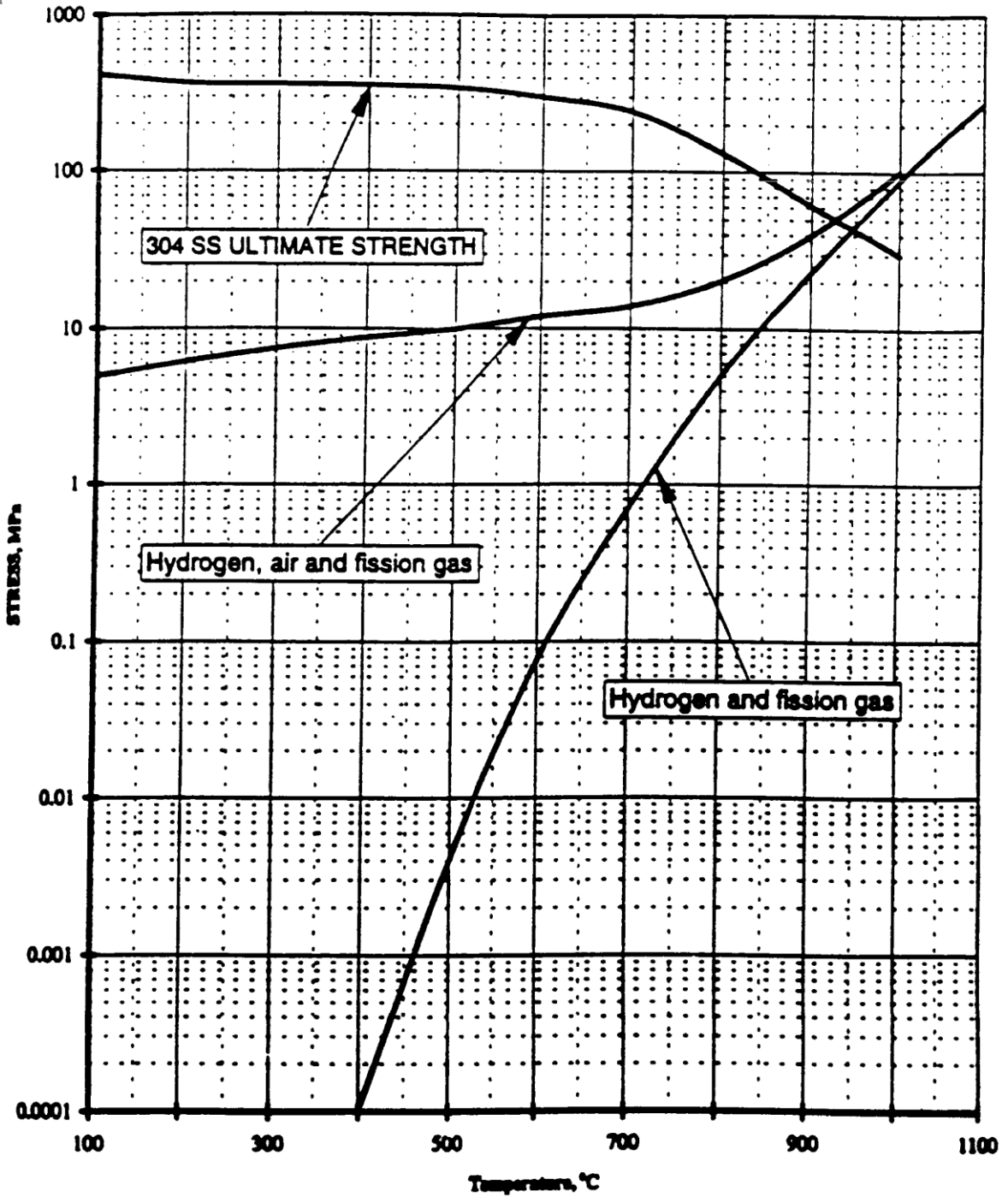


FIGURE 13.5 CLAD STRENGTH AND APPLIED STRESS RESULTING FROM EQUILIBRIUM HYDROGEN DISSOCIATION PRESSURE AS A FUNCTION OF TEMPERATURE

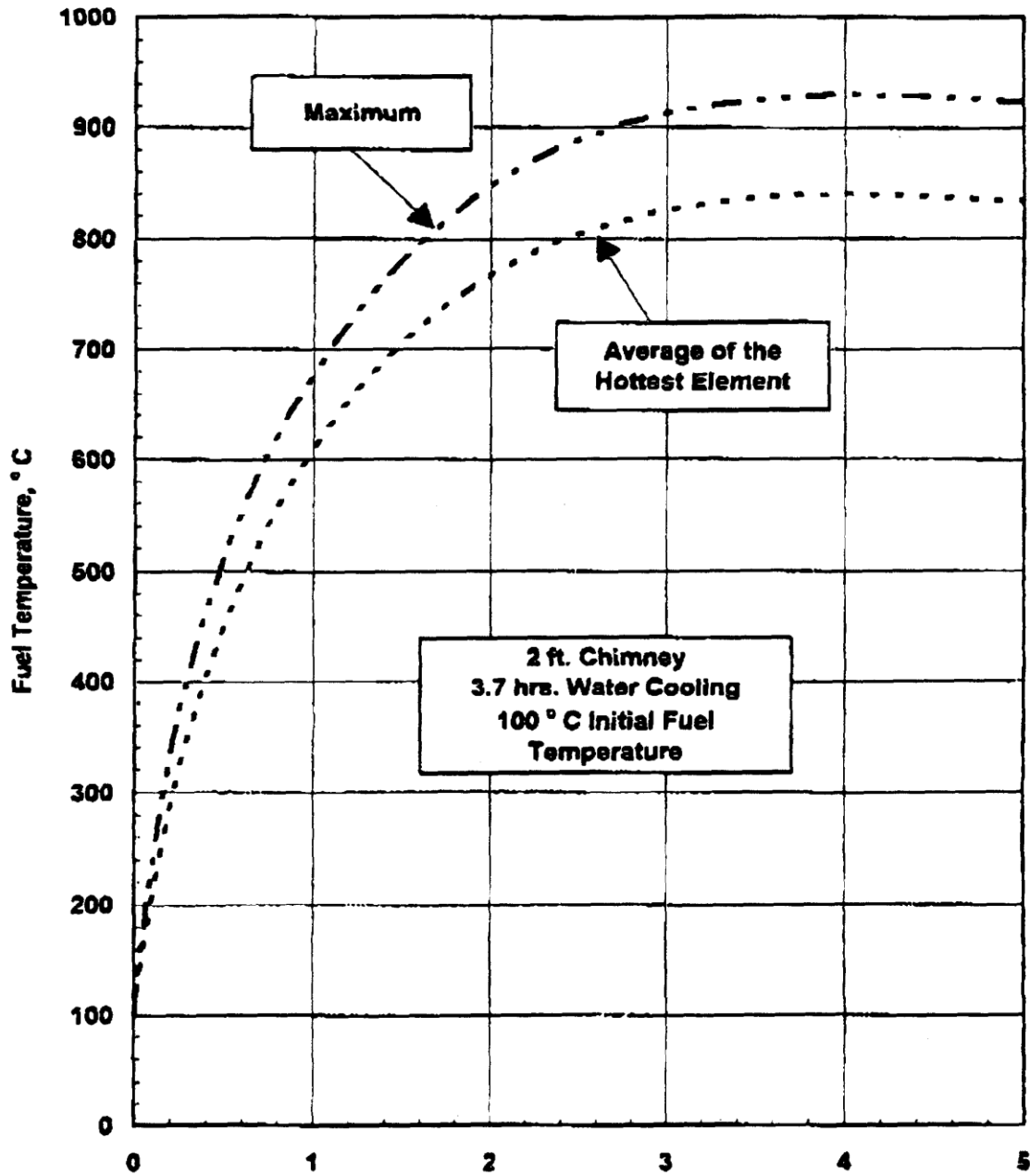


FIGURE 13.6 MAXIMUM AND AVERAGE FUEL TEMPERATURES FOR THE HOTTEST FUEL ELEMENT AS FUNCTIONS OF TIME AFTER END OF SPRAY COOLING FOR 3.7 HOURS

Next, a calculation was made to determine the length of time for the lost coolant to reach ground water.

The relationship to determine the time (t) for water to move from a point under the reactor tank a distance, D, to ground water is:

$$t=D/(K \times I);$$

where:

t = penetration time (sec.);

D = depth of penetration with time (ft);

I = hydraulic gradient = 1.0;

K = hydraulic conductivity =  $4.57 \times 10^{-4}$  ft/sec (Reference 13.14).

If it is assumed that the ground water is 80 feet below the UCD/MNRC site, it would require more than 36 hours for it to be reached if the reactor tank containment were breached. The radionuclide concentrations present in the reactor tank water upon reaching the ground water were then calculated utilizing a 36 hour delay time. These values are presented in Table 13-6.

As shown, Aluminum-28, Magnesium-27, and Nitrogen-16 are gone by the time the tank water reaches the ground water, and most of the other radionuclides will have undergone some degree of decay during the first 36 hours. Decay will, of course, vary depending on the radionuclide, but Argon-41 activity would fall to about  $6 \times 10^{-12}$   $\mu\text{Ci/ml}$  during the first 36 hours. Because of its low solubility in water, argon has no limiting water concentration under 10 CFR Part 20. However, this concentration level is well below the 10 CFR Part 20 air concentration limit for the unrestricted area. Since Argon-41 is only a concern from a dose standpoint when an individual is immersed in an Argon-41 cloud, and since the concentration in this situation is well below the air or cloud limit for the unrestricted area, Argon-41 is not a problem in the ground water.

The concentration of Manganese-56 in the reactor primary water will be about  $4.7 \times 10^{-4}$   $\mu\text{Ci/ml}$ . This means that at initial release the Manganese-56 concentration is 6.7 times higher than the  $7 \times 10^{-8}$   $\mu\text{Ci/ml}$  unrestricted area concentration limit in 10 CFR Part 20. However, as shown in Table 13-6, the Manganese-56 concentration is far below the 10 CFR Part 20 limit by the time it reaches ground water.

The estimated Hydrogen-3 (tritium) level is dependent upon how long the reactor has operated since initial startup and how much non-radioactive makeup water has been added prior to the LOCA. As shown in Table 11-4, after 20 years of operation at 2 MW with no addition of clean makeup, water the tritium concentration may reach  $1.3 \times 10^{-2}$   $\mu\text{Ci/ml}$ , but this is definitely an upper limit estimate and a concentration closer to  $1.0 \times 10^{-3}$   $\mu\text{Ci/ml}$  (the 10 CFR 20 concentration limit) is expected for at least the first several years. However, the tritium concentration in the water when it is released will be largely unchanged when and if the tank water reaches the ground water. Even so, the potential tritium dose to members of the general public who might consume the ground water will still be low because this accident will be a one-time event with a limited duration of release, and because only a limited amount of the 7,000 gallons of water potentially released from the reactor tank will likely escape from the radiography bays in the facility.

**TABLE 13- 6 PREDOMINANT RADIONUCLIDES IN PRIMARY COOLANT AT EQUILIBRIUM AND UPON REACHING GROUND WATER**

Radionuclide	Half Life	Equilibrium Concentration at 2 MW ( $\mu\text{Ci/ml}$ )	Concentration Reaching Ground Water ( $\mu\text{Ci/ml}$ )
Aluminum-28	2.3 min	$6.0 \times 10^{-3}$	0
Argon-41	1.8 hr	$3.0 \times 10^{-3}$	$6.17 \times 10^{-12}$
Hydrogen-3	12 yr	$1.0 \times 10^{-3}$ to $1.3 \times 10^{-2}$	$1.0 \times 10^{-3}$ to $1.3 \times 10^{-2}$
Magnesium-27	9.46 min	$4.0 \times 10^{-4}$	0
Manganese-56	2.58 hr	$4.7 \times 10^{-4}$	$4.09 \times 10^{-10}$
Nitrogen-16	7.14 sec	131	0
Sodium-24	14.96 hr	$2.6 \times 10^{-3}$	$5.00 \times 10^{-4}$

There will obviously also be a reduction in the tritium concentration when the reactor tank water mixes with the ground water, and normally, chemical processes take place as water percolates through soil which result in partial removal of many radionuclides. While these processes are usually not as significant for tritium as they are for many other radionuclides, some small reduction in tritium concentration may occur.

The potential release of tritium between  $1.0 \times 10^{-3} \mu\text{Ci/ml}$  and  $1.3 \times 10^{-2} \mu\text{Ci/ml}$  also assumes the tritium concentration in the primary water reaches the predicted 2 MW levels. This may or may not occur and will definitely not occur rapidly. The Hydrogen-3 concentration will gradually build up as it is produced. Periodic monitoring of the primary coolant for this radionuclide (semi-annually until the trend stabilizes) will allow continuous long-term assessment of the Hydrogen-3 concentration and its relation to 10 CFR Part 20 limits.

At the time the reactor tank water reaches the ground water, the Sodium-24 concentration will meet the 10 CFR Part 20 release limit for discharge into a sewer system, but will exceed the 10 CFR Part 20 effluent release concentration. However, after just 2.1 days of decay, the concentration of Sodium-24 in the ground water (ignoring dilution) will be within the NRC effluent concentration limit in 10 CFR Part 20. In addition, the Sodium-24 ground water concentration will continue to drop due to the continued rapid decay of this radionuclide. Therefore, Sodium-24 does not represent a significant source of potential radiation exposure to the general public.

### 13.2.3.2.2.12 Radiation Levels from the Uncovered Core

Even though there is a very remote possibility that the primary coolant and reactor shielding water will be totally lost, direct and scattered radiation doses from an uncovered core following 2 MW operations were calculated in Appendix B and are summarized here. Direct radiation doses were calculated for a person standing on the grating directly above the reactor core. The core, shut down and drained of water, was treated as a bare cylindrical uniform source of 1 MeV photons. No accounting was made of sources other than fission product decay gammas, and no credit was taken for gamma attenuation through the fuel element end pieces and the upper grid plate. The first of these assumptions is optimistic, the second conservative, and the net effect is conservative. The results are given in Table 13-7 and agree with results for the 2 MW Torrey Pines TRIGA® Reactor (Reference B.18).

**TABLE 13-7 DOSE RATES ON THE UCD/MNRC REACTOR TOP AFTER A LOSS OF POOL WATER ACCIDENT FOLLOWING 2 MW OPERATIONS**

<b>Time After Shutdown</b>	<b>Effective Dose Equivalent Rate (rem/h)</b>
10 seconds	$3.64 \times 10^4$
1 hour	$3.77 \times 10^3$
1 day	$1.69 \times 10^3$
1 week	$8.96 \times 10^2$
1 month	$4.70 \times 10^2$

A second calculation was made to determine the dose rate to a person in the reactor room who is not in the direct beam from the exposed core but is still subject to scattered radiation from the reactor room ceiling. The dose point was chosen to be three feet above the reactor room floor at a distance of six feet away from the edge of the reactor tank. This is the furthest distance a person can get from the edge of the tank and still remain in the reactor room. The ceiling of the reactor room is about twenty four feet from the reactor top and is assumed to be a thick concrete slab. The concrete slab assumption gives the worst case scattering, but it should be carefully noted that the roof over the reactor is only corrugated metal and not a thick concrete slab. Therefore, in reality the scattering will not be as great as calculated because the radiation from the unshielded core will be collimated upward by the shield structure and will undergo minimal interaction with the roof, greatly reducing the actual dose rates away from the edge of the tank. The results of the calculated dose rates due to scatter in the reactor room are found in Table 13-8. These dose rates show that personnel could occupy areas within the reactor room shortly after the accident for a sufficient period of time to undertake mitigating actions without exceeding NRC occupational dose limits.

**TABLE 13- 8 SCATTERED RADIATION DOSE RATES IN THE UCD/MNRC REACTOR ROOM AFTER A LOSS OF POOL WATER ACCIDENT FOLLOWING 2 MW OPERATIONS**

<b>Time After Shutdown</b>	<b>Effective Dose Equivalent Rate (rem/h)</b>
10 seconds	9.640
1 hour	1.000
1 day	0.449
1 week	0.238
1 month	0.124

A final calculation was carried out to estimate the dose rates to a person at the UCD/MNRC facility fence due to scattered radiation from the reactor room ceiling. The dose point was chosen to be three feet above the ground at the facility fence. This is the closest point a member of the public would be able to occupy. The calculated dose rates are presented in Table 13-9, but once again are overestimates because scatter off of the reactor room ceiling will be much less than assumed.

**TABLE 13- 9 SCATTERED RADIATION DOSE RATES AT THE UCD/MNRC FACILITY FENCE AFTER A LOSS OF POOL WATER ACCIDENT FOLLOWING 2 MW OPERATIONS**

<b>Time After Shutdown</b>	<b>Effective Dose Equivalent Rate (rem/h)</b>
10 seconds	0.460
1 hour	0.047
1 day	0.021
1 week	0.011
1 month	0.006

## 13.2.4 Loss of Coolant Flow

### 13.2.4.1 Accident Initiating Events and Scenarios

Loss of coolant flow could occur due to failure of a key component in the reactor primary or secondary cooling system (e.g. a pump), loss of electrical power, or blockage of a coolant flow channel. Operator error could also cause loss of coolant flow.

Scenarios for loss of coolant flow events during operation are difficult to imagine since the bulk water temperature adiabatically increases at a rate of about  $1.1^{\circ}\text{C}/\text{min}$  at a power level of 2 MW. Under these conditions, the operator has ample time to reduce the power and place the heat-removal system into operation before any abnormal temperature is reached in the reactor water. A core inlet temperature alarm at  $45^{\circ}\text{C}$  and primary and secondary low flow alarms will alert the operator to an abnormal condition and should allow for corrective action prior to reaching the bulk water temperature limit.

### 13.2.4.2 Accident Analysis and Determination of Consequences

#### 13.2.4.2.1 Loss of Coolant Flow Without Immediate Operator Action

If the reactor were operated without coolant flow for an extended period of time (and there was no heat removal by reactor coolant systems), voiding of the water in the core would occur and the water level in the tank would decrease because of evaporation. The sequence of events postulated for this very unlikely condition is as follows:

- a) The reactor would continue to operate at a power of 2 MW (provided that the rods were adjusted to maintain power) and would heat the tank water at a rate of about 1.1°C/min until the water entering the core approached the saturation temperature (this would take 60 minutes, assuming an initial temperature near 35°C and adiabatic conditions). At this time, voids in the core would cause power oscillations and the negative void coefficient of reactivity would cause a reduction in power if control rods were not adjusted to maintain power;
- b) If it is assumed that the operator or automatic control system maintained power at 2 MW, about 3180 kg/hr of water would be vaporized (assuming that the system is adiabatic except for the evaporation process), and the water level would decrease. It would take about 9 hours to heat and vaporize the entire tank at this rate. In fact, the reactor would shut down as the water level passed the top of the fuel.

It is considered inconceivable that such an operating condition would go undetected. Water level, water flow, and water temperature alarms would certainly alert the operator. Also, as the water level lowers, the reactor room radiation monitors will alarm. Because of all of these factors, water should be added to the tank to mitigate the problem.

### 13.2.5 Mishandling or Malfunction of Fuel

#### 13.2.5.1 Accident Initiating Events and Scenarios

Events which could cause accidents in this category at the UCD/MNRC reactor include 1) fuel handling accidents where an element is dropped underwater and damaged severely enough to breach the cladding, 2) simple failure of the fuel cladding due to a manufacturing defect or corrosion, and 3) overheating of fuel with subsequent cladding failure during steady state operations or pulsing; overheating might occur due to incorrect loading of fuel elements with different <sup>235</sup>U enrichments in a mixed core.

### 13.2.5.2 Accident Analysis and Determination of Consequences

#### 13.2.5.2.1 Single Element Failure in Water

At some point in the lifetime of the UCD/MNRC reactor, used fuel within the core will be moved to new positions or removed from the core. Fuel elements are moved only during periods when the reactor is shut down. The most serious fuel-handling accident involves spent or used fuel that has been removed from the core and then dropped or otherwise damaged, causing a breach of the fuel element cladding and a release of fission products. As noted previously, the standard or accepted maximum hypothetical accident for TRIGA® reactors involves failure of the cladding of a single fuel element after extended reactor operations, followed by instantaneous release of the fission products directly into the air of the reactor room. A less severe, but more credible accident involving a single element cladding failure assumes the failure occurs underwater in the reactor tank 48 hours after reactor shutdown (i.e., 48 hours of decay has occurred). This accident has been analyzed in Appendix B and results in much lower doses to the public and the reactor staff than those estimated for the MHA.

Assumptions used for assessing the consequences of the single element failure in water are almost exactly the same as those used for the MHA, except for the presence of pool water which contains most of the halogens and thereby reduces the halogen dose contribution. The fission product release fraction to the cladding gap remains at  $7.7 \times 10^{-5}$  and the halogen release fraction from the fuel-cladding gap is still a very conservative 0.5. However, for the single element failure in water there are two assumptions which differ from the MHA. First, the fuel is assumed to have decayed for 48 hours prior to the accident and secondly it is assumed that most of the halogens released from the cladding gap remain in the water and are removed by the demineralizer. However, a small fraction, approximately 2.5% of the total halogens released to the cladding gap are, in this case, assumed to escape from the reactor tank water into the reactor room air, which is more conservative than assuming total (100%) solubility of the halogens as is sometimes done for TRIGA® reactors (Reference B.18). However, even assuming a 2.5% halogen release from the pool water will almost certainly result in an overestimate of the actual radioiodine activity released into the room because of the use of a 50% halogen gap release fraction rather than the 1.7% documented in References B.7 and B.8. In addition, about 50% of the airborne halogens released from the pool water are expected to plate out in the reactor building before reaching the outside environment. See References B.4 and B.5. The experience at TMI-2, along with experimental data, indicate that the 50% halogen release fraction is much too large. Smaller releases, possibly as little as 0.6% of the iodine reaching the cladding gap may be released into the reactor room air due in part to a large amount of the elemental iodine reacting with cesium to form CsI, a compound much less volatile and more water soluble than elemental iodine (Reference B.8).

As with the MHA, radiological consequence calculations were done using the Radiological Safety Analysis Computer Program (RSAC-5) version 5.2, 02/22/94 (Reference B.9).

RSAC-5 calculates consequences of the release of radionuclides to the atmosphere and can generate a fission product inventory; decay and ingrow the inventory with time; model the downwind dispersion of the activity; and calculate doses to downwind individuals.

For this accident at the UCD/MNRC, dispersion coefficients ( $\chi/Q$  values) for locations in the unrestricted area, 10 m (the UCD/MNRC perimeter fence line nearest the building which defines the interface of the restricted and unrestricted area) out to 100 m, were input directly into the code and were calculated using Regulatory Guide 1.145 methodology (Reference B.11). Calculations were performed for Pasquill weather classifications A through F. Diffusion coefficients were taken from Reference B.12 and are presented in Table B-2. Calculations were performed assuming a ground level release at an 800 cfm reactor room release rate without any credit for stack height or building wake effects, which would only improve mixing and lower projected doses. Furthermore, it was assumed that all of the fission products were released to the unrestricted area by a single reactor room air change, which would maximize the dose rate to persons exposed to the plume during the accident and minimize the exposure time to receive the highest estimated dose from this accident. These latter assumptions regarding release are very, very conservative since the reactor room is not at ground level and, rather than 10 meters, is closer to 30 meters from the perimeter fence. Furthermore, there are no normal or direct flow pathways to support an 800 cfm ground level flow from the reactor room to the unrestricted area.

The results of the RSAC-5 calculations are shown in Tables B-4 and B-6. Included are doses inside the reactor room (Table B-4) and doses at several locations in the unrestricted area outside the UCD/MNRC (10 to 100 m from the building) as a function of weather class (Table B-6). Results are reported for the Committed Dose Equivalent (CDE) to the thyroid, the Committed Effective Dose Equivalent (CEDE) due to inhalation, the Deep Dose Equivalent (DDE) due to air immersion, and the Total Effective Dose Equivalent (TEDE) resulting from adding the CEDE and the DDE.

As indicated by the results in Table 13-10, the occupational dose to workers who evacuate the reactor room within 5 minutes following the cladding failure of a single fuel element in water should be approximately 32.5 millirem Total Effective Dose Equivalent and 660 millirem Committed Dose Equivalent to the thyroid. If evacuation occurs within 2 minutes, as it no doubt will because the reactor room is small and easy to exit, the doses drop to 13.2 millirem TEDE and 260 millirem CDE. All of these doses are well within the NRC guidelines for occupational exposure as stated in 10 CFR 20.1201.

**TABLE 13-10 Occupational Radiation Doses in the UCD/MNRC Reactor Room Following a Single Element Failure in Water.**

Accident: Cladding Failure in Water 48 Hours after Reactor Shutdown				
	CDE Thyroid (millirem)	CEDE (millirem)	DDE (millirem)	TEDE (millirem)
2 minute room occupancy	260	13	0.2	13.2
5 minute room occupancy	660	32	0.5	32.5

Projected doses to the general public in the unrestricted area around the UCD/MNRC following a single element failure in water are shown in Table 13-11. To receive the indicated dose, a person must be exposed to the airborne plume from the reactor room for the entire 9.2 minute period it is being vented. Even using this exposure requirement at the closest distance to the UCD/MNRC building (10 m), and assuming the most unfavorable atmospheric conditions (Category F), the maximum TEDE to a member of the general public would be only 4.7 millirem. Although this accident and the corresponding radiation doses are very unlikely to occur, the maximum estimated dose to a member of the general public of 4.7 millirem is still well within the 100 millirem TEDE limit for the general public published in 10 CFR 20 (Reference 10 CFR 20.1301). It should also be noted that if one assumes a 50% halogen plateout in the reactor room, the TEDE drops to 2.4 millirem.

**TABLE 13-11 RADIATION DOSES TO MEMBERS OF THE GENERAL PUBLIC UNDER DIFFERENT ATMOSPHERIC CONDITIONS AND AT DIFFERENT DISTANCES FROM THE UCD/MNRC FOLLOWING A CLADDING FAILURE IN WATER 48 HOURS AFTER REACTOR SHUTDOWN.**

Distance (Meters)	CDE Thyroid (millirem)	CEDE (millirem)	DDE <sup>1</sup> (millirem)	TEDE (millirem)
10	97	4.7	0.0	4.7
20	76	3.7	0.0	3.7
40	52	2.5	0.0	2.5
80	30	1.4	0.0	1.4
100	24	1.1	0.0	1.1

<sup>1</sup>Doses less than 0.1 mrem were entered as zero.

- CDE - Committed Dose Equivalent
- CEDE - Committed Effective Dose Equivalent
- DDE - Deep Dose Equivalent
- TEDE - Total Effective Dose Equivalent

#### 13.2.5.2.2 Fuel Loading Error

##### 13.2.5.2.2.1 1998 Fuel Loading Error

The fuel loading error description and analysis is provided below is given as reference. It is no longer applicable as it involved the misplacement of a 20/20 element in the mix J core. As the mix J core and the use of 8.5 wt% is no longer permitted, this fuel loading error is only given to provide a previously accepted methodology for analyzing fuel loading errors.

Operation of the UCD/MNRC Reactor after a 20/20 fuel element has been loaded into the wrong grid position could result in increased temperatures in surrounding fuel elements. Neutronics calculations were done to identify the worst-case error for use in analyzing this type of accident. It was assumed that no fuel elements can be loaded in rings A or B of the UCD/MNRC reactor because of the cutout in the upper grid plate. The highest power peaking would result from a fresh 20/20 fuel element being substituted for a graphite dummy element at a ring C flat (even numbered) position. Because of the surrounding 8.5/20 fuel environment, higher element power would be generated if this substitution were made in the mixed-fuel reference core than in the all-20/20 reference core. The worst case is fresh 20/20 fuel replacing the dummy element in position C10 of the MixJ Core loading. The loading error would increase the excess reactivity by \$1.51 (18%) and would increase the peak element power by 11.5 kW (42%) to 39.1 kW. Accordingly, the loading error is assumed to result in a peak element power of 40 kW.

The RELAP5 steady-state thermal-hydraulic analysis described in Section 4.6 was repeated with the nominal inlet temperature (32.2 °C) and the peak element power increased to 40 kW (core radial peaking factor increased to 2.0). The peak fuel temperature was 734°C, which is still below the operational safety limit (the LCO) of 750°C. The critical heat flux ratio was 2.6, indicating that there is still ample margin before film boiling. Since the hot channel outlet void fraction was 5% and the core outlet subcooling was 8°C, it appears unlikely that any detectable chugging will occur. Should chugging occur, it will be easily detected and appropriate operational constraints established.

Operation in pulse mode with the maximum allowed reactivity insertion,  $\beta$ 1.75, and the above loading error was also considered. The core-average fuel  $\Delta T$  with this insertion is 161 °C. The four factors used to produce the total peaking factor were:

- Core radial peaking factor of 2.0, based on a peak element power of 40 kW;
- Axial and pin tilt factors of 1.27 and 1.5, respectively, from the worst MixJ Core in Section 4.5.5.5 Table 4-17;
- 1.33 pin radial peaking factor, since the erroneously loaded fuel is the 20/20 type.

This leads to a peak fuel temperature of 837 °C, well below the 1100°C pulsing limit. Thus, pulse operation is also predicted to be benign.

#### 13.2.5.2.2.2 Current 30B Fuel Loading Error

The 30B core is the only core configuration in the foreseeable future for the MNRC. Given that the central graphite insert and aluminum slug would have to be removed on purpose and the A/B ring grid plate would need to be installed (also on purpose) before fuel could be loaded (accidentally), placement of fuel into the A or B ring is not credible. The most credible and serious fuel loading error for the 30 B core is placement of a 30/20 element into the C ring. Based on the October 1<sup>st</sup> 2017 MCNP model of the 30B the worst position to place a 30/20 element in the C ring is the I-6 (grid naming system) position. This placement results in an element thermal output of 41 kW which is slightly higher than what was found and analyzed for in section 13.2.5.2.2.1. This results in a core radial peaking factor of 2.07 instead of 2.0. It is unlikely that that this slight (<3%) increase in element power output would result in lowering the critical heat flux ratio from 2.6 (section 13.2.5.2.2.1) to below 2.0, which would be considered potentially unacceptable.

It is important to note the analysis in section 13.2.5.2.2.1 assumes axial peaking to be 1.33 with the control rods to be 2/3<sup>rds</sup> of the way withdrawn for the reference 20E core. The 20E reference core was designed to intentionally maximize peaking factors to make all other permissible core configurations more conservative in terms of peaking factors (references 4.4 and 4.5). A radial peaking factor of 1.33 is highly unlikely due to burnup in the core and the fact that the current core can only achieve 1.0 MW operations (without xenon buildup) with the control rods 2/3<sup>rds</sup> of the way withdrawn. With the control rods fully withdrawn the axial peaking factor was calculated to be 1.23. Therefore, the true axial peaking factor of the current core is between 1.23 and 1.33. This would place the actual worst case heating somewhere between 6% below and 3% above what was analyzed for in the previous accepted accident analysis for a fuel loading error section. Therefore the consequences of this accident for steady state operations would likely be indistinguishable from the accident analyzed in section 13.2.5.2.2.1. Furthermore if this fuel loading error somehow did result in a single element failure, the consequences would be bound by the MHA.

Operation in pulse mode with the maximum allowed reactivity insertion,  $\beta_{1.75}$ , and the above loading error was also considered. The core-average fuel  $\Delta T$  with this insertion is 161 °C (based on 94 elements). The four factors used to produce the total peaking factor were:

- Core radial peaking factor of 2.07, based on a peak element power of 41 kW (based on 101 elements);
- Axial and pin tilt factors of 1.33 and 1.63, respectively, from the worst 20E Core (with aluminum slug/graphite assembly installed in A and B ring) in Section 4.5.5.5;
- 1.33 pin radial peaking factor that is selected from section 4.5.5.5 based on the controls being withdrawn  $2/3^{\text{rds}}$  of the way to achieve 2.0 MW operation.

This leads to a peak fuel temperature of 993 °C, below the 1100°C pulsing limit. Thus, pulse operation is also predicted to be benign. This result is conservative as the peaking factors were selected to be larger than our current non-zero burnup 30B core.

It is prudent to discuss the series of events that would be required to produce this fuel loading error. As discussed in chapter 4 there is currently no new supply of TRIGA fuel in the world. If new 30/20 elements become available they will be used to finish populating first the E ring with 30/20 elements, then they will be used to populate rings outside of E ring. This will be done to minimize core axial peaking for safety and operational purposes. It is inconceivable that for this planned evolution of the 30B core that a 20/20 element would be accidentally removed from the C ring, placed in storage, and a fresh 30/20 element would be accidentally placed in the now vacant C ring position.

## 13.2.6 Experiment Malfunction

### 13.2.6.1 Accident Initiating Events and Scenario

Improperly controlled experiments involving the UCD/MNRC reactor could potentially result in damage to the reactor, unnecessary radiation exposure to facility staff and members of the general public, and unnecessary releases of radioactivity into the unrestricted area. Mechanisms for these occurrences include the production of excess amounts of radionuclides with unexpected radiation levels, and creation of unplanned for pressures in irradiated materials which subsequently vent into reactor irradiation facilities or into the reactor building causing damage from the pressure release or an uncontrolled release of radioactivity. Other mechanisms for damage, such as corrosion and large reactivity changes, are also possible.

### 13.2.6.2 Accident Analysis and Determination of Consequences

Because of the potential for accidents which could damage the reactor if experiments are not properly controlled, there are strict procedural and regulatory requirements addressing experiment review and approval (Chapter 10). These requirements are focused on ensuring that experiments will not fail, but they also incorporate requirements to assure that there is no reactor damage and no radioactivity releases or radiation doses which exceed the limits of 10 CFR Part 20, should failure occur. For example, specific requirements in UCD/MNRC administrative procedures such as the Utilization of the University of California

- Davis/McClellan Nuclear Radiation Center Research Reactor Facility (MNRC- 0027) (Reference 11.7) establish detailed administrative procedures, technical requirements, and the need for safety reviews for all types of proposed reactor experiments.

Safety related reviews of proposed experiments usually require the performance of specific safety analyses of proposed activities to assess such things as generation of radionuclides and fission products (i.e., radioiodines), and to ensure evaluation of reactivity worth, chemical and physical characteristics of materials under irradiation, corrosive and explosive characteristics of materials, and the need for encapsulation. This process is an important step in ensuring the safety of reactor experiments and has been successfully used for many years at research reactors to help assure the safety of experiments placed in these reactors. Therefore, the process is expected to be an effective measure in assuring experiment safety at the UCD/MNRC reactor.

A specific limitation of less than \$1.00 on the reactivity of individual moveable experiments placed in the reactor tank has been established and is safe because analysis has shown that pulse reactivity insertions of \$1.75 in the 2 MW UCD/MNRC reactor result in fuel temperatures which are well below the fuel temperature safety limit of 930°C (Section 13.2.2). In addition, limiting the worth of each moveable experiment to less than \$1.00 will assure that the additional increase in transient power and temperature will be slow enough so that the fuel temperature scram will be effective. Likewise, an additional reactivity limitation of less than \$1.75 for any single secured experiment and an absolute total reactivity worth of \$1.92, including the potential reactivity which might result from malfunction, flooding or voiding, is safe because Section 13.2.2 shows that a maximum reactivity of \$1.92 can be safely inserted.

Limiting the generation of certain radionuclides in experiments and certain fission products in fueled experiments also helps to assure that occupational radiation doses (as well as doses to the general public) due to postulated experiment failure, with subsequent radionuclide or fission product release, will be within the limits prescribed by 10 CFR 20. A limit of 1.5 curies of I-131 through I-135 for a single fueled experiment is small compared to the approximately 8,500 curies of I-131 through I-135 which are present in the single fuel element failure analyzed in Section 13.2.1 (failure in air) and Section 13.2.5 (failure in water). In both cases, the occupational doses and the doses to the general public in the unrestricted area due to radioiodine are within 10 CFR 20 limits. Therefore, establishing conservative limits for radioiodine in experiments will result in projected doses well within 10 CFR 20 limits. Strontium-90 in a fueled experiment is limited to 0.005 curies which is far below the 34 curies present in the single fuel element failures mentioned above. Since no dose limits will be exceeded in the single element failure accidents, doses from experiments where the Strontium-90 is limited to 0.005 curies are expected to be safely within 10 CFR 20 limits.

Projected damage to the reactor from experiments involving explosives varies significantly depending on the quantity of explosives being irradiated and where the explosives are placed relative to critical reactor components and safety systems. For example, an explosives limit of 25 milligrams when irradiation is to be in the reactor tank carries the additional restriction that experiment containment must be able to withstand the pressure produced upon detonation. Based on the following discussion, containment of detonation pressure from this small quantity of explosives is possible using conventional materials and methods, and such containment will eliminate potential damage to reactor components or other experiments (Reference 13.15).

A 25 milligram quantity of explosives, upon detonation, releases approximately 25 calories (104.2 joules) of energy with the creation of 25 cm<sup>3</sup> of gas. For the explosive TNT, the density is 1.654 gm/cm<sup>3</sup> so that 25 mg represents a volume of 0.015 cm<sup>3</sup>. If the assumption is made that the energy release occurs as an instantaneous change in pressure, the total force on the encapsulation material is the sum of two pressures. For a one cm<sup>3</sup> volume, the energy release of 104.2 joules represents a pressure of 1032 atmospheres. The instantaneous change in pressure due to gas production in the same volume adds another 25 atmospheres. The total pressure within a 1 cm<sup>3</sup> capsule is then 1057 atmospheres for the complete reaction of 25 mg of explosives.

Typical construction materials of capsules are stainless steel, aluminum and polyethylene. Table 13-12 lists the mechanical properties of these encapsulation materials.

**TABLE 13-12 MATERIAL STRENGTHS**

Material	Yield	Ultimate	Density
Stainless Steel (type 304)	35 ksi	85 ksi	7.98 g/cm <sup>3</sup> (500 lb/ft <sup>3</sup> )
Aluminum (alloy 6061)	40 ksi	45 ksi	2.739 g/cm <sup>3</sup> (171 lb/ft <sup>3</sup> )
Polyethylene	1.7 ksi	1.4 ksi	0.923 g/cm <sup>3</sup>

Analysis of the encapsulation materials determines the material stress limits that must exist to confine the reactive equivalent of 25 mg of explosives. The stress limit in a cylindrical container with thin walls is one half the pressure times the ratio of the capsule diameter to wall thickness,

$$\sigma_{\max} = \frac{pd}{2t};$$

where:

- $\sigma_{\max}$  = maximum stress in container wall;
- p = total pressure within the container;
- d = diameter of the container;
- t = wall thickness.

When evaluating an encapsulation material's ability to confine the reactive equivalent of 25 mg of explosives, the maximum stress in the container wall is required to be less than or equal to the yield strength of the material:

$$\frac{pd}{2t} \leq \sigma_{\text{yield}} ;$$

where  $\sigma_{\text{yield}}$  is the yield strength. Solving this equation for d/t provides an easy method of evaluating an encapsulation material:

$$\frac{d}{t} \leq \frac{2}{p} \sigma_{\text{yield}} ;$$

Assuming an internal pressure of 1057 atmospheres (15,538 psi), maximum values of d/t are displayed in Table 13-13 for the encapsulation materials of Table 13-12. The results indicate that a polyethylene vial is not a practical container since its wall thickness must be 4.5 times the diameter. However, both the aluminum and the stainless steel make satisfactory containers.

**TABLE 13-13 Container Diameter to Thickness Ratio**

Material	d/t
Stainless Steel (type 304)	4.3
Aluminum (alloy 6061)	5.1
polyethylene (low density)	0.22

As a result of the preceding analysis, a limit of 25 milligrams of TNT equivalent explosives is deemed to be a safe limitation on explosives which may be irradiated in facilities located inside the reactor tank.

Irradiation of larger quantities of explosives in the reactor tank is not allowed. However, safety analyses have been performed which show that three pounds of TNT equivalent explosives may be safely irradiated in radiography Bays 1, 2, 3 and 4, provided the beam tube cover plates are at least 0.5 inch thick (Reference 13.16).

Southwest Research Institute (SRI) completed a safety analysis to determine the maximum amount of TNT equivalent explosive allowable in radiography Bay 3, (i.e., the amount that will not cause failure of the beam tube cover plate and will cause only repairable structural damage to the bay) (Reference 13.17). Bay 3 is the smallest in volume of all the radiography bays at the UCD/MNRC. The study concluded that Bay 3 can withstand a detonation of ■ pounds of TNT equivalent explosive with certain modifications. The study performed by SRI concluded that the Bay 3 door track must be strengthened. The recommended strengthening consists of welding three additional anchor bolt plates to the door track and bolting these plates into the wall with additional drilled anchor bolts. This strengthening assures that the door will respond in a ductile manner to an unexpected high blast load, absorbing the additional load with larger deflections, rather than responding in a brittle failure mode.

The UCD/MNRC completed a similar study to determine the maximum amount of TNT equivalent explosives allowable in all radiography bays (Reference 13.16). This study concluded that Bays 1, 2 and 4 can withstand a detonation of ■ pounds of TNT equivalent explosives without any damage provided the criteria in Table 13-14 are implemented in each bay. However, to meet category 1 protection requirements for ■ pounds of explosives, the west door of Bay 2 also requires modification by means of an additional wheel and post assembly. The analysis performed by the UCD/MNRC demonstrates that for ■ pounds of TNT equivalent explosives, no modifications are necessary to the radiography bay doors for Bays 1, 2 or 4. These doors will also respond in a ductile manner. As a result of the above studies, it is concluded that installation of beam tube cover plates with the thicknesses shown in Table 13-14 and implementing an explosives limitation of ■ pounds of TNT equivalent for each of the four radiography bays will satisfy the safety limitations established by the two previous safety analyses.

**TABLE 13-14 Changes to Beam Tube Cover Plates**

BAY	Cover Plate Thickness (in)	Explosive Location	Explosive distance* ref.@ 0°	Deflection (in)	Resistance (psi)	Ultimate Resistance (psi)
1	0.60	L/D = 100	13.00	0.294	43.6	108
2	0.60	L/D = 100	10.40	0.353	52.3	108
3	0.75	L/D = 100	8.80	0.433	125	168
4	0.60	L/D= 100	13.70	0.248	37	108

\*Minimum distance from the beam tube cover plate to the explosive.

The Argon-41 Production Facility (see Chapter 10) can produce argon-41 in excess of the amounts analyzed in Appendix A. However, if the system releases argon-41, the gas will be contained in the reactor room and the existing reactor room ventilation system will be used in recirculation mode to prevent the release of argon-41 to the environment by recirculating the gas until it decays. The existing stack continuous air monitor will also be used to verify that none has been released outside the UCD/MNRC boundary.

If the system had a catastrophic failure and 4 Curies of argon-41 were released to the volume of the reactor room, the argon-41 concentration in the reactor room would be  $2 \times 10^{-2} \mu\text{Ci/ml}$  and the gamma dose rate in the reactor room would be approximately 22 R/hr (based on a semi-infinite cloud, see following calculation). Personnel would be evacuated from the reactor room and access would be restricted. The reactor room ventilation system (as described in Chapter 9) would be operated in the recirculation mode for approximately one day before the dose rate from argon-41 decays to less than 1 mR/hr. Therefore, the argon-41 discharge limit defined in the UCD/MNRC Technical Specifications will not be exceeded due to the recirculation mode of the reactor room ventilation system.

One accident that could be postulated includes failure of the irradiation canister due to over-pressurization from the argon gas supply cylinder, since a new argon supply cylinder is typically delivered at a pressure of 2200 psi and the canister is rated for 1800 psi. However, this requires multiple failures and is considered non-credible: a) the operator would have to violate an operational procedure; b) the regulator would have to fail, and c) at the same time the pressure relief valve would have to fail. Also, another potential accident is that liquid nitrogen could spill into the reactor tank, causing expansion of the water and expelling a portion of tank water. To prevent this, a catch basin surrounds the cold trap. A third accident could result if the pressure relief valve became choked with supersonic flow; however, the flow rates are estimated to be less than sonic as shown in the following calculation.

**ARGON-41 CONCENTRATION IN REACTOR ROOM**

Given:

$$1. \text{ Reactor room volume} = 7.39 \times 10^3 \text{ ft}^3 \quad (1)$$

2. 4 Ci Argon-41 in argon production system

$$3. D(y)_{\infty/2} = 0.25E_{\gamma}\chi \quad (2)$$

where

$D(y)_{\infty/2}$  = gamma dose rate from a semi-infinite cloud (rad/sec)

$E_{\gamma}$  = average gamma energy per disintegration (MeV/dis)

= 1.2936 MeV/dis for Argon-41

(3)

$\chi$  = concentration of gamma emitting isotope in the cloud (Ci/m<sup>3</sup>)

Therefore:

$$\chi = (4\text{Ci}) / (7.39 \times 10^3 \text{ ft}^3) (1 \text{ m}^3 / 35.314 \text{ ft}^3) = 1.91 \times 10^{-2} \text{ Ci/m}^3$$

$$\begin{aligned} D(y)_{\infty/2} &= 0.25E_{\gamma}\chi \\ &= (0.25)(1.2936 \text{ MeV/dis})(1.91 \times 10^{-2} \text{ Ci/m}^3) \\ &= (0.0062 \text{ rads/sec})(3600 \text{ sec/hr}) \\ &= 22.24 \text{ rads/hr} \end{aligned}$$

Since

$$D = D_0 e^{-\lambda t}$$

$$t = -(1/\lambda) \ln(D/D_0)$$

$$= -(T_{1/2} / \ln 2) \ln(D/D_0)$$

Then for:

$$D = 1 \text{ mrad/hr}$$

$$\begin{aligned} t &= -(1.8 \text{ hr} / \ln 2) \ln(1 \text{ mrad/hr} / 22.240 \text{ mrad/hr}) \\ &= 26 \text{ hr} \end{aligned}$$

(1) See Figure 9.11

(2) Shleien, B., L. Slaback, and B. Birky, Handbook of Health Physics and Radiological Health, Williams &amp; Wilkin January 1997, p. 439.

(3) Nuclides and Isotopes, 14<sup>th</sup> edition, Chart of the Nuclides, GE Nuclear Energy, p. 22.

### SONIC FLOW

Assume: Perfect Gas

Constants:	Property	Value	Units
	R	208	N-m/kg-degK
	K(cp/cv)	1.67	Dimensionless

Problem: Determine if the pressure relief valve will experience choking due to supersonic flow.

Solution:

First calculate the speed of sound in argon at 40 °C and -200 °C given that  $c$  = speed of sound in a medium =  $(kRTg_c)^{1/2}$

$$c = [1.67 \times 208(\text{N-m/kg-degK}) \times (40+273)\text{K} \times 1(\text{kg-m/N-s}^2)]^{1/2}$$

$$= 329.7327 \text{ m/s at } 40 \text{ }^\circ\text{C}$$

$$c = [1.67 \times 208(\text{N-m/kg-degK}) \times (-200+273)\text{K} \times 1(\text{kg-m/N-s}^2)]^{1/2}$$

$$= 159.2397 \text{ m/s at } -200 \text{ }^\circ\text{C}$$

Next calculate the velocity of the argon in the tubing at the pressure relief valve given volumetric flow rate  
 $V$  = velocity  $\times$  area.

From technical data on valve, assume  $V = 1 \text{ ft}^3/\text{min}$ , based on air and relief at 1125 psi.

$$V = 1 \text{ ft}^3/\text{min} \times (12 \text{ in./ft})^3 \times (2.54 \text{ cm/in.})^3 \times 1 \text{ min}/60 \text{ sec} = 471.9474 \text{ cm}^3/\text{sec}$$

$$\text{area} = \pi r^2 = 3.14 \times (0.18 \text{ in./2})^2 = 0.025434 \text{ in.}^2 \quad (\text{based on } 1/4 \text{ in. tubing})$$

$$= 0.16409 \text{ cm}^2$$

$$\text{velocity} = V/\text{area} = 2876.15 \text{ cm/sec} = 28.7615 \text{ m/s}$$

$$\text{mach number} = \text{velocity}/c = 0.180618 \text{ at } -200 \text{ }^\circ\text{C}$$

$$= 0.087227 \text{ at } 40 \text{ }^\circ\text{C}$$

Conclusion: Gas velocity at the relief valve is less than the speed of sound in argon and therefore should not experience choking at the valve

Reference: Zucher, Robert D., Fundamentals of Gas Dynamics, Weber Systems, Incorporated, 1977, pp. 89, 130-133, 375.

## 13.2.7 Loss of Normal Electrical Power

### 13.2.7.1 Accident Initiating Events and Scenarios

Loss of electrical power to the UCD/MNRC could occur due to many events and scenarios which routinely affect commercial power.

### 13.2.7.2 Accident Analysis and Determination of Consequences

Since the UCD/MNRC does not require emergency backup power systems (see Chapter 6) to safely

maintain core cooling, there are no credible reactor accidents associated with the loss of electrical power. A backup power system is present at the UCD/MNRC which mainly provides conditioned power to the reactor console and control instrumentation. Therefore, the reactor will not automatically scram when there is a loss of normal electrical power. In fact, the backup power system is capable of providing electrical power for the reactor control and various operational measurements for a period of time after loss of normal electrical power and until its batter power supply is exhausted.

Loss of normal electrical power during operations is addressed in the reactor operating procedures, which require that upon loss of normal power an orderly shutdown is to be initiated by the operator on duty. The battery backup power will allow monitoring of the orderly shutdown of the reactor and verification of the reactors shutdown condition.

### 13.2.8 External Events

#### 13.2.8.1 Accident Initiating Events and Scenarios

Hurricanes, tornadoes and floods are virtually nonexistent in the area around the UCD/MNRC reactor. Therefore, these events are not considered to be viable causes of accidents for the reactor facility. In addition, seismic activity in Sacramento is low relative to other areas of California (Chapter 2). Seismic activity has already been mentioned in connection with the postulated reactor tank damage 13.2.3.

The UCD/MNRC facility is surrounded by a security fence and a physical security plan is continuously in force for personnel and activities inside the fence. The reactor site is located in an Industrial Park on a former US Air Force Base where access and overall security is far stricter than the surrounding civilian business and residential areas. Therefore, accidents caused by human controlled events which would damage the reactor, such as explosions of other unusual actions, are considered to be of very low probability.

Since the UCD/MNRC reactor is located at the edge of the runway at the former McClellan AFB, airplane crashes involving the reactor may potentially cause reactor damage.

#### 13.2.8.2 Accident Analysis and Determination of Consequences

A study of the probability of aircraft crashes which could cause reactor damage at the UCD/MNRC was conducted by GA Technologies as a part of the original Stationary Neutron Radiography System Proposal (Reference 13.19). The conclusions show that the calculated reactor damage probability due to aircraft accidents is  $5 \times 10^{-8}$  per reactor year. This value was obtained using conservative assumptions and the "best estimate" value is expected to be considerably lower than  $5 \times 10^{-8}$ . Safety analysis of nuclear power reactors have generally concluded that a reactor damage probability due to an aircraft accident which is less than  $1 \times 10^{-7}$  per year does not represent a significant contribution to the overall reactor risk. Therefore, it is concluded that no specific aircraft accident and no radiological consequences need to be considered for the UCD/MNRC reactor.

### 13.2.9 Mishandling of Malfunction of Equipment

#### 13.2.9.1 Accident Initiating Events and Scenarios

No credible accident initiating events were identified for this accident class. Situations involving an operator error at the reactor controls, a malfunction or loss of safety related instruments or controls and an electrical fault in the control rod system were anticipated at the reactor design stage. As a result, many safety features, such as control system interlocks and automatic reactor shutdown circuits, were designed into the overall TRIGA® Control System (Chapter 7).

TRIGA® fuel also incorporates a number of safety features (Chapter 4) which together with the features designed into the control system assured safe reactor response, including in some cases reactor shutdown.

Malfunction of confinement or containment systems would have the greatest impact during the maximum hypothetical accident (MHA), if they were used to lessen the impact of such an accident. However, as shown in section 13.2.1, no credit is taken for confinement or containment systems in the analysis of the MHA for the UCD/MNRC reactor. Furthermore, no safety consideration at the UCD/MNRC depend on confinement or containment systems, although simple confinement devices like a fume hood might be used as part of normal operations.

Rapid leaks of liquids have been previously addressed in Section 13.2.3. Although no damage to the reactor occurs as a result of these leaks, the details of the analysis provide a more comprehensive explanation.

### 13.3 Summary and Conclusions

Chapter 13 of the Safety Analysis Report contains a conservative analysis of many different types of hypothetical accidents as they relate to the UCD/MNRC reactor and the surrounding environment. Beginning with the maximum hypothetical accident and continuing on through an entire array of other accidents, it has been shown that the consequences of such accidents will not result in occupational radiation exposure of the UCD/MNRC staff or radiation exposure of the general public in excess of applicable NRC limits in 10 CFR Part 20. Furthermore, there is no projected significant damage to the reactor as an outcome of the accidents evaluated, except the damage or malfunction assumed as part of the different accident scenarios analyzed. Details of the assumptions used for each accident scenario and the specific consequences of each accident are presented in the text of this Chapter.

**CHAPTER 14**

**Technical Specifications**

**14 Technical Specifications:**

MNRC Technical Specifications are provided in a separate document.

**CHAPTER 15**

**Financial Qualifications**

**15 Financial Qualifications:**

MNRC financial qualifications are provided in a separate document.

**CHAPTER 16**

**Other License Considerations**

## **16 Other License Considerations:**

### **16.1 Prior Use of Reactor Components**

MNRC does not use any equipment previously utilized at other reactor facilities.

### **16.2 Medical Use of Non-Power Reactors**

MNRC does not engage in nor is it licensed to engage in any activities for medical use of the facility.

**APPENDIX A**

**RADIOLOGICAL IMPACT OF Ar-41, N-16,  
FISSION PRODUCTS AND ACTIVATED  
MATERIALS DURING NORMAL OPERATIONS**

Appendix A - Valid Pages  
Rev. 3 3/05/18

i	Rev. 3	3/5/18
ii	Rev. 3	3/5/18
A-1	Rev. 3	3/5/18
A-2	Rev. 3	3/5/18
A-3	Rev. 3	3/5/18
A-4	Rev. 3	3/5/18
A-5	Rev. 3	3/5/18
A-6	Rev. 3	3/5/18
A-7	Rev. 3	3/5/18
A-8	Rev. 3	3/5/18
A-9	Rev. 3	3/5/18
A-10	Rev. 3	3/5/18
A-11	Rev. 3	3/5/18
A-12	Rev. 3	3/5/18
A-13	Rev. 3	3/5/18
A-14	Rev. 3	3/5/18
A-15	Rev. 3	3/5/18
A-16	Rev. 3	3/5/18
A-17	Rev. 3	3/5/18
A-18	Rev. 3	3/5/18
A-19	Rev. 3	3/5/18
A-20	Rev. 3	3/5/18
A-21	Rev. 3	3/5/18
A-22	Rev. 3	3/5/18
A-23	Rev. 3	3/5/18
A-24	Rev. 3	3/5/18
A-25	Rev. 3	3/5/18

Table of Contents

A.1. INTRODUCTION ..... A-1  
 A.1.1 Purpose ..... A-1  
 A.1.2 Radiological Standards ..... A-2  
 A.1.3 MNRC Design Bases..... A-2  
 A.2 PRODUCTION RATE AND CONCENTRATION OF Ar-41 FROM BEAMS..... A-4  
 A.3 PRODUCTION RATE OF Ar-41 FROM COOLANT WATER ..... A-9  
 A.4. MAXIMUM IMPACT OF Ar-41 OUTSIDE THE OPERATIONS BOUNDARY ..... A-14  
 A.5. NITROGEN-16 ACTIVITY..... A-17  
 A.6 RELEASE OF FISSION PRODUCTS TO TANK WATER ..... A-21  
 A.7 ACTIVATION OF MATERIALS IN RADIOGRAPHY BAYS ..... A-22

List of Tables

A-1 Neutron Beam Sizes ..... A-3  
 A-2 Enclosure Exhaust Rates..... A-4  
 A-3 Neutron Interactions Per Second in Beam Volumes ..... A-5  
 A-4 Ar-41 Production Rate in Beams ..... A-6  
 A-5 Ar-41 Concentrations in the Unrestricted Area After Dispersion in Air at Various  
 Atmospheric Stability Classes..... A-16  
 A-6 Typical Induced Radionuclides During Neutron Radiography of Aircraft Components .... A-23

REFERENCES

- A.1 Dorsey, N. E., "Properties of Ordinary Water-Substances," pp. 537-544, Reinhold Publ. Co., New York, New York.
- A.2 Moore, W. J., Physical Chemistry, 3rd Edition, p. 341, Prentice-Hall, New Jersey, 1962.
- A.3 Boerboom, A. J. H. and G. Kleyn, "Diffusion Coefficients of Noble Gases in Water," J. Chem Phys., V. 50, No. 3, February 1, 1969.
- A.4 Climatology of the National Reactor Testing Station, January 1966.
- A.5 Meteorology and Atomic Energy - 1968, TID-24190.
- A.6 Kocher, D. C., "Dose-Rate Conversion Factors for External Exposure to Photons and Electrons," Health Physics 45, pp. 665-686, 1983.
- A.7 CAP88-PC, Clean Air Act Assessment Package - 1988, (V1.0), 1988.
- A.8 Mittl, R.L., and M. H. Theys, "N-16 Concentrations in EBWR," p. 81, Nucleonics, March 1961.

## APPENDIX A

RADIOLOGICAL IMPACT OF Ar-41, N-16, FISSION PRODUCTS,  
AND ACTIVATED MATERIALS DURING NORMAL OPERATIONSA.1. INTRODUCTION

## A.1.1 Purpose

The purpose of this appendix is to show the methods and calculations that were used to predict the production and concentrations and dose rates from Ar-41, N-16, and fission and activation products as a result of normal MNRC operation.

Argon-41 is produced by the reaction of thermal neutrons with the argon contained in air ( $\approx 1\%$ ) entrained in the reactor cooling water as it passes through the core and the air in the path of the radiography beams. This Ar-41 ends up in the reactor room and radiography bays and is subsequently released to the atmosphere through the facility exhaust stack.

Nitrogen-16 is produced by the reaction of fast neutrons with oxygen. The only N-16 source in the MNRC facility that needs consideration results from neutron interactions with the oxygen in the water molecule of the reactor cooling water as it passes through the core. The production of N-16 as a result of the reaction of neutrons with oxygen present in air, either in the beam path or air entrained in the reactor cooling water, is insignificant and has been neglected.

A portion of the N-16 produced in the core is eventually released from the top of the reactor tank into the reactor room. The half-life of N-16 is only 7.14 seconds so its radiological consequences outside the MNRC are insignificant.

Although not expected, the cladding on a fuel element could fail during normal operation as a result of corrosion or a manufacturing defect. Should a failure occur, a fraction of the fission products would be released to the reactor tank. Most of the halogens would remain in the cooling water while the noble gases, krypton and xenon, would be released to the reactor room and subsequently to the atmosphere through the exhaust stack. Although this operational occurrence is mentioned in this appendix, it is addressed in detail in Appendix B as part of the analysis of a single fuel element failure in water.

There will be a varying amount of neutron activation products generated due to neutron interactions with materials being intentionally irradiated in reactor irradiation facilities. Normally this will be fixed radioactivity and mainly a source of direct radiation to operations personnel.

### A.1.2 Radiological Standards

The International Commission on Radiological Protection (ICRP) has been a principal organization studying the effects of ionizing radiation for many years. In 1959, Committee II of the ICRP published recommendations for maximum permissible concentrations (MPC) of radionuclides in air and water. These recommendations became the technical bases for radionuclide concentration limits published in 10 CFR Part 20. More recently, Committee II reviewed the current state of knowledge and published updated recommendations in Publication 30 (1978/79), which supersedes Publication 2. In this publication, the ICRP recommends that the concentration limit in air for radioactive noble gases be based only on the total effective dose equivalent computed for a person immersed in a large cloud of gamma-ray emitters. This guidance is justified in Publication 30, where it is shown that the internal and skin doses from the beta rays would add less than 1% of the total effective dose equivalent. At the MNRC a cloud of finite size is more applicable, because room sizes are not large enough to meet the required dimensions for an infinite cloud for the noble gas routinely present, i.e., Ar-41. Because of this, the total effective dose equivalent at the concentration limit is correspondingly lower.

In 1994, the U.S. Nuclear Regulatory Commission (NRC) implemented a major revision in 10 CFR 20 which incorporated many of the new dosimetry concepts published by the ICRP over the past several years. Since the new version of 10 CFR Part 20 is applicable to non-power reactors licensed by the NRC and is widely used as a basis for regulatory limits for similar reactors not under NRC jurisdiction, the calculations and interpretations in this appendix will be based on the requirements of the new 10 CFR Part 20.

The current 10 CFR Part 20 concentration limits for Ar-41 are:

- For accessible regions inside the operations boundary  $3 \times 10^{-6}$   $\mu\text{Ci/ml}$ ;
- For accessible regions outside the operations boundary  $1 \times 10^{-8}$   $\mu\text{Ci/ml}$ .

### A.1.3 MNRC Design Bases

The calculations for Ar-41 and N-16 releases from MNRC operation are based on the following system parameters:

#### Reactor System:

- (1) Reactor power - 2 MW;
- (2) Core coolant mass flow rate( $w$ ) -  $10.8 \times 10^3$  g/s;
- (3) Core coolant density ( $\rho$ ) -  $1.0$  g/cm<sup>3</sup>;
- (4) Average thermal neutron ( $\phi$ ) -  $2.0 \times 10^{13}$  n/cm<sup>2</sup>·sec;  
Flux > 0.6 eV =  $4.2 \times 10^{13}$  n/cm<sup>2</sup>·sec (for N-16 calculation);

- (5) Core flow area ( $A^f$ ) 546 cm<sup>2</sup>;
- (6) Fuel element length, heated ( $\ell_c$ ) - 38.1 cm;
- (7) Reactor tank - 213.4 cm dia. x 746.8 cm h. (7 ft dia. x 24 ½ ft h.);
- (8) Water depth above fuel - 609.6 cm (20 ft).

Facility:

(1)	<u>Enclosure volume</u>	<u>Vol(cm<sup>3</sup>)</u>
	Radiography Bay 1	2.09 x 10 <sup>9</sup> ;
	Radiography Bay 2	1.11 x 10 <sup>9</sup> ;
	Radiography Bay 3	1.70 x 10 <sup>8</sup> ;
	Radiography Bay 4	4.63 x 10 <sup>8</sup> ;
	Reactor Room	2.09 x 10 <sup>8</sup> .

	Equivalent Diameter (cm) @ Film Plane	Area cm <sup>2</sup>	Length* cm	Volume cm <sup>3</sup>	For Film Radiography cm <sup>3</sup>
Radiography Bay 1	25.4	510	941	4.80 x 10 <sup>5</sup>	2.52 x 10 <sup>6</sup>
Radiography Bay 2	25.4	510	762	3.89 x 10 <sup>5</sup>	2.04 x 10 <sup>6</sup>
Radiography Bay 3	25.4	510	581	2.96 x 10 <sup>5</sup>	1.56 x 10 <sup>6</sup>
Radiography Bay 4	58.4	2680	762	2.04 x 10 <sup>6</sup>	2.04 x 10 <sup>6</sup>

Table A-1 Neutron Beam Sizes

NOTE: On occasion, Bays 1, 2, and 3 will be used for standard film radiography. During these occasions, the neutron beams will have the same cross section as the Radiography Beam in Bay 4.

\* For these calculations it is assumed that the plane of radiography and the beam stop plane are at the same position. This is conservative since the distance of radiography is less than to the beam stop.

	cm <sup>3</sup> /s	
Radiography Bay 1	7.88 x 10 <sup>5</sup>	1.35 air changes per hour
Radiography Bay 2	4.72 x 10 <sup>5</sup>	1.53 air changes per hour
Radiography Bay 3	2.36 x 10 <sup>5</sup>	5.00 air changes per hour
Radiography Bay 4	2.83 x 10 <sup>5</sup>	2.20 air changes per hour
Reactor Room	3.78 x 10 <sup>5</sup>	6.50 air changes per hour
Sample Preparation Room	5.19 x 10 <sup>5</sup>	3.22 air changes per hour
TOTAL	2.68 x 10 <sup>6</sup>	

Table A-2 Enclosure Exhaust Rates

(2) Beam Intensity

Operating experience over the last five (5) years has shown that there is no benefit in performing neutron radiography at higher neutron fluxes than 10<sup>6</sup> to 10<sup>7</sup> n/cm<sup>2</sup> · sec. Therefore, the four beam tubes will be filtered to produce a thermal neutron flux of approximately 4 x 10<sup>6</sup> n/cm<sup>2</sup> · sec at 2 MW and an L/D = 100.

A.2 PRODUCTION RATE AND CONCENTRATION OF Ar-41 FROM BEAMS

The neutron beam intensity (J) at the plane of radiography is assumed to be 4 x 10<sup>6</sup> n/cm<sup>2</sup>·s. The total number of neutrons per second (I) passing the plane of radiography is then:

$$I = JR ;$$

where:

$$R = \text{area of the plane of radiography} = 2.68 \times 10^3 \text{ cm}^2 \text{ (23 in. dia) for film;}$$

$$= 5.07 \times 10^2 \text{ cm}^2 \text{ (10 in. dia) for electronic imaging;}$$

therefore:

$$I = 1.07 \times 10^{10} \text{ n/s for film radiography;}$$

$$= 2.03 \times 10^9 \text{ n/s for electronic imaging.}$$

Because the beam tubes will either be helium-filled or evacuated and sealed, there is no air to produce Ar-41 within the beam tubes. The neutrons in the beam in the length of the radiography bay will interact with the air to produce Ar-41. The number of interactions over the beam path length is:

$$I_0 - I;$$

where:

$I_0$  = the number of neutrons entering the air volume.

The relationship between  $I_0$  and  $I$  is:

$$I = I_0 e^{-\Sigma t f}$$

where:

$\Sigma$  = Ar-40 macroscopic cross section for thermal neutron interactions ( $1.7 \times 10^{-5}/\text{cm}$ );

$t$  = path length;

$f$  = fraction of argon in the air ( $9.4 \times 10^{-3}$ );

then:

$$I_0 - I = I_0(e^{-\Sigma t f} - 1) = \text{total interactions/s in beam volume.}$$

Bay	For Film Radiography	For Electronic Imaging
	$I_0 - I$ (int/s)	$I_0 - I$ (int/s)
1	$1.61 \times 10^6$	$3.05 \times 10^5$
2	$1.30 \times 10^6$	$2.47 \times 10^5$
3	$9.95 \times 10^5$	$1.89 \times 10^5$
4	$1.30 \times 10^6$	$1.89 \times 10^5^*$

Table A-3 Neutron Interactions Per Second in Beam Volumes

\* If Bay 4 is used for electronic imaging the beam diameter must be no larger than Bays 1, 2, and 3.

The production rate,  $P$ , of Ar-41 is:

$$P = \frac{(I_o - I)\lambda}{c} = \frac{\mu Ci}{s};$$

where:

$$c = 3.7 \times 10^4 \text{ dis/s per } \mu\text{Ci};$$

$$\lambda = \text{decay constant of Ar-41 (} 1.06 \times 10^{-4} \text{/s)}.$$

Bay	For Film Radiography P( $\mu\text{Ci/s}$ )	For Electronic Imaging P( $\mu\text{Ci/s}$ )
1	$4.61 \times 10^{-3}$	$8.73 \times 10^{-4}$
2	$3.90 \times 10^{-3}$	$7.41 \times 10^{-4}$
3	$2.99 \times 10^{-3}$	$5.67 \times 10^{-4}$
4	$3.90 \times 10^{-3}$	$5.67 \times 10^{-4}$

Table A-4 Ar-41 Production Rate in Beams

Assuming that the Ar-41 atoms are evenly distributed over a room volume, the rate of change of the number of Ar-41 atoms per  $\text{cm}^3$  can be determined as follows:

$$S = \text{source of Ar-41 atoms/s} = (I_o - I);$$

$$N = \text{Ar-41 concentration in atoms/cm}^3;$$

$$\lambda = \text{Decay constant} = 1.06 \times 10^{-4} \text{ sec}^{-1};$$

$$V_R = \text{Room volume} = (\text{See Section A 1.3});$$

$$q = \text{Exhaust rate} = (\text{See Section A 1.3}).$$

At equilibrium conditions  $\frac{dN}{dt} = 0$ ;

then:

$$N = \frac{S}{\lambda V_R + q} .$$

The Ar-41 activity (A) produced by a beam in  $\mu\text{Ci}/\text{cm}^3$  is given by:

$$A = \frac{\lambda N}{c} ;$$

then:

For film radiography in all bays (exhaust system on):

	<u>Ar-41 atoms/cm<sup>3</sup></u>	<u>Ar-41 concentration</u>
Bay 1	N = 1.6 atoms/cm <sup>3</sup>	A = 5.0 x 10 <sup>-9</sup> $\mu\text{Ci}/\text{ml}$
Bay 2	N = 2.2 atoms/cm <sup>3</sup>	A = 7.0 x 10 <sup>-9</sup> $\mu\text{Ci}/\text{ml}$
Bay 3	N = 3.9 atoms/cm <sup>3</sup>	A = 1.2 x 10 <sup>-8</sup> $\mu\text{Ci}/\text{ml}$
Bay 4	N = 3.7 atoms/cm <sup>3</sup>	A = 1.1 x 10 <sup>-8</sup> $\mu\text{Ci}/\text{ml}$ ;

For electronic imaging devices in Bays 1, 2, and 3 and film radiography in Bay 4 (exhaust system on):

	<u>Ar-41 atoms/cm<sup>3</sup></u>	<u>Ar-41 concentration</u>
Bay 1	N = 0.3 atoms/cm <sup>3</sup>	A = 9.0 x 10 <sup>-10</sup> $\mu\text{Ci}/\text{ml}$
Bay 2	N = 0.4 atoms/cm <sup>3</sup>	A = 1.0 x 10 <sup>-9</sup> $\mu\text{Ci}/\text{ml}$
Bay 3	N = 0.7 atoms/cm <sup>3</sup>	A = 2.0 x 10 <sup>-9</sup> $\mu\text{Ci}/\text{ml}$
Bay 4	N = 3.7 atoms/cm <sup>3</sup>	A = 1.1 x 10 <sup>-8</sup> $\mu\text{Ci}/\text{ml}$ .

If film radiography is used in all bays, the highest Ar-41 concentration is in Bay 3 and is  $\cong 200$  times lower than the 10 CFR Part 20 occupational concentration limit of  $3 \times 10^{-6} \mu\text{Ci}/\text{ml}$ . When electronic imaging devices are used in Bays 1, 2, and 3, Ar-41 concentrations are about three orders of magnitude below the 10 CFR 20 limit. The assumption of even distribution over the enclosure volume is, of course, only an approximation. Some regions will have higher concentrations, and some will have lower values. Occupancy factors will be combined with actual survey meter readings of radiation levels inside the radiography bay when establishing safe operating procedures. In the case of even distribution of Ar-41, but zero exhaust (i.e.,  $q = 0$ ), the Ar-41 concentrations are as follows:

For film radiography all bays (exhaust system off):

	<u>Ar-41 concentration</u>
Bay 1	$A = 2.2 \times 10^{-8} \mu\text{Ci/ml}$
Bay 2	$A = 3.1 \times 10^{-8} \mu\text{Ci/ml}$
Bay 3	$A = 1.7 \times 10^{-7} \mu\text{Ci/ml}$
Bay 4	$A = 7.6 \times 10^{-8} \mu\text{Ci/ml};$

For electronic imaging devices in Bays 1, 2, 3 and film radiography in Bay 4 (exhaust system off):

	<u>Ar-41 concentration</u>
Bay 1	$A = 4.0 \times 10^{-9} \mu\text{Ci/ml}$
Bay 2	$A = 6.0 \times 10^{-9} \mu\text{Ci/ml}$
Bay 3	$A = 3.2 \times 10^{-8} \mu\text{Ci/ml}$
Bay 4	$A = 7.6 \times 10^{-8} \mu\text{Ci/ml}.$

As can be seen from the above, the concentrations of Ar-41 in the radiography bays are well below the 10 CFR 20 occupational concentration limit, even with the bay ventilation system off.

(Note: The normal operating mode for the MNRC reactor will be with the radiography bays air handling system turned on. However, the reactor can be operated with this system turned off.)

The external dose equivalent rate for an occupationally exposed individual in radiography bay can be estimated by assuming that the room is a hemisphere with the equivalent volume of the room and the individual is immersed in the cloud at the center of the hemisphere. Because none of the radiography bays have dimensions large enough to equal the volume of a semi-infinite cloud for Ar-41, immersion of an individual at the center of a hemispherical cloud using the volume of the largest radiography bay will still give a total effective dose equivalent (TEDE) after 2000 hours of occupational exposure which is well below 5000 mrem. However, using this approach, the dose rate is determined by:

$$D = \frac{BS\mu(1-e^{-\mu_s R_o})}{2\mu_s g} = \frac{BS\mu(1-e^{-\mu_s R_o})}{2(8 \times 10^{-5})(5.5 \times 10^2)} = 11.36BS\mu(1 - e^{-\mu_s R_o}) \quad ;$$

where:

- B = Dose buildup factor (never less than 1) ;
- $R_o$  = Radius of hemisphere;
- $S\mu$  = Source strength ( $\text{dis/s-cm}^3$ ) ;
- $\mu_s$  = Linear absorption coefficient ( $\text{cm}^{-1}$ ) =  $8 \times 10^{-5}$  for air;
- g = dose conversion factor  $\left( \frac{\text{dis-cm}^3}{\frac{\text{mR}}{\text{hr}}} \right) = 5.5 \times 10^2$  for Ar-41

Using the above, it has been determined that the TEDE for a worker in the radiography bay with the highest Ar-41 concentration and the radiography bay exhaust system on will be approximately 0.5 millirem for 2000 hours of annual exposure. Even if this individual worked the 2000 hours with the radiography bays exhaust system off (which would not be a mode of normal operation) the annual TEDE would be only about 7.0 millirem.

### A.3 PRODUCTION RATE OF Ar-41 FROM COOLANT WATER

The Ar-41 activity in the reactor tank water results from irradiation of the air dissolved in the water. The following calculations were performed to evaluate the rate at which Ar-41 escapes from the reactor tank water into the reactor enclosure. The calculations show that the Ar-41 decays while in the water, and most of the radiation is safely absorbed in the water. The changes in Ar-41 concentration in the core region, in the tank water external to the reactor core, and in the air of the reactor enclosure are calculated using the variables as defined below:

- V = Volume of region (cm<sup>3</sup>);
- N = Atomic density (atoms/cm<sup>3</sup>);
- λ = Decay constant (s<sup>-1</sup>);
- σ = Absorption cross section (cm<sup>2</sup>);
- q = Volume flow rate from MNRC reactor room exhaust (cm<sup>3</sup>/s);
- w = Mass flow rate (g/s);
- ρ = Density (g/cm<sup>3</sup>);
- v = Volume flow rate through the core (cm<sup>3</sup>/s);
- Φ = Average thermal neutron flux in the core (n/cm<sup>2</sup>-s);
- ℓ<sub>c</sub> = Fuel element length (heated);
- A<sub>f</sub> = Flow area (standard TRIGA<sup>®</sup> fuel element).

The volume flow rate through the core is:

$$v_1 = \frac{w}{\rho} = \frac{11.3 \times 10^3 \text{ g/s}}{1 \text{ g/cm}^3} = 11.3 \times 10^3 \text{ cm}^3/\text{s};$$

where a typical mass flow rate w has been used; the exposure time in the core is:

$$t = \frac{V_1}{v_1} = \frac{A_f \ell_c}{v_1} = \frac{(546)(38.1)}{11.3 \times 10^3} = 1.84 \text{ s}$$

It remains to find the atom density N for dissolved argon in the reactor tank water.

According to Henry's Law for gases in contact with liquids, the equilibrium concentration in the liquid is proportional to the partial pressure of the gas. The saturated concentration of argon in water at one atmosphere of argon is (Reference A.1):

°C	cm <sup>3</sup> /1000 g H <sub>2</sub> O
0	52.4
25	30.8
50	22.5

Since the argon content of air is 0.94% by volume, the partial pressure of argon above the water is:

$$0.0094 (760 \text{ mm} - 23 \text{ mm, vapor pressure of water}) = 6.9 \text{ mm (Hg)}.$$

The argon concentration (N) in the water at a conservative estimate of the core inlet temperature (27°C) is:

$$N = \left(0.03 \text{ cm}^3 \frac{\text{argon}}{\text{cm}^3} \text{H}_2\text{O}\right) \frac{6.9 \text{ mm}}{760 \text{ mm}} \left(2.7 \times 10^{19} \frac{\text{atoms}}{\text{cm}^3}\right)$$

$$N = 7.35 \times 10^{15} \text{ atom/cm}^3$$

At 110°C, the core exit water temperature, the solubility of argon in H<sub>2</sub>O is 0.01 and the concentration is  $2.5 \times 10^{15}$  atoms/cm<sup>3</sup>.

The Ar-41 density (at equilibrium) at the exit from the core is given by:

$$A_{\infty} = A_0 e^{-\lambda t} + N \sigma \Phi (1 - e^{-\lambda t})$$

where t is the exposure time in the core (1.84 s).

The Ar-41 density at the entrance to the core is given by:

$$A_0 = A_{\infty} e^{-\lambda t}$$

The average out-of-core cycle time, T, is given by:

$$T = \frac{V_2}{v_1} = \frac{2.7 \times 10^7 \text{ cm}^3}{11.3 \times 10^3 \text{ cm}^3/\text{s}} = 2.39 \times 10^3 ;$$

where  $V_2$  is the tank volume (7-ft diameter and 24-ft deep) and  $v_1$  is, again, the volume flow rate through the core. The solution to this set of equations is:

$$A_\infty = N\sigma\Phi \left( \frac{1 - e^{-\lambda t}}{1 - e^{-\lambda(t+T)}} \right)$$

Substituting the values from above, one obtains:

$$A_\infty = (7.35 \times 10^{15}) (0.61 \times 10^{-24}) (2.0 \times 10^{13}) \frac{1 - e^{[-(1.06 \times 10^{-4})(1.84)]}}{1 - e^{[-(1.06 \times 10^{-4})(2.39 \times 10^3)]}}$$

$$A_\infty = 78.0 \text{ dps/cm}^3$$

and:

$$N_{41} = \frac{78.0}{1.06 \times 10^{-4}} = 7.4 \times 10^5 \text{ atoms/cm}^3$$

One source of Ar-41 in the room results from the reduced solubility of argon in water as the temperature increases. Considering the expected temperature rise of the water passing through the core, an immediate release of about 29% of the Ar-41 produced could be expected during passage. Some of this Ar-41 will be redissolved as it is transported into cooler water, but since the cooler water is in equilibrium with the air above, it is nearly saturated with argon and will not absorb all of the argon released. Measurements of Ar-41 in the water as a function of height above the core indicate that approximately 60% of the released Ar-41 is reabsorbed.

Assuming that 12% ( $29\% \times [1 - 0.6]$ ) of the Ar-41 comes out of solution, remains undissolved after leaving the core, and escapes to the air, this source would be:

$$S_1 = 0.12N_{41}v_1 = (0.12) \left( 7.4 \times 10^5 \frac{\text{atoms}}{\text{cm}^3} \right) \left( 11.3 \times 10^3 \frac{\text{cm}^3}{\text{s}} \right) ;$$

$$= 1.0 \times 10^9 \frac{\text{atoms}}{\text{s}} .$$

The tendency of the balance of the argon activity in the tank to escape to the air owing to its proximity to the water-air boundary will constitute the additional source of Ar-41 at the water surface.

An estimate of the fraction of argon atoms in the tank water that escape each second can be obtained by considering the relation between the average distance traversed by a diffusing particle and the diffusion coefficient obtained from the random walk treatment. The relation is (Reference A.2):

$$\Delta X^2 = 2Dt ;$$

where  $\Delta X^2$  is the mean square displacement in time  $t$  and  $D$  is the diffusion coefficient. We then have for the mean displacement:

$$\Delta X = (2Dt)^{1/2} .$$

The diffusion coefficient for argon atoms in water (at 23°C) has been measured to be  $1.1 \times 10^{-5}$   $\text{cm}^2/\text{s}$  so that in one second the average displacement is  $(2.2 \times 10^{-5})^{1/2}$  or  $4.7 \times 10^{-3}$   $\text{cm}$  (Reference A.3). The average diffusion velocity is approximately  $4.7 \times 10^{-3}$   $\text{cm}/\text{s}$  and thus about half of the atoms within  $4.7 \times 10^{-3}$   $\text{cm}$  of the surface in any one second will reach the surface and escape. Where  $A_s$  is the surface area of the tank, the diffusion of argon across the water-air interface would constitute a source of :

$$S_2 = 0.88 \left( \frac{\Delta X}{\Delta t} \right) N_{41} A_s = 0.88 \left( \frac{4.7 \times 10^{-3}}{2} \right) (7.4 \times 10^5) (3.58 \times 10^4) ;$$

$$= 5.48 \times 10^7 \frac{\text{atoms}}{\text{s}} .$$

The total source is then:

$$S = S_1 + S_2 = (10.0 + 0.548) \times 10^8 = 10.55 \times 10^8 \frac{\text{atoms}}{\text{s}} ;$$

$$= 3.02 \mu\text{Ci}/\text{s} .$$

Assuming complete mixing with air, the equilibrium Ar-41 concentration in the reactor room with the reactor room exhaust system operating is given by the following equation:

$$N = \frac{S}{\lambda V_R + q} = \frac{10.55 \times 10^8}{(1.06 \times 10^{-4})(2.09 \times 10^8) + (3.78 \times 10^5)};$$

$$= 2,637 \frac{\text{atoms}}{\text{cm}^3}.$$

where the room volume is  $2.09 \times 10^8 \text{ cm}^3$  and the room air exhaust rate is  $3.78 \times 10^5 \text{ cm}^3/\text{sec}$ . This corresponds to an activity concentration of:

$$A = \frac{\lambda N}{c} = \frac{(1.06 \times 10^{-4})(2,637)}{(3.7 \times 10^4)} = 7.55 \times 10^{-6} \mu\text{Ci/ml}.$$

The maximum concentration is reached when the reactor room exhaust system is not operating ( $q=0$ ). For this condition, the following is obtained:

$$N = 4.76 \times 10^3 \text{ atoms/cm}^3;$$

$$A = 1.36 \times 10^{-4} \mu\text{Ci/ml}.$$

The 10 CFR Part 20 Derived Air Concentration (DAC) for Ar-41 is  $3.0 \times 10^{-6} \mu\text{Ci/ml}$ . Therefore, the calculated Ar-41 concentration in the reactor room under normal operating conditions (i.e., 2 MW steady state with the reactor room exhaust system operating) is 2.52 times the NRC occupational concentration limit, but even at 2000 hours of annual occupancy in the reactor room, the TEDE will still be well below NRC regulatory limits, as shown below. With the reactor room exhaust system off, the calculated Ar-41 concentration in the reactor room will build up to about 45 times the DAC in 10 CFR Part 20, but this is not a normal mode of operation for the reactor since technical specification requirements will mandate that the reactor room exhaust system be fully operating when the reactor is operating.

Actual measurements of Ar-41 in the reactor room after the reactor had operated for about 9 hours at 1 MW (reactor room exhaust system on) showed Ar-41 concentrations averaging about  $1.5 \times 10^{-6} \mu\text{Ci/ml}$  for areas which are occupied during normal work in the room. This would then correlate to about  $3.0 \times 10^{-6} \mu\text{Ci/ml}$  at 2 MW.

Using the same calculational method employed for estimating Ar-41 dose to personnel in the radiography bays, and recognizing that the dimensions of the reactor room do not provide a

cloud volume large enough to create a semi-infinite cloud for Ar-41, the TEDE after 2000 hours of immersion in an Ar-41 concentration of  $7.55 \times 10^{-6}$   $\mu\text{Ci/ml}$  is about 318 millirem, and for 2000 hours in a concentration of  $3.0 \times 10^{-6}$   $\mu\text{Ci/ml}$  the TEDE is about 126 millirem.

#### A.4. MAXIMUM IMPACT OF Ar-41 OUTSIDE THE OPERATIONS BOUNDARY

The Ar-41 will be discharged from the MNRC through the exhaust stack, which is 60 feet above ground level. Dilution with other building ventilation air and atmospheric dilution will reduce the Ar-41 concentration considerably before the exhaust plume returns to ground level locations which could be occupied by personnel or the general public.

It is important to note that only a modest amount of dilution is required to reduce the Ar-41 concentration to a level that is well below the 10 CFR Part 20 limit of  $1 \times 10^{-8}$   $\mu\text{Ci/ml}$  for unrestricted areas. This is due in part to the fact that the Ar-41 concentration leaving the stack is not expected to exceed about  $1.0 \times 10^{-6}$   $\mu\text{Ci/ml}$  when the ventilation flow from the radiography bays air handling system is available (i.e., the system in on), and this flow is mixed with the other building ventilation flow. If the radiography bay air handling system is not operational, then the projected Ar-41 concentration leaving the stack will increase slightly to about  $3.0 \times 10^{-6}$   $\mu\text{Ci/ml}$ , and this will occur only while the radiography bays ventilation is turned off. Since the normal mode of operation for the reactor will be with the radiography bays ventilation system turned on, (which provides the maximum stack ventilation flow of 5678 cfm), it should also be noted that the concentration of Ar-41 leaving the stack may actually be closer to  $4.0 \times 10^{-7}$   $\mu\text{Ci/ml}$  if one chooses the 1 MW measured concentration for Ar-41 in the reactor room and extrapolates that value to 2 MW ( $3.0 \times 10^{-6}$   $\mu\text{Ci/ml}$ ). It appears that virtually any of the preceding concentration values are a reasonable estimate because adjustment of 1995 measured Ar-41 release concentrations for the current maximum flow rate out the stack (5678 cfm), for an increase in power to 2 MW and for more projected operating hours at 2 MW, results in an estimated Ar-41 release concentration out the stack of about  $9.0 \times 10^{-7}$   $\mu\text{Ci/ml}$ . Clearly, this value compares favorably with the other projected Ar-41 concentrations obtained by different methods, and thus adds confidence to these projected release rates.

The method outlined in References A.4 and A.5 was used to predict the maximum concentration of Ar-41 in the unrestricted area. The prediction shows that the concentration is well below the NRC concentration limit of  $1 \times 10^{-8}$   $\mu\text{Ci/ml}$ .

The basic equations used were:

$$\chi_{max} = \frac{2Q}{e\pi\bar{u}h^2} \left( \frac{C_z}{C_y} \right) = \frac{Ci}{m^3} = \frac{\mu Ci}{cm^3} ;$$

$$d_{max} = \left( \frac{h^2}{C_z^2} \right)^{\frac{1}{2-n}} = m ;$$

where:

- Q = Emission Rate =  $2.68 \times 10^{-6}$  Ci/s\*;
- h = Stack Height = 18.2 m;
- $\bar{u}$  = Mean Wind Speed (m/s);
- $\begin{cases} C_y \\ C_z \end{cases}$  = Virtual diffusion coefficients in the crosswind and vertical directions ( $m^{n/2}$ );
- n = The dimensionless stability parameter.

\* Based on a projected (and seemingly most probable) Ar-41 release concentration at the stack of  $1.0 \times 10^{-6}$   $\mu$ Ci/ml and a stack flow rate of 5678 cubic feet per minute (assuming the radiography bays air handling system is operational, which will be the normal mode of operation). However, it should be noted that if the radiography bays air handling system is not operable the slight increase in the Ar-41 concentration leaving the stack will be offset by a proportional decrease in stack flow rate so the projected emission rate for Ar-41 remains constant at  $2.68 \times 10^{-6}$  Ci/s.

The values for the parameters and the maximum concentration for various atmospheric conditions are as follows:

Atmospheric Stability Classification	n Value	$\bar{u}$ (m/s)	$Cy^*$ ( $m^{n/2}$ )	$Cz^*$ ( $m^{n/2}$ )	$\chi_{max}$ ( $\mu Ci/cm^3$ )	d (m)
Extremely Unstable (A)	0.20	7.0	0.31	0.31	$1.5 \times 10^{-10}$	92
Slightly Unstable (C)	0.25	5.0	0.15	0.15	$2.3 \times 10^{-10}$	240
Slightly Stable (E)	0.33	3.0	4Cz	0.075	$9.4 \times 10^{-11}$	720
Extremely Stable (G)	0.50	2.0	8Cz	0.035	$7.0 \times 10^{-11}$	4200

Table A-5 Ar-41 Concentrations in the Unrestricted Area After Dispersion in Air at Various Atmospheric Stability Classes

\* From Reference A.3

Using the Ar-41 concentrations from Table A-5 and Ar-41 dose conversion factors for immersion in a semi-infinite cloud (Reference A.6), calculations show that a person immersed for a full year in a semi-infinite cloud of Ar-41 at the maximum projected concentration in the unrestricted area ( $2.3 \times 10^{-10} \mu Ci/cm^3$ ) would receive a total effective dose equivalent of approximately 1.4 mrem. This dose is well within all applicable limits in 10 CFR Part 20.

Determination of radiation dose to the general public from airborne effluents may also be carried out using several other computer codes recognized by regulatory authorities. One such method involves the use of the Clean Air Assessment Package - 1988 (CAP88-PC) (Reference A.7). Application of this code (V1.0) to the projected Ar-41 releases from the MNRC predicts a dose to the general public of less than 0.1 mrem per year.

A.5. NITROGEN-16 ACTIVITY

Nitrogen-16 is generated by the reaction of fast neutrons with oxygen. The oxygen present in air, either in a beam path or entrained in the water near the reactor core, is insignificant compared to the oxygen in the water molecule in the liquid state. Production of Nitrogen-16 resulting from the oxygen in air or air entrained in the cooling water can therefore be neglected.

The cross-section energy threshold for the Oxygen-16 (n,p) Nitrogen-16 (N-16) reaction is 9.4 MeV; however, the minimum energy of the incident neutrons must be about 10 MeV because of center of mass corrections. This high energy threshold limits the production of Nitrogen-16, since only about 0.1% of all fission neutrons have an energy in excess of 10 MeV. Moreover, a single hydrogen scattering event will reduce the energy of these high-energy neutrons to below the necessary threshold. The effective cross section for the Oxygen-16 (n,p) Nitrogen-16 reaction averaged over the TRIGA<sup>®</sup> spectrum is  $2.1 \times 10^{-29} \text{ cm}^2$ . This value agrees well with the value obtained from integrating the effective cross section over the fission spectrum.

The concentration of N-16 atoms per  $\text{cm}^3$  of water as it leaves the reactor core is given by:

$$N^N = \frac{\phi_v N^O \sigma}{\lambda} (1 - e^{-\lambda t})$$

where:

$N^N$  = Nitrogen-16 atoms per  $\text{cm}^3$  of water;

$\phi_v$  = Neutron flux (0.6-15 MeV) -  $4.2 \times 10^{13} \text{ n/cm}^2 \text{-s}$  at 2000 kW ;

$N^O$  = Oxygen atoms per  $\text{cm}^3$  of water =  $3.3 \times 10^{22} \text{ atoms/cm}^3$ ;

$\sigma$  = (n,p) cross section of oxygen =  $2.1 \times 10^{-29} \text{ cm}^2$  (averaged over 0.6-15 MeV) ;

$\lambda$  = Nitrogen-16 decay constant =  $9.71 \times 10^{-2} \text{ s}^{-1}$ ;

t = Average time of exposure in reactor;

v = Flow velocity (20.6 cm/s);

$$N^N = 3.0 \times 10^8 (1 - e^{-[(9.71 \times 10^{-2})(1.9)]});$$

=  $0.5 \times 10^8$  atoms of N-16 per  $\text{cm}^3$  in the water leaving the core.

If it is assumed that the water continues to flow at the same velocity (20.6 cm/s) to the surface, (i.e., the diffuser pump is not on), the transit time from core to surface is:

$$t_{\text{rise}} = \frac{(20 \text{ ft}) \left( 30.5 \frac{\text{cm}}{\text{ft}} \right)}{20.6 \frac{\text{cm}}{\text{s}}} = 29.5 \text{ s.}$$

This assumption is quite conservative as energy losses from the fluid stream resulting from turbulent mixing will reduce the velocity significantly. Furthermore, delays in transit time resulting from operation of the diffuser pump are sizeable. Measurements made of the dose rates at the tank surface of several TRIGA<sup>®</sup> reactors show that the operation of the diffuser pump reduces the N-16 contribution to the surface dose rate by an order of magnitude or more depending on the size of the tank.

However if 29.5 seconds is used as the transit time for N-16 from the core to the surface of the reactor tank, in this time, the N-16 decays to about 0.06 times the value of the activity leaving the core. Thus, the concentration of N-16 atoms that reach the region near the surface of the tank is no greater than about  $2.85 \times 10^6$  atoms/cm<sup>3</sup>.

Only a small proportion of the N-16 atoms present near the tank surface are transferred into the air of the reactor room. When the N-16 atom is formed, it appears as a recoil atom with various degrees of ionization. For high-purity water ( $\approx 2 \mu\text{mho}$ ) practically all of the N-16 combines with oxygen and hydrogen atoms of the water. Most of it combines in an anion form, which has a tendency to remain in the water (Reference A.8).

It is assumed that at least one-half of all ions formed are anions. Because of its 7.14 second half-life, the N-16 decays before reaching a uniform concentration in the tank water. The activity will be dispersed over the surface area of the tank and much of it will decay during the lateral movement.

For the purpose of the analysis, it is postulated that the water-bearing N-16 rises from the core to the surface and then spreads across a disk source with a radius of 107 cm  $\approx$  (3.5 ft), and an area  $A_s = 3.60 \times 10^4 \text{ cm}^2$ .

For a constant velocity of 20.6 cm/sec the cycle time for distributing the N-16 over the tank surface would be:

$$t_s = 107 \text{ cm} / 20.6 \text{ cm/s} = 5.2 \text{ s}.$$

The average concentration during this time is:

$$\begin{aligned} \bar{N} &= \int_0^{t_s} \frac{N_o}{t_s} e^{-\lambda t} dt = \frac{N_o}{\lambda t_s} (1 - e^{-\lambda t_s}) = \frac{2.85 \times 10^6}{(9.71 \times 10^{-2})(5.2)} (1 - e^{-[(9.71 \times 10^{-2})(5.2)]}); \\ &= 3.4 \times 10^6 \frac{\text{atoms}}{\text{cm}^3}. \end{aligned}$$

The thickness of the layer of N-16-bearing water is:

$$h = \frac{v_1 t_s}{A_s} = \frac{(10.8 \times 10^3)(5.2)}{3.60 \times 10^4} = 1.56 \text{ cm}$$

The dose rate at the tank surface arising from the N-16 near the surface is:

$$D = \frac{\lambda \bar{N}}{2\mu K} (1 - E_2(\mu h));$$

Where  $\mu$  is the attenuation coefficient for 6 MeV photons in water with a value of  $(0.0277 \text{ cm}^{-1})$  and:

$$K \text{ is the flux-to-dose-rate conversion } \left( 1.6 \times 10^5 \frac{\text{photons}}{\text{cm}^2 \text{ s}} / \frac{\text{R}}{\text{hr}} \right);$$

and  $E_2$  is the second exponential function. This yields an N-16 dose rate near the tank surface at 2 MW of 1350 mR/hr (with the diffuser system off).

Aside from this dose rate at the tank surface, there is interest from a radiation protection standpoint in the number of N-16 atoms escaping into the air from the diffusing surface source above the core. The number escaping to the air would be about:

$$(3.4 \times 10^6 \text{ atoms/cm}^3) (0.9 \times 10^{-2} \text{ cm/s}) = 30.6 \times 10^3 \text{ atoms/cm}^2 \cdot \text{s};$$

where the escape velocity is  $0.9 \times 10^{-2} \text{ cm/s}$  (Reference A.1).

In the room, the activity is affected by dilution, ventilation, and decay. The accumulation of N-16 in the enclosure under equilibrium conditions is determined by the following equation:

$$N = \frac{S}{\lambda V_R + q};$$

where:

$N$  = Number of N-16 atoms/cm<sup>3</sup>;

$S$  = Number of N-16 atoms entering the enclosure from the tank per second ( $30.6 \times 10^3 \text{ atoms/cm}^2 \cdot \text{s}$ ) ( $3.60 \times 10^4 \text{ cm}^2$ ) =  $1.1 \times 10^9 \text{ atoms/s}$ ;

$V_R$  = Volume of the reactor enclosure =  $2.1 \times 10^8 \text{ cm}^3$ ;

$q$  = Volume flow rate from the reactor enclosure exhaust  $3.8 \times 10^5 \text{ cm}^3/\text{s}$ ;

$\lambda$  = Decay constant for N-16 =  $9.71 \times 10^{-2}$ ;

then:

$$N = \frac{1.1 \times 10^9}{(2.078 \times 10^7) + (3.8 \times 10^5)} = 5.29 \times 10^1 \text{ nuclei/cm}^3$$

This corresponds to an N-16 concentration of  $1.4 \times 10^{-4} \mu\text{Ci/cm}^3$ .

The gamma dose rate (D) from this equilibrium concentration of N-16 in the air is:

$$D = \frac{BS_{\mu}(1 - e^{-\mu_s R_o})}{2\mu_s g} \text{ mR/hr};$$

where:

$$B = 1;$$

$$\mu_s = 3.03 \times 10^{-5} \text{ cm}^{-1} @ 6 \text{ MeV};$$

$$g = 1.62 \times 10^2 \frac{\text{dis/s-cm}^2}{\text{mR/hr}} @ 6\text{MeV};$$

$$R_o = 4.65 \times 10^2 \text{ cm};$$

$$S_u = (34.2)(9.71 \times 10^{-2}) = 5.14 \text{ dis/s - cm}^3;$$

$$D = \frac{(1)(5.14)[1 - e^{-(3.03 \times 10^{-5})(4.65 \times 10^2)}]}{(2)(3.03 \times 10^{-5})(1.6 \times 10^2)} \text{ mR/hr.}$$

D = 7.7 mr/hr when the effective radius of the enclosure is assumed to be a hemisphere with a volume of  $2.1 \times 10^8 \text{ cm}^3$ .

If saturation activity is reached,  $q=0$ , the dose will not change significantly. This is due to the short half-life of N-16.

Again, with the diffuser system operating, the dose rate from N-16 in the enclosure will be significantly less. Exposure to the general public is negligible because of the rapid decay of N-16.

#### A.6 RELEASE OF FISSION PRODUCTS TO TANK WATER

Although not expected, the cladding on a fuel element could fail as a result of a manufacturing defect or corrosion. Since these types of failures would occur over a long period of time it is unlikely that there would be an undetected failure of more than one element. Therefore, only a single element is considered in this analysis. An analysis of this release can be found in Appendix B, since it is enveloped by the analysis of an accidental rupture of the cladding of a single element under water.

### A.7 ACTIVATION OF MATERIALS IN RADIOGRAPHY BAYS

Small amounts of radioactivity will be produced when materials in the radiography bays are exposed to neutrons. This section shows the methods used to estimate the activity produced and personnel exposures incurred as a result of the induced activity. Because exposure times and decay times will vary to optimize radiography and operational objectives, the values calculated are to be considered typical cases, which are unlikely to be exceeded. Therefore, they represent a reasonable worst case situation.

The induced activity is determined as follows:

$$A = \frac{N_a M \sigma \phi}{A_o} (1 - e^{-\lambda t}) e^{-\lambda \tau};$$

where:

- A = activity (dis/s);
- $N_a$  = Avogadro number =  $6.02 \times 10^{23}$ ;
- M = mass of isotope of interest (g);
- $\sigma$  = cross section (barns);
- $\phi$  = thermal neutron flux (n/s·cm<sup>2</sup>);
- $A_o$  = atomic weight of element of interest (grams/gram atom);
- $\lambda$  = decay constant of activation product (1/s);
- t = exposure time (s);
- $\tau$  = decay time (s).

If it is assumed that there is a 6 minute exposure period followed by a 30 minute decay period prior to personnel entering the bays, the only target isotope in a typical airplane component made from 2024 aluminum that is of significance, from the activation standpoint, is Mn-55. Although the Al-28 activity will reach 84% of its saturation value during exposure, it will decay by a factor of approximately 10,000 during the post-irradiation decay period.

If it is assumed that the target material is a plate of aluminum the same size as the beam used for film radiography (2680 cm<sup>2</sup>) and ½ in. thick (1.27 cm), it will weigh  $\approx 9.19 \times 10^3$  g.

The following apply for Mn-55:

- m = Mn-55 = 74 g;
- $\sigma$  = 13.3 barns;
- $\lambda$  =  $7.5 \times 10^{-5} \text{ s}^{-1}$  (Mn-56);
- $A_o$  = 55;
- t = 360 s;
- $\tau$  = 1800 s;
- $\phi$  =  $4 \times 10^6 \text{ n/s} \cdot \text{cm}^2$ ;

where:

$$m = \text{mass of plate (gms)} \times \text{wt \% Mn} \times \text{abundance of Mn-55};$$

$$= 9.19 \times 10^3 \left(\frac{0.8}{100}\right) \left(\frac{100}{100}\right) = 74 \text{ gms.}$$

Applying these values to the above equations gives a Mn-56 activity of  $9.96 \times 10^5$  dis/s or about 27  $\mu\text{Ci}$ .

If this same approach is applied to the other isotopes of interest in 2024 aluminum, the following activities can be calculated:

Stable Isotope	$\sigma$	$\lambda$	% Abundant	Al 2024 Element (wt %)	Mass Isotope (gms)	Radionuclide & Activity ( $\mu\text{Ci}$ )
Cu-63	4.4	$1.50 \times 10^{-5}$	69.1	4.5	286	Cu-64 6.5
Cu-65	2.17	$2.27 \times 10^{-3}$	30.9	4.5	128	Cu-66 2.6
Al-27	0.231	$5.16 \times 10^{-3}$	100	91.9	$8.5 \times 10^3$	Al-28 0.6

Table A-6 Typical Induced Radionuclides During Neutron Radiography of Aircraft Components

If these induced activities are assumed to be present as a point source (which is unlikely), then the dose at 5 ft for each individual radionuclide will be:

$$D = \frac{6CE_{\gamma}\%Yield}{25};$$

where:

- D = dose (mr/hr);  
 C = source (mCi);  
 $E_{\gamma}$  = energy of  $\gamma$  (MeV);  
 % Yield = % yield of  $\gamma$ .

For Mn-56 the following apply:

<u><math>E_{\gamma}</math></u> <u>(MeV)</u>	<u>% Yield</u>
.85	98.9
1.81	27.2
2.11	14.3
2.80	2.1 .

This yields a Mn-56 dose rate of  $\approx 0.012$  mr/hr at 5 ft. The dose rate from the other radionuclides is small when compared to Mn-56.

If a similar approach is used for the wing pivot, 38.5 kg of B6AC stainless steel, the dose is found to be  $\approx 0.04$  mr/hr at 5 ft. As with the aluminum plate example, Mn-56 (wt % - 0.75) produces the only significant dose.

The dose from an entire wing (area is 33 ft x 13 ft and there is 3800 lb. of aluminum), when using an electronic imaging device (area exposed is  $510 \text{ cm}^2$ ) can be estimated by applying the above method for determining the activity but in a stepped manner. This method proceeds as follows:

1. Assume the examination of the entire wing takes place in steps and requires 8 hrs and there is a 30 min decay period after the examination is complete;
2. Each step is exposed for 36.78 seconds and is determined as follows:

$$\text{No. Steps} = \frac{\text{Wing Area}}{\text{Exposed Area}} = \frac{3.99 \times 10^5 \text{ cm}^2}{510 \text{ cm}^2} = 783;$$

$$\text{Time per step} = \frac{(8 \text{ hrs})(3600 \text{ s/hr})}{783 \text{ steps}} = 36.78 \text{ s};$$

or 48.9 steps per 30 min period;

$$\text{Mass of step} = \frac{(3800)(453.5)}{783} = 2.2 \times 10^3 \text{ gms};$$

$$\text{Mass Mn-55} = (2.2 \times 10^3) \left(\frac{0.8}{100}\right) \left(\frac{100}{100}\right) = 17.6 \text{ gms/step};$$

3. The activity produced during the 36.78 s with a  $\phi$  of  $4 \times 10^6$  is  $2.82 \times 10^4$  dis/sec or  $0.76 \mu\text{Ci}$ ;
4. Since there are 48.9 steps in 30 min, the activity produced during this time (not accounting for decay after exposure) is  $48.9 \times 0.76$  or  $37.3 \mu\text{Ci}$ ;
5. This activity will then decay for 8 hrs prior to the time personnel are permitted to enter the radiography bay. The activity will be reduced by  $e^{-\lambda t}$  or a factor of 0.115 leaving an activity of  $4.3 \mu\text{Ci}$ ;
6. If the same process is repeated for each 30 min period (the decay time decreased by 30 min for each period), the total activity at the end of 8-1/2 hrs will be  $228 \mu\text{Ci}$ ;
7. Assuming a point source and using the same  $\gamma$  energies and yields as used for the plates, the dose rate at five (5) feet is approximately  $0.1 \text{ mr/hr}$ . The actual dose rate would be somewhat less since the activity would be spread over the wing volume and thus would not be a point source.

**APPENDIX B**

**RADIOLOGICAL IMPACT OF  
ACCIDENTS**

Appendix B - Valid Pages  
Rev.3 03/5/18

i	Rev. 3	3/5/18
ii	Rev. 3	3/5/18
iii	Rev. 3	3/5/18
B-1	Rev. 3	3/5/18
B-2	Rev. 3	3/5/18
B-3	Rev. 3	3/5/18
B-4	Rev. 3	3/5/18
B-5	Rev. 3	3/5/18
B-6	Rev. 3	3/5/18
B-7	Rev. 3	3/5/18
B-8	Rev. 3	3/5/18
B-9	Rev. 3	3/5/18
B-10	Rev. 3	3/5/18
B-11	Rev. 3	3/5/18
B-12	Rev. 3	3/5/18
B-13	Rev. 3	3/5/18
B-14	Rev. 3	3/5/18
B-15	Rev. 3	3/5/18
B-16	Rev. 3	3/5/18
B-17	Rev. 3	3/5/18

TABLE OF CONTENTS

B.1 Maximum Hypothetical Accident (MHA) .....B-1

B.2 Single Element Cladding Failure in Water .....B-10

B.3 Radiation Dose Rate from the Core Following a Loss of Coolant Accident.....B-11

    B.3.1 Introduction .....B-11

    B.3.2 Dose Rate From Scattered Radiation in Reactor Room .....B-14

    B.3.3 Dose Rate at Facility Fence After a Loss of Pool Water Accident .....B-16

LIST OF TABLES

B-1. SOURCE TERMS FOR ONE-ELEMENT ACCIDENT..... B-2

B-2. DISPERSION COEFFICIENTS FOR SMALL DOWNWIND DISTANCES FOR VARIOUS WEATHER  
CONDITIONS ..... B-4

B-3. VALUES OF RELEASE FRACTION COMPONENTS ..... B-6

B-4. OCCUPATIONAL RADIATION DOSES TO PERSONNEL INSIDE THE MNRC REACTOR ROOM ..... B-7

B-5. RADIATION DOSES TO MEMBERS OF THE GENERAL PUBLIC UNDER DIFFERENT ATMOSPHERIC  
CONDITIONS AND AT DIFFERENT DISTANCES FROM THE MNRC FOLLOWING A FUEL ELEMENT  
CLADDING FAILURE IN AIR (MHA) ..... B-8

B-6. RADIATION DOSES TO MEMBERS OF THE GENERAL PUBLIC UNDER DIFFERENT ATMOSPHERIC  
CONDITIONS AND AT DIFFERENT DISTANCES FROM THE MNRC FOLLOWING A CLADDING  
FAILURE IN WATER 48 HOURS AFTER REACTOR SHUTDOWN ..... B-9

B-7. TOTAL FISSION PRODUCT ACTIVITY AFTER SHUTDOWN ..... B-12

B-8. DOSE RATES ON THE MNRC REACTOR TOP AFTER A LOSS OF POOL WATER ACCIDENT  
FOLLOWING 2 MW OPERATIONS..... B-13

B-9. SCATTERED RADIATION DOSE RATES IN THE MNRC REACTOR ROOM AFTER A LOSS OF POOL  
WATER ACCIDENT FOLLOWING 2 MW OPERATION ..... B-16

B-10. SCATTERED RADIATION DOSE RATES AT THE MNRC FACILITY FENCE AFTER A LOSS OF POOL  
WATER ACCIDENT FOLLOWING 2 MW OPERATIONS ..... B-17

## REFERENCES

- B.1 Blomeke, J.O., and Mary F. Todd, "Uranium-235 Fission Product Production as a Function of Thermal Neutron Flux, Irradiation Time, and Decay Time," ORNL-2127, August 1957-November 1958.
- B.2 DiMunno, J.J., F.D. Anderson, R.E. Baker, and R.L. Materfield, "The Calculations of Distance Factors for Power and Test Reactor Sites," U.S. Atomic Energy Commission, TID-14844, March 1962.
- B.3 Regulatory Guide 3.33, "Assumptions Used for Evaluating the Potential Radiological Consequences of Accidental Nuclear Criticality in a Fuel Reprocessing Plant," April 1977.
- B.4 Regulatory Guide 3.34, "Assumptions Used for Evaluating the Potential Radiological Consequences of Accidental Nuclear Criticality in a Uranium Fuel Fabrication Plant," July 1979.
- B.5 Regulatory Guide 1.5, "Assumptions Used for Evaluating the Potential Radiological Consequences of a Loss of Coolant Accident for Pressurized Water Reactor," June 1974 (See also Regulatory Guide 1.3 on BWR's).
- B.6 Elder, J.C., et al, "A Guide to Radiological Accident Considerations for Siting and Design of DOE Nonreactor Nuclear Facilities," Los Alamos National Laboratory, LA- 10294-MS, January 1986.
- B.7 Lewis, E.E., Nuclear Power Reactor Safety, p. 521, ISBN-0-471-53335-1, John Wiley and Sons, Inc., 1977.
- B.8 Knief, R.A., Nuclear Engineering, Theory and Technology of Commercial Nuclear Power, pp. 353 and 431, ISBN 1-56032-089-3, Hemisphere Publishing Corp., 1992.
- B.9 Wenzel, D.R., "The Radiological Safety Analysis Computer Program (RSAC-5) User's Manual," Idaho National Engineering Laboratory, WINCO-1123, Rev. 1, February 1994.
- B.10 SRA (Shonka Research Associates, Inc.), "Software Verification and Validation Report for the WINCO RSAC-5 Code", Marietta, GA., 1993.
- B.11 U.S. Nuclear Regulatory Commission, "Regulatory Guide 1.145, Atmospheric Dispersion Models for Potential Accident Consequence Assessments at Nuclear Power Plants," Issued for Comment, August 1979.

- B.12 Wong, Bright M.K., et al, "Calculated Atmospheric Radioactivity from the OSU TRIGA<sup>®</sup> Research Reactor Using the Gaussian Plume Diffusion Model," Oregon State University Department of Nuclear Engineering Report 7903, August 1979.
- B.13 U.S. Department of Energy, "Internal Dose Conversion Factors for Calculation of Dose to the Public," DOE/EH-0071, Washington, D.C., 1988.
- B.14 U.S. Department of Energy, "External Dose-Rate Conversion Factors for Calculation of Dose to the Public," DOE/EH-0070, Washington, D.C., 1988.
- B.15 Credible Accident Analyses for TRIGA<sup>®</sup> and TRIGA<sup>®</sup>-fueled Reactors, NUREG/CR-2387, Pacific Northwest Laboratory, 1982.
- B.16 Glasstone, S., Principles of Nuclear Reactor Engineering, p. 120, D. Van Nostrand Co.Inc., 1955.
- B.17 International Commission on Radiation Protection, "Data for Use in Protection Against External Radiation," ICRP Report No. 51, Pergamon Press, March 1987.
- B.18 Safety Analysis Report for the Torrey Pines TRIGA<sup>®</sup> Mark III Reactor, GA-9064, January 5, 1970.

## APPENDIX B

RADIOLOGICAL IMPACT OF ACCIDENTSB.1 Maximum Hypothetical Accident (MHA)

Numerous safety committees that have reviewed TRIGA<sup>®</sup> reactor operations have considered potential accidents including rapid insertion of reactivity, loss of heat removal, loss of coolant, metal-water reactions, rearrangement of fuel, fuel aging, and accidents during handling of irradiated fuel. Chapter 13 of this document discusses such accidents. This appendix addresses the consequences of the accepted maximum hypothetical accident (previously called the design basis accident) for a TRIGA<sup>®</sup> reactor: a cladding rupture of one fuel element with no decay and subsequent instantaneous release of fission products into the air. This is commonly referred to as a single element failure in air. This is also the most severe of all accidents for TRIGA<sup>®</sup> reactors and is analyzed to examine potential radiation doses to the reactor staff and the general public. A less severe, but more credible accident involving a single element cladding failure in water 48 hours after reactor shutdown will also be analyzed, and will result in lower doses to the public and the reactor staff.

At some point in the lifetime of the MNRC reactor, used fuel within the core may be moved to new positions or removed from the core. Fuel elements are moved only during periods when the reactor is shut down. The most serious fuel-handling accidents involve spent or used fuel that has been removed from the core and then dropped or otherwise damaged, causing a breach of the fuel element cladding and a release of fission products. As noted previously, the standard or accepted maximum hypothetical accident for TRIGA<sup>®</sup> reactors involves failure of the cladding of a single fuel element after extended reactor operations, no time to decay, and subsequent release of the fission products directly into the air of the reactor room. While a credible scenario for this accident is hard to establish, it will be assumed that such an event can take place and does so immediately after reactor operation with a fuel element that has been run at full power (2 MW) for a period of 1 year. This operating history is very appropriate in view of the proposed facility mission.

The fission product inventory at shutdown is listed in Table B-1. These data are based on compilations from Reference B.1 and have been adjusted for 2 MW operation. The data are for the volatile fission products contained in a fuel element run to saturation at the highest core power density.

For both accidents being analyzed in this appendix, a release fraction of  $7.7 \times 10^{-5}$  is assumed for the release of noble gases and halogens from the fuel to the cladding gap. This release fraction is developed in Chapter 4 and is based on a RELAP5/3.1 calculation of fuel temperature in the hottest core element. In addition, for the accident where the cladding failure occurs in air, it is very conservatively assumed that 25% of the halogens released to the cladding gap are eventually available for release from the reactor room to the outside environment.

Group I		Group II	
Nuclide	Activity (Ci)	Nuclide	Activity (Ci)
Br-83	153.4	Kr-83M	153.5
Br-84	352.7	Kr-85M	477.1
Br-84M	7.3	Kr-85	98.9
Br-85	477.2	Kr-87	866.7
Br-87	858.0	Kr-88	1186.8
I-129	319.7	Kr-89	1473.9
I-131	927.3	Kr-90	1657.3
I-132	1405.9	Kr-91	986.5
I-133	2071.7	Xe-131M	9.3
I-134	2428.0	Xe-133M	49.9
I-135	1888.2	Xe-133	2073.6
I-136	994.5	Xe-135M	566.5
		Xe-135	1530.7
		Xe-137	188.8
		Xe-138	1753.4
		Xe-139	1813.9
		Xe-140	1904.4
TOTAL	11880.5		16698.4

Table B-1 Source Terms for One-Element Accident

This value is based on historical usage and recommendations from References B.2, B.3, B.4, B.5, and B.6, where Reference B.2 recommends a 50% release of the halogens. References B.3 and B.4 apply a natural reduction factor of 50% due to plate out in the building. This latter 50% applied to the 50% of the inventory released from the fuel element cladding gap results in 25% of the available halogen inventory reaching the outside environment. However, this value appears to be quite conservative based on the 1.7% gap release fraction for halogens quoted in References B.7 and B.8. For the single element accident in water, it is conservatively assumed that most of the halogens released from the cladding gap remain in the water and are removed by the demineralizer. However, a small fraction, approximately 2.5% of the total halogens released to the cladding gap are, in this case, assumed to escape from the reactor tank water into the reactor room air, which is more conservative than assuming total (100%) solubility of the halogens as is sometimes done for TRIGA<sup>®</sup> reactors (Reference B.18). However, even assuming 2.5% halogen release from the pool water will almost certainly result in an overestimate of the actual radioiodine activity released into the room because of the use of a 50% halogen gap release fraction rather than the 1.7% documented in References B.7 and B.8. In addition, about 50% of the halogens released from the water are expected to plate out in the reactor building before reaching the outside environment (References B.3 and B.4). The experience at TMI-2, along with recent experiments, indicate that the 50% halogen release fraction is much too large. Smaller releases, possibly as little as 0.6% of the iodine reaching the cladding gap may be released into the reactor room air due in part to a large amount of the elemental iodine reacting with cesium to form CsI, a compound much less volatile and more water soluble than elemental iodine (Reference B.8).

Radiological consequence calculations were done using the Radiological Safety Analysis Computer Program (RSAC-5) version 5.2, 02/22/94 (B.9). RSAC-5 calculates the consequences of the release of radionuclides to the atmosphere and it can generate a fission product inventory; decay and ingrow the inventory with time, model the downwind dispersion of the activity; and calculate doses to downwind individuals. RSAC-5 has been subjected to extensive independent verification and validation for use in performing safety-related dose calculations to support safety analysis reports. Shonka Research Associates, Inc. (Reference B.10) conducted this verification and validation in accordance with the guidelines presented in ANSI/ANS-10.4, "American National Standard Guidelines for the Verification and Validation of Scientific and Engineering Programs for the Nuclear Industry" (ANSI/ANS 1987).

For the MHA at the MNRC, dispersion coefficients ( $\chi/Q$  values) for locations in the unrestricted area, 10 m (the MNRC perimeter fence line nearest the facility which defines the interface of the restricted and unrestricted areas) out to 100 m, were input directly into the code and were calculated using NRC Regulatory Guide 1.145 methodology (Reference B.11). Diffusion coefficients were taken from Reference B.12 and are presented in Table B-2. Calculations were performed assuming a ground level release at an 800 cfm reactor room release rate without any credit for stack height or building wake effects, which would only improve mixing and lower projected doses.

<u>x(m)</u>	$\sigma_y(m)$ Pasquill Factor					
	<u>A</u>	<u>B</u>	<u>C</u>	<u>D</u>	<u>E</u>	<u>F</u>
10	3.00	2.50	2.10	1.70	1.50	1.29
20	5.00	4.00	3.20	2.40	2.00	1.58
30	7.00	5.50	4.30	3.10	2.50	1.87
40	9.00	7.00	5.40	3.80	3.00	2.16
50	11.00	8.50	6.50	4.50	3.50	2.45
60	13.00	10.00	7.60	5.20	4.00	2.74
70	15.00	11.50	8.70	5.90	4.50	3.03
80	17.00	13.00	9.80	6.60	5.00	3.32
90	19.00	14.50	10.90	7.30	5.50	3.61
100	21.00	16.00	12.00	8.00	6.00	3.90

<u>x(m)</u>	$\sigma_z(m)$ Pasquill Factor					
	<u>A</u>	<u>B</u>	<u>C</u>	<u>D</u>	<u>E</u>	<u>F</u>
10	2.40	1.90	1.68	1.37	1.20	1.04
20	3.80	2.80	2.36	1.74	1.40	10.8
30	5.20	3.60	3.04	2.11	1.60	1.12
40	6.60	4.60	3.72	2.48	1.80	1.16
50	8.00	5.50	4.40	2.85	2.00	1.20
60	9.40	6.40	5.08	3.22	2.20	1.24
70	10.80	7.30	5.76	3.59	2.40	1.28
80	12.20	8.20	6.44	3.96	2.60	1.32
90	13.60	9.10	7.12	4.33	2.80	1.36
100	15.00	10.00	7.80	4.70	3.00	1.40

Table B-2. Dispersion Coefficients for Small Downwind Distances for Various Weather Conditions

Furthermore, it was assumed that all of the fission products were released to the unrestricted area by a single reactor room air change, which would maximize the dose rate to persons exposed to the plume during the accident and minimize the exposure time to receive the highest estimated dose from this accident. These latter assumptions are very, very conservative since the reactor room is not at ground level and, rather than 10 meters, is closer to 30 meters from the perimeter fence. Furthermore, there are no normal or direct flow pathways to support an 800 cfm ground level flow from the reactor room to the unrestricted area.

Calculations were done for Pasquill weather classifications A through F. A summary of the pertinent assumptions used in the analysis are listed below. These include:

1. Initial Fission Product Source;
  - a. Reactor Power level - 2 MW;
  - b. Operating time - 365 days;
2. Release Fractions;
  - a. For the purposes of the maximum hypothetical accident and the accident where the pool water remains present, it was assumed that at the time of fuel cladding failure, a fraction of the  $i$ th radionuclide in the inventory given in Table B-1 was instantaneously released into the air of the reactor room. In one scenario this instantaneous release occurs directly into the reactor room air, while in the other projected accident the pathway to the air requires migration through the pool water which will reduce the halogen release. Also, for the halogens, a further reduction in activity is expected to occur due to plateout in the building. Thus, the fraction ( $w_i$ ) of the fission product inventory released from a single fuel element which reaches the reactor room air and then the atmosphere in the unrestricted environment outside the facility will be as follows:

$$w_i = e_i \times f_i \times g_i \times h_i ;$$

where:

$e_i$  = the fraction released from the fuel to the fuel-cladding gap;

$f_i$  = the fraction released from the fuel-cladding gap to the pool if water is present, or directly to the reactor room air if no water is present;

$g_i$  = the fraction released from the pool water to the reactor room air; and

$h_i$  = the fraction released from the reactor room air to the outside (unrestricted) environment.

- b. Based on information provided previously in this appendix,  $e_i$  was set at  $7.7 \times 10^{-5}$  for both noble gases and halogens and at zero for other fission products. The values of  $f_i$ ,  $g_i$ , and  $h_i$  for the two accident scenarios being considered are given in Table B-3.

Fission Product	$f_i$		$g_i$		$h_i$
	w/o pool water	w/ pool water	w/o pool water	w/ pool water	
Noble Gases	1.0	1.0	N/A	1.0	1.0
Halogens	0.5*	0.5*	N/A	0.05*	0.5
Others	0.0	0.0	0.0	0.0	0.0

Table B-3. Values of Release Fraction Components

3.  $\chi/Q$  values calculated using NRC Regulatory Guide 1.145;
  - a. Ground level release at 800 cfm, all building ventilation dampers open;
  - b. No credit for stack height or building wake effects;
4. Receptor exposure time - single instantaneous release over 9.2 minutes for both accidents;
5. Dose conversion factors;
  - a. Internal - Based on DOE/EH-0071 (Reference B.13);
  - b. External - Based on DOE/EH-0070 (Reference B.14);
6. Receptor breathing rate -  $3.3 \times 10^{-4} \text{ m}^3/\text{s}$  (0.7 cfm);
7. Fission product decay time: no decay for cladding failure in air and 48 hours decay for cladding failure in water.

---

\* These values are conservative based on References B.7 and B.8, which quote a halogen release fraction of 0.017 from the cladding gap. Reference B.8 also quotes a halogen release from TMI-2 fuel to the reactor building of 0.006.

The results of the RSAC-5 calculations are summarized in Tables B-4, B-5, and B-6. Shown are the doses inside the reactor room for both projected accidents and doses at several locations in the unrestricted area outside the MNRC (10 to 100 m from the building) as a function of weather class. Results are reported for the Committed Dose Equivalent (CDE) to the thyroid, the Committed Effective Dose Equivalent (CEDE) due to inhalation, the Deep Dose Equivalent (DDE) due to air immersion, and the Total Effective Dose Equivalent (TEDE) resulting from adding the CEDE and the DDE.

As indicated by the results in Table B-4, the occupational dose to workers who evacuate the reactor room within 5 minutes following the MHA should be approximately 454 millirem TEDE and 11,500 millirem Committed Dose Equivalent to the thyroid. If evacuation occurs within 2 minutes, as it no doubt will because the reactor room is small and easy to exit, the doses drop to 180 millirem TEDE and 4,640 millirem CDE. Furthermore, if the pool water remains in place and there is 48 hours of decay, the 5 minute and 2 minute occupational doses (TEDEs) drop to 32.5 and 13.2 millirem, respectively. All of these doses are well within the NRC limits for occupational exposure as stated in 10CFR 20.1201.

Accident: Cladding Failure in Air (MHA)				
	CDE Thyroid (millirem)	CEDE (millirem)	DDE (millirem)	TEDE (millirem)
2 minute room occupancy	4,640	140	40	180
5 minute room occupancy	11,500	360	94	454

Accident: Cladding Failure in Water 48 Hours after Reactor Shutdown				
	CDE Thyroid (millirem)	CEDE (millirem)	DDE (millirem)	TEDE (millirem)
2 minute room occupancy	260	13	0.2	13.2
5 minute room occupancy	660	32	0.5	32.5

Table B-4 Occupational Radiation Doses to Personnel Inside the MNRC Reactor Room

- CDE means Committed Dose Equivalent
- CEDE means Committed Effective Dose Equivalent
- DDE means Deep Dose Equivalent
- TEDE means Total Effective Dose Equivalent (Sum of DDE and CEDE)

10 meters

Weather Class	A	B	C	D	E	F
CDE Thyroid	107	160	165	198	418	1694
CEDE	3.3	5.1	5.1	5.8	13	53
DDE	0.8	1.2	1.2	1.5	3.2	13
TEDE	4.1	6.3	6.3	7.3	16.2	66

20 meters

Weather Class	A	B	C	D	E	F
CDE Thyroid	40	68	75	109	275	1330
CEDE	1.2	2.2	2.3	3.4	8.5	42
DDE	0.3	0.5	0.6	0.8	2.0	9.9
TEDE	1.5	2.7	2.9	4.2	10.5	52.0

40 meters

Weather Class	A	B	C	D	E	F
CDE Thyroid	13	23	28	48	143	90
CEDE	0.4	0.7	0.9	1.5	4.4	2.9
DDE	0.1	0.2	0.2	0.4	1.0	6.7
TEDE	0.5	0.9	1.1	1.9	5.4	9.6

80 meters

Weather Class	A	B	C	D	E	F
CDE Thyroid	3.6	6.4	9.0	17.6	58	52
CEDE	0.1	0.2	0.3	0.5	1.9	1.7
DDE	0.0	0.0	0.0	0.1	0.4	3.7
TEDE	0.1	0.2	0.3	0.6	2.3	5.4

100 meters

Weather Class	A	B	C	D	E	F
CDE Thyroid	2.4	4.7	6.0	12	42	42
CEDE	0.0	0.2	0.2	0.4	1.3	1.3
DDE	0.0	0.0	0.0	0.1	0.3	3.0
TEDE	0.0	0.2	0.2	0.5	1.6	4.3

Table B-5 Radiation Doses to Members of the General Public Under Different Atmospheric Conditions and at Different Distances from the MNRC Following a Fuel Element Cladding Failure in Air (MHA)

- All doses in mrem
  - CDE - Committed Dose Equivalent
  - CEDE - Committed Effective Dose Equivalent
  - DDE - Deep Dose Equivalent
  - TEDE - Total Effective Dose Equivalent
- FP Inventory/2 MW no decay  
 800 cfm from Rx room  
 Halogen RF  $1.92 \times 10^{-5}$  (50% x 50%)  
 Gas RF  $7.7 \times 10^{-7}$   
 Ground level release

Weather Class	A	B	C	D	E	F
CDE Thyroid	6.0	9.1	9.2	11	24	97
CEDE	0.3	0.4	0.4	0.5	1.3	4.7
DDE	0.0	0.0	0.0	0.0	0.0	0.0
TEDE	0.3	0.4	0.4	0.5	1.3	4.7

20 meters

Weather Class	A	B	C	D	E	F
CDE Thyroid	2.2	4.0	4.3	6.3	15	76
CEDE	0.1	0.2	0.2	0.3	0.7	3.7
DDE	0.0	0.0	0.0	0.0	0.0	0.0
TEDE	0.1	0.2	0.2	0.3	0.7	3.7

40 meters

Weather Class	A	B	C	D	E	F
CDE Thyroid	0.7	1.3	1.7	2.8	8.0	52
CEDE	0.0	0.0	0.0	0.0	0.4	2.5
DDE	0.0	0.0	0.0	0.0	0.0	0.0
TEDE	0.0	0.0	0.0	0.0	0.2	2.5

80 meters

Weather Class	A	B	C	D	E	F
CDE Thyroid	0.2	0.4	0.5	1.0	3.3	30
CEDE	0.0	0.0	0.0	0.0	0.2	1.4
DDE	0.0	0.0	0.0	0.0	0.0	0.0
TEDE	0.0	0.0	0.0	0.0	0.2	1.4

100 meters

Weather Class	A	B	C	D	E	F
CDE Thyroid	0.1	0.3	0.3	0.7	2.4	24
CEDE	0.0	0.0	0.0	0.0	0.1	1.1
DDE	0.0	0.0	0.0	0.0	0.0	0.0
TEDE	0.0	0.0	0.0	0.0	0.1	1.1

Table B-6 Radiation Doses to Members of the General Public Under Different Atmospheric Conditions and at Different Distances from the MNRC Following a Cladding Failure in Water 48 hours after Reactor Shutdown

- All doses in mrem
- CDE - Committed Dose Equivalent
- CEDE - Committed Effective Dose Equivalent
- DDE - Deep Dose Equivalent
- TEDE - Total Effective Dose Equivalent

FP Inventory/2MW 48 hr decay  
800 cfm from Rx room  
Halogen RF  $1.92 \times 10^{-6}$  (5% x 50%)  
Gas RF  $7.7 \times 10^{-5}$   
Ground level release

Projected doses to the general public in the unrestricted area around the MNRC from the two postulated accidents are shown in Tables B-5 and B-6. Table B-5 summarizes the doses based on the "standard" maximum hypothetical accident (MHA) for TRIGA® reactors, which incorporates the conservative assumptions that the reactor pool water is suddenly gone from around the fuel element when the cladding failure occurs (an assumption generally thought to be incredible), that no decay occurs between the time the reactor is shut down and the time the cladding fails, and that all of the fission products released are discharged to the unrestricted area at ground level by a single reactor room air change over a period of 9.2 minutes. Even using these assumptions, at the closest distance to the MNRC building (10 meters), and under the most unfavorable atmospheric conditions (Category F), the maximum TEDE to a member of the general public would be 66 millirem. Although this accident and the corresponding radiation doses are never expected to occur, the maximum estimated dose of 66 millirem to the general public is still within the 100 millirem TEDE limit for the general public published in the NRC's most recent revision to 10 CFR 20 (Reference 10 CFR 20.1301). As a point of interest, should this accident occur after 48 hours of decay, the TEDE to the public drops to approximately 34 millirem.

## B.2 Single Element Cladding Failure in Water

While the above analysis of the MHA clearly shows that the MNRC can be subjected to current MHA criteria and remain within dose limits established by the NRC for occupational radiation exposure and exposure of the general public, results of more realistic accident scenarios are summarized in Tables B-4 and B-6. In this accident, it is assumed that the pool water remains in the reactor tank (thus lowering the halogen dose significantly) and that the cladding failure occurs 48 hours after reactor shutdown (a decay time consistent with Reference B.15). Conservative assumptions regarding the release of fission product activity at ground level due to one air change in the room, assumption of the closest distance to the MNRC building and the most unfavorable atmospheric conditions are all retained for this analysis.

Since most of the halogens will be retained in the primary coolant water, the majority of the activity will end up in the demineralizer resin beds. If it is assumed that all of the halogens in the primary coolant are removed in one resin bottle and that they can be represented as a point source, the dose rate can be estimated by:

$$D = 6 \text{ CEN};$$

where:

$$\begin{aligned} D &= \text{Dose, R/hr at 1 ft;} \\ C &= \text{Number of curies retained in resins;} \\ &= (\text{Total Ci} \times \text{release fraction}) \times 0.975; \\ &= 11,880.5 \times 7.7 \times 10^{-5} \times 0.975^*; \\ &= 0.915 \text{ Ci} \times 0.975; \\ &= 0.892 \text{ Ci;} \\ E &= \text{Energy of source in MeV} = 1; \\ N &= \text{Number of photons/dis} = 1. \end{aligned}$$

---

\* It is assumed that 2.5% of the total halogens released from the fuel escape from the pool water into the reactor room air.

From this equation and the above values, the dose rate 1 ft from a single resin bottle will be 5.35 R/hr. If necessary, temporary shielding could be placed in the demineralizer resin area to protect personnel during resin replacement. However, in reality, this is a worst case estimate because the halogens will be distributed over more than one resin bottle and thus will not create a point source geometry, which maximizes the dose rate. In addition, decay could be used to reduce the halogen dose rate before personnel would need to be in the area. But, should this operation be required, personnel will be closely monitored and exposures kept within limits specified by 10 CFR Part 20.

As discussed in Chapter 11, an area radiation monitor is located inside the demineralizer resin cubicle to alert personnel if the radiation level in the area reaches the alarm point.

Results of the analysis of the single element failure in water show in Table B-4 that the occupational TEDE will fall between 13.2 and 32.5 millirem depending on reactor room occupancy time after the accident. Using the worst case atmospheric conditions for release of radioactivity into the unrestricted area, Table B-6 shows that the CDE to the thyroid of a member of the general public will total about 97 millirem, the CEDE will be about 4.7 millirem, the DDE will be significantly less than 1 millirem and the TEDE will total about 4.7 millirem. It should also be noted that if one assumes a 50% halogen plateout in the reactor room, the TEDE drops to 2.4 millirem. Based on values quoted earlier, it is obvious that these doses are well below the 10 CFR 20 limits for the general public.

### B.3 Radiation Dose Rate from the Core Following a Loss of Coolant Accident

#### B.3.1 Introduction

Even though there is a very remote possibility that the primary coolant and reactor shielding water will be totally lost, direct and scattered dose rates from an uncovered core following 2 MW operations have been calculated. The first calculation involves determining the dose rate to a person standing on the grating directly above the reactor, while the second requires finding the dose rate to a person shielded from the direct core radiation but subjected to the radiation scattered from the reactor room ceiling while occupying the reactor room. There are several common calculations required for each situation. These are discussed below.

#### Total Core Activity

The total fission product activity as a function of time after shutdown was determined using the standard equation below (Reference B.16):

$$\text{Activity at time } \tau = 1.4 P_o [(\tau - T_o)^{-0.2} - \tau^{-0.2}] \text{ Ci ;}$$

where:

$P_o$  = Thermal power (W);

$\tau$  = Time after reactor startup (s);

$T_o$  = Time reactor operating at power  $P_o$  (s);

hence:

$$\tau - T_0 = \text{Time after reactor shutdown (s).}$$

This equation gives results that are better than a factor of two for times between 10 seconds (or less) and 100 days. The MNRC will operate about 644 MWd per year; therefore, the operating profile used in the above equations was 7728 hours (322 days) at the full power of 2 MW. Increasing the operating time further makes little difference to the total fission product activity.

The core was modeled as a cylinder with a radius of 26 cm and a height of 38 cm. This assumes that fuel is filling all of the grid positions. Therefore, the source term for the analysis ( $S_v$ ) was determined by dividing the activity by the volume of this cylinder.

The resultant fission product activity and source term can be seen in Table B-7.

Table B-7 Total Fission Product Activity After Shutdown		
Time After Shutdown	Total Activity (Ci)	Source Strength $S_v$ ( $\gamma s^{-1} cm^3$ )
10 seconds	$4.22 \times 10^7$	$1.94 \times 10^{13}$
1 hour	$4.40 \times 10^6$	$2.02 \times 10^{11}$
1 day	$1.97 \times 10^6$	$9.05 \times 10^{11}$
1 week	$1.04 \times 10^6$	$4.79 \times 10^{11}$
1 month	$5.48 \times 10^5$	$2.51 \times 10^{11}$

#### Core Attenuation Coefficient ( $\mu_c$ )

A new linear attenuation coefficient was calculated for the LEU core to allow for the different amount of uranium present. To be conservative, allowance was made for the fact that the core is not solid fuel but has air gaps between the elements. In essence, the fuel material was smeared over the volume of the cylindrical core as described above. The resulting value for the core attenuation coefficient ( $\mu_c$ ) for 1 MeV photons was  $0.2794 \text{ cm}^{-1}$ .

#### B.3.2 Dose Rate Directly Above the Core

As discussed in the introduction, the core, shut down and drained of water, was treated as a uniform bare cylindrical source of 1 MeV photons. Its dimensions were taken to be equal to those of the active core lattice. No accounting was made of sources other than fission product decay gammas, and no credit was taken for attenuation through the fuel element end pieces and the upper grid plate. The first of these assumptions is optimistic, the second conservative, and the net effect is conservative. The conservative assumption of a uniformly distributed source of 1 MeV photons was balanced by not assuming any buildup in the core.

The dose rate was calculated for a point on the axis of the core cylinder at a distance of 732 cm (24 feet) from the top. This is the distance from the core to a point about three feet above the tank cover grating. Because of the small angle the core subtends at this range, the results are not very sensitive to the distance.

The dose rate was determined from the equation:

$$\phi = \frac{S_v R^2}{4\mu_c a^2} (1 - e^{-\mu_c h}) \text{ cm}^{-2} \text{ s}^{-1};$$

where:

- R = radius of cylinder (26 cm);
- h = height of the cylinder;
- a = distance from top of cylinder to dose point (732 cm);
- S<sub>v</sub> = source strength;
- μ<sub>c</sub> = core attenuation coefficient.

#### Dose Factors

The conversion factor, K<sub>e</sub>, for effective dose equivalent per unit photon fluence was obtained from ICRP 51, Table 2 (Reference B.17). These have been calculated for photons incident on an anthropomorphic phantom from various geometries. Therefore, the worst case factor (anterior to posterior) was used for the 1 MeV photons from the core.

#### Results

The results are given in Table B-8 and agree with results for the 2 MW Torrey Pines TRIGA<sup>®</sup> Reactor (Reference B.18).

Table B-8 Dose Rates on the MNRC Reactor Top After a Loss of Pool Water Accident Following 2 MW Operations	
Time After Shutdown	Effective Dose Equivalent Rate (rem/h)
10 seconds	3.64 x 10 <sup>4</sup>
1 hour	3.77 x 10 <sup>3</sup>
1 day	1.69 x 10 <sup>3</sup>
1 week	8.96 x 10 <sup>2</sup>

1 month	$4.70 \times 10^2$
---------	--------------------

### B.3.3 Dose Rate From Scattered Radiation in Reactor Room

#### Geometry

The purpose of this section is to calculate the dose rate to a person in the reactor room who is not in the direct beam from the exposed core but is subject to scattered radiation from the reactor room ceiling. The dose point was chosen to be three feet above the reactor room floor at a distance of six feet away from the edge of the reactor tank. This is the furthest distance a person can get from the edge of the tank and remain in the MNRC reactor room. The ceiling is about twenty four feet (732 cm) above the reactor top. The worst case scattering occurs if the ceiling is assumed to be a thick concrete slab. However, it should be carefully noted that the scattering calculation is very conservative because the roof over the reactor is not a thick concrete slab, and for persons inside as well as outside the building the radiation from the unshielded core would be collimated upward by the shield structure with minimal interaction with the roof. This would greatly reduce the dose rates calculated for the reactor room and at the facility fence. But even if the calculated dose rates were present, personnel could occupy areas within the reactor room for a sufficient period of time to take actions to help mitigate the accident without exceeding NRC occupational dose limits. Since there is no routine personnel occupancy of areas adjacent to the fence; since the projected fence dose rates drop off quickly; and since the calculated fence line values are clearly overestimates; members of the general public are not expected to receive doses exceeding NRC limits.

#### Method

After a review of various methodologies for determining the dose rate from scattered radiation, a decision was made to use the scattering formula shown in the Torrey Pines SAR (Reference B.18). This equation provides the gamma fluence rate from a beam of radiation which is incident at an angle  $\theta_0$  to a thick slab of scattering material and is scattered back at an angle of  $\theta_1$  to a dose point a distance  $x$  from the point of scatter:

$$\phi = 6.03 \times 10^{23} \rho \left(\frac{Z}{A}\right) \left(\frac{I_0 C}{x^2}\right) \frac{1}{\left(\mu_0 + \mu_1 \left(\frac{\sin \theta_0}{\cos \theta_1}\right)\right)} \frac{\delta \sigma}{\delta \Omega}$$

where:

- $\rho$  = Density of the scattering material (concrete) =  $2.3 \text{ g cm}^{-3}$  ;
- $Z/A$  = Ratio of the average atomic number to the atomic mass of the scatterer = 0.5;
- $I_0 C$  = Incident current times the cross section of the beam, photons/sec;
- $x$  = Distance from scattering point to dose point, cm = 702.3 cm;
- $\mu_0, \mu_1$  = Attenuation coefficient in scattering material for incident and scattered photons,  $\text{cm}^{-1}$  (0.146, 0.292);
- $\theta_0, \theta_1$  = Incident and scattered angle (measured from the normal to the scatterer), ( $0^\circ, 24.3^\circ$ );

$$\delta\sigma/\delta\Omega = \text{Differential Klein-Nishina scattering cross section cm}^2 \text{ electron-steradian}^{-1} \\ (7.989 \times 10^{-27}).$$

It was assumed that all of the source photons which directly reached the top of the reactor tank were incident normally to the concrete roof ( $\theta_0 = 0$ ) at a point directly over the core. Thus:

$$I_0 C = S_0 \omega;$$

where  $S_0$  is the strength of a point source equal to the radioactivity found within one mean free path of the top of the reactor ( $1/\mu_c$ ), i.e., :

$$S_0 = \frac{\pi R^2 S_v}{\mu_c};$$

$\omega$  = Fractional solid angle subtended by the equivalent point source to the top of the reactor tank (0.0073);

$$\omega = \frac{1}{2} \left[ 1 - \frac{z}{\sqrt{z^2 + r^2}} \right];$$

where:  $r$  = Radius of the reactor tank;  
 $z$  = Distance from the top of the tank to the equivalent point source located on the cylindrical axis one half a mean free path down from the top of the fuel.

The energy of the scattered photons is given by:

$$E = \frac{E_0}{1 + \frac{E_0}{0.51}(1 - \cos \theta)};$$

where  $E_0$  is the incident photon energy (1 MeV) and  $\theta$  is the scattering angle =  $\pi - (\theta_0 + \theta_1)$ . In this case  $\theta_0 = 0$ . For the geometry of the current situation,  $E$  is approximately 0.2 MeV.

The differential scattering cross section is given by:

$$\frac{\delta\sigma}{\delta\Omega} = \frac{r_e^2}{2} \left[ \frac{E}{E_0} - \left( \frac{E}{E_0} \sin \theta \right)^2 + \left( \frac{E}{E_0} \right)^3 \right];$$

where  $r_e$ , the classical electron radius, =  $2.818 \times 10^{-13}$  cm.

#### Dose Factors

As before, the ICRP 51, Table 2 effective dose equivalent per unit photon fluence dose factors were used. Again, the anterior to posterior irradiation geometry provided the greatest dose rate for the 0.2 MeV scattered photons.

#### Results

The results of the calculations for the scattered radiation dose rates can be seen in Table B-9.

Table B-9 Scattered Radiation Dose Rates in the MNRC Reactor Room After a Loss of Pool Water Accident Following 2 MW Operation	
Time After Shutdown	Effective Dose Equivalent Rate (rem/h)
10 seconds	9.64
1 hour	1.00
1 day	0.45
1 week	0.24
1 month	0.12

#### B.3.4 Dose Rate at Facility Fence After a Loss of Pool Water Accident

##### Geometry

The purpose of this section is to calculate the dose rate to a person at the facility fence who is not in the direct beam from the exposed core but is subject to scattered radiation from the reactor room ceiling. The dose point was chosen to be three feet above the ground at the facility fence. This is the closest point a member of the public would be able to occupy. The slant distance to this point from the center of the reactor room ceiling above the tank (scatterer) is about 96 feet. The ceiling is about twenty four feet (732 cm) above the reactor top. The worst case scattering occurs if the ceiling is assumed to be a thick concrete slab, but once again the calculated values are overestimates because scatter of the reactor room ceiling will be much less than assumed.

##### Method

The methodology was exactly as that used in Section B.3.3. Values used were the same except as indicated below:

$$\begin{aligned}
 \mu_1 &= 0.269 \text{ cm}^{-1}; \\
 \theta_1 &= 65^\circ; \\
 x &= 96 \text{ ft (2926.08 cm)}; \\
 K(e) &= 2.147 \times 10^6.
 \end{aligned}$$

##### Results

The results of the calculation for the scattered radiation dose rate at the MNRC facility fence are presented in Table B-10.

Table B-10 Scattered Radiation Dose Rates at the MNRC Facility Fence After a Loss of Pool Water Accident Following 2 MW Operations	
Time After Shutdown	Effective Dose Equivalent Rate (rem/h)
10 seconds	0.460
1 hour	0.047
1 day	0.021
1 week	0.011
1 month	0.006

**APPENDIX C**

**PROBABILISTIC ASSESSMENT OF  
THE AIRPLANE CRASH RISK FOR  
MCCLELLAN AIR FORCE BASE  
TRIGA<sup>®</sup> REACTOR**

Appendix C - Valid Pages

Rev. 3 03/22/18

i	Rev. 3	03/22/18
ii	Rev. 3	03/22/18
C-1	Rev. 3	03/22/18
C-2	Rev. 3	03/22/18
C-3	Rev. 3	03/22/18
C-4	Rev. 3	03/22/18
C-5	Rev. 3	03/22/18
C-6	Rev. 3	03/22/18
C-7	Rev. 3	03/22/18
C-8	Rev. 3	03/22/18
C-9	Rev. 3	03/22/18
C-10	Rev. 3	03/22/18
C-11	Rev. 3	03/22/18
C-12	Rev. 3	03/22/18
C-13	Rev. 3	03/22/18
C-14	Rev. 3	03/22/18

TABLE OF CONTENTS

SUMMARY .....C-1

1. INTRODUCTION.....C-2

2. ASSESSMENT METHODOLOGY .....C-3

3. ANALYSIS.....C-7

4. CONCLUSIONS.....C-13

LIST OF TABLES

C-1 AIRCRAFT (USAF) CRASH PROBABILITIES (REFERENCES C.4 AND C.5) .....C-7

C-2 AIRCRAFT MOVEMENTS AT MCCLELLAN AFB FOR THE SEVEN-MONTH PERIOD .....C-10

LIST OF FIGURES

C.1 TRIGA® REACTOR BUILDING .....C-5

C.2 CONDITIONAL WALL PENETRATION FOR HEAVY AIRCRAFT IMPACT .....C-6

C.3 TRIGA® LOCATION .....C-8

C.4 MCCLELLAN AFB AIR TRAFFIC PATTERNS .....C-9

NOTE: This appendix was extracted from the Stationary Neutron Radiography System (SNRS) proposal to Sacramento Air Logistics Center, McClellan AFB, California, Volume I - Design and Management, Submitted March 31, 1986 by GA Technologies. The original authors were W. H. Strohmayer and M. G. Stamatelatos.

REFERENCES

- C.1 "Air Installation Compatible Use Zone (AICUZ)," McClellan Air Force Base Report, September 15, 1983.
- C.2 Wall, I. B., "Probabilistic Assessment of Aircraft Risk for Nuclear Power Plants," Nuclear Safety 15, 1974, p. 276.
- C.3 American Nuclear Society Report of the Special Committee on Source Terms, September 1984.
- C.4 "Aircraft Crash Probabilities," Review, Nuclear Safety 17, No. 3, May-June 1976.
- C.5 Standard Review Plan, chapter 3, NUREG-0800, Office of Nuclear Reactor Regulation, USNRC, July 1981.
- C.6 Solomon, K. A., et al., "Airplane Crash Risk to Ground Population," UCLA-ENG-7424, March 1974.
- C.7 Hornyik, K., "Preliminary Evaluation of Hazards Associated with Siting of a 250 kW In-the-Ground TRIGA<sup>®</sup> Facility Near the Runway of the McClellan AFB," report prepared for N-Ray Engineering Company, December 9, 1983.
- C.8 Code of Federal Regulation Title 10, Parts 0 to 199, U.S. Government Printing Office, 1985.

## SUMMARY

An assessment of the risk of aircraft accidents at a TRIGA<sup>®</sup> radiography facility (stationary neutron radiography system) located at the McClellan Air Force Base in Sacramento, California was performed to evaluate its contribution to the overall reactor risk. The facility is partially below grade, with the top of the reactor core located 2 ft below ground level. The core itself is surrounded by a cylinder of reinforced concrete 7.5 ft thick, and it has a 7-ft concrete mat below.

The most severe credible accident sequence has been estimated to be the direct impact on the reactor building by a heavy aircraft leading to structure penetration and major damage to the reactor; i.e., the release of gaseous fission product nuclides from the gap between the fuel and the cladding as a result of fuel element breach. The doses related to this release are below 10 CFR 20 limits and much below the 10 CFR 100 limits which would actually apply under reactor accident conditions.

The present analysis consisted of the evaluation of three probabilities the product of which yields the sought-after probability. These are the probability of aircraft impact onto the reactor building and its vicinity, the conditional probability of building penetration when subject to impact, and the probability of major reactor damage given reactor structure penetration.

Each of the three probabilities was calculated by using conservative methods and data. Therefore, the resulting product, i.e., the probability of major reactor damage due to aircraft accidents, which was evaluated to be  $5 \times 10^{-8}$  per reactor year, is an upper limit. The “best estimate” value is expected to be considerably lower.

Probabilistic safety analyses of nuclear power reactors have generally concluded that a reactor damage probability due to an aircraft accident less than  $10^{-7}$  per year does not represent a significant contribution to the overall reactor risk.

In a “partially below grade” configuration, the design safety requirement for the SNRS (specification 4.2.2 in solicitation No. F04606-86-R-0266) is that either (1) the probability of a significant radiological accident is less than  $10^{-7}$  per year, or (2) the maximum credible radiological accident will have inconsequential effects, considering both air and water releases as per 10 CFR 20 and ANSI 15.7 limits. Our analysis has shown that the GA TRIGA<sup>®</sup> reactor can actually meet both requirements. Therefore, the aircraft radiological accident is an “incredible” event

## 1. INTRODUCTION

The objective of this assessment is to estimate the risk of aircraft accidents at a stationary neutron radiography system (SNRS) facility using a 1-MW TRIGA<sup>®</sup> nuclear reactor located at the McClellan Air Force Base in Sacramento, California.

The main concern motivating this assessment is the potential release to the public of radioactive material as a result of an aircraft striking the reactor building or its vicinity.

Over the past two decades, probabilistic methods have gained increasing use for evaluating the risks of nuclear power reactors. Probabilistic risk assessment (PRA) is aimed at evaluating the probability of adverse reactor conditions leading to prompt or delayed severe health hazards to the public.

As a result of numerous reactor studies, it has been concluded that airplane crashes become a significant contributor to public risks when the probability of a significant aircraft radiological accident exceeds approximately 1 in 10,000,000 reactor years; i.e.,  $10^{-7}$  per reactor year. If this probability is smaller than  $10^{-7}$ , the aircraft accident risk becomes insignificant or, equivalently, the aircraft radiological accident becomes an incredible accident scenario.

In a “partially below grade” configuration, the design safety requirement for the SNRS (specification 4.2.2 in solicitation No. F04606-86-R-0266) is that either (1) the probability of a significant radiological accident is less than  $10^{-7}$  per year, or (2) the maximum credible radiological accident will have inconsequential effects, considering both air and water releases per 10 CFR 20 and ANSI 15.7 limits. Our analysis has shown that the GA TRIGA<sup>®</sup> reactor can actually meet both requirements. Therefore, the aircraft radiological accident is an “incredible” event.

The analysis performed here has been realistic (best estimate) where possible and very conservative where there were data limitations. The derived conclusions about aircraft accident-related risk are therefore very conservative from the safety standpoint.

## 2. ASSESSMENT METHODOLOGY

The probability  $P$  per year that an airplane crash will lead to critical reactor damage is essentially the product of three probabilities:

1.  $P_c$ , the probability of an airplane crash at the reactor site,
2.  $P_{p/c}$ , the conditional probability that the reactor building will be penetrated as a result of an airplane crash.
3.  $P_{d/p}$ , the conditional probability of critical damage to the reactor as a result of airplane-crash-induced reactor building penetration,

$$P = P_c \cdot P_{p/c} \cdot P_{d/p} \quad (C-1)$$

The crash probability,  $P_c$ , is the product of three factors: the number of aircraft movements, the accident probability per aircraft movement per unit area, and the effective area of the target of interest.

$$P_c = \sum_i \sum_j \sum_k (N_{ijk} C_{ijk} A_{ijk}) \quad , \quad (C-2)$$

where  $N_{ijk}$  = number of annual movements of type  $j$  for aircraft type  $i$  in flight pattern  $k$ ,

$C_{ijk}$  = crash probability per movement of type  $j$  for aircraft type  $i$  in flight pattern  $k$ ,

$A_{ijk}$  = effective target area associated with the structure of interest for aircraft type  $i$  in movement type  $j$  and flight pattern  $k$ .

The types of aircraft for an Air Force Base (Reference C.1) include fighters, trainers, heavy aircraft, and other miscellaneous aircraft. The aircraft movements include takeoff, landing, and closed pattern maneuvers. Flight patterns refer to flights to and from different runways.

In the present analysis the aircraft were grouped into two categories: those exceeding 12,500 lb in gross weight and the lighter ones which represent an insignificant fraction of the total operations. Three flight maneuvers were considered: namely, takeoff, landing, and closed patterns. There is only one flight path of interest since there is only one runway in the TRIGA<sup>®</sup> vicinity.

The conditional probability of penetration as a result of an airplane crash is generally evaluated for both direct and indirect hits. The latter refer to the impact of missiles generated as a result of the airplane crash in the immediate vicinity of the target of interest, as well as the possibility of lateral aircraft skid into the structure.

For the present analysis it was conservatively estimated that indirect hits are inconsequential because of the target configuration and building structure (Figure C.1). The reactor building (with wall thickness of 3.5 ft or more) is surrounded on all sides by rooms and, therefore, it was estimated that no missile generated by an aircraft crash in the immediate vicinity of the TRIGA<sup>®</sup>

building could penetrate to and through the reactor walls. Thus, only direct hits were considered in the analysis.

For direct hits the conditional probability of structure penetration by an aircraft was calculated based on the method of Reference C.2. This method very conservatively evaluates the conditional probability of penetration of a reinforced concrete wall when impacted by a heavy aircraft at full flight speed. The probability is given as a function of wall thickness as shown in Figure C.2.

The conditional probability of radionuclide release from the reactor by fuel element breach due to reactor structure penetration by an impacting aircraft ( $P_{d/p}$ ) is difficult to evaluate analytically because it strongly depends on the collision history and on the likelihood that all or most of the reactor water will be lost and that a radioactive release from the damaged fuel will enter the atmosphere or groundwater resulting in radiological environmental hazard.

The McClellan AFB TRIGA<sup>®</sup> core is surrounded on all lateral sides and on the bottom by a continuous concrete structure 7 ft thick. Therefore, total loss of coolant is highly unlikely since this structure is designed to comply with seismic requirements. Also, Reference C.2 conservatively estimates that 7 ft of reinforced concrete are impenetrably by an aircraft. If the reactor water is not lost, then it will be an effective radionuclide filter. Water scrubbing under accident conditions was estimated to be a very efficient radionuclide remover when estimating nuclear reactor accident source terms (Reference C.3).

Nevertheless, the present analysis took the very conservative approach of assigning  $P_{d/p}$  the value of unity. This approach could be fine-tuned at a later time when a "best estimate" value (less than one) could be used instead. This is, however, not necessary to meet the SNRS aircraft accident design specification.

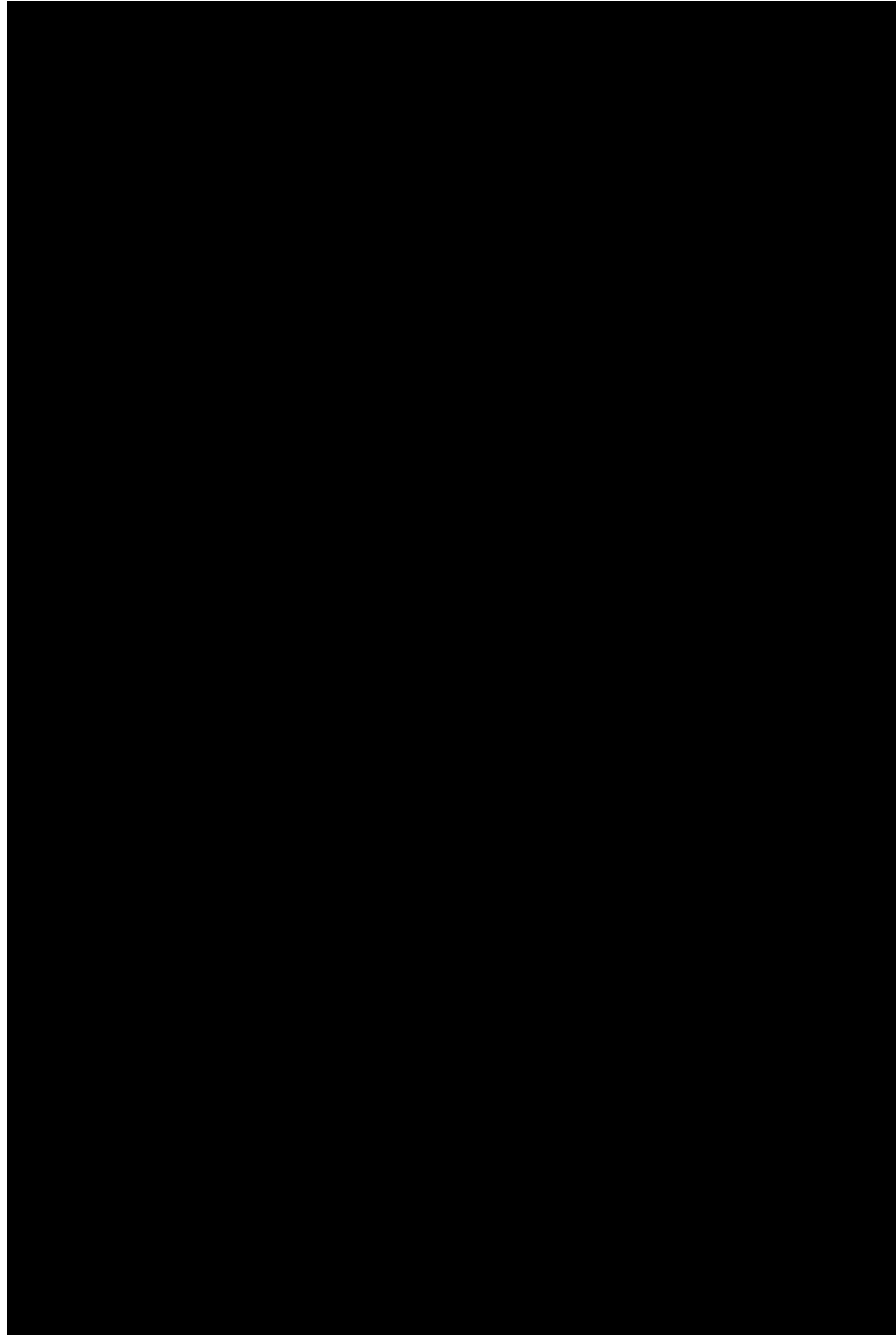


FIGURE C.1: TRIGA<sup>®</sup> REACTOR BUILDING

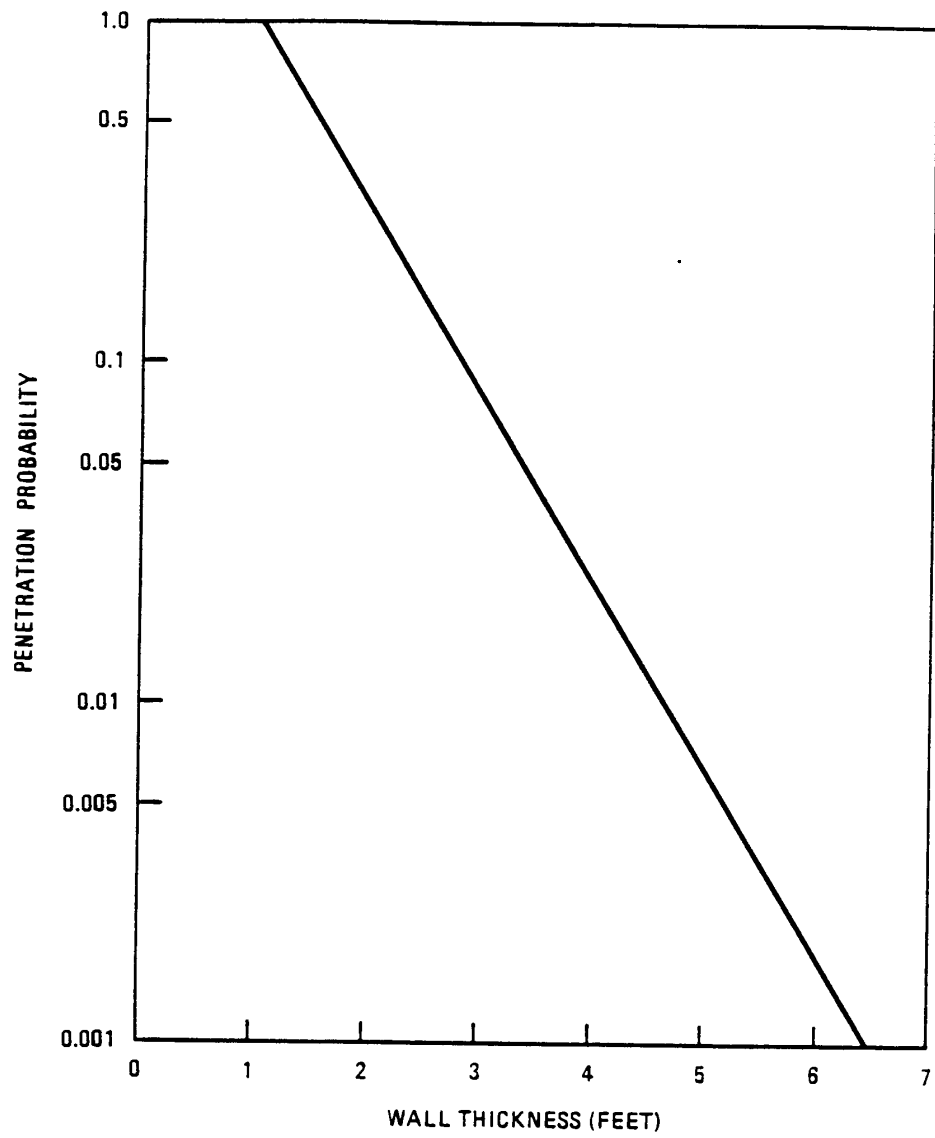


FIGURE C.2: CONDITIONAL WALL PENETRATION FOR HEAVY AIRCRAFT IMPACT

### 3. ANALYSIS

The proposed location of the McClellan SNRS TRIGA<sup>®</sup> is shown in Figure C.3. The reactor building is located approximately 2000 ft east of the main north-south runway and 4000 ft north of the runway's southern end. Figure C.4 shows the air traffic patterns at McClellan.

The aircraft crash probability was evaluated using Equation C-2. We considered essentially only one class of aircraft, those with a gross weight in excess of 12,500 lb. Lighter aircraft operations at McClellan form an insignificant part of total operations. We also considered three maneuvers (takeoff, landing, and closed patterns) and one flight path (one runway).

Table C-1 shows data accumulated for USAF aircraft crash probabilities as a function of distance from the runway (References C.4 and C.5). These probabilities have been combined to generate an overall probability of crash per square mile per aircraft movement within an area with a radius of five miles from the runway. This probability, evaluated to be  $10^{-8}$  per square mile per movement, was used as the probability of crash for closed patterns. Based on information from Reference C.6, the probability of crash during a landing maneuver is  $1.5 \times 10^{-7}$  per square mile per movement. We assumed that takeoffs have a negligible contribution to the crash probability at the reactor site because the reactor is always at an orientation of 180 deg away from the takeoff flight path.

Table C-2 shows operations data for McClellan AFB. These data, in raw form, were collected for the seven-month period from February 1 through August 31, 1981. Assuming that the air activity in Reference C.1 is fairly constant in time, the annual activity was obtained by multiplying the seven months data by 12/7. This step was omitted in the analysis of Reference C.7, which was also performed for McClellan AFB. We subdivided the aircraft activity into categories: closed pattern and landings. The total annual activities for all aircraft are also given in Table C-2.

TABLE C- 1 AIRCRAFT (USAF) CRASH PROBABILITIES (References C.4 and C.5)	
Distance from Runway (miles)	Crash Probability ( $10^{-8}$ /square mile movement)
0 to 1	5.7
1 to 2	2.3
2 to 3	1.1
3 to 4	0.42
4 to 5	0.4



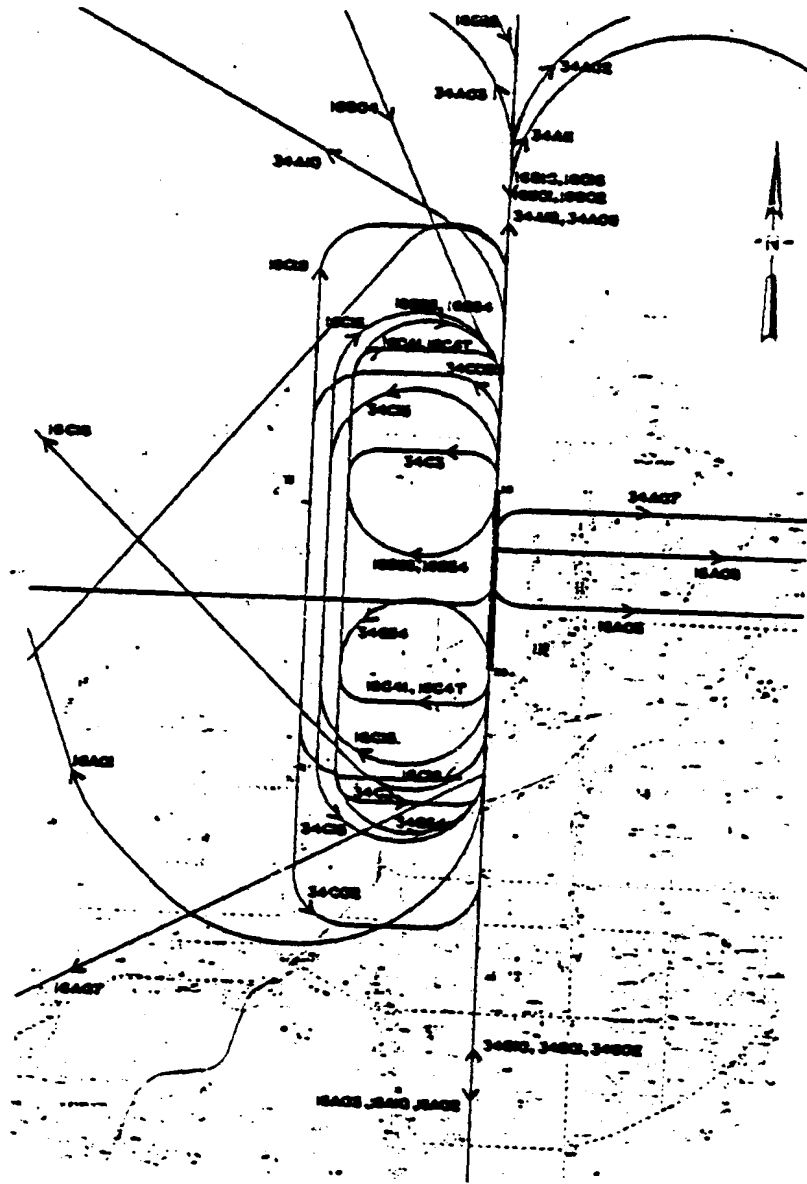


FIGURE C. 4 MCCLELLAN AFB AIR TRAFFIC PATTERNS

TABLE C-2 AIRCRAFT MOVEMENTS AT MCCLELLAN AFB FOR THE SEVEN-MONTH PERIOD  
FEBRUARY 1 THROUGH AUGUST 31, 1981  
(Reference C.2)

Maneuver	Fighter		Trainer		Heavy		Miscellaneous	
	7-Month	Annual	7-Month	Annual	7-Month	Annual	7-Month	Annual
Takeoff	3,226	5,530	2,218	3,802	3,768	6,459	6,870	11,777
Landing	3,226	5,530	2,218	3,802	3,768	6,459	6,870	11,777
Closed patterns	12,154	20,835	7,447	12,766	18,560	31,817	9,387	16,092
Total	18,606	31,895	11,883	20,370	26,096	44,735	23,127	39,636

The target area for the crash probability calculation was evaluated from exact drawings of the proposed SNRS TRIGA<sup>®</sup> facility and the "shadow" area was calculated using a glide angle of 20 deg (Reference C.6). The base dimensions of the reactor building are 72 ft 3 in. X 85 ft 6 in. with a height of 33 ft. Thus the effective target area is:

$$A_{eff} = \frac{(72.25)(85.5)ft^2}{(5280 ft/mi)^2} + \frac{(33)(85.5)ft^2}{\tan(20^\circ)(5820 ft/mi)^2} = 5 \times 10^{-4} mi^2.$$

This effective area does not include the room above the reactor which houses the control rod drives and the refueling crane (Figure C.1). This room was deemed to be more vulnerable to airplane crash structural damage than the rest of the reactor building (thinner walls), and it was treated separately from the rest of the reactor building.

The calculation of the probability of an aircraft crash on the reactor building yields:

$$\begin{aligned} P_c &= (81,510 \text{ closed patterns/year}) \left( 1 \times 10^{-8} \frac{\text{crash}}{\text{closed pattern} - mi^2} \right) (5 \times 10^{-4} mi^2) \\ &+ (27,568 \text{ landings/year}) \left( 1.5 \times 10^{-7} \frac{\text{crash}}{\text{landing} - mi^2} \right) (5 \times 10^{-4} mi^2) \\ &= 2.5 \times 10^{-6} \text{ crashes/year} \end{aligned}$$

Estimates of the conditional probability of penetration given a crash are given in Figure C.2. For the case where the minimum thickness of reinforced concrete is 3.5 ft and the aircraft weight is greater than 12,500 lb the conditional probability of penetration is approximately 0.045/crash. Thus the uncorrected probability of breach of the reactor building structure is:

$$\Delta \dot{P}_1 = (0.045/\text{crash})(2.5 \times 10^{-6} \text{ crash/year}),$$

$$\Delta \dot{P}_1 = 1.1 \times 10^{-7} / \text{year}.$$

This number requires correction because only approximately one-third of the target area has the minimum wall thickness of 3.5 ft, while the remainder has a minimum wall thickness of 8 ft which, according to Reference C.2, is impenetrable to an airplane crash. Applying the one-third correction factor to the previous calculation, we obtain the probability of core damage due to the breach of the reactor building structure:

$$\Delta P_1 = (1/3)(1.1 \times 10^{-7})/\text{year},$$

$$\Delta P_1 = 3.7 \times 10^{-8}/\text{year}.$$

The refueling room, located above the reactor, has thin walls which are estimated to yield no significant missiles upon impact. However, a three-ton crane is in position over the core for at most two days every six months. The rest of the time, this crane is stowed away. Only when the crane is in position can it contribute to the likelihood of core damage by an impact-generated missile. The probability of this event was estimated from the annual probability of crashing into the refueling room using the fraction of time when the crane is in place. The effective target area of the refueling room is  $4.4 \times 10^{-5} \text{ mi}^2$ , whence the crash probability for this room is  $2.18 \times 10^{-7}/\text{year}$ . Since the room is a thin-walled structure, we can assume that the conditional probability of penetration is unity. The fraction of time the crane is in place is 0.01 (i.e., four days per year). Thus an additional contribution to probability of core damage due to a missile generated from a collision with the refueling crane is:

$$\Delta P_2 = (0.01)(2.18 \times 10^{-7})/\text{year} = 2.2 \times 10^{-9}/\text{year}$$

The probability of an aircraft crash directly onto the opening at the top of the reactor vessel will now be evaluated. Since it is assumed that the refueling room structure has unit conditional probability of penetration, the effective target area is the opening area at the top of the reactor vessel, which has a diameter of 7.5 ft. This area is  $2.3 \times 10^{-6} \text{ mi}^2$ . Therefore, the third contribution to the probability of damage to the reactor core, a crash directly onto the pool opening, is:

$$\Delta P_3 = \left( \frac{2.5 \times 10^{-6} \text{crashes}}{5 \times 10^{-4} \text{mi}^2 \text{year}} \right) (2.3 \times 10^{-6} \text{mi}^2) (1 \text{ penetration/crash}) (1 \text{ release/penetration}).$$

or

$$\Delta P_3 = 1.2 \times 10^{-8}/\text{year}.$$

The total probability of aircraft-related core damage is then the sum of these separate probabilities:

$$P = \Delta P_1 + \Delta P_2 + \Delta P_3,$$

which yields:

$$P = 5.1 \times 10^{-8}/\text{year}.$$

This value is considerably less than  $10^{-7}$ , the threshold value for a significant risk contributor.

It should be borne in mind that the value of P calculated here is very conservative in view of the fact that the probability of critical damage to the reactor given structural penetration ( $P_{d/p}$ ) was assumed to be unity. For a best estimate, inclusion of a more realistic value of  $P_{d/p}$  could lead to a reduction in the value of P by one order of magnitude or more.

#### 4. CONCLUSIONS

The reactor damage probability due to aircraft accidents was conservatively calculated to be  $5 \times 10^{-8}$ , a factor of two below the probability of a credible aircraft radiological accident. This, by itself, satisfies the SNRS aircraft safety requirement.

To further reinforce the statement that the aircraft radiological accident is an “incredible” event, several comments can be made regarding the potential radionuclide release during the aircraft-induced most severe TRIGA<sup>®</sup> accident.

The most severe credible accident for a TRIGA<sup>®</sup> is expected to be the simultaneous breach of integrity of the majority of the fuel elements and the complete loss of water from the reactor tank.

Insofar as melting of the reactor core following complete loss of coolant is not feasible for the TRIGA<sup>®</sup>, the only radiological hazard associated with the above most severe credible accident is due to gaseous radioisotopes that could be released from the gap between the nuclear fuel and the cladding in the event of fuel element breach. Aerosolization of the nuclear fuel is highly unlikely because the TRIGA<sup>®</sup> fuel elements consist of a UZrH<sub>x</sub> metallic matrix with outstanding retention capability not only structurally but also for the entrapped fission and activation products.

Release of radionuclides into the ground by coolant loss is also unlikely. Since the reactor is surrounded from the sides and the bottom by a thick reinforced concrete structure that is not penetrable by a direct aircraft crash, the only mode of water loss can be due to aircraft-generated missiles which are not capable of penetrating or cracking the reinforced concrete reactor cradle. If water is released from the reactor by severing one of the beam conduits connecting the reactor with the surrounding rooms without cracking the floor of the reactor structure, contaminated water cannot be released into the environment because the floor and part of the walls of the room adjacent to the reactor core are waterproof.

Therefore, the most credible aircraft-induced TRIGA<sup>®</sup> accident may involve partial release of gaseous radionuclides directly into the reactor atmosphere by partial exposure of damaged fuel elements and, indirectly, through the water remaining in the core which has been shown to be a very effective radionuclide “scrubber.”

By very conservatively assuming that all fuel rods can suffer clad rupture and that all halogens and noble gases are released, Reference C.7 has shown that the resulting whole body dose, as well as thyroid dose, is less than the limits in 10 CFR 20 (Reference C.8) and much less than those in 10 CFR 100. The results in Reference C.7, obtained for a 250-kW TRIGA<sup>®</sup>, were modified here to represent a 1-MW reactor. Despite the factor of 4 increase in power, the radiological doses for the 1-MW system are still below the 10 CFR 20 limits and well below the 10 CFR 100 limits. The 10 CFR 20 limits apply to radioactive material handling, while the 10 CFR 100 limits apply to reactor accident conditions. Although the latter are the suitable ones for use in assessing aircraft-induced radiological hazards, the maximum credible aircraft-induced release doses from a TRIGA<sup>®</sup> are also below the 10 CFR 20 limits.

**APPENDIX D**

**LAYOUT OF REACTOR AND  
REACTOR HALL**

Appendix D - Valid Pages  
Rev. 3 03/22/18

i	Rev. 3 03/22/18
D-1	Rev. 3 03/22/18
D-2	Rev. 3 03/22/18
D-3	Rev. 3 03/22/18

TABLE OF CONTENTS

D.0 Layout of Reactor and Reactor Hall .....D-1

LIST OF FIGURES

D.1 Floor Plan Of Reactor Hall Showing Relation Of Wall Mounted Air Supply Duct And  
500 Cfm Exhaust Duct .....D-2

D.2 Elevation View Showing Reactor Tank, Reactor Hall, Inlet And Outlet Ventilation Ducts .....D-3

#### D.0 Layout of Reactor and Reactor Hall

Personnel at MNRC have supplied sketches of the relationship between the reactor tank, reactor hall, and the inlet and exhaust ventilation ducts. These are exhibited in Figures D.1 and D.2. Figure D.1 is important for two reasons. First, it shows why it is reasonable to assume that a portion of the hot air plume is diverted from the reactor hall into the 500 cfm exhaust duct at the top of the reactor tank. Second, it shows that the exhaust from the 1600 cfm return duct should be diverted from across the core to an angular direction (perhaps 30° to 45°). Such a redirected air path minimizes the disturbance of the plume as it rises into the reactor hall and does not interfere with the action of the 500 cfm exhaust duct to withdraw a portion of the plume before it enters the reactor hall. In the redirected path, the 1600 cfm continues to promote rapid mixing of the reactor hall air.

Figure D.2 provides additional information concerning the physical relationship of the hot air plume from the core and the various inlet and exhaust ducts. It should be noted that an additional 300 cfm of air is supplied to the reactor hall by leaks through the walls, ceiling, and around the two doors in the east wall.

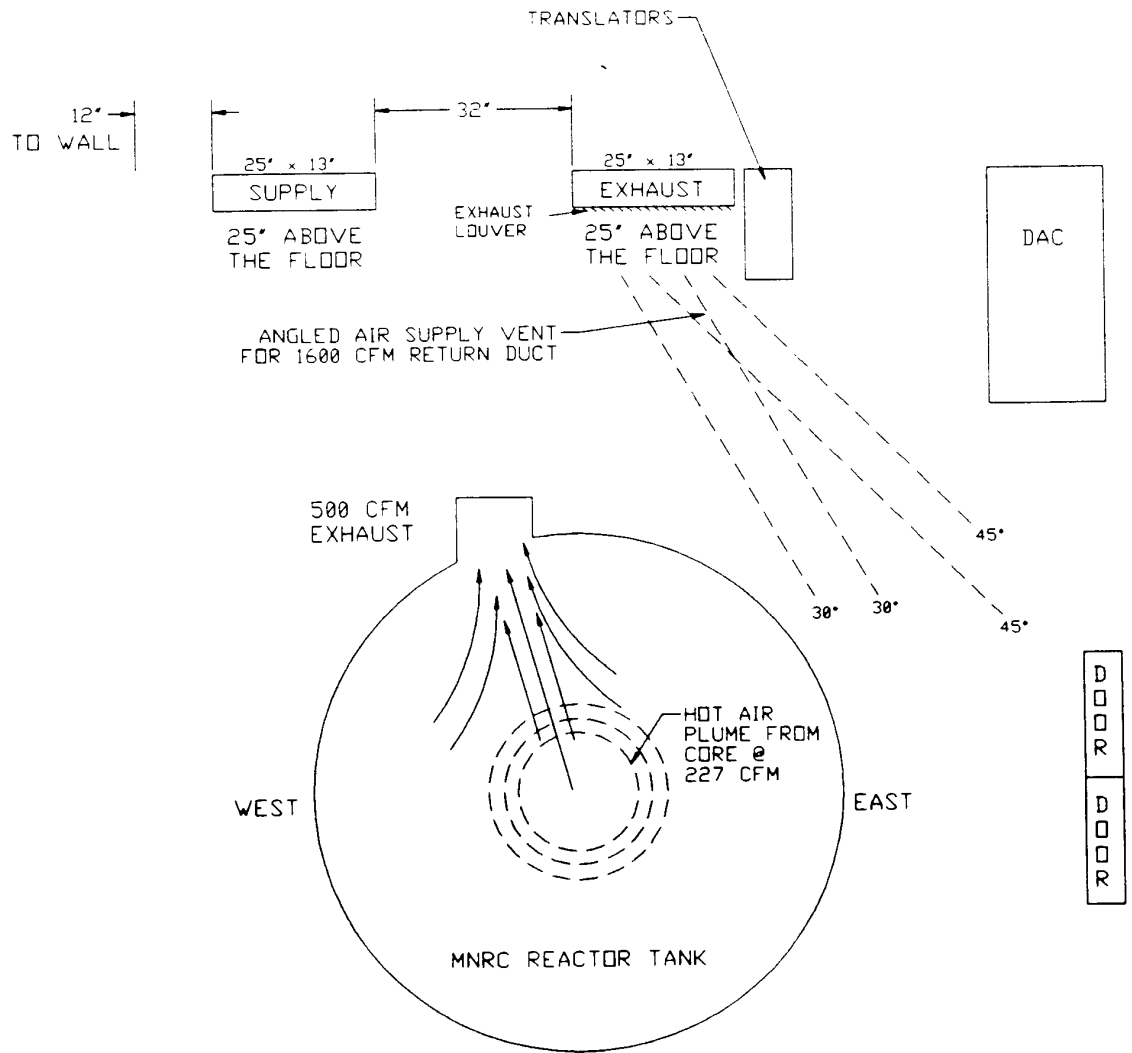


**Figure D. 1: FLOOR PLAN OF REACTOR HALL SHOWING RELATION OF WALL MOUNTED AIR SUPPLY DUCT AND 500 CFM EXHAUST DUCT**

